



<https://theses.gla.ac.uk/>

Theses Digitisation:

<https://www.gla.ac.uk/myglasgow/research/enlighten/theses/digitisation/>

This is a digitised version of the original print thesis.

Copyright and moral rights for this work are retained by the author

A copy can be downloaded for personal non-commercial research or study,  
without prior permission or charge

This work cannot be reproduced or quoted extensively from without first  
obtaining permission in writing from the author

The content must not be changed in any way or sold commercially in any  
format or medium without the formal permission of the author

When referring to this work, full bibliographic details including the author,  
title, awarding institution and date of the thesis must be given

Enlighten: Theses

<https://theses.gla.ac.uk/>  
[research-enlighten@glasgow.ac.uk](mailto:research-enlighten@glasgow.ac.uk)

**FRictional BEHAVIOUR OF REINFORCEMENT  
IN REINFORCED EARTH FILL MATERIALS**

by

**Meijiu Wei**

**A Thesis Submitted for the degree of Doctor of Philosophy**

**Univerisity of Glasgow  
Department of Civil Engineering**

**May 1990**

ProQuest Number: 11007358

All rights reserved

INFORMATION TO ALL USERS

The quality of this reproduction is dependent upon the quality of the copy submitted.

In the unlikely event that the author did not send a complete manuscript and there are missing pages, these will be noted. Also, if material had to be removed, a note will indicate the deletion.



ProQuest 11007358

Published by ProQuest LLC (2018). Copyright of the Dissertation is held by the Author.

All rights reserved.

This work is protected against unauthorized copying under Title 17, United States Code  
Microform Edition © ProQuest LLC.

ProQuest LLC.  
789 East Eisenhower Parkway  
P.O. Box 1346  
Ann Arbor, MI 48106 – 1346

**DEDICATED TO MY PARENTS**

# CONTENTS

	<u>PAGE</u>
ACKNOWLEDGEMENTS	1
SUMMARY	2
NOTATION	4
CHAPTER 1: INTRODUCTION	6
1.1 GENERAL	6
1.2 SCOPE OF THESIS	8
CHAPTER 2: LITERATURE REVIEW	11
2.1 INTRODUCTION	11
2.2 THE DEVELOPMENT OF EARTH REINFORCEMENT	11
2.2.1 Historical Earth Reinforcement	11
2.2.2 Application of Reinforced Earth	13
2.3 THEORY REVIEW	14
2.3.1 Concept of Reinforced Earth	14
i) Fundamental mechanics	14
ii) Design theory of reinforced earth	16
2.4 MATERIALS USED IN REINFORCED EARTH	21
2.4.1 Fill	21
i) Cohesionless fill	22
ii) Cohesive frictional fill	22

iii)	Cohesive fill	23
iv)	Waste materials	24
2.4.2	Reinforcement	25
i)	Metallic reinforcement	26
ii)	Non-metallic reinforcement	26
2.5	SOIL-REINFORCEMENT FRICTIONAL CHARACTERISTICS	27
2.5.1	Friction Coefficient	28
2.5.2	Measurements of Soil-Reinforcement Interaction	29
2.5.3	Direct Shear Box Tests	30
2.5.4	Pull-out Tests	33
i)	Pull-out tests on a full-scale structure	34
ii)	Pull-out tests on a reduced scale model structure	35
iii)	Pull-out tests from a box	36
2.5.5	Discussion	39
CHAPTER 3:	DESCRIPTION OF THE MATERIALS USED IN THE PRESENT WORK	59
3.1	INTRODUCTION	59
3.2	FILL MATERIALS	59
3.2.1	Minestones	59
3.2.1a	Wardley Minestone	60
3.2.1b	Wearmouth Minestone	61
3.2.2	Horden Red Shale	61
3.2.3	Loudon Hill Sand	62
3.2.4	Methil PFA	63
3.3	REINFORCING MATERIALS	64
CHAPER 4:	DIRECT SHEAR BOX TESTS	74
4.1	INTRODUCTION	74
4.2	APPARATUS AND PROCEDURES	74

4.2.1	Shear Box Apparatus	74
4.2.2	Test Procedures	75
4.3	TEST RESULTS	76
4.3.1	Wardley Minestone	76
4.3.2	Wearmouth Minestone	78
4.3.3	Horden Red Shale	79
4.3.4	Loudon Hill Sand	79
4.3.5	Methil PFA	80
4.4	COMPARISON OF THE RESULTS FROM THE VARIOUS FILL MATERIALS	81
4.5	CONCLUSIONS	83
CHAPTER 5:	LABORATORY PULL-OUT BOX TESTS	104
5.1	INTRODUCTION	104
5.2	APPARATUS AND PROCEDURES	104
5.2.1	Pull-out Box Apparatus	104
5.2.1a	Load Controlled Pull-out Box	104
5.2.1b	Displacement Controlled Pull-out Box	105
5.2.2	Test Procedures	105
5.3	TEST RESULTS	106
5.3.1	Wardley Minestone	106
i)	Force-Displacement Behaviour	106
ii)	Maximum Pull-out Force and Friction Coefficient	107
5.3.2	Wearmouth Minestone	109
i)	Force-Displacement Behaviour	109
ii)	Maximum Pull-out Force and Friction Coefficient	110
5.3.3	Horden Red Shale	112

i)	Force Displacement Behaviour	112
ii)	Maximum Pull-out Force and Friction Coefficient	113
5.3.4	Loudon Hill Sand	114
i)	Force-Displacement Behaviour	114
ii)	Maximum Pull-out Force and Friction Coefficient	115
5.3.5	Methil PFA	116
i)	Force-Displacement Behaviour	116
ii)	Maximum Pull-out Force and Friction Coefficient	117
5.3.6	Comparison of the Results from the Various Fill Materials	117
5.4	DISCUSSION AND CONCLUSIONS	118
5.4.1	Discussion	118
5.4.2	Conclusions	125
CHAPTER 6:	SOME SPECIFIC PULL-OUT TESTS	171
6.1	INTRODUCTION	171
6.2	TEST DESCRIPTION	171
6.3	TEST RESULTS	174
6.3.1	Pull-out tests with "Piano Wire" Monitoring	174
i)	Paralink behaviour in pull-out tests	174
ii)	Extension and strain distribution along a Paralink strap	175
6.3.2	Results from Tests with "Sandwich" Straps	176
6.3.3	Results from a Test with a Ribbed Steel Strap Monitored by Pressure Cells	177

6.3.4	Results of Pull-out with Facing Plate Tests	177
6.3.5	Comparison of Load and Displacement Controlled Pull-out Box Tests	178
6.4	CONCLUSIONS	179
CHAPTER 7: FIELD FULL-SCALE PULL-OUT TESTS		205
7.1	INTRODUCTION	205
7.2	FIELD TEST BOX, DEVICES AND TEST PROCEDURES	205
7.2.1	The Full-Scale Boxes and Test Devices	205
7.2.2	Test Procedures	206
7.3	TEST RESULTS	207
7.3.1	Results with Wardley Minstone	207
7.3.2	Results with Wearmouth Minestone	208
7.3.3	Results with Horden Red Shale	209
7.3.4	Results with Loudon Hill Sand	210
7.3.5	Results with Methil PFA	211
7.4	COMPARISON AND DISCUSSION	212
7.4.1	Comparison of the Results from the Various Fill Materials	212
7.4.2	Discussion of the Field Test Results	213
7.5	CONCLUSIONS	215
CHAPTER 8: COMPARISON OF THE TEST METHODS AND DESIGN CONSIDERATION		244
8.1	INTRODUCTION	244
8.2	COMPARISON OF THE RESULTS FROM THE DIFFERENT TEST METHODS	244
8.2.1	Test Results	244
8.2.2	Analyses of The Test Methods	246

8.3	RELATIONSHIP BETWEEN THE FRICTION COEFFICIENT AND SOME OF THE FACTORS	254
8.3.1	Apparent Friction Coefficient of Fill-Reinforcement	254
8.3.2	The Friction Coefficient from Shear Box Tests	258
8.3.3	The Relationship between Pull-out Force and Strap Displacement	259
CHAPTER 9:	GENERAL DISCUSSION, CONCLUSION AND FUTURE WORK	287
9.1	INTRODUCTION	287
9.2	GENERAL DISCUSSION	287
9.2.1	Reinforcing Materials	287
9.2.2	Fill Materials	289
9.2.3	Characteristics of Bond Resistance	292
	i) Influence of overburden pressure on friction coefficient	292
	ii) Influence of density on friction coefficient	293
	iii) Influence of reinforcement extensibility and softness on apparent friction coefficient	298
	iv) Influence of strap length on apparent friction coefficient	299
	v) Influence of moisture content on bond resistance	300
	vi) Influence of facing plate in pull-out tests	300
9.3	CONCLUSIONS	301
9.4	SUGGESTIONS FOR FUTURE STUDY	304
	REFERENCES	307

## ACKNOWLEDGEMENTS

I would like to express my appreciation to the head of department, Dr. D. Green, Professor H. B. Sutherland and Professor D. Muir Wood for the opportunity to do this work and for their encouragement and continued interest in the progress of this research.

I am deeply indebted to my supervisor Mr. T. W. Finlay for his invaluable guidance, encouragement and help throughout this work.

I would like to specially thank Professor K. Skarzynska, Dr. N. Hytiris, Mr. A. Bouazza and Mr. S. Barnett for their collaboration, assistance and discussion, particularly during the field experimental work.

My special thanks go to Dr. W. M. Stewart and Dr. I. McConnochie for their help during this period.

I am grateful to Mr. W. Henderson and T. Montgomery for their generous assistance in setting up the apparatus. Thanks also due to Mr. A. Yuill for helping with the electronic equipment.

Many thanks also to my friends and fellow research students, O. A. Awolaye, H. Jasem, E. Osman, M. Zhu, I. Hass whose warmth and companionship made my stay so memorable.

The author also wishes to acknowledge financial support from Glasgow University and also partly from the U.K. Government ORS Awards. Many thanks to British Coal Minestone Services for providing the testing materials without which this research would not have been possible.

Finally, I would like to express my sincerest thanks to my wife, my son and my mother-in-law for their love, encouragement and boundless patience overall these years.

## SUMMARY

This thesis reports on an investigation into the interaction between reinforcement and fill in reinforced earth.

The theory and development of reinforced earth and previous research work pertaining to soil–reinforcement bond resistance have been reviewed.

This investigation was mainly carried out using three different test methods, viz. large shear box tests, laboratory pull–out tests and field full–scale pull–out tests. Three types of reinforcing straps, viz. galvanized ribbed steel, Paralink 500s and Paralink 300s were tested with five different fill materials, viz. Wardley minestone, Wearmouth minestone, Horden red shale, Loudon Hill sand and Methil PFA. The tests were carried out under various conditions of overburden pressure, density, moisture content and strap length. A total of 550 tests were completed and the results obtained from the different test methods, different reinforcing and fill materials and various conditions are compared.

The fill–reinforcement friction coefficient was found to be influenced by test method, overburden pressure, density, moisture content, strap length, extensibility and compressibility. Comparing the three test methods, no matter which reinforcement and fill material were used the field full–scale pull–out test produced the lowest friction coefficient. Higher results were generally obtained from laboratory pull–out tests than from direct shear box tests when ribbed steel was used, whereas when Paralink straps were used higher results were encountered from direct shear box tests. Ribbed steel strap produced the highest friction coefficient with Paralink 500s being superior to Paralink 300s, no matter which fill material was used. As regards fill materials, Horden red shale appeared to produce higher bond resistance, while the efficiency of the minestones, the PFA and the Loudon Hill sand varies with the type of reinforcement and test method.

The pulling behaviour of Paralink straps in a pull–out test was monitored by using a "piano wire" method. The extensible Paralink straps were found to perform differently from rigid straps. The "piano wire" monitoring method is a readily

available method to investigate the pulling behaviour of an extensible strap, strain distribution along a strap being calculated from the results. The strap extensibility is an important characteristic which causes the reduction of the apparent friction coefficient.

It is believed that dilatancy and arching play an important part in a pull-out test. However, the arching effect acts differently with rigid ribbed steel and compressible Paralink straps. It increases the normal pressure on a ribbed steel strap, whereas when a Paralink strap is used the normal pressure is reduced.

When Paralink straps are used, pull-out tests appear to be more suitable than shear box tests to obtain the fill-reinforcement friction coefficient, since the influence of extensibility and compressibility of a strap is involved in the former tests.

A relationship was established between the friction coefficient and the overburden pressure and density for the present used materials.

## NOTATION

The symbols in general use throughout the thesis are listed below. Symbols peculiar to a particular theory or part of the thesis are defined in the text when they occur.

- c — cohesion of soil
- $c_r$  — cohesion between the fill and reinforcement
- $f^*$  — apparent friction coefficient
- $f^{**}$  — friction coefficient from model wall tests
- $f_c$  — the constant value of the apparent friction coefficient  
from a  $f^*$ - $\log\sigma_v$  curve
- $m/c$  — natural moisture content
- $m/c_{opt}$  — optimum moisture content
- n — number of effective layers of reinforcing elements
- t — thickness of an element of reinforcement
- B — width of an element of reinforcement
- D — pull-out displacement
- $D(x)$  — extension distribution along a reinforcing strap
- E — Young's modulus
- $E_p$  — pull-out stiffness
- FS — factor of safety
- H — height of the fill
- $\Delta H$  — zone of action of an individual layer of reinforcement
- $K_a$  — coefficient of active earth pressure
- $K_0$  — coefficient of earth pressure at rest
- $K_p$  — coefficient of passive earth pressure
- $K_u$  — ratio of the angle of skin friction  
and internal friction of soil
- L — length of an element of reinforcement

- LL — liquid limit
- N — the number of the first layer of reinforcement  
to cross the theoretical failure line
- PI — plasticity index
- PL — plastic limit
- $S_h$  — horizontal spacing of reinforcement
- $S_v$  — vertical spacing of reinforcement
- T — tensile force in the reinforcement
- $T_i$  — the total maximum tension in the  $i$ th layer of reinforcement
- $T_{max}$  — the maximum pull-out force in a pull-out test
- U — uniformity coefficient
- $\alpha$  — the angle of the decreasing line to horizontal  
in  $f^*-\log\sigma_v$  curve
- $\sigma_1$  — major principal effective stress
- $\sigma_3$  — minor principal effective stress
- $\sigma_c$  — the overburden pressure at which the  $f^*$  starts  
to be constant in a  $f^*-\log\sigma_v$  curve
- $\sigma_h$  — lateral stress on an element of soil
- $\sigma_v$  — vertical stress on an element of soil (or overburden pressure)
- $\gamma$  — unit weight of the fill in a structure
- $\gamma_d$  — dry density
- $\gamma_{max}$  — maximum dry density
- $\tau$  — shear stress
- $\tau_r$  — residual shear stress in a shear box test
- $\tau_s$  — maximum shear stress in a shear box test
- $\mu$  — friction coefficient between the fill and reinforcing elements  
from shear box tests
- $\varphi$  — Mohr-Coulomb angle of internal friction of fill material
- $\delta$  — angle of friction between fill and reinforcement
- $\epsilon(x)$  — strain distribution along a reinforcing strap

## CHAPTER 1

### INTRODUCTION

#### 1.1 GENERAL

The term "reinforced earth" generically refers to any mass of soil which has been artificially strengthened by the incorporation of one or more reinforcement elements within it. However, after Vidal (1966, 1969a and 1969b) introduced the new composite construction material, this term has become closely associated with the particular system which consists mainly of three different parts: fill, reinforcement and facing. According to Vidal's concept, long thin galvanized steel strips are placed at a horizontal orientation and spaced evenly in a horizontal and vertical direction in selected frictional soil. The strips are most commonly fixed to a facing to enable a vertical retaining wall or abutment to be constructed (*Figure 1.1*). The strengthening of the reinforcement to the soil is achieved by the mobilization of friction between soil and reinforcement.

As an alternative to conventional structures such as retaining walls, and bridge abutments built of reinforced concrete, reinforced earth provides cost reduction, ease of construction and suitability for poor subsoil. It is also extensively adaptable to various fields, such as industrial works, harbour facilities, town development, hydraulic structures, etc ... . During its twenty years development, the particular advantages of reinforced earth technique have become more attractive to civil engineers and used more frequently in building construction in recent years.

Significant developments have been made on reinforced earth in both utilization of new materials and design theory. On the aspect of reinforcing materials in addition to the metallic strips, some non-metallic reinforcements with various forms have been invented, such as polymers, glass fibre reinforced plastic (GRP), Paralink (or Paraweb), Geotextile, Geogrids and Tensar, some of which have been widely used in the construction. On the other hand, apart from the conventional fill

material — cohesionless soil, some other fills such as cohesive soil and waste materials are also used or have been tried as the fill materials in reinforced earth structures.

A number of design theories have been developed. However, the general design procedures for earth retaining walls include the checking of internal and external stability. External stability of a reinforced earth wall is checked using conventional procedures. Internal stability requires checking against tension failure and adhesion failure. In order to design against the latter type of failure a knowledge of frictional (or bond) resistance between the reinforcement and the fill material is required. This is normally represented by appropriate friction coefficients.

The bond resistance between fill and reinforcing elements is regarded as the most fundamentally important aspect of reinforced earth. Therefore besides other aspects of reinforced earth, extensive research work on this complex mechanism has been carried out by a number of investigators. Various test methods have been employed by the investigators to obtain the fill–reinforcement friction coefficient, these mainly are: direct shear box tests, pull–out tests and model tests.

A direct shear box test is conducted using a shear box apparatus. During testing the shear force is applied to the interface of the soil and reinforcing elements. Shear resistance can be obtained under different normal stresses, and in turn the friction coefficient can be calculated.

Pull–out tests can be carried out from a laboratory pull–out box, a model structure or an actual structure. In a test, a reinforcing strip embedded in the soil is extracted under a series of overburden pressures. As a result the apparent friction coefficient can be obtained from the maximum pull–out force.

From model tests to failure by reinforcement slippage, the soil–reinforcement friction coefficient can also be calculated by taking the maximum strip tension as the maximum pull–out resistance.

Like many other applications, however, practice leads theory, so that the optimum designs may not always result, prediction of performance may not be precise, and all aspects of behaviour may not be fully understood. As Lee (1978)

said, "Although conceptually simple, the behaviour of reinforced earth is actually very complex and I imagine many more years will elapse before the basic mechanisms are clearly established to every one's satisfaction". On the other hand, new applications are continually being conceived, and new fill materials and new reinforcing materials and configurations are under investigation. Therefore it is still an attractive subject for researchers to investigate.

## 1.2 SCOPE OF THESIS

This thesis reports on an investigation into the characteristics of the interaction between the fill materials and reinforcements. Three types of reinforcement were used in the present research, these are a galvanized ribbed steel strap and two I.C.I developed polypropylene straps — Paralink 500s and Paralink 300s. These reinforcements were tested with five different fill materials, viz. Wardley minestone, Wearmouth minestone, Horden red shale, Loudon Hill sand and Methil PFA. The investigation was undertaken using three different test methods, large shear box, laboratory pull-out box and field full-scale pull-out tests. The large shear box tests and laboratory pull-out tests were carried out in the Soil Mechanics Laboratory of Glasgow University. The field full-scale pull-out tests were performed with the assistance of British Coal's Minestone Services at Wardley Colliery in England and Barony Colliery in Scotland.

The present investigation is associated with a programme of research at Glasgow University, being done with the assistance of a grant from British Coal's Extra-Mural Research Committee. This research programme is to investigate the possibility of using minestone as a fill in conjunction with polypropylene reinforcing straps, since minestone is a readily available fill material found in many areas of the U.K., while polypropylene offers better corrosion resistance.

Chapter 1 presents the general introduction and the scope of the present research. Chapter 2 reviews the development of reinforced earth and the material used in reinforced earth, and theoretical and experimental work done by previous

investigators, with particular emphasis on the investigation of bond resistance characteristics between fill and reinforcements. Chapter 3 contains details of the properties of the materials (fills and reinforcements) used in the present work. The description of the shear box apparatus and procedures of the shear box test, and the presentation of the results, some discussions and conclusions from the tests are contained in Chapter 4. Chapter 5 contains the description of the laboratory pull-out apparatus and testing procedures, and the results and some conclusions from the tests are also presented in this Chapter. Some specific pull-out test results and more discussions are contained in Chapter 6. Chapter 7 describes the field tests, and presents the results obtained. The comparison of the results from the different tests are made, the relations between the friction coefficient and some of the influential factors are established in Chapter 8. Finally, Chapter 9 presents the general discussion, conclusions from this investigation and suggestions for further study.

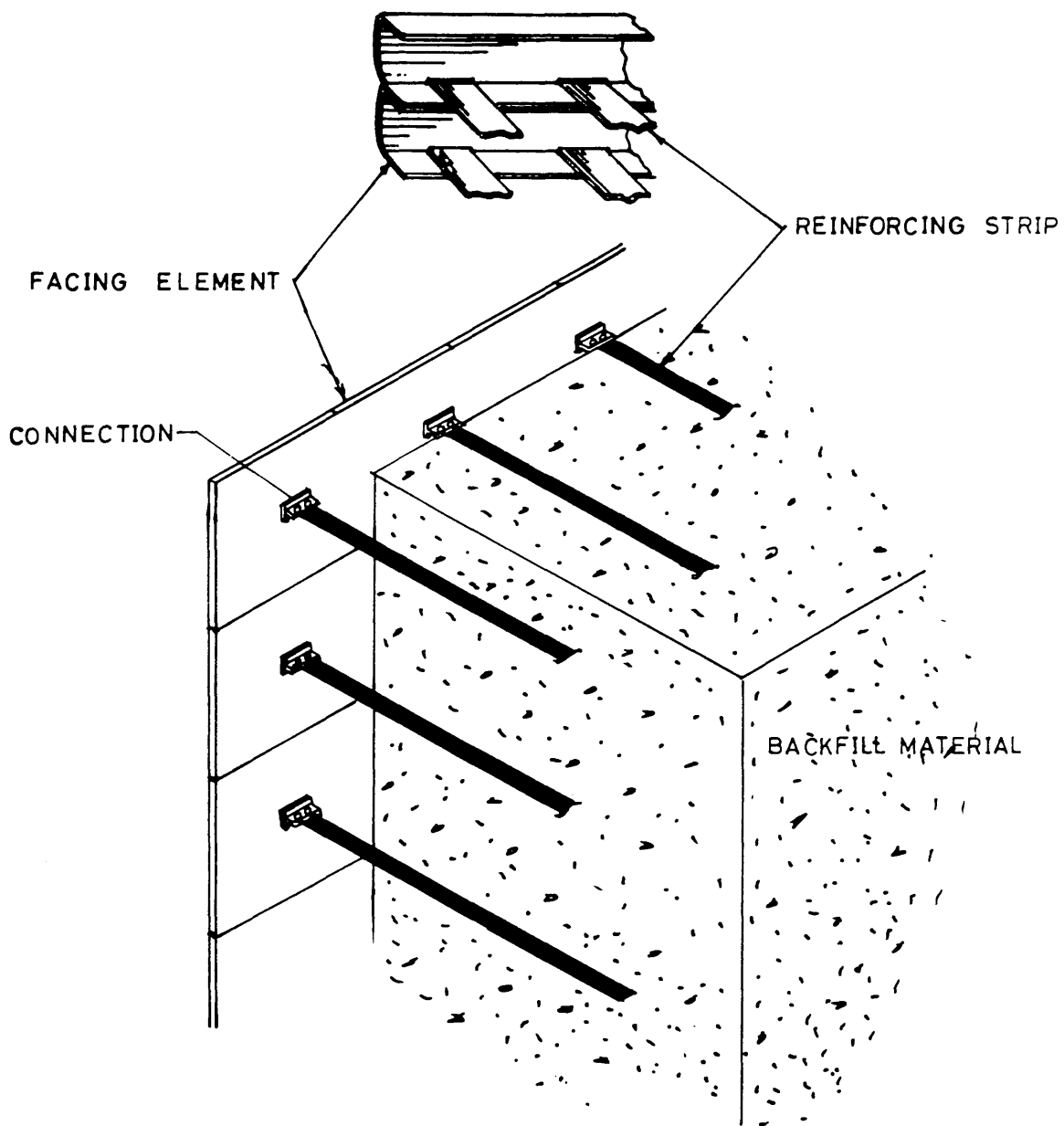


**Figure 1.1** Schematic representation of major elements of reinforced earth wall

## CHAPTER 2

### LITERATURE REVIEW

#### 2.1 INTRODUCTION

During the last two decades significant developments have been made on reinforced earth and research work has been undertaken by a number of investigators over the years. Most of the work has involved the design theory and the fundamental mechanism, i.e. bond resistance of fill–reinforcement. These are reviewed in this chapter.

This chapter includes five sections. Section 2.1 is the introductory section. In section 2.2, the author makes a brief review of the development of reinforced earth structures, and describes their applications. Section 2.3 reviews the concept and the design theories. The materials are described in section 2.4. The main part in this chapter is section 2.5 which is closely related to the present research and reviews and describes in detail previous researches into the interaction of soil–reinforcement.

#### 2.2 THE DEVELOPMENT OF EARTH REINFORCEMENT

##### 2.2.1 *Historical Earth Reinforcement*

Reinforced earth is a relatively new construction material invented in 1966 by French architect and engineer, Henry Vidal (1966, 1969a and 1969b). It is a composite material consisting mainly of three different parts: fill, reinforcement, and facing. The concept of earth reinforcement, however, is far from new. The basic principles are demonstrated abundantly in nature by animals and birds and the action of tree roots. As a matter of fact, earth reinforced constructions have existed in the world for about 5,000 years.

As long ago as the fifth millennium B.C. compacted clay reinforced with reed was used in the construction of crude mud huts in Sivalik on the Iranian Plateau. By the fourth millennium B.C. this method of construction was superseded by the simple adobe brick. The earliest remaining example of earth reinforcement is the Agar-Quf structure which is 45m tall, thought to be 3,000 years old (Hanna 1977). The great wall of China, parts of which were completed circa 200 B.C., contains example of reinforced soil. The reinforcement, in this case, was made using mixtures of clay and gravel embedded with tamarisk branches (Dept. of Transport 1977).

An early contributor to the use of earth reinforcement as a general building medium was Lt. Col. Pasley of the Royal Engineers who introduced a form of reinforced soil for military construction in the British Army. He demonstrated that a significant reduction could be made in the pressure exerted behind retaining walls, when the fill was reinforced by horizontal layers of brushwood, wooden planks or canvas, Pasley (1822).

A significant development in the modern concept of reinforced earth structures was made in the United States in 1925 by Andreas Munster. The reinforced earth wall shown in *Figure 2.1*, consisted of a light facing unit to which reinforcement was attached. This in plan looks very much like a ladder in which the "rungs" of the ladder were intended to generate high frictional forces between the fill and the reinforcement. Sliding attachments between the reinforcing members and the facing allowed vertical movement of the reinforcement relative to the back of the wall in order to minimize the problem associated with settling of the backfill.

In the 1930's, Coyne introduced the "mur a echelle" (ladder wall), in which the retaining wall consisted of a mass of granular fill unified by a row of tie members each having a small end anchor, together with a thin cladding membrane (see *Figure 2.2*).

Although reinforced earth structures have existed for thousands of years and have been developed by a number of investigators, what is regarded as the first credible reinforced earth system, was introduced by Henry Vidal in 1960's.

"Reinforced Earth" (or "Terre Armee") was the term given by Vidal to describe all forms of earth reinforcement or soil structures. The concept of reinforced earth, according to Vidal, is a composite material formed from flat reinforcing strips laid horizontally in a frictional soil, the interaction between the soil and the reinforcements being solely by friction generated by gravity (*Figure 1.1*).

The first reinforced earth wall was built in 1964 for research by Vidal in France (Price 1975), but the first major retaining wall structure using Vidal's concept was started on the Autoroute de Menton, in South of France, in 1968. In 1972 the first reinforced earth structure was completed in the United States (Chang et al 1972, 1974 and Beaton et al 1974). Meanwhile, in 1973 a reinforced earth wall was completed at Granton near Edinburgh, in the UK. The wall having a 7m height and a 106m length, was completed in five weeks and was reported by T.W. Finlay and H.B. Sutherland (1978, 1979). Since then more and more reinforced earth structures have been erected. Up to 1979, 2,300 reinforced earth structures had been completed throughout the world, with a construction area of 1.35 million square metres (McKittrick et al 1979). In 1980, the first reinforced earth structure was erected in China. This was a retaining wall 12m high and 82m long. The highest reinforced earth structure in the world is a 43 metres high retaining wall in Pakistan.

### 2.2.2 Applications of Reinforced Earth

As a composite construction material, reinforced earth has proved to be economical and beneficial in a wide range of areas. Reinforced earth walls are expected to cost about half as much as cantilever or crib walls of the same height (Lee 1973). Apart from the cost advantage for a general ideal case, reinforced earth offers several significant technical advantages that may make it even more attractive for special situations. Because it is flexible and the structural components are built simultaneously with the backfill, it is particularly suited for use over compressible foundations.

The following cases are some areas of application and structural forms which have been used in practice:

(1). Reinforced walls (*Figure 1.1*);

The main use of reinforced earth.

(2). Embankments (*Figure 2.3*);

(3). Foundations (*Figure 2.4*).

(4). Bridge abutments (*Figure 2.5*);

(5). Dams (*Figure 2.6*).

It can also be used in some other areas, such as highways—reinforced—embankments supporting carriageways, housing applications used to form terraced housing to support sloping sites, industrial, military, railways, pipe works, underground structures and so on. Generally speaking, reinforced earth can be used in quite a wide range of areas and with development, new applications are continually being conceived.

## 2.3 THEORY REVIEW

### 2.3.1 Concept of Reinforced Earth

#### i) Fundamental mechanics

Vidal was enlightened by the phenomenon when, on the beach he laid rows of pine needles in the sand and discovered that the slope of the sand embedded with pine needles was steeper than the one without (see *Figures 2.7* and *2.8*). This started his research work, and after five years of theoretical studies and model tests the basic conclusion reached by Vidal (1966, 1978) was that when dry granular soil is combined with a roughened material having tensile strength, the resulting composite material is stronger than the soil alone. Some forty years ago Professor

Arthur Casagrande idealised the problem in the form of a weak soil reinforced by strong membranes laid horizontally in layers (Westergaard 1938). It was basically the same idea as Vidal.

Reinforced earth is somewhat analogous to reinforced concrete in which the reinforcement is bonded to the soil. However, this direct comparison between the two situations is not completely valid, because with reinforced concrete the reinforcement is designed to carry the tensile forces in the structural element, whereas, in the case of reinforced soil, it is likely that a completely compressive stress field will exist. The mode of action of reinforcement in soil is therefore, not the one of carrying developed tensile stresses but one of anisotropic reduction of normal strain rate (C.J.F.P. Jones 1985).

The fundamental mechanism of reinforced earth has been accurately identified and explained by Bassett and Last (1978), McKittrick (1978), and Swiger (1978). The global effect of the reinforcement is to restrain the lateral deformations of the soil.

It was pointed out that soil obeys the Mohr–Coulomb failure criterion which, for a cohesionless soil, may be simply defined by two linear failure envelopes inclined at  $+\varphi$  and  $-\varphi$  to the normal stress axis (*Figure 2.9*), where  $\varphi$  is the internal angle of shearing resistance of the soil. If such a soil is loaded by a vertical principal stress  $\sigma_1$ , then for the soil not to fail there must also be a lateral confining stress  $\sigma_3$  consistent with stability which is  $K_a\sigma_1$ , where  $K_a$  is the coefficient of active earth pressure. These limiting conditions are represented by the Mohr stress circle shown by the solid line in *Figure 2.9*. If the externally applied confining pressure  $\sigma_3$  is reduced to zero then under the action of  $\sigma_1$ , the stress circle, shown by the broken line in *Figure 2.9* would fall outside the Mohr–Coulomb envelope thus indicating failure in the soil.

Considering a semi–infinite mass of cohesionless soil at depth  $H$ , vertical stress can be expressed as:

$$\sigma_v = \gamma H.$$

At–rest lateral stress is:  $\sigma_H = K_0\gamma H$

where  $K_0 \approx 1 - \sin\varphi$  (Jaky 1944).

If the soil expands laterally the lateral stress ( $K_0\sigma_v$ ) reduces to the limiting value ( $K_a\sigma_v$ ).

The fundamental mechanism of reinforced earth can be illustrated by the following example. Let us assume an element of cohesionless soil (*Figure 2.10*). If a vertical load is applied to the soil, the element will expand laterally. In a dense state, because of dilation, the lateral strain is more than half the axial strain. If, however, reinforcing elements, which are inextensible relative to soil, are placed within its mass, in the form of horizontal layers, the reinforcement will prevent any lateral strains because of adhesion – or interaction – between the reinforcement and the soil. The soil will be restrained as if a lateral force had been imposed on the element. The lateral force equivalent to the pressure at rest  $K_0\sigma_v$ , (i.e. the effect of the reinforcement) will restrict anisotropically any normal strains. It can be seen that as  $\sigma_v$  increases the lateral stress also increases in direct proportion. Therefore, for any value of the angle of internal friction ( $\varphi$ ), normally associated with granular soils, the stress circle for the reinforced condition always lies below the rupture curve, as shown in *Figure 2.11*. Failure can only occur by loss of friction between the soil and the reinforcement or by tensile failure of the reinforcement. Therefore, the strength of the soil is considerably increased in reinforced earth as illustrated in *Figure 2.12*.

## ii) Design theory of reinforced earth

As mentioned in Chapter 1 the applications of reinforced earth structures exist in quite a wide civil engineering area. The majority of reinforced earth structures encountered are vertically faced reinforced earth retaining walls. The essential design theory of reinforced earth established is based on this kind of structure. The other types are normally related to the basic principle.

In designing a reinforced earth wall, generally two conditions are considered: External stability and Internal stability.

For external stability, conventional design methods are used. The reinforced

earth structure is considered as a unit. The effects of self-weight and of the loads acting on the structure are taken into account. The external failure conditions include the whole structure sliding, tilt/bearing, and slip within the surrounding sub-soil, or slip planes passing through the reinforced earth structure.

The internal stability is considered with the estimation of the number, size, strength, spacing and length of the reinforcement needed to ensure stability of the whole structure, together with pressures exerted on the facing. Considering internal stability, two failure modes may occur in reinforced earth. These are: reinforcement break and reinforcement slip. That means if the force established in the strips exceeds the breaking strength of the reinforcement, the structure will fail by rupture of the reinforcement. On the other hand if sufficient friction does not occur between the strips and the soil to generate the force required, failure will occur by the strips pulling out of the soil.

Two methods of analysis have been proposed in order to check internal stability. These are:

- a. Those in which local stability is considered for soil near a single strip or element of reinforcement (Lee et al 1973 and Bolton and Choudhury 1977).
- b. Those in which overall stability of blocks or wedges of soil is considered.

According to the local stability analysis and Schlosser and Vidal's assumption of reinforcement maintaining the active earth pressure ( $K_a$ ) in soil, Lee et al and Bolton and Choudhury derived the force, T, in reinforcement, as –

$$T = K_a \sigma_v S_h S_v \quad (2.1)$$

where  $S_v$  is the vertical spacing,  $S_h$  the horizontal spacing of the reinforcement and  $\sigma_v$  the vertical stress caused by the overlying soil. Once the force in the strip is established, two modes of failure are considered: firstly the force may exceed the tensile strength of the reinforcement and secondly it may fail by the strip pulling out.

If the overall stability is considered, the method of calculation is to assume

that the wedge ABC is restrained by the reinforcement protruding through it into stable soil (Figure 2.13). The same failure mechanisms are assumed possible, i.e. reinforcement break or reinforcement slip.

Previous researchers have derived several design approaches according to the two failure modes, i.e. tension failure and adhesion failure.

a) Tension failure

When considering tension failure, the reinforcement is assumed to be of sufficient length so not to cause failure by lack of adherence. The following approaches are based on tension failure mode:

(1). Rankine theory

$$T'_{\max} = K_a \gamma H \Delta H \tag{2.2}$$

Where  $T'_{\max}$  — maximum tensile force in the bottom layer of reinforcing elements or elements under consideration;

$\gamma$  — unit weight of the fill in a structure;

$H$  — height of the fill;

$\Delta H$  — zone of action of an individual layer of reinforcement.

This approach was advocated by Laboratoire Central des Ponts et Chaussees in 1967.

(2). Coulomb wedge theory

$$T_i = \frac{n}{n + 1} K_a \gamma H \Delta H \tag{2.3}$$

where  $T_i$  — the total maximum tension in the  $i$ th layer of reinforcement;

$n$  — number of effective layers of reinforcing elements.

$$\text{or } \Sigma T = \gamma H^2 \left[ \frac{FS - \tan \beta' \tan \varphi'}{\cot \beta' \tan \varphi' + 1} \right]^{1/2} \quad (2.4)$$

where FS — Factor of safety;

$\varphi'$  — effective angle of internal friction;

$$\tan \beta' = \sqrt{(\tan^2 \varphi' + \frac{FS - \tan \varphi'}{\cot \beta' \tan \varphi' + 1})}$$

(3). Coulomb moment balance

$$T'_{\max} = \frac{n^2}{(n^2 - 1)} K_a \gamma H \Delta H \quad (2.5)$$

(4). Trapezoidal distribution

$$T'_{\max} = K_a \gamma H \Delta H \left[ 1 + K_a \left( \frac{H}{L} \right)^2 \right] \quad (2.6)$$

where L — length of an element of reinforcement.

(5). Meyerhof distribution

$$T'_{\max} = K_a \gamma H \frac{\Delta H}{\left[ 1 - 0.3 K_a \left( \frac{H}{L} \right)^2 \right]} \quad (2.7)$$

Among the several design methods, the Coulomb wedge theory gives the minimum area of reinforcement needed, whereas the trapezoidal distribution is more conservative.

#### b) Adhesion failures

Based on the other failure mode, i.e. adhesion failure, the following design approaches are introduced:

(1). Rankine theory (I)

$$FS = 2 \left( \frac{BL\mu}{K_a \Delta H} \right) \quad (2.8)$$

where B — width of an element of reinforcement;

$\mu$  — friction coefficient between the fill and reinforcement.

or if the part of the reinforcement which lies within the failure wedge is not taken into account in preventing failure by lack of adherence, then consider:

Rankine theory (II)

$$FS = \frac{2B\mu [ L - H \tan(45 - \varphi'/2) ]}{K_a \Delta H} \quad (2.9)$$

(2). Coulomb force balance

$$FS = \frac{4B\mu \Delta H}{K_a H^2} \sum_{i=N}^n i [ L - (n-i) \Delta H \tan (45 - \varphi'/2) ] \quad (2.10)$$

where N — the number of the first layer of reinforcement to cross the theoretical failure line.

(3). Coulomb moment balance

$$FS = \frac{12B\mu H^2}{K_a H^3} \sum_{i=N}^n (n-i) i \times [ L - (n-i) \Delta H \tan (45 - \varphi'/2) ] \quad (2.11)$$

(4). Coulomb wedge

$$FS = \frac{2B\mu\gamma H \left[ \frac{L}{2} (n+1) + H \tan\beta' \left( \frac{1-N^2}{6N} \right) \right]}{\frac{1}{2} \gamma H^2 \left[ \frac{FS - \tan\beta' \tan\varphi'}{\cot\beta' + \tan\varphi' + 1} \right]} \quad (2.12)$$

(5). Meyerhof distribution

$$FS = \frac{L}{\frac{H^2 K_a}{3L} + \left[ \frac{1}{1-1/3K_a} \left( \frac{H}{L} \right)^2 \right] \frac{K_a \Delta H}{2B\mu}} \quad (2.13)$$

As the height of a structure increases, the adherence developed between the soil and the reinforcement will increase; as a result, for low walls at a limiting factor of safety, the adhesion criteria rather than the tension criteria, will normally be critical.

There are other design methods such as logarithmic spiral method, elastic analysis, energy method, semi-empirical methods, etc, but since the present research is not primarily concerned with design theory, no more design details will be discussed.

## 2.4 MATERIALS USED IN REINFORCED EARTH

As has been mentioned, reinforced earth consists of three basic components, fill matrix, reinforcement and facing. In addition, other parts are required to cover associated elements such as the foundations, drainage, connecting elements and capping units and to act as barriers and fencing. However, among the three basic components, since facing panels have only a secondary function; limiting deformation and influencing the aesthetics, developments and improvements will not have a significant effect on the concept of reinforced earth structures. Fill and reinforcement are the main components which significantly influence the properties and costs of reinforced earth structures. In this section, these two main materials will be discussed.

### 2.4.1 Fill

Fill is the largest item in reinforced earth structures relative to the other

components. For this reason the properties of the fill chosen will considerably affect the quality and stability of the structure. Also a large increase in cost of fill will lead to a major increase in the total cost of the wall, particularly with large structures where the quantity of fill required may become the dominant factor in the economic aspect. Three principal considerations which influence the selection of fills for use in reinforced earth structures are reported by McKittrick (1979). These are: (1) long-term stability of the completed structure; (2) short-term (or construction phase) stability and (3) physicochemical properties of materials.

i) Cohesionless fill

Cohesionless fill is also termed frictional fill or granular backfill. Vidal's concept of reinforced earth was established based on cohesionless soil, particularly on sand. For practical purposes, only a limited range of fills is likely to be used.

Cohesionless fill is defined as good quality fill for reinforced earth, because of its advantages, such as being stable, free draining, not susceptible to frost, relatively non-corrosive to reinforcement, and usually possessing a good angle of internal friction. For the purpose of reinforced earth, it is defined in UK (Department of Transport 1978) as a material in which no more than 10% passes a  $63\mu\text{m}$  B.S. sieve, and in France refers to fill in which no more than 15% (by weight) is smaller than  $15\mu\text{m}$ . In UK the effective angle of internal friction,  $\phi \geq 25^\circ$ . In France the angle of internal friction,  $\phi$  of saturated consolidated frictional fill must be  $>25^\circ$ .

However, cohesionless fills are usually imported materials, therefore they are expensive.

ii) Cohesive frictional fill

Apart from cohesionless fills, there is another sort of material accepted for use in reinforced earth, i.e. cohesive frictional fill. According to British Technical

Memorandum BE 3/78, the fills used for reinforced earth structures are limited to either wholly frictional or wholly cohesive frictional material. Cohesive frictional fill can be defined as material with more than 10% passing 63 $\mu$ m BS sieve. The effective angle of internal friction of cohesive frictional fill,  $\phi \geq 20^\circ$ . Liquid limit  $LL \leq 45\%$ . Plasticity index,  $PI \leq 20\%$ . Although it is not as good quality as cohesionless fill, the main advantage of cohesive frictional fill is better availability when compared with cohesionless fill. This may represent an economy.

iii) Cohesive fill

Cohesive fills are regarded as poor materials when used for reinforced earth, and are not included in British Technical Memorandum BE 3/78. The main problem in using cohesive fills is generally short-term stability, due to the bond between cohesive fill and reinforcement strip being poor and subject to reduction if positive pore water pressure develops. Durability is considered to be another problem, since cohesive fills are significantly more aggressive than frictional fills.

However, as stated in BE 3/78, "the technique of reinforced earth is a developing art which will, from time to time, make use of new proprietary materials for which no adequate British Standards exist".

Despite these recommendations some successful trials with non-recommended fill materials can be found in the literature. Work at the Transport and Road Research Laboratory using cohesive fill and by Ingold (1980, 1981) has encouraged consideration of the utilization of cohesive and other economic materials. Murray and Boden (1979) used silty clayey sand as a fill material for a reinforced earth wall and concluded that, despite construction difficulties and pore pressure development, cost savings could be achieved in comparison with the utilization of granular material imported over substantial distances. Blivet and Gestin (1979) have found high friction coefficients between phosphogypse and Geotextile. Fourie et al (1987) and Terashi (1988) also reported that the shear strength of clay may be increased by geotextile reinforcement. Cohesive soils can be reinforced and may be economical. If suitable

reinforcement and construction techniques can be adapted to use cohesive fill, many widespread benefits and applications arise, particularly in areas where frictional fill is in short supply.

iv) Waste materials

The use of waste materials as fill for reinforced earth structures is attractive from an environmental as well as economic viewpoint.

(1) Minestone

Minestone or mine waste rock, is a by-product of mining coal. It is by far the largest source of waste material in the United Kingdom both in terms of existing surface accumulations and current annual production. Some 67 million tonnes were produced in Britain in 1979 – 80 by underground mining operations Rainbow (1983). Although minestone has been accepted for use in reinforced earth construction in some countries, e.g. Belgium and France, Rainbow (1987), it has hitherto not been utilized in reinforced earth structures in the U.K., since certain authorities have yet to be convinced that its mechanical, physical, and chemical characteristics are suited to backfill requirements in such structures. In order to assess such characteristics, together with the suitability of strap design and composition, British Coal's Minestone Services commenced technical studies in 1978. As part of the investigation, a series of reinforced earth structures have been constructed at five coalmines to date in Britain. The reinforced elements employed in the research programme include non-metallic Paraweb, Tensar and Fibretain, and high-adherence galvanized mild steel.

When considering minestone as a backfill for reinforced earth, spontaneous combustion, aggression and breakdown are factors which may effect its suitability, although investigations into minestone have shown that these problems can be solved with proper construction and reinforcing material. Because of the concern for the

durability of construction elements used with mine waste, reinforcing materials formed from materials which have high corrosion and degradation resistance are preferred, Jewell and Jones (1981).

## (2) Pulverized Fuel Ash (PFA)

Pulverized Fuel Ash (PFA) is a waste material produced in significant quantities by coal-fired power stations in many industrial areas. In addition, it has certain consistent material properties which are potentially attractive to the designer of reinforced earth structures, providing PFA can be supplied at an economic rate, relative to alternative materials, and at a price such that the final structure is economic when compared with alternative structural forms. In addition to the economic benefit, PFA also possesses some advantageous physical properties which offer the following potential technical benefits: lower density; cohesive-cementation action; easier handling; reduced site damage to reinforcement; and reduce internal stresses within the reinforced soil mass.

Because of its nature and fine structure, non-metallic and grid reinforcement may prove the most satisfactory form of reinforcement. Some structures have been completed, e.g. a reinforced earth retaining wall using Tensar Geogrids and PFA backfill was constructed at Dewsbury, West Yorkshire County, Jones (1984).

### 2.4.2 Reinforcement

Reinforcement is another component of reinforced earth. The conventional material and form of reinforcement is metallic strip, although a variety of other materials and forms have been used as reinforcement, including steel, concrete, glass fibre, polypropylene, wood, rubber, aluminium and thermoplastics. The form may be of strips, grids, anchors, vegetation, and combinations of these or other material forms.

i) Metallic reinforcement

The most common metallic reinforcement comes in the form of strips. Metallic strips are linear elements normally having their breadth,  $B$  greater than their thickness,  $t$ . Dimensions vary with applications and structure type, but are usually within the range  $t = 3$  to  $5\text{mm}$ , and  $B = 5$  to  $100\text{mm}$ . The form of strips can be either plain or have several protrusions such as ribs or grooves to increase the frictional resistance between the reinforcement and the fill. In addition to the strip form, metallic reinforcement can also be in the form of sheets, anchors, or other shapes. Related to steel reinforcement, the main concern is corrosion. This is not only a function of steel properties but also of environmental characteristics. The usual but not economical solution is to increase the thickness of the reinforcement, as a safety measure against corrosion. Galvanising, plastic coating, the utilization of stainless steel, aluminium or copper strips, can also be employed, but also with increasing cost of the structure.

ii) Non-metallic reinforcement

Besides the most common and conventional reinforcement, metallic strips, plastic reinforcement can also be employed. The continuous industrial development has provided a large variety of high tensile strength and stiff reinforcement materials, such as polymers, glass fibre reinforced plastic (GRP), Paralink, Geotextile and Tensor, all of which have been utilized in practice. Paralink strips are used in the present research and will be discussed further in Chapter 3.

The possibility that non-metallic reinforcement, in the form of fibre inclusions, might improve the strength and deformation resistance of soils has been considered by Hausmann (1976), who studied in the triaxial apparatus the effect of the diameter of inclusions on failure by lack of adherence, and showed that the apparent friction angle increases with the dimension of the inclusion.

Mallinder (1977) found that Fibretain strap had a coefficient of friction

against non-cohesive soils measurably higher than that between the same soil and conventional metallic straps.

Non-metallic strips normally possess strong corrosion resistance and are insensitive to the presence of compounds such as sodium chloride or sulphates. Since corrosion is regarded as a problem for reinforced earth structure and the problem becomes critical when cohesive fills, or waste materials are considered, in these cases non-metallic reinforcing elements appear more suitable than metallic reinforcement. Plastic reinforcement is of a more complex nature, where time and temperature may play an important role in its behaviour. The remaining uncertainties regarding plastic reinforcement are its durability and long term behaviour (creep). Durability will depend on the reinforcement material and environmental characteristics. Some data on degradation resistance of some synthetic fibres are presented by Ingold (1982). Creep behaviour depends on type of reinforcement, stress level and temperature. Studies by McGown et al (1984) have shown that since the factors affecting the time dependent behaviour of reinforcement have been identified and quantified, safe designs incorporating creep allowances can be achieved. Non-metallic strips are normally more flexible. They may behave differently from rigid strips when embedded in soil. The in-soil properties of fabrics are also very different from the in-air properties, McGown et al (1982).

## 2.5 SOIL-REINFORCEMENT FRICTIONAL CHARACTERISTICS

The essential phenomenon in the mechanism of reinforced earth is the friction mobilized at the soil-reinforcement interface. Unless shear stresses can be transferred to the reinforcement slip will develop. On the other hand if the slipping resistance exceeds the tensile strength of the reinforcement, then reinforcement breakage will occur before slip. It is obvious that the bond between the soil and the reinforcement is of major importance to reinforced earth structures design. Actually it is a complex mechanism depending on soil type, reinforcement type and how they interact with each other. It may behave differently for the same type of

reinforcement and fill in different conditions. As professor Lee (1978) once said "... the most fundamentally important, the most critical and the least understood aspect of reinforced earth in any form is the mechanism of sliding shear resistance between soil backfill and the tensile reinforcing elements".

Further, Lee proposed a list of reinforced earth topics for further study, the first item being "sliding shear resistance between soil and reinforcing material", including how it is developed; how to measure it; how to quantify and express it; how it varies with certain design factors; and how to apply it in practical designs.

The topic of sliding shear resistance between the soil and reinforcement has been the subject of numerous research studies in several countries over the last two decades. Previous research work pertaining to soil–reinforcement friction mobilization, including the test methods and the relative influences of different factors affecting the value of the soil–reinforcement friction coefficient will be reviewed in this section.

### 2.5.1 Friction Coefficient

Up to now all researchers have chosen to express the soil–reinforcement sliding resistance in terms of a sliding friction angle or a friction coefficient ( $f^*$  or  $\mu$ ).

From pull–out tests an apparent friction coefficient can be defined by the ratio, Alimi et al (1977):

$$f^* = \frac{T_{\max}}{2BL\gamma H} = \frac{T_{\max}}{2BL\sigma_v} \quad (2.14)$$

where  $T_{\max}$  is the maximum pull–out load,  $\sigma_v$  is the overburden pressure, and B and L are the strip width and length respectively, 2 is because two sides of the strip are mobilized in pull–out test.

Actually a friction coefficient can be worked out from the frictional angle obtained in shear box test. That is for a purely frictional soil,

$$\mu = \tan \delta \quad (2.15)$$

where  $\delta$  — friction angle between soil and reinforcing elements.

$$f^* = \tan \delta = \mu \quad (2.16)$$

for a cohesive frictional soil:

$$\mu = c_r/\sigma_v + \tan \delta \quad (2.17)$$

where  $c_r$  is the unit adhesion.

It is possible to relate  $\mu$  and  $f^*$  for a cohesive frictional soil. At any overburden pressure in the shear box,  $\mu = c_r/\sigma_v + \tan \delta$ . In terms of pull-out a reinforcing strip, length  $L$ , width  $B$  embedded in a fill under an overburden pressure  $\sigma_v$ , the maximum pull-out force

$$T_{\max} = 2BL\sigma_v\left(\frac{c_r}{\sigma_v} + \tan \delta\right) \quad (2.18)$$

$$\text{Hence } f^* = c_r/\sigma_v + \tan \delta = \mu \quad (2.19)$$

### 2.5.2 Measurements of Soil-Reinforcement Interaction

In order to investigate the friction characteristics of soil-reinforcement several types of tests have been used. Some tests used by previous investigators are presented in Table 2.1.

Additionally, model wall test results at failure have also been used by several investigators to measure the soil-reinforcement frictional angle, Bacot et al (1978). Some studies using triaxial tests can also be found in the literature, by Hausmann

(1976). More recently, another new technique called "extension test" was introduced by Shen et al (1988).

From table 2.1, it is evident that the most common testing methods are generally divided into two types of test, i.e. direct shear box and pull-out tests. The test adopted by British Standard for designing reinforced earth is the direct shear box test. The pull-out test has also been adopted to get the friction coefficient used in design of structures, Mitchell and Schlosser (1979).

### 2.5.3 Direct Shear Box Tests

There are two main types of direct shear test. The most common test procedure is described as follows:

In a shear box test, the bottom half of the box is filled with a block of hard wood (or metal) on which the reinforcing material is fixed. The top face of the material is flush with the top edge of the lower half of the box and aligned so that shearing occurs in a direction parallel to the longitudinal axis of the reinforcing element. The fill is then compacted in the upper half of the box, and a known normal stress is applied. Shear stress and displacement are monitored and recorded.

Another method was employed by Jewell (1980) and Dyer (1985), in which the inclined reinforcement was embedded within dense sand across the central plane (see *Table 2.1*).

Potyondy (1961) first used the direct shear box to measure the angle of skin friction between various construction materials such as steel, wood and concrete and different types of soils.

When Vidal introduced the technique of reinforced earth, this method was proposed for measuring the angle of friction between soil and reinforcement and since then many investigators including Osman (1977), Bacot et al (1978), Al-Huassani and Perry (1978b), Shen et al (1979), Jones and Smith (1979), Ingold and Templeman (1979), and Jewell (1980) have carried out tests on different strip materials, metallic and non-metallic to measure the angle of skin friction either for

use in design, or for comparison with pull-out tests or other research purposes.

Work carried out at the Central Laboratory of "Ponts et Chaussees", by Schlosser and Vidal (1969) on smooth and grooved aluminium strips tested in a shear box has shown that compared to the smooth strip the presence of grooves on the strip surface enables the almost complete utilization of the internal friction of the soil thereby increasing considerably the adhesion between the earth and the strip. It was further found in this series of tests, that a large number of very thin striations oriented in the direction of the displacement, occurred on the smooth strips indicating that sliding of the soil particles took place along the strip. However, in the case of the grooved strips, it was found that no such striations existed indicating that the soil particles remained attached to the strip as displacement proceeded. In this case, shearing of the soil took place on a plane parallel to the longitudinal axis of the strip.

The results from Schlosser's early study also indicated that an important parameter is the relative volume of fine grained portion to the granular portion, and that the friction developed decreases with increase in the fine-grained portion. Further, these studies indicated that the critical grain size which separates purely frictional behaviour is the  $15\mu\text{m}$  size, Schlosser and Long (1973).

In work carried out by Alimi and Bacot (1977) using a large shear box (600 x 600 mm), three factors which influence the friction coefficient were pointed out: (1) the nature of the surface of the reinforcing material; (2) rigidity of the reinforcing material and (3) the grain size of the soil.

Lee (1978) carried out a series of tests on samples of sand at various densities. Aluminium foil reinforcing material was tested. He discovered that density has no effect on the value of angle of skin friction. He also suggested that the angle of skin friction should be expressed as a ratio of the angle of internal friction of soil ( $K_u = \delta/\varphi$ ) which varies between the limits of approximately zero for a frictionless surface to a maximum of 1.0. The ratio of 0.66 is normally accepted in design.

Compared to the conventional shear box testing, Soydemir and Espinosa

(1979) conducted another shear box testing method in which instead of shearing the sand at the strip surface, the strip was sandwiched at the level of the controlled shearing plane. They observed that this method gave an angle of skin friction  $10^\circ$  higher than the conventional methods.

A very important work was carried out by Jewell (1980) to study the patterns of strain which result from the interaction between sand and reinforcement in the direct shear box test. He suggested that the sand may strain and due to this, he performed a set of tests in a large shear box in which the reinforcement was embedded within dense sand across the central plane. He observed two important features in the shear box test. (i) a new well defined zone of strain patterns and (ii) strip force–displacement relationship, as shown in *Figure 2.14*, which were then compared with pull–out tests carried out using the same material subject to the same stress level. For a potential failure surface intersecting the reinforcement layer, Jewell has demonstrated that a limit equilibrium analysis may be successfully used to obtain reinforcement forces in a direct shear box.

Investigations of the interaction between fabric reinforcing materials and soils have been carried out by several investigators using direct shear box tests.

A special  $1.10 \times 0.25\text{m}$  direct shear box was designed by Holtz (1977) so that  $0.15\text{m}$  wide fabric strips could be tested. The normal pressure was applied with a pressure bag and the strain distribution along the fabric strip was determined with magnets glued to the fabric. The test data indicated that the interface friction angle ( $\delta$ ) of the investigated sand, was the same as the angle of internal friction determined by direct shear tests.

Myles (1982) used direct shear tests ( $100 \times 100 \text{ mm}$ ) to investigate the soil–fabric interface friction. The fabric was located in the lower frame of the direct shear apparatus while sand was placed in the upper frame. The investigation indicated that the interface friction angle varied with the type of fabric material, woven and non–woven.

Miyamori et al (1986) also investigated the soil–fabric interface friction of non–woven fabric with direct shear tests. A relatively large shear box was used

(316 × 316 mm). The interface friction resistance ( $\delta$ ) was found to be lower than the angle of internal friction of the investigated soil as determined by triaxial or direct shear tests. For dense sand the interface friction resistance was only 72% to 87% of the peak shear strength of the sand.

Direct shear tests were also carried out by Chandrasekaran (1988) to determine the soil–fabric interface friction. The size of the direct shear box was 100 × 100 mm. It was found that the interface friction angle of the investigated angular sand decreased with the increasing normal pressure from about 41° at low normal pressure (50 KPa) to about 32° when the normal pressure was 500 KPa.

Large shear box tests (316 × 316 mm) were used by Makizuchi and Miyamori (1988). A series of tests with geofabrics against sand and cohesive soil were conducted at different conditions. The results indicated that mobilized friction on the fabric–soil interface is much lower than that of soil itself in a range of small displacement, but increases as the displacement develops and approaches finally toward the friction value of the soil itself, the denser the sand, the higher the friction angle for woven and non–woven fabrics. Increasing the moisture content of sand delays the appearance of peak friction of the interface.

#### 2.5.4 Pull-out Tests

The pull-out test is another method used to measure the soil–reinforcement friction coefficient. It is supposed by Mitchell and Schlosser (1979) to represent adequately the conditions which actually occur in reinforced earth, which can either be carried out from a real structure, a model structure or a pull-out box. In a reinforced earth structure, the reinforcement is pulled out in the actual condition. In a pull-out box test, a reinforcement is embedded in a compacted fill mass, and a normal pressure is applied. The pull-out force and the displacement are monitored and recorded. According to the maximum pull-out force, the apparent friction coefficient can be worked out. The pull-out box test is analogous to the pull-out test from a full scale structure, however, it enables a better control of the friction

mobilization than the full scale test where the reinforcements are embedded in a large mass.

i) Pull-out tests at full scale structure

Chang (1974) performed the first full-scale field pull-out tests during the construction of a reinforced earth wall at Highway 39, California, U.S.A. The results were obtained in the form of load-displacement curves with yielding, peak and residual points clearly defined (*Figure 2.15*). These points correspond to three loads which are: the yield load, the maximum load and the residual load. Chang concluded that the angle of skin friction decreases with increasing overburden height and increases with length of the reinforcement. The influence of strip length is shown in *Figure 2.16*. Further Chang et al reported (1977a and 1977b) that for the same strip length, the relation between the peak pull-out load and the overburden load is approximately linear. However the rate of increase in peak pull-out load caused by an increase in overburden is much smaller than that caused by an increase in strip length. It was suggested that the minimum strip length required for a low-height reinforced earth wall should be at least 3.1 m.

Some 500 field pull-out tests, using two types of reinforcement, plain and ribbed galvanized steel strips, in granular fill material have been performed by the Reinforced Earth Companies in France and Spain, (Schlosser 1977) to study the effect of strip roughness. Typical load-displacement curves (*Figure 2.17*) show that the peak resistance for ribbed strip is greater than for smooth strip, occurring at a displacement of approximately 50 mm and 5 mm with the ribbed strip and the smooth strip respectively. The value of apparent friction coefficient ( $f^*$ ) for both types of reinforcement was greater than  $\tan \delta$  measured using a direct shear box.

Full-scale pull-out tests both with plain strips and ribbed strips in galvanized steel were tested in several granular soils, Schlosser and Elias (1978). The conclusions were consistent with Chang. All pull-out tests performed indicated a decrease of  $f^*$  values with increasing overburden pressure  $\gamma H$  (*Figures 2.18, 2.19,*

2.20). Extremely high values of  $f^*$  are obtained at low overburden pressures, particularly for the ribbed strip.  $f^*$  appears to reach a constant value at an approximate value of  $\gamma H = 100 \text{ kN/m}^2$  (5 m to 6 m). With the smooth strip the constant value of  $f^*$  (obtained for  $\gamma H$  greater than  $100 \text{ kN/m}^2$ ) is approximately equal to  $\tan \delta$ ; with the ribbed strip it is equal to  $\tan \varphi$ .

Bacot and Iltis (1978) conducted a series of pull-out tests from a full scale structure with galvanized steel strip and sand. The fill mass was divided into two compacted and uncompacted zones. Different sizes of strip were tested. The results indicated that  $f^*$  was smaller in compacted fill than in non-compacted fill. The average decrease of  $f^*$  in a compacted zone with respect to the value of  $f^*$  in an uncompacted zone is 34%. This conclusion is quite surprising and is contrary to some other investigators. Considering different sizes he obtained the same conclusion as Alimi and Bacot, that is that the values of  $f^*$  decrease with the width and increase with the length of the reinforcing strips. He attributed this to the influence of the undulation of reinforcement.

Rainbow (1983) performed two series of full scale pull-out tests with ribbed steel and Donisthorpe minestone. The results are presented in *Figure 2.21* and *Figure 2.22*. From *Figure 2.21* it can be seen that the apparent angle of friction decreases with increasing normal stress (or fill height) and would appear to level out at a constant value estimated to be about  $f^* = 0.75$  and  $f^* = 0.6$ . *Figure 2.22* shows the plot of shear stress ( $\tau$ ) against normal stress ( $\sigma_v$ ). The resultant plots represent reasonable straight lines suggesting that the adhesion between the strap and fill makes a considerable contribution to the overall strength of system.

## ii) Pull-out tests on a reduced scale model structure

Alimi and Bacot et al (1977) performed a series of pull-out tests from a model with ribbed steel and sand. Various conditions and various sizes of reinforcement were considered to investigate the influences. Conclusions were drawn that the length and width of the strip, the overburden pressure, and the density are

some factors which influence the value of friction coefficient. This increases with the length (*Figure 2.23*), and decreases with the width (*Figure 2.24*). The influence of density is significant (*Figure 2.25*). The apparent friction coefficient  $f^*$  increases with increasing density. A surprising result produced contrary to the previous investigators was that  $f^*$  increases with the overburden pressure. However, the difference of the heights were small ( $H = 3, 6$  and  $9$  cm).

Smooth bronze reinforcement with sand tests were carried out at three different densities on reduced scale models (by Schlosser and Elias 1978) and it was found that the density of the granular fill material has a very large influence on the soil–reinforcement friction. At high density, the values of the apparent friction coefficient  $f^*$  are much greater than  $\tan \delta$ ; while at low density they are smaller than  $\tan \delta$ . The phenomenon can be explained by the fact that at high density the granular soil is dilatant and that the tangential stresses exerted by the reinforcement on the soil lead to increase in the normal stresses acting on the faces of the reinforcement by dilatancy. The apparent coefficient of friction  $f^*$  in this case decreases with width.

Tumay et al (1977) carried out a series of tests on model walls with both non–woven fibre and plain metal reinforcement against sand. Results from the two reinforcements, at different lengths of reinforcement and different densities of sand were compared. The following conclusions were drawn; the effectiveness in mobilizing sand–reinforcement interaction for fibre–fabric is three times higher than that of metal, because of the "grabbing" effect of fibre fabric. The frictional resistance of fibre fabric reinforcement increases with increasing relative density of sand; whereas in the case of metallic reinforcement the relative density has very little effect in improving friction capacity. By increasing the length, the efficiency in mobilizing soil–strip interaction for both types of reinforcement will increase.

### iii) Pull–out tests from a box

Pull–out tests from a special shear box ( $915 \times 915 \times 45$  mm) were

performed by the Reinforced Earth Company, U.S.A., (Schlosser and Elias 1978). Both smooth and ribbed strips were tested with five granular soils. The apparent friction coefficient  $f^*$  was found to decrease with increase in the average applied normal stress, as has been found in pull-out tests on actual structures. Constant values of  $f^*$  were obtained for the normal stress values of  $\sigma_v = 100 \text{ kN/m}^2$ . The values of apparent friction coefficient were greater than  $\tan\phi$  with ribbed strips (which lead to a soil-soil shear in the vicinity of the strip) and greater than  $\tan\delta$  with smooth strips, which can be explained by the dilatancy of the granular soil.

Walter (1978) conducted a series of pull-out tests to compare the performance of ribbed and smooth reinforcing strips in various types of soil. The same conclusions were drawn as Schlosser and Elias that the ribbed strip performed better than smooth strip and  $f^*$  decreased with increase in the surcharge load.

Shen and Mitchell et al (1979) carried out a series of pull-out tests on steel strips of various lengths and widths in a pull-out box. The  $f^*$  obtained from different sizes of strip showed a very random variation. A few tests on an undulating strip were carried out and compared with a plain strip. The results from the undulating strip were much larger than from the plain strip. Shen and Mitchell suggested that the apparent angle of skin friction would be affected not only by the testing method but also by soil arching, dilation, boundary conditions, soil compaction, strip geometry (length and width) and undulations in the strip.

Ingold and Templeman (1979) performed pull-out tests using five types of reinforcement: a woven fabric (Terram RF/12); two net structures (Netlon 1168 and FBM 5); sand coated mild steel, 0.8mm thick; and plain mild steel, 0.8mm thick. The sand used was coarse to medium with some fine gravel. Results in the form of shear stress versus normal stress are shown in *Figure 2.26* and apparent angle of bond stresses versus normal stress in *Figure 2.27*. It may be seen that the apparent bond angle decreases significantly with increase in normal stress. The very large values of bond angle for low normal stresses suggest that some mechanism over and above simple dilatancy is active. Perhaps the inclusion of soil grains within the fabric openings could be a factor. Shear box tests were also done, and in general, different

values of resistance (usually lower, at least at low normal stresses) were obtained.

Jewell (1980) carried out a series of pull-out tests with reinforcement possessing different stiffness. Three important features of the results (shown in *Figure 2.28*) were concluded. They were:

(1). The longitudinal stiffness of the reinforcement has a marked influence on the pull-out load displacement response.

(2). For both extensible and stiff bar reinforcement there is a dramatic reduction in pull-out force with displacement after the peak pull-out force has been mobilized .

(3). The peak pull-out force for the extensible bar is significantly less than that for the stiff bar, although both have identical dimensions and surface properties; the pull-out displacement required to mobilize this peak force is considerably greater than for the stiff bar.

A series of pull-out tests from a steel box with ribbed steel against sand were carried out, (Khattri 1982 and Finlay et al 1984). Similar results to most of the previous researchers were obtained. The dense soil yielded higher values of apparent friction coefficient than loose soil, both gave higher values compared with the direct shear method and indicated a trend of decreasing apparent friction coefficient with increasing normal pressure. In order to investigate the influence of the facing plate on the pull-out test results, two types of tests were conducted. In one the strip was pulled through a slot in the facing plate, while in the other the strip was fixed to the facing plate and both were moved forward together. The results showed that the strip-with-facing plate pull-out testing method can result in a reduction in  $f^*$  of approximately 28 % (*Figure 2.29*). With density variation along the length of the strip in order to investigate the effect of density variation, the results showed that the pull-out force decreases with decreasing density along the length of the strip (*Figure 2.30*).

Kutara et al (1988) carried out a series of pull-out tests with Polymer grids and sand. It was concluded that when polymer grids embedded in sand are pulled out with a constant force, the pull-out displacement increases with time. However

the displacement at the free end of polymer grids hardly increases with time. Thus, long-term stability can be maintained for the friction/adhesion between short-term stability.

Pull-out tests were also carried out by Palmeira et al (Palmeira 1987, Palmeira et al 1989) with grids and sand. It was found that pull-out test results could be influenced by boundary conditions. They concluded that apparent friction coefficients between soil and reinforcement can be severely overestimated because of friction on the internal front wall of the box in small scale tests. This effect can be minimised by lubricating the front face and increasing the scale of the test.

#### 2.5.5 Discussion

The significant results produced from several different testing methods by previous investigators have been briefly reviewed. Comparing direct shear box and pull-out testing methods a conclusion which can be drawn from most of the investigators is that both tests indicate remarkably different results and pull-out tests always give a higher value of friction coefficient than shear box tests. The high value from the pull-out test is attributed by McKittrick (1979) and Jewell (1980) and other researchers to the dilatancy of the soil during the pulling action (*Figures 2.31 and 2.32*). Due to the dilatancy occurring in the soil when the strip is pulled, the normal stress imposed on the surface of the strip will increase above the initial value. Consequently the value of  $f^*$  increases. It was reported in France (Rainbow 1983) that in recent tests where volumetric expansion was not allowed to develop during direct shear tests, calculated values of  $\varphi$  were 10 – 15 degrees higher than tests where free expansion could occur.

It appears extremely important from the point of view of design that further understanding of the performance and characteristics of the different tests is needed so that an adequate testing method can be adopted to determine the friction coefficient. The testing method used has been a point disputed by various previous investigators.

McKittrick (1978) proposed that of all the testing methods used, the direct shear test is the one most available to practising engineers for the evaluation of design parameters. Other testing methods require more specialized equipment, and generally involve higher cost.

Some other researchers, such as Osman (1977) and Hoshiya (1978) carried out model tests using plain reinforcement and sand. The value of the angle of skin friction or friction coefficient was back-calculated from the results of model tests, then compared with direct shear box test results. The same value was found.

Chapuis (1977) also compared some model test results with direct shear box test results and indicated approximately the same value of friction coefficient. Therefore he drew the conclusion that the direct shear testing method in the case of the smooth strip measures a realistic value of angle of skin friction but this may not be the same with ribbed strip for which no such comparison between model and direct shear test has been made.

Bacot and Iltis et al (1978) observed model wall test results and shear box test results. They found an important fact that the friction coefficient  $f^{**}$  from a model wall test was always greater than  $\tan\delta$  obtained from shear box tests, and believe that the value of  $\tan\delta$  is the minimal value of the friction coefficient when the different values obtained from different testing methods are compared. However they believe that  $f^{**}$  varies with the characteristics of the reinforcement, according to the following law:

$$f^{**} = \tan\delta + \alpha L + \beta/B \quad (2.19)$$

with  $\alpha$  and  $\beta$  constant.

A strong discussion on the use of the pull-out test was made by Jewell (1980). He pointed out that the load-displacement response, the displacement field and the strain field which develops in sand reinforced by a bar or a grid reinforcement and loaded in shear are not modelled by a test in which the reinforcement is pulled out of the sand. If the above three fundamental and

characteristic features of the interaction which occurs between sand and reinforcement in reinforced sand undergoing shear are not modelled by the pull-out test, then it must be concluded that the results of pull-out tests might well have no direct relevance, or bearing on the action of reinforced sand.

In reinforced sand the reinforcement improves the strength of sand by modifying the strains which develop as the sand plastically deforms under an applied load, whereas in a pull-out test the body of sand is "at rest".

Therefore Jewell concluded that the apparent coefficient of friction  $f^*$  between sand and reinforcement is not a fundamental parameter; and the pull-out test does not model the action of reinforcement placed in sand undergoing shear. Moreover he believed that the use of a high value of soil-reinforcement friction coefficient in design would be misleading.

On the other hand, a number of investigators believe that the pull-out test is the method which should be adopted to measure the friction coefficient for use in design. They believe that the pull-out test represents a frictional behaviour which exists in actual reinforced earth structures, and that the use of a high value would permit economy in design.

Mitchell and Schlosser (1979) described the shear box test as a test representing the two-dimensional case of an infinite reinforcement sheet, and it does not represent the different phenomena involved in the complex three dimensional mechanism of the soil-reinforcement interaction in actual reinforced earth structures. Schlosser considered that it was advantageous to use the pull-out test for measuring an angle of skin friction because the various factors occurring in real structures could be included in it. Such factors are difficult to analyse otherwise. The apparent friction coefficient takes into consideration the effects of dilatancy and compaction, which are difficult to include separately in a calculation.

Shen et al (1979) compared model test results with pull-out tests. A good agreement was met. Therefore he suggested that the pull-out test should be used for measuring an angle of skin friction.

The pull-out testing method was also supported by Al-Yassin (1977). He

analysed the rigid facing model using a finite element technique and found very good agreement between the model test data and the results when the angle of skin friction as determined by pull-out testing was used.

Having studied the literature, the author's view on which test method should be adopted to determine friction coefficient between soil and reinforcement is the direct shear box test. According to the literature, the direct shear box test reflects the fundamental mechanism of friction resistance. On the other hand, the use of a high value of soil-reinforcement friction coefficient will be misleading, this should be severely avoided in design.

However from the discussion in this section, in addition to influence of testing method there are various factors which affect the value of friction coefficient or angle of skin friction. The factors are generally as follows:

- (1). nature and mechanical characteristics of soil;

Normally soil possessing a higher internal friction angle produces a higher friction coefficient. Soil including more fine grained material shows a lower friction coefficient.

- (2). nature and mechanical characteristics of reinforcement;

The rougher the reinforcement surface is the higher the friction coefficient can be obtained.

- (3). overburden pressure;

Apparent friction coefficient decreases with increasing overburden pressure (pull-out test).

- (4). length of reinforcement;

Apparent friction coefficient increases with increasing reinforcement length (pull-out test).

- (5). width of reinforcement;

Apparent friction coefficient decreases with increasing reinforcement width (pull-out test).

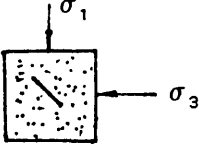
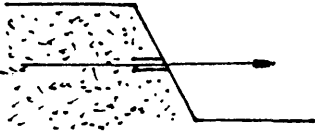
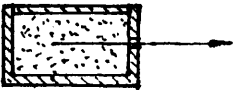
(6). density;

Friction coefficient increases with increasing density for ribbed steel or grid reinforcement, but this is not so apparent for smooth reinforcement. Some investigators, on the other hand oppose this and believe that the friction coefficient decreases with increasing density.

Besides these factors above, the value of the friction coefficient is also influenced by edge effects and size of the apparatus.

Generally speaking, the soil–reinforcement frictional characteristics are of a quite complex character. Although significant research work has been carried out, these characteristics are not fully understood. With new material, fill and reinforcement, introduced into reinforced earth, further investigations are still required.

**Table 2.1**                    **Some Testing Configurations**  
for the Study of Soil -Reinforcement Interaction

testing procedure	authors
plane strain unit cell	
	McGown et al (1978)
direct shear box	
	Jewell (1980), Dyer (1985)
	Ossman (1977), Alimi & Bacot (1977), Holtz (1977), Al-Huassani & Perry (1978), Lee (1978), Shen et al (1979), Soydemir & Epinosa (1979), Myles (1982), Miyamori et al (1986), Chandrasekaran (1988), Makizuchi & Miyamori (1988)
pull-out	
	Chang et al (1974), Terre Armee/ Schlosser & Elias (1978), Bacot & Iltis (1978), Rainbow (1983)
	Schlosser & Elias (1978), Alimi & Bacot (1977), Tumay et al (1979)
	Chang et al (1977), Schlosser & Elias (1978), Walter (1978), Shen & Mitchell (1979), Templeman (1979), Jewell (1980), Khattri & Finlay (1982), Kutara (1988)

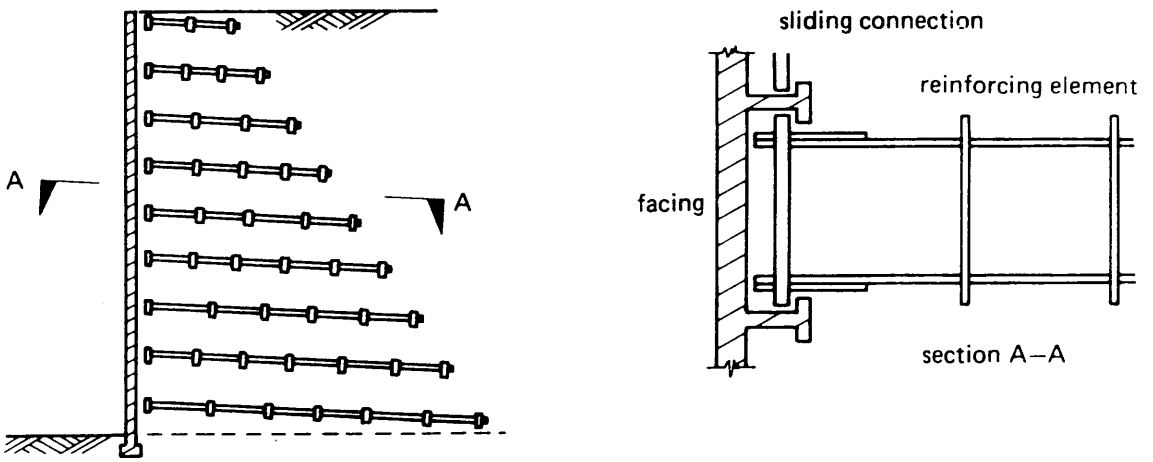


Figure 2.1 Munster earth retaining structure

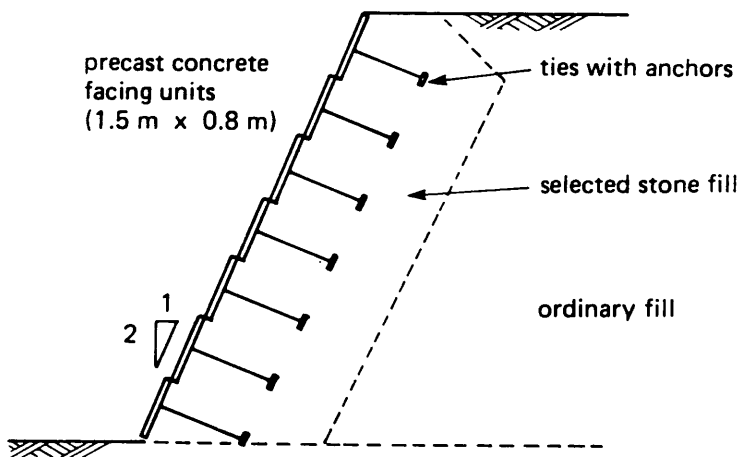


Figure 2.2 Coyne retaining wall at Brest

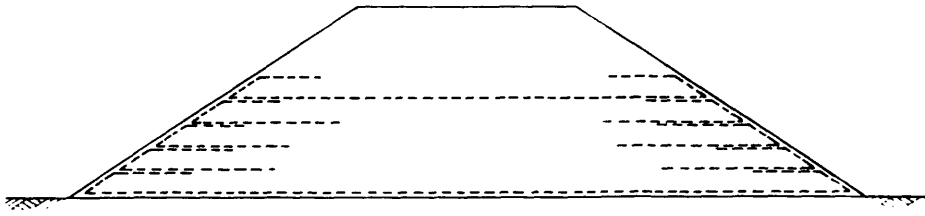


Figure 2.3 Embankment reinforced to produce stability

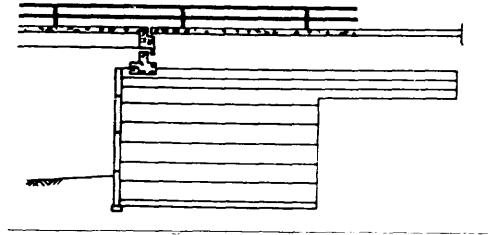
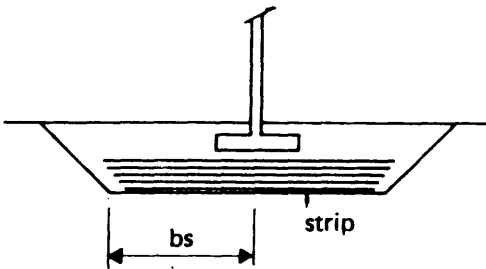


Figure 2.4 Reinforced foundation      Figure 2.5 Bridge abutment. (After Goughnour and Di Maggio)

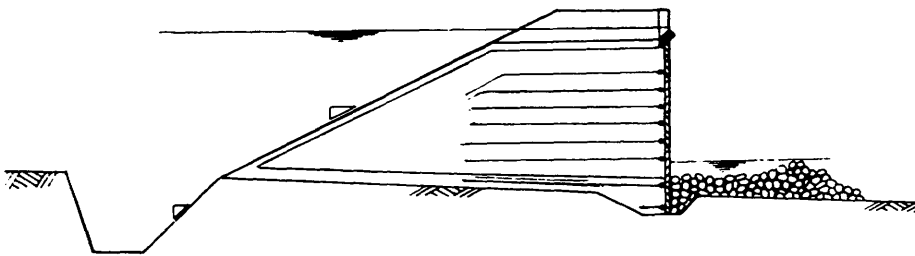


Figure 2.6 Reinforced earth dam. (After Cassard et al.)

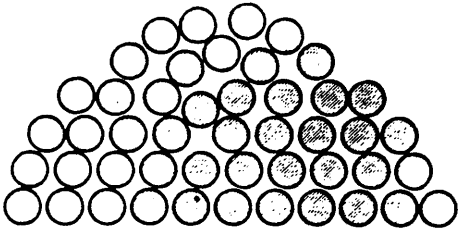


Figure 2.7

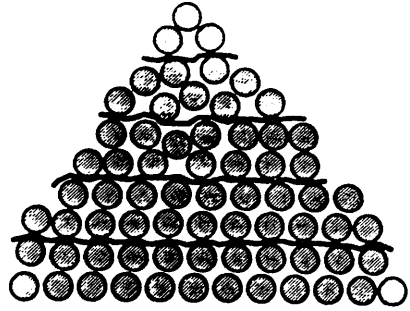


Figure 2.8

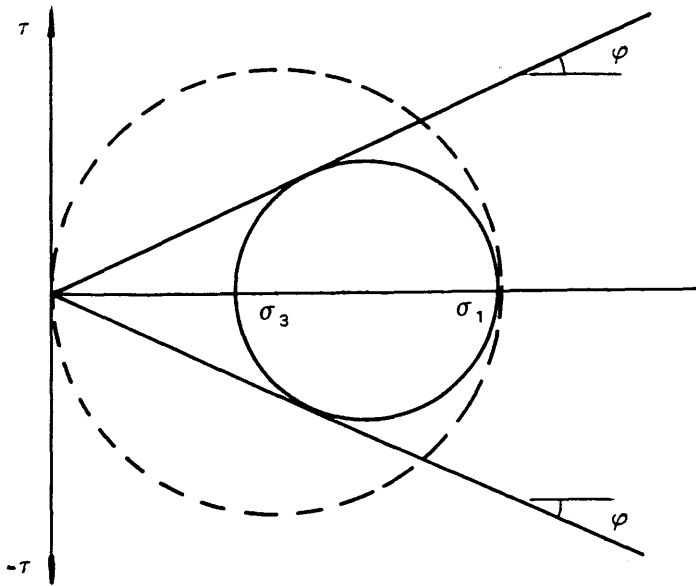


Figure 2.9 Failure in unreinforced soil

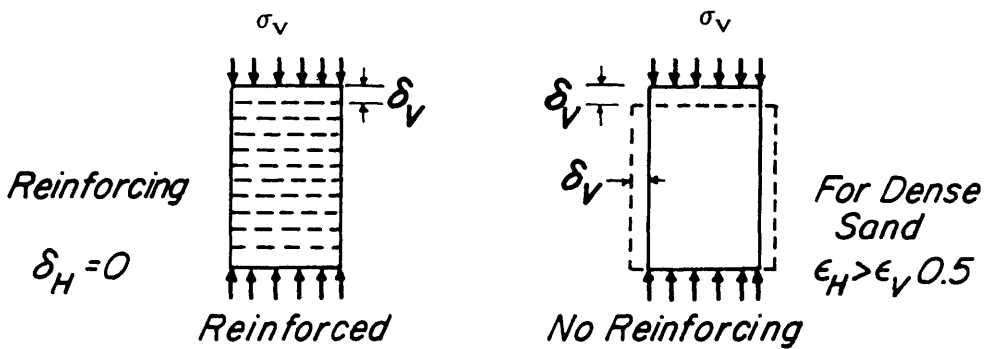


Figure 2.10

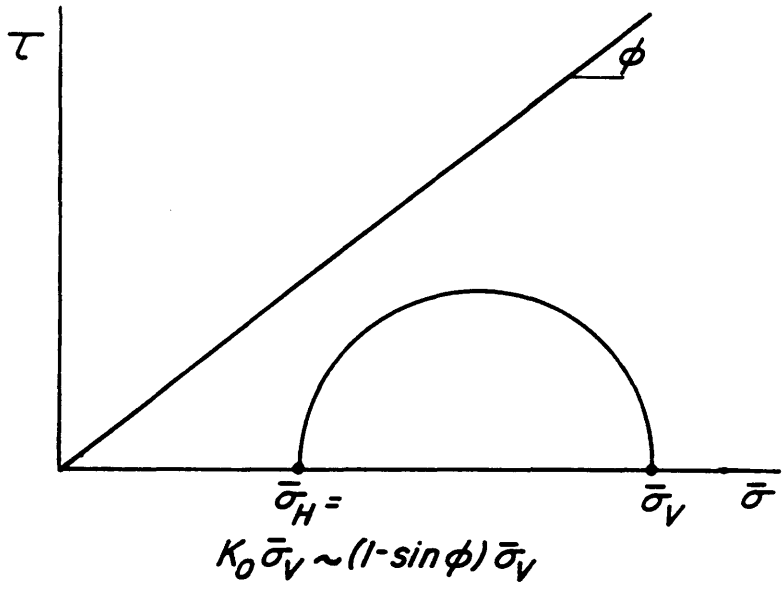


Figure 2.11 State of stress in earth reinforced with tension elements

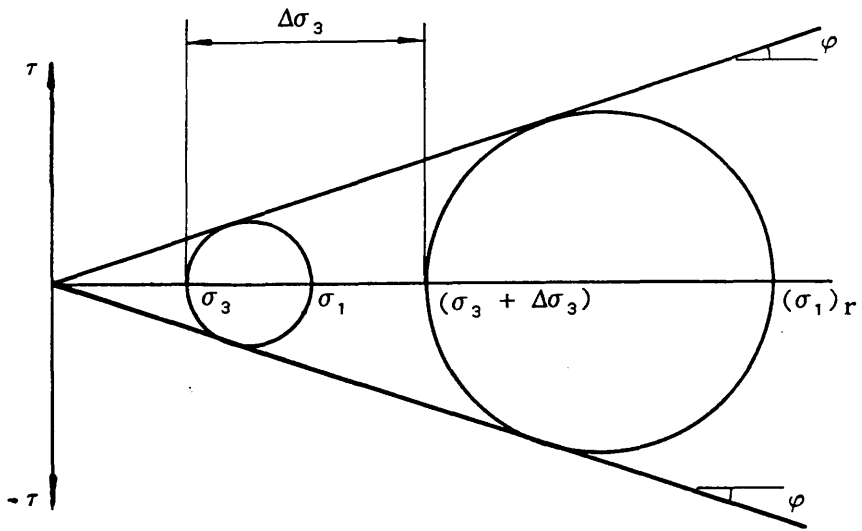


Figure 2.12 Improvement in strength

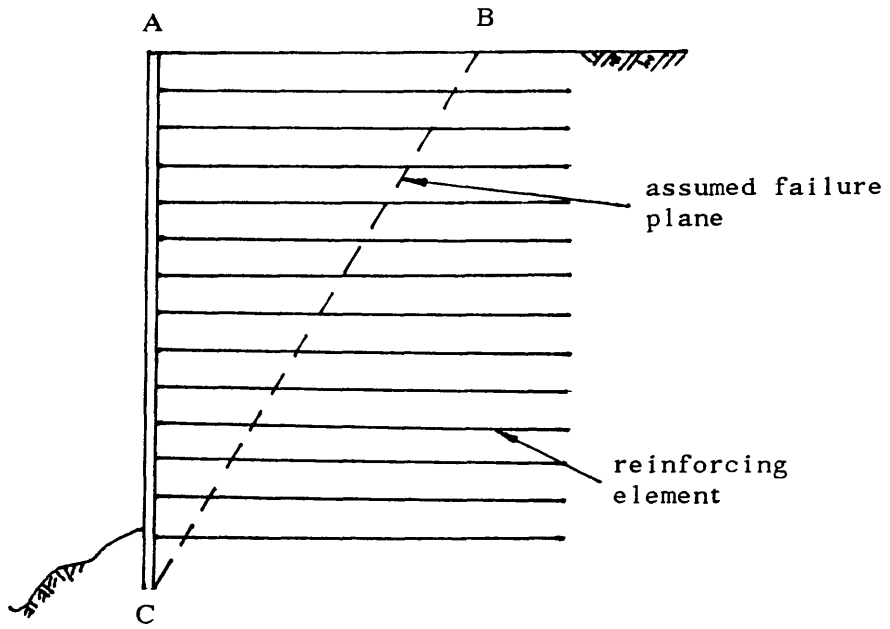
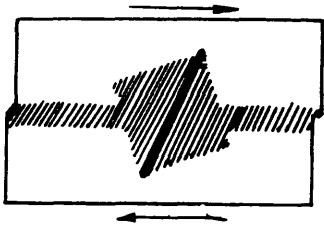


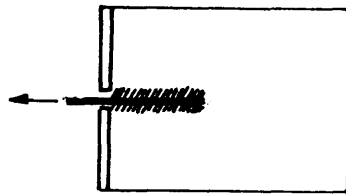
Figure 2.13

DIRECT SHEAR  
BOX TEST

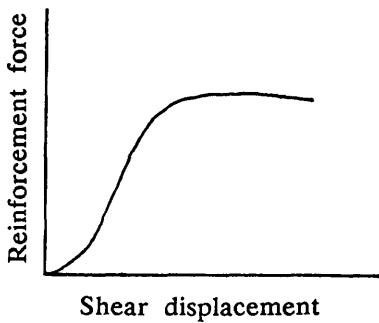


a. zone of strain in the sand

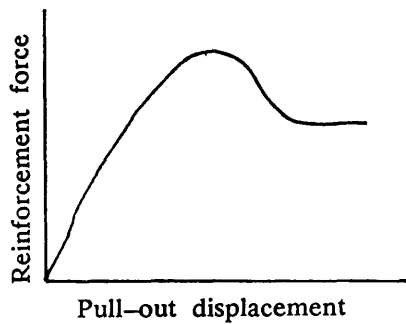
PULL-OUT TEST



c. zone of strain in the sand



b.



d.

Figure 2.14 A comparison of the strained zone in the sand and the reinforcement force displacement relationship, for reinforced sand loaded in shear and a pull-out test ( After Jewell )

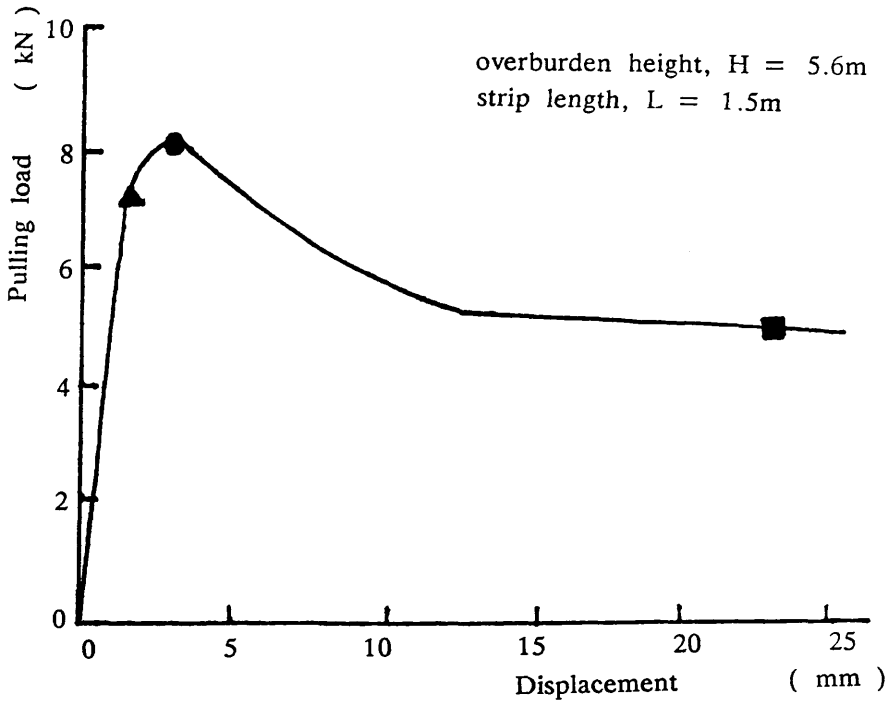


Figure 2.15 Load-displacement curves from field pull-out test (After Chang)

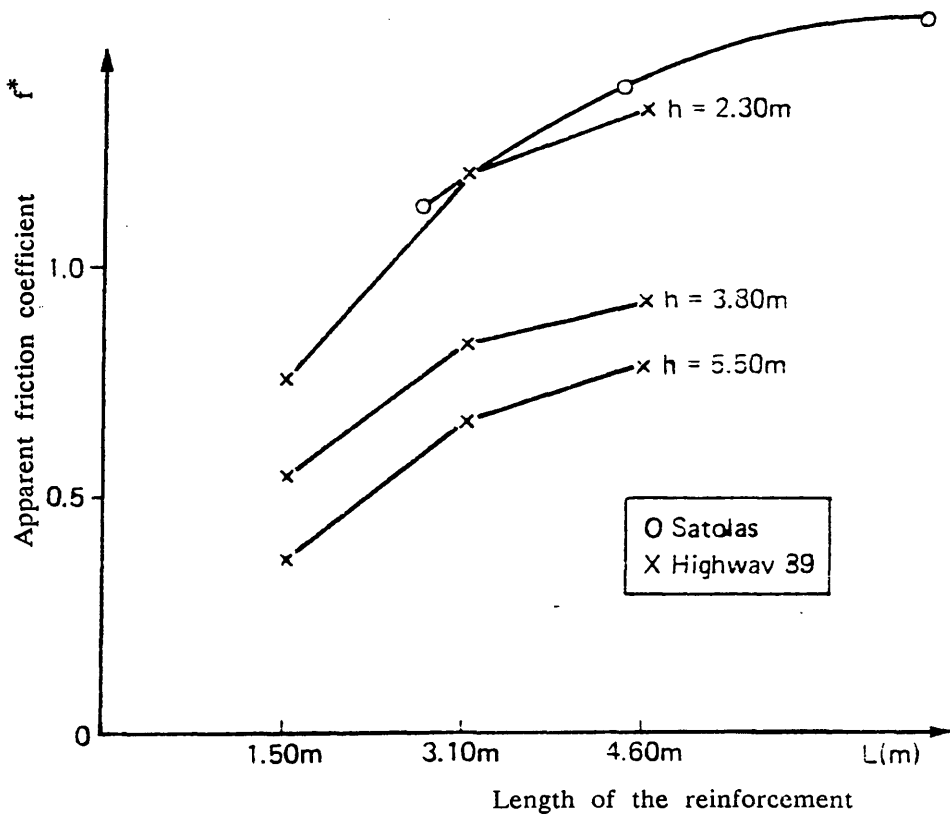


Figure 2.16 Influence of the length of the strip (After Chang and Schlosser)

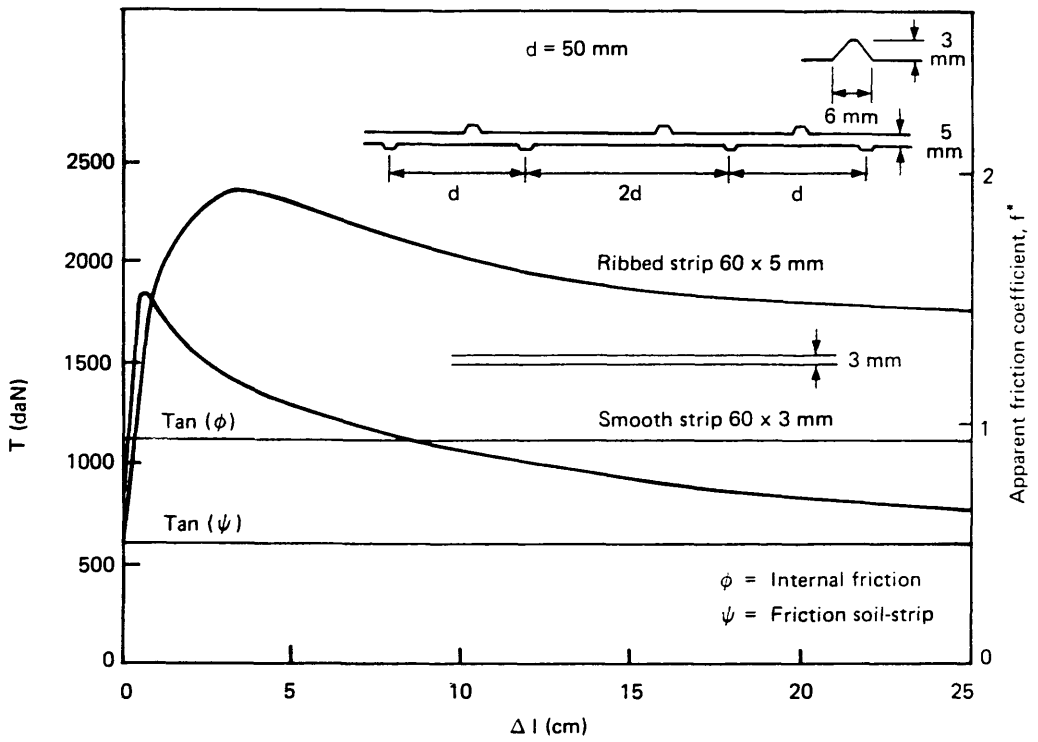


Figure 2.17 Influence of the nature of the strip surface in pull-out tests (After Schlosser)

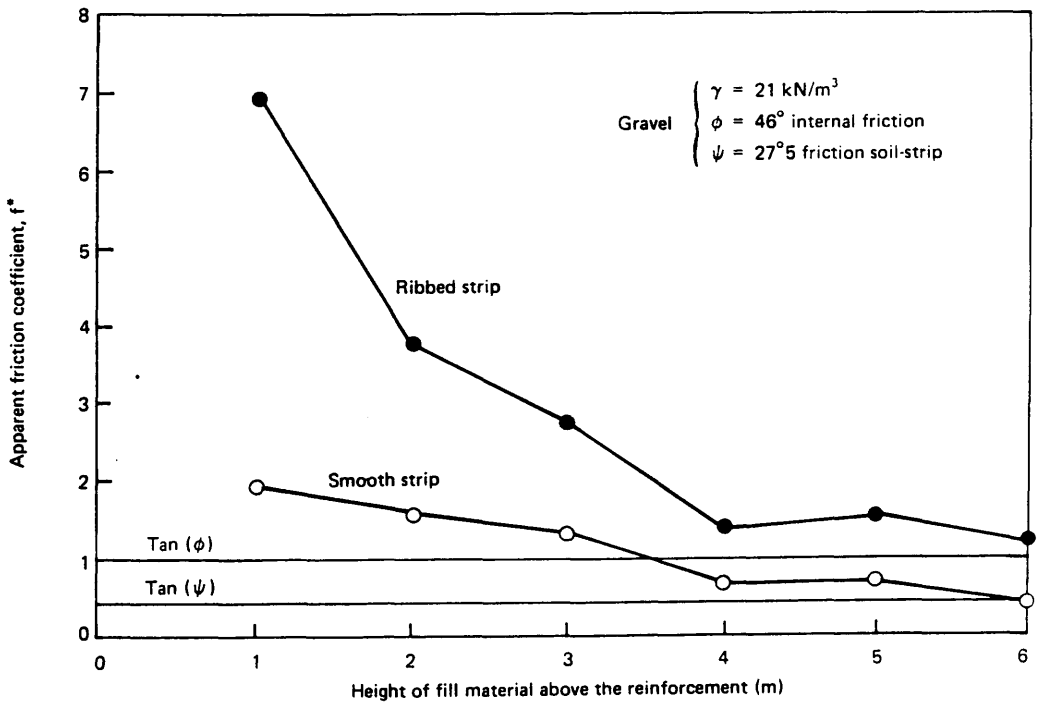


Figure 2.18 Influence of the overburden pressure in pull-out tests (After Schlosser)

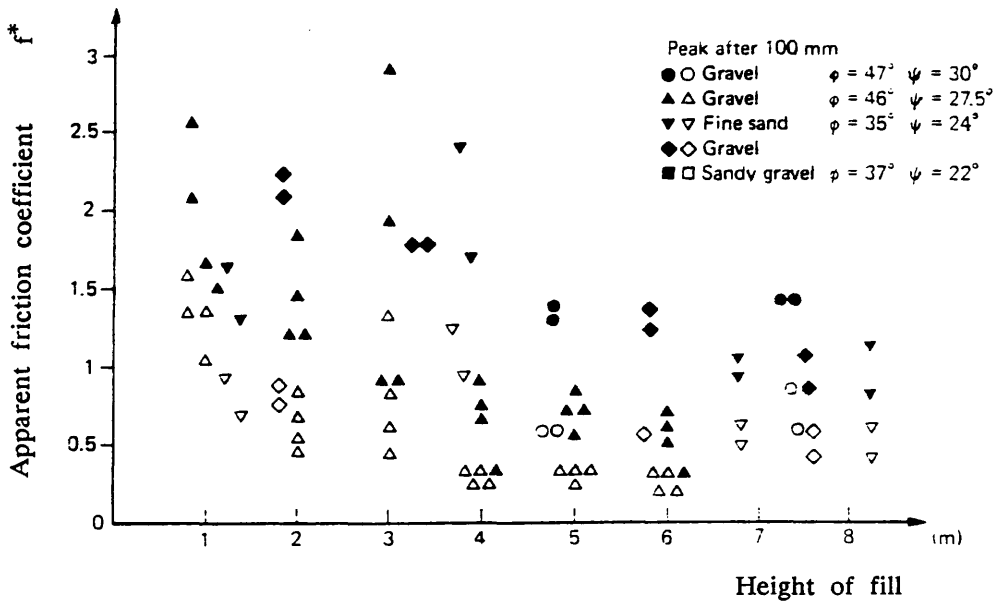


Figure 2.19 Influence of the overburden pressure (smooth strip) in pull-out tests (After Schlosser)

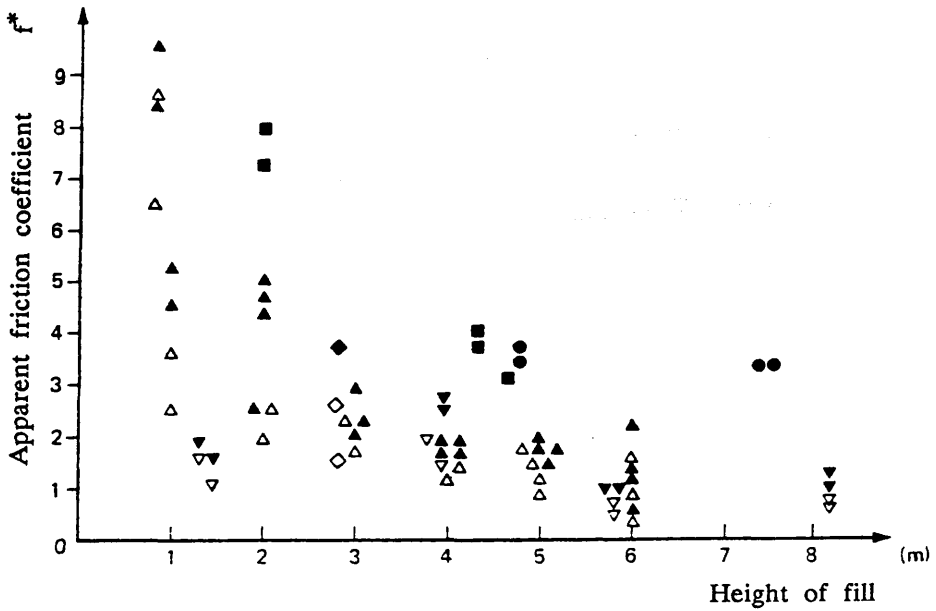


Figure 2.20 Influence of the overburden pressure (ribbed strip) in pull-out tests (After Schlosser)

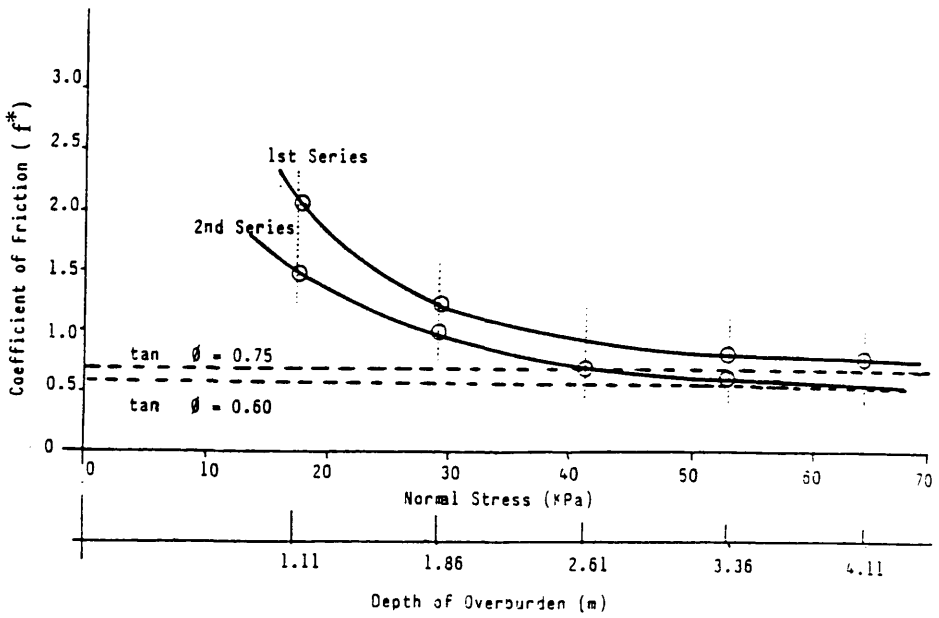


Figure 2.21 Apparent friction coefficient vs overburden pressure in pull-out tests (After Rainbow)

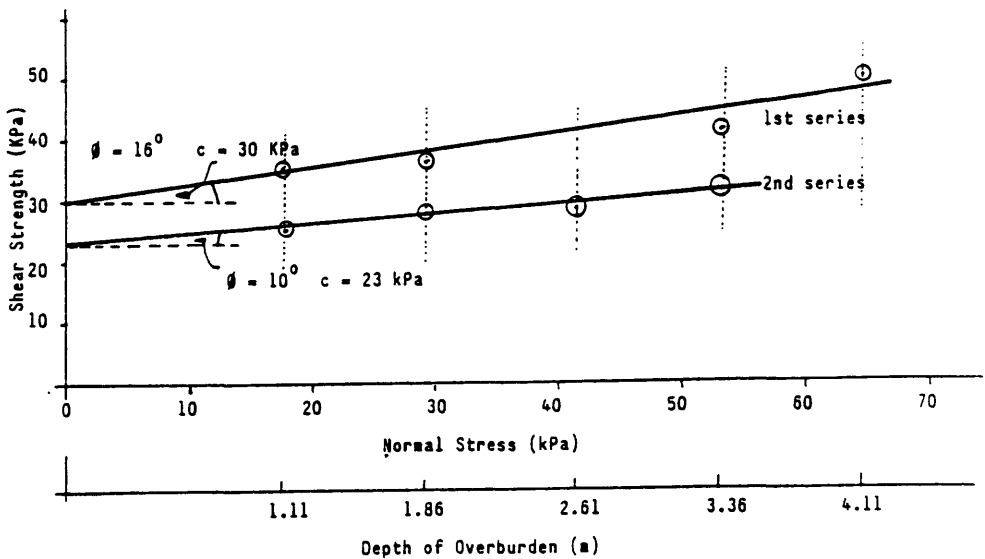


Figure 2.22 Shear stress vs overburden pressure in pull-out tests (After Rainbow)

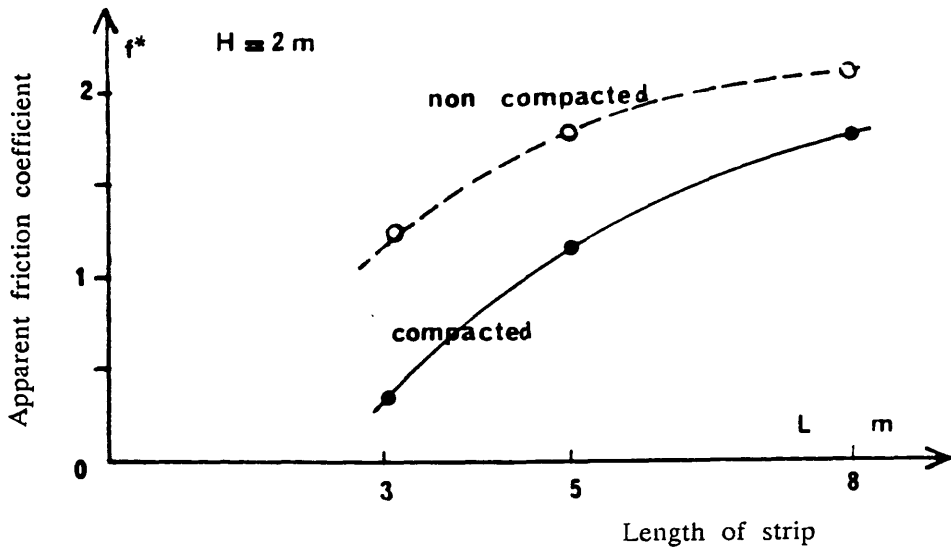


Figure 2.23 Influence of length of strip in pull-out tests (After Alimi)

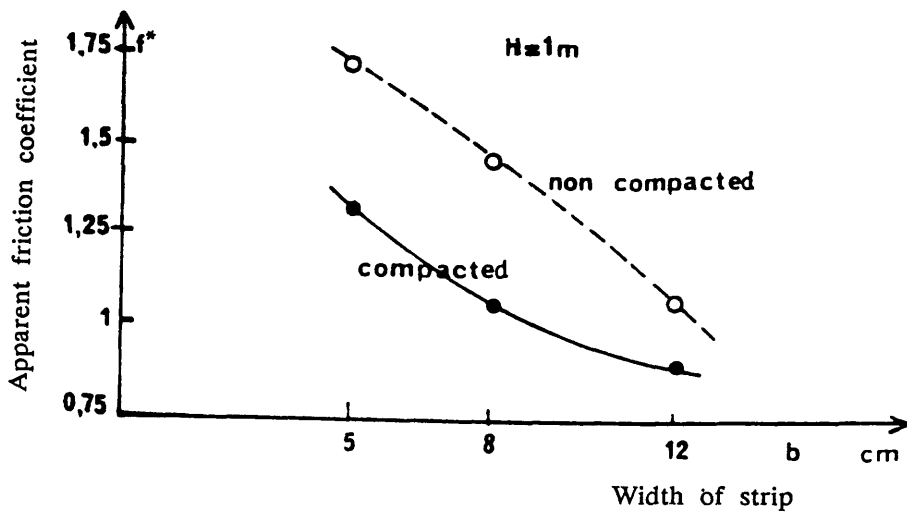


Figure 2.24 Influence of width of strip in pull-out tests (After Alimi)

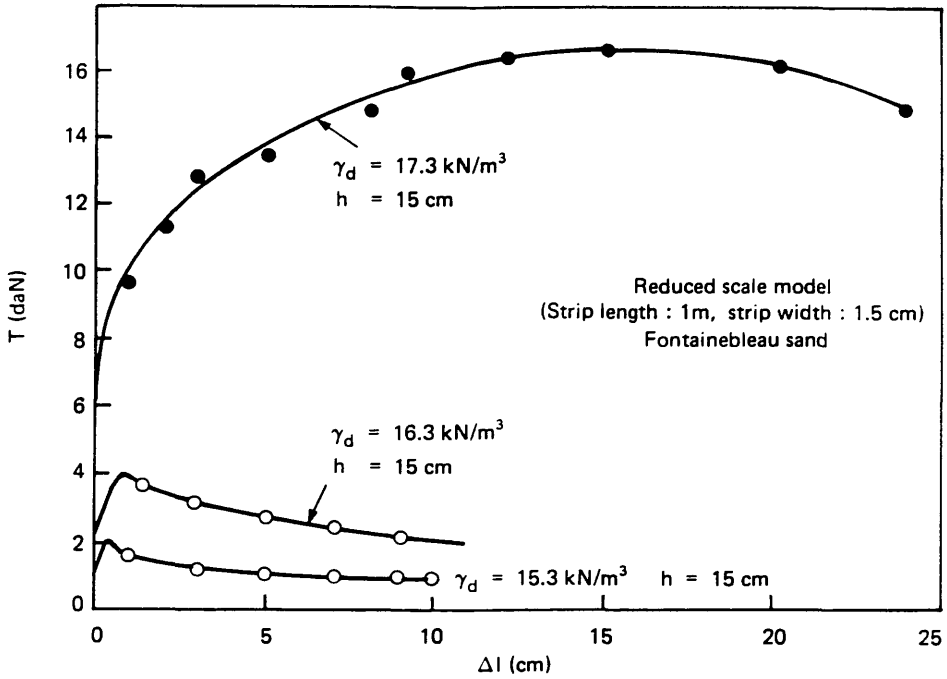


Figure 2.25 Influence of density in pull-out tests (After Alimi)

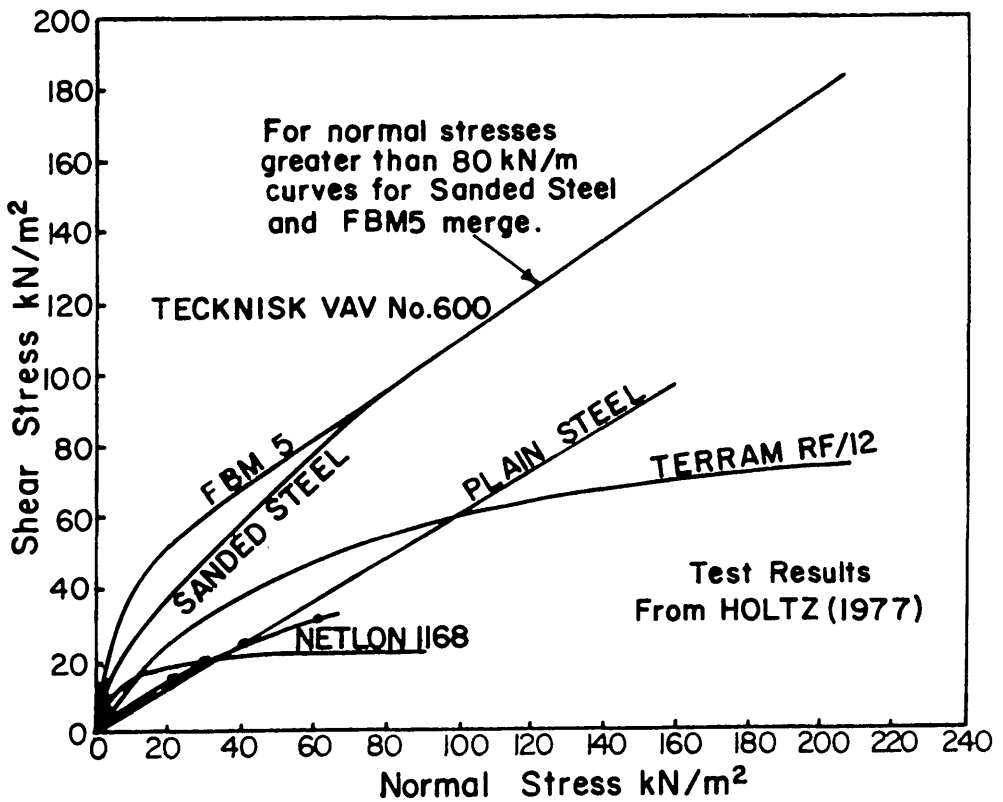


Figure 2.26 Comparison of pull-out test results (After Ingold and Templeman)

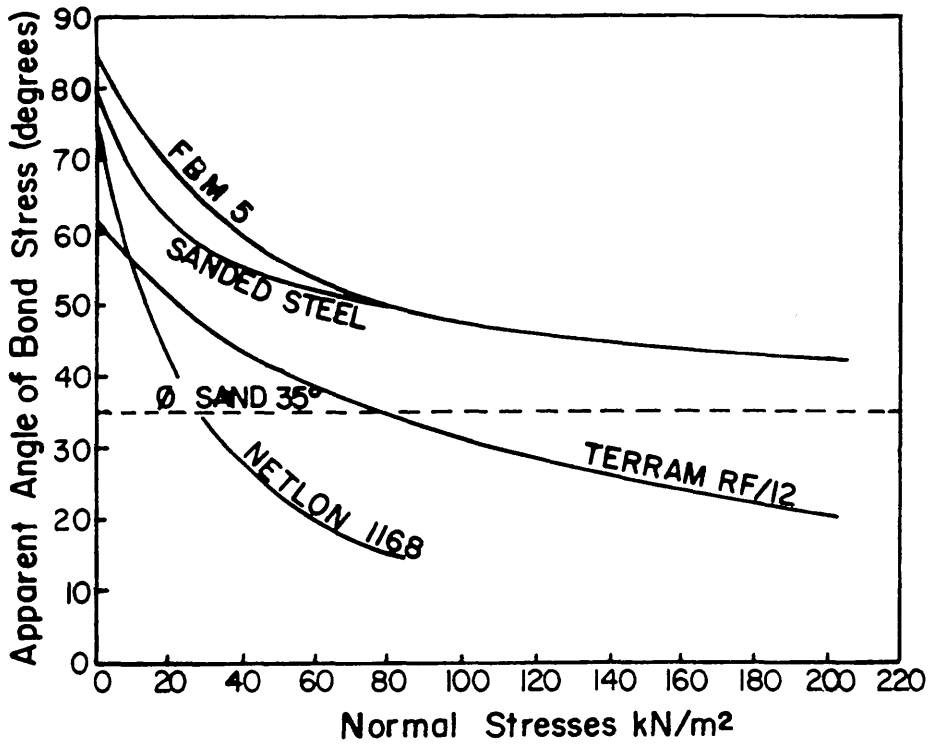


Figure 2.27 Comparison of pull-out test results (After Ingold and Templeman)

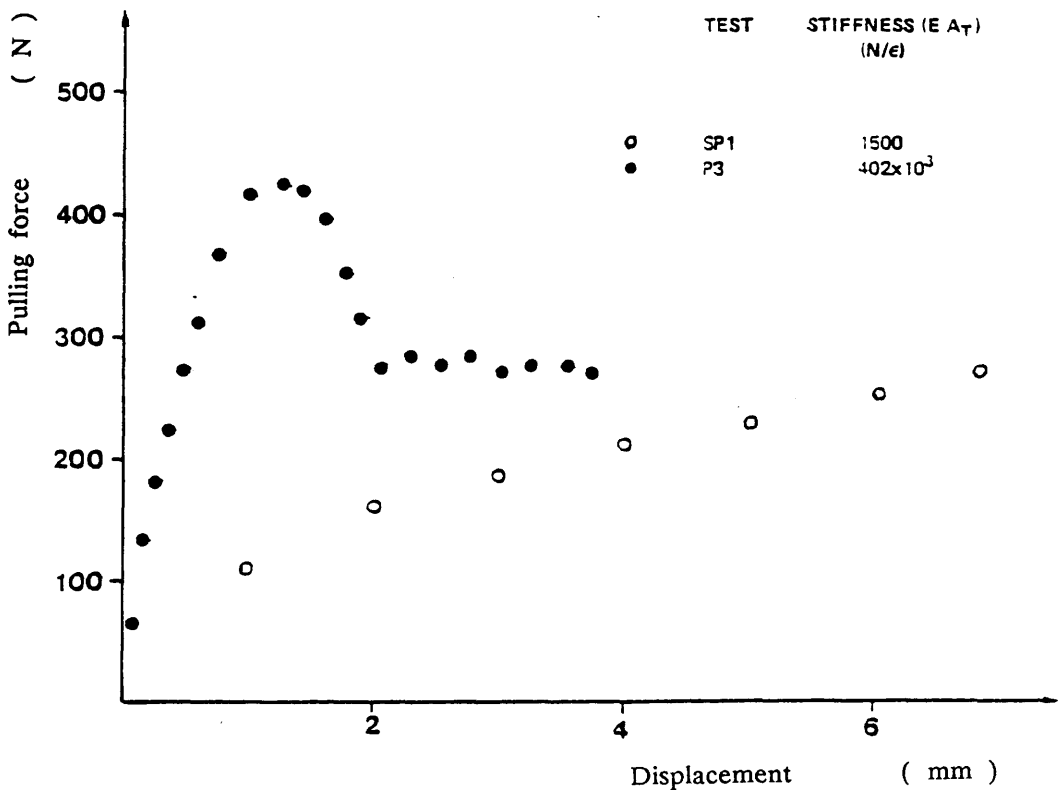


Figure 2.28 Comparison of pull-out test results from different longitudinal stiffness bars (After Jewell)

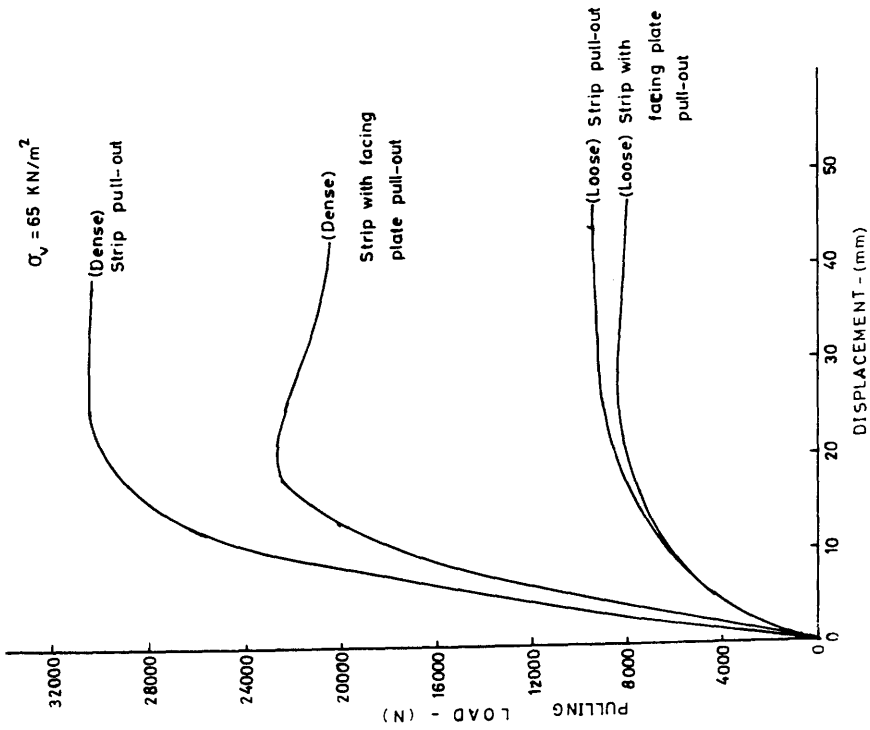


Figure 2.29 Comparison for strip pull-out and strip with facing plate pull-out tests (After Khattri)

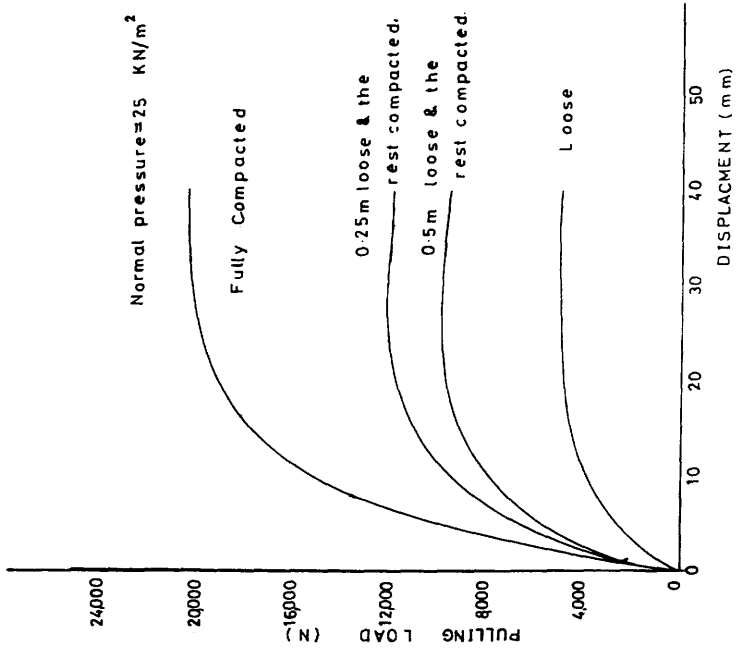


Figure 2.30 Influence of density variation along the strip in pull-out tests (After Khattri)

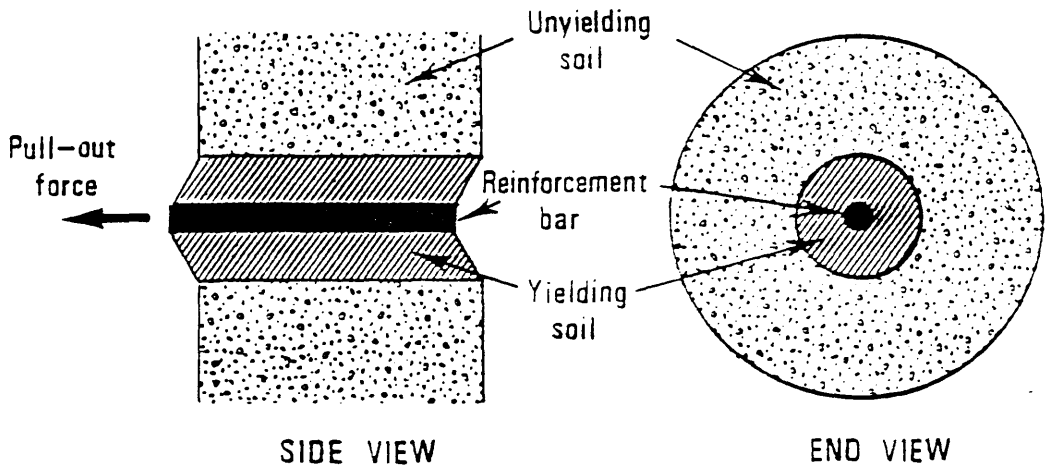
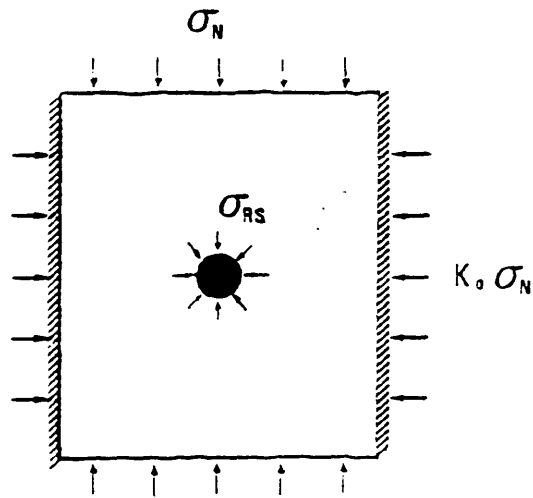


Figure 2.31 Idealised cavity expansion due to dense soil plastically yielding adjacent to a rough bar during a pull-out test (After Jewell)



$$\sigma_{RS} = \left( \frac{1 + K_0}{2} \right) \sigma_N$$

Figure 2.32 Simple pull-out configuration showing an applied normal stress  $\sigma$  acting on the surface of a circular reinforcement (After Jewell)

## CHAPTER 3

### DESCRIPTION OF THE MATERIALS USED IN THE PRESENT WORK

#### 3.1 INTRODUCTION

Five different fill materials were provided for the present research by British Coal's Minestone Services. These were two types of unburnt colliery spoil (Wardley and Wearmouth minestones), one type of burnt colliery spoil (Horden red shale), Loudon Hill sand and Methil PFA. Two kinds of polypropylene reinforcing strap (Paralink 300s and Paralink 500s) were used to investigate their working behaviour with the fill materials, and for comparison a type of conventional reinforcement, galvanized ribbed steel or high adherence steel, was also adopted. The properties of the various fill and reinforcing materials will be described and discussed in this chapter.

#### 3.2 FILL MATERIALS

##### 3.2.1 Minestones

Minestone is a by-product of coal. It includes the rock and other non-coal minerals which are hauled to the surface during mining, and comprises mainly siltstone, mudstone and sometimes sandstone. It is also loosely referred to as "rock", "stone" or "pit-dirt". As has been mentioned in the previous chapter, minestone was reported to be the largest waste source in the U.K. (Rainbow, 1983 and 1987). It is estimated that associated with an output of 109 million tonnes of coal make, a minestone make of 67 million tonnes was produced in 1979 to 1980. Its extraction continues throughout the life-time of the mine. The cost of disposal of colliery wastes is quite high, varying from £2 per tonne for local disposal to up to £7 per tonne for remote tipping. It is therefore attractive from both an economic and an

environmental point of view to utilize this waste. An attempt has been made by British Coal to use minestone as a fill material in reinforced earth structures. Certain authorities in the U.K. have, however, yet to be convinced of its suitability because of its natural properties, such as chemical content (sulphate, chloride etc.) which may attack metallic reinforcing elements or concrete materials, breakdown due to compaction, degradation due to weathering and risk of spontaneous combustion. Further investigation is therefore still required.

### 3.2.1a Wardley minestone

This was produced in Wardley colliery in N.E. England, and consists mainly of mudstone and clay minerals. Some of its natural properties have been described in previous literature (Rainbow, 1983).

Some properties of the material were tested in accordance with the British Standards (BS 1377:1975 and BS 1377:1967 To the Testing of Colliery Spoil). A wet sieving method was adopted for the grading tests, and compaction tests were conducted using a CBR mould. All the results are presented in *Tables* 3.1a and 3.1b. *Figure* 3.1 illustrates the grading curve, and indicates a well-graded soil (with a uniformity coefficient of 75), containing particles of all sizes from cobbles down to clay, but having a predominance of gravel sizes. Liquid and plastic limit test results imply a clay of low plasticity. Most of the results shown in these tables were provided by British Coal's Minestone Services. Some chemical properties are also presented, such as the pH value, sulphur content which is aggressive to concrete material, and chloride content which causes corrosion of metallic reinforcement. This material contained total sulphur of 0.95% and chloride of less than 0.1%, it had a pH value of 8.8 which showed it to be slightly alkaline in reaction. The loss on ignition is also presented, since it is an important property of minestone.

Shear box tests were also carried out to measure the shear strength of the material using a large shear box apparatus (303 × 303 × 303 mm). The same apparatus was also employed to measure the fill-reinforcement bond resistance, and

details of this and the testing procedures will be discussed in chapter 4. In order to correspond to the field test (Chapter 7) conditions, these were conducted after accomplishing the field tests, so that the moisture content and density in the field could be measured and adopted in the direct shear tests. In the case of Wardley minestone, however, the moisture content from the field tests (natural moisture content of 9.7%) was quite close to the optimum moisture content of 10%, and the dry density was 96% of the maximum dry density. Under this condition an internal angle of friction of  $33^\circ$  and a cohesion of  $15 \text{ kN/m}^2$  were obtained.

### 3.2.1b Wearmouth minestone

This unburnt colliery spoil was extracted from Wearmouth colliery. Obvious differences were observed compared with Wardley minestone, in that sandstones were present and the stones were relatively hard and resisted break-down during compaction.

The results are shown in *Tables 3.1a and 3.1b* and *Figure 3.1*. Similar to Wardley minestone, the grading curve shows a well graded material with a predominance of gravel particles. The plasticity index and liquid limit indicate clay characteristics. A high total sulphur content (3.72%) was found, the chloride content was less than 0.1%, and the pH value (8.2) shows a slightly alkalinity in reaction. A higher loss on ignition (27.1%) was obtained than Wardley minestone.

For shear strength testing, the natural moisture content of 5.6% (which was different from the optimum of 8%) and 96% of the maximum dry density were prepared, these being the same conditions found in the field pull-out tests. The same shear box apparatus as used for the previous minestone was employed and an internal angle of friction of  $37^\circ$  and a cohesion of  $11 \text{ kN/m}^2$  were obtained.

### 3.2.2 Horden Red shale

The suitability of well-burnt shale has long been recognised and extensively

used in the field of civil engineering. The present red shale was a well-burnt type of colliery spoil produced from Horden colliery and consisted of angular hardened particles.

Some of the properties are shown in *Tables 3.1a* and *3.1b* and *Figure 3.1*. Its grading curve shows a relatively fine but well-graded material with a uniformity coefficient of 150 which is much higher than the previous minestones. No plastic limit could be found. The total sulphur content obtained was about the same as Wardley minestone and the chloride content was less than 0.1%. The pH value shows neutral in reaction.

Shear strength tests were carried out using the  $303 \times 303 \times 303$  mm shear box with a natural moisture content of 11.6% and 95% of the maximum dry density state. A quite high internal angle of friction of  $41.4^\circ$  and a cohesion of  $11.4 \text{ kN/m}^2$  were obtained.

### 3.2.3 Loudon Hill Sand

As a type of conventional fill material, cohesionless soil has been widely used in reinforced earth structures. It is regarded as the best fill material for use in reinforced earth, its main advantages being its high internal angle of friction, good permeability and the fact that it is non-corrosive to metallic reinforcement. This is, however, a more expensive material than colliery spoil and is not always available.

Some of the properties of Loudon Hill sand were tested and are shown in *Tables 3.1a* and *3.1b* and *Figure 3.1*. A well-graded sand with a uniformity coefficient of 6 is shown in the grading curve. The total sulphur was 1.3%, but a very low chloride content (0.02%) was found. The pH value (7%) shows neutral in reaction.

An internal angle of friction of  $37.6^\circ$  and a small cohesion of  $4.6 \text{ kN/m}^2$  were produced at the natural moisture content of 7.1% and a density of  $16.19 \text{ kN/m}^3$  using the same shear box apparatus as for the previous materials.

### 3.2.4 Methil PFA

PFA (Pulverized Fuel Ash) is the ash extracted by electrostatic or mechanical means from the flue gases in a coal-fired power plant. This material consists principally of minute glass spheres in the silt size range together with some crystalline matter and a varying amount of carbon, and its three predominant chemical elements are silicon, aluminium and iron. It is a material with fine particles and light weight, its fineness and high silica content lead to a very important property, viz. it is pozzolanic i.e. it will combine with lime and water to form cementitious material. This may have a connection with another significant property i.e. that of hardening over a period when compacted at optimum (or near optimum) moisture content. PFA has been widely used in civil engineering construction (Knight, 1979 and Weatherley, 1979) and reinforced earth structures have been erected with PFA as a fill material (Jones, 1984). The main advantages of using PFA as a fill are that it is an economic material, possesses the property of light weight and increases in shear strength with time.

The present PFA material was tested and some of the properties are presented in *Tables* 3.1a and 3.1b and *Figure* 3.1. The grading curve shows very fine particles with a predominance of silt sizes. The maximum dry density was found to be much lower than the other materials. It did not possess clay characteristics, no plastic limit being found. A total sulphur was obtained as 1.1% and the chloride content was 0.5% which was higher than the other fill materials. The pH value of 8.7 shows a slightly alkalinity in reaction.

The same shear box test method as used for testing the previous materials was employed in the shear strength tests, the field moisture content and density being adopted, i.e. samples with a natural moisture content of 27% and 104.5% of the maximum dry density were prepared. An internal angle of friction of  $36.5^\circ$  and cohesion of  $3.6 \text{ kN/m}^2$  were measured.

### 3.3 REINFORCING MATERIALS

Two types of Paralink straps were adopted in the present research, these were Paralink 300s and Paralink 500s, the latter being known as Paraweb to some previous researchers. For comparison, a type of conventional reinforcing strap (galvanized ribbed steel or high adherence steel) was also employed.

Paralink straps consist of tendons developed by I.C.I. and made from ten bundles of continuous, aligned, high tenacity polyester fibres enclosed in a durable polyethylene sheath. It is claimed by the manufacturers that the straps are corrosion resistant against chemicals in the fill, have good resistance to abrasion caused by the action of hard angular stones, and are unaffected by water. Paralink 300s is beige in colour and has a tensile strength of 30 kN, whereas Paralink 500s is black and possesses a 50 kN tensile strength. Because of its black colour, the manufacturers also claim that it provides a good resistance against ultra violet radiation. They claim that these reinforcing straps will retain load without adverse effects on the long term stability of structure, implying that the material is not liable to creep (Rainbow, 1983).

The straps are shown on *Plate 3.1* and some of their features and properties are presented in *Table 3.2*. Comparing the three reinforcing materials, the ribbed steel produces higher tensile strength, and lower extensibility (relatively rigid behaviour) than the Paralink straps, and Paralink 500s was found to be better than Paralink 300s in terms of tensile strength and stiffness. Paralink 500s possesses a slightly rougher surface than Paralink 300s. Comparing the surface nature of the both sides of a Paralink strap (Paralink 500s or Paralink 300s) a slightly different roughness can be found.

Several tensile tests were carried out using a 250 kN Instron tensile machine (*Plate 3.3*). The results from the tests are also shown in *Table 3.2*.

A set of clamps (see *Plate 3.2*) was manufactured with serrated faces in order to fix the Paralink straps without slip or keep it to a minimum. These were used in the tensile tests as well as in the pull-out box tests (Chapter 5 and 6). The

aim of the tensile tests was, on the one hand to investigate the characteristics of the tensile force versus the strain of the straps, on the other hand to examine the efficiency of the clamps holding the straps. In the field pull-out tests (Chapter 7), another type of connection ("buckle" see *Plate 3.2*) was employed to fix the Paralink strap to the pull-out device. For comparison of the two types of the connection, several tensile tests with the sample held by the buckles were also carried out. The ends of the strap were fastened by threading through the buckle, and a gradual tightening occurred as the tensile force increased. Samples of 100mm and 200mm length were tested at a strain rate of 5% per minute until failure.

The maximum loads were found to be about 26 kN and 33 kN on Paralink 300s and Paralink 500s respectively with "clamp fixing". Typical curves of tensile load against strain are shown in *Figure 3.2*. The failure was, however, caused by the slipping between the outer casing and the inner fibres of the straps rather than by rupture, although no slippage was observed at tensile loads less than 20 kN. The same failure mode was found with "buckle fixing", the results of Paralink 500s with the two different connection fixings are illustrated in *Figure 3.3*.

It is shown that Paralink 500s is stiffer in tension than Paralink 300s. In order to represent the behaviour of the straps in tension a term, "stiffness", is introduced, which in meaning is very close to the term of Young's modulus. The only difference between them is that the tensile load is used here instead of stress in a Young's modulus expression (see expressions 3.1 and 3.2). This means that Young's modulus is the stress produced per unit strain, whereas stiffness is the load produced per unit strain. The reason for choosing the term stiffness is due to the non-homogeneous cross section of the Paralink straps, and also the use of stiffness can relate the force to the strain more directly for a specific strap.

$$\text{Young's Modulus} = \frac{\text{Tensile Stress (kN/m}^2\text{)}}{\text{Strain}} \quad (3.1)$$

$$\text{Stiffness} = \frac{\text{Tensile Load (kN)}}{\text{Strain}} \quad (3.2)$$

A considerably larger strain, but similar failure load was produced from the test with "buckle fixing". The large strain was attributed to the fact that a certain amount of displacement was required to "tighten up" the strap through the buckles, particularly at the earlier part of the test.

It was therefore concluded that the buckles and the clamps possessed about the same efficiency in reaching a high tensile load, but the clamps appear better able to control the slippage. Both of the connections are, however, not efficient enough to reach the maximum bearing loads of the straps, which are claimed by the manufacturers, 87% and 66% of the maximum bearing loads being obtained for Paralink 300s and Paralink 500s respectively in the tensile tests.

Several tensile tests on ribbed steel were also carried out using the same tensile testing machine (see *Plate 3.3*). The results are also presented in *Table 3.2*.

Table 3.1a

Properties of Fill Materials

properties	Wardley minestone	Wearmouth minestone	Horden red shale	Loudon Hill sand	Methil PFA
natural moisture m/c content (%)	9.7	5.6	11.6	7.1	27.0
loose bulk density $\gamma_b$ (kN/m <sup>3</sup> )	14.0	12.7	13.7	13.1	6.3
specific gravity $G_s$	2.37	2.40	2.69	2.76	2.24
liquid limit LL (%)	31	49	41	25	50
plastic limit PL (%)	22	26	—	—	—
plasticity index PI (%)	9	23	—	—	—
optimum moisture m/c <sub>opt</sub> content (%) (2.5 kg rammer)	10.0	8.0	15.0	15	36
maximum dry $\gamma_{max}$ density (kN/m <sup>3</sup> ) (2.5 kg rammer)	18.6	18.3	18.6	18.2	11.1
optimum moisture m/c <sub>opt</sub> content (%) (4.5 kg rammer)	6.5	8.0	13.0	15	29
maximum dry $\gamma_{max}$ density (kN/m <sup>3</sup> ) (4.5 kg rammer)	19.3	18.5	18.9	18.7	11.8
optimum moisture m/c <sub>opt</sub> content (%) (vibrating)	8.3	9.0	13.0	14	29
maximum dry $\gamma_{max}$ density (kN/m <sup>3</sup> ) (vibrating)	19.6	17.5	19.7	19.2	11.7

Table 3.1b

## Properties of Fills

properties	Wardley minestone	Wearmouth minestone	Horden red shale	Loudon Hill sand	Methil PFA
field test density $\gamma$ (kN/m <sup>3</sup> )	17.9	17.6	17.6	16.2	11.6
internal friction angle $\varphi$	33.0°	37.0°	41.4°	37.6°	36.5°
cohesion c (kN/m <sup>2</sup> )	15.0	11.0	11.4	4.6	3.6
uniformity coefficient U	75	10	150	6	7
total sulphur (% SO <sub>3</sub> )	0.95	3.72	0.96	1.30	1.10
water soluble sulphate 1:1 extraction (% SO <sub>3</sub> )	0.1	<0.05	0.15	<0.1	0.18
acid soluble sulphate (% SO <sub>3</sub> )	0.1	0.1	0.78	<0.1	0.59
pyritic sulphur (% SO <sub>3</sub> )	0.62	2.60	0.10	0.68	0.40
chloride content (% CL )	<0.10	<0.10	<0.10	0.02	0.50
pH value	8.8	8.2	6.9	7.0	8.7
loss on ignition (% by weight) (at 815°C)	17.4	27.1	3.0	5.5	14.2

Table 3.2 Characteristics of Reinforcing Elements

Type	Paralink 300s (Beige)	Paralink 500s (Black)	High Adherence (Ribbed) steel
Width (mm)	85	88	40
Thickness (mm)	2.5	3.5	5
Maximum Load <sup>▽</sup> (kN)	30	50	—
Maximum Load <sup>*</sup> (kN)	26	33	98
Stiffness <sup>*</sup> (kN)	132	161	34600
Strain <sup>*</sup> at Maximum Load (%)	24	22	16

▽ — Results claimed by the manufacturers ;

\* — Results from the present tensile tests;

$$\text{Stiffness} = \frac{\text{Tensile Load (kN)}}{\text{Strain}}$$

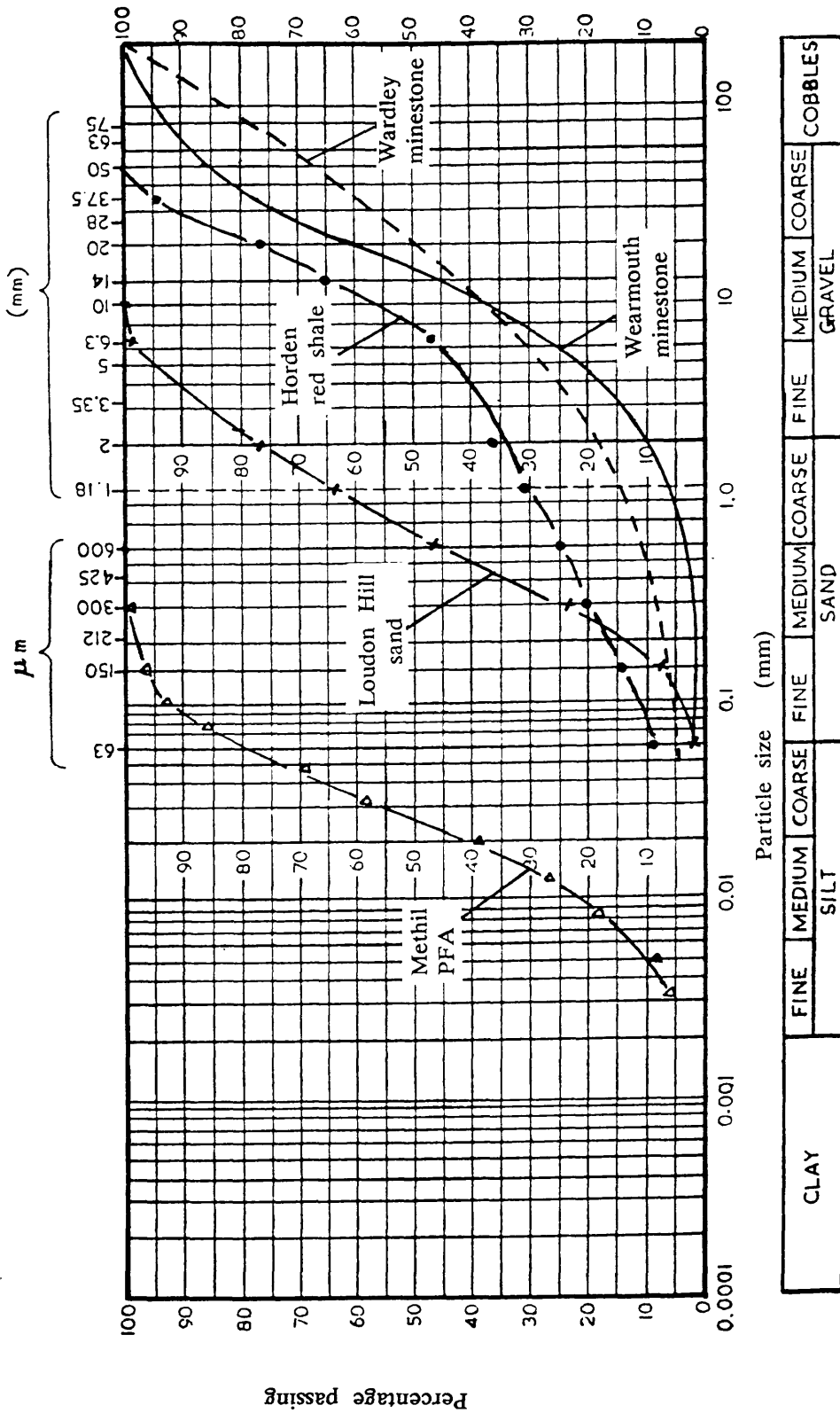


Figure 3.1 PARTICLE SIZE DISTRIBUTION CURVES

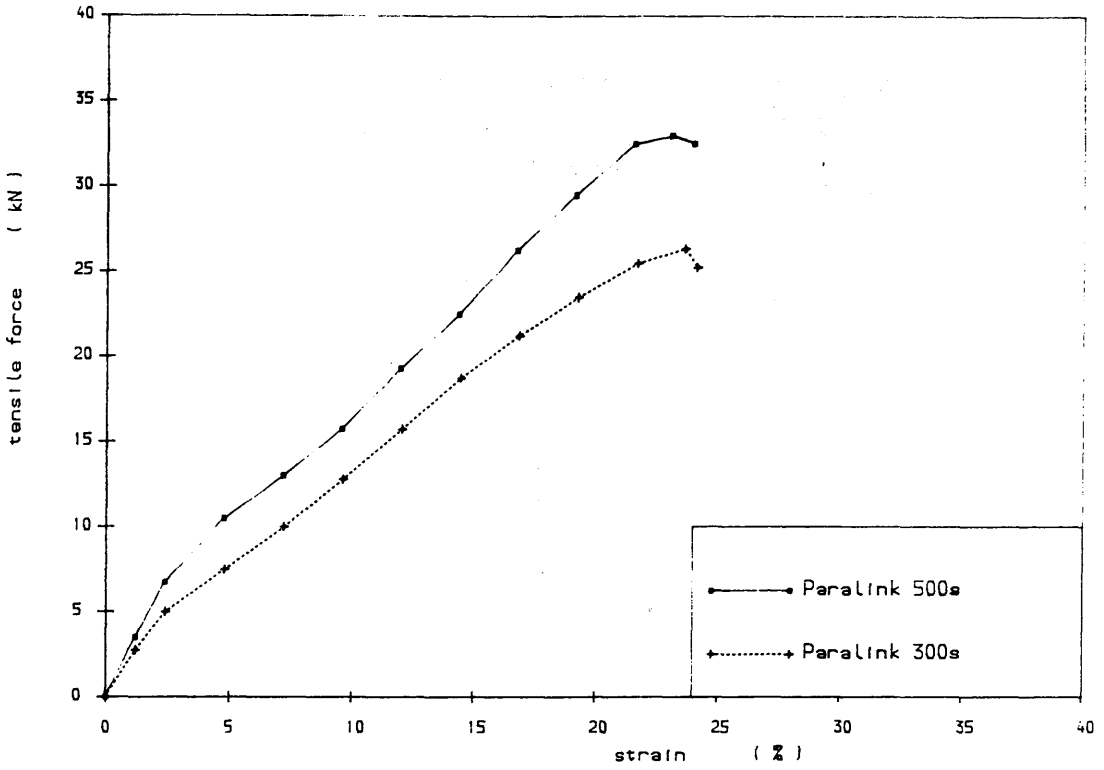


Figure 3.2 STRAP TENSION FORCE VS. TENSILE STRAIN  
from tensile tests, fixing with clamp

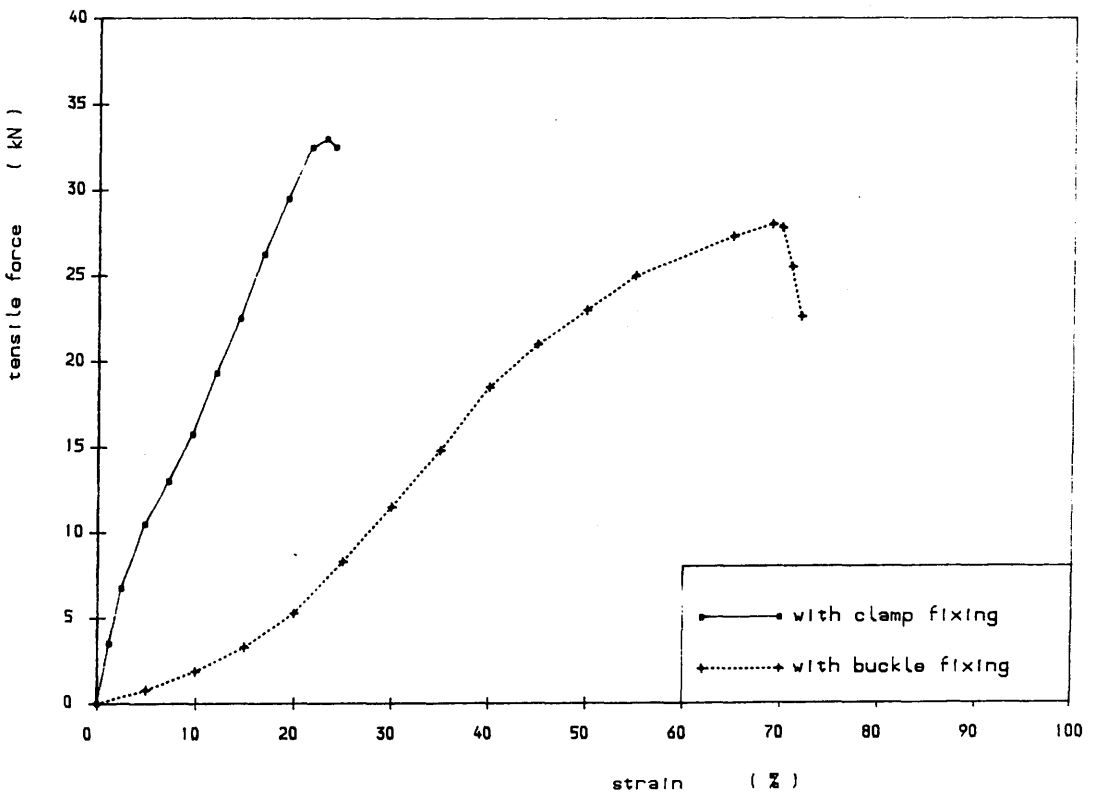


Figure 3.3 STRAP TENSION FORCE VS. TENSILE STRAIN  
from tensile tests on ParaLink 500s

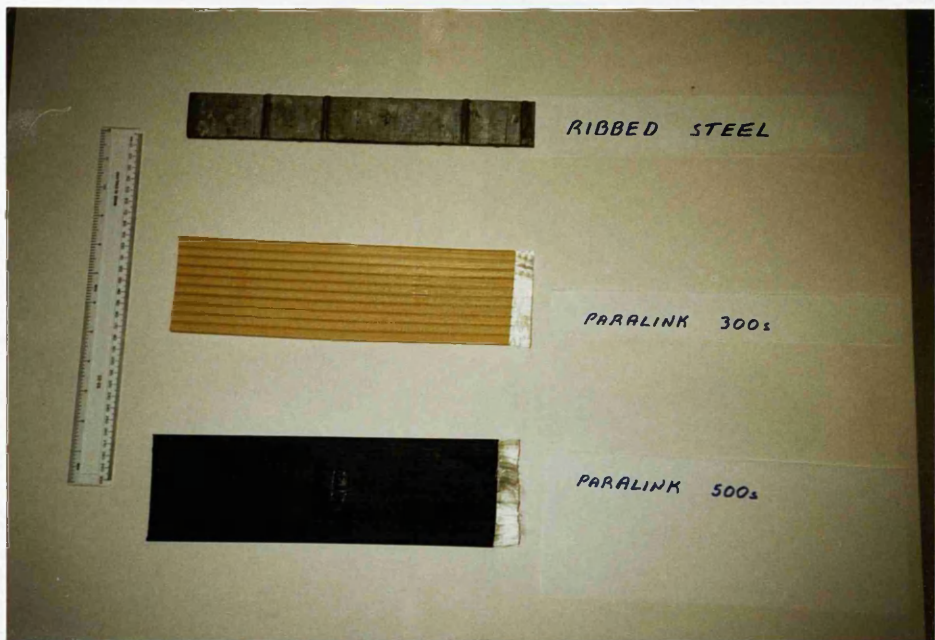


Plate 3.1 REINFORCING STRAPS

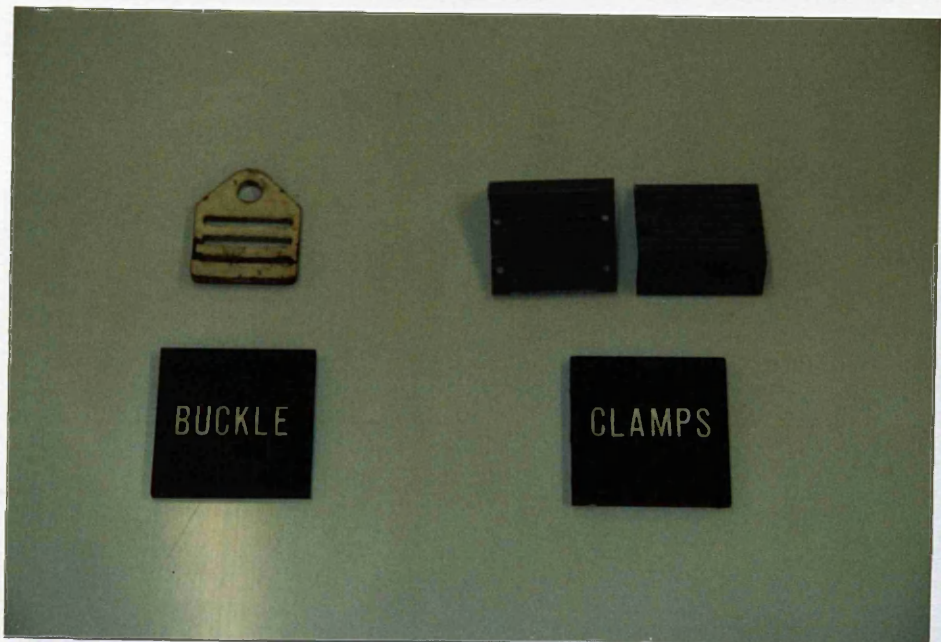


Plate 3.2 CLAMPS AND BUCKLES

INDIRECT SHEAR BOX TESTS



Plate 3.3 TENSILE TESTING ON PARALINK



Plate 3.4 TENSILE TESTING ON RIBBED STEEL

## CHAPTER 4

### DIRECT SHEAR BOX TESTS

#### 4.1 INTRODUCTION

A direct shear box test is the conventional method used to measure the shear strength of a soil. After Vidal (1966) invented the technique of reinforced earth, this method was also introduced into this field and adopted as the British criterion for reinforced earth (Department of Transport 1978) to measure the bond resistance between fills and reinforcing elements. It has also been widely employed by a number of researchers (Alimi et al 1977 and Lee 1978 etc.) in their research on the interaction of soil-reinforcement.

In the present research programme, the direct shear box test was adopted as one of the three main types of test (shear box, pull-out box and field pull-out). This was used to measure the shear strength of the fills as well as the bond resistance of the fill-reinforcement. The various fill and reinforcement materials provided were tested under different conditions of normal stress and density. The test apparatus and procedures are described, and the results presented and discussed in this chapter.

#### 4.2 APPARATUS AND PROCEDURES

##### 4.2.1 Shear Box Apparatus

This was a 303 × 303 × 303 mm large shear box apparatus. The overall view of the equipment is illustrated in *Figure 4.1* and also shown on *Plate 4.1*. The box consisted of two parts, the upper-half-box and the lower-half-box. The lower-half-box was placed in a outer box which was mounted on two rows of bearings which were in a "V" configuration to keep the shear box aligned. The

lower-half-box with the outer box could be pushed or pulled by means of a screw jack driven by a motor loading system to produce shearing forces. A test could be carried out at a constant displacement rate of 1.05 mm/min. The normal load was applied by means of a loading lever and frame system via a 100 kN load cell to a loading plate. The precise normal load imposed on the sample could be adjusted by the weight and monitored and recorded by the load cell connected to a data logger. Shear resistance was monitored by a 50 kN load cell and displacement transducers were used to measure the shearing displacement and the vertical movement of the soil, and these were connected to the same data logger.

#### 4.2.2 Test Procedures

The preparation procedure of the shear box test is as follows. The density required was achieved by means of compaction using a Kango hammer. The amount of soil required was determined according to the density, moisture content and the volume of the box. Particles larger than 25 mm size were not included. The upper-half-box was fixed together with the lower part using two bolts at the diagonal corners to avoid any side movements during compaction. The two bolts were removed before any shear testing started. In order to reduce the side friction influence, the inner sides of the box were lubricated.

In the case of testing the fill material alone, the material was placed in three layers. The compaction procedure was that a grid plate was placed on the bottom of the box, a layer of the fill material was placed in the box, then a rigid metal plate was put on it so that the hammer could vibrate on the plate and consequently compact the fill uniformly. Another grid plate was then positioned on the top of the fill after compaction and before placing the loading cover.

When testing the Paralink reinforcements with the fills, the procedure adopted was in accordance with the Department of Transport Technical Memorandum BE/3 78. The lower-half-box was filled with a hard wooden block on which the reinforcing elements were fixed firmly using adhesive (see *Plate 4.2*). The elements

were aligned so that shearing occurred in a direction parallel to the longitudinal axis along the shearing direction. The block was adjusted so that the surface of the reinforcement was flush with the top edge of the bottom half box, so that the shearing could only occur at the interface. Then the same procedure as in fill material alone testing was adopted, except that the fill in this case was compacted in two layers in the upper-half-box.

In the case of ribbed steel, a similar procedure to the one used when testing Paralink reinforcements with fill was adopted, but instead of glueing the elements on the block, they were simply placed on the top of it (see *Plate 4.2*). The level of the rib-tips was flush with the top edge of the lower-half-box. The fill was then placed and compacted in two layers.

Once the compaction of the fill was completed, the grid plate, loading cover, load cell, and loading frame were placed in position. Meanwhile, the load cell and transducer for measuring shear load and displacement were also fixed. The tests were carried out mainly at normal stresses of 20, 60 and 120 kN/m<sup>2</sup>. From these tests the internal angle of friction of the fills and also the bond resistance between them and the reinforcing materials could be obtained.

### 4.3 TEST RESULTS

With each of the fill materials, the three types of reinforcement (Paralink 300s, Paralink 500s and ribbed steel) were tested under various conditions, and the results obtained are presented in this section.

#### 4.3.1 Wardley Minestone

In the case of testing Wardley minestone with the reinforcing elements, three different densities (17.847, 16.579 and 15.206 kN/m<sup>3</sup>) were prepared at the natural moisture content of 9.7% which was close to the optimum (10%). In order to make a comparison among the different types of test (shear box, pull-out box and field

pull-out tests), either in shear box or pull-out box tests one of the test conditions (density or moisture content) was prepared in accordance with the field pull-out tests (Chapter 7). For example from the three densities above,  $17.847 \text{ kN/m}^3$  was the same as the density measured in the field pull-out tests. The results of shear stress against normal stress are illustrated in *Figures 4.2 to 4.5*, and the frictional angles and cohesions are presented in *Table 4.1*.

It is obvious (see *Figure 4.2* and *Table 4.1*) that the bond resistance angle ( $\delta$ ) between any of the reinforcing elements and the fill material was smaller than the internal angle of friction ( $\varphi$ ) from fill material alone tests. The  $\delta$  produced from ribbed steel with Wardley minestone was, however, close to the  $\varphi$ . When comparing the three different reinforcements, ribbed steel indicated a higher bond resistance than both of the Paralink elements. The two Paralink reinforcements did not produce a big difference, Paralink 500s was, however, slightly superior to Paralink 300s in terms of bond resistance.

In order to compare the bond resistance of fill-reinforcement with the internal angle of friction and cohesion, the relative friction ( $\tan \delta / \tan \varphi$ ) and the relative cohesion ( $c_r / c$ ) ( $c_r$  is the cohesion produced between the reinforcement and fill) were obtained and are shown in *Table 4.6*. Higher values were produced from ribbed steel both in relative friction and cohesion. The relative friction from the two different Paralink elements were both around 0.5, but the relative cohesion is quite low.

*Figures 4.3 to 4.5* illustrate the influence of the density, and show that the fill-reinforcement bond resistance increases with increasing density. This result was contrary to Lee (1978), who discovered that density had no effect on the angle of friction between sand and aluminium foil reinforcing material, but it was consistent with Makizuchi and Miyamori (1988) when using woven and non-woven fabrics. The density played an important role in the case of ribbed steel, and it seemed that an increase of the fill density caused a higher value of cohesion, the cohesion increasing from 0 to  $14 \text{ kN/m}^2$  with an increase in the density from  $15.206 \text{ kN/m}^3$  to  $17.847 \text{ kN/m}^3$ . For Paralink reinforcements, some increases of bond resistance with density

were also observed, although they were not as evident as for ribbed steel.

The friction coefficients ( $\mu$ ) were calculated according to equation (2.15) at three different normal stresses and densities for the three types of reinforcement, and are presented in *Table 4.7*. It is seen that the friction coefficient decreased with the normal stress (except for the ribbed steel in the loose density state) and increased with the density. The reason for this decrease with normal stress is virtually due to the existence of the cohesion ( $c_f$ ).

Several tests with varying moisture content were performed on Paralink 500s with Wardley minestone to examine the effect of the moisture content. The results are shown in *Figures 4.6* and *4.7*. In addition to a slight decrease in bond resistance with increase in moisture content, a phenomenon also observed was that a large displacement was needed to reach the maximum shear force when the moisture content increased. It is believed that this was because of the softening of the fill material when containing more water.

#### 4.3.2 Wearmouth Minestone

Similar to the previous fill material, Wearmouth minestone was also tested at three different densities (17.658, 16.380 and 15.000 kN/m<sup>3</sup>) at the natural moisture content of 5.6%. The density of 17.658 kN/m<sup>3</sup> and the moisture content of 5.6% corresponded to the field pull-out test condition (Chapter 7). For each density, the tests were conducted mainly under three normal stresses (20, 60 and 120 kN/m<sup>2</sup>), and the results are shown in *Figures 4.8* to *4.11*.

*Figure 4.8* implies the same trend as with Wardley minestone, namely that the fill alone tests produced the highest shear resistance, the ribbed steel was superior to the Paralink elements, with Paralink 500s being better than Paralink 300s in terms of bond resistance.

A relative friction was found to be 0.86 for ribbed steel, whereas about 0.5 and 0.4 were obtained for Paralink 500s and Paralink 300s respectively (see *Table 4.6*).

The influence of density was also observed, the higher the density, the larger the bond resistance.

Table 4.2 presents the frictional angles and cohesions, and the values of  $\tan \delta / \tan \varphi$  and  $c_r / c$  are exhibited in Table 4.6. The friction coefficients ( $\mu$ ) were calculated and are shown in Table 4.7, the value of  $\mu$  was found to decrease with an increase in normal stress and to increase with increasing density for all the reinforcements.

#### 4.3.3 Horden Red Shale

A series of tests were carried out with Horden red shale and the three types of reinforcements, under three different densities (17.640, 17.317 and 16.180 kN/m<sup>3</sup>) and at the natural moisture content of 11.6%. Among the densities, 17.640 kN/m<sup>3</sup> corresponded to the field pull-out test condition. The results are shown in Figures 4.12 to 4.15, the frictional angle and cohesion being presented in Table 4.3.

Figure 4.11 shows the same trend as with the previous fill materials, the bond resistance of ribbed steel was found to be close to, but slightly less than the shear resistance of the fill material. Ribbed steel produced much higher bond resistance than the two Paralink elements, while Paralink 500s was superior to Paralink 300s. The value of  $\tan \delta / \tan \varphi$  and  $c_r / c$  are presented in Table 4.6.

The influence of the density was also observed (see Figures 4.13 to 4.15), particularly  $c_r$  was observed to increase with increasing density. The  $c_r$  was increased by 7 to 8 kN/m<sup>2</sup> for an increase in the density from 16.180 kN/m<sup>3</sup> to 17.640 kN/m<sup>3</sup> for all three reinforcements.

The friction coefficient is shown in Table 4.7, and it was found to decrease with an increase in normal stress, and to increase with an increase in density.

#### 4.3.4 Loudon Hill sand

This fill material was also tested with the three types of reinforcement

provided. Three different densities (17.085, 16.190 and 15.288 kN/m<sup>3</sup>) at the natural moisture content of 7.1% were prepared in these tests. Among them the density of 16.190 kN/m<sup>3</sup> was the same as that obtained from the field pull-out tests (Chapter 7). The results from these tests are illustrated in *Figures* 4.16 to 4.19, and the frictional angles ( $\delta$ ) and cohesions ( $c_r$ ) are presented in *Table* 4.4.

The same trend can be seen, that is all the results of bond resistance between the sand and the reinforcements were smaller than the shear resistance from sand alone tests. Ribbed steel produces much higher bond resistance than the Paralink reinforcements, with Paralink 500s producing slightly higher results than Paralink 300s. The values of  $\tan\delta/\tan\phi$  and  $c_r/c$  were obtained and are presented in *Table* 4.6.

The influence of the density is illustrated in *Figures* 4.17 to 4.19. The three types of reinforcement all indicated an increase of bond resistance with an increase in the sand density.

The friction coefficients ( $\mu$ ) calculated from the test results are presented in *Table* 4.7. As with the previous fill materials, the  $\mu$  increased with increasing density and decreased with increasing normal stress.

#### 4.3.5 Methil PFA

Methil PFA was tested with the three types of reinforcement at the density of 11.590 kN/m<sup>3</sup> and natural moisture content of 27%, these corresponding to the field pull-out test condition (Chapter 7).

The results are shown in *Figures* 4.20 and *Table* 4.5. The same trend was found as from the other fill materials discussed previously, PFA alone test giving the highest shear resistance when compared with the bond resistance from PFA with reinforcement tests. Ribbed steel produced much higher bond resistance than the two types of the Paralink, with Paralink 500s being superior to Paralink 300s.

The values of  $\tan\delta/\tan\phi$  and  $c_r/c$  are presented in *Table* 4.6. The friction coefficients at normal stresses of 20, 60 and 120 kN/m<sup>2</sup> were calculated and are

shown in *Table 4.7*.

#### 4.4 COMPARISON OF THE RESULTS FROM THE VARIOUS FILL MATERIALS

Some typical curves of shear stress against displacement are illustrated in *Figures 4.21, 4.22 and 4.23*. All the results were produced under a normal stress of  $60 \text{ kN/m}^2$  and at the same moisture content and density condition as in the field tests.

*Figure 4.21* shows the behaviour of ribbed steel with the various fill materials. From these curves it can be seen that Horden red shale yielded a considerably high bond resistance, the two types of minestone, Wardley and Wearmouth, produced quite similar results which were smaller than the red shale but higher than the PFA and the sand. There was no apparent peak to the curves, and after the yield points the shear stresses increased continuously or kept about constant.

In the case of Paralink 500s (see *Figure 4.22*) the stress versus displacement curves showed a similar tendency to the ribbed steel, i.e. the red shale produced the highest bond resistance while the lowest shear stress was encountered with the Wearmouth. An obvious difference was, however, that peaks could be found in some of the materials.

*Figure 4.23* shows the case of Paralink 300s, where red shale again gave a higher result than the the two minestones and the PFA, but the sand produced a higher result. However, the differences among the fill materials were not so apparent as shown by the other two types of reinforcement. Peaks can be found with minestones and the sand.

For both the ribbed steel and the Paralink reinforcements, a linear relationship was observed in the earlier part of the shear stress versus displacement curve. In the case of the Paralink elements the maximum shear stresses were normally achieved before 10mm displacement under normal stresses up to  $120 \text{ kN/m}^2$ , the smaller the normal stress was, the smaller the displacement required for

the maximum shear stress. For ribbed steel the shear stress was increasing continuously, hence a large displacement was needed to achieve the ultimate shear stress.

*Figures 4.24, 4.25 and 4.26* show the results of shear stress against normal stress on the three types of reinforcement. The results from the five types of fill materials were plotted together for convenience of comparison. One can see that no matter which reinforcement is used, red shale always showed the highest bond resistance. It is difficult to compare the other four materials and draw a conclusion of superiority in terms of bond resistance, because it depends on the type of reinforcement. For instance, the sand produced a lower interface resistance with ribbed steel, whereas with Paralink elements it appeared superior to the two minestones and the PFA.

In the case of ribbed steel reinforcement, it seemed that the fill materials possessing higher internal angles of friction produced higher bond resistance, but for the Paralink reinforcements this relationship did not show clearly. When comparing the values of the relative friction and cohesion obtained from the different materials, one can find that for ribbed steel, the ratios of  $\tan \delta / \tan \varphi$  and  $c_r / c$  are all close to a high value of 0.9. Therefore, there might be a direct relationship between the internal shear resistance of a fill material and the bond resistance of fill-ribbed steel. However, the ratios obtained from the Paralink reinforcements were rather variable, hence it is difficult to find a relationship as above. Especially for PFA, low values of  $\tan \delta / \tan \varphi$  (0.40 and 0.33) and quite high values of  $c_r / c$  ratio (2.6 and 2.0) were obtained. It is not easy to explain the reason why higher cohesion was obtained between the PFA and the Paralink elements than from the PFA alone tests.

The reason why the ribbed steel showed a relation to the internal shear resistance is probably due to the fact that for ribbed steel because of the resistance of the ribs the shearing occurs mainly between the fill particles rather than between the fill and the reinforcement, therefore the results imply, to a certain extent, the shear behaviour of the soil alone. Whereas for Paralink elements, the shear is

generated at the interface of the fill and the reinforcement, therefore what affects the results is the nature of the surface of the elements and also the fill material and their interaction; in other words these may not be directly related to the internal angle of friction.

The results from soil alone tests have shown that the internal angle of friction from a soil is always higher than the friction angle produced between the soil and any of the reinforcing elements. The reason why a higher friction angle is obtained with ribbed steel than Paralink elements is the existence of the ribs which cause shearing between soil, hence produces larger shearing resistance.

Little cohesion was produced for the sand, but in the case of the other fill materials, the contribution of the cohesion to the bond resistance should not be ignored. Using the friction coefficient ( $\mu$ ) to represent the bond resistance appears appropriate, because it includes the effect of cohesion.

#### 4.5 CONCLUSIONS

From the results of the shear box tests and the discussion above, some conclusions can be drawn:

1. Comparing fill alone and fill–reinforcement tests, the internal shear resistance is always higher than the bond resistance, no matter which fill material and what type of reinforcement is used.
2. For all five types of fill material, ribbed steel elements produce considerably higher bond resistance than the Paralink reinforcements, with Paralink 500s being superior to Paralink 300s.
3. Comparing the five different fill materials, Horden red shale produces the highest bond resistance no matter which type of reinforcing element is used, while the efficiency of the other fill materials varies with type of reinforcing element.

4. In the curve of shear stress versus displacement, no peak appeared for ribbed steel, whereas peaks can be found for the Paralink elements.

5. In the case of ribbed steel there may exist a direct relationship between the internal shear resistance and the bond resistance, the ratios of  $\tan \delta / \tan \varphi$  and  $c_r / c$  being both around 0.9. However, in the case of Paralink straps this relation does not exist, the ratios of  $\tan \delta / \tan \varphi$  and  $c_r / c$  vary according to the different fill materials.

6. Density is a factor which influences the result of bond resistance between any of the three reinforcements and the fill materials (except the PFA). The higher the density, the higher the bond resistance is obtained.

7. There is an influence of moisture content in the case of Wardley minestone with Paralink 500s. Some small reduction of bond resistance is caused by an increase in moisture content. Moreover greater displacement is needed to achieve ultimate shear stress when moisture content increases.

8. Cohesion ( $c$ ) is also found to be an important part of the bond resistance, therefore the contribution of it should be taken into account for design.

9. The friction coefficient  $\mu$  increases with an increase in the density, whereas it decreases with normal stress. The decrease with normal stress is actually due to the presence of the cohesion.

Table 4.1

## SHEAR BOX TEST RESULTS

Wardley Minestone

Dry Density	Fill Alone		Fill/RS		Fill/500s		Fill/300s	
$\gamma$ kN/m <sup>3</sup>	$\varphi$ Deg.	$c$ kN/m <sup>2</sup>	$\delta$ Deg.	$c_r$ kN/m <sup>2</sup>	$\delta$ Deg.	$c_r$ kN/m <sup>2</sup>	$\delta$ Deg.	$c_r$ kN/m <sup>2</sup>
17.847	33	15	29	14	20	4	18	4
16.579	—	—	29.5	10	18.7	4	17.5	3
15.206	—	—	29.5	0	18.1	3.5	16.2	1.6

Table 4.2

## SHEAR BOX TEST RESULTS

Wearmouth Minestone

Dry Density	Fill Alone		Fill/RS		Fill/500s		Fill/300s	
$\gamma$ kN/m <sup>3</sup>	$\varphi$ Deg.	$c$ kN/m <sup>2</sup>	$\delta$ Deg.	$c_r$ kN/m <sup>2</sup>	$\delta$ Deg.	$c_r$ kN/m <sup>2</sup>	$\delta$ Deg.	$c_r$ kN/m <sup>2</sup>
17.658	37	11	33	10	22	7	18	3
16.380	—	—	31	7	18.5	4	17	3
15.000	—	—	29.5	5.7	16	4	16	3

RS — ribbed steel; 500s — Paralink 500s; 300s — Paralink 300s

Table 4.3

## SHEAR BOX TEST RESULTS

Horden Red Shale

Dry Density	Fill Alone		Fill/RS		Fill/500s		Fill/300s	
$\gamma$ kN/m <sup>3</sup>	$\varphi$ Deg.	c kN/m <sup>2</sup>	$\delta$ Deg.	$c_r$ kN/m <sup>2</sup>	$\delta$ Deg.	$c_r$ kN/m <sup>2</sup>	$\delta$ Deg.	$c_r$ kN/m <sup>2</sup>
17.640	41.4	11.4	39	8.6	26	10	23.4	8
17.317	—	—	37.1	5	26	5	25	1.4
16.180	—	—	36.5	1.7	26	2.1	25	0

Table 4.4

## SHEAR BOX TEST RESULTS

Loudon Hill Sand

Dry Density	Fill Alone		Fill/RS		Fill/500s		Fill/300s	
$\gamma$ kN/m <sup>3</sup>	$\varphi$ Deg.	c kN/m <sup>2</sup>	$\delta$ Deg.	$c_r$ kN/m <sup>2</sup>	$\delta$ Deg.	$c_r$ kN/m <sup>2</sup>	$\delta$ Deg.	$c_r$ kN/m <sup>2</sup>
17.085	—	—	34	8.3	26.8	4.6	23.5	5
16.190	37.6	4.6	34	3.9	24.6	4.5	22	5
15.288	—	—	30.3	2	22.5	2	21.8	2

Table 4.5

## SHEAR BOX TEST RESULTS

Methil PFA

Dry Density	Fill Alone		Fill/RS		Fill/500s		Fill/300s	
$\gamma$ kN/m <sup>3</sup>	$\varphi$ Deg.	c kN/m <sup>2</sup>	$\delta$ Deg.	$c_r$ kN/m <sup>2</sup>	$\delta$ Deg.	$c_r$ kN/m <sup>2</sup>	$\delta$ Deg.	$c_r$ kN/m <sup>2</sup>
11.590	36.5	3.6	33	3.6	16.5	9.3	13.6	7.1

Table 4.6

## SHEAR BOX TEST RESULTS

Values of Relative friction and Relative Cohesion

Type of Fill	Fill/RS		Fill/500s		Fill/300s	
	$\tan\delta/\tan\phi$	$c_r/c$	$\tan\delta/\tan\phi$	$c_r/c$	$\tan\delta/\tan\phi$	$c_r/c$
Wardley Minestone	0.85	0.93	0.56	0.27	0.51	0.27
Wearmouth Minestone	0.86	0.91	0.54	0.64	0.43	0.27
Horden Red Shale	0.92	0.75	0.55	0.91	0.49	0.70
Loudon Hill Sand	0.88	0.85	0.60	0.99	0.53	1.09
Methil PFA	0.88	1.00	0.40	2.60	0.33	2.00

Table 4.7

**FRICITION COEFFICIENT ( $\mu$ )**  
Calculated From Shear Box Test Results

Type of Fill Material	Dry Density (kN/m <sup>3</sup> )	Moisture Content (%)	Ribbed Steel			Paralink 500s			Paralink 300s		
			Normal Stress (kN/m <sup>2</sup> )	20	60	120	Normal Stress (kN/m <sup>2</sup> )	20	60	120	Normal stress (kN/m <sup>2</sup> )
Wardley	17.847		1.254	0.787	0.671	0.564	0.431	0.397	0.525	0.392	0.358
Minestone	16.579	9.7	1.066	0.733	0.649	0.539	0.406	0.372	0.465	0.365	0.340
	15.206		0.566	0.566	0.566	0.502	0.385	0.356	0.371	0.318	0.304
Wearmouth	17.658		1.149	0.816	0.732	0.754	0.521	0.462	0.475	0.375	0.350
Minestone	16.380	5.6	0.951	0.718	0.659	0.535	0.402	0.368	0.456	0.356	0.331
	15.000		0.851	0.661	0.614	0.487	0.354	0.320	0.437	0.337	0.312
Horden	17.640		1.240	0.953	0.881	0.988	0.655	0.571	0.833	0.566	0.500
Red	17.317	11.6	1.006	0.839	0.798	0.738	0.571	0.530	0.536	0.489	0.478
Shale	16.180		0.825	0.768	0.754	0.593	0.523	0.500	0.466	0.466	0.466
Loudon	17.085		1.090	0.813	0.744	0.735	0.582	0.543	0.685	0.518	0.477
Hill	16.190	7.1	0.870	0.740	0.708	0.683	0.533	0.496	0.654	0.487	0.446
Sand	15.288		0.684	0.617	0.601	0.514	0.447	0.431	0.500	0.433	0.417
Methil PFA	11.590	27.0	0.829	0.709	0.679	0.761	0.451	0.374	0.597	0.360	0.301

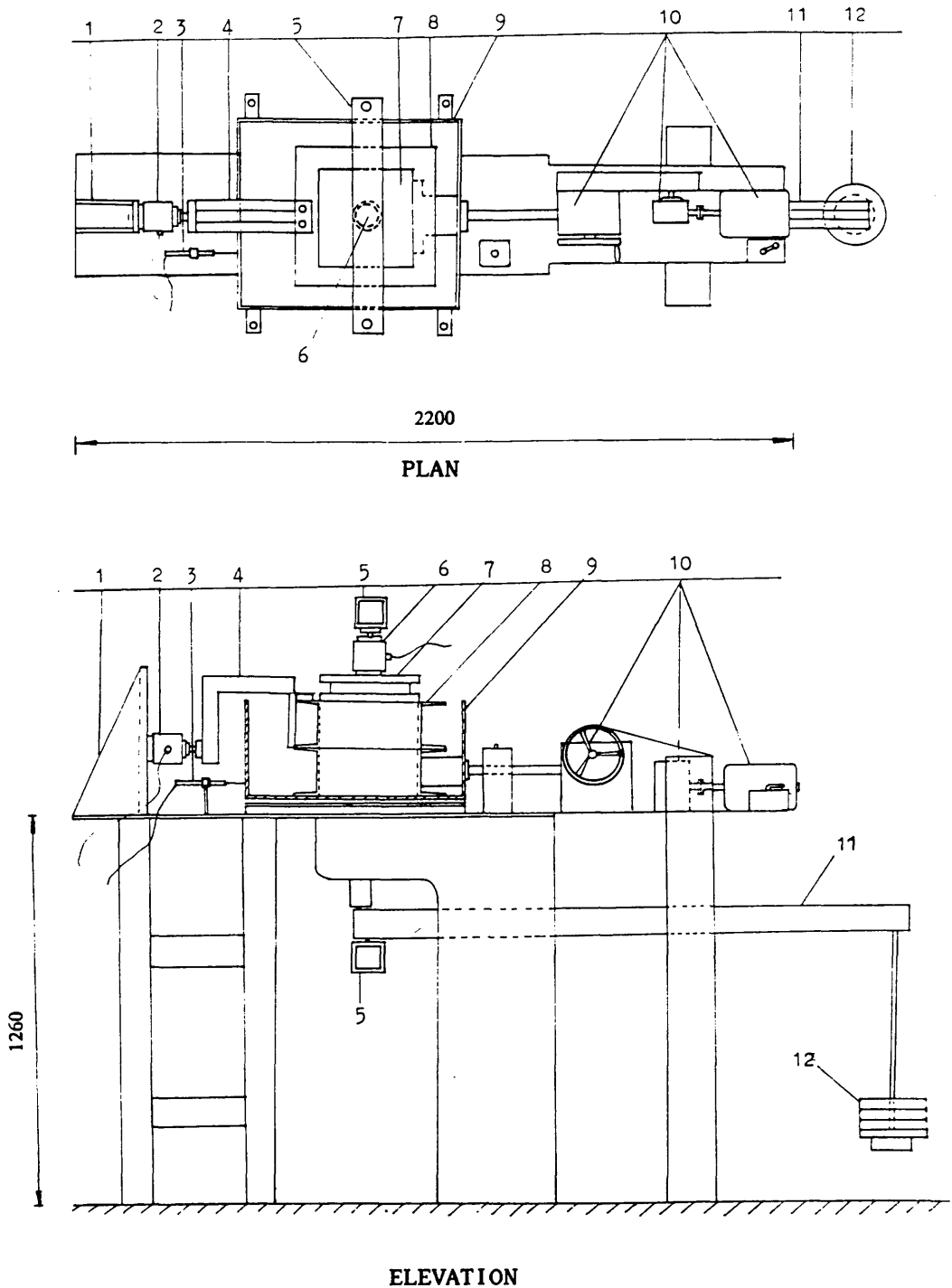


**Figure 4.1 SHEAR BOX APPARATUS**

**Description of Shear Box**

1. load cell support, 2. load cell, 3. displacement transducer, 4. resistance bar, 5. loading frame, 6. load cell, 7. loading plate, 8. shear box (303 × 303 × 303 mm), 9. outer box (if water required), 10. loading system, 11. loading lever (ratio: 0.03), 12. weights.

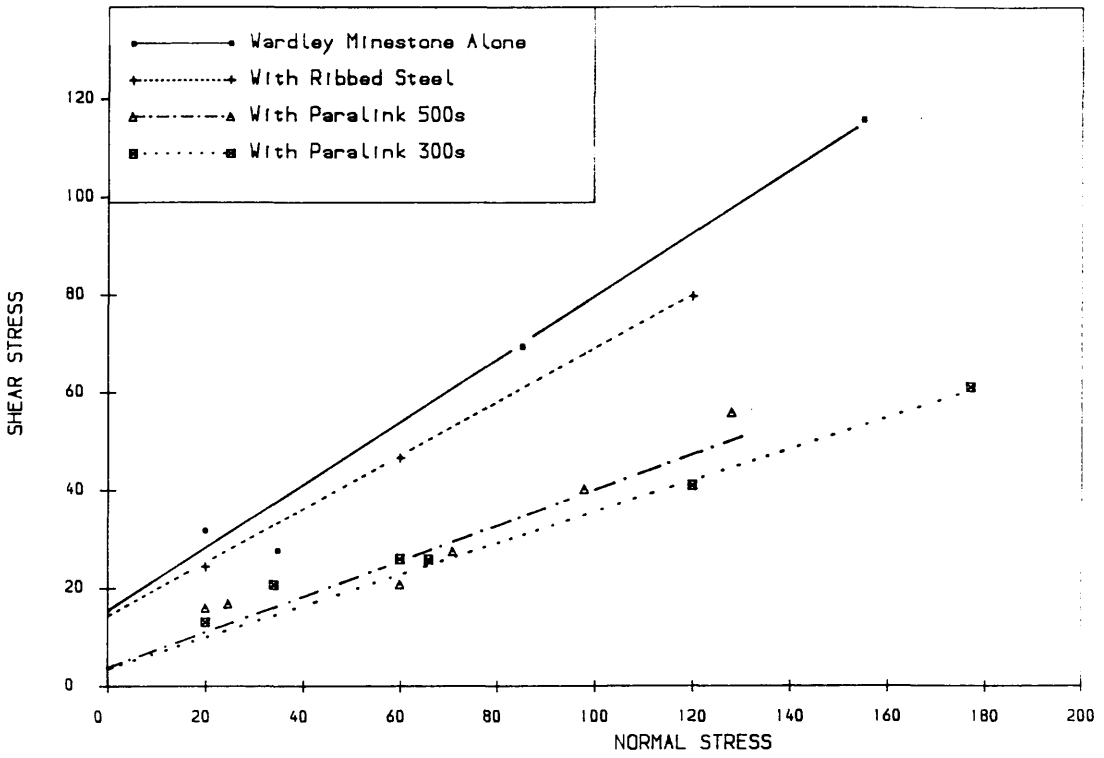


Figure 4.2 SHEAR STRESS VS. NORMAL STRESS

Shear Box Test, Wardley Minestone,  $\gamma_d = 17.847 \text{ kN/m}^3$

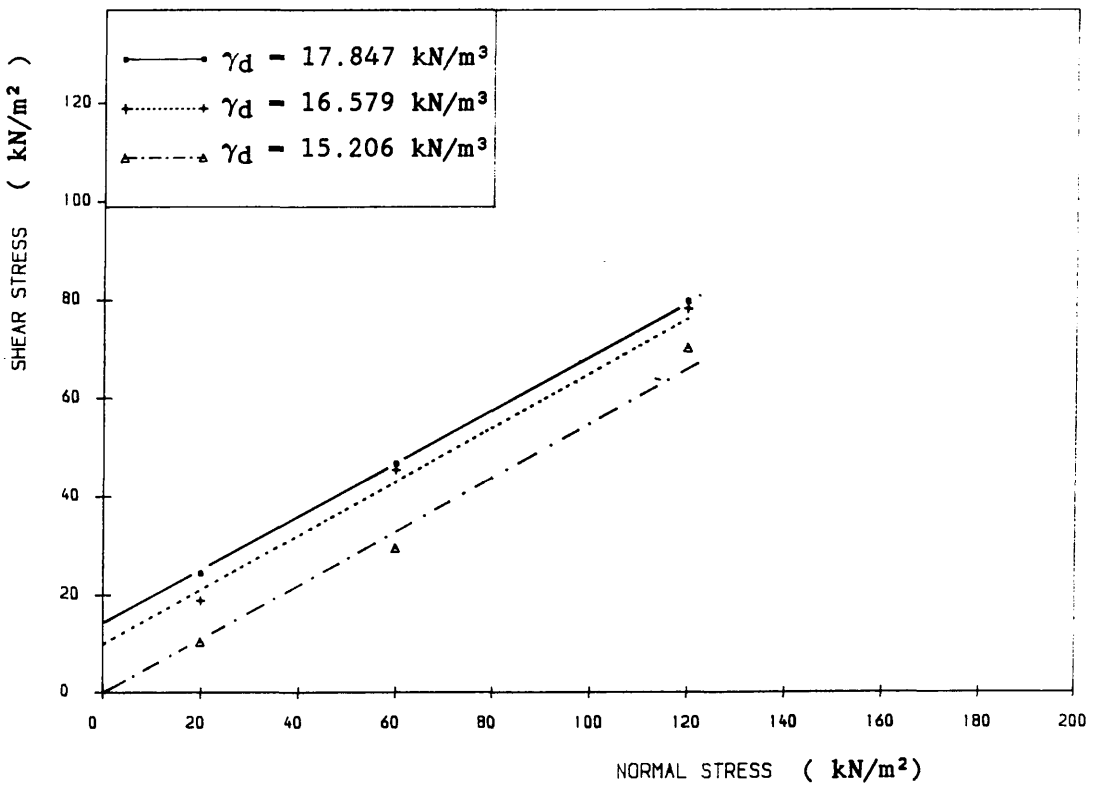


Figure 4.3 SHEAR STRESS VS. NORMAL STRESS

Shear Box Test, Wardley Minestone, Ribbed Steel

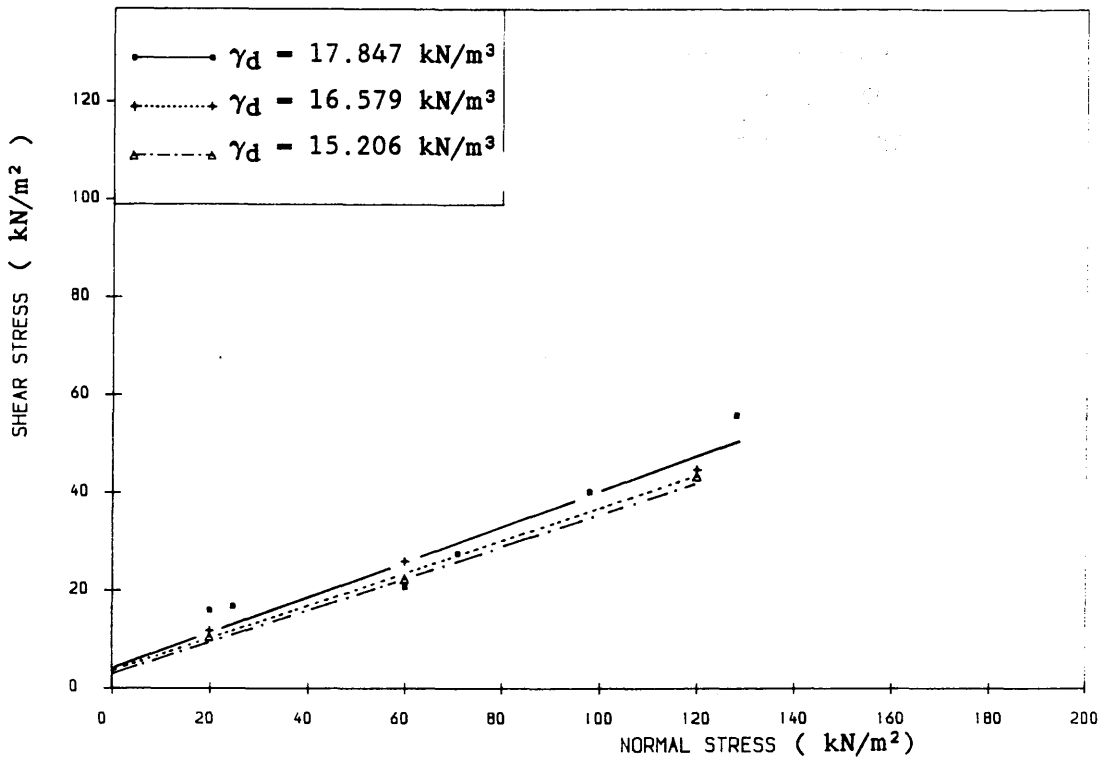


Figure 4.4 SHEAR STRESS VS. NORMAL STRESS  
 Shear Box Test, Wardley Minestone, Paralink 500s

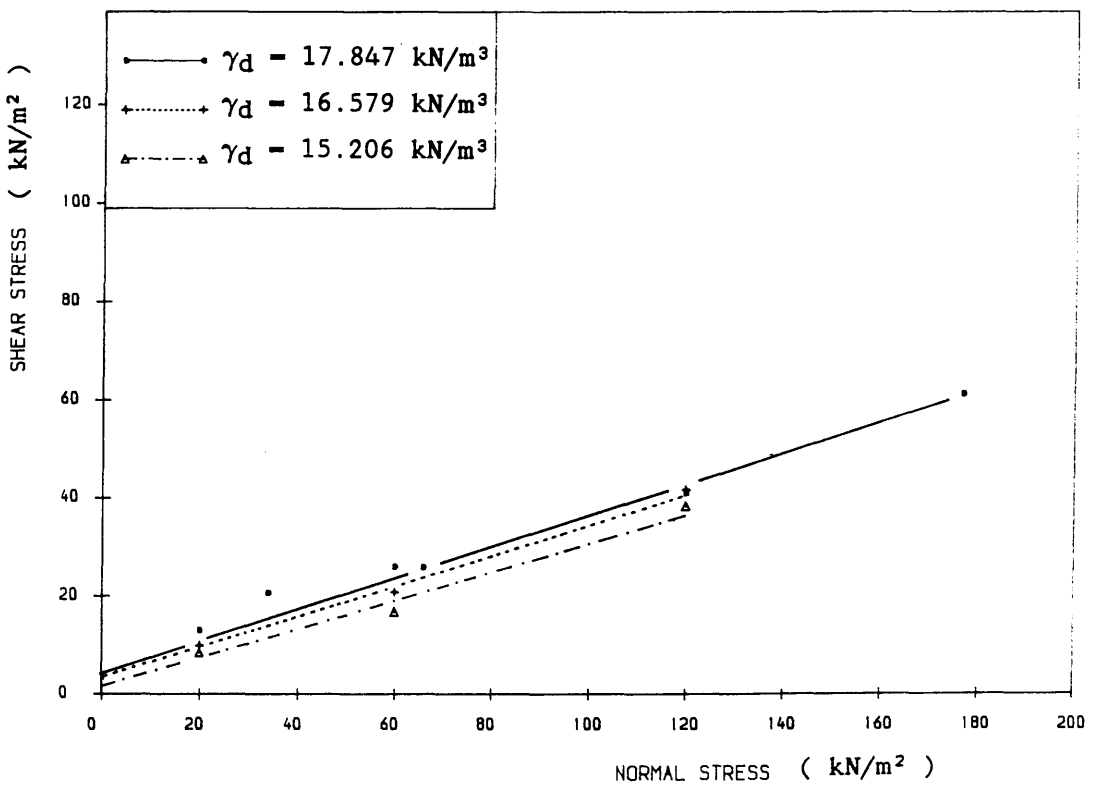


Figure 4.5 SHEAR STRESS VS. NORMAL STRESS  
 Shear Box Test, Wardley Minestone, Paralink 300s

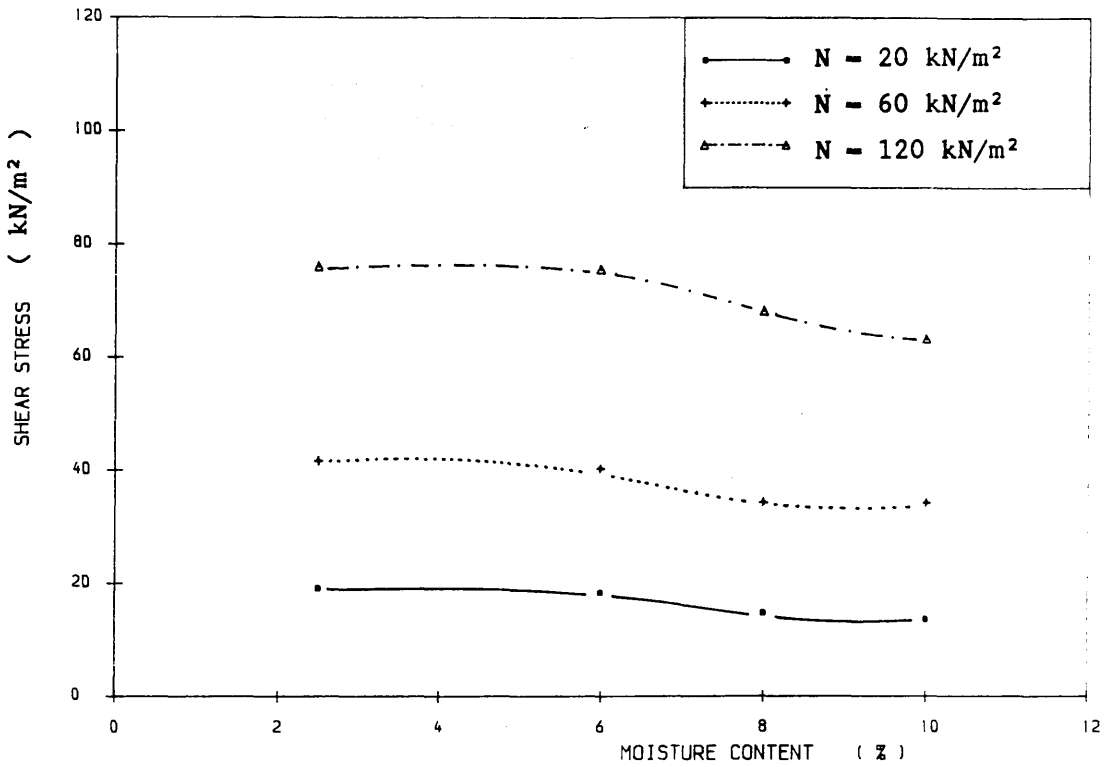


Figure 4.6 SHEAR STRESS VS. MOISTURE CONTENT

Shear Box Test, Wardley Minestone,  $\gamma_d = 16.579 \text{ kN/m}^3$ , Paralink 500s

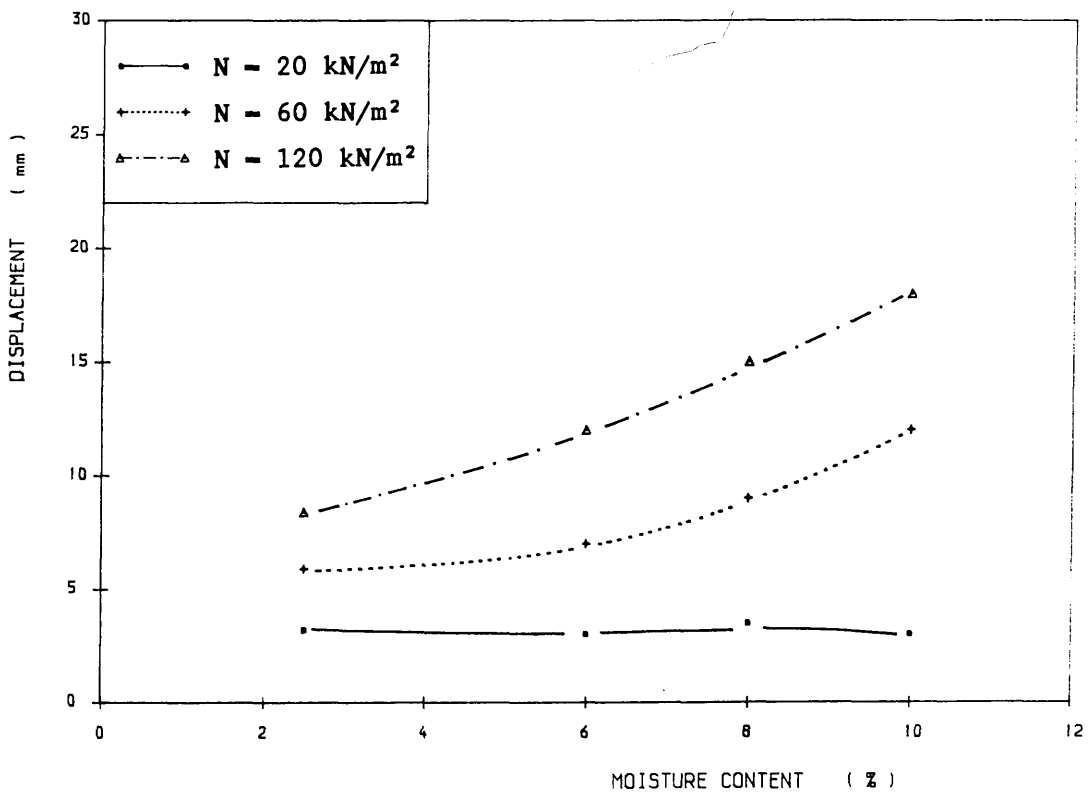


Figure 4.7 DISPLACEMENT AT MAXIMUM SHEAR STRESS VS. MOISTURE CONTENT

Shear Box Test, Wardley Minestone,  $\gamma_d = 16.579 \text{ kN/m}^3$ , Paralink 500s

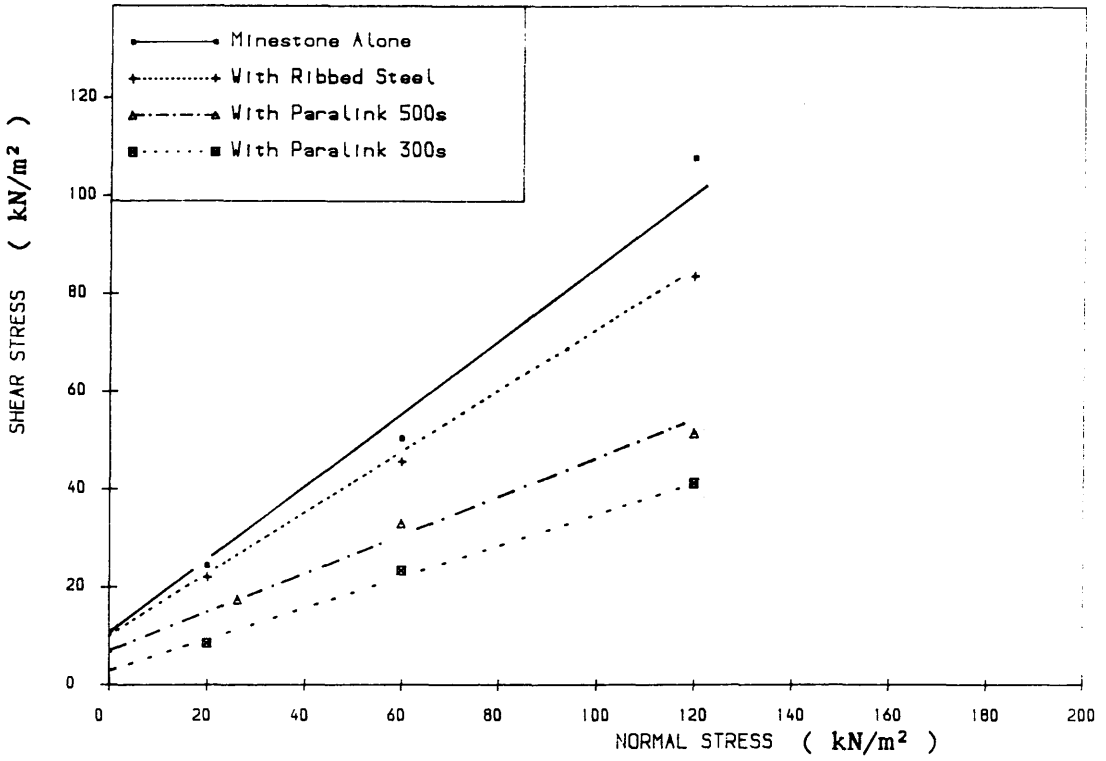


Figure 4.8 SHEAR STRESS VS. NORMAL STRESS

Shear Box Test, Wearmouth Minestone,  $\gamma_d = 17.658 \text{ kN/m}^3$

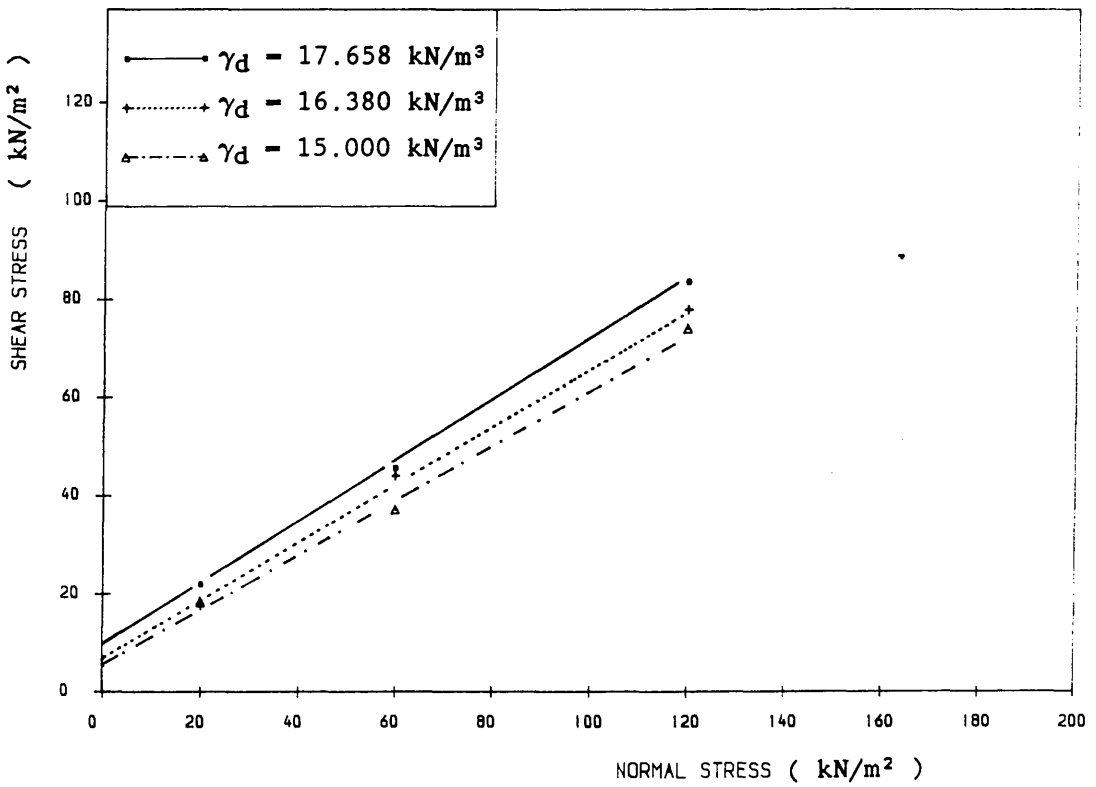


Figure 4.9 SHEAR STRESS VS. NORMAL STRESS

Shear Box Test, Wearmouth Minestone, Ribbed Steel

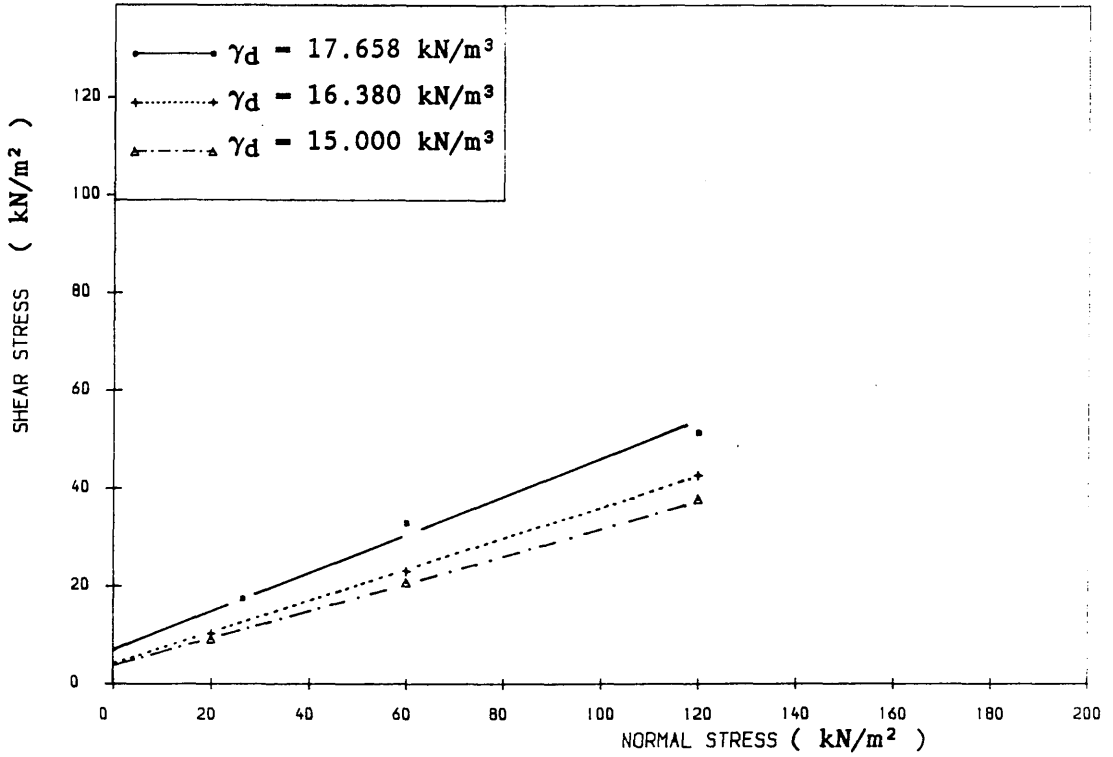


Figure 4.10 SHEAR STRESS VS. NORMAL STRESS  
 Shear Box Test, Wearmouth Minestone, Paralink 500s

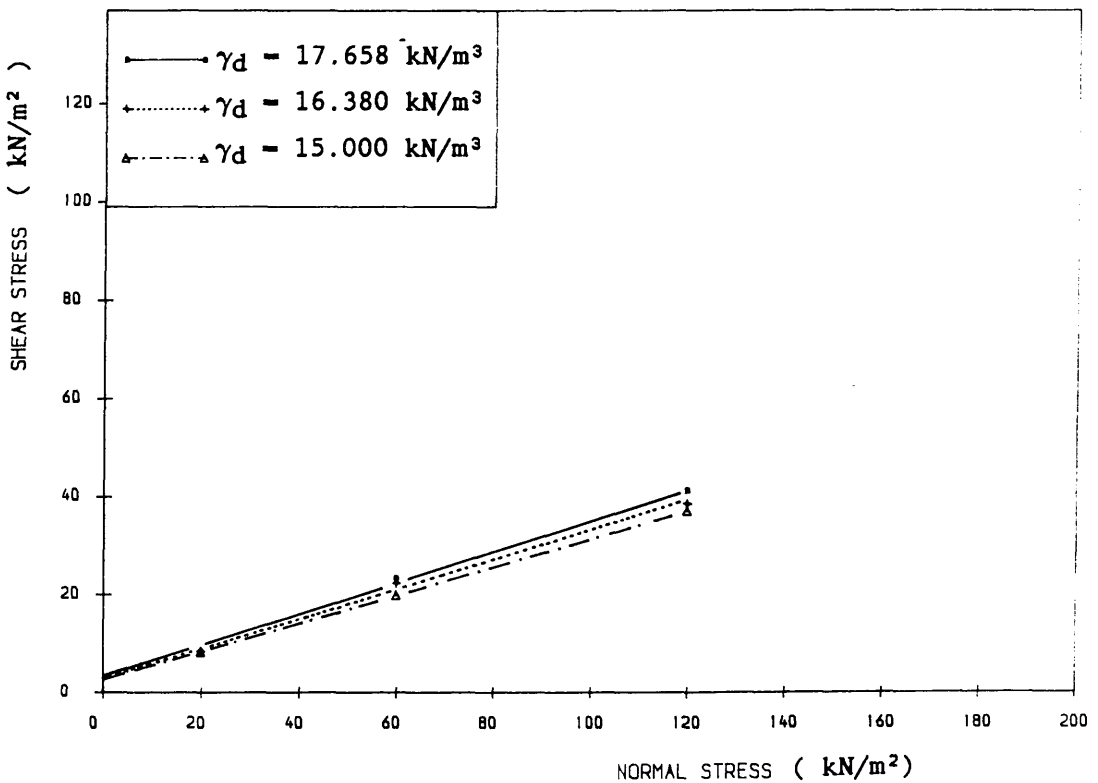


Figure 4.11 SHEAR STRESS VS. NORMAL STRESS  
 Shear Box Test, Wearmouth Minestone, Paralink 300s

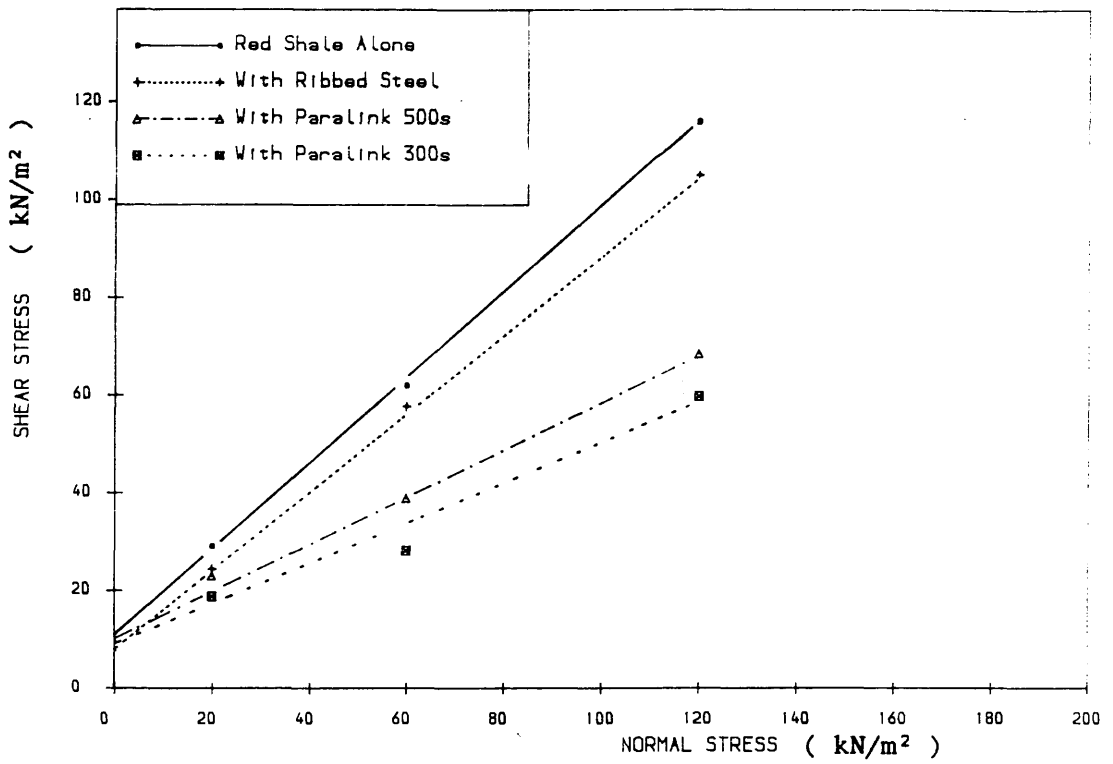


Figure 4.12 SHEAR STRESS VS. NORMAL STRESS  
 Shear Box Test, Horden Red Shale,  $\gamma_d = 17.640 \text{ kN/m}^3$

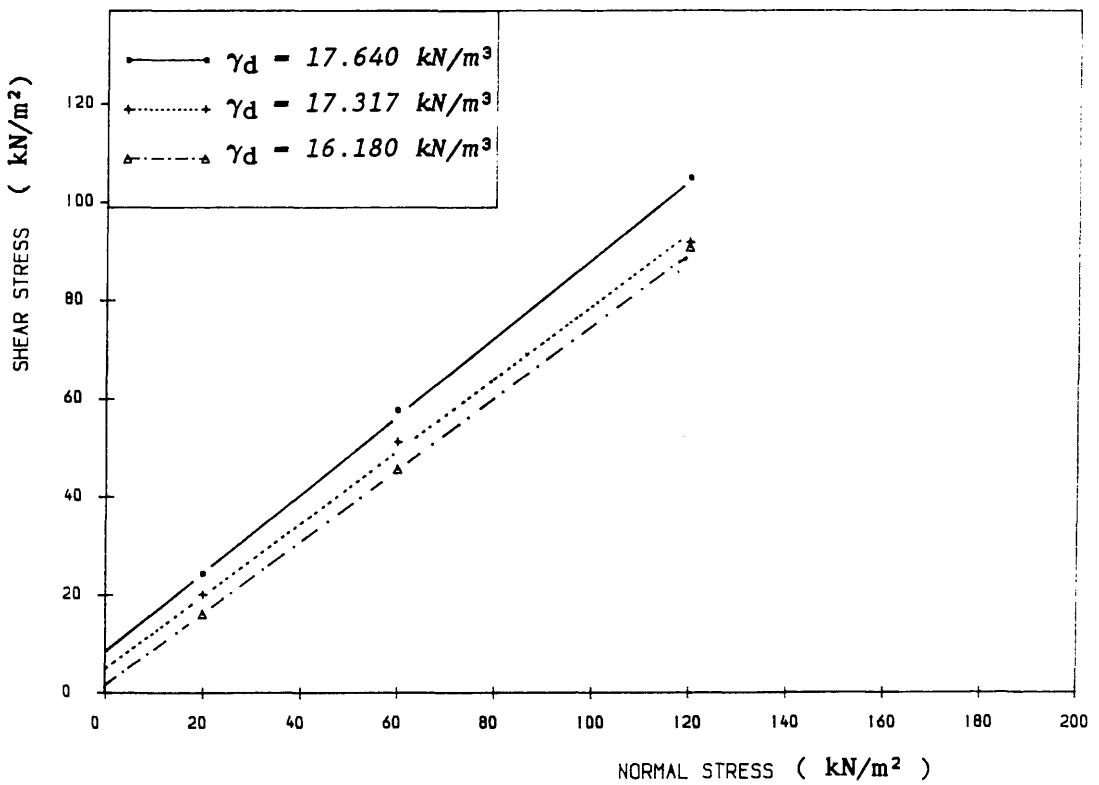


Figure 4.13 SHEAR STRESS VS. NORMAL STRESS  
 Shear Box Test, Horden Red Shale, Ribbed Steel

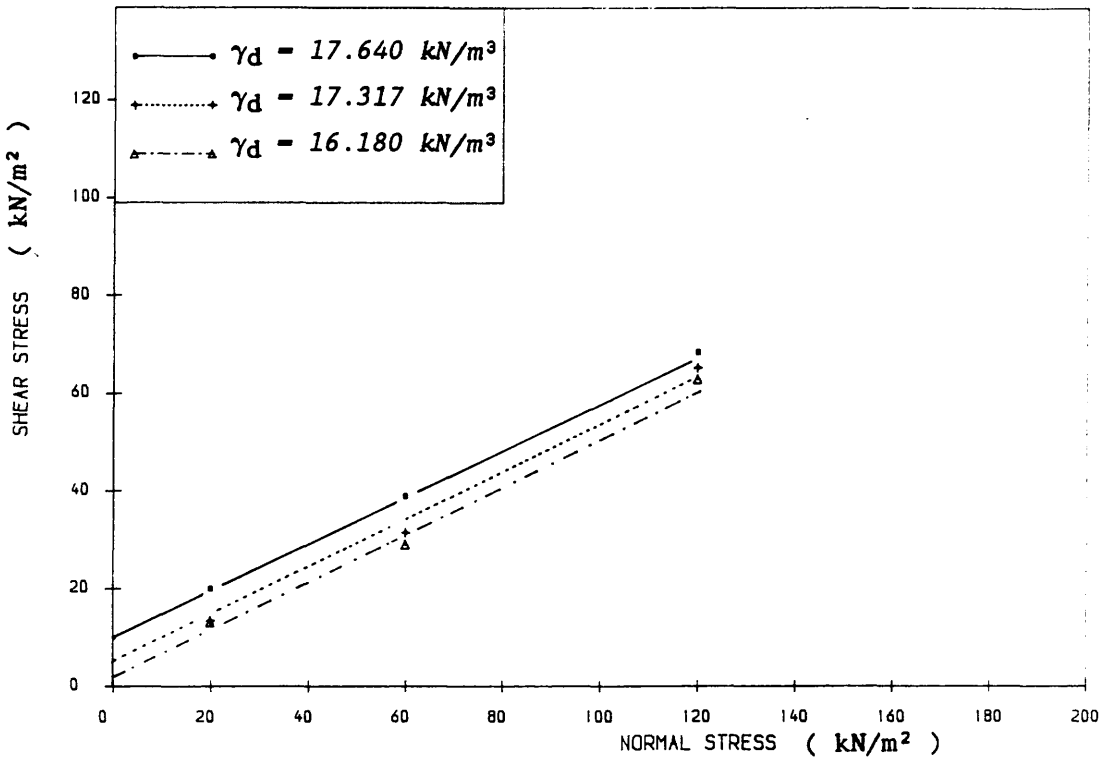


Figure 4.14 SHEAR STRESS VS. NORMAL STRESS

Shear Box Test, Horden Red Shale, Paralink 500s

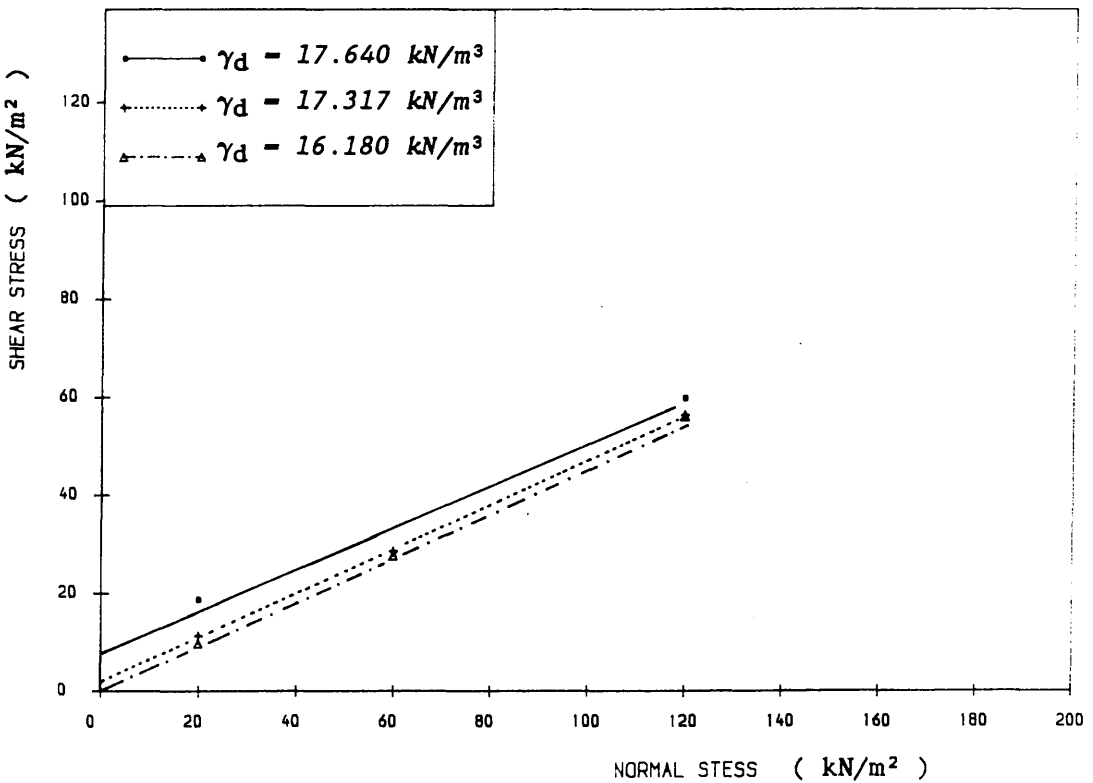


Figure 4.15 SHEAR STRESS VS. NORMAL STRESS

Shear Box Test, Horden Red Shale, Paralink 300s

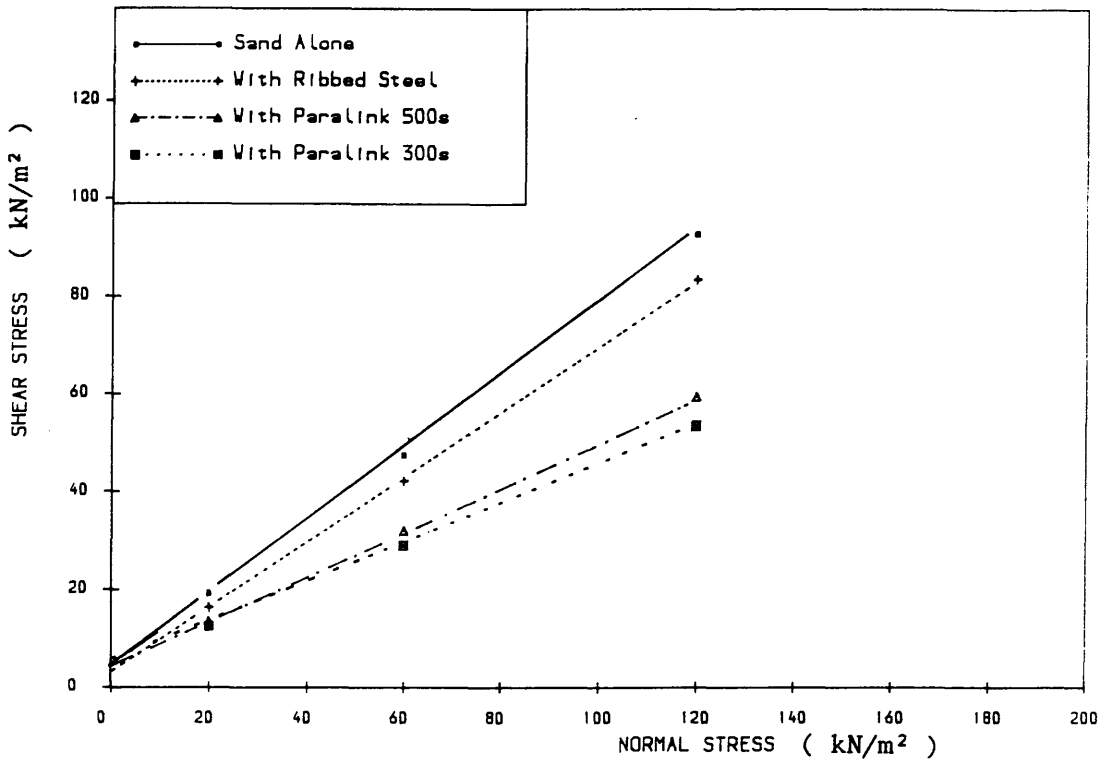


Figure 4.16 SHEAR STRESS VS. NORMAL STRESS  
 Shear Box Test, Loudon Hill Sand,  $\gamma = 16.190$

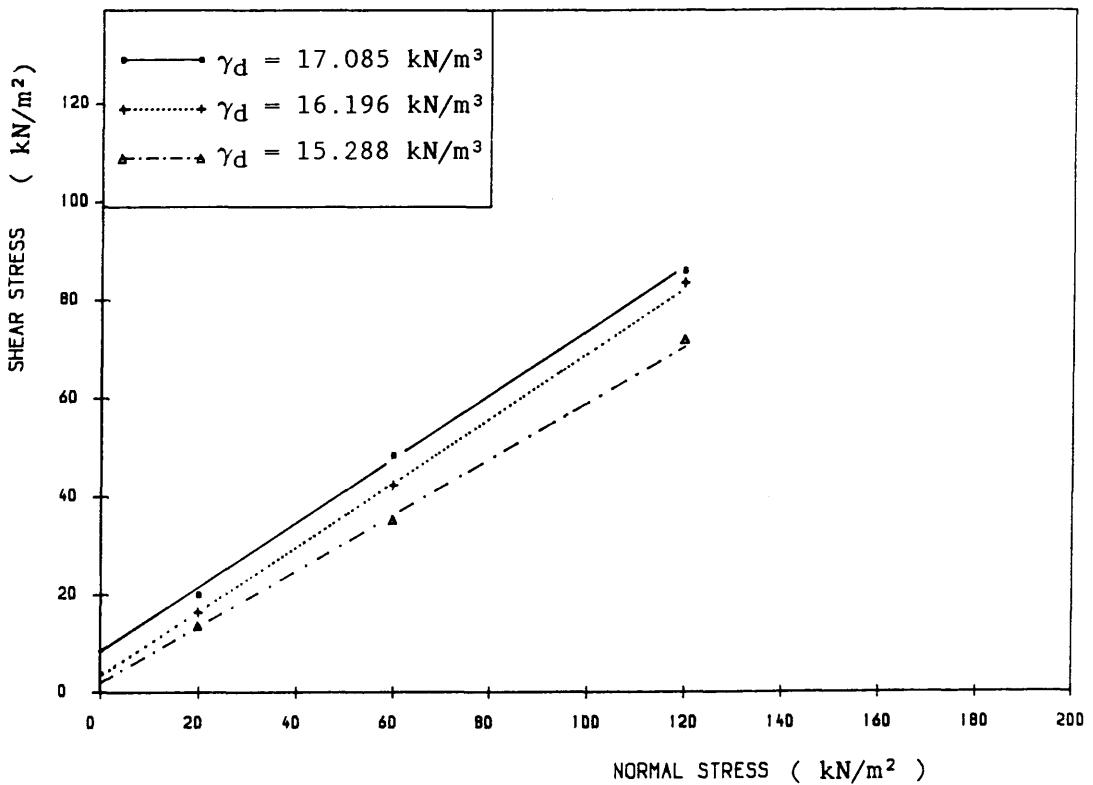


Figure 4.17 SHEAR STRESS VS. NORMAL STRESS  
 Shear Box Test, Loudon Hill Sand, Ribbed Steel

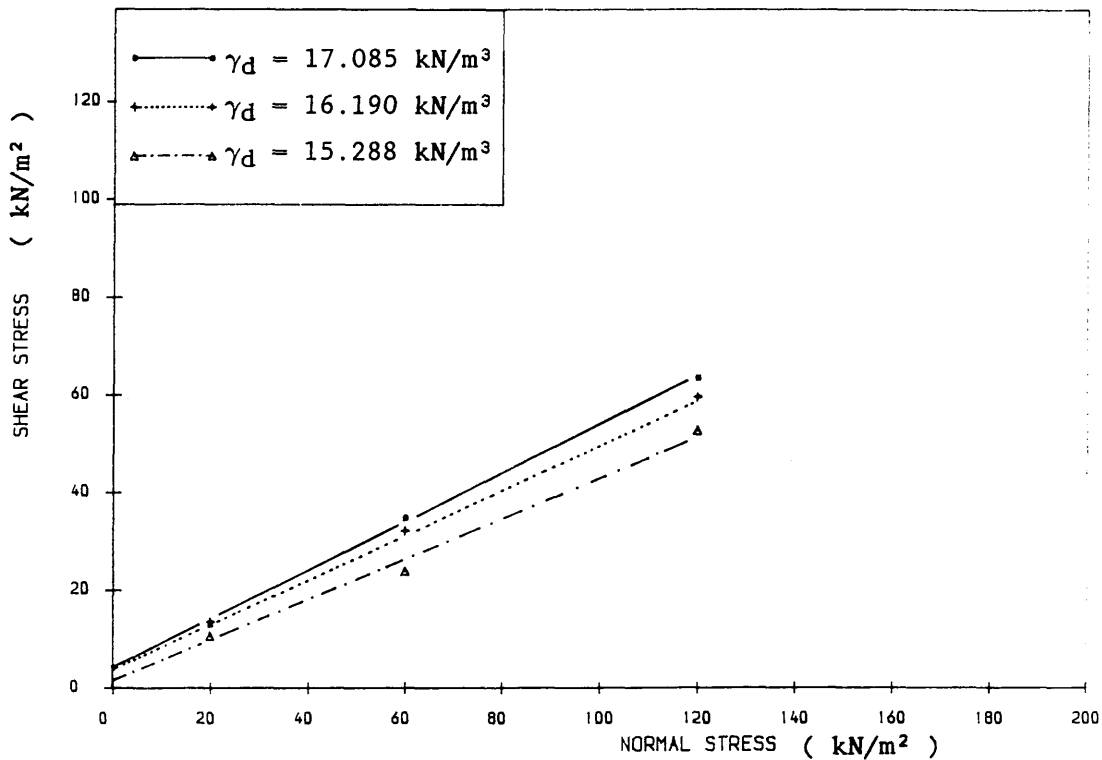


Figure 4.18 SHEAR STRESS VS. NORMAL STRESS

Shear Box Test, Loudon Hill Sand, Paralink 500s

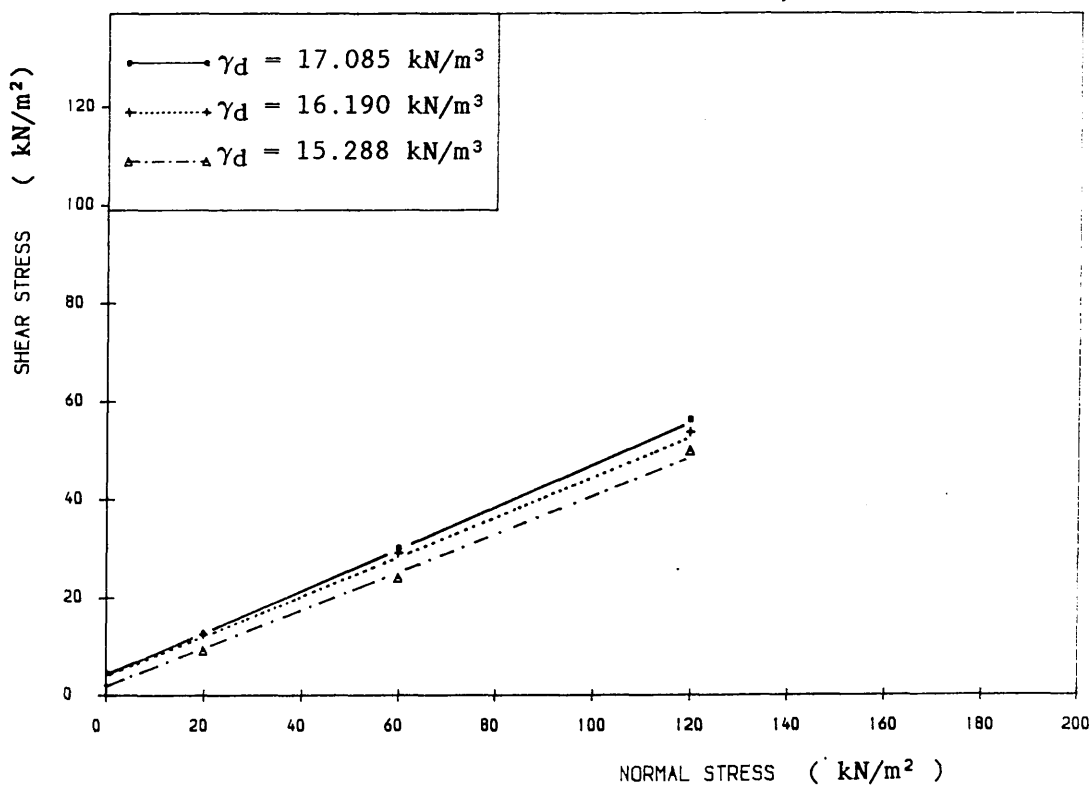


Figure 4.19 SHEAR STRESS VS. NORMAL STRESS

Shear Box Test, Loudon Hill Sand, Paralink 300s

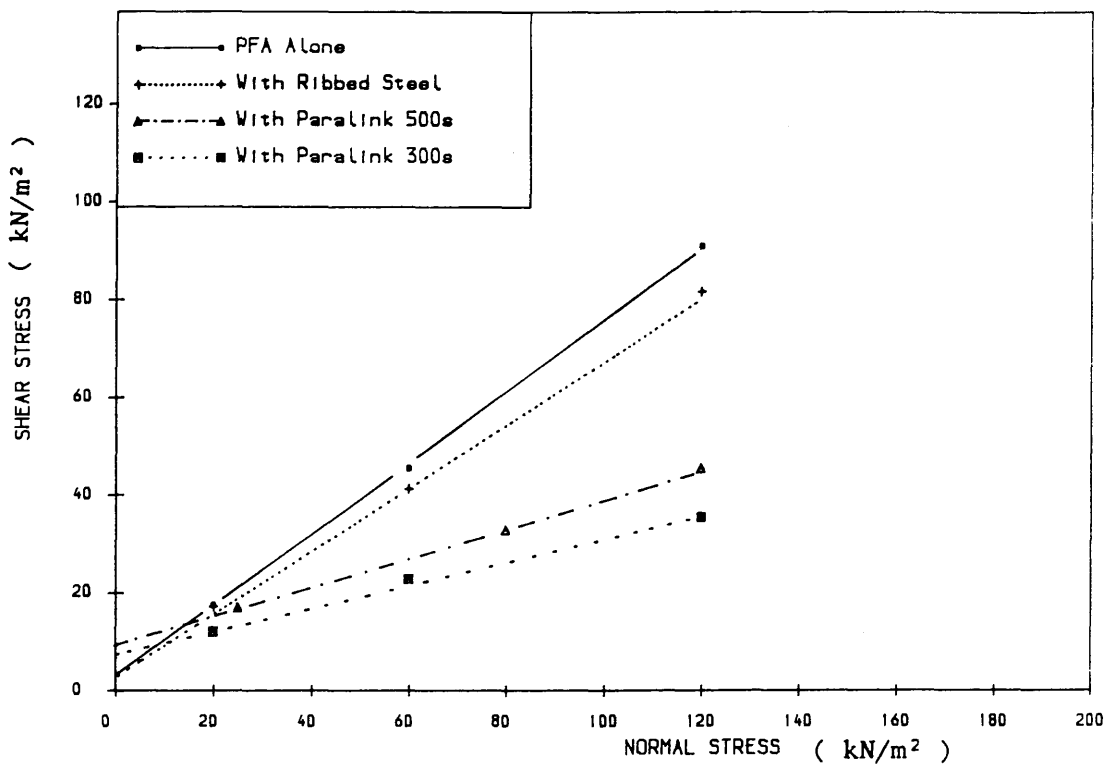


Figure 4.20 SHEAR STRESS VS. NORMAL STRESS

Shear Box Test, Methil PFA,  $\gamma = 11.590$

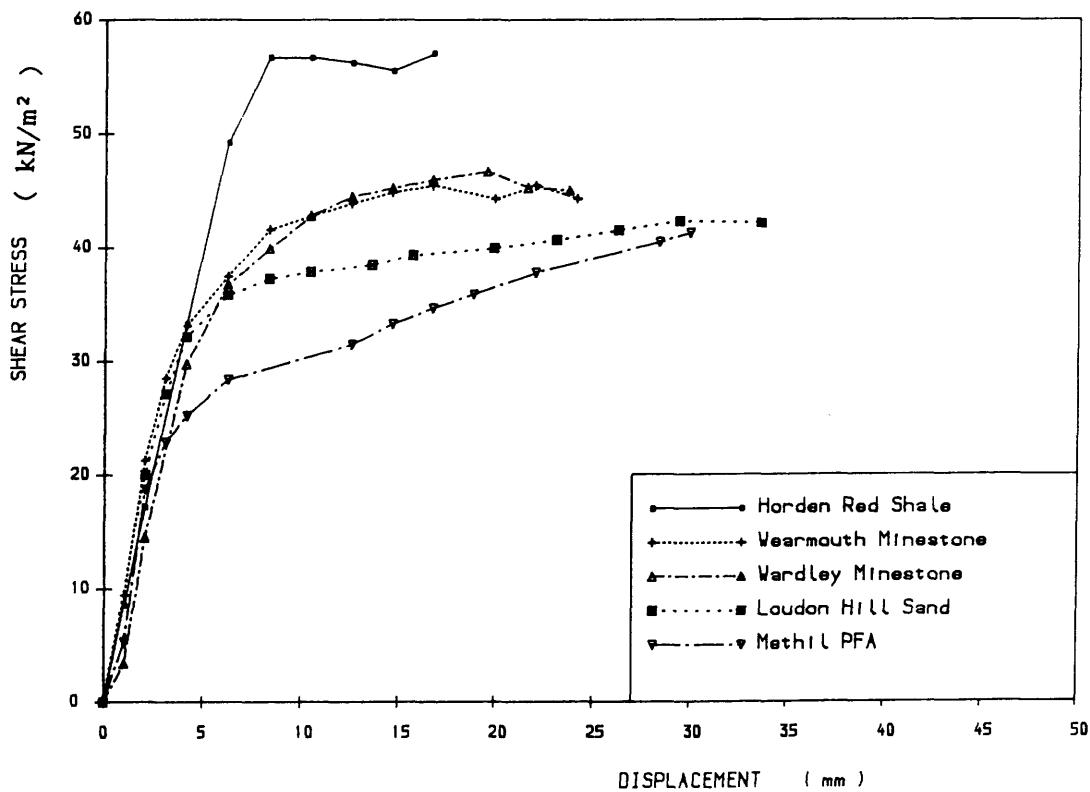


Figure 4.21 SHEAR STRESS VS. DISPLACEMENT

Shear Box Test, Ribbed Steel,

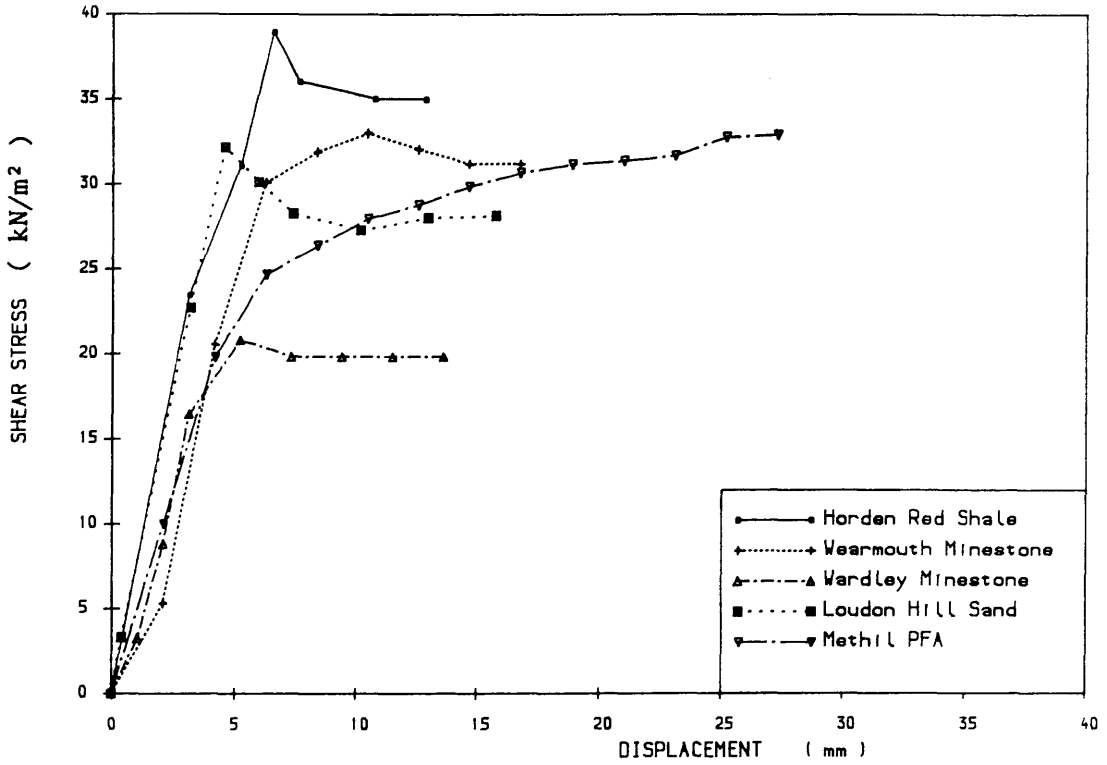


Figure 4.22 SHEAR STRESS VS. DISPLACEMENT

Shear Box Test, Paralink 500s,

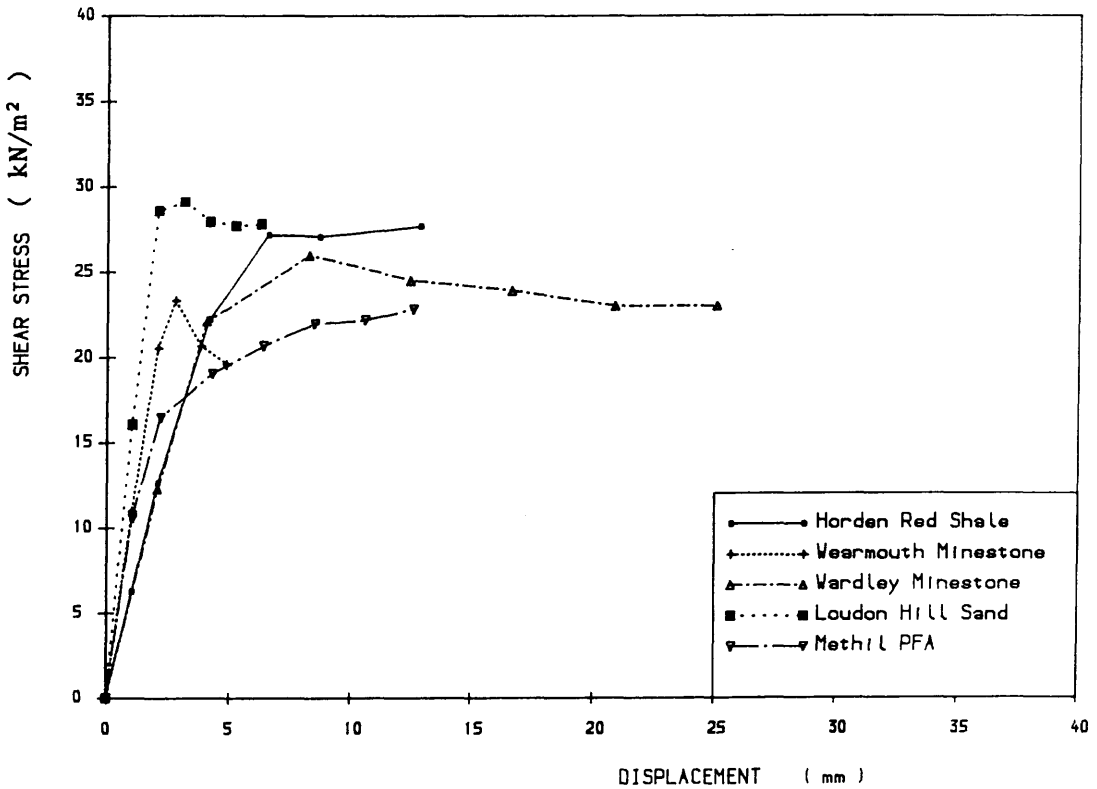


Figure 4.23 SHEAR STRESS VS. DISPLACEMENT

Shear Box Test, Paralink 300s,

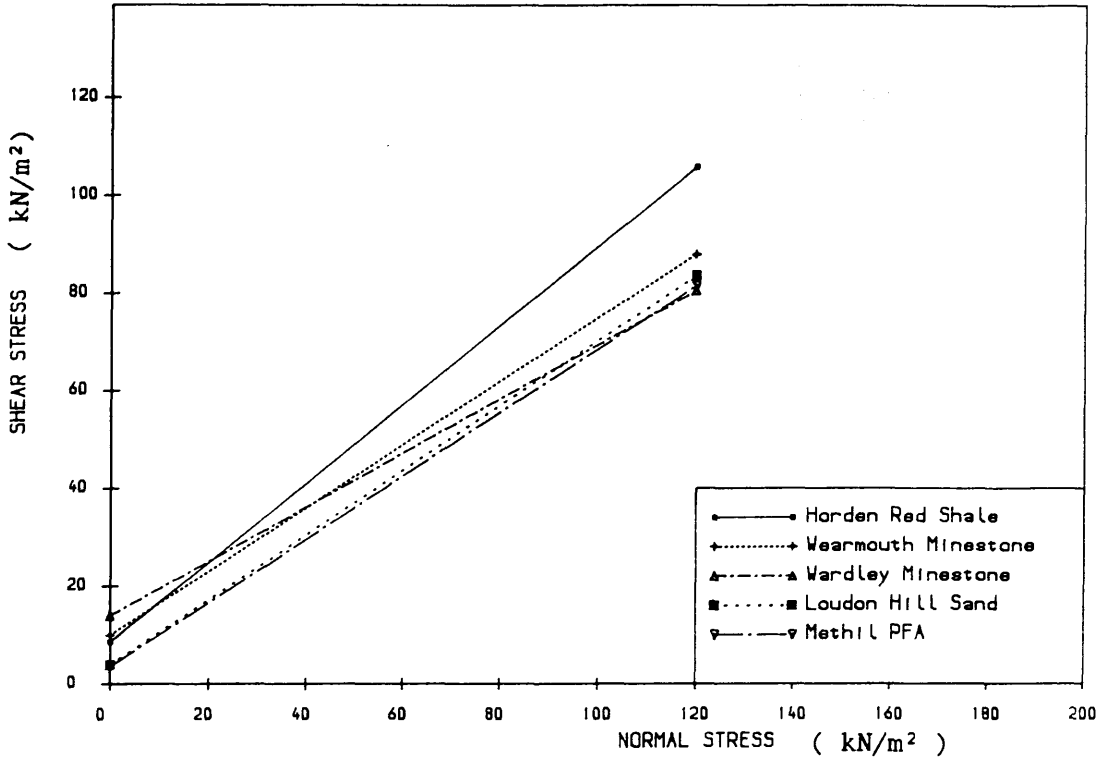


Figure 4.24 SHEAR STRESS VS. NORMAL STRESS

Shear Box Test, Ribbed Steel

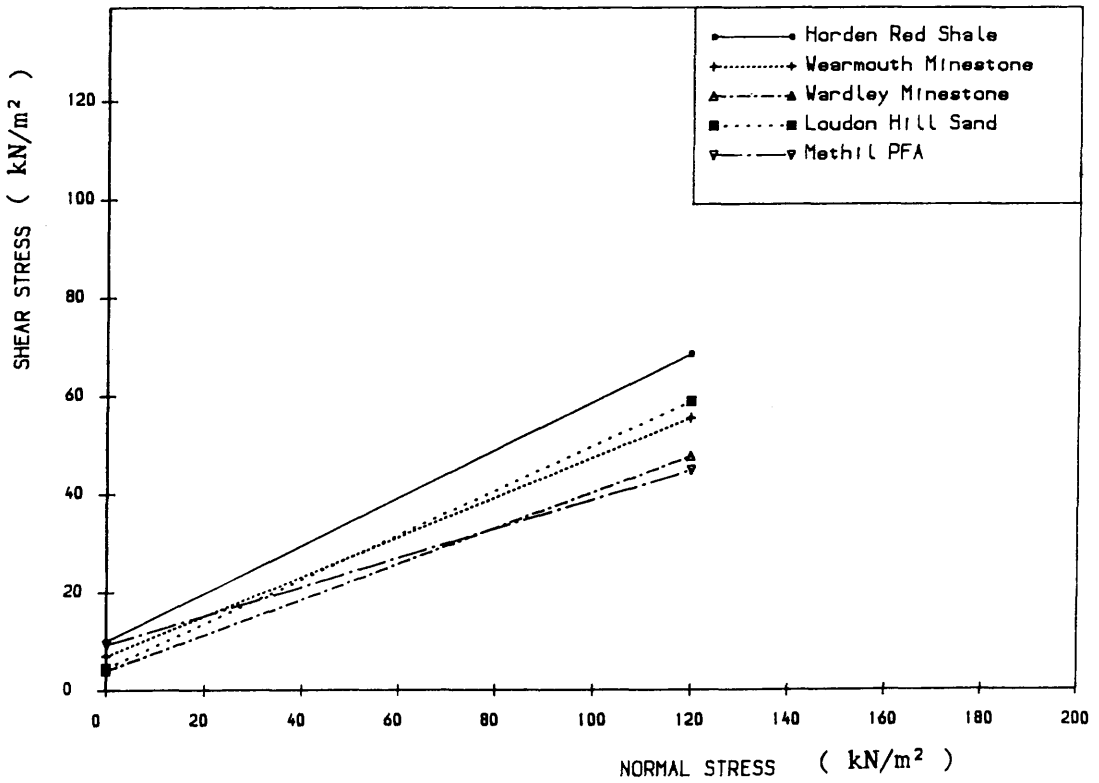


Figure 4.25 SHEAR STRESS VS. NORMAL STRESS

Shear Box Test, Paralink 500s

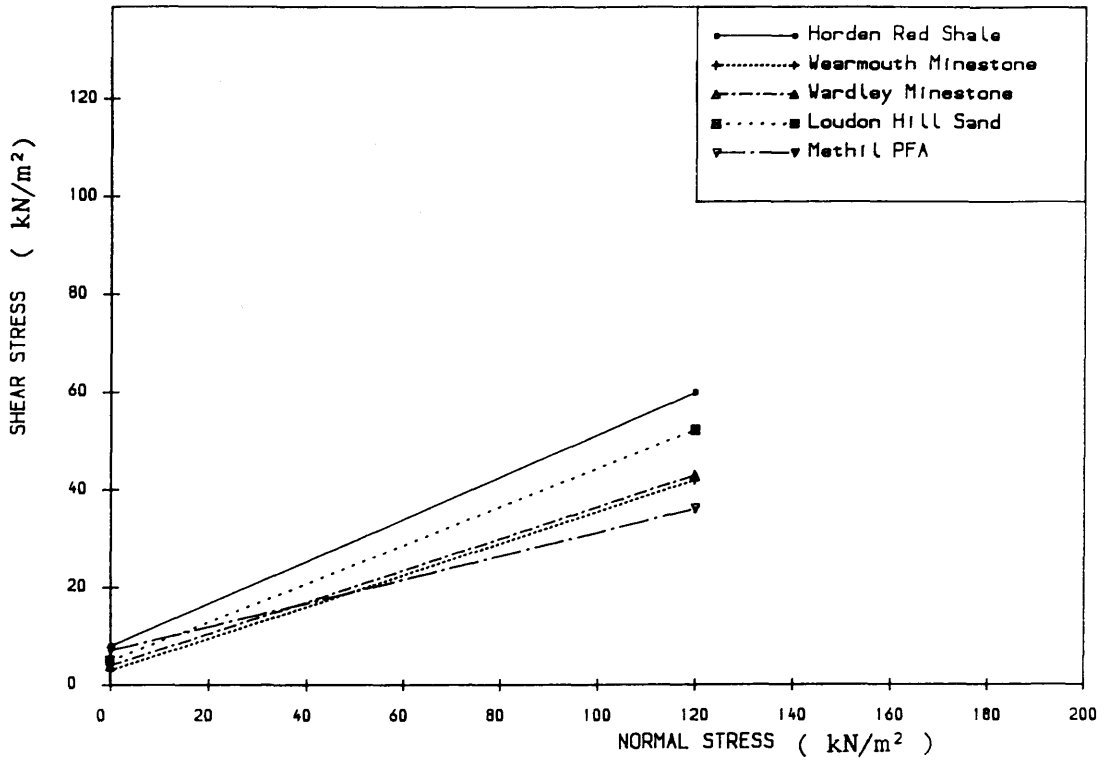


Figure 4.26 SHEAR STRESS VS. NORMAL STRESS

Shear Box Test, Paralink 300s



Plate 4.1 SHEAR BOX APPARATUS



Plate 4.2 WOODEN BLOCK WITH REINFORCING ELEMENTS

## CHAPTER 5

### LABORATORY PULL-OUT BOX TESTS

#### 5.1 INTRODUCTION

The pull-out box test is an alternative method used to investigate the interaction between fill and reinforcement, and it has been used by a number of investigators both in research and for design.

In the present work, a pull-out box test was employed to measure the bond resistance of fill-reinforcement and to investigate the performance of a reinforcing strap under a pulling force. The same three types of reinforcement and the various fill materials used in the shear box tests were also used in the pull-out box tests. The tests were carried out under various conditions of density, overburden pressure and strap length and the results are presented and discussed in this chapter. The test apparatus and procedures are also described.

#### 5.2 APPARATUS AND PROCEDURES

##### 5.2.1 Pull-out Box Apparatus

In the present research, two pull-out boxes were set up; one with load control and the other with displacement control. They are shown in *Figures 5.1* and *5.2* respectively and also on *Plates 5.1* and *5.2*.

##### 5.2.1a Load Controlled Pull-Out Box

A large rigid steel box 2000mm long by 400mm wide by 250mm deep was used (see *Figure 5.1* and *Plate 5.1*). The top part of the box comprised a rubber

membrane below a steel cover plate which could be bolted in position. Through the inlets compressed air at a controlled pressure was introduced between the rubber membrane and the top of the box, in order to simulate the overburden pressure. The pulling force was also applied by compressed air through a cylinder and a yoke. Load and displacement were monitored and recorded by a load cell and a displacement transducer which were connected to a data logger.

#### 5.2.1b Displacement Controlled Pull-Out Box

This was identical to the load controlled box, except for the method of applying the pulling force. As shown in *Figure 5.2* and *Plate 5.2*, a displacement controlled loading machine was used instead of the cylinder used for the previous box. The normal pressure was applied by means of compressed air, and the pulling load and displacement were monitored using a load cell and a displacement transducer.

#### 5.2.2 Test Procedures

The preparation of the pull-out tests was the same for the two different control systems. As in the shear box tests, the amount of the fill was determined according to the volume of the box, the density required and the moisture content. The same compaction method was used as in shear box tests. The box was rubbed with grease to reduce the friction affect and the fill was compacted in four layers, with a single strap being embedded in the compacted fill at the top of the second layer. Through the slot of the facing plate, one end of the strap was fixed by a connection to the loading system. For Paralink straps the connection used was a pair of serrated clamps, whereas in the case of ribbed steel, the strap was fixed by bolting through two holes at the end of the strap. The cover plate was then positioned with a rubber sheet below and at the top of the compacted fill. It was

fixed tightly by using a number of bolts and nuts. Normal stresses of 20, 60 and 120 kN/m<sup>2</sup> were applied by means of compressed air for each test respectively. The strap was then pulled out until failure occurred at a constant rate of either 50 N/min with the load controlled box or 1.5 mm/min with the displacement controlled box.

### 5.3 TEST RESULTS

The results obtained from these tests with the five different fill materials and the three types of reinforcing strap are presented and discussed in this section.

#### 5.3.1 Wardley Minestone

A series of tests was carried out using the load controlled pull-out box and the three types of reinforcement. The reinforcing straps were 1.5 metre length and the tests were conducted under different overburden pressures (20, 60 and 120 kN/m<sup>2</sup>) and different densities (17.847, 16.579 and 15.206 kN/m<sup>3</sup>) at the natural moisture content (9.7%). These conditions corresponded to those used in the shear box tests described in the last chapter.

##### i) Force–Displacement Behaviour

Some typical curves of pulling force versus displacement are illustrated in *Figures 5.3 to 5.6*.

*Figure 5.3* indicates the behaviour of the three reinforcements in pulling action when embedded in the minestone. These results were produced under an overburden pressure of 60 kN/m<sup>2</sup> and a density of 17.847 kN/m<sup>3</sup> at a moisture content of 9.7%. The density and the moisture content coincided with the field pull-out test (Chapter 7) condition. As can see from the figure, Paralink 500s gave

a higher pull-out resistance than Paralink 300s, although both were less than the ribbed steel. In addition the curve for ribbed steel shows a stiffer behaviour than the Paralinks, with Paralink 500s being stiffer than Paralink 300s. In the tests with the load controlled system, the straps always pulled out suddenly with the failure of bond resistance at the maximum force, therefore it was impossible to obtain the residual part of the force-displacement curve. In the case of ribbed steel, however, a large displacement was needed to achieve the failure point.

*Figures 5.4, 5.5 and 5.6* illustrate the force-displacement curves at different overburden pressures on the three different reinforcements. For all the reinforcements, a larger pull-out force was produced under a higher overburden pressure. In the case of ribbed steel, the initial parts of the curves meet together in an approximately linear relation. An interesting point is that the pattern of the force-displacement curves from Paralink straps appeared to be affected by the overburden pressure, the higher the overburden pressure applied, the stiffer the curve appeared. Pull-out stiffness was introduced and designated as  $E_p$  which was calculated at 10mm displacement (the curves at this part being close to a linear relation), i.e.

$$E_p = T/D \quad (\text{kN/mm}) \quad (5.1)$$

where  $T$  is the pulling force and  $D$  is the displacement. The values of  $E_p$  for the different materials are presented in *Table 5.6*.

## ii) Maximum Pull-out Force and Friction Coefficient

All the tests were repeated twice (or three times for some) and the mean values of the results are presented in *Table 5.1* and *Figures 5.7 to 5.14*.

Maximum pull-out force was plotted against overburden pressure. It was assumed that when the overburden pressure was zero, the pull-out force would also

be zero, because without normal stress, the shear stress would not exist and would not therefore produce a pull-out force. Therefore the points could be joined from the origin. *Figure 5.7* shows the differences among the three reinforcements. It gives the same conclusion as *Figure 5.3*, that is the ribbed steel produced the highest pull-out force, with Paralink 500s being superior to Paralink 300s in terms of pull-out resistance, although the width of the ribbed steel strap is only about half that of the Paralink straps. This graph also indicates an increase in maximum pull-out force with an increase in overburden pressure. *Figures 5.8* to *5.10* are the results produced from the three types of reinforcement with three different densities. A similar trend is indicated, i.e. the maximum pull-out force increased with an increase in overburden pressure. In addition, the influence of density was apparent, particularly for ribbed steel. The higher the density, the higher the pull-out force obtained. In the case of Paralink Straps, an increase of pull-out force with density was also observed, but it became negligible when the overburden pressure increased up to about 120 kN/m<sup>2</sup>. In *Figures 5.9* and *5.10* higher pull-out force can be found from a lower density when  $\sigma_v$  was 120 kN/m<sup>2</sup>, this implies that the influence of density has become modest.

The friction coefficient  $f^*$  was obtained according to equation (2.14), and these are presented in *Table 5.1* and also shown in *Figures 5.11* to *5.14*.

Comparing the three straps, the highest value of  $f^*$  was produced from ribbed steel, with higher results being obtained from Paralink 500s than Paralink 300s. The difference between the two Paralinks was small relative to that between the ribbed steel and the Paralinks. A decrease of  $f^*$  was observed with increasing overburden pressure. This was consistent with the conclusion from some other researchers (Chang 1974, Schlosser and Elias 1978). However, the rate of decrease in the friction coefficient became less when the overburden pressure became higher. One can see from the curves that from 20 to 60 kN/m<sup>2</sup> of overburden pressure the decreases of  $f^*$  were 2.143, 0.356 and 0.378 for ribbed steel, Paralink 500s and Paralink 300s respectively. Whereas from 60 to 120 kN/m<sup>2</sup> the decreases of  $f^*$

became rather smaller, and they were found to be 0.723, 0.081 and 0.075 for ribbed steel, Paralink 500s and Paralink 300s respectively. The apparent friction coefficient was also found to be increasing with increase in density. The influence of density on  $f^*$  appeared significant in the case of ribbed steel. For all three straps the effect of density was quite obvious at the lower overburden pressures, and it became negligible when  $\sigma_v$  increased up to 120 kN/m<sup>2</sup>. This implies that density is a factor which affects the value of  $f^*$ , but this influence was also related to the overburden pressure.

### 5.3.2 Wearmouth Minestone

Similar to the tests with Wardley minestone, these were conducted under three different overburden pressures (20, 60 and 120 kN/m<sup>2</sup>) and three different densities (17.658, 16.380 and 15.000 kN/m<sup>3</sup>) at the natural moisture content (5.7%). The load controlled pull-out box was employed and the three reinforcing straps of 1.5 metre length were tested. The results obtained from these tests are presented in this section.

#### i) Force–Displacement Behaviour

*Figures 5.15 to 5.18* illustrate some typical force–displacement curves. The curves in *Figure 5.16* are from the tests at a density of 17.658 kN/m<sup>3</sup> and under an overburden pressure of 60 kN/m<sup>2</sup>. These show the same trend as obtained with Wardley minestone, i.e. Paralink 500s produced a higher resistance than Paralink 300s, with both being less than the ribbed steel strap. It also shows the highest stiffness in pulling behaviour with the ribbed steel, and Paralink 500s appeared stiffer than Paralink 300s. However, in the case of Wearmouth minestone, the difference between the ribbed steel and the Paralink straps was not significant in terms of the maximum pull-out force.

From *Figure 5.16*, it can be seen that higher pull-out force is produced by higher overburden pressure for the ribbed steel strap. The curves show the same linear form at the initial part and after a certain point the curves become almost horizontal. *Figures 5.17* and *5.18* show the force-displacement curves for Paralink 500s and Paralink 300s respectively. The two figures show an analogous pattern, and for both Paralink straps, a higher overburden pressure produced a higher pull-out force, the same as with Wardley minestone. The curves also indicate an increased in pull-out stiffness ( $E_p$ ) of Paralink straps and the value of  $E_p$  are also presented in *Table 5.6*.

## ii) Maximum Pull-out Force and Friction Coefficient

The results are shown in terms of maximum pull-out force ( $T_{max}$ ) versus overburden pressure ( $\sigma_v$ ) in *Figures 5.19* to *5.22*.

*Figure 5.19* shows the comparison of the different straps. For all the straps a trend is that the maximum pull-out force increases with increasing overburden pressure. It can be seen that up to  $60 \text{ kN/m}^2$  the pull-out forces obtained ranged in descending order from ribbed steel to Paralink 500s and Paralink 300s, but at an overburden pressure of  $120 \text{ kN/m}^2$  the result from ribbed steel dropped below Paralink 500s. The reason for this is that since the Paralink straps are wider than the ribbed steel one, when the overburden pressure increases, the overall force imposed on the area of the Paralink straps becomes much larger relative to the ribbed steel, while the friction coefficient decreases with increase in overburden pressure, particularly for ribbed steel this decrease appears more apparently, and the difference of the  $f^*$  produced from ribbed steel and Paralink becomes less when  $\sigma_v$  increases. Therefore at higher overburden pressure, the strap area plays more important role than the rib protrusions to produce more pull-out resistance. This can also be illustrated by the results obtained by Schlossor (see *Figure 2.18*). Assuming the widths of ribbed strap be  $40 \text{ mm}$  and smooth strap be  $100 \text{ mm}$ , and both with

1.5 m length, according to the equation (2.14), the expression of pull-out force

$$T = 2f^*BL\sigma_v \quad (2.14)$$

It can be obtained from *Figure 2.18* that at 20 kN/m<sup>2</sup> of  $\sigma_v$ , the values of  $f^*$  are 7 for ribbed strap and 2 for smooth strap, whereas at 100 kN/m<sup>2</sup> of  $\sigma_v$ ,  $f^*$  is found to be 1.5 for ribbed and 0.7 for smooth straps. Using  $T_r$  and  $T_m$  to designate the pull-out forces produced with ribbed and smooth steel straps respectively, the maximum pull-out forces can be calculated at 20 kN/m<sup>2</sup> of overburden pressure to be 16.8 kN and 12 kN for  $T_r$  and  $T_m$  respectively. Higher pull-out force is produced with ribbed strap. But when  $\sigma_v$  increases to 100 kN/m<sup>2</sup>,  $T_r$  is found to be 18 kN, and  $T_m$  be 21 kN. On the contrary to the former results, the wider smooth strap produces higher pull-out force. This is obviously caused by the larger decrease of the friction coefficient  $f^*$  with increase in overburden pressure when the ribbed steel strap is used, although the friction coefficient from the ribbed steel strap is still higher, the bigger area of the smooth strap leads a higher pull-out resistance.

*Figures 5.20 to 5.22* show the results of tests at different densities. All these graphs indicate an increase in maximum pull-out force with an increase of overburden pressure, regardless of reinforcement type or density. At low overburden pressures, an increase in density resulted in a larger maximum pull-out force, but with an increase in overburden pressure, some contrary results appeared. This became quite obvious at the overburden pressure of 120 kN/m<sup>2</sup>, particularly for Paralink straps. In the case of Paralink 500s, at 20 kN/m<sup>2</sup> overburden pressure, a 29% higher pull-out force,  $T_{max}$ , was obtained as the density increased from 15.000 kN/m<sup>3</sup> to 17.658 kN/m<sup>3</sup>, but an 18% lower  $T_{max}$  was produced with the same increase of density when the overburden pressure was 120 kN/m<sup>2</sup>. Similarly for Paralink 300s, a 42% increase in  $T_{max}$  was found at 20 kN/m<sup>2</sup> of  $\sigma_v$  with an increase in density from 15.000 kN/m<sup>3</sup> to 17.658 kN/m<sup>3</sup>, whereas a 47% of reduction of  $T_{max}$  was obtained at 120 kN/m<sup>2</sup> of  $\sigma_v$  with the same increase of

density.

*Figures 5.23 to 5.26* display the results of friction coefficient versus overburden pressure. Results from the three different straps at the same conditions are shown in *Figure 5.23*. The highest values of  $f^*$  were found for ribbed steel with Paralink 500s slightly higher than Paralink 300s. A decrease of  $f^*$  was found with increasing overburden pressure from all the three straps. The rate of decrease was large when  $\sigma_v$  was low, but the decrease became negligible when  $\sigma_v$  was higher than about 60 kN/m<sup>2</sup>, this point was analogous to that obtained with Wardley minestone.

*Figures 5.24 to 5.26* show the results of  $f^*$  versus  $\sigma_v$  at different densities from the three straps. It appears to be true for all the three straps that at low overburden pressure, a higher density caused a higher friction coefficient. However, contrary results could be found at higher  $\sigma_v$ , i.e. the higher density caused lower  $f^*$ . The reason for this will be discussed later in this chapter. Regardless of the density, a decrease in  $f^*$  was found to occur with an increase in overburden pressure, but this decrease appeared to be greater when the density was high. When  $\sigma_v$  was higher than 60 kN/m<sup>2</sup> the value of  $f^*$  tended towards a constant value.

### 5.3.3 Horden Red Shale

A series of tests was conducted on the three types of reinforcement with Horden red shale fill, at the density of 17.640 kN/m<sup>3</sup>, and a moisture content of 12.5% corresponding to the field conditions. A strap 1.5 metre long was tested at 20, 60 and 120 kN/m<sup>2</sup> overburden pressure using the displacement controlled pull-out box. The results obtained are presented and discussed in this section.

#### i) Force–Displacement Behaviour

Some load–displacement curves are illustrated in *Figures 5.27 to 5.30*. *Figure*

5.27 shows the curves obtained from the three different reinforcing straps at the same overburden pressure. A higher pull-out force was obtained with Paralink 500s than with Paralink 300s, both being less than the ribbed steel strap. These curves also showed that larger displacements were required to achieve the maximum forces in turn from the ribbed steel, Paralink 300s and Paralink 500s straps. A reduction in force after the peaks occurred in the case of the Paralink straps.

*Figures 5.28 to 5.30* show the curves at different overburden pressures for ribbed steel, Paralink 500s and Paralink 300s. For all the straps, it appears that a higher force was produced under higher overburden pressure, the difference was, however, not significant in the case of ribbed steel. Only a small reduction of pulling force after the peak was found for ribbed steel, whereas the reduction was more pronounced in the case of the Paralink straps. The influence of pull-out stiffness with overburden pressure was also indicated for the Paralink straps in *Figures 5.29 and 5.30*, and these are also presented in *Table 5.6*.

## ii) Maximum Pull-out Force and Friction Coefficient

All the results obtained with Horden red shale fill material and the three reinforcing straps are presented in *Table 5.3* and also shown in *Figures 5.31 to 5.34*.

As with the previous fill materials, *Figure 5.31* shows an increase in maximum pull-out force with increasing overburden pressure. At the lower  $\sigma_v$ , it is obvious that the ribbed steel strap produces the highest pull-out force, with Paralink 500s producing a higher pull-out force than Paralink 300s. However a higher force is obtained with Paralink 500s than ribbed steel strap at high overburden pressure (e.g.  $\sigma_v = 120 \text{ kN/m}^2$ ). The influence of density is shown in *Figure 5.32*, with higher density causing a higher pull-out force when the overburden pressure is low. At  $120 \text{ kN/m}^2$  of  $\sigma_v$  the opposite occurs. When observing the friction coefficient (*Figures 5.33 and 5.34*), a trend is clearly shown that increasing the overburden

pressure causes a decrease of  $f^*$ , the rate of the decrease being significant when  $\sigma_v$  was low, whereas above 60 kN/m<sup>2</sup>, the rate of the decrease reduced, and the values of  $f^*$  remained about constant. An increase of  $f^*$  was also observed with an increase in density, although at 120 kN/m<sup>2</sup> overburden pressure the influence became small.

#### 5.3.4 Loudon Hill Sand

A series of tests with Loudon Hill Sand was carried out using the displacement controlled pull-out box. The three types of reinforcing strap were tested under conditions of three overburden pressures (20, 60 and 120 kN/m<sup>2</sup>) and three different densities (17.085, 16.190 and 15.288 kN/m<sup>3</sup>) at a natural moisture content (7.1%). These densities and moisture content corresponded to these in the shear box tests. Several tests with different lengths of Paralink strap were also conducted.

##### i) Force–Displacement Behaviour

Some typical force–displacement curves are shown in *Figures 5.35 to 5.38*. Comparing the three different reinforcing straps tested under the same overburden pressure of 60 kN/m<sup>2</sup>, it can be seen that the highest force was obtained from Paralink 500s, with the ribbed steel strap superior to Paralink 300s (see *Figure 5.35*), a somewhat different result to those obtained from the other fills. Regardless of the strap type, a higher force was obtained by imposing higher overburden pressure. For the Paralink straps, there was a slight decrease of force after the maximum. Higher pull-out stiffness  $E_p$  was also observed with increasing overburden pressure (see *Table 5.6*).

## ii) Maximum Pull-out Force and Friction Coefficient

The results obtained from the pull-out tests with the sand are all presented in *Table 5.4* and *Figures 5.39* to *5.50*.

*Figures 5.39* to *5.42* show the results of maximum pull-out force versus overburden pressure. It was found that the Paralink 500s appeared to be superior to the other two reinforcing straps in terms of pull-out force when tested with the sand, and the ribbed steel strap was better than the Paralink 300s. The influence of density was also observed for the three straps, and it was noted that the higher the density, the higher the pull-out force even at an overburden pressure of  $120 \text{ kN/m}^2$ , a result which was different from that shown in the previous fill materials. At the loose state ( $\gamma_d = 15.288 \text{ kN/m}^3$ ), the line from the origin through the points was nearly straight (see *Figures 5.40*, *5.41* and *5.42*), giving a linear relationship for maximum pull-out force against overburden pressure, and implying an unchanged friction coefficient with increasing overburden pressure. This was also shown in *Figures 5.45* and *5.46* by the nearly horizontal lines of  $f^*$  versus  $\sigma_v$ .

*Figure 5.43* shows friction coefficient versus overburden pressure from the three different straps. These results were for a density of  $16.190 \text{ kN/m}^3$ , the same as in the field tests (Chapter 7). The results obtained with ribbed steel were higher than both Paralinks, with Paralink 500s being better than Paralink 300s. The friction coefficient was found to decrease with increasing overburden pressure, probably remaining constant after  $100 \text{ kN/m}^2$ . Comparing the results from different densities (see *Figures 5.44*, *5.45* and *5.46*), one can see that a higher density caused a higher value of  $f^*$ . This influence appeared to be greater when  $\sigma_v$  was low, whereas when  $\sigma_v$  increased the influence became less.

The force-displacement curves from various lengths of Paralink straps show a very interesting phenomenon (see *Figures 5.47* and *5.48*). In addition to an increase in pull-out force with increasing strap length, there is a clear indication that the same pattern of force-displacement curve is obtained from the different lengths of

straps. This shows that the force–displacement relationship was not affected by a change in strap length, i.e. the same displacement could be produced under the same force from different length of straps. When comparing the influences of both overburden pressure and strap length, the difference was quite obvious. Although increasing both could cause larger pull–out forces, the strap performance under the action was apparently different. As mentioned previously, a change of overburden pressure could cause a change in the force–displacement curve of a pull–out test, whereas altering the strap length did not change any of the pull–out behaviour. In order to explain this phenomenon the extensibility of the Paralink straps should be taken into consideration. This will be discussed in Chapter 6.

The influence of the length of the Paralink straps on the apparent friction coefficient can be seen in *Figures 5.49 and 5.50*. Higher values of  $f^*$  could be obtained from longer straps.

### 5.3.5 Methil PFA

The pull–out tests with Methil PFA fill material were tested at the condition corresponding to the field tests, i.e. a density of  $11.590 \text{ kN/m}^3$  at a moisture content of 27%. Three 1.5 metre long straps, ribbed steel, Paralink 300s and Paralink 500s were tested under overburden pressures of 20, 60 and  $120 \text{ kN/m}^2$ , using the displacement controlled pull–out box. The results obtained are presented in *Table 5.5 and Figures 5.51 to 5.56*.

#### i) Force–Displacement Behaviour

*Figure 5.51* shows the force–displacement curves from the three straps under an overburden pressure of  $60 \text{ kN/m}^2$ . This shows that Paralink 500s was superior to Paralink 300s, with both being better than ribbed steel strap in terms of force resistance. The ribbed steel strap behaved stiffer than the Paralink straps, with

Paralink 500s being stiffer than Paralink 300s.

*Figure 5.52, 5.53 and 5.54* show the force–displacement curves produced under different overburden pressures on the three straps. They show as expected that a higher pull–out force was obtained under higher overburden pressure. In the case of the ribbed steel strap, a nearly constant or slightly increasing force occurred after the ultimate point. For the Paralink straps a slightly decreasing force was found after the peak. The pull–out stiffness of Paralink straps was also found to increase with increasing overburden pressure (see *Table 5.6*).

#### ii) Maximum Pull–out Force and Friction Coefficient

*Figure 5.55* shows the results of maximum force versus overburden pressure. An increase in pull–out force was clearly shown with increasing overburden pressure. It shows clearly that Paralink 500s produced the highest force, with Paralink 300s producing higher values than the ribbed steel strap. In terms of friction coefficient, however, the ribbed steel appeared to be still superior to the Paralink straps, and Paralink 500s was better than Paralink 300s (see *Figure 5.56*). This is because the friction coefficient is independent of the surface area of a strap, therefore the effect due to the difference of the areas from each strap is eliminated in  $f^*$ . A decrease in the value of  $f^*$  was found with overburden pressure, however, after 60 kN/m<sup>2</sup> the decrease became very small.

#### 5.3.6 Comparison of the results from the Various Fill Materials

The pull–out test results obtained from the various materials are presented together for comparison. The results shown here were obtained at the condition which corresponded to that in the field tests. *Figures 5.57, 5.58 and 5.59* show some typical force–displacement curves when ribbed steel, Paralink 500s and Paralink

300s straps were tested with these fill materials.

The results of maximum pull-out force and friction coefficient versus overburden pressure are shown respectively in *Figures 5.60 to 5.65*. Comparing the efficiency of the fill materials, it is difficult to make a general conclusion of superiority, because the efficiency of the material seems to be different when different types of reinforcing elements are considered. *Table 5.7* shows the order of the fill materials according to their efficiency in bond resistance with the reinforcing straps. It can be found that the order of the Loudon Hill sand, PFA and Wardley minestone varies according to the type of reinforcements. Red shale was, however, superior to all the other materials, no matter which type of reinforcement was used, on the other hand Wearmouth minestone appeared the least efficient relative to the others.

## 5.4 DISCUSSION AND CONCLUSIONS

### 5.4.1 Discussion

The pull-out tests with the three reinforcing straps and five different fill materials have been described and the results obtained have been presented above.

Comparing the three types of reinforcement in terms of apparent friction coefficient, it is obvious that no matter which fill material is used the ribbed steel showed very high efficiency relative to the other two Paralink straps. This can be explained by the existence of the protruding ribs on which a passive resistance was imposed by the compacted fill during the pulling action. This passive resistance is more efficient than any frictional resistance occurring at the interface of the fill-reinforcement. If the protruding ribs are regarded as small walls, during pulling action the passive resistance will occur in the front of the ribs as shown in *Figure a*.

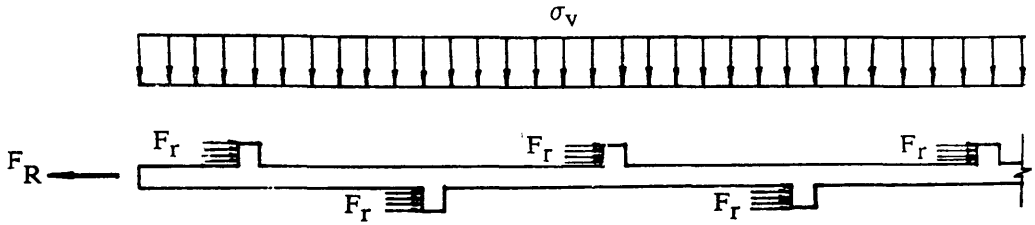


Figure a Analysis of Passive Resistance Caused by the Ribs  
in a Ribbed Steel Strap Pull-out Test

Based on the theory of passive pressure, the passive resistance produced by one protruding rib with unit strap width is expressed as (5.2)

$$F_r = \left( \frac{\gamma \cdot d^2}{2} + d \cdot \sigma_v \right) K_p \quad (5.2)$$

where  $F_r$  — is the passive resistance produced to one protruding rib  
with per unit strap width;

$d$  — the height of the rib;

$K_p$  — is the coefficient of passive pressure;

when the friction coefficient between the soil and the rib is zero then

$$K_p = \frac{1 + \sin\varphi}{1 - \sin\varphi} \quad (5.3)$$

However, when this friction coefficient between the soil and the rib is not zero, the value of  $K_p$  was found to be related to the internal friction angle of the

soil ( $\varphi$ ) and the friction angle between the soil and the resistant face ( $\delta$ ). Some values were given with  $\varphi$  and  $\delta$  by C.P.2 (1951) which are presented in Table 5.8.

Since the height of the ribs,  $d$ , is small (3 mm), the first term with  $d^2$  between the brackets in expression (5.2) can be eliminated. Therefore it becomes

$$F_R = d \cdot \sigma_v \cdot K_p \quad (5.4)$$

Taking the strap width (the length of rib) and the number of ribs into consideration, it can be deduced

$$F_R = d \cdot B \cdot N_r \cdot \sigma_v \cdot K_p \quad (5.5)$$

where  $B$  — the width of the strap;

$N_r$  — the number of ribs;

$F_R$  — the total passive resistance produced  
by the ribs of a strap.

Based on expression (5.5) and taking the strap used in the present work, which was 1.5m long by 0.04m wide with rib's height of 0.003m and the number of ribs  $N_r = 36$ . In the case of Loudon Hill sand,  $\varphi = 37.6^\circ$ , and  $\delta$  is assumed to be  $20^\circ$  then  $K_p$  was found to be about 7.6.

When  $\sigma_v = 20 \text{ kN/m}^2$ , the passive resistance is calculated to be  $F_R = 0.66 \text{ kN}$ , compared with  $T_{\max} = 4.34 \text{ kN}$ , and when  $\sigma_v = 120 \text{ kN}$ , the passive resistance  $F_R = 3.94 \text{ kN}$  compared with  $T_{\max} = 14.48 \text{ kN}$ . It is obvious that the passive resistance from the ribs contributes to the pull-out force. However, comparing the results from ribbed and smooth steel straps by Schlosser (*Figure 2.18*), it is noted that at low overburden pressure, the influence of the ribs is specially larger than at high overburden pressure, which can not be explained only by the passive resistance theory. To explain this the factor of dilatancy and arching effect should also be considered. Schlosser's results imply that the protruding ribs

can cause more dilatancy which leads to a higher normal stress. The factor of dilatancy and arching effect will be discussed in more detail in chapter 6.

The value of  $f^*$  obtained from ribbed steel could be 3 to 5 times higher than from the Paralink straps. Comparing the two Paralink straps, in addition to the difference in stiffness, one could feel from the different nature of the surfaces, that the Paralink 500s strap was rougher than Paralink 300s. The rougher surface should produce higher frictional resistance with fill materials. Higher values of  $f^*$  were obtained from Paralink 500s than Paralink 300s, no matter which fill material was used. However, the difference of  $f^*$  from the two straps was not as great as between them and the ribbed steel.

The results obtained from the tests under different overburden pressures show a decrease of friction coefficient with  $\sigma_v$ . This conclusion is consistent with some previous researchers, such as Schlosser and Elias (1978). As suggested by McKittrick (1978) and Gilloux et al (1979), in a pull-out test, dilatancy occurs in a comparatively small zone in the immediate vicinity of the reinforcing strap. Arching occurs across the strip by which the ambient backfill suppresses the volumetric expansion normally associated with dilatancy. This suppressed dilatancy results in a locally enhanced vertical stress which gives rise to an increased pull-out resistance and hence an enhanced apparent friction coefficient. When the overburden pressure is low, the enhanced vertical stress is relatively high compared with the pressure, and therefore plays an important part, making  $f^*$  quite high. When the overburden pressure is high, this enhanced vertical stress by dilatancy will be relatively small compared with the pressure, hence its influence becomes modest, consequently  $f^*$  becomes smaller.

In addition to the dilatancy influence, the author believes there is also another factor which enhances the vertical stress. When the fill is compacted, some stress will be locked in the fill, especially if the fill possesses cohesive behaviour. This locked-in-stress can also impose on the strap an enhanced normal stress in a pull-out test.

In order to prove this, a pull-out test was done with no overburden pressure being applied by the air pressure. The pressure imposed on the strap was only the weight of the small height of fill material above, which was 120 mm thick, and the  $\sigma_v$  was about 2.4 kN/m<sup>2</sup>. The test was conducted with the load controlled box, and a 1.5 m long Paralink 300s strap and Wardley minestone with a density of 17.847 kN/m<sup>3</sup> and moisture content of 9.7% were used. A maximum pull-out force was found to be 1.481 kN, and a considerably high value of friction coefficient,  $f^* = 2.420$ , was obtained, which was about 4 times the value obtained at 20 kN/m<sup>2</sup> of  $\sigma_v$  or 13 times the value at 120 kN/m<sup>2</sup> of  $\sigma_v$ . The pull-out resistance produced could not be attributed to the fill weight alone ( $\gamma H = 2.4$  kN/m<sup>2</sup>). It is obvious that in addition to this, an extra normal stress was actually exerted on the strap which was caused by the dilatancy and the locked-in stress.

This point can also be proved from the results at different densities. At higher density the rate of decrease of  $f^*$  with  $\sigma_v$  is large, and at low density the rate of decrease becomes small. This is because in a high density test the enhanced stress by dilatancy and locked-in-stress is high.

However, the decrease of  $f^*$  with increase in overburden pressure does not continue indefinitely and it was found that in the present work after about 60 to 100 kN/m<sup>2</sup> of  $\sigma_v$  the  $f^*$  remained reasonably constant.

Investigating the influence of density on the apparent friction coefficient, a higher  $f^*$  is obtained with higher density. this result being observed from all the reinforcing straps and fill materials. For ribbed steel the influence of density appears to be quite significant. It was, however, observed that this influence was also related to the overburden pressure, in that when  $\sigma_v$  is low the influence of density is high, whereas with increasing  $\sigma_v$ , the effect of density becomes less. For Paralink straps, the values of  $f^*$  were very close at 100 kN/m<sup>2</sup> overburden pressure. In the case of Wearmouth minestone, when  $\sigma_v$  is over 60 kN/m<sup>2</sup>,  $f^*$  does not increase with density. Even some higher values of  $f^*$  can be produced at lower density when overburden pressure is high. However, in the case of ribbed steel strap and Loudon

Hill sand the influence of density can exist up to a high overburden pressure.

The reasons for the influence of density can probably be explained as follows:

(1) After compaction a dense state is established, a stress is locked in the fill material, and this locked-in-stress and the dilatancy effect in the dense state act as an enhanced normal stress during pull-out testing. The denser the fill material is compacted, the higher the enhanced normal stress can be achieved, in turn high pull-out resistance can be produced, therefore higher apparent friction coefficient can be obtained. When the overburden pressure applied is low, as discussed previously, the enhanced normal stress is relatively high compared to the pressure, thus the effect of this stress appears significant. But with increasing  $\sigma_v$ , the enhanced stress is relatively less compared to the pressure, therefore the influence of this stress becomes less, or in other words the influence of the density becomes modest.

(2) The loose density state can only be kept under a low overburden pressure, since when the pressure is high, it compresses the fill material to a denser state which is probably close to a compacted higher density. Consequently the influence caused by the difference of prepared density became eliminable.

(3) Since minestone is susceptible to breakdown when compacted (Taylor 1978 and Rainbow 1983), during vibrating compaction the sharp angles of the stones might be broken, causing a reduction in friction. Hence higher values of  $f^*$  may be obtained in lower density when the overburden pressure is high.

The influence of overburden pressure on pull-out stiffness was also found for the Paralink straps with all the fill materials. This result was quite analogous to the conclusion made by some of the previous researchers, such as Siel (1987), who found that an increase in confining pressure can increase the secant modulus of geotextile. *Figures 5.66 and 5.67* show the results of  $E_p$  versus overburden pressure tested from the two Paralink straps with all the fill materials. A linear relationship

of  $E_p$  with  $\sigma_v$  was discovered, but this relationship varies with different fill materials.

Only a few tests with various lengths of Paralink straps were conducted with Loudon Hill sand. The results obtained show the same trend as reported by some previous researchers (Bacot and Iltis 1978). The value of  $f^*$  is found to increase with the length of reinforcement when galvanized steel strip was tested with sand. This was attributed to the influence of the undulation of the reinforcement. In the present case, with Paralink straps, because they are flexible in bending, there must, in preparation of a test, be some undulation; resulting in a higher pulling resistance. The longer the strap is, the more it is prone to undulation in preparation, thus higher results are produced.

So far two testing methods, direct shear box and pull-out box tests have been used to investigate the bond resistance of the fill and reinforcement materials. Comparing the results from the two different tests it was found that when Paralink reinforcing straps were used, these results appeared to contradict the findings of previous investigators working, with steel straps. The results with Wardley minestone were taken as an example, the friction coefficients have been put in terms of  $\mu$  for the shear box tests and  $f^*$  for the pull-out box tests and shown in *Figures 5.68 and 5.69*. It can be seen from this figure that the  $f^*$  values for the Paralink straps are lower than the  $\mu$  values (except at very low  $\sigma_v$ ). This is in direct contradiction to the generally accepted behaviour of metallic straps, on which pull-out box tests produce higher friction coefficient than direct shear box tests. This was also indicated with the ribbed strap test results in the present work. Therefore this behaviour is believed to be related to the extensibility of the reinforcements. Further investigation into this behaviour is intended, some special tests are designed and more discussions will be made in Chapter 6.

#### 5.4.2 CONCLUSIONS

The following conclusions can be drawn from the pull-out test results:

(1) Comparing the three types of reinforcing straps, regardless of the fill material, the ribbed steel strap always gives the highest apparent friction coefficient, with Paralink 500s being superior to Paralink 300s.

(2) Comparing the five different fill materials, Horden red shale is the most efficient material in producing high frictional resistance, whereas Wearmouth minestone is the least efficient one. The efficiency of the other three materials, i.e. Wardley minestone, Loudon Hill sand and Methil PFA, varies with different reinforcing elements.

(3) No matter which reinforcements and fill materials are used, the apparent friction coefficient decreases with increasing overburden pressure. This decrease is, however, modest when the overburden pressure is high. After 60 to 100 kN/m<sup>2</sup> of  $\sigma_v$ , the values of  $f^*$  become about constant.

(4) No matter which reinforcement is used, when tested with Wardley minestone, Wearmouth minestone and Loudon Hill sand, the apparent friction coefficient increases with the density of the fill materials. For ribbed steel strap, the influence of density is more significant. The same conclusion can also be drawn when using Paralink 300s with Horden red shale. The influence of density is, however, related to the overburden pressure. When  $\sigma_v$  is low this influence is considerable, otherwise when  $\sigma_v$  is high this influence can be very small.

(5) When using the Paralink straps with Loudon Hill sand, the length of the strap can influence the value of apparent friction coefficient. A higher value of  $f^*$  is

obtained from longer straps. Increasing the length of the straps does not influence the pattern of the force–displacement curve in pull–out tests.

(6) The pull–out stiffness with Paralink straps is influenced by the overburden pressure, and  $E_p$  increases with increasing  $\sigma_v$ . The relationship between  $E_p$  and  $\sigma_v$  is linear. But pull–out stiffness is independent of strap length.

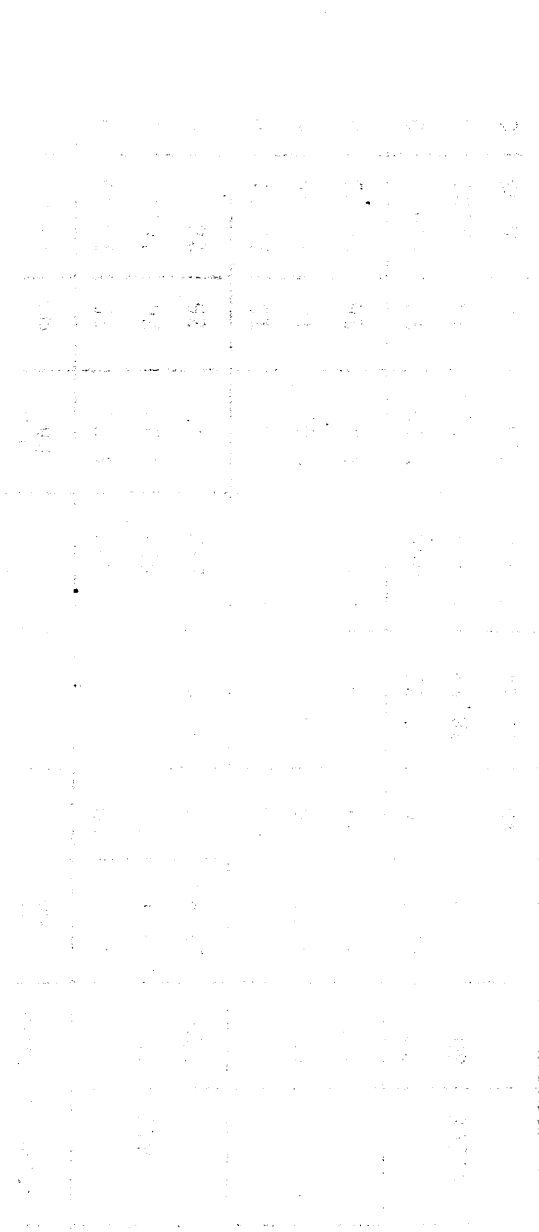


Table 5.1

## RESULTS FROM PULL-OUT BOX TESTS

Wardley Minestone

m/c %	$\gamma$ kN/m <sup>3</sup>	$\sigma_v$ kN/m <sup>2</sup>	Ribbed Steel				Paralink 500s				Paralink 300s			
			T <sub>max</sub> kN	D mm	$\tau$ kN/m <sup>2</sup>	f* kN/m <sup>2</sup>	T <sub>max</sub> kN	D mm	$\tau$ kN/m <sup>2</sup>	f* kN/m <sup>2</sup>	T <sub>max</sub> kN	D mm	$\tau$ kN/m <sup>2</sup>	f* kN/m <sup>2</sup>
9.7	17.847	20	8.87	40	73.95	3.698	3.71	15	13.45	0.672	3.25	32	12.73	0.637
		60	11.19	52	93.25	1.555	5.23	24	18.95	0.316	3.96	31	15.50	0.259
		120	11.98	62	99.83	0.832	7.77	26	28.15	0.235	5.62	40	22.06	0.184
	16.579	20	5.71	41	47.59	2.380	3.23	13	11.71	0.585	2.91	21	11.43	0.572
		60	6.69	36	55.77	0.929	4.02	14	14.56	0.243	3.68	28	14.44	0.241
		120	7.63	49	63.62	0.530	8.49	26	30.75	0.256	6.51	46	25.54	0.213
15.206	20	2.56	20	21.32	1.066	1.79	12	6.45	0.322	1.51	23	5.01	0.295	
	60	3.42	31	28.53	0.475	3.32	16	12.03	0.201	3.00	30	11.74	0.196	
	120	7.48	46	62.34	0.520	7.33	28	26.56	0.221	5.88	27	23.08	0.192	

Table 5.2

## RESULTS FROM PULL-OUT BOX TESTS

Wearmouth Minestone

m/c %	$\gamma$ kN/m <sup>3</sup>	$\sigma_v$ kN/m <sup>2</sup>	Ribbed Steel				Paralink 500s				Paralink 300s			
			T <sub>max</sub> kN	D mm	$\tau$ kN/m <sup>2</sup>	f* kN	T <sub>max</sub> kN	D mm	$\tau$ kN/m <sup>2</sup>	f* kN	T <sub>max</sub> kN	D mm	$\tau$ kN/m <sup>2</sup>	f* kN
5.7	17.658	20	4.50	52	37.50	1.869	2.42	16	9.17	0.459	2.13	41	8.35	0.418
		60	4.80	81	39.96	0.668	4.03	26	15.27	0.254	3.58	26	13.81	0.230
		120	7.23	98	60.25	0.502	8.31	52	31.49	0.262	6.07	35	23.79	0.198
5.7	16.380	20	2.85	22	23.72	1.186	1.90	8	6.99	0.361	1.96	17	7.69	0.385
		60	5.29	38	44.07	0.735	4.17	13	15.79	0.263	4.06	24	15.94	0.266
		120	8.13	35	67.79	0.565	8.85	26	33.51	0.280	8.67	47	34.01	0.283
5.7	15.000	20	2.13	21	17.71	0.885	1.88	8	7.10	0.356	1.50	14	5.88	0.294
		60	4.62	36	38.46	0.641	4.92	16	18.65	0.311	4.10	23	16.09	0.268
		120	8.08	56	67.31	0.561	10.11	31	38.29	0.319	11.44	45	33.63	0.280

RESULTS FROM PULL-OUT BOX TESTS

Horden Red Shale

Table 5.3

m/c %	$\gamma$ kN/m <sup>3</sup>	$\sigma_v$ kN/m <sup>2</sup>	Ribbed Steel				Paralink 500s				Paralink 300s			
			T <sub>max</sub> kN	D mm	$\tau$ kN/m <sup>2</sup>	f* kN/m <sup>2</sup>	T <sub>max</sub> kN	D mm	$\tau$ kN/m <sup>2</sup>	f* kN/m <sup>2</sup>	T <sub>max</sub> kN	D mm	$\tau$ kN/m <sup>2</sup>	f* kN/m <sup>2</sup>
12.5	17.640	20	11.65	34	97.08	4.854	7.88	28	29.85	1.492	5.50	36	21.57	1.078
		60	12.39	47	103.25	1.721	9.92	27	37.59	0.626	6.06	46	23.77	0.396
		120	13.88	50	115.67	0.964	15.77	52	59.74	0.498	8.83	52	34.63	0.289
12.5	17.317	20	—	—	—	—	—	—	—	—	3.44	22	13.50	0.675
		60	—	—	—	—	—	—	—	—	5.17	24	20.29	0.338
		120	—	—	—	—	—	—	—	—	7.46	34	29.26	0.244
12.5	16.180	20	—	—	—	—	—	—	—	—	3.19	15	12.52	0.626
		60	—	—	—	—	—	—	—	—	4.54	23	17.80	0.297
		120	—	—	—	—	—	—	—	—	8.33	41	32.65	0.271

Table 5.4

## RESULTS FROM PULL-OUT BOX TESTS

Loudon Hill Sand

m/c %	$\gamma$ kN/m <sup>3</sup>	$\sigma_v$ kN/m <sup>2</sup>	Ribbed Steel				Paralink 500s				Paralink 300s			
			T <sub>max</sub> kN	D mm	$\tau$ kN/m <sup>2</sup>	f* kN/m <sup>2</sup>	T <sub>max</sub> kN	D mm	$\tau$ kN/m <sup>2</sup>	f* kN/m <sup>2</sup>	T <sub>max</sub> kN	D mm	$\tau$ kN/m <sup>2</sup>	f* kN/m <sup>2</sup>
7.1	17.085	20	7.44	13	62.00	3.100	6.64	24	25.15	1.258	4.70	31	18.43	0.931
		60	16.05	31	133.75	2.229	12.11	44	45.87	0.765	7.68	44	30.10	0.502
		120	24.74	23	206.11	1.718	16.77	73	63.50	0.529	11.37	42	44.59	0.372
	16.190	20	4.34	11	36.17	1.808	6.15	21	23.30	1.165	3.24	14	12.48	0.624
		60	7.22	39	60.13	1.003	10.02	30	38.64	0.644	5.35	28	20.71	0.345
		120	14.48	36	120.67	1.006	13.14	46	49.77	0.415	9.61	51	37.18	0.310
15.288	20	2.15	34	17.93	0.897	1.85	6	6.99	0.350	1.75	18	6.85	0.343	
	60	3.46	31	28.85	0.481	5.33	11	20.18	0.336	4.79	25	18.78	0.313	
	120	7.38	25	61.50	0.513	11.09	18	42.72	0.356	9.32	42	36.56	0.305	

Table 5.5

## RESULTS FROM PULL-OUT BOX TESTS

Methil PFA

m/c %	$\gamma$ kN/m <sup>3</sup>	$\sigma_v$ kN/m <sup>2</sup>	Ribbed Steel				Paralink 500s				Paralink 300s			
			T <sub>max</sub> kN	D mm	$\tau$ kN/m <sup>2</sup>	f* kN/m <sup>2</sup>	T <sub>max</sub> kN	D mm	$\tau$ kN/m <sup>2</sup>	f* kN/m <sup>2</sup>	T <sub>max</sub> kN	D mm	$\tau$ kN/m <sup>2</sup>	f* kN/m <sup>2</sup>
27	11.590	20	2.70	21	22.49	1.125	4.85	20	18.37	0.919	3.70	22	14.51	0.725
		60	4.80	23	39.98	0.666	7.55	27	28.60	0.477	5.40	26	21.18	0.353
		120	8.06	15	67.20	0.560	13.75	64	52.08	0.434	10.70	69	41.96	0.350

Table 5.6

## PULL-OUT STIFFNESS OF PARALINK STRAPS

 $E_p$  (kN/mm) Calculated at 10mm Displacement

Type of Fills	Paralink 300s			Paralink 500s		
	$\sigma_v$ (kN/m <sup>2</sup> )			$\sigma_v$ (kN/m <sup>2</sup> )		
	20	60	120	20	60	120
Wardley Minestone	159	212	242	273	318	379
Wearmouth Minestone	106	197	261	167	242	333
Horden Red Shale	238	324	389	378	476	584
Loudon Hill Sand	174	244	296	374	609	713
Methil PFA	148	235	383	235	313	504

Table 5.7

## ORDER OF THE FILL MATERIAL

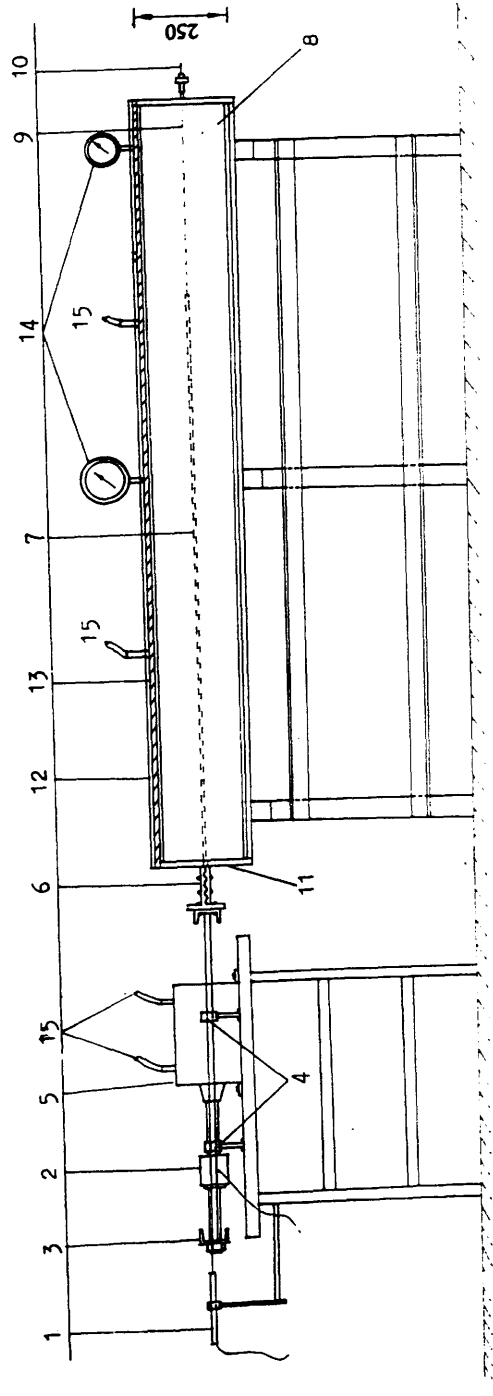
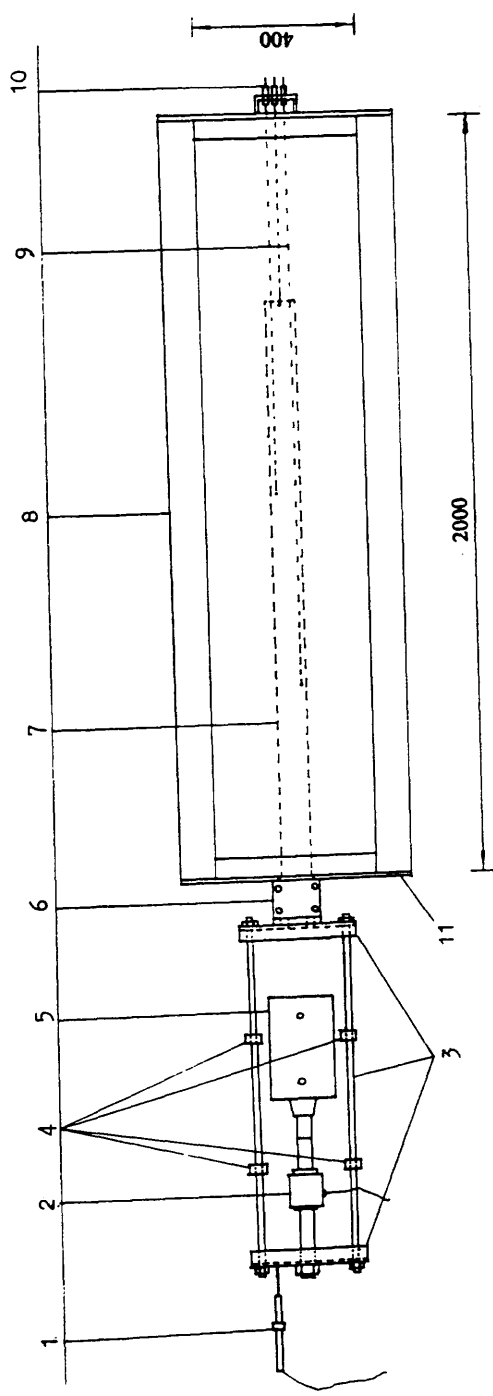
According to the Frictional Efficiency

type of straps	1	2	3	4	5
Ribbed Steel	Horden Red Shale	Wardley Minestone	Loudon Hill Sand	Methil PFA	Wearmouth Minestone
Paralink 500s	Horden Red Shale	Loudon Hill Sand	Methil PFA	Wardley Minestone	Wearmouth Minestone
Paralink 300s	Horden Red Shale	Methil PFA	Loudon Hill Sand	Wardley Minestone	Wearmouth Minestone

Table 5.8

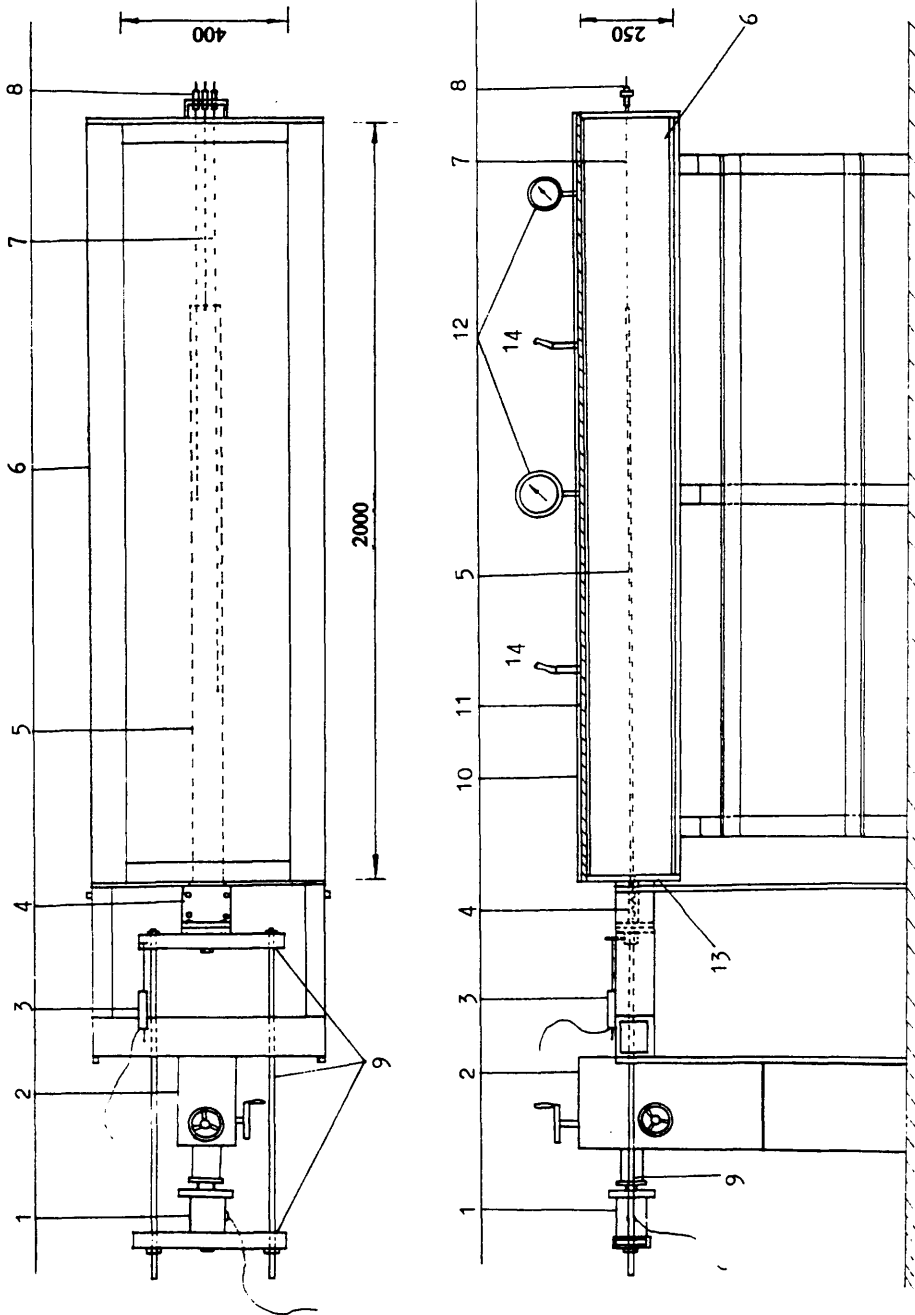
VALUES OF  $K_p$  GIVEN BY C.P.2 (1951)

Values of $\delta$	Values of $\varphi$			
	25	30	35	40
	Values of $K_p$			
0	2.5	3.0	3.7	4.6
10	3.1	4.0	4.8	6.5
20	3.7	4.9	6.0	8.8
30	—	5.8	7.3	11.4



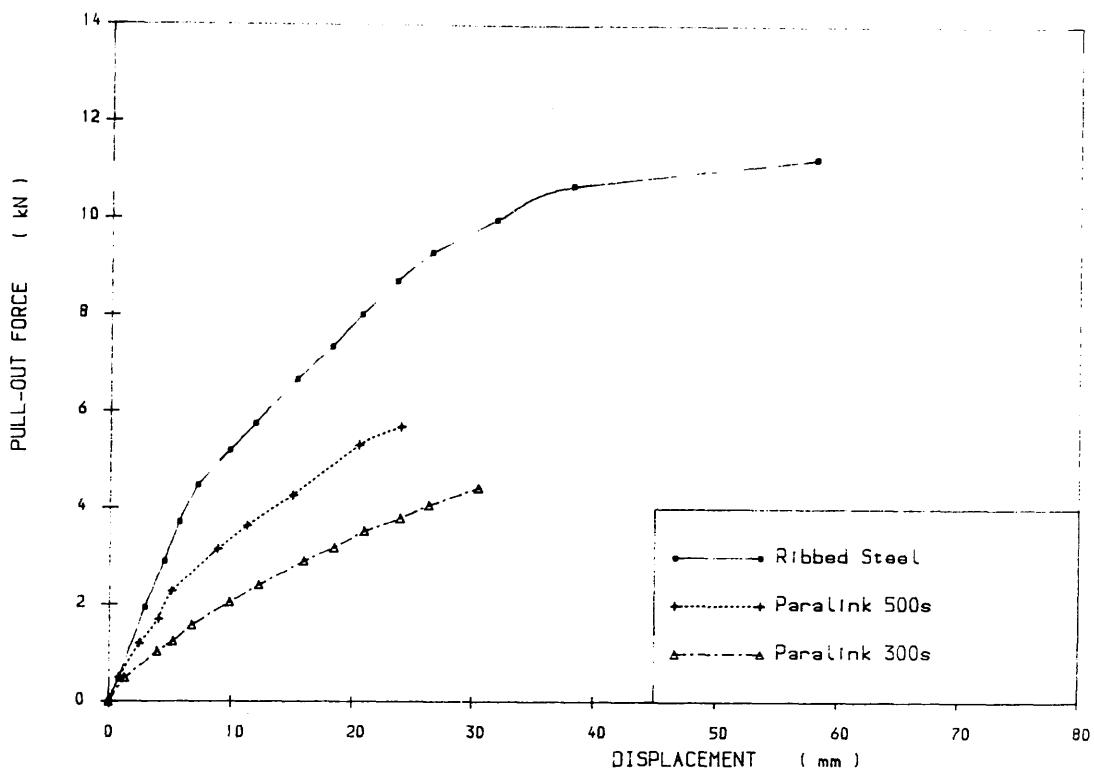
1. displacement transducer,
2. load cell,
3. yoke,
4. yoke bearings,
5. compressor air cylinder,
6. clamp,
7. reinforcing strap,
8. pull-out box,
9. wires from strap touch to displacement transducers,
10. displacement transducers,
11. facing plate,
12. cover plate,
13. rubber mamberane,
14. pressure gauges,
15. air inlets.

Figure 5.1 LOAD-CONTROLLED PULL-OUT BOX



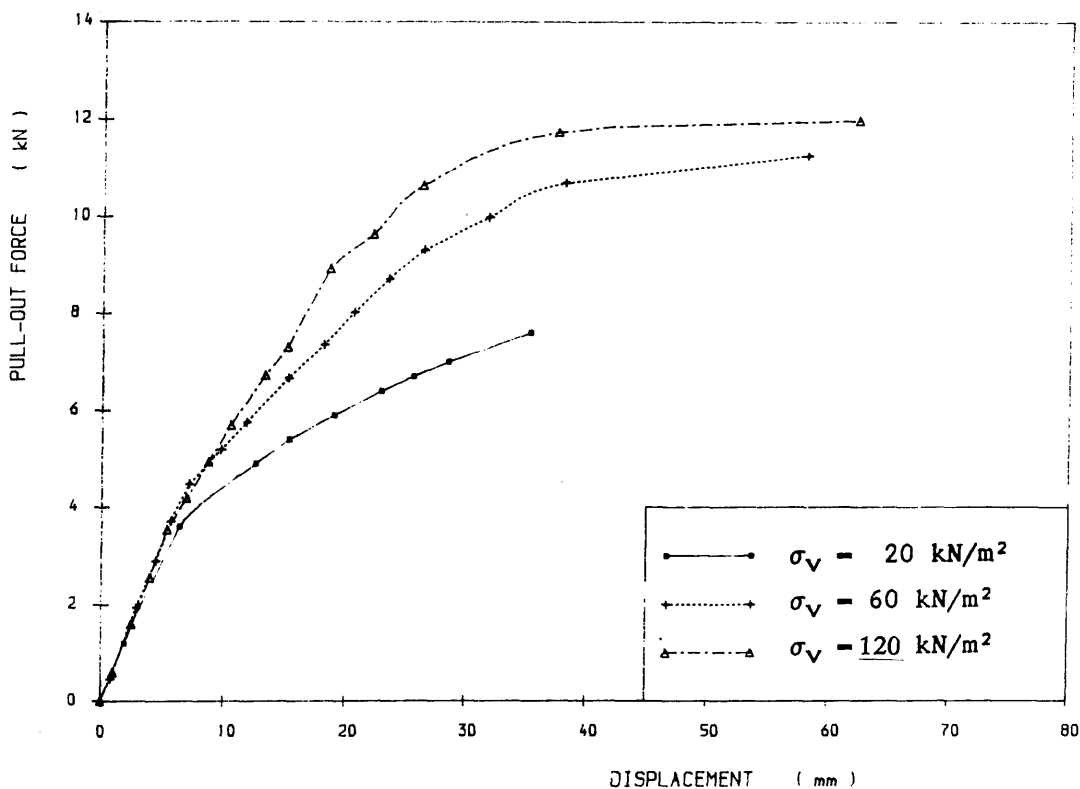
1. load cell,
2. loading machine,
3. displacement transducer,
4. clamp,
5. reinforcing strap,
6. pull-out box,
7. wires from strap touch to displacement transducers,
8. displacement transducers,
9. yoke,
10. coverplate,
11. rubber membrane,
12. pressure gauges,
13. facing plate,
14. air inlets

Figure 5.2 DISPLACEMENT-CONTROLLED PULL-OUT BOX



**Figure 5.3 PULL-OUT FORCE VS. STRAP DISPLACEMENT**

Laboratory Test, Wardley Minestone,  $L=1.5m$ ,  $\gamma_d=17.847kN/m^3$ ,  $\sigma_v=60kN/m^2$



**Figure 5.4 PULL-OUT FORCE VS. STRAP DISPLACEMENT**

Laboratory Test, Wardley Minestone,  $L=1.5m$ ,  $\gamma_d=17.847kN/m^3$ , Ribbed Steel

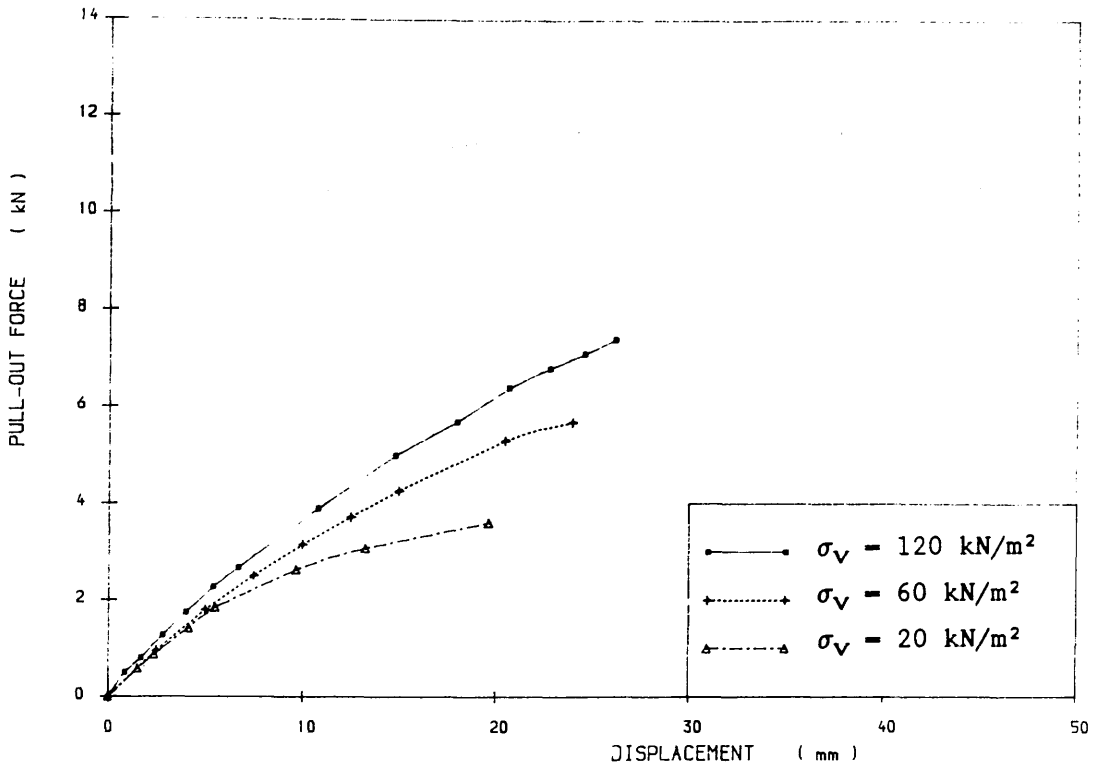


**Figure 5.5 PULL-OUT FORCE VS. STRAP DISPLACEMENT**

Laboratory Test, Wardley Minestone,  $L=1.5\text{m}$ ,  $\gamma_d=17.847\text{kN/m}^3$ , Paralink500s

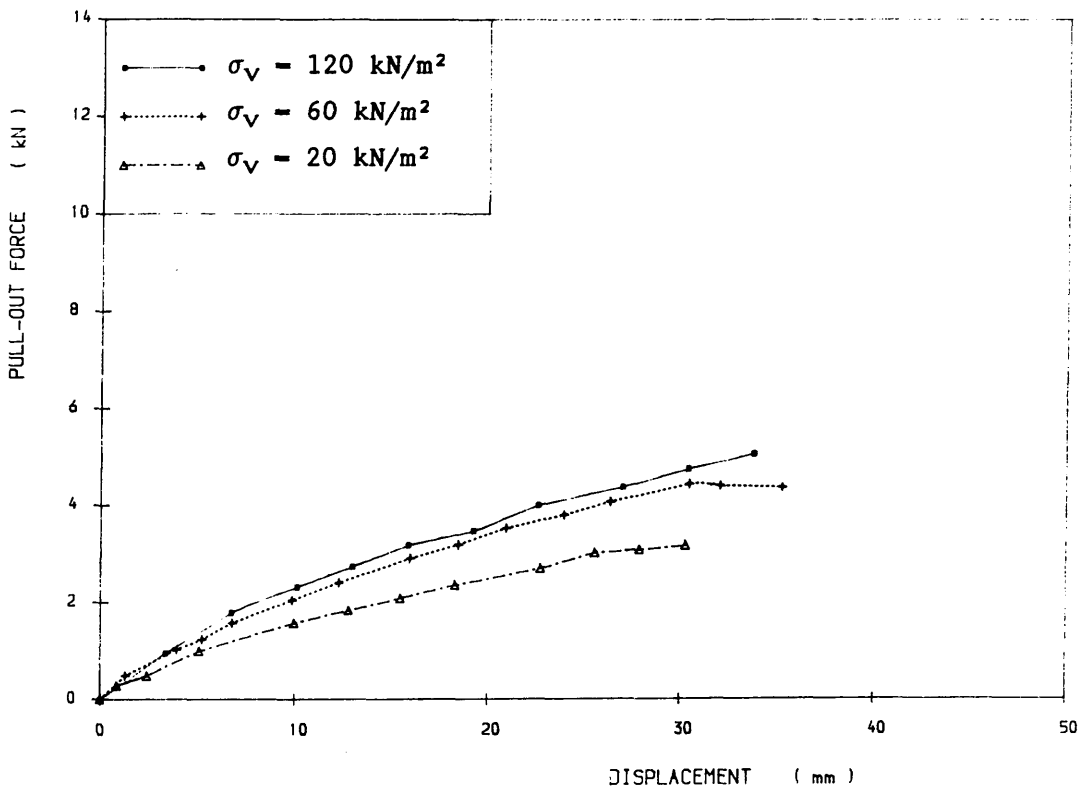


**Figure 5.6 PULL-OUT FORCE VS. STRAP DISPLACEMENT**

Laboratory Test, Wardley Minestone,  $L=1.5\text{m}$ ,  $\gamma_d=17.847\text{kN/m}^3$ , Paralink300s

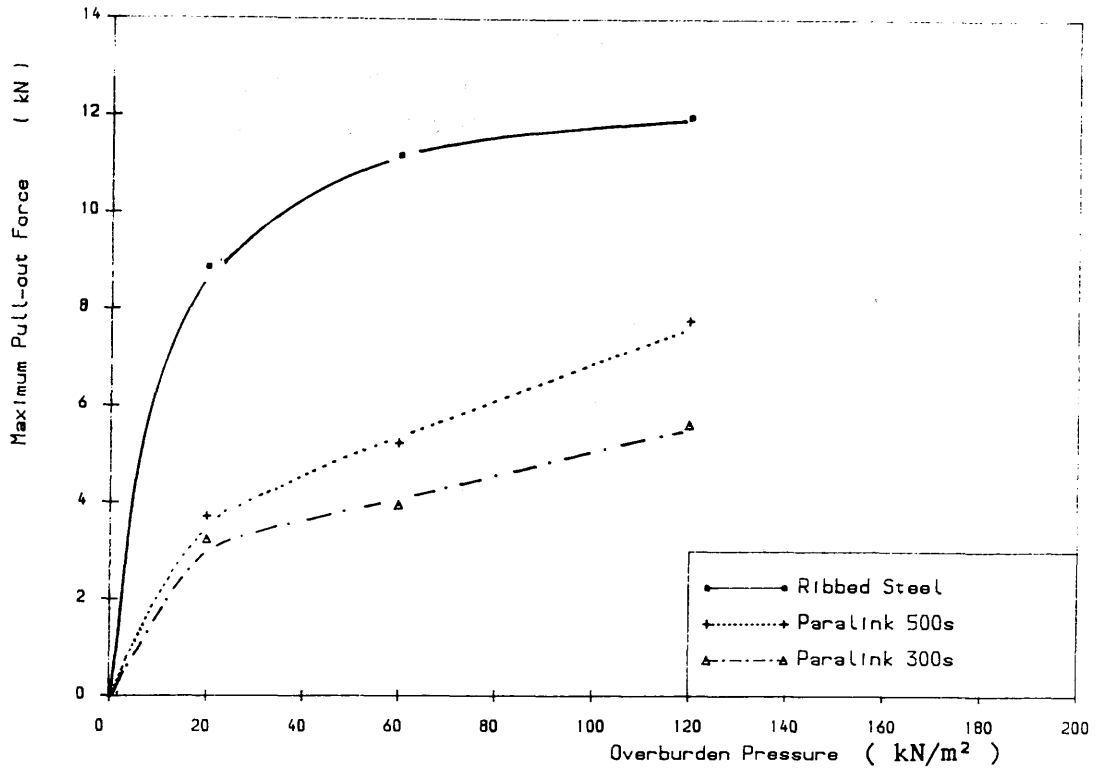


**Figure 5.7 MAXIMUM PULL-OUT FORCE VS. OVERBURDEN PRESSURE**

Laboratory Pull-out Test, Wardley Minestone,  $\gamma_d=17.847\text{kN/m}^3$ ,  $L=1.5\text{m}$

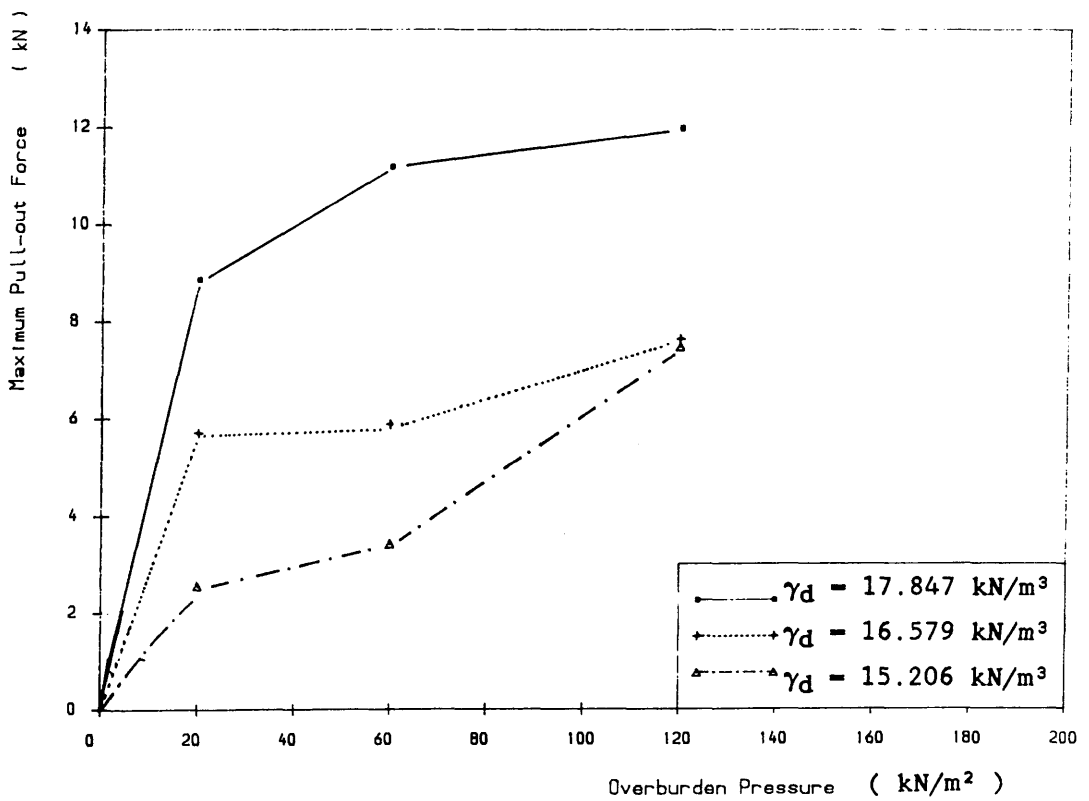


**Figure 5.8 MAXIMUM PULL-OUT FORCE VS. OVERBURDEN PRESSURE**

Laboratory Pull-out Test, Wardley Minestone, Ribbed Steel,  $L=1.5\text{m}$

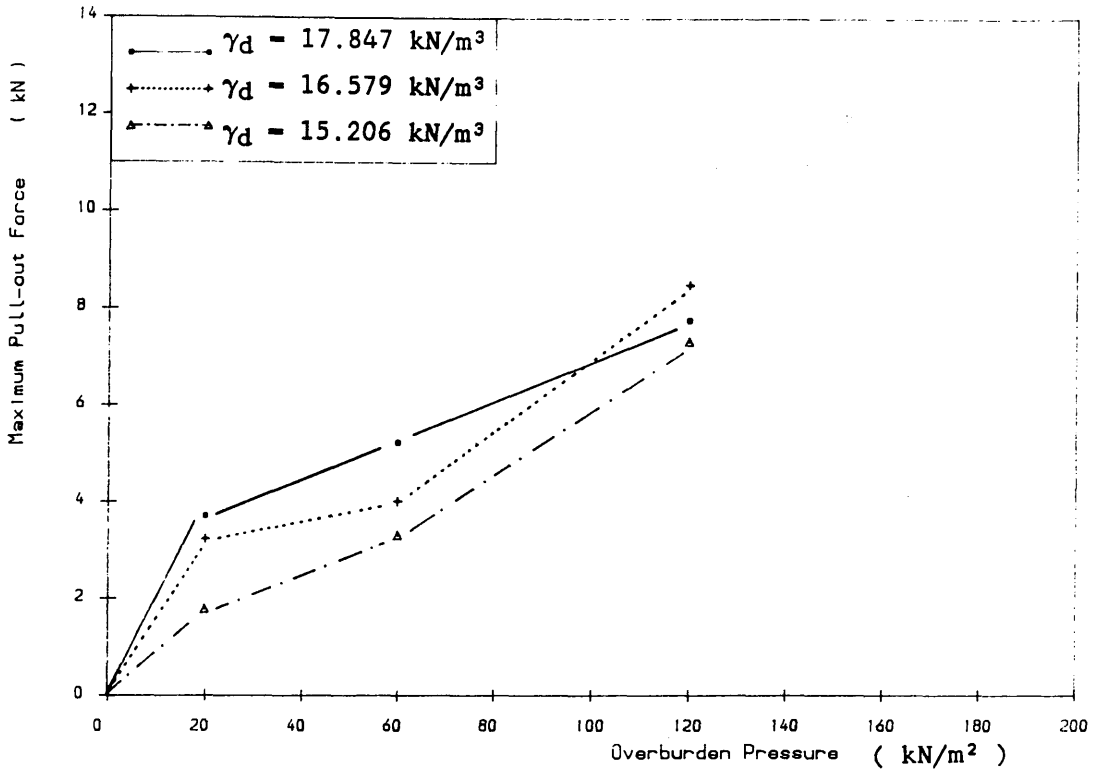


Figure 5.9 MAXIMUM PULL-OUT FORCE VS. OVERBURDEN PRESSURE  
 Laboratory Pull-out Test, Wardley Minestone, Paralink 500s, L=1.5m

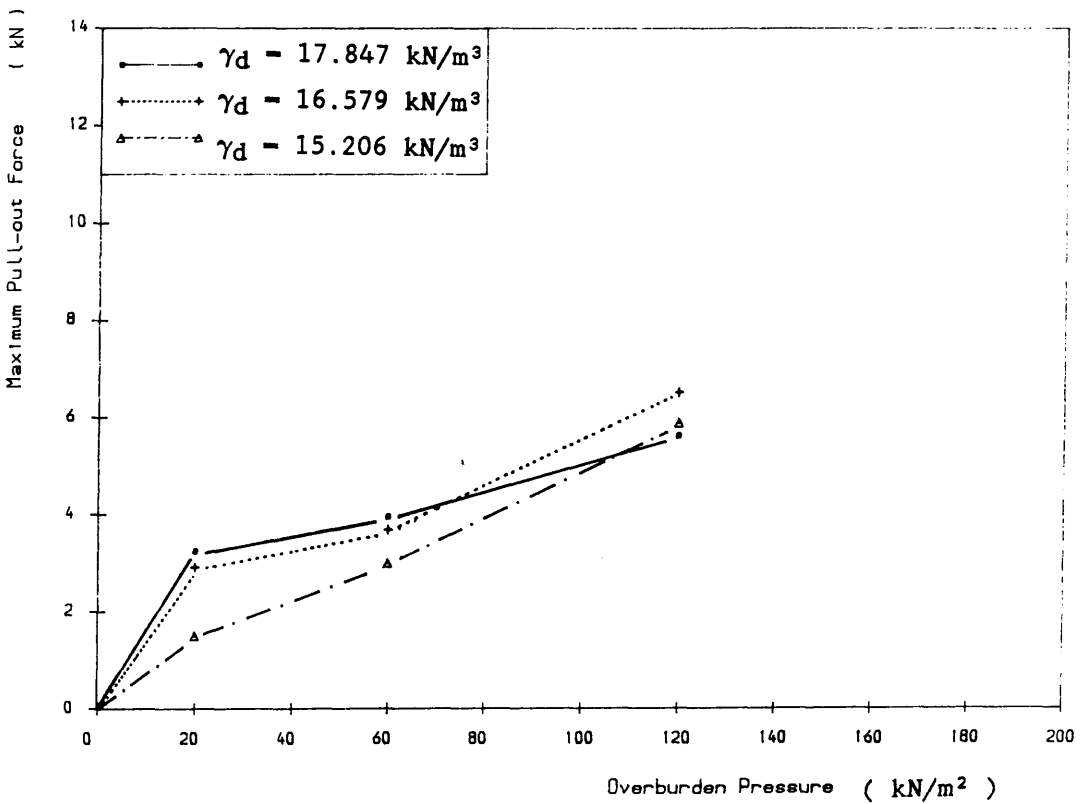


Figure 5.10 MAXIMUM PULL-OUT FORCE VS. OVERBURDEN PRESSURE  
 Laboratory Pull-out Test, Wardley Minestone, Paralink 300s, L=1.5m

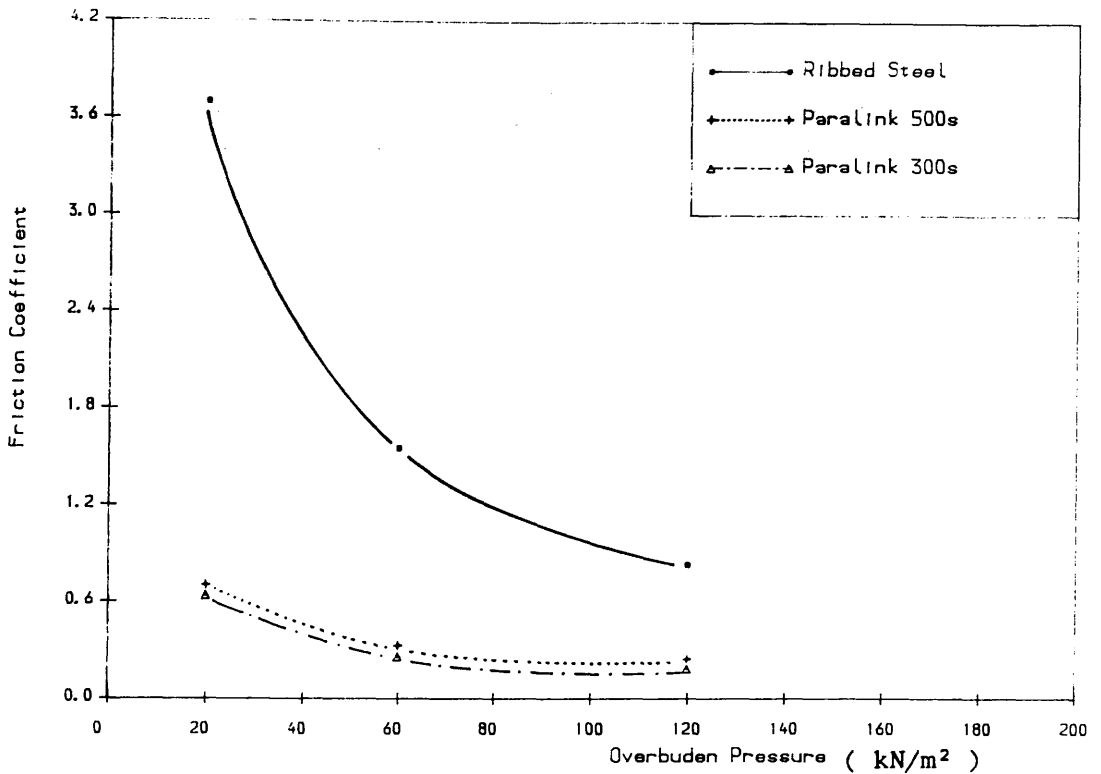


Figure 5.11 FRICTION COEFFICIENT VS. OVERBURDEN PRESSURE

Laboratory Pull-out Test, Wardley Minestone,  $\gamma_d=17.847/m^3$ ,  $L=1.5m$

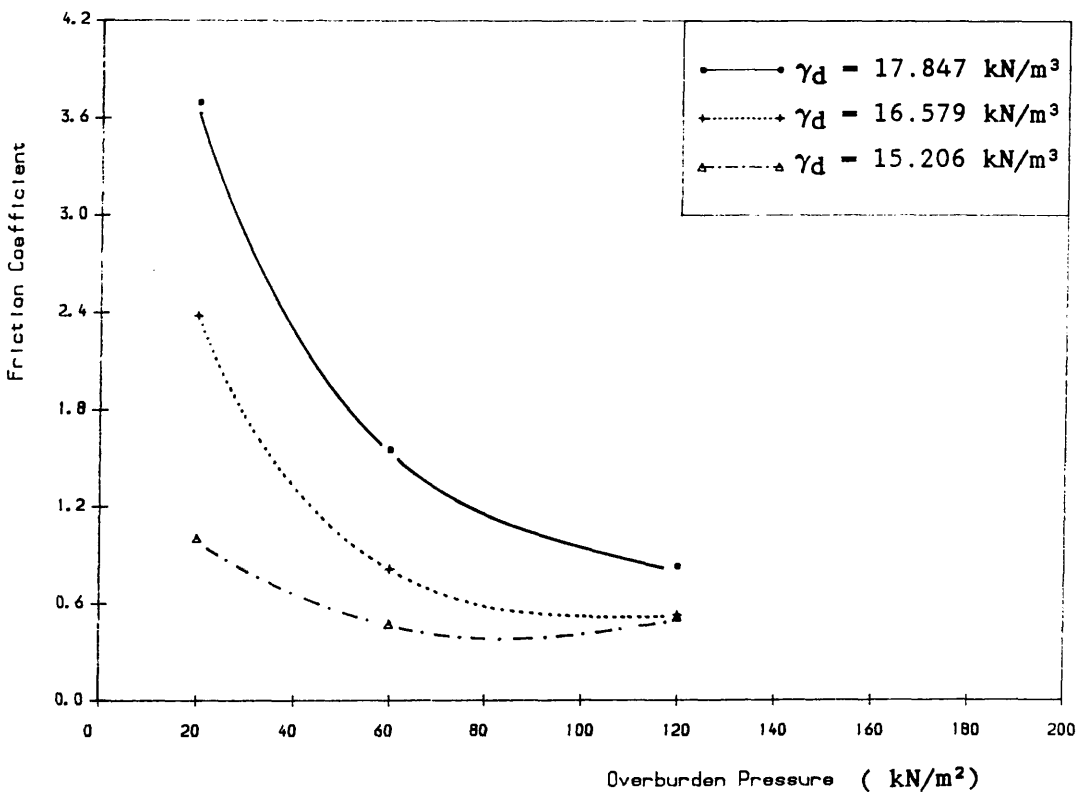


Figure 5.12 FRICTION COEFFICIENT VS. OVERBURDEN PRESSURE

Laboratory Pull-out Test, Wardley Minestone, Ribbed Steel,  $L=1.5m$

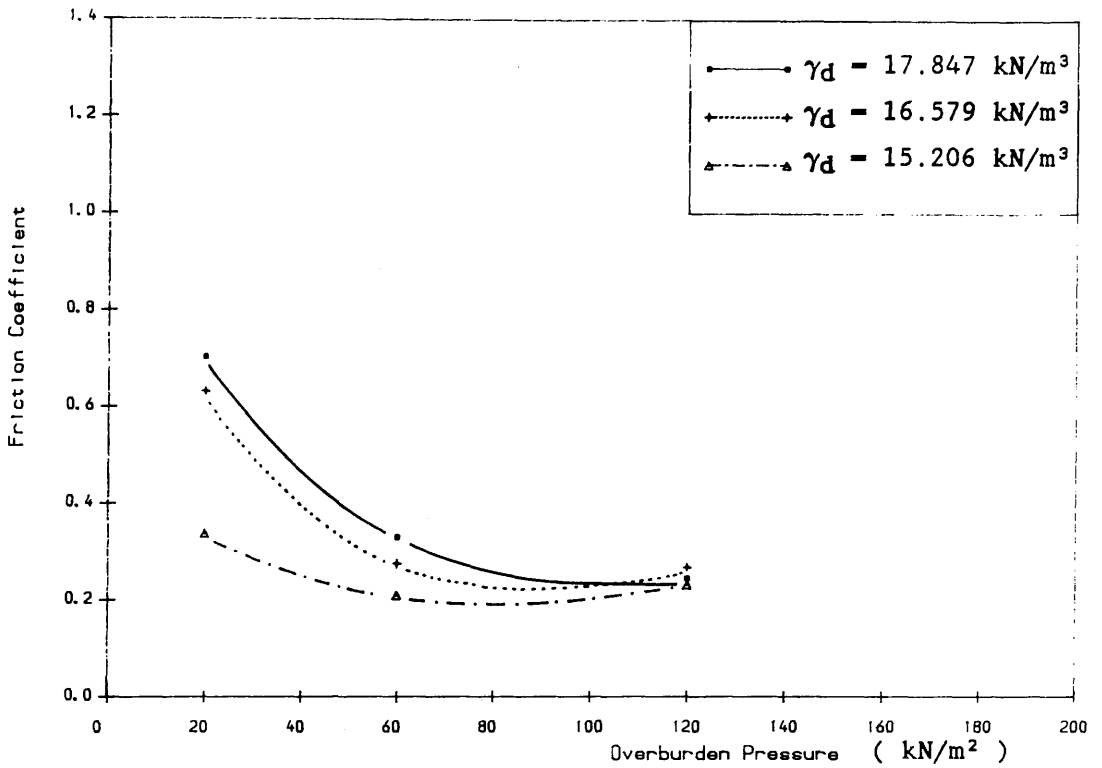


Figure 5.13 FRICTION COEFFICIENT VS. OVERBURDEN PRESSURE

Laboratory Pull-out Test, Wardley Minestone, Paralink 500s, L=1.5m

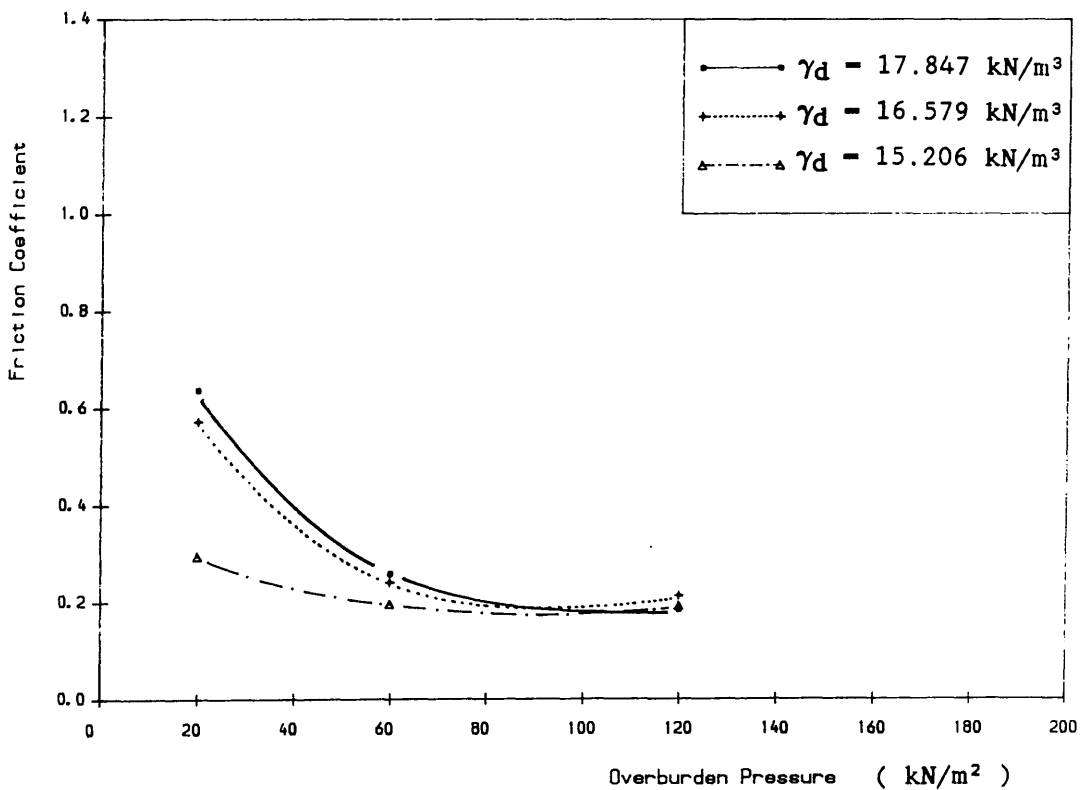


Figure 5.14 FRICTION COEFFICIENT VS. OVERBURDEN PRESSURE

Laboratory Pull-out Test, Wardley Minestone, Paralink 300s, L=1.5m

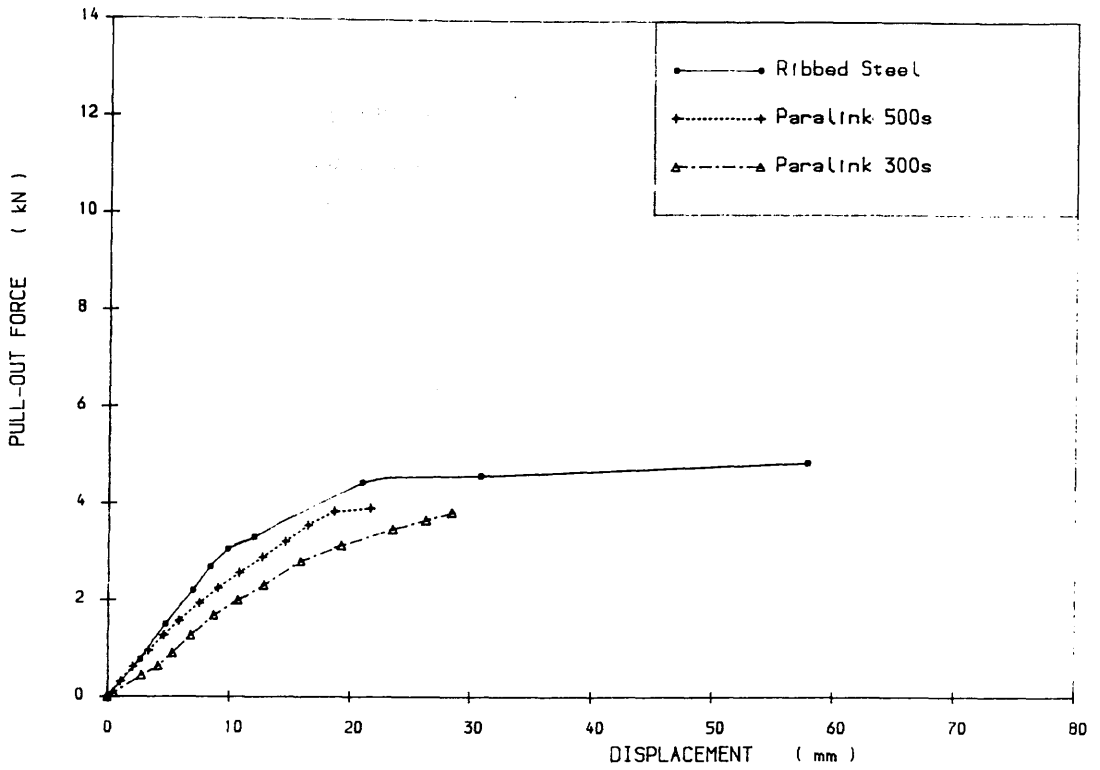


Figure 5.15 PULL-OUT FORCE VS. STRAP DISPLACEMENT

Laboratory Test, Wearmouth Minestone,  $L=1.5m$ ,  $\gamma_d=17.658kN/m^3$ ,  $\sigma_v=60kN/m^2$

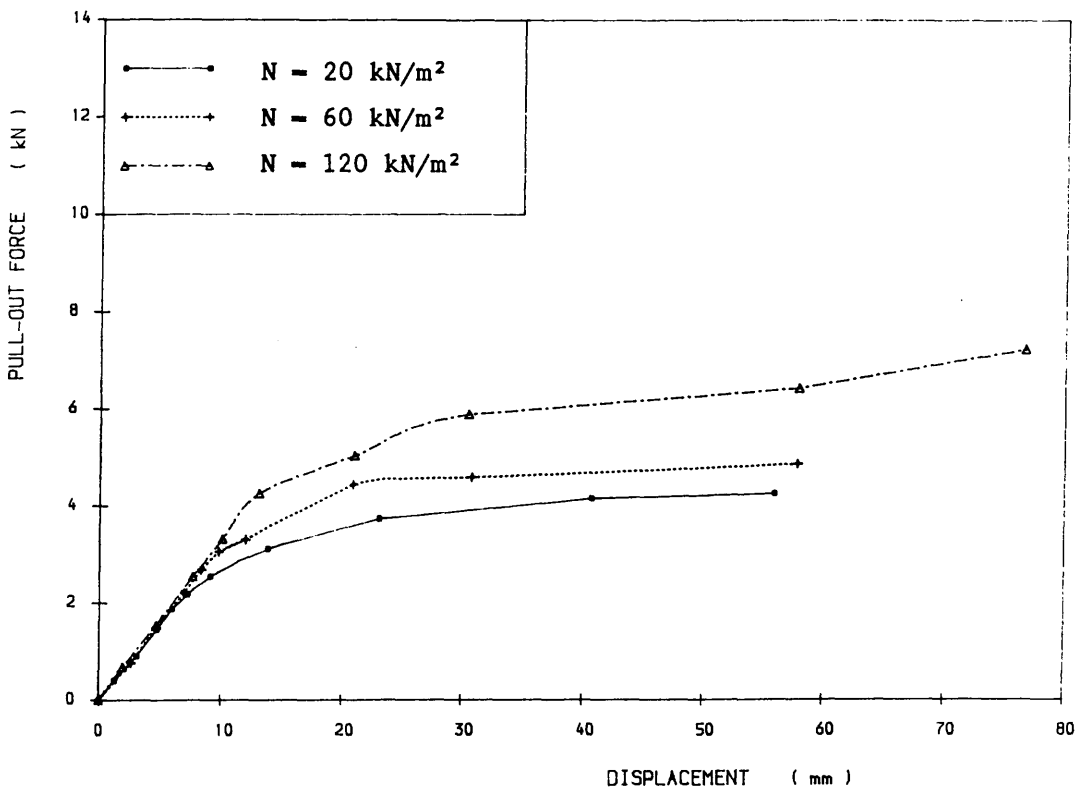


Figure 5.16 PULL-OUT FORCE VS. STRAP DISPLACEMENT

Laboratory Test, Wearmouth Minestone,  $L=1.5m$ ,  $\gamma_d=17.658kN/m^3$ , Ribbed Steel

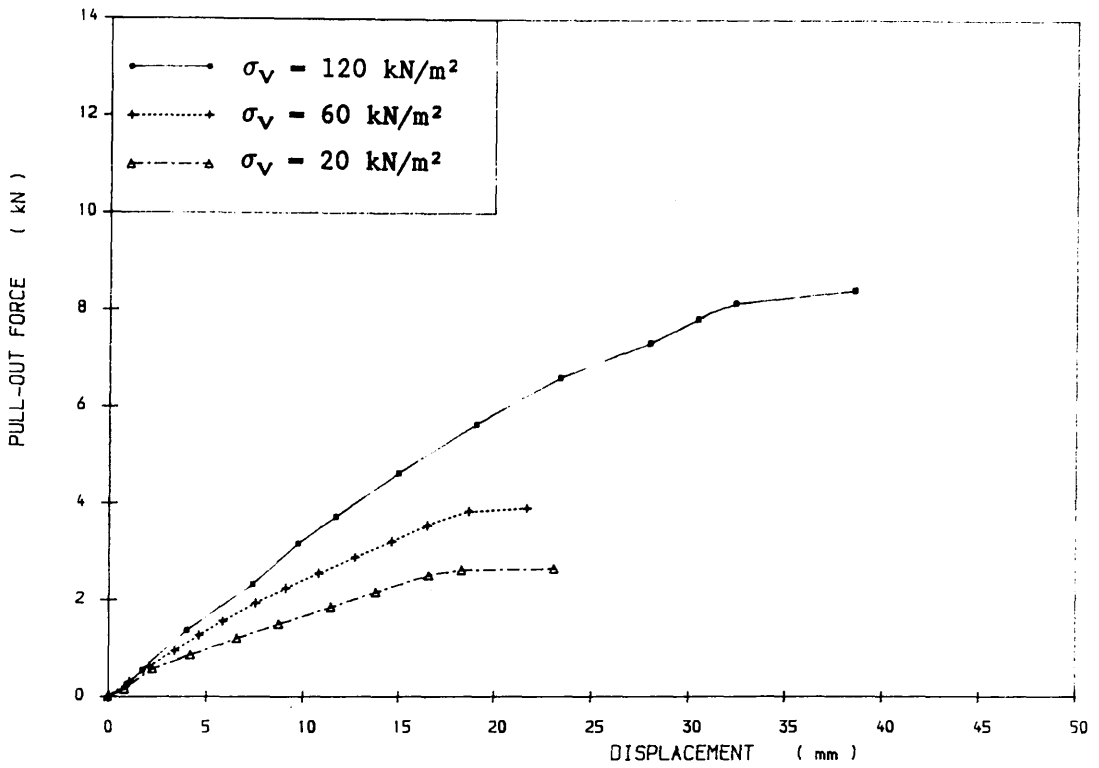


Figure 5.17 PULL-OUT FORCE VS. STRAP DISPLACEMENT

Laboratory Test, Wearmouth Minestone,  $L=1.5\text{m}$ ,  $\gamma_d=17.658\text{kN/m}^3$ , Paralink 500 s

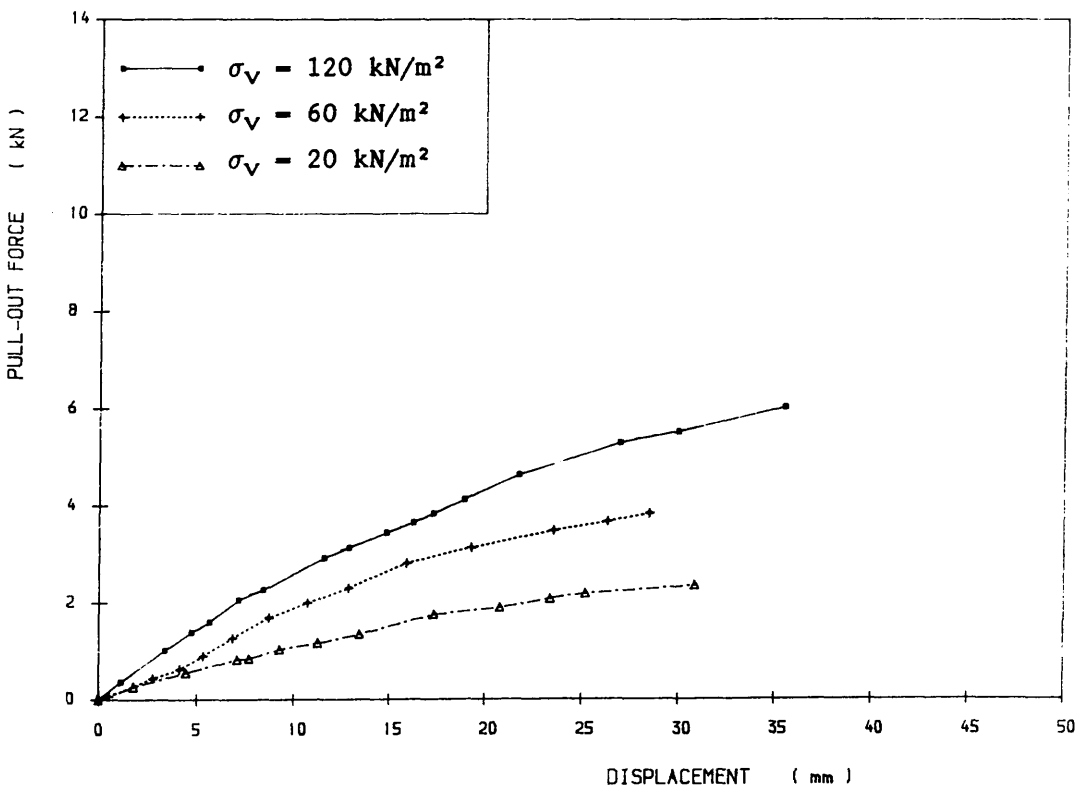


Figure 5.18 PULL-OUT FORCE VS. STRAP DISPLACEMENT

Laboratory Test, Wearmouth Minestone,  $L=1.5\text{m}$ ,  $\gamma_d=17.658\text{kN/m}^3$ , Paralink 300 s

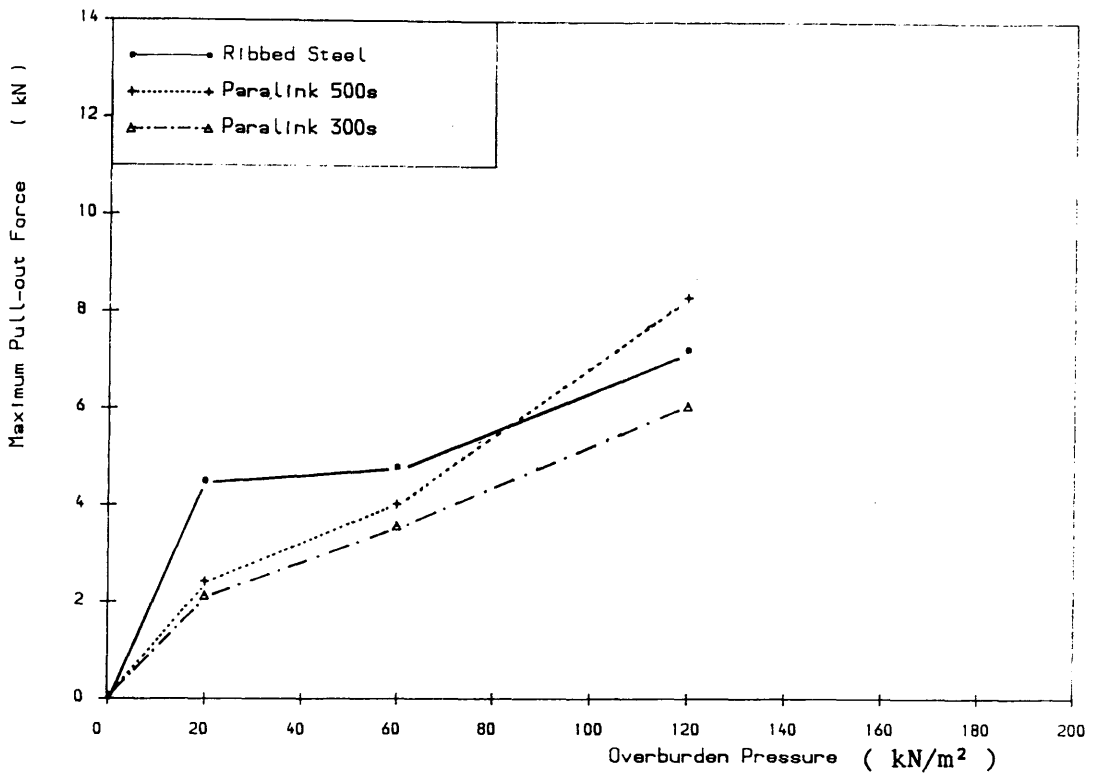


Figure 5.19 MAXIMUM PULL-OUT FORCE VS. OVERBURDEN PRESSURE  
 Laboratory Pull-out Test, Wearmouth Minestone,  $\gamma_d=17.658\text{kN/m}^3$ ,  $L=1.5\text{m}$

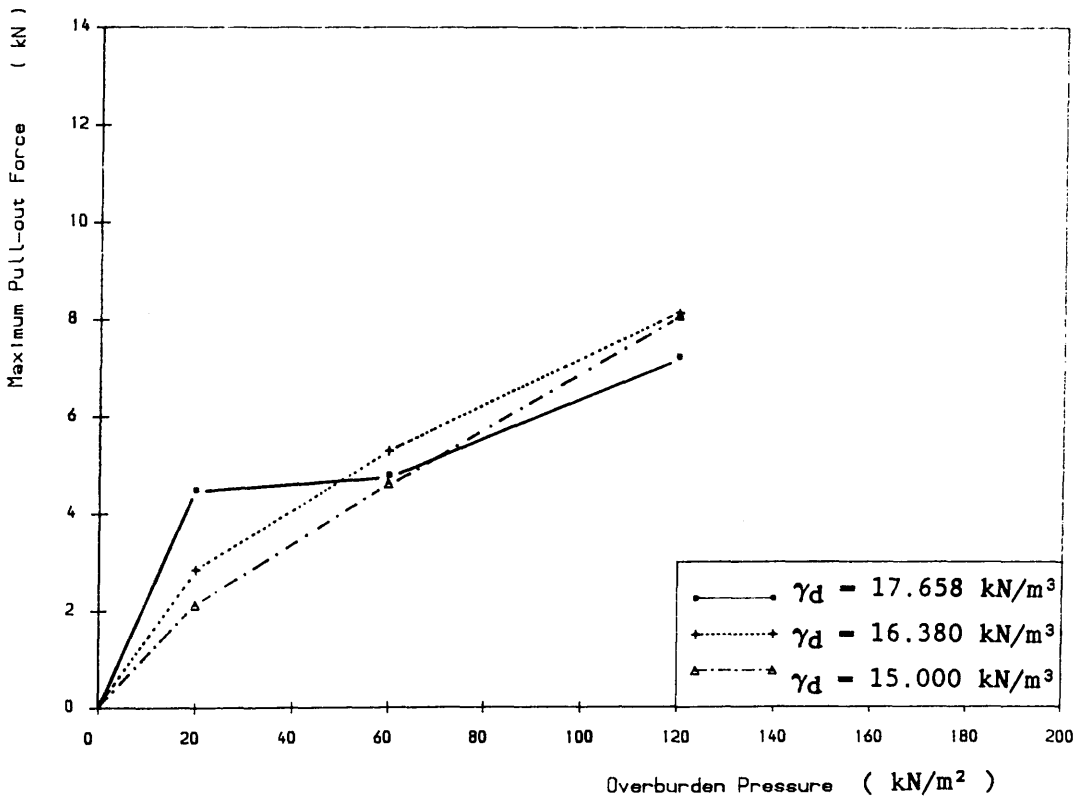


Figure 5.20 MAXIMUM PULL-OUT FORCE VS. OVERBURDEN PRESSURE  
 Laboratory Pull-out Test, Wearmouth Minestone, Ribbed Steel,  $L=1.5\text{m}$

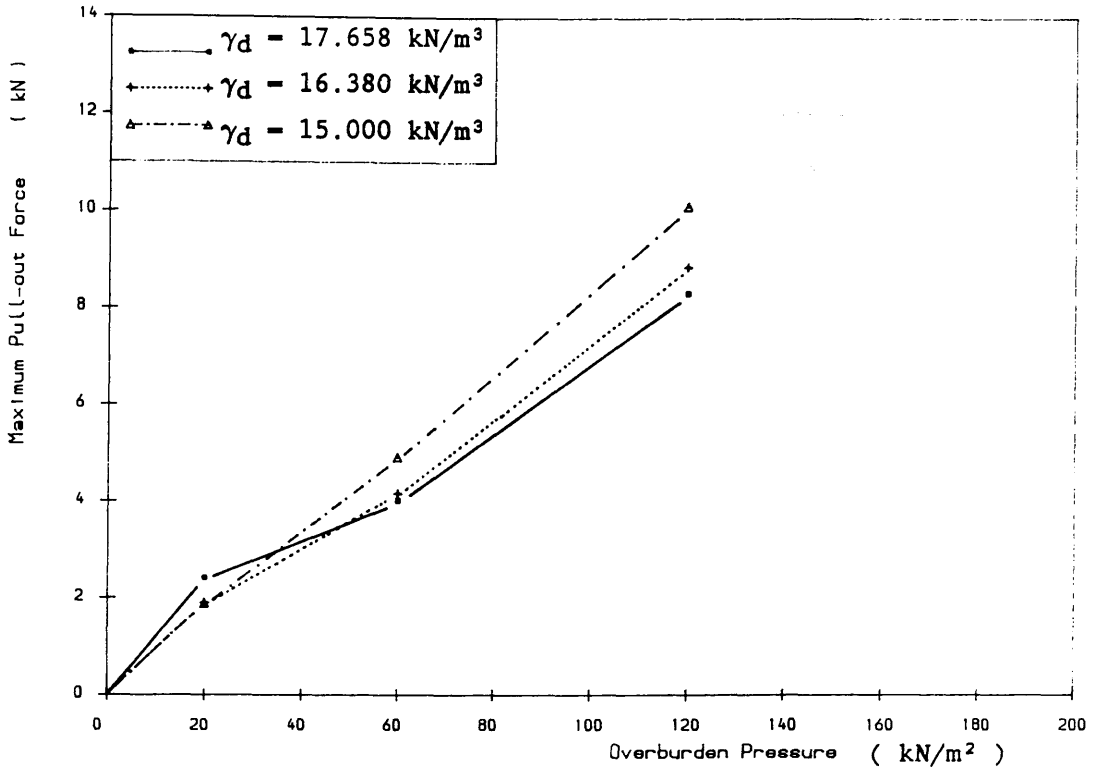


Figure 5.21 MAXIMUM PULL-OUT FORCE VS. OVERBURDEN PRESSURE  
 Laboratory Pull-out Test, Wearmouth Minestone, Paralink 500s, L=1.5m

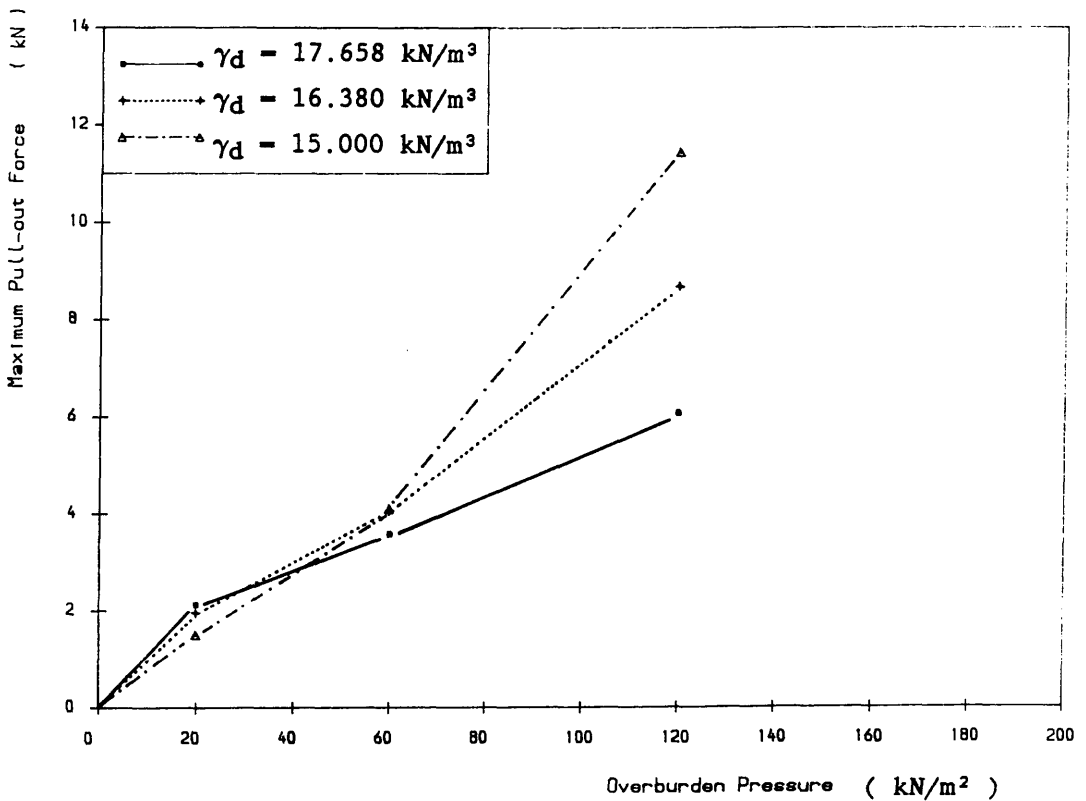


Figure 5.22 MAXIMUM PULL-OUT FORCE VS. OVERBURDEN PRESSURE  
 Laboratory Pull-out Test, Wearmouth Minestone, Paralink 300s, L=1.5m

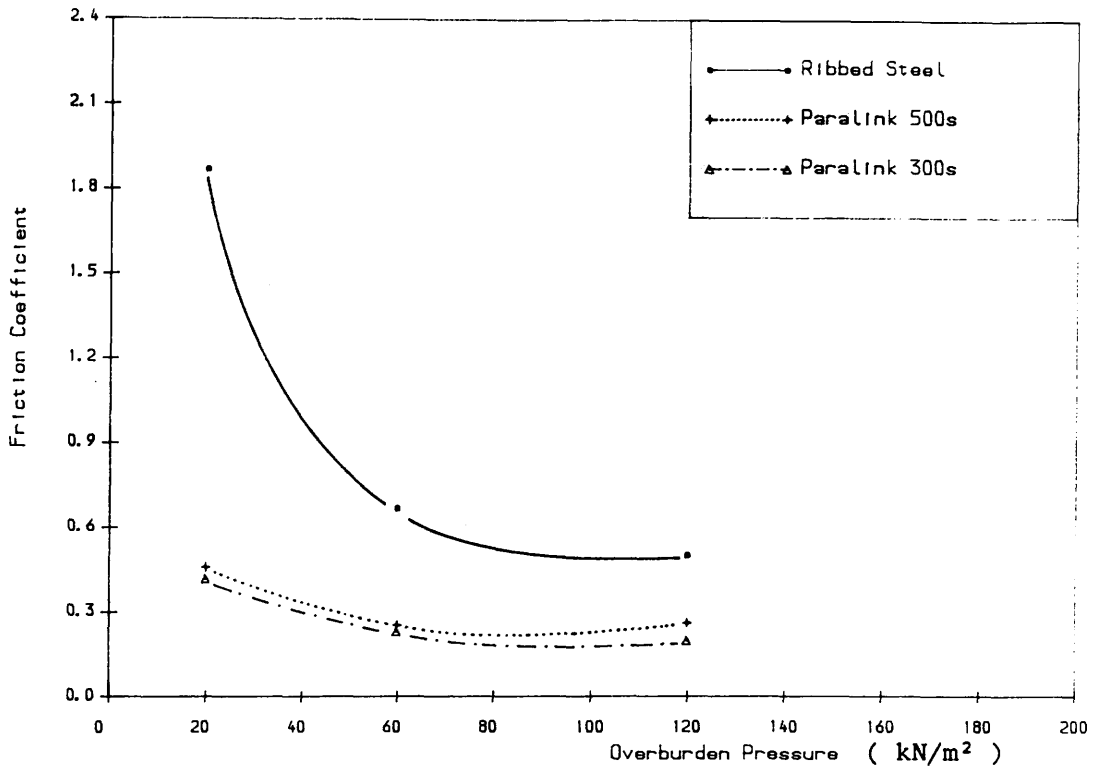


Figure 5.23 FRICTION COEFFICIENT VS. OVERBURDEN PRESSURE

Laboratory Pull-out Test, Wearmouth Minestone,  $\gamma_d=17.658\text{kN/m}^3$ ,  $L=1.5\text{m}$

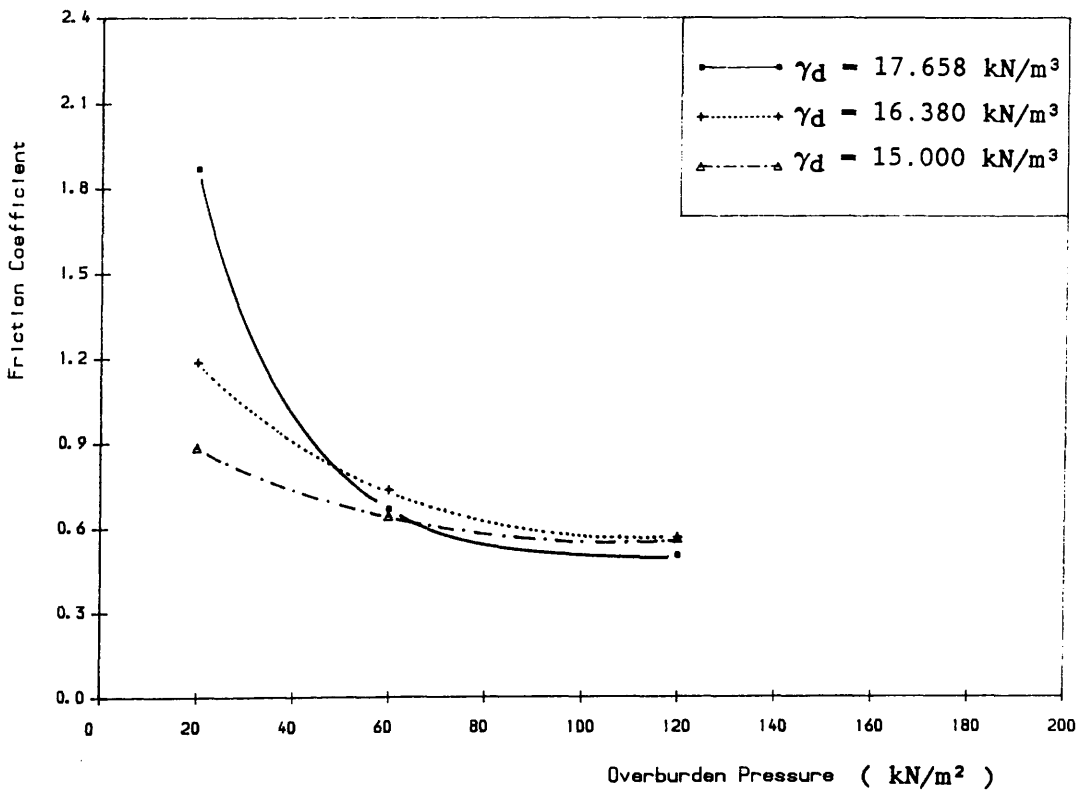


Figure 5.24 FRICTION COEFFICIENT VS. OVERBURDEN PRESSURE

Laboratory Pull-out Test, Wearmouth Minestone, Ribbed Steel,  $L=1.5\text{m}$

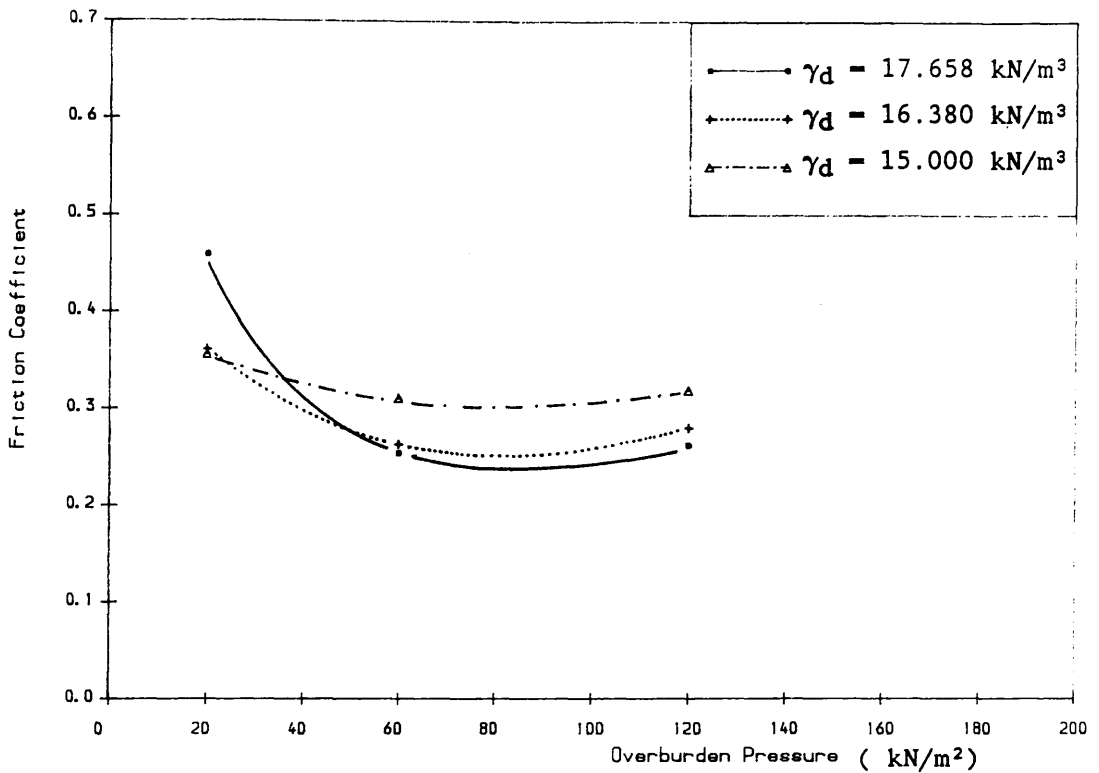


Figure 5.25 FRICTION COEFFICIENT VS. OVERBURDEN PRESSURE

Laboratory Pull-out Test, Wearmouth Minestone, Paralink 500s, L=1.5m

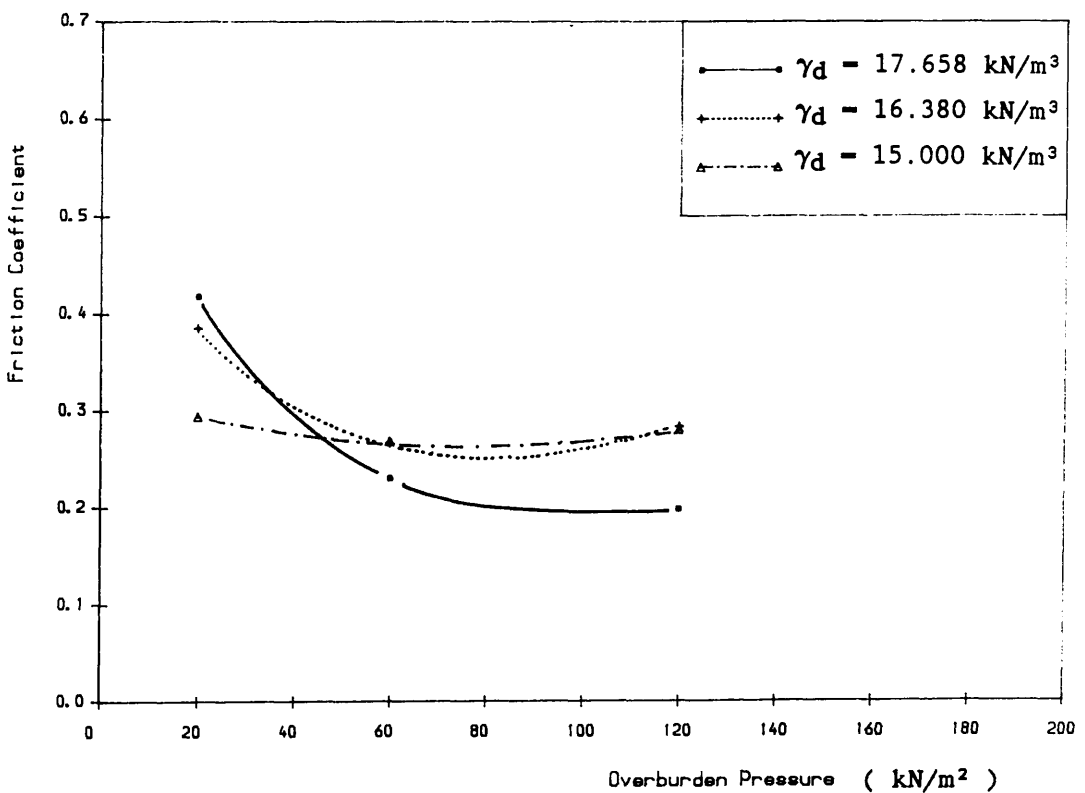


Figure 5.26 FRICTION COEFFICIENT VS. OVERBURDEN PRESSURE

Laboratory Pull-out Test, Wearmouth Minestone, Paralink 300s, L=1.5m

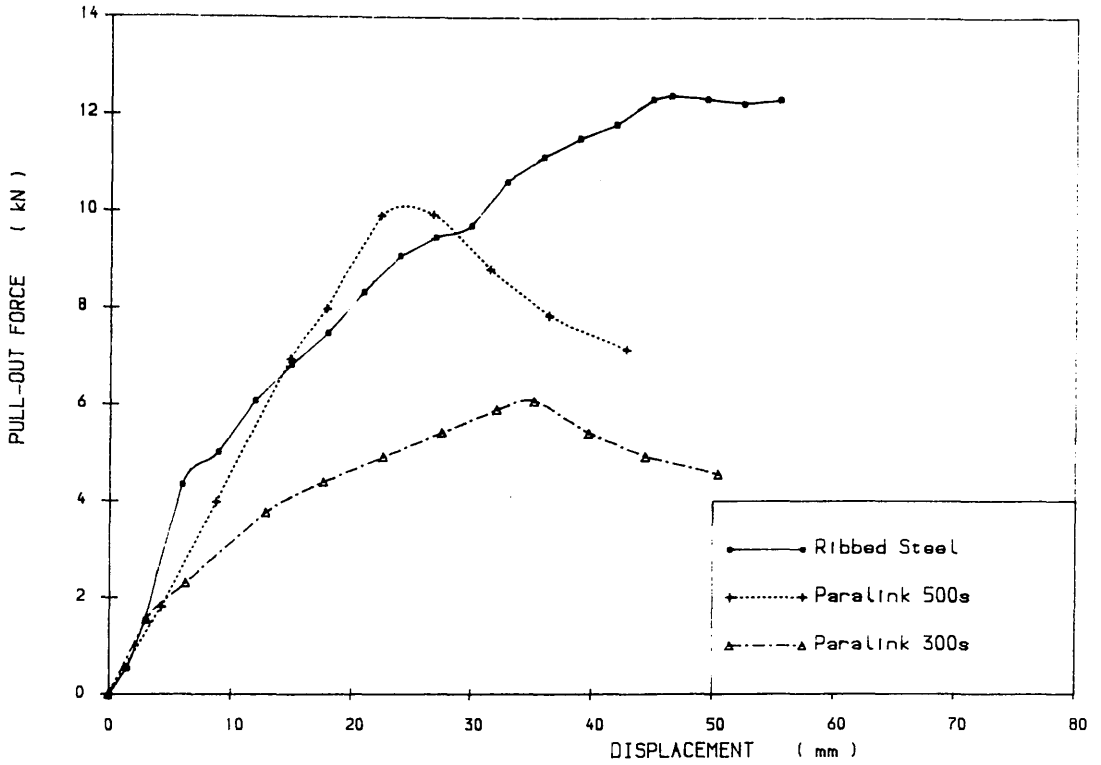


Figure 5.27 PULL-OUT FORCE VS. STRAP DISPLACEMENT

Laboratory Test, Horden Red Shale,  $L=1.5m$ ,  $\gamma_d=17.640kN/m^3$ ,  $\sigma_v=60kN/m^2$

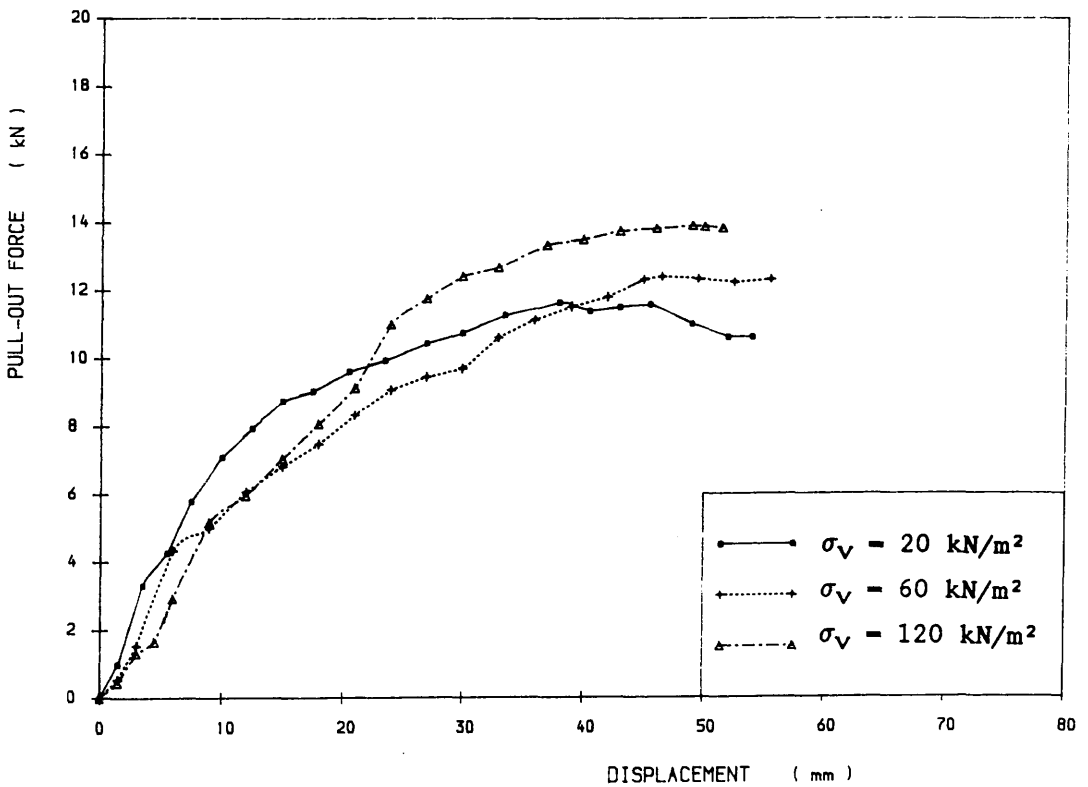


Figure 5.28 PULL-OUT FORCE VS. STRAP DISPLACEMENT

Laboratory Test, Horden Red Shale,  $L=1.5m$ ,  $\gamma_d=17.640kN/m^3$ , Ribbed Steel

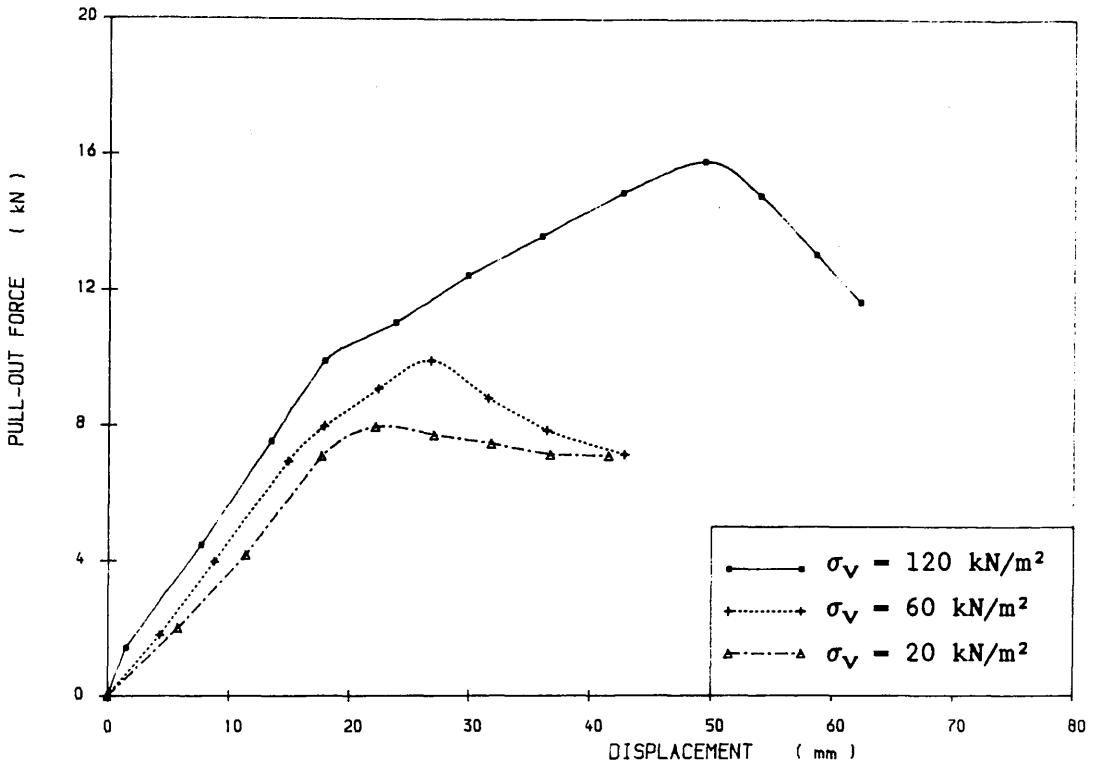


Figure 5.29 PULL-OUT FORCE VS. STRAP DISPLACEMENT

Laboratory Test, Horden Red Shale,  $L=1.5\text{m}$ ,  $\gamma_d=17.640\text{kN/m}^3$ , Paralink 500s

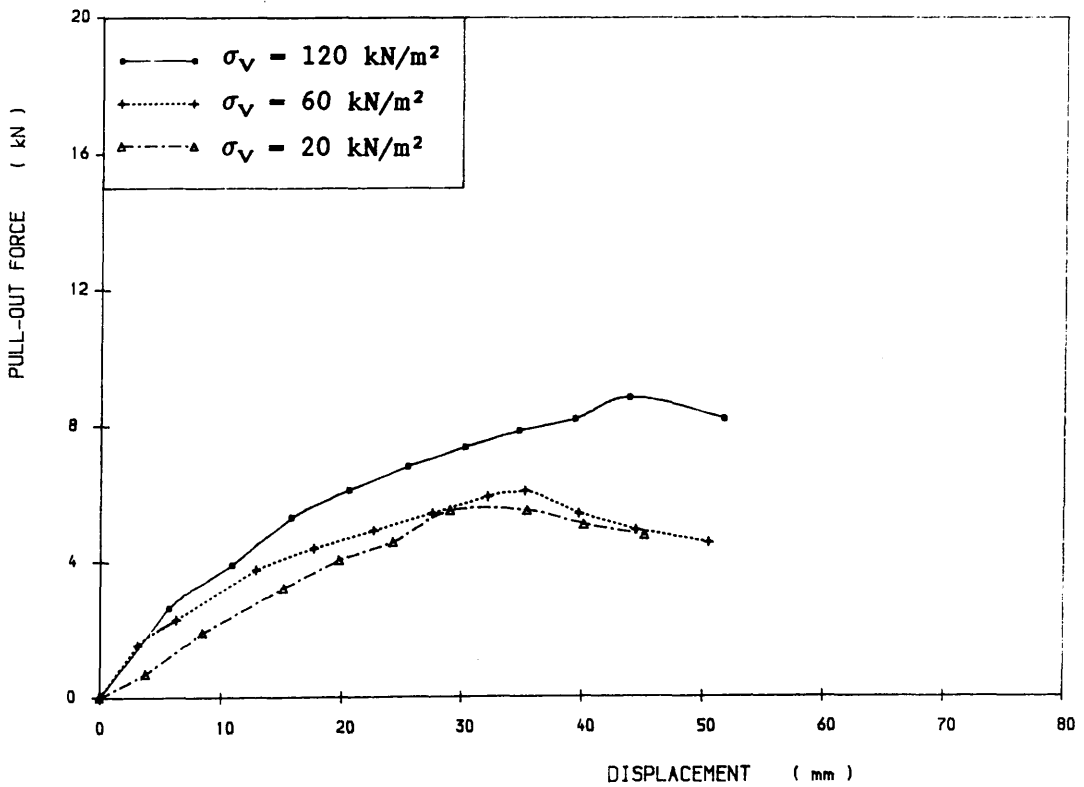
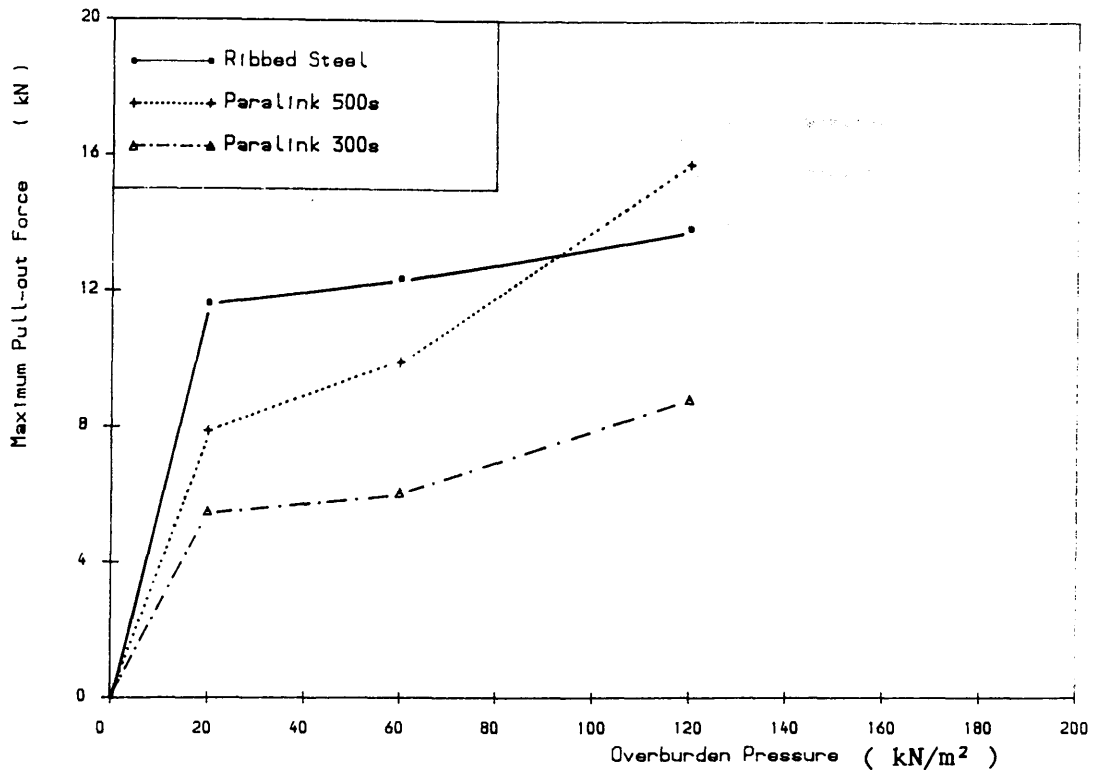
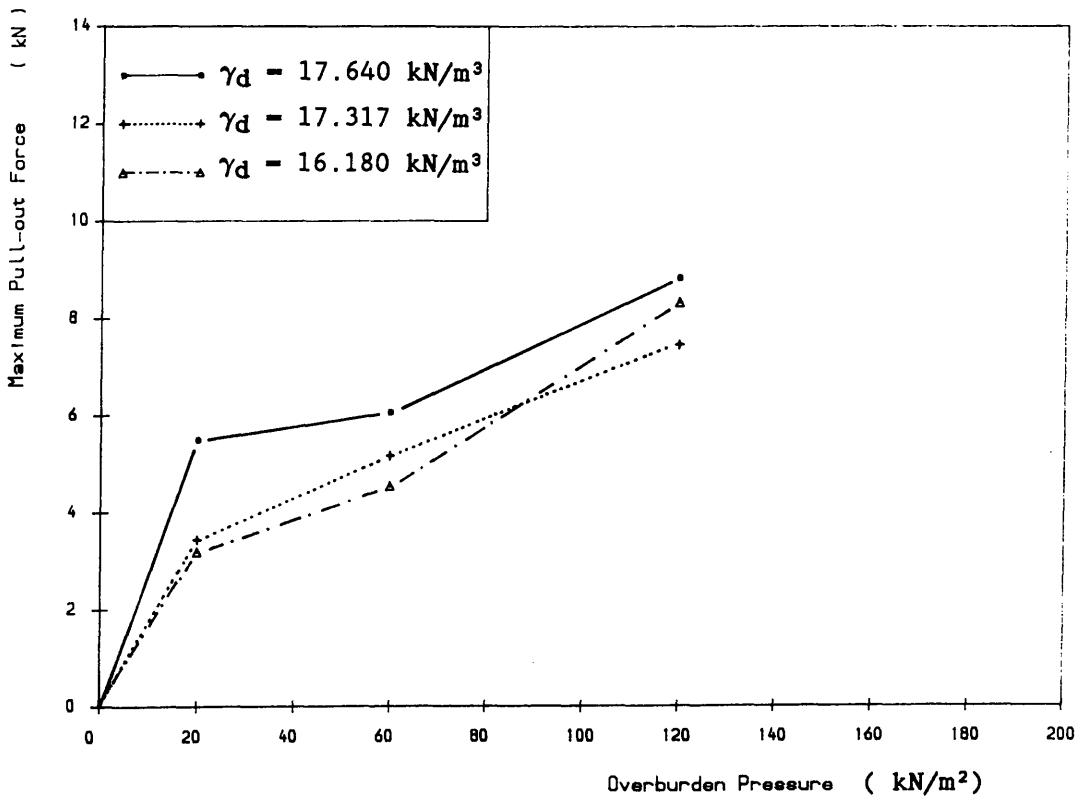


Figure 5.30 PULL-OUT FORCE VS. STRAP DISPLACEMENT

Laboratory Test, Horden Red Shale,  $L=1.5\text{m}$ ,  $\gamma_d=17.640\text{kN/m}^3$ , Paralink 300s



**Figure 5.31 MAXIMUM PULL-OUT FORCE VS. OVERBURDEN PRESSURE**  
 Laboratory Pull-out Test, Horden Red Shale,  $\gamma_d=17.640\text{kN/m}^3$ ,  $L=1.5\text{m}$



**Figure 5.32 MAXIMUM PULL-OUT FORCE VS. OVERBURDEN PRESSURE**  
 Laboratory Pull-out Test, Red Shale, Paralink 300s,  $L=1.5\text{m}$

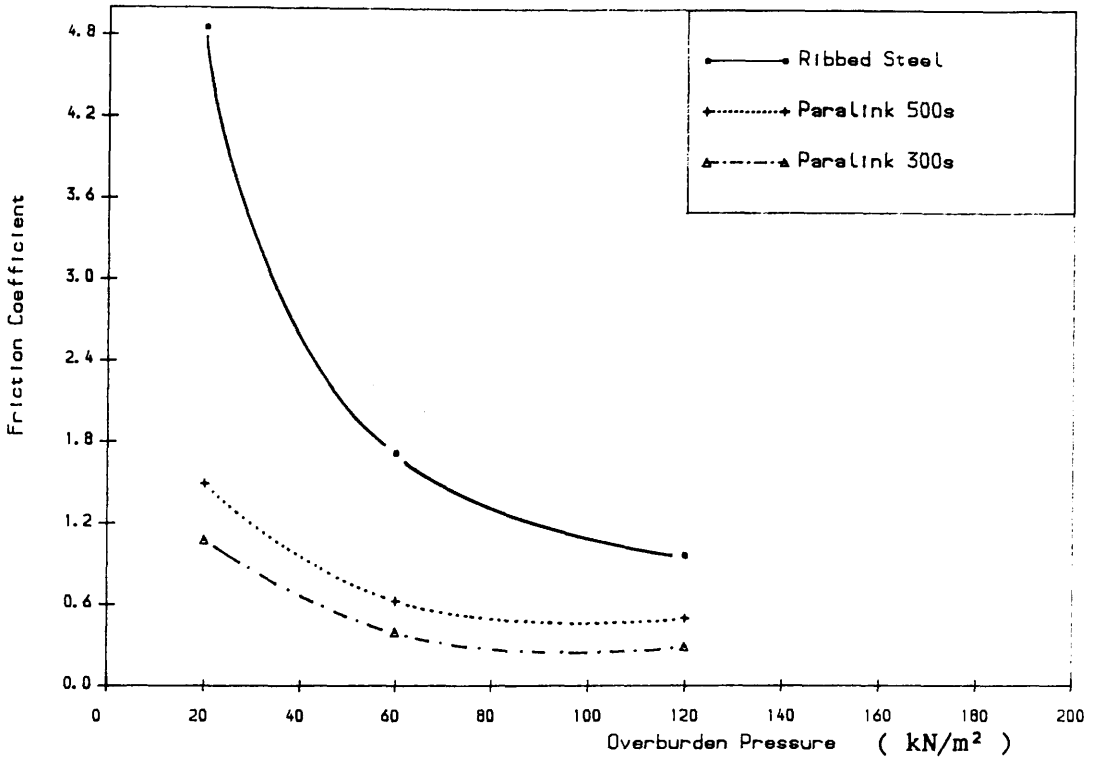


Figure 5.33 FRICTION COEFFICIENT VS. OVERBURDEN PRESSURE

Laboratory Pull-out Test, Horden Red Shale,  $\gamma_d=17.640\text{kN/m}^3$ ,  $L=1.5\text{m}$

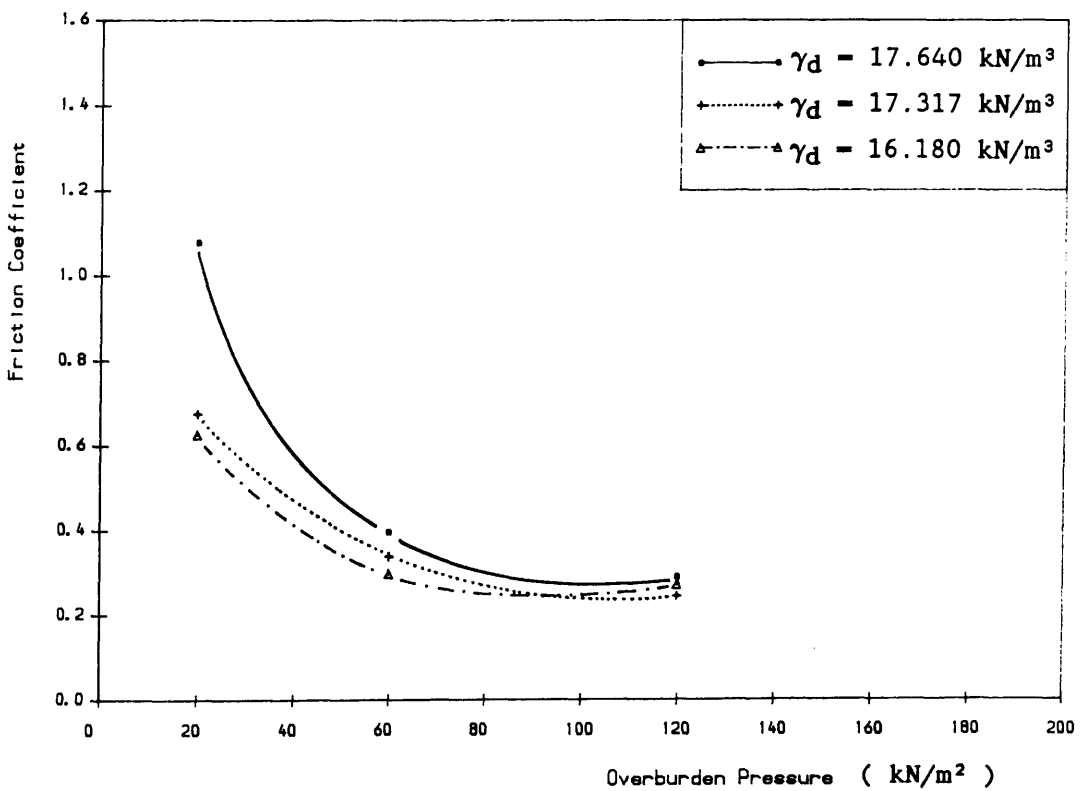


Figure 5.34 FRICTION COEFFICIENT VS. OVERBURDEN PRESSURE

Laboratory Pull-out Test, Red Shale, ParaLink 300s,  $L=1.5\text{m}$

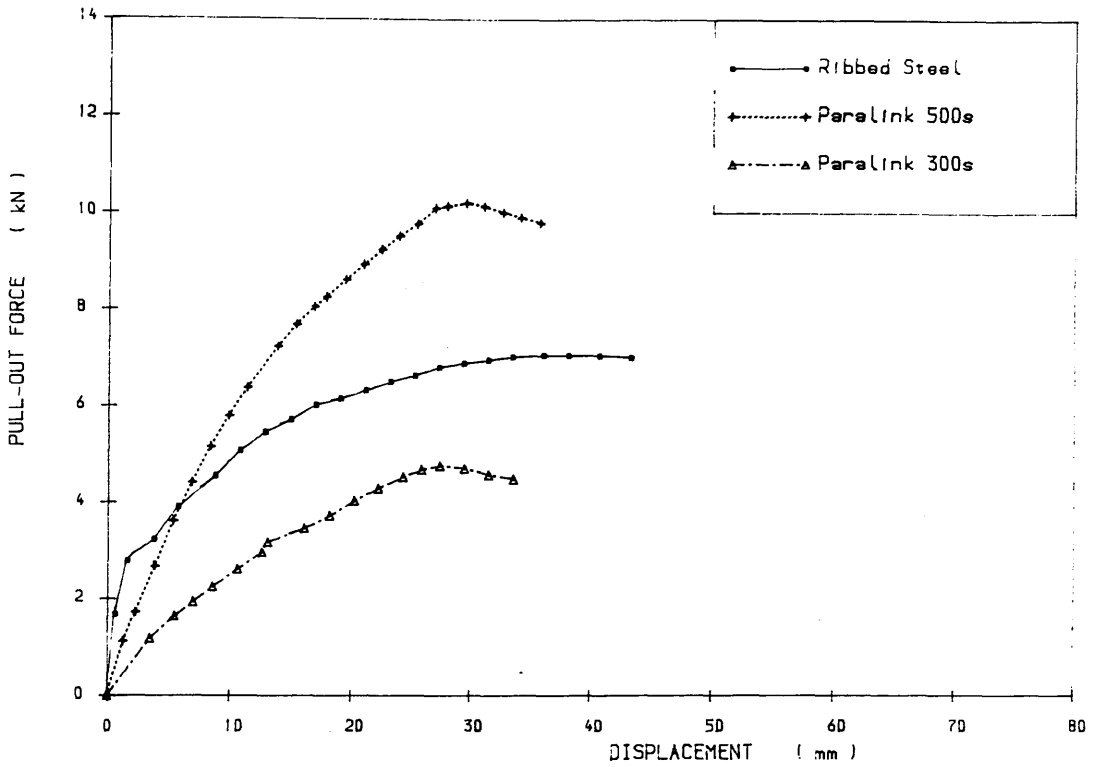


Figure 5.35 PULL-OUT FORCE VS. STRAP DISPLACEMENT

Laboratory Test, Loudon Hill Sand,  $L=1.5m$ ,  $\gamma=16.190kN/m^3$ ,  $N=60kN/m^2$

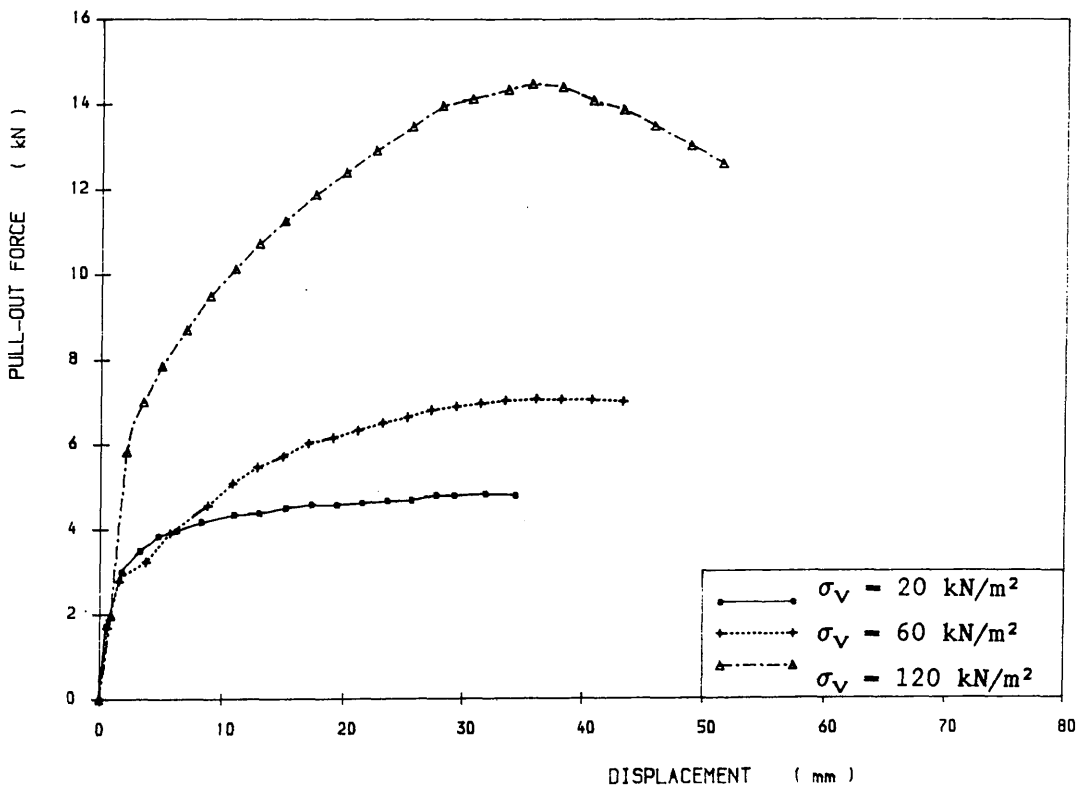


Figure 5.36 PULL-OUT FORCE VS. STRAP DISPLACEMENT

Laboratory Test, Loudon Hill Sand,  $L=1.5m$ ,  $\gamma_d=16.190kN/m^3$ , Ribbed Steel

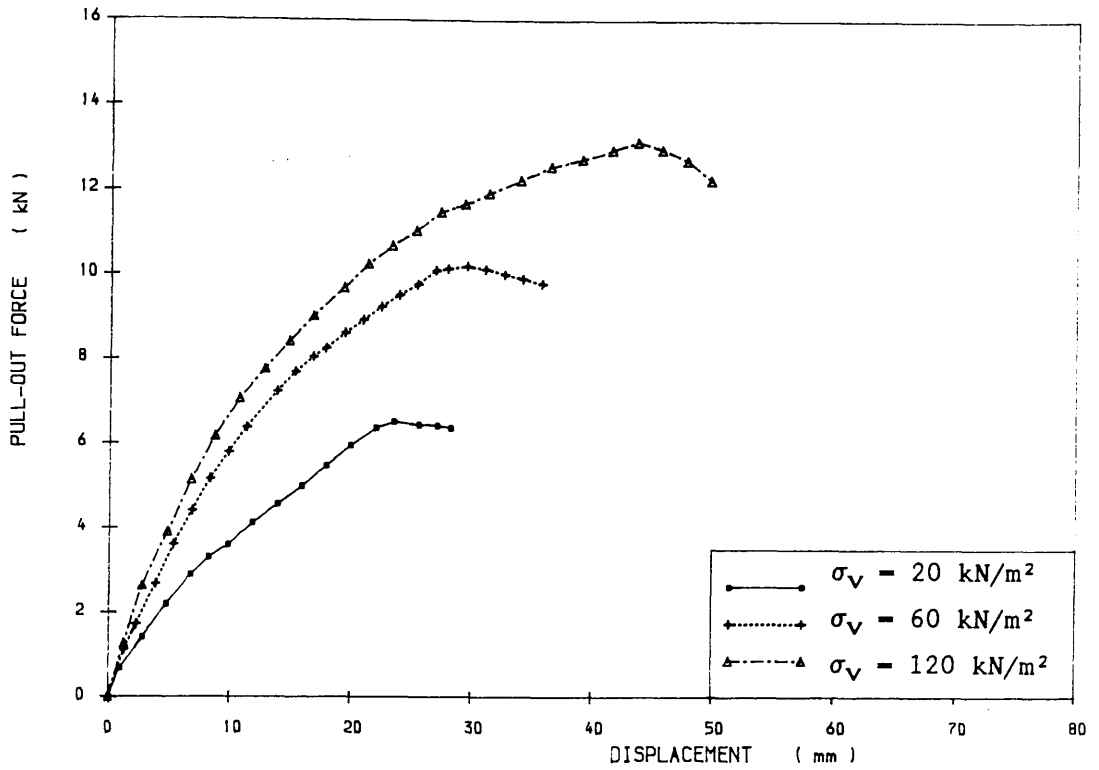


Figure 5.37 PULL-OUT FORCE VS. STRAP DISPLACEMENT

Laboratory Test, Loudon Hill Sand,  $L=1.5\text{m}$ ,  $\gamma_d=16.190\text{kN/m}^3$ , Paralink 500s

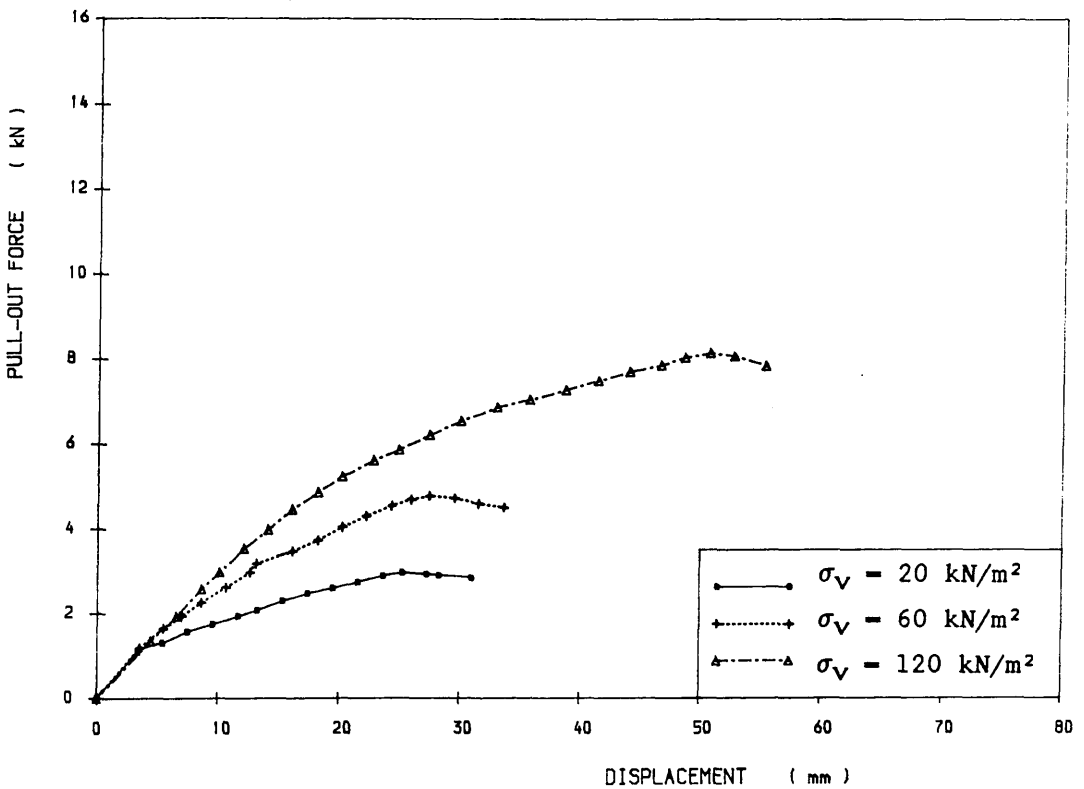


Figure 5.38 PULL-OUT FORCE VS. STRAP DISPLACEMENT

Laboratory Test, Loudon Hill Sand,  $L=1.5\text{m}$ ,  $\gamma_d=16.190\text{kN/m}^3$ , Paralink 300s

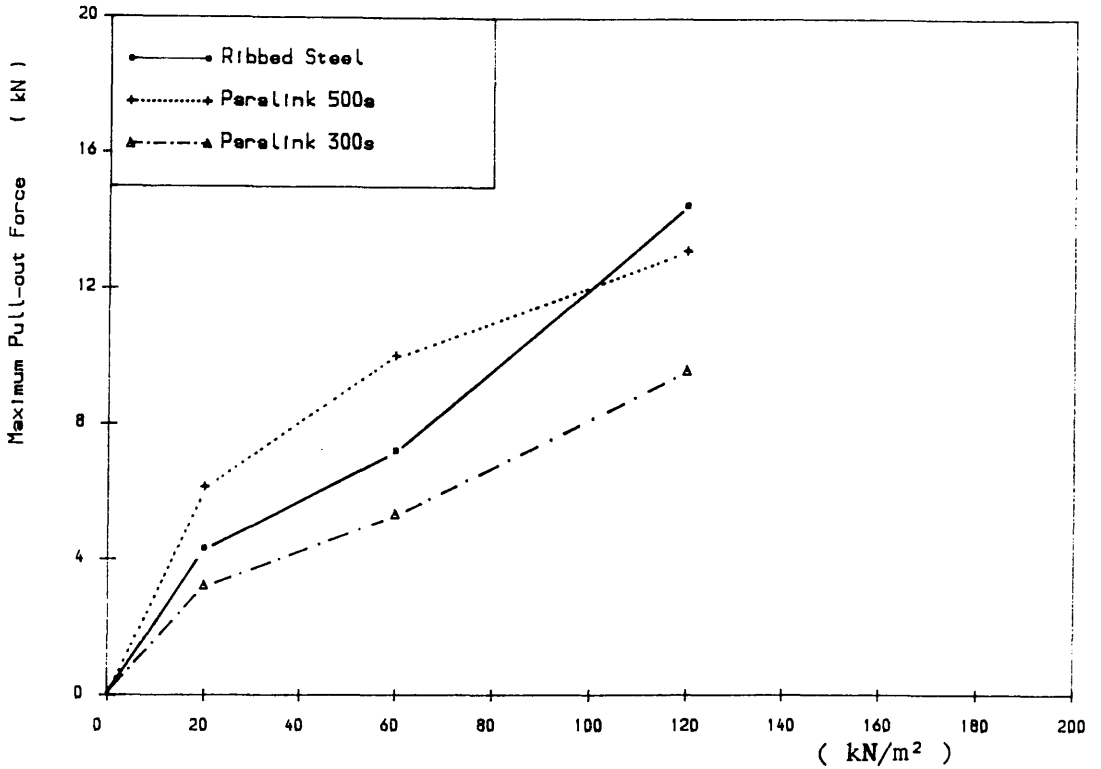


Figure 5.39 MAXIMUM PULL-OUT FORCE VS. OVERBURDEN PRESSURE  
 Laboratory Pull-out Test, Loudon Hill Sand,  $\gamma_d=16.190\text{kN/m}^3$ ,  $L=1.5\text{m}$

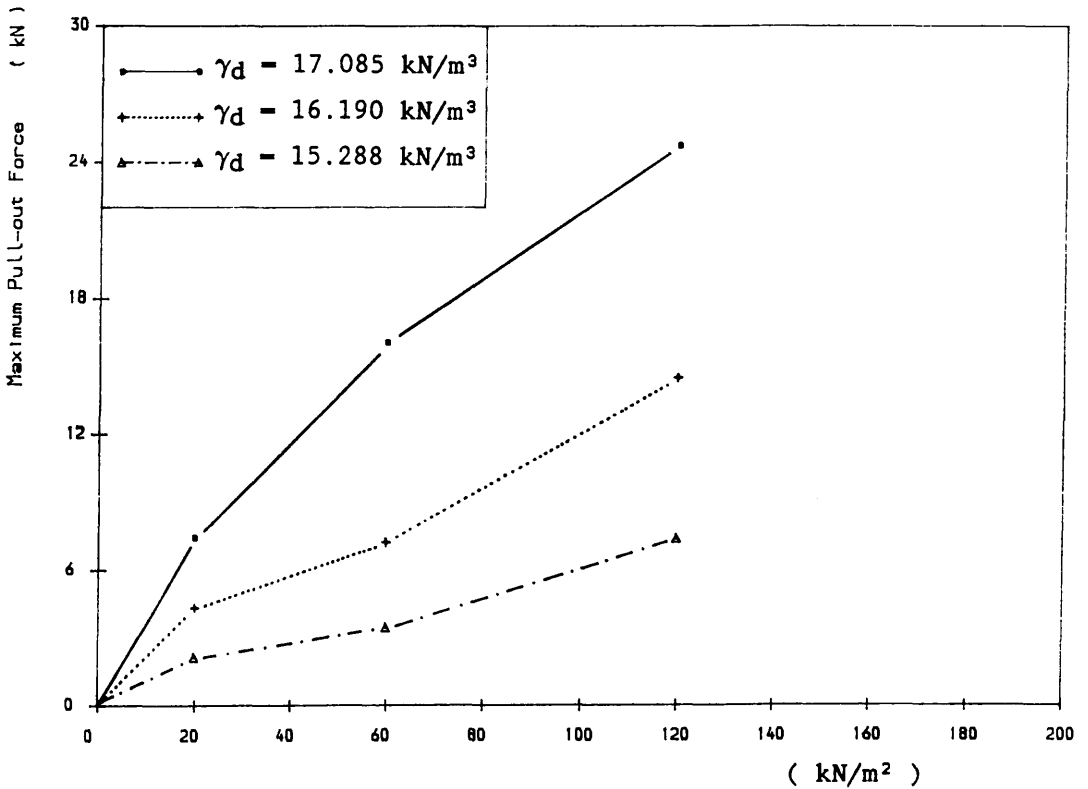


Figure 5.40 MAXIMUM PULL-OUT FORCE VS. OVERBURDEN PRESSURE  
 Laboratory Pull-out Test, Loudon Hill Sand, Ribbed Steel,  $L=1.5\text{m}$

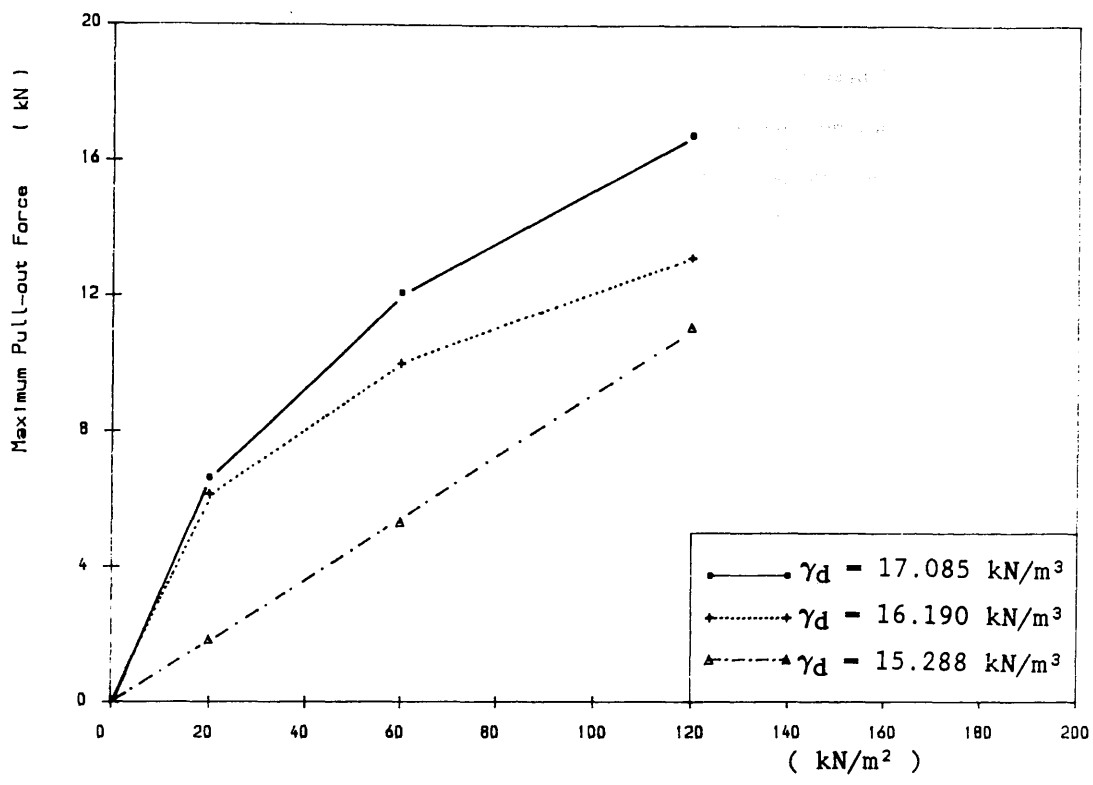


Figure 5.41 MAXIMUM PULL-OUT FORCE VS. OVERBURDEN PRESSURE  
 Laboratory Pull-out Test, Loudon Hill Sand, Paralink 500s, L=1.5m

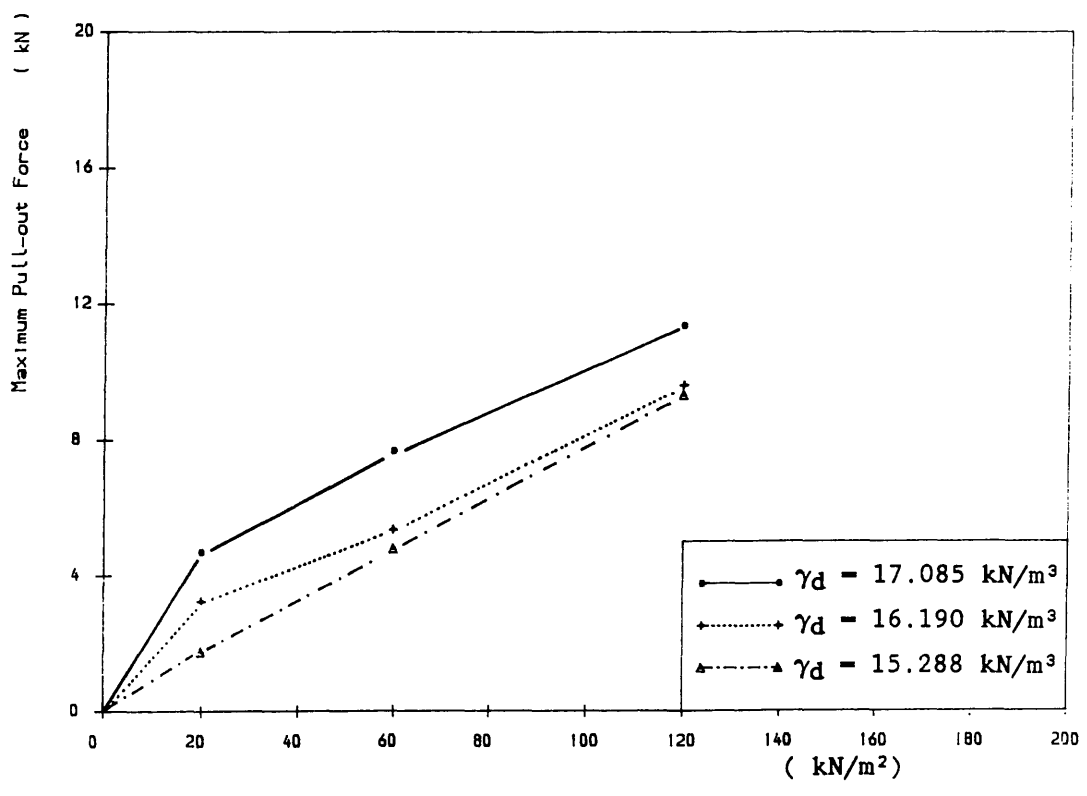


Figure 5.42 MAXIMUM PULL-OUT FORCE VS. OVERBURDEN PRESSURE  
 Laboratory Pull-out Test, Loudon Hill Sand, Paralink 300s, L=1.5m

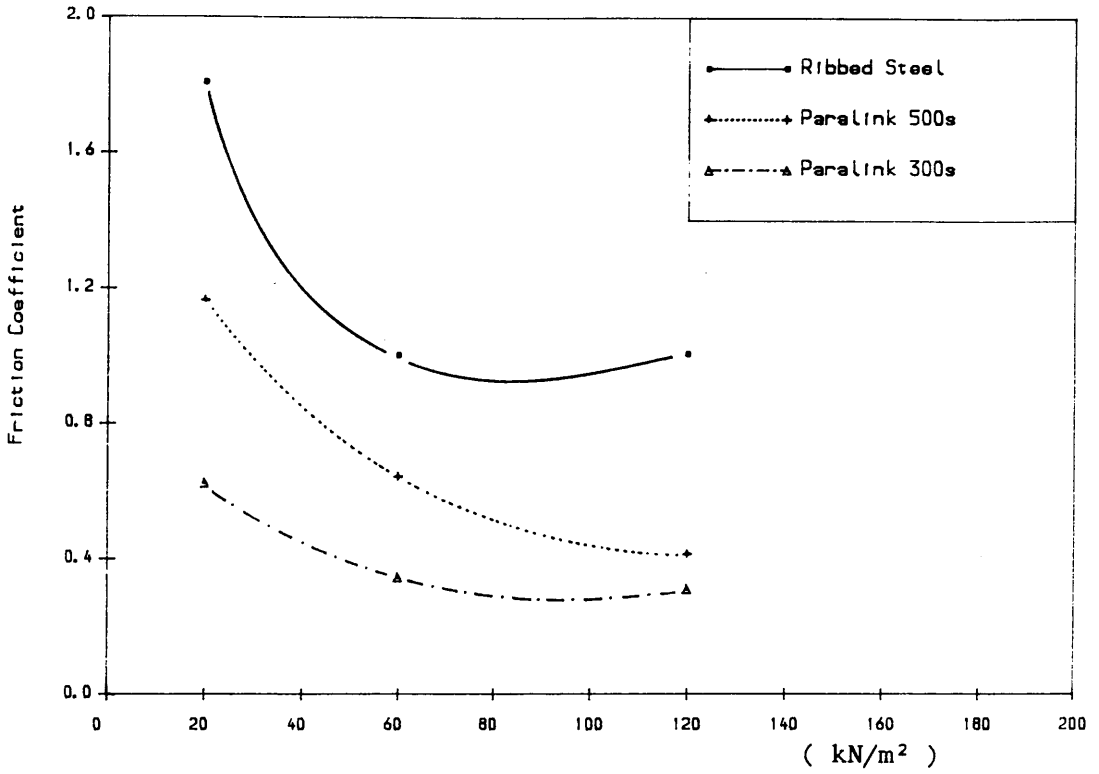


Figure 5.43 FRICTION COEFFICIENT VS. OVERBURDEN PRESSURE  
 Laboratory Pull-out Test, Loudon Hill Sand,  $\gamma_d=16.190\text{kN/m}^3$ ,  $L=1.5\text{m}$

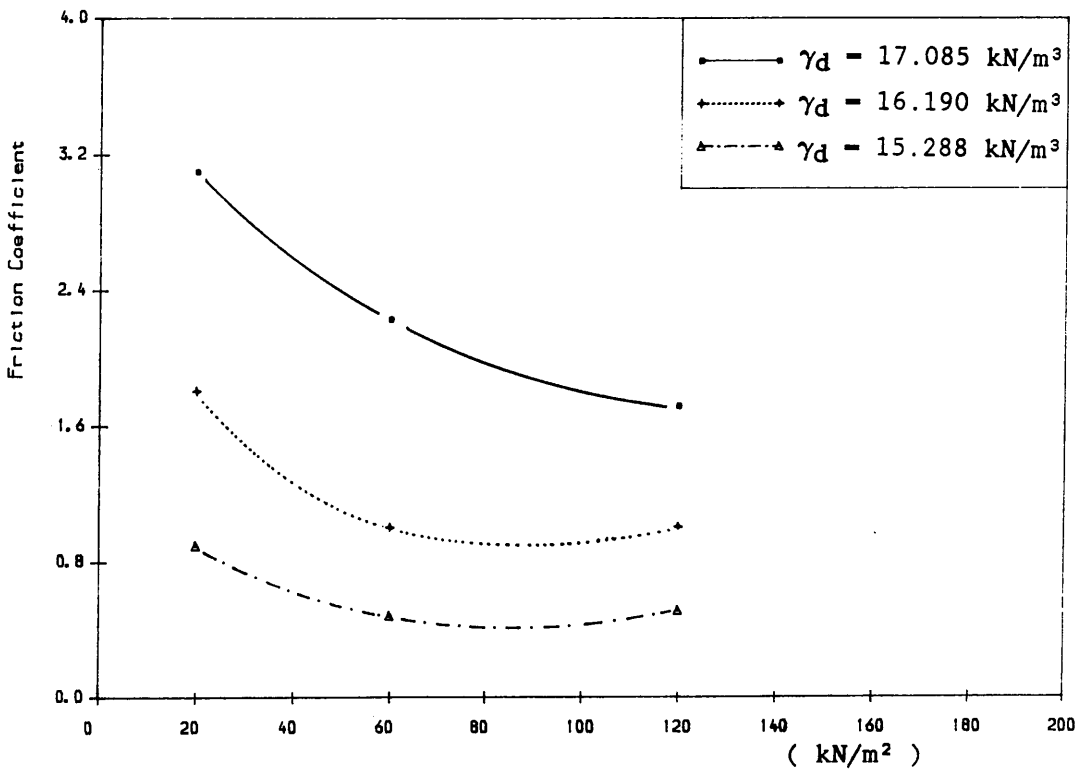


Figure 5.44 FRICTION COEFFICIENT VS. OVERBURDEN PRESSURE  
 Laboratory Pull-out Test, Loudon Hill Sand, Ribbed Steel,  $L=1.5\text{m}$

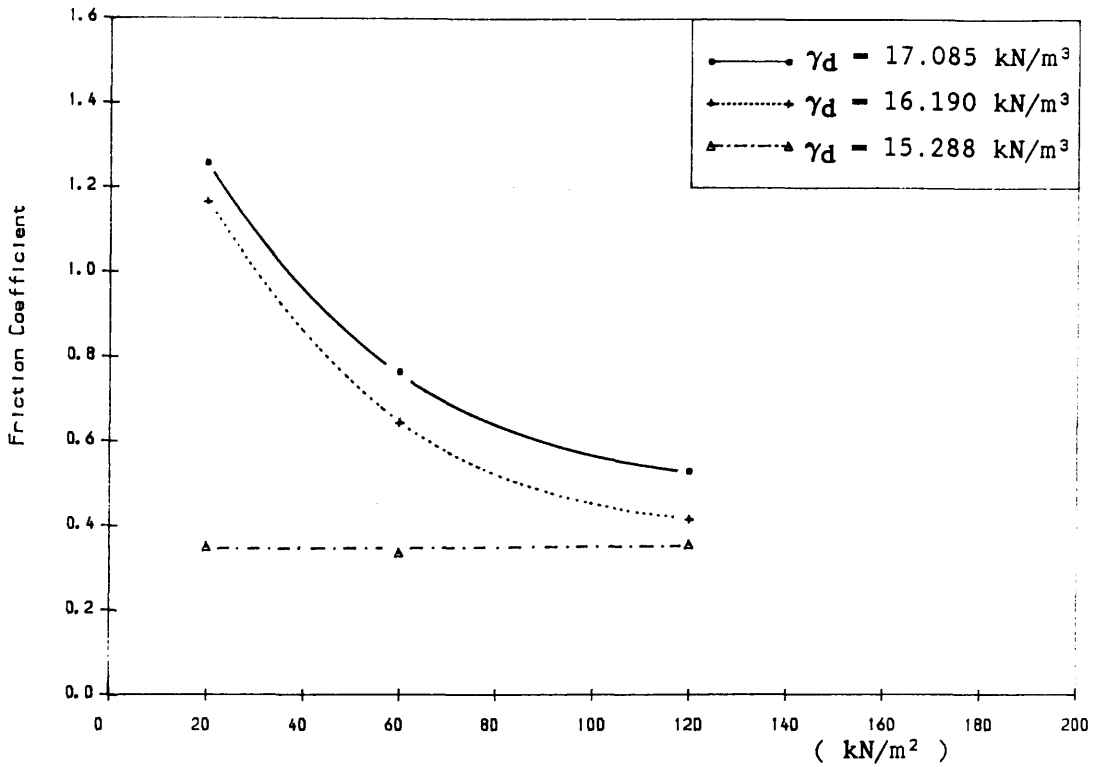


Figure 5.45 FRICTION COEFFICIENT VS. OVERBURDEN PRESSURE  
 Laboratory Pull-out Test, Loudon Hill Sand, Paralink 500s, L=1.5m

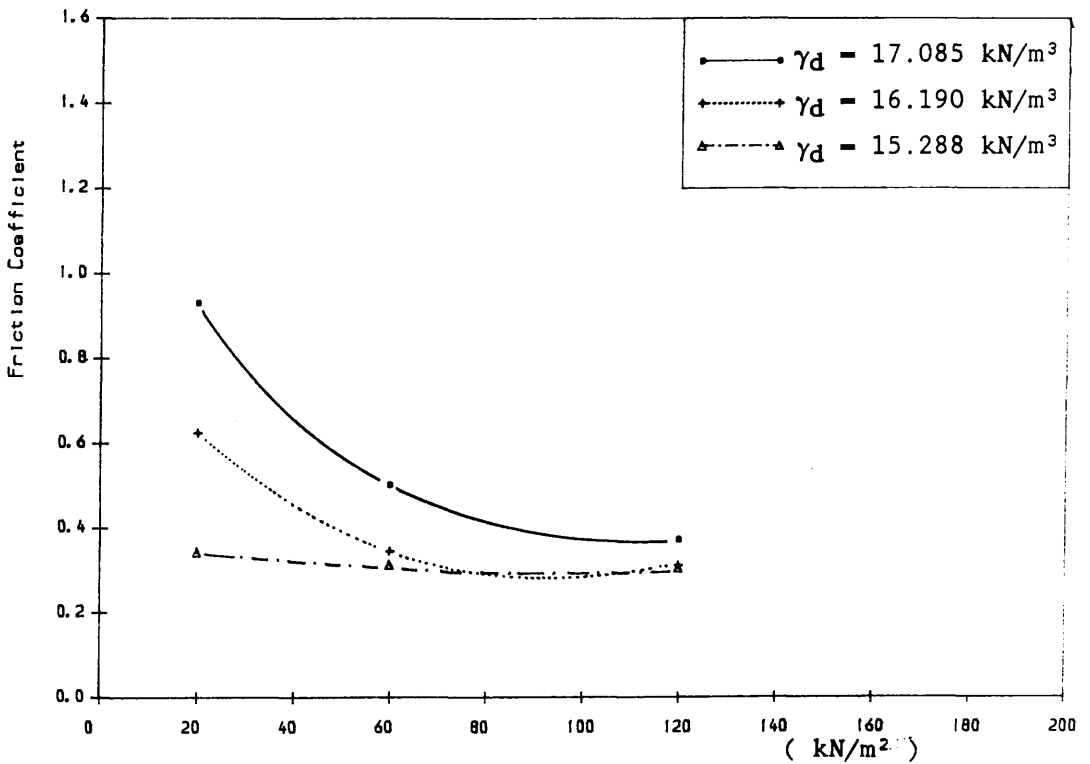


Figure 5.46 FRICTION COEFFICIENT VS. OVERBURDEN PRESSURE  
 Laboratory Pull-out Test, Loudon Hill Sand, Paralink 300s, L=1.5m

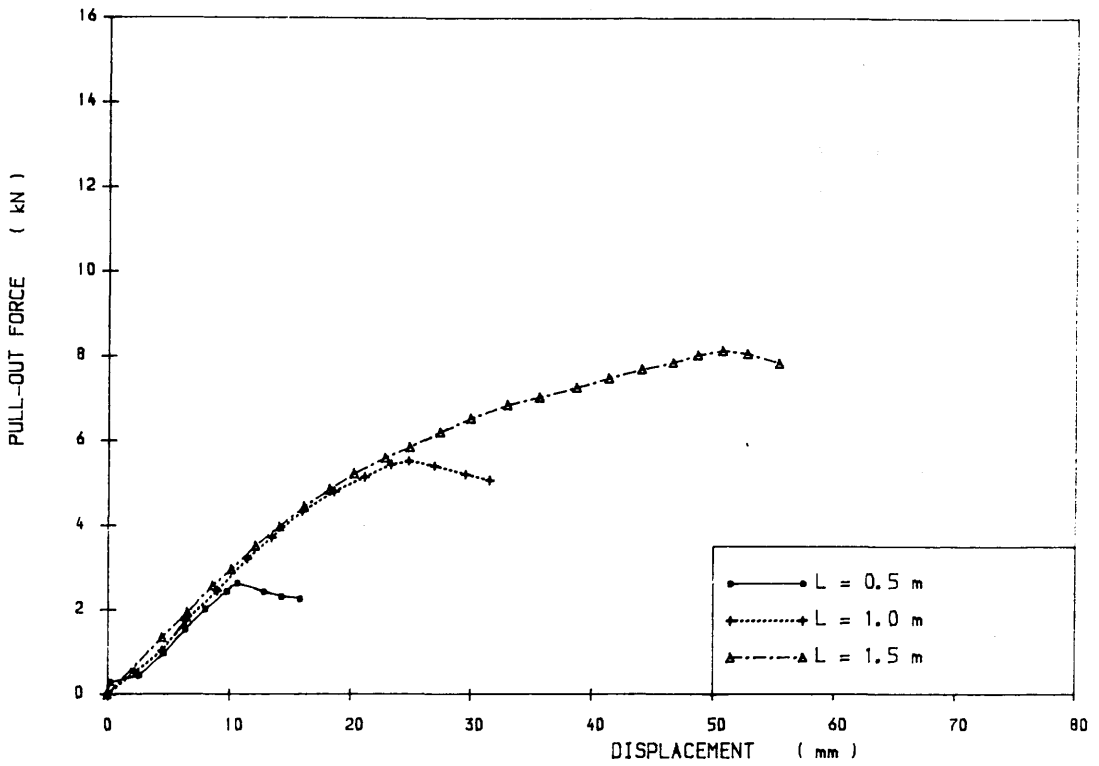


Figure 5.47 PULL-OUT FORCE VS. STRAP DISPLACEMENT  
 Loudon Hill Sand,  $\gamma_d=16.190\text{kN/m}^3$ , Paralink 300s,  $\sigma_v=120\text{kN/m}^2$

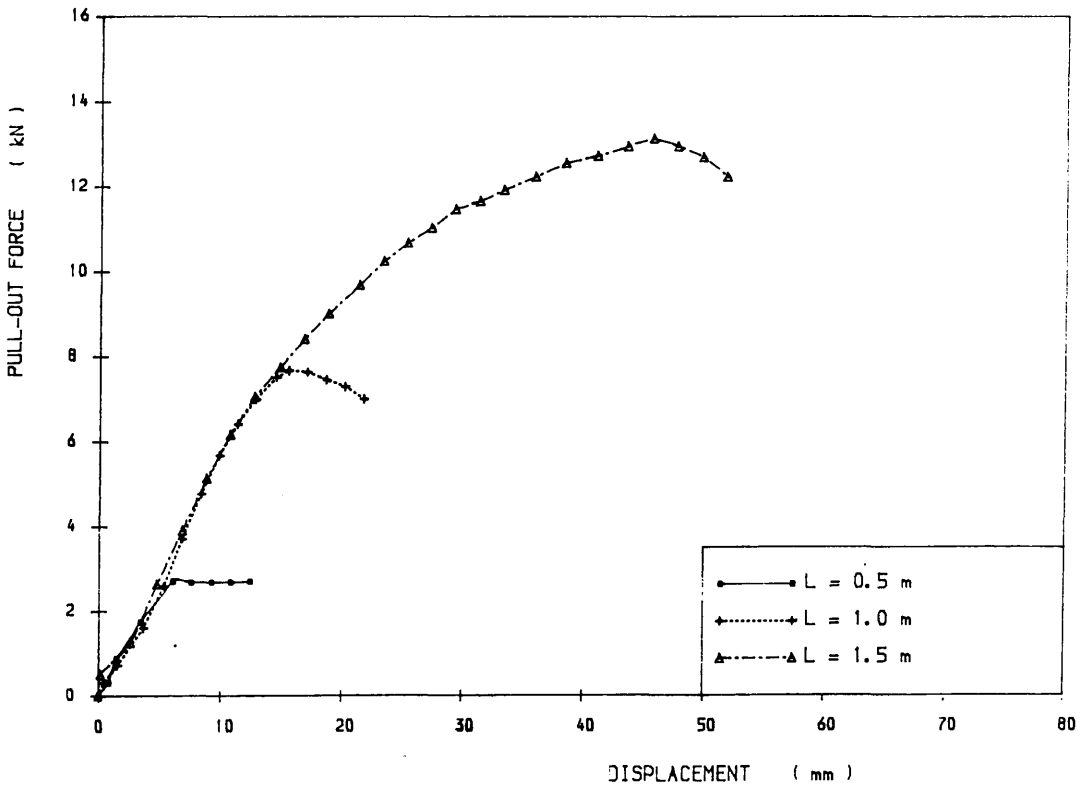


Figure 5.48 PULL-OUT FORCE VS. STRAP DISPLACEMENT  
 Loudon Hill Sand,  $\gamma_d=16.190\text{kN/m}^3$ , Paralink 500s,  $\sigma_v=120\text{kN/m}^2$

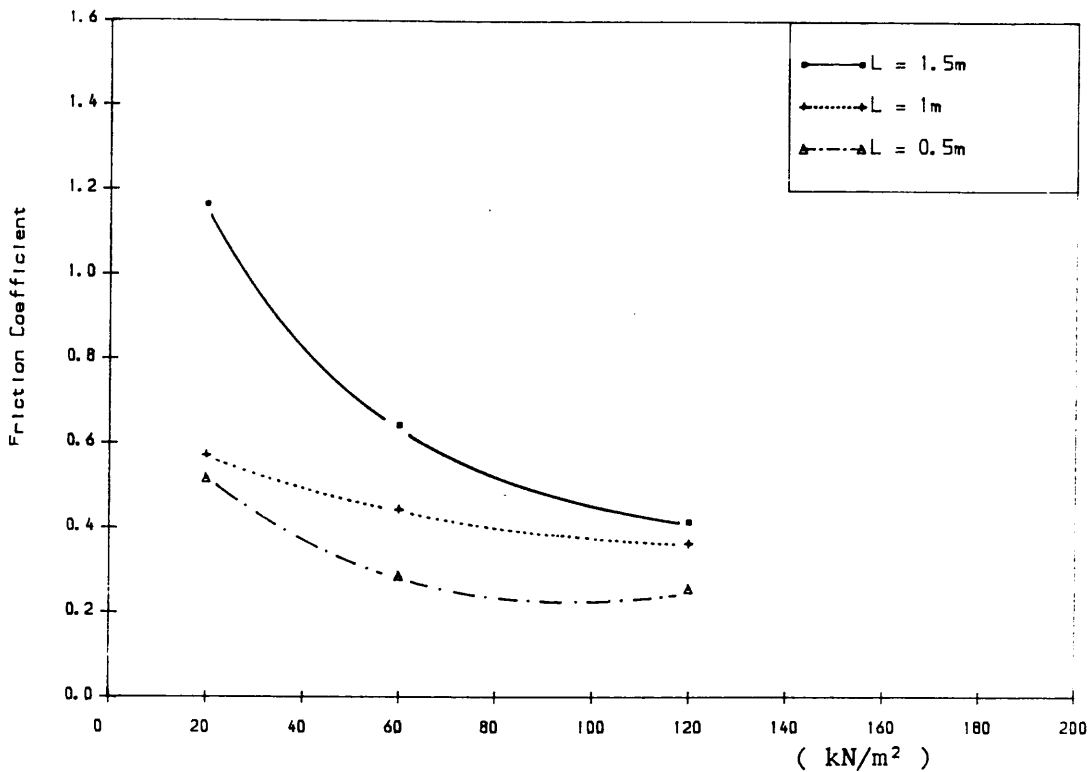


Figure 5.49 FRICTION COEFFICIENT VS. OVERBURDEN PRESSURE

Laboratory Pull-out Test, Loudon Hill Sand, Paralink 500s,  $\gamma_d=16.190\text{kN/m}^3$

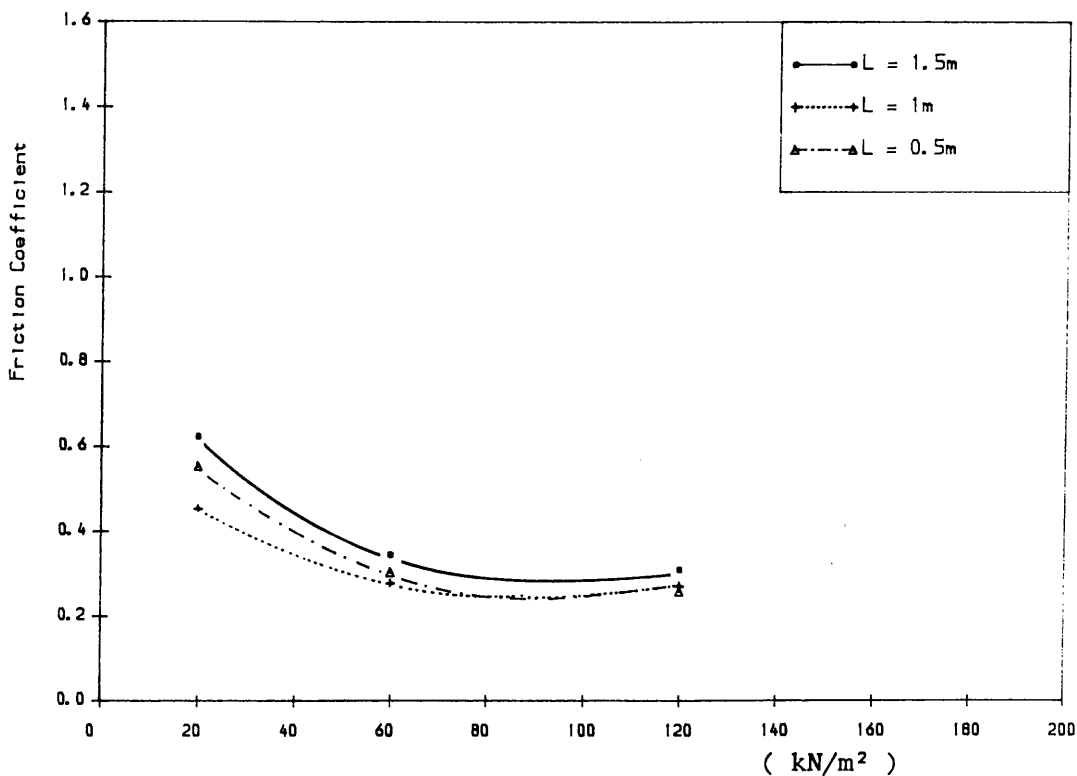


Figure 5.50 FRICTION COEFFICIENT VS. OVERBURDEN PRESSURE

Laboratory Pull-out Test, Loudon Hill Sand, Paralink 300s,  $\gamma_d=16.190\text{kN/m}^3$

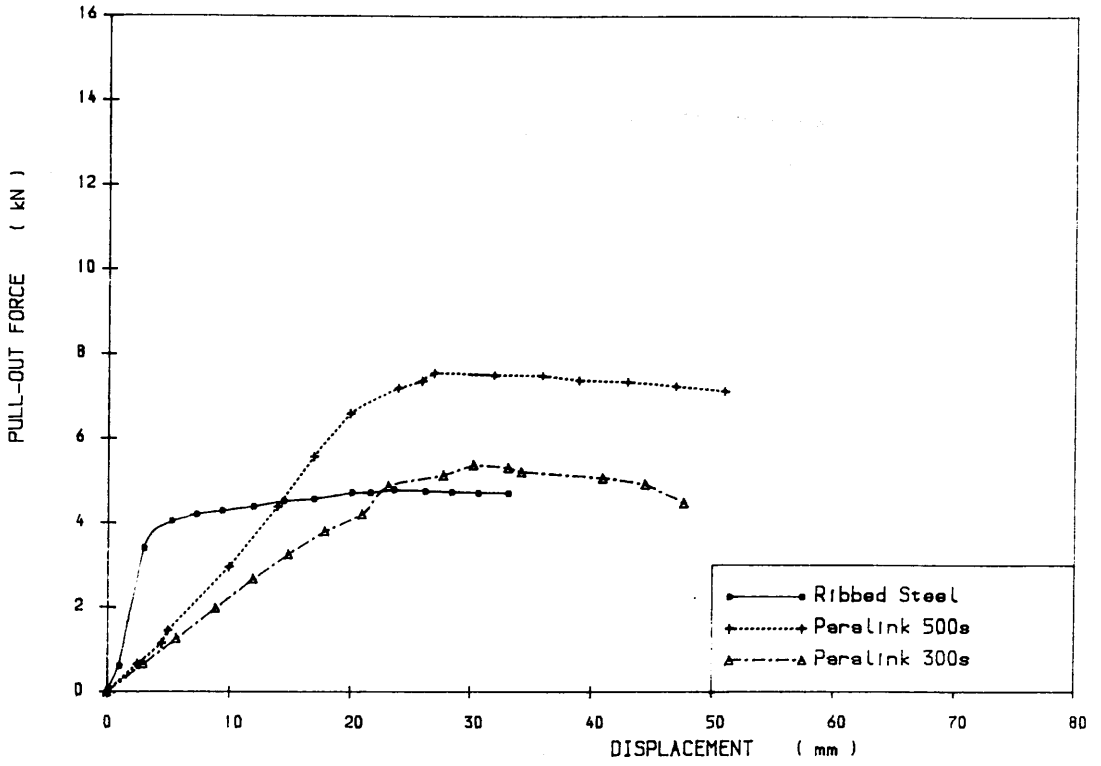


Figure 5.51 PULL-OUT FORCE VS. STRAP DISPLACEMENT

Laboratory Test, Methil PFA,  $L=1.5m$ ,  $\gamma_d=11.590kN/m^3$ ,  $\sigma_v=60kN/m^2$

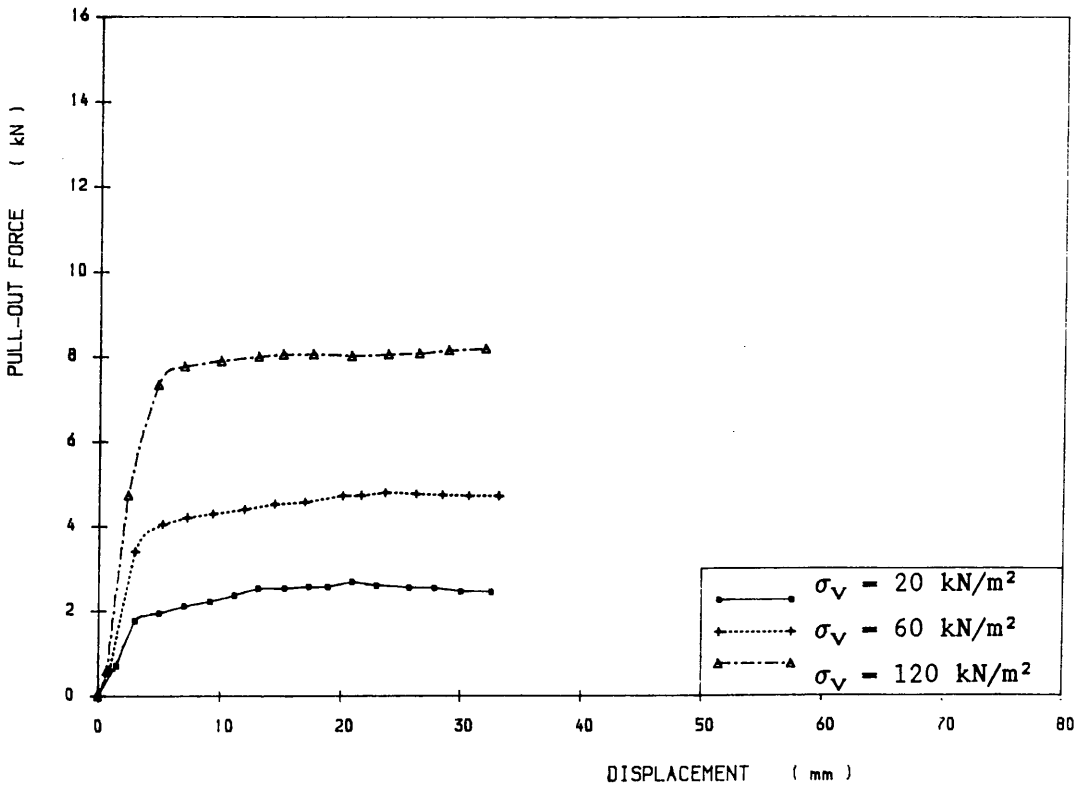


Figure 5.52 PULL-OUT FORCE VS. STRAP DISPLACEMENT

Laboratory Test, Methil PFA,  $L=1.5m$ ,  $\gamma_d=11.590kN/m^3$ , Ribbed Steel

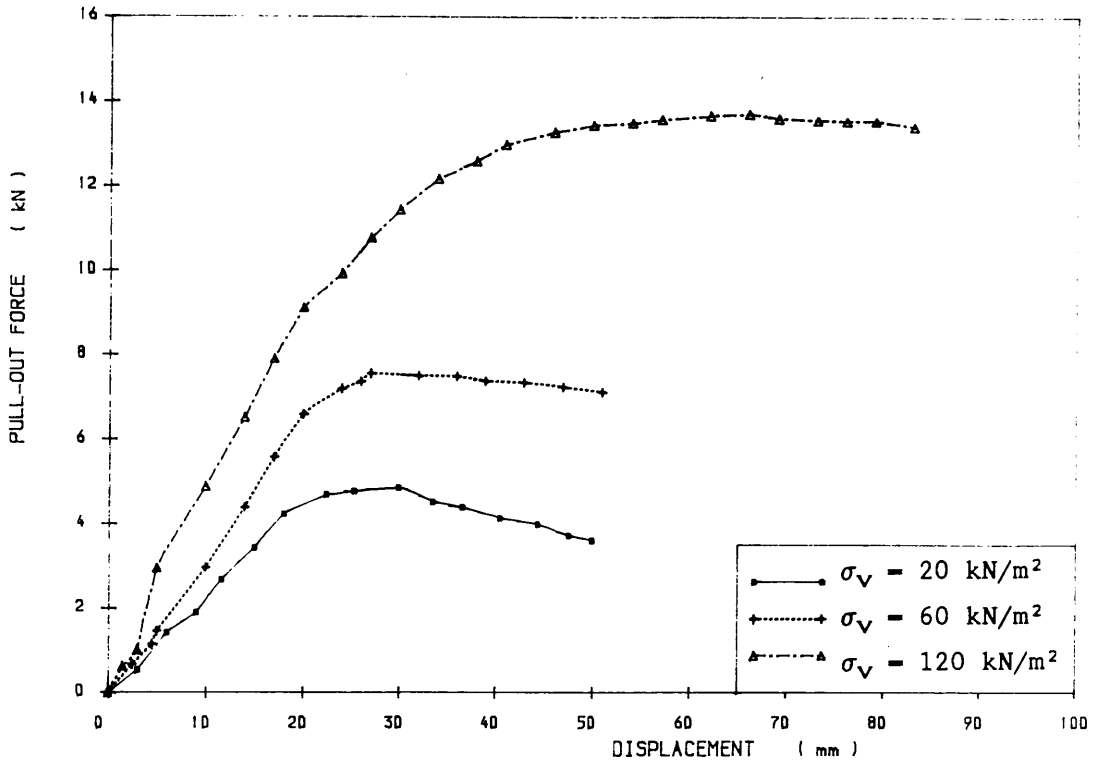


Figure 5.53 PULL-OUT FORCE VS. STRAP DISPLACEMENT

Laboratory Test, Methil PFA,  $L=1.5\text{m}$ ,  $\gamma_d=11.590\text{kN/m}^3$ , Paralink 500s

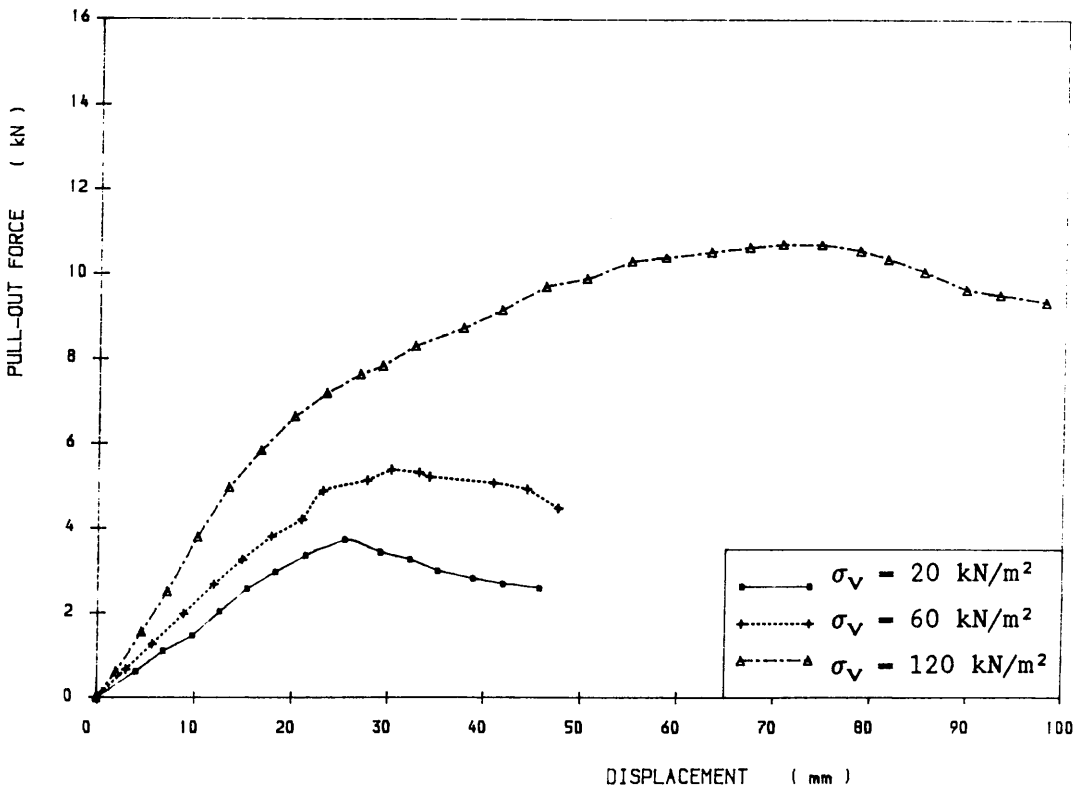


Figure 5.54 PULL-OUT FORCE VS. STRAP DISPLACEMENT

Laboratory Test, Methil PFA,  $L=1.5\text{m}$ ,  $\gamma_d=11.590\text{kN/m}^3$ , Paralink 300s

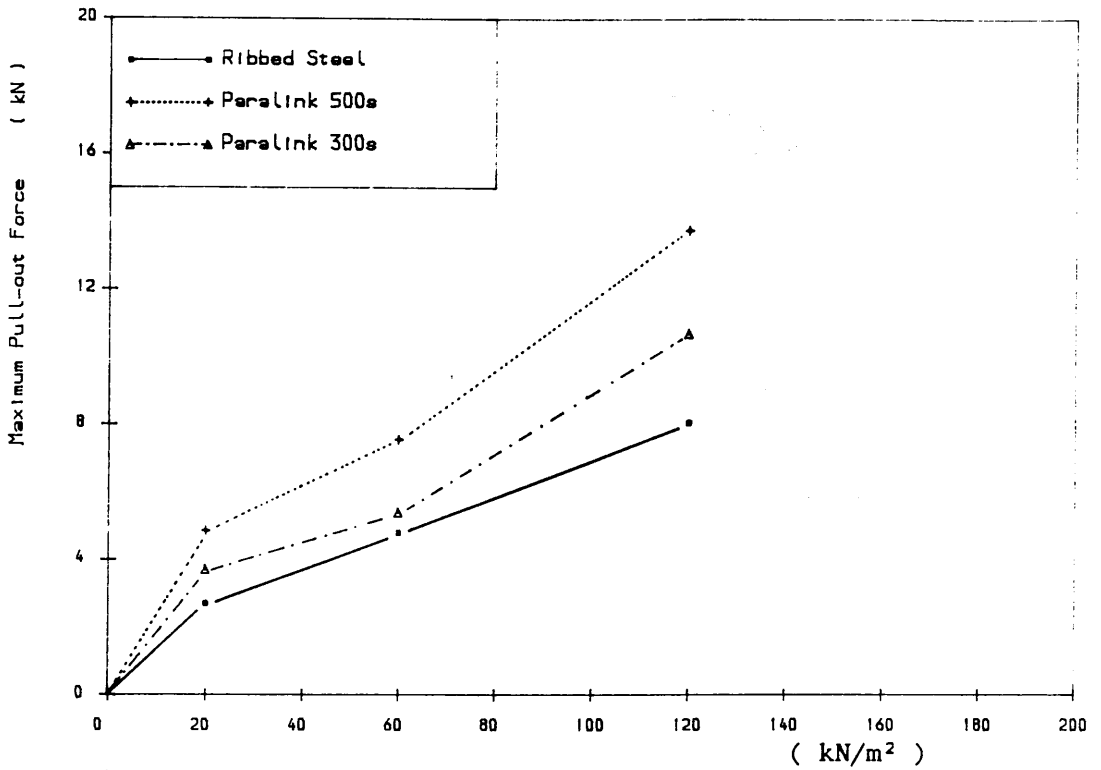


Figure 5.55 MAXIMUM PULL-OUT FORCE VS. OVERBURDEN PRESSURE  
 Laboratory Pull-out Test, Methil PFA,  $\gamma_d=11.590\text{kN/m}^3$ ,  $L=1.5\text{m}$

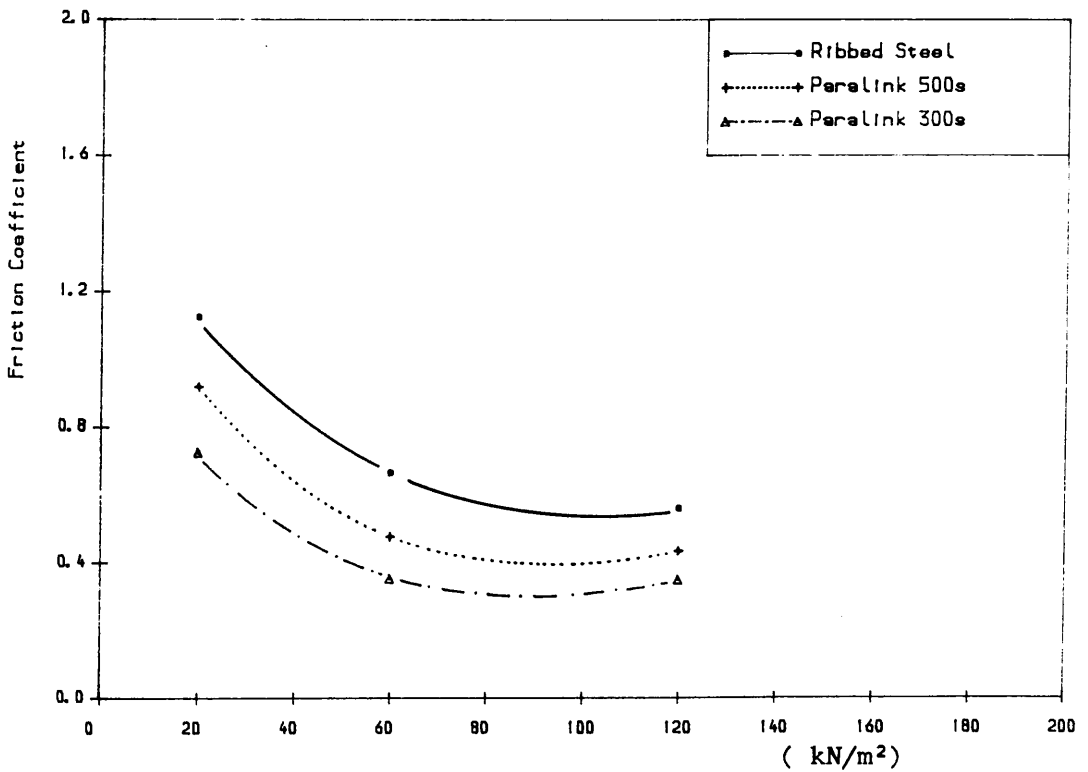


Figure 5.56 FRICTION COEFFICIENT VS. OVERBURDEN PRESSURE  
 Laboratory Pull-out Test, Methil PFA,  $\gamma_d=11.590\text{kN/m}^3$ ,  $L=1.5\text{m}$

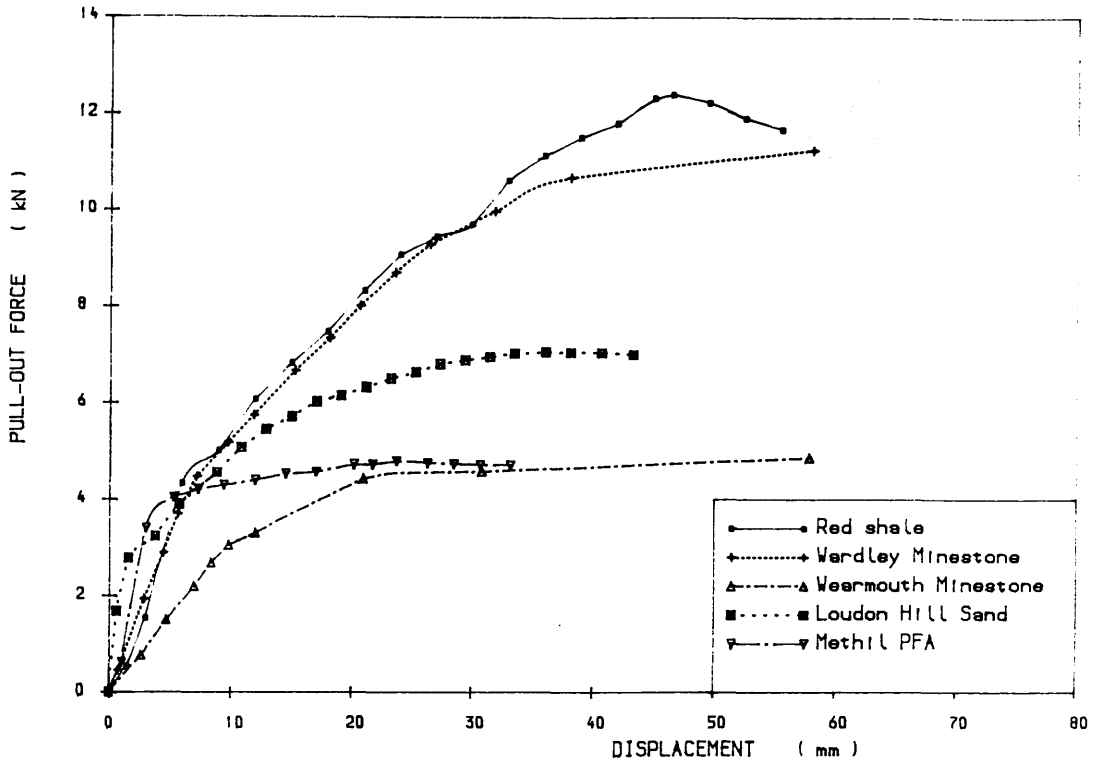


Figure 5.57 PULL-OUT FORCE VS. STRAP DISPLACEMENT  
 Laboratory Test, Ribbed Steel,  $\sigma_v = 60 \text{ kN/m}^2$

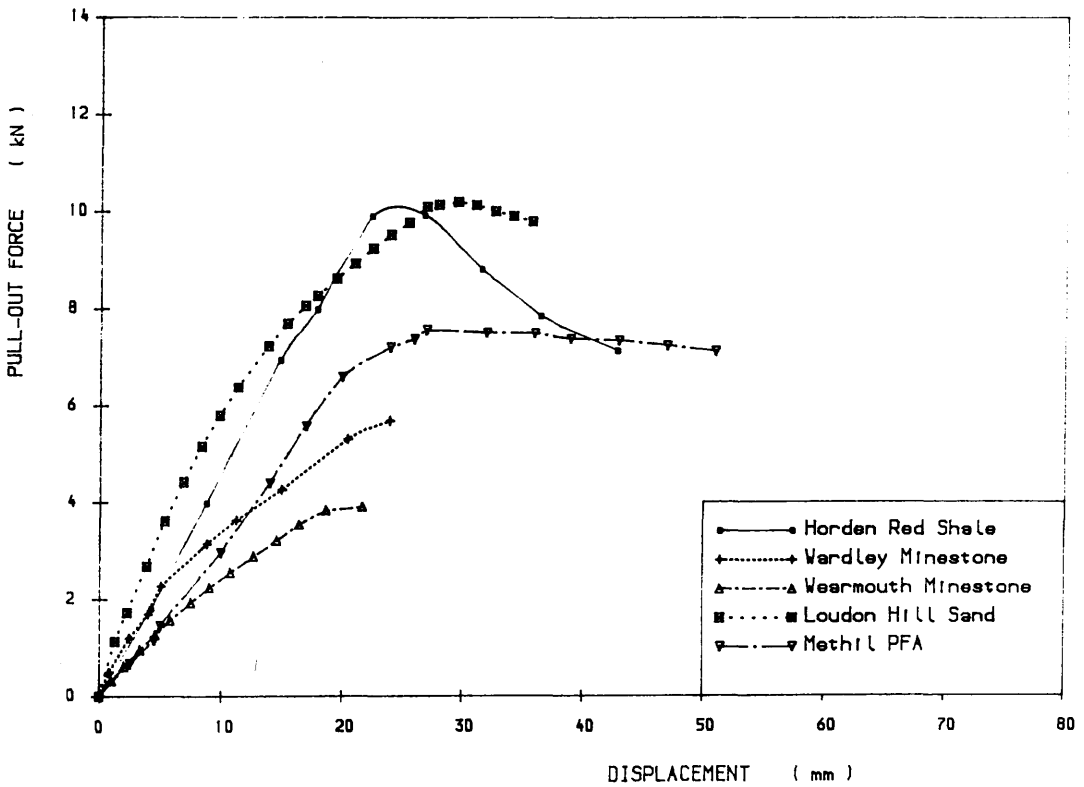


Figure 5.58 PULL-OUT FORCE VS. STRAP DISPLACEMENT  
 Laboratory Test, Paralink 500s,  $\sigma_v = 60 \text{ kN/m}^2$

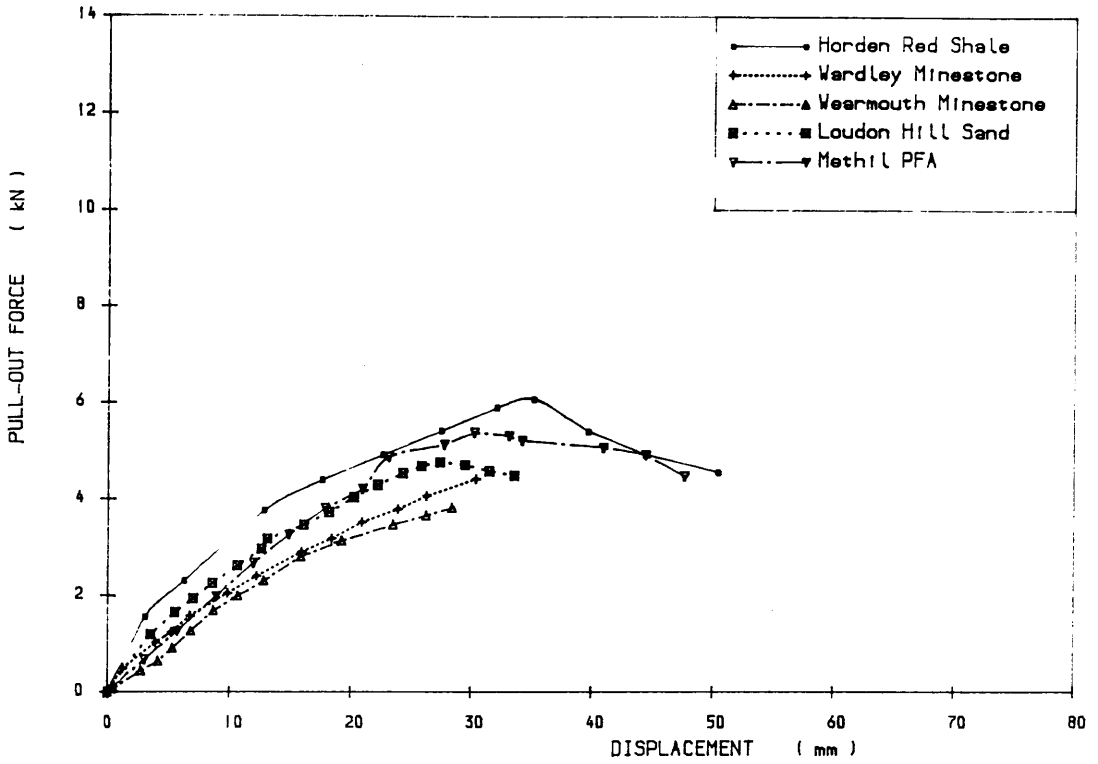


Figure 5.59 PULL-OUT FORCE VS. STRAP DISPLACEMENT

Laboratory Test, Paralink 300s,  $\sigma_v = 60 \text{ kN/m}^2$

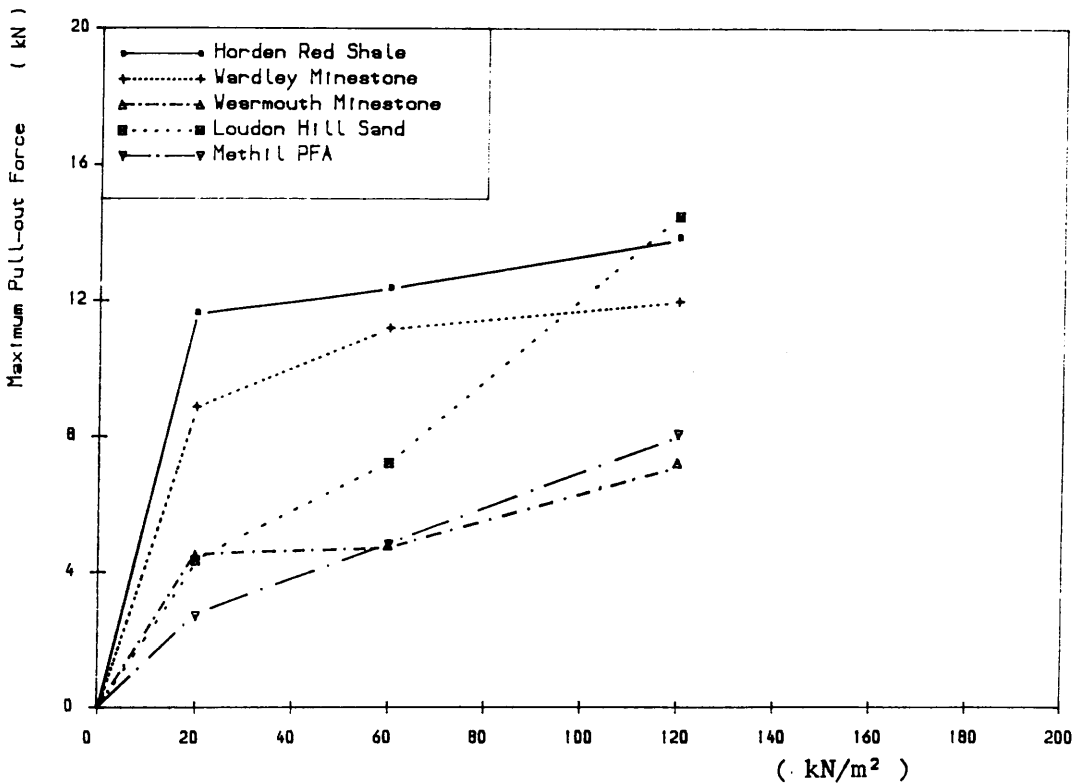


Figure 5.60 MAXIMUM PULL-OUT FORCE VS. OVERBURDEN PRESSURE

Laboratory Test, Ribbed Steel,  $L = 1.5\text{m}$

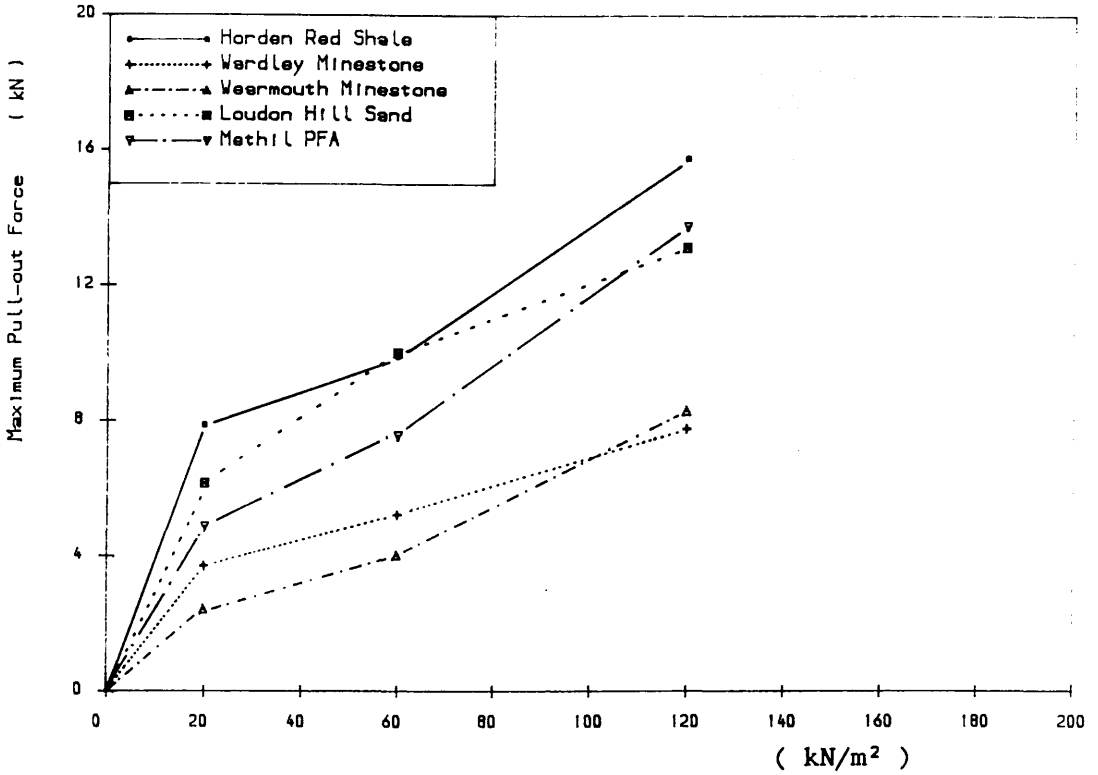


Figure 5.61 MAXIMUM PULL-OUT FORCE VS. OVERBURDEN PRESSURE

Laboratory Test, Paralink 500s, L = 1.5m

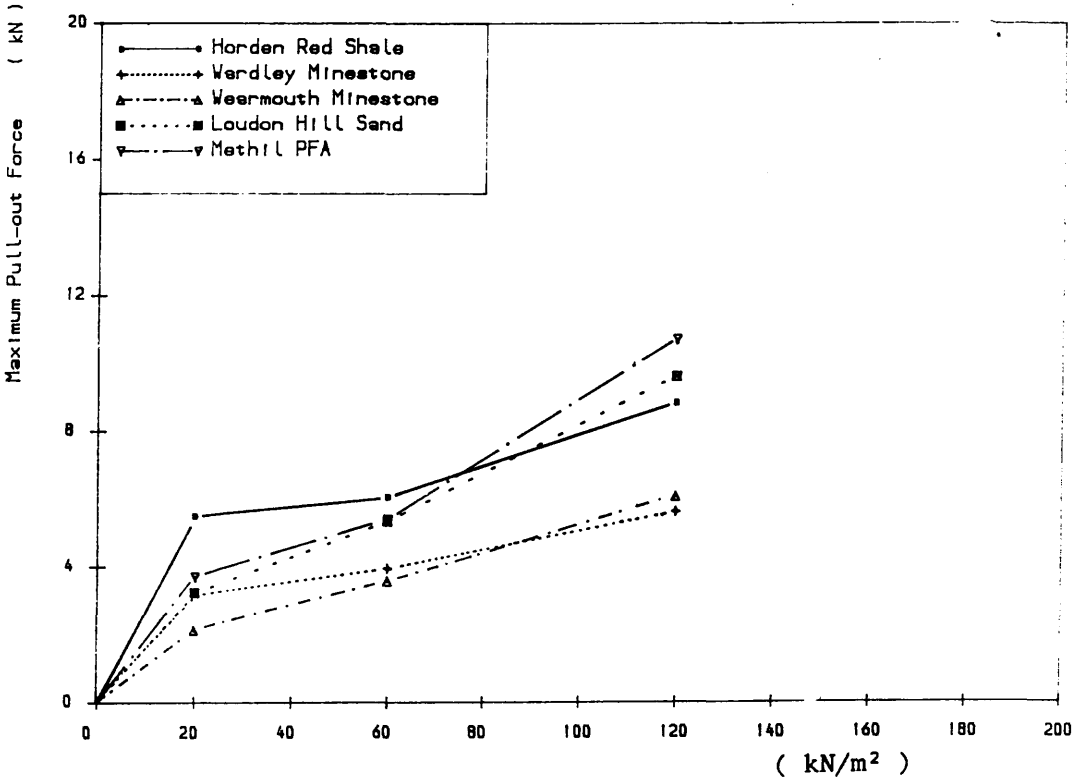


Figure 5.62 MAXIMUM PULL-OUT FORCE VS. OVERBURDEN PRESSURE

Laboratory Test, Paralink 300s, L = 1.5m

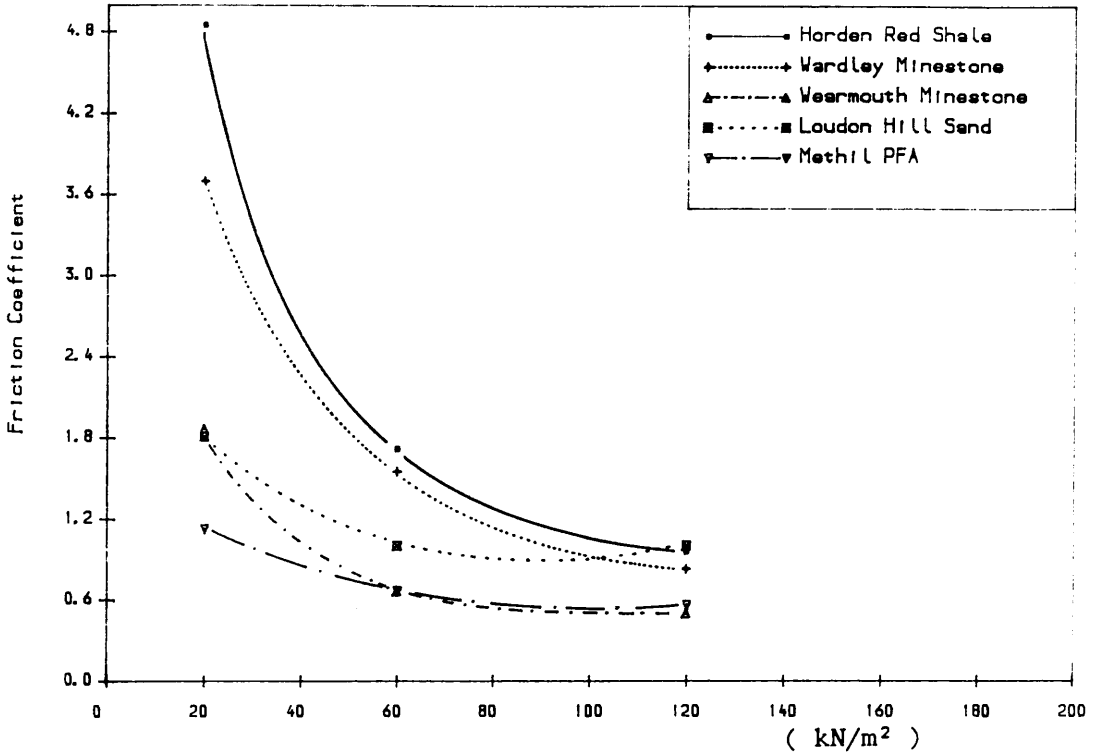


Figure 5.63 FRICTION COEFFICIENT VS. OVERBURDEN PRESSURE  
Laboratory Pull-out Test, Ribbed Steel, L = 1.5m

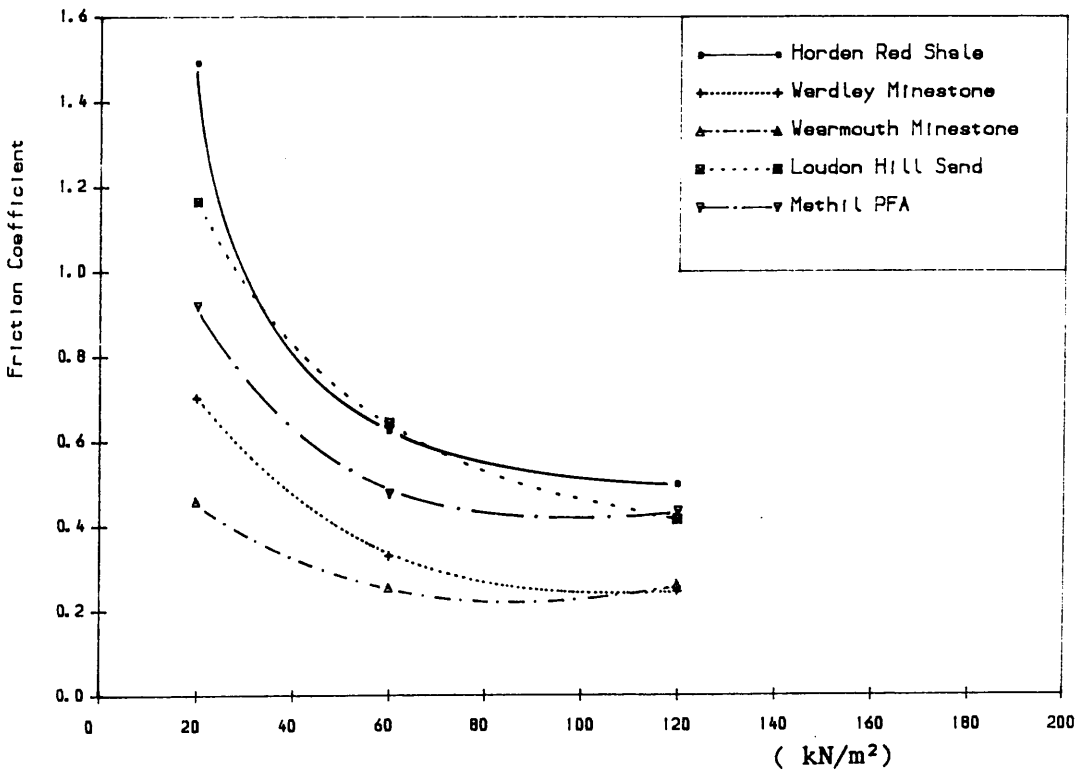


Figure 5.64 FRICTION COEFFICIENT VS. OVERBURDEN PRESSURE  
Laboratory Pull-out Test, Paralink 500s, L = 1.5m

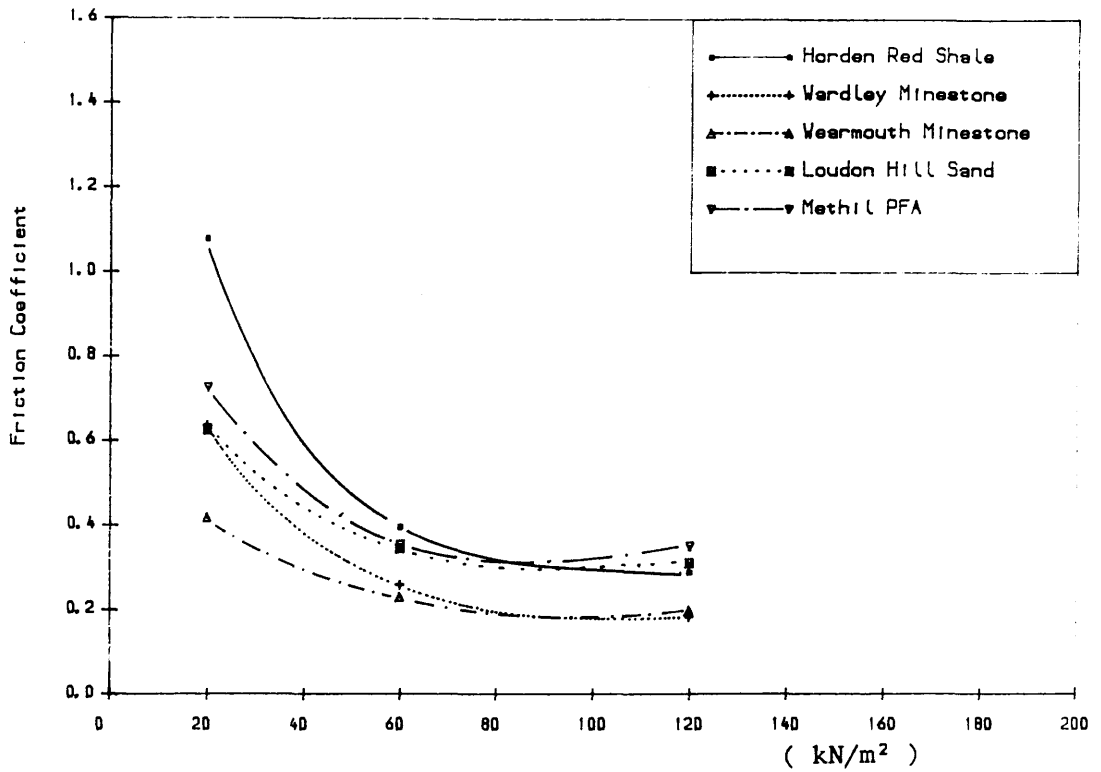


Figure 5.65 FRICTION COEFFICIENT VS. OVERBURDEN PRESSURE  
 Laboratory Pull-out Test, Paralink 300s, L = 1.5m

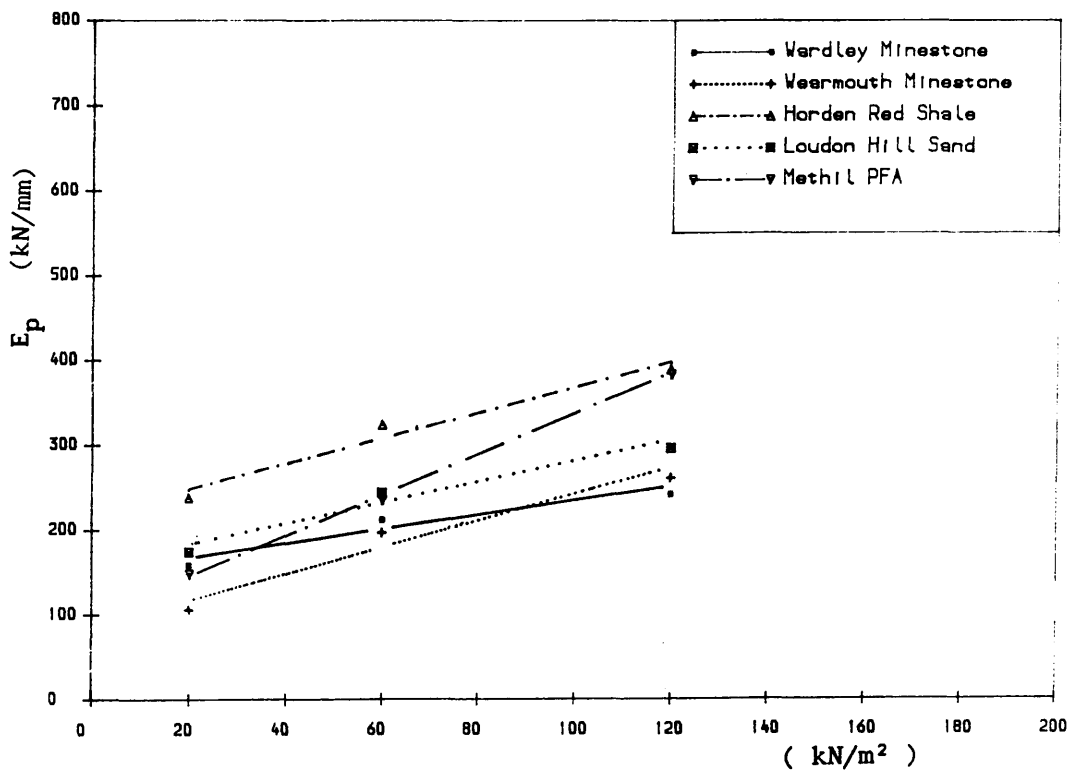


Figure 5.66 PULL-OUT STIFFNESS VS. OVERBURDEN PRESSURE  
 Laboratory Pull-out Test, Paralink 300s, L = 1.5m

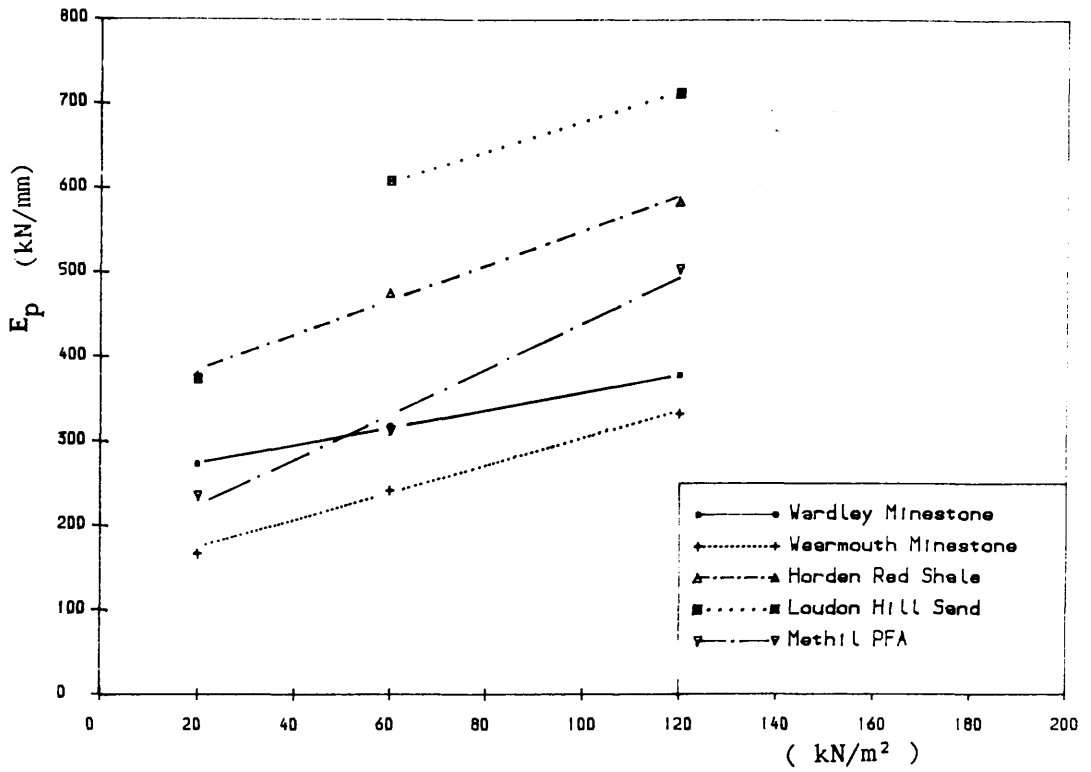


Figure 5.67 PULL-OUT STIFFNESS VS. OVERBURDEN PRESSURE  
 Laboratory Pull-out Test, Paralink 500s, L = 1.5m

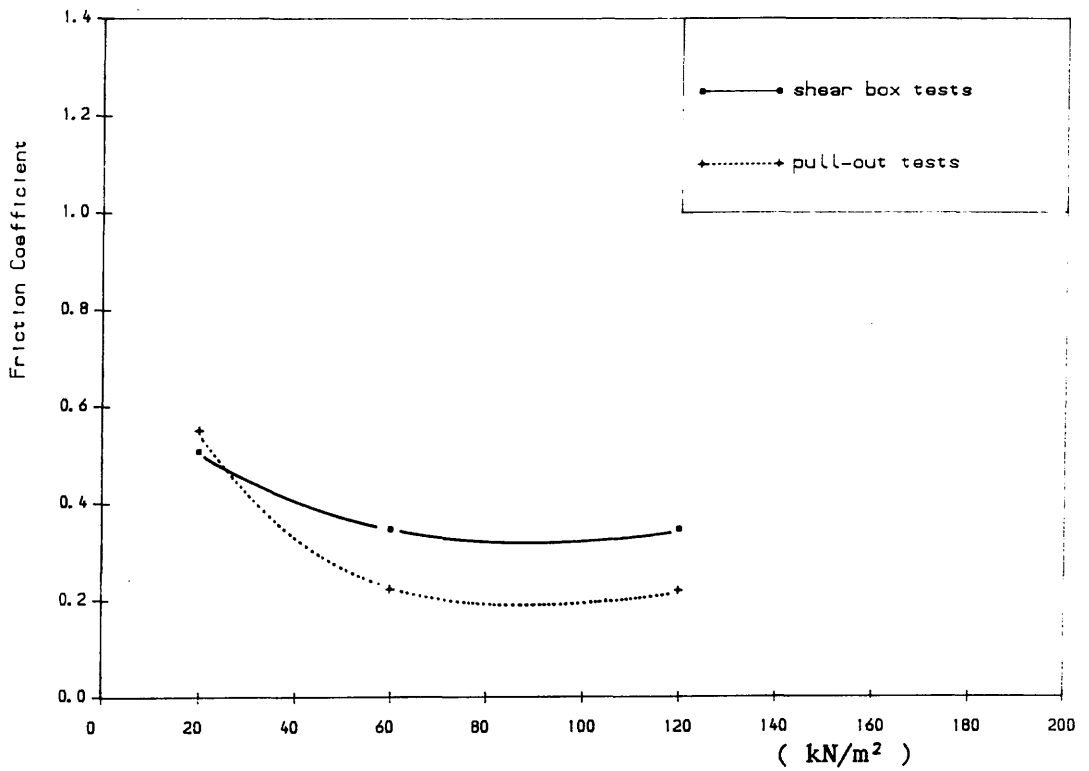


Figure 5.68 COMPARISON OF PULL-OUT AND SHEAR BOX TEST RESULTS  
 Paralink 300s with Wardley Minestone

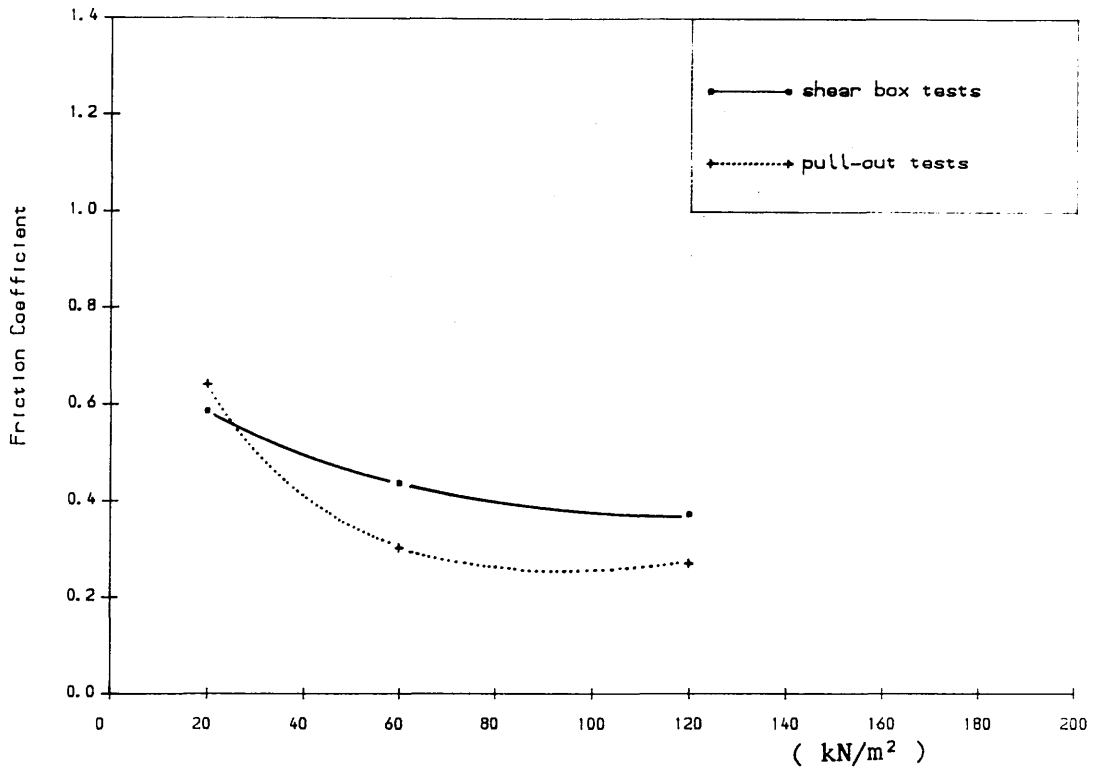


Figure 5.69 COMPARISON OF PULL-OUT AND SHEAR BOX TEST RESULTS  
Paralink 500s with Wardley Minestone

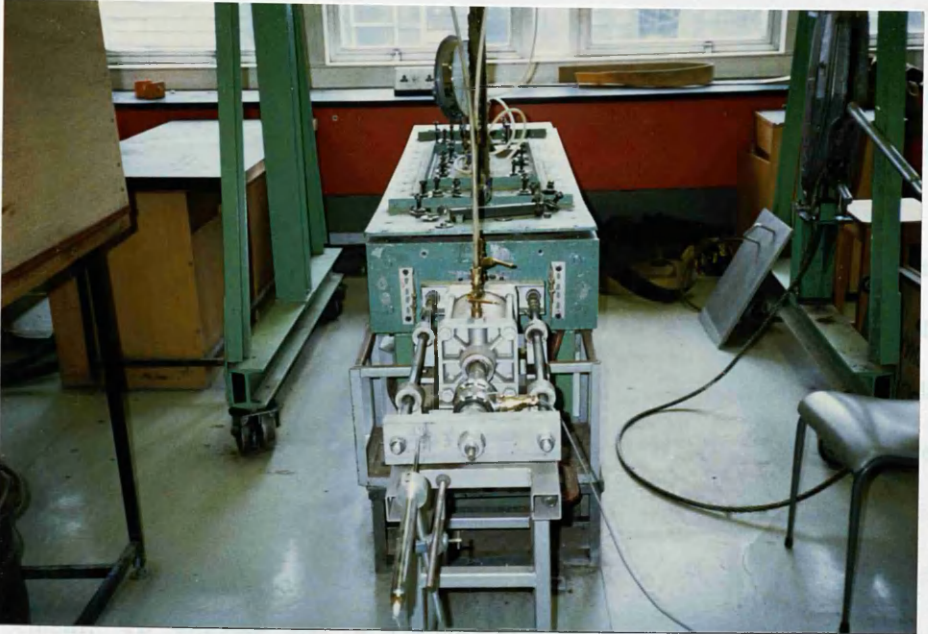


Plate 5.1 LOAD-CONTROLLED PULL-OUT BOX



Plate 5.2 DISPLACEMENT-CONTROLLED PULL-OUT BOX

## CHAPTER 6

### SOME SPECIFIC PULL-OUT TESTS

#### 6.1 INTRODUCTION

Pull-out box tests have been described and a number of test results presented in the last chapter. However, some queries are raised when analysing these results, especially comparing the shear box and pull-out tests, since when Paralink reinforcement was used the former produced higher results than the latter, in direct contradiction to the generally accepted behaviour of metallic reinforcing material. It was thought that these contradictory results must be related to the extensibility of the reinforcement. To explain this, a further understanding of the behaviour of Paralink strap in a pull-out test is required. In order to reach this understanding, Paralink strap pull-out tests monitored with "piano wires" were carried out. For a direct comparison between rigid and extensible straps, some pull-out tests with "sandwich" straps were also conducted. In addition, in order to investigate the effect of dilatancy, pull-out of a strap with pressure cells was performed. Pull-out with facing plate was also used to check the influence of the facing plate on the pull-out results. These specific tests were carried out using the same pull-out boxes as described in the last chapter. The tests and results are shown in this chapter

#### 6.2 TEST DESCRIPTION

##### (1) Pull-out tests monitored with "piano wires"

An attempt was made to investigate the pull-out behaviour of the Paralink straps by measuring the extensibility or the strain (or stress) distribution in the straps. A common way of doing this is by using strain gauges, but in the case of

the Paralink straps, difficulties were encountered in fixing strain gauges due to the large extension behaviour of the material. To overcome this problem of the measurement of large movements, "piano wires" 0.3mm diameter were used in the following way. In a test, three wires were fixed to a 1.5 m strap at intervals of 0.5 m (see *Figures 5.1* and *5.2* in Chapter 5) through eyelets in the strap. The other ends of the wires were led out of the box through three metallic tubes embedded in the box at the end and the same level of the strap. During preparation the wires were kept straight by using three small weights fixed at the ends. When compaction was completed, the weights were taken off and the wires were fixed to displacement transducers (see *Plate 6.1*). The movements of the wires at different points along the strap were monitored during application of the pull-out force. Since the wires were so thin, had a smooth peripheral surface, and were inextensible relative to the strap, the movements of the wires could be expected as to give displacements (or extension) of the strap at these points, and consequently the strain distribution could be determined.

## (2) "Sandwich" straps

In order to investigate the influence of extensibility on the pull-out force (or the friction coefficient) and displacement, two 1.5 m length "sandwich" straps were prepared with Paralink 300s and 500s respectively (see *Plate 6.2*). A "sandwich" strap consisted of two Paralink straps with a metallic strap sandwiched between. The metallic strap was 2 mm thick, the same length and width as the Paralink straps and relatively rigid in tension. The Paralinks were glued firmly on both sides of the metallic strap with adhesive and also fixed with a number of rivets. The surfaces of the "sandwich" strap were therefore kept the same as the Paralink's. The rivets were ground flush with the strap surface to reduce any excess resistance caused by them. The same clamp as used for ribbed steel strap in the pull-out tests was employed to connect via the holes at the pulling end of the strap. Since, in

pull-out tests with the "sandwich" straps, the Paralink straps did not stretch, a comparison of the straps in the two conditions, extensible and rigid, could be made.

### (3) Pull-out of a strap with pressure cells

A special ribbed steel strap with pressure cells fixed was designed and a test was performed with it. Four pressure cells 4 mm thick by 20 mm diameter were manufactured from aluminium alloy and instrumented with Redshaw strain gauges. Along the strap four 21 mm diameter by 4 mm deep holes were made to fit the pressure cells. The cells were glued in with the active face flush with the strap surface (see *Plate 6.2*). During the test preparation, a tube was embedded beside and at the same level as the strap, so that the cables from the pressure cells could be led out through the box and connected to a data logger. Before testing, a calibration test was conducted by increasing the normal pressure in 10 kN/m<sup>2</sup> steps up to 120 kN/m<sup>2</sup>. A test was then performed under a pressure of 60 kN/m<sup>2</sup>.

### (4) "Pull-out with facing plate"

A few tests were performed on "pull-out with facing plate" in the load controlled box. Unlike the other tests in which the facing was fixed to the box, during this test it was fixed to the yoke and the strap so that the strap and the facing plate moved together under the pulling force. Therefore, the effects of any resistance to pull-out caused by the facing could be eliminated, and the situation would be similar to that in a real structure.

## 6.3 TEST RESULTS

### 6.3.1 Pull-out Tests with "Piano Wire" Monitoring

A series of pull-out tests on Paralink straps monitored with "piano wires" were performed. The results obtained are presented.

#### i) Paralink behaviour in pull-out tests

Two sets of typical force-displacement curves are shown in *Figures 6.1 and 6.2*. The results were obtained by testing Loudon Hill sand with Paralink 300s and Paralink 500s respectively. These curves show the performance of a strap during pulling when embedded in the fill. Because of the extensibility, a differential movement of a Paralink strap was produced, with the extension of the strap produced by the pulling force starting from the "clamped" end and being transmitted towards the other end (the free end). In other words, the frictional mechanism, as well as the stress distribution during pulling action was mobilized increasingly along the strap's length. This phenomenon could be observed from these curves. The "clamped" end started moving once the pulling force was imposed, but there was no movement at the point 500 mm (No.1 wire) from the "clamped" end until the force reached a certain amount. Then with a further increase of the pulling force, the point at 1000 mm (No.2 wire) began to move. Eventually the free end (No.3 wire) started moving, at about the same time as the maximum force was produced. Therefore at the beginning when the pulling force was imposed, it was not the whole strap but only some of the front part of it which was being stressed. This indicates the different performance when compared with a metallic strap, which can be regarded as so rigid that the whole strap moves simultaneously during pulling.

ii) Extension and strain distribution along a Paralink strap

The movements monitored with "piano wires" at the three points at intervals of 500 mm and the movement of the "clamped" end were obtained at the moment the free end started moving. These movements actually represented the differential extension along the strap at about failure and they are shown in *Figures 6.3 to 6.8*. Some third power curves were obtained from these results by means of a regression analysis. In each figure the distribution curves at different overburden pressures are shown. Higher pull-out forces and greater extensions were produced at higher overburden pressures, but it was observed that nearer the free end, the difference in extension caused by the overburden pressure (or pulling force) became less. These curves can be expressed by the following polynomial expression:

$$D(x) = b_0 + b_1x + b_2x^2 + b_3x^3 \quad (6.1)$$

where  $D(x)$  — extension at the point,

$x$  — the distance of the point from the clamped end.

The constants  $b_0$ ,  $b_1$ ,  $b_2$  and  $b_3$  obtained by regression analysis are presented in *Table 6.1*.

The strain distribution at the failure load, therefore, can be easily gained by differentiation of equation (6.1).

$$\epsilon(x) = D'(x) = b_1 + 2b_2x + 3b_3x^2 \quad (6.2)$$

where  $\epsilon(x)$  — strain along the strap.

The strain distributions calculated from equation (6.2) are shown in *Figures 6.9 to 6.14*. The highest strain was found at the "clamped" end and decreased

towards the free end. The small strains apparently present at the free end in some results were not unexpected, because, since the strain was calculated indirectly from the extension, some small errors might appear in the strain results.

### 6.3.2 Results from Tests with "Sandwich" Straps

In order to investigate the influence of strap extensibility on the test results, two "sandwich" straps were manufactured as described previous. A series of tests was carried out with these straps and Wardley minestone at a density of 16.579 kN/m<sup>3</sup> and natural moisture content of 9.7%. The load-controlled pull-out box was used in these tests. The results of the tests are presented and compared with the results from the Paralink straps under the same testing conditions.

*Figures 6.15 and 6.16* show the force-displacement curves from the tests with the Paralink straps and the "sandwich" straps under three different overburden pressures. A different behaviour of the two types of strap in pulling action was observed. The two figures indicate that the force-displacement curves with the "sandwich" strap show a linear relationship and a stiffer behaviour than the Paralink straps. This is due to the "sandwich" straps possessing relatively rigid characteristics, and therefore little extension during the pull-out action. The Paralink straps on the other hand behaved relatively extensibly, the higher extension during pulling causing larger displacement in the force-displacement curves.

In addition to the different pattern of the force-displacement curves, another important point also noted was that higher pull-out forces were obtained from the "sandwich" straps than from the Paralink straps. The test results in terms of maximum pull-out force, shear stress and apparent friction coefficient are all presented in *Table 6.2*. Comparing the two, extensible and rigid, straps in terms of apparent friction coefficient, up to 27% higher value of  $f^*$  could be obtained from the rigid "sandwich" straps. This result was consistent with that obtained by Jewell (1980) who found the maximum pull-out force for an extensible bar reinforcement

was significantly less than that for a stiff bar (see *Figure 2.28*).

### 6.3.3 Results from Test with Strap Monitored by Pressure Cells

This test has been described in section 6.1, and it was used to investigate the possible enhancement of normal stress due to dilatancy in a pull-out test.

The special ribbed steel strap fitted with four pressure cells was tested with Loudon Hill sand. The sand was prepared at the natural moisture content of 7.1% and a density of  $16.19 \text{ kN/m}^3$ . A test was conducted under the overburden pressure of  $60 \text{ kN/m}^2$ . Unfortunately one of the pressure cells was damaged because its cable snapped. The other three cells, however, showed some interesting results and these are shown in *Figure 6.17*.

The normal pressure measured by the cells showed an increasing trend during pulling action. It can be seen from *Figure 6.17* that when the pulling action started, the applied pressure remained unchanged until a certain amount of pulling force or displacement, and then started to increase rapidly. The pressure, according to the measurement of the cells, increased up to three times that of the initial applied overburden pressure. These results proved what McKittrick (1979) suggested, i.e. in a pull-out test the dilatancy of the fill material could act locally to enhance the normal stress. Because of the enhanced normal stress, a higher pull-out resistance could be produced.

### 6.3.4 Results of Pull-out with Facing Plate Tests

A series of pull-out with facing plate tests were carried out using Paralink 500s strap with Wardley and Wearmouth minestones respectively. Wardley minestone was prepared at a natural moisture content of 9.7% and a density of  $17.847 \text{ kN/m}^3$ , and Wearmouth minestone at a natural moisture content of 5.7% and a density of  $17.658 \text{ kN/m}^3$ . The tests were conducted using the load controlled pull-out box.

Figures 6.18 and 6.19 show the results of apparent friction coefficient versus overburden pressure. The results of pull-out tests with and without facing plate moving are shown together for comparison. Lower results were obtained from the tests with facing plate pull-out. This was consistent with results reported by Khattri (1982). At 20 kN/m<sup>2</sup> of  $\sigma_v$ , about 24% and 46% lower values of  $f^*$  were obtained from Wardley minestone and Wearmouth minestone respectively when using pull-out with facing plate tests. When the overburden pressure was high the two different types of tests did not show a great difference.

Therefore with the two minestones the facing resistance influenced the value of  $f^*$  only when the overburden pressure was low. At high  $\sigma_v$  the pull-out through a slot and with facing plate produced almost the same results.

#### 6.3.5 Comparison of Load and Displacement-Controlled Pull-out Box Tests

As has been described previously, two different kinds of pull-out apparatus were employed in the present research, i.e. load and displacement controlled boxes. Some tests were conducted using the load controlled box and others using the displacement controlled box. When making comparison of these results, a query might be raised that if the two control systems can influence the testing results, are results tested from the different boxes comparable? With the load controlled system, the pulling force was applied by compressed air pressure through a cylinder at a constant rate of 50 N/min, whereas with the displacement controlled system, the pulling force was applied using a pulling machine at a constant rate of 1.5 mm/min.

In order to make sure of this point, two comparative tests were performed. The tests were prepared with loose density state (uncompacted), so that any difference that might be caused by non-uniform compaction could be eliminated.

Tests were carried out with Paralink 300s and the red shale using the two different control systems. The tests were prepared at the same condition, i.e. a moisture content of 12.5% and a density of 14.327 kN/m<sup>3</sup>.

The force–displacement curves at an overburden pressure of 60 kN/m<sup>2</sup> from the two types of test are shown in *Figure 6.20*. From this figure one can see that the same pattern of curves and very good agreement of the maximum pull–out forces were produced. The values of  $f^*$  obtained were 0.352 and 0.341 from the load and displacement–controlled tests respectively. Hence the difference of the control systems did not have any evident influence on the testing results.

#### 6.4 DISCUSSION

An important finding from the pull–out tests with "piano wires" was the behaviour of an extensible strap, which appeared to be different from a rigid one. Unlike a rigid metallic strap with which an increase in pulling force causes a movement of the whole strap, with the Paralink strap at the earlier stage, increasing the pulling force causes the elongation of only part of the strap. This behaviour should be taken into account in the analysis of the testing results.

When comparing the results from the two different types of test, it was found that in the case of ribbed steel, the pull–out tests produced higher friction coefficients than the shear box tests, but when the Paralink straps were used, opposite results were encountered (except at very low  $\sigma_v$ ). Besides the surface nature, one main difference between the ribbed steel and the Paralink straps was the extensibility. The steel strap might be regarded as rigid relative to the extensible Paralink straps. Therefore the pull–out behaviour was different between the two types of strap. However, in the direct shear box tests the Paralink elements were glued on a wooden block, and the shearing was generated by pushing the soil. There was no tensile stress imposed on the elements, and the behaviour of extensibility was not reflected. In addition, another difference between the two straps was that the ribbed steel behaved as an incompressible inclusion, whereas the Paralink was compressible under normal stress. This behaviour may also cause some differences in the two test methods. It was therefore suspected that the lower friction coefficient obtained from

the pull-out box tests might be due to the extensibility and compressibility of Paralink straps.

Firstly let us discuss the pull-out test of a ribbed steel strap. In a test the strap was embedded in a compacted fill. When a pulling force was applied, the strap tended to move towards the pulling direction, on the other hand, due to the bond resistance generated on the interfaces between the fill and the strap, the fill acted to hold the strap. Therefore any movements of the strap would cause a certain disturbance of the fill around. The disturbance could be more apparent because of the existence of the rib protrusions. Since the fill was compacted, this disturbance would cause some dilatancy of the fill, mostly above and below the strap zone, which in turn could lead to an arching effect producing a considerable pressure on the strap.

Arching is one of the most universal phenomena encountered in soils. If one part of the support of a mass of soil yield while the remainder stays in place the soil adjoining the yielding part moves out of its original position between adjacent stationary masses of soil. The relative movement within the soil is opposed by a shearing resistance within the zone of contact between the yielding and stationary masses. Since the shearing resistance tends to keep the yielding mass in its original position, it reduces the pressure on the yielding part of the support and increases the pressure on the adjoining stationary part (see *Figure a*). This transfer of pressure from a yielding mass of soil onto adjoining stationary parts is commonly called the arching effect, and the soil is said to arch over the yielding part of the support (Terzaghi, 1956). This definition seems to be somewhat different from the case of a pull-out test of a ribbed steel strap, in which arching was caused by the dilatancy of the soil rather than yielding of a support. However, it can be understood that the dilation of the mass of soil adjacent to the strap will also cause a relative movement to the adjoining non-dilating parts which tends to keep the dilating soil in its original position. In this case the arching effect causes an increase of pressure on the dilating part of the soil. Therefore the arching effect due to dilatancy

actually transfers pressure from the adjoining non-dilating parts onto the dilating part, in the present case onto the ribbed steel strap (see *Figure b*).

A theory was proposed by Terzaghi to calculate the reduced pressure due to arching caused by yielding of a support. If it is assumed that the surfaces of sliding between the yielding mass of soil and the adjacent stationary masses are vertical, the problem of computing the vertical pressure on the yielding support becomes identical with the problem of computing the vertical pressure on the yielding bottom of prismatic bins.

*Figure c* is a section through the space between two vertical surfaces of sliding. The shearing resistance of the earth is determined by the equation

$$s = c + \sigma \cdot \tan\phi \quad (6.3)$$

The unit weight of the soil is  $\gamma$  and surface of the soil carries a uniform surcharge  $q$  per unit of area. The ratio between the horizontal and the vertical pressure is assumed to be equal to an empirical constant  $K$  at every point of the soil. The vertical stress on a horizontal section at any depth  $z$  below the surface is  $\sigma_v$ , and the corresponding normal stress on the vertical surface of sliding is

$$\sigma_h = K \cdot \sigma_v \quad (6.4)$$

The weight of the slice with a thickness  $dz$  at a depth  $z$  below the surface is  $2B\gamma dz$  per unit of length perpendicular to the plane of the drawing. The slice is acted upon by the forces indicated in the figure. The condition that the sum of the vertical components which act on the slice must be equal to zero can be expressed by the equation

$$2B \cdot \gamma \cdot dz = 2B(\sigma_v + d\sigma_v) - 2B \cdot \sigma_v + 2c \cdot dz + 2K \cdot \sigma_v \cdot dz \cdot \tan\phi \quad (6.5)$$

or

$$\frac{d\sigma_v}{dz} = \gamma - \frac{c}{B} - K \cdot \sigma_v \frac{\tan\phi}{B} \quad (6.6)$$

and  $\sigma_v = q$  for  $z = 0$

Solving the equations the pressure imposed on a yielding support is:

$$\sigma_v = \frac{B(\gamma - c/B)}{K \cdot \tan\phi} (1 - e^{-K \cdot \tan\phi \cdot z/B}) + q \cdot e^{-K \cdot \tan\phi \cdot z/B} \quad (6.7)$$

The same theory can be applied to the case of arching caused by dilatancy, except that the shearing resistance on the sliding surfaces between the dilating mass and the adjacent stationary masses of the soil acts in the opposite direction. This is shown in *Figure d*, where the shear forces act downwards instead of upwards.

Therefore equation (6.5) becomes

$$2B \cdot \gamma \cdot dz = 2B(\sigma_v + d\sigma_v) - 2B \cdot \sigma_v - 2c \cdot dz - 2K \cdot \sigma_v \cdot dz \cdot \tan\phi \quad (6.8)$$

thus

$$\frac{d\sigma_v}{dz} = \gamma + \frac{c}{B} + K \cdot \sigma_v \frac{\tan\phi}{B} \quad (6.9)$$

and  $\sigma_v = q$  for  $z = 0$ .

Solving these equations

$$\sigma_v = \frac{B(\gamma + c/B)}{K \cdot \tan\phi} (e^{K \cdot \tan\phi \cdot z/B} - 1) + q \cdot e^{K \cdot \tan\phi \cdot z/B} \quad (6.10)$$

Assuming  $K = 0.4$ , and substituting the following conditions from the present test with ribbed steel and Loudon Hill sand:  $B = 0.02\text{m}$ ,  $z = 0.125\text{m}$ ,  $\gamma = 16.19 \text{ kN/m}^3$ ,  $c = 4.6 \text{ kN/m}^2$ ,  $\phi = 37.6^\circ$  and taking the example of overburden pressure  $q = 60 \text{ kN/m}^2$ , the normal stress imposed on the strap was calculated according to

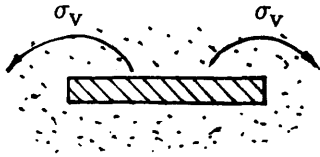


Figure a Arching Effect Caused by Support Yielding.

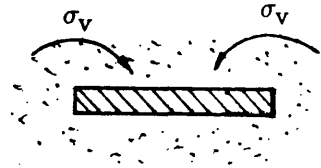


Figure b Arching Effect Caused by Dilatancy

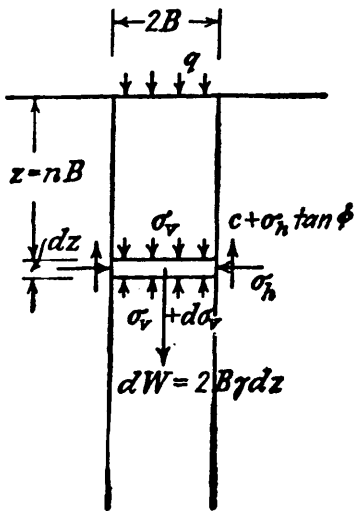


Figure c

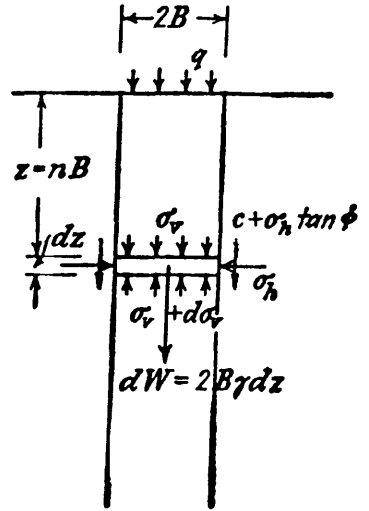


Figure d

equation (6.10) to be  $508 \text{ kN/m}^2$ . This indicates that the normal stress caused by arching effect could be very large. However, this equation gives a limit state, when the shearing resistance is fully generated on the sliding surface. In a pull-out test the arching effect caused by dilatancy might not reach this limit state. The present test with pressure cells monitoring have shown that a vertical stress about three times higher than the applied normal stress was produced during pulling action. Because of the increased normal stress on the strap, a higher pull-out resistance was produced. This may be an explanation of why pull-out tests produced higher friction coefficients than shear box tests when ribbed steel strap was used.

For Paralink straps, the arching effect may act differently. Compared to the rigid ribbed steel straps, the Paralink elements behave more compressibly under normal stresses. Some comparative tests with Loudon Hill sand and the Paralink elements were conducted using consolidation cell apparatus. For the Paralink material a circular element with the same diameter as the consolidation cell was prepared. In a test the strain was measured with increasing normal stress. The results showed that at a normal stress of  $60 \text{ kN/m}^2$ , the strain was found about 1.8% for the sand and 30% for the Paralink elements. This obviously indicated that the Paralink elements were much more compressible than the sand under normal stresses. It can be understood that in a pull-out test, when overburden pressure is applied, the strap, because of its compressibility, will yield relative to the sand around. Therefore arching takes place, but unlike the effect of dilatancy in a ribbed steel strap test, in this case the transfer of pressure is from the compressible strap onto the adjoining soil. This effect reduces the normal stress exerted on the strap. In the case of Loudon Hill sand, if a strap behaves like a fully yielding support, the  $\sigma_v$  exerted on the strap can be computed by equation 6.7, and it can be as low as  $18 \text{ kN/m}^2$  when an overburden pressure of  $60 \text{ kN/m}^2$  is applied. For a thin Paralink strap, however, the compressibility can not give a fully yielding support, and the reduction of normal stress may not be as large as calculated. As mentioned above, the strain of Paralink was found to be 30% under  $60 \text{ kN/m}^2$  normal stress, i.e. the strap

thickness can be reduced by about 1mm. Therefore in the example above 1mm yielding of the strap should be taken into consideration. If the shear stresses at 1mm shearing displacement are taken, an internal shearing angle  $\varphi_1$  and cohesion  $c_1$  are found to be  $8.5^\circ$  and  $2 \text{ kN/m}^2$  respectively with Loudon Hill sand alone. Substituting these values in equation (6.7) the normal stress acting on the strap was calculated to be  $45 \text{ kN/m}^2$  under an overburden pressure of  $60 \text{ kN/m}^2$ . If this overburden pressure ( $45 \text{ kN/m}^2$ ) was taken into account, the apparent friction coefficient was found to be 0.466 rather than 0.345 obtained at  $60 \text{ kN/m}^2$  of  $\sigma_v$ . This calculated value was close to the value of  $\mu = 0.487$  obtained from the shear box tests. Therefore, the arching effect in a Paralink strap pull-out test can cause a reduction in the normal stress and in turn reduce the pull-out resistance. This arching effect is considered to be one of the reasons which lead to a lower value of friction coefficient from pull-out tests than from shear box tests when Paralink reinforcement is used. Some dilatancy may also occur in the fill surrounding a Paralink strap in a pull-out test. But the dilatancy in this case will not be as big as with a ribbed steel, and the compressibility of the strap may offset some of the effect of the dilatancy. However, when the overburden pressure is very low the dilatancy effect may appear to be more dominant and result in a higher friction coefficient from pull-out tests when the overburden pressure is low ( see *Figures 5.69 and 5.70*).

It has also been discovered that the pulling behaviour of a Paralink strap is different from a rigid one. Due to its extensibility, the displacement at different points along a Paralink strap was not uniform but differential during the pulling action. In other words, the displacement generated by the pull-out force proceeds incrementally along the strap from the "clamped" end towards the free end, and when the free end started moving, the maximum force was produced. On the other hand, from a shear box test stress-displacement curve (see *Figures 4.22 and 4.23*), the shear stress increased from zero up to a maximum with a drop after the peak shear stress point. This implies that in a pull-out test, the maximum shear stress is not produced along the whole strap. As a matter of fact, the maximum shear stress

is only generated at the point which has the same displacement as that producing a maximum shear stress in a shear box test. The part which has larger displacement produces residual shear stress, while the part which has smaller displacement produces lower shear stress, and there is no shear stress at the free end because there is zero displacement.

If these characteristics are introduced to analyse a Paralink strap pull-out test, it may help us to further understand the reason why pull-out tests produce lower friction coefficients than shear box tests. Take the shear stresses obtained in a shear box test, and suppose the same shear stresses also occurred in the pull-out test. The maximum shear stress is produced at only one point, in front of this point (towards the "clamped" end), residual shear stress is produced, and beyond this point the shear stress reduces from the maximum to zero at the free end. Using  $\tau_s$  and  $\tau_r$  to stand for the maximum and residual shear stress obtained by shear box tests, find the position along the strap in *Figures 6.5 to 6.8*, which had the same displacement ( $D$ ) as the maximum shear stress in a shear box test, and designate the length from this position to the free end as "a". Assuming the shear stress to be distributed linearly from the maximum to zero at the free end, this can then be illustrated as in *Figure e*.

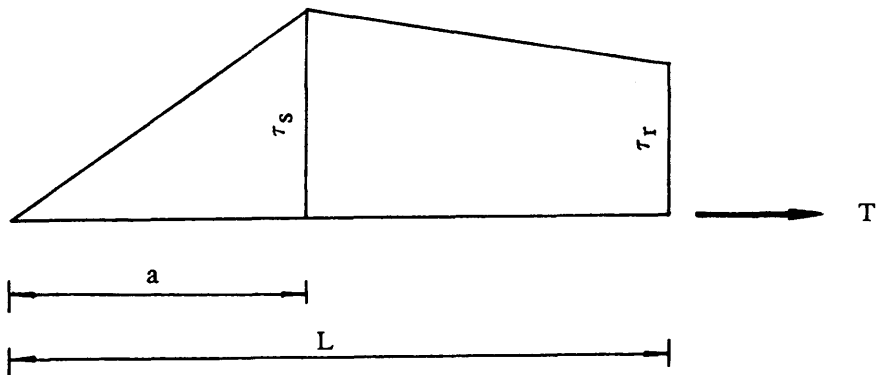


*Figure e* Assumption of Shear Stress Distribution along a Paralink Strap in a Pull-out Test

Based on this analysis, an equation can be derived to compute the pull-out force:

$$T' = \left[ \frac{1}{2} a \cdot \tau_s + \frac{\tau_s + \tau_r}{2} (L - a) \right] \cdot 2B$$

$$T' = B [\tau_s \cdot L + \tau_r (L - a)] \quad (6.11)$$

where  $T'$  — the pull-out force calculated from the shear stresses obtained from a shear box test in relation to the displacements in a pull-out test;

$B$  — the width of strap;

$L$  — the length of strap;

$a$  — the length from the free end to the maximum shear stress point;

$\tau_s$  — maximum shear stress in a shear box test;

$\tau_r$  — residual shear stress in a shear box test.

From equation (6.11), a "pull-out force" can be calculated according to shear box test results and pull-out test behaviour of Paralink 300s in Wardley minestone at a density of 16.579 kN/m<sup>3</sup>. The pull-out force" ( $T'$ ) was calculated at 60 and 120 kN/m<sup>2</sup> of overburden pressure, and these are presented in Table 6.3 together with pull-out forces calculated directly from the shear box test ( $T_s$ ) and those from pull-out tests ( $T_{max}$ ). It is obvious that this analysis gives closer results to the real values obtained in the pull-out tests.

This indicates that the flexibility of a strap is also a factor which causes a lower pull-out resistance in a pull-out test. This point was also proved by the higher results produced in the "sandwich" strap pull-out tests. However, the results from the shear box tests are still found to be higher compared with the "sandwich" strap pull-out tests. This might be due to the compressibility of the straps. Although

a "sandwich" strap behaved as rigid, the compressibility under normal stress was still present, and the double thickness of Paralink material in a "sandwich" strap would lead to a greater arching effect tending to reduce the normal stress on the strap and in turn reducing the pull-out resistance. On the other hand, the surface nature of a Paralink strap is different on both sides, i.e. one side of the strap is slightly rougher than the other. In the present shear box tests, the rougher side of the strap elements were arranged to be in contact with the fill, therefore the shearing force occurred on the interface of the fill and rougher side of the Paralink. In a pull-out test, the bond resistance was mobilized on the both sides, therefore a lower friction coefficient was produced in the pull-out tests.

In addition, the cross section of a Paralink strap can be reduced under a pull-out force, this may influence the contact of the strap and the fill material and in turn cause a reduction of the friction coefficient.

From the discussion above, it is understood that the bond resistance is really complex in a pull-out test. Particularly in the case of Paralink straps, this resistance is affected by the following factors, viz. dilatancy of the soil, arching effect, extensibility, and compressibility of the strap. The combination of these factors causes lower values of apparent friction coefficient in pull-out tests. However when the overburden pressure is low the effect of dilatancy may be more apparent than the others and lead to higher results.

It has been discovered in the previous chapter that the pull-out stiffness shown by the force-displacement curve from Paralink strap pull-out tests increased with increase in overburden pressure. The reason for this could be explained by the conclusions reported by previous researchers (McGown 1984, Fabian 1988). From tensile tests with geotextile, they found that the tensile stiffness of the reinforcement was influenced by the confining pressure imposed, i.e. the higher the confining pressure imposed, the stiffer the reinforcement behaved.

However, the author believes that there exists another factor which causes the increase of pull-out stiffness with the overburden pressure. If the differential

movements along a Paralink strap in a pull-out test are taken into consideration, it may help to further understand this phenomenon. As has been described, once the pulling action started, the fixed end of the strap was immediately in tension. But the part away from this end was free of stress. With further increase of the pulling force, the stress was gradually transmitted towards the free end. Therefore at a certain applied pulling force before the maximum, only a certain part of the strap was in stress. When the overburden pressure was low, a smaller maximum force was required to set the whole strap eventually moving (the free end started to move). On the contrary, a large maximum force was required when the overburden pressure was high (see the results of  $T_{max}$  in Tables 5.1 to 5.5). This implies that under the same pulling force, when the overburden pressure is low a large part of the strap will be in stress, whereas with a higher overburden pressure, only a smaller part of it will be in stress. Consequently, the same tensile force could cause a larger extension or displacement with a longer strap and the higher overburden pressure would lead to a smaller displacement at the same pull-out force, and result in a higher value of  $E_p$ .

This analysis can also be applied to explain the force-displacement curves from various lengths of Paralink straps shown in *Figures 5.47* and *5.48*. At a constant overburden pressure, altering the strap length did not change any the pull-out behaviour. According to the differential movement of the extensible strap in a pull-out test the following discussion can be made. If the 1m and 1.5m long straps are compared, one can imagine that in the case of the 1.5m strap, before the extension transmitted to the one metre point the extra 0.5m length of the strap had not taken part in the action. Therefore the performance (or force-displacement) of this strap is the same as the 1m long strap. With an increase in the pull-out force, the extension (or movement) was transmitted beyond the 1m point, and the extra part of this strap was brought into play. From *Figures 5.47* and *5.48*, one can see that the increase in length extended the force-displacement curve.

## 6.5 CONCLUSIONS

The following conclusions can be drawn from the results discussed in this chapter:

(1) Pull-out test with "piano wires" monitoring is a readily available method to investigate the behaviour of a Paralink strap in pulling action. Until a more suitable technique of measuring the strain distribution along a Paralink strap is found, the measurement with "piano wires" can be used to determine the strain distribution in a pull-out test.

(2) Due to the extensible characteristics of the Paralink straps, their performance in a pull-out test is different from a rigid steel strap. For a rigid strap once the pulling force is imposed, the whole strap, from the "clamped" end to the free end, will move simultaneously. In the case of a Paralink strap, the movement (or extension) is differential along the strap. The extension is mobilized from the "clamped" end incrementally towards the free end, until eventually the free end starts moving, and bond failure occurs. This also implies that the stress in the strap generated by the pulling force is also transmitted from the "clamped" end towards the free end.

(3) Arching effect plays an important part in a pull-out test, but this effect acts differently with the ribbed steel and Paralink straps. In the case of a ribbed steel strap, the arching effect is due to the soil dilatancy and it causes a transfer of normal pressure from the adjacent fill onto the strap, leading to an increase of normal stress on the strap during pulling. With a Paralink strap however, because of its compressibility, the arching effect is mainly caused by yielding of the strap under the overburden pressure and this leads to a transfer of normal stress from the strap onto the adjacent fill.

(4) The characteristics of the Paralink straps, i.e. extensibility and compressibility were found to be the factors causing lower apparent friction coefficient in the pull-out tests than in the shear box tests.

(5) With the two minestones and the Paralink straps tests, a lower value of  $f^*$  is produced from the pull-out with facing than through a slot. When  $\sigma_v$  is low the influence of facing resistance is considerable, when  $\sigma_v$  is high this influence does not appear.

(6) Pull-out tests with load and displacement controlled systems produce very similar results.

Table 6.1

THE CONSTANTS IN EQUATIONS (6.1) AND (6.2)

Type of Fill	Type of strap	$\sigma_v$ kN/m <sup>2</sup>	$b_0$	$b_1$	$b_2$	$b_3$
Wardley	Paralink 300s	20	20	-0.02113	$2.00 \times 10^{-6}$	$2.134 \times 10^{-9}$
		60	28	-0.02917	$3.00 \times 10^{-6}$	$2.667 \times 10^{-9}$
		120	46	-0.07626	$4.56 \times 10^{-5}$	$-1.013 \times 10^{-8}$
Minestone	Paralink 500s	20	10	-0.01837	$1.16 \times 10^{-5}$	$-2.533 \times 10^{-9}$
		60	14	-0.02463	$1.60 \times 10^{-5}$	$-3.866 \times 10^{-9}$
		120	26	-0.0533	$4.00 \times 10^{-5}$	$-1.067 \times 10^{-8}$
Wearmouth	Paralink 300s	20	13	-0.01437	$1.60 \times 10^{-6}$	$1.467 \times 10^{-9}$
		60	24	-0.03130	$1.08 \times 10^{-5}$	$-4.00 \times 10^{-10}$
		120	47	-0.09643	$7.20 \times 10^{-5}$	$-1.906 \times 10^{-8}$
Minestone	Paralink 500s	20	6.3	-0.0084	$2.20 \times 10^{-6}$	$4.00 \times 10^{-10}$
		60	12.4	-0.02447	$1.76 \times 10^{-5}$	$-4.533 \times 10^{-9}$
		120	25.7	-0.04953	$3.22 \times 10^{-5}$	$-7.066 \times 10^{-8}$
Loudon Hill sand	Paralink 300s	20	11.9	-0.01660	$6.20 \times 10^{-6}$	$-2.66 \times 10^{-10}$
		60	23	-0.02820	$7.80 \times 10^{-6}$	$5.340 \times 10^{-10}$
		120	49.2	-0.08770	$5.64 \times 10^{-5}$	$-1.320 \times 10^{-8}$
	Paralink 500s	20	23.6	-0.03400	$1.14 \times 10^{-5}$	$5.340 \times 10^{-10}$
		60	29.6	-0.06443	$5.00 \times 10^{-5}$	$-1.347 \times 10^{-8}$
		120	42.6	-0.09260	$7.16 \times 10^{-5}$	$-1.920 \times 10^{-8}$

Table 6.2

## COMPARISON OF THE PULL-OUT TEST RESULTS

From the "Sandwich" and Paralink Straps

Type of Strap	$\sigma_v$ kN/m <sup>2</sup>	$T_{max}$ kN	$\tau$ kN/m <sup>2</sup>	$f^*$
Paralink 300s	20	2.44	11.02	0.551
	60	3.39	13.38	0.223
	120	6.75	26.40	0.220
Paralink 300s "sandwich"	20	3.12	12.24	0.612
	60	4.35	15.90	0.265
	120	8.21	32.16	0.268
Paralink 500s	20	3.54	12.82	0.641
	60	4.92	18.18	0.303
	120	8.90	32.52	0.271
Paralink 500s "sandwich"	20	4.50	16.30	0.815
	60	5.20	18.84	0.314
	120	10.83	39.24	0.327

Table 6.3

Overburden Pressure $\sigma_v$ (kN/m <sup>2</sup> )	"Pull-out Force" from Shear Box Test $T_s$ (kN)	Pull-out Force from Pull-out Box Test $T_{max}$ (kN)	Pull-out Force Calculated from Equation (6.11) $T'$ (kN)
60	5.306	3.680	3.262
120	10.611	6.510	7.094

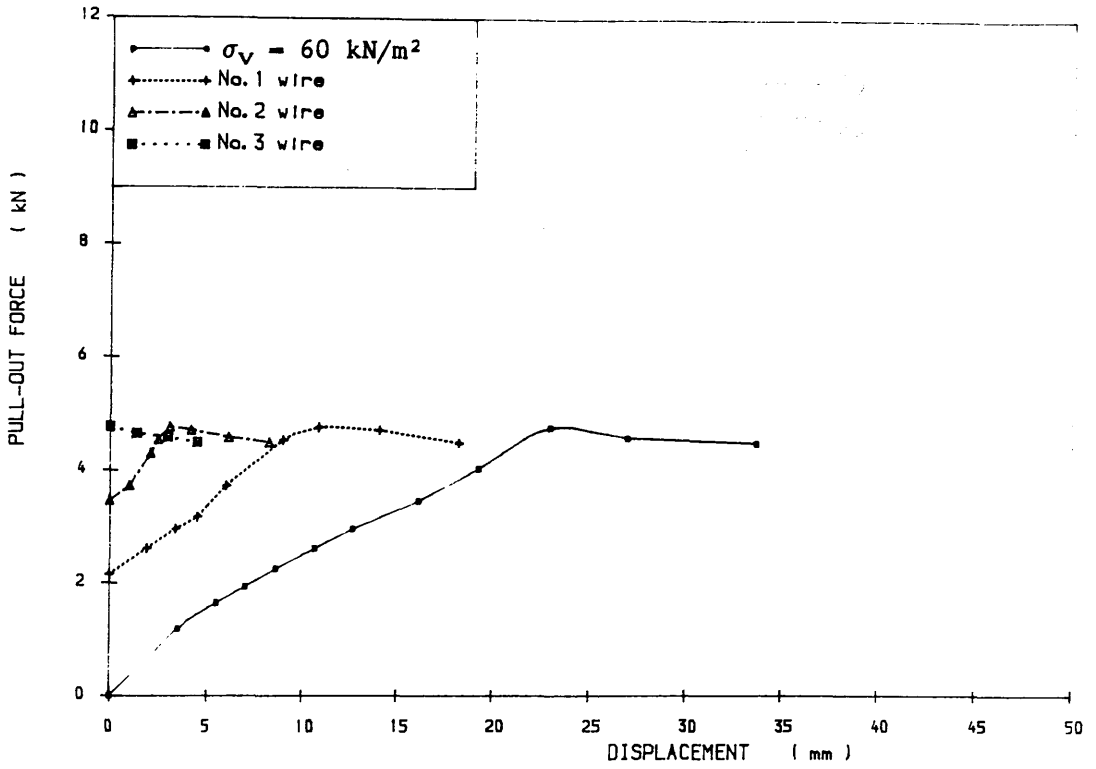


Figure 6.1 PULL-OUT FORCE VS. STRAP DISPLACEMENT

Laboratory Test, Loudon Hill Sand,  $L=1.5\text{m}$ ,  $\gamma_d=16.190\text{kN/m}^3$ , Paralink 300s

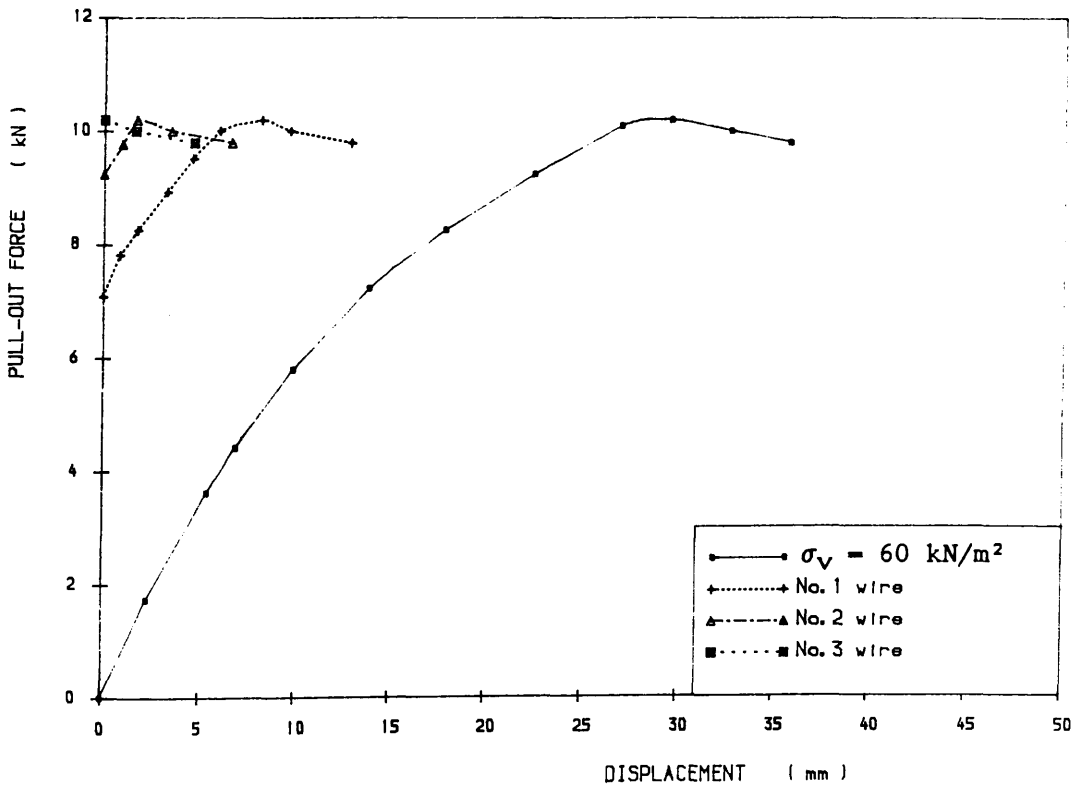


Figure 6.2 PULL-OUT FORCE VS. STRAP DISPLACEMENT

Laboratory Test, Loudon Hill Sand,  $L=1.5\text{m}$ ,  $\gamma_d=16.190\text{kN/m}^3$ , Paralink 500s

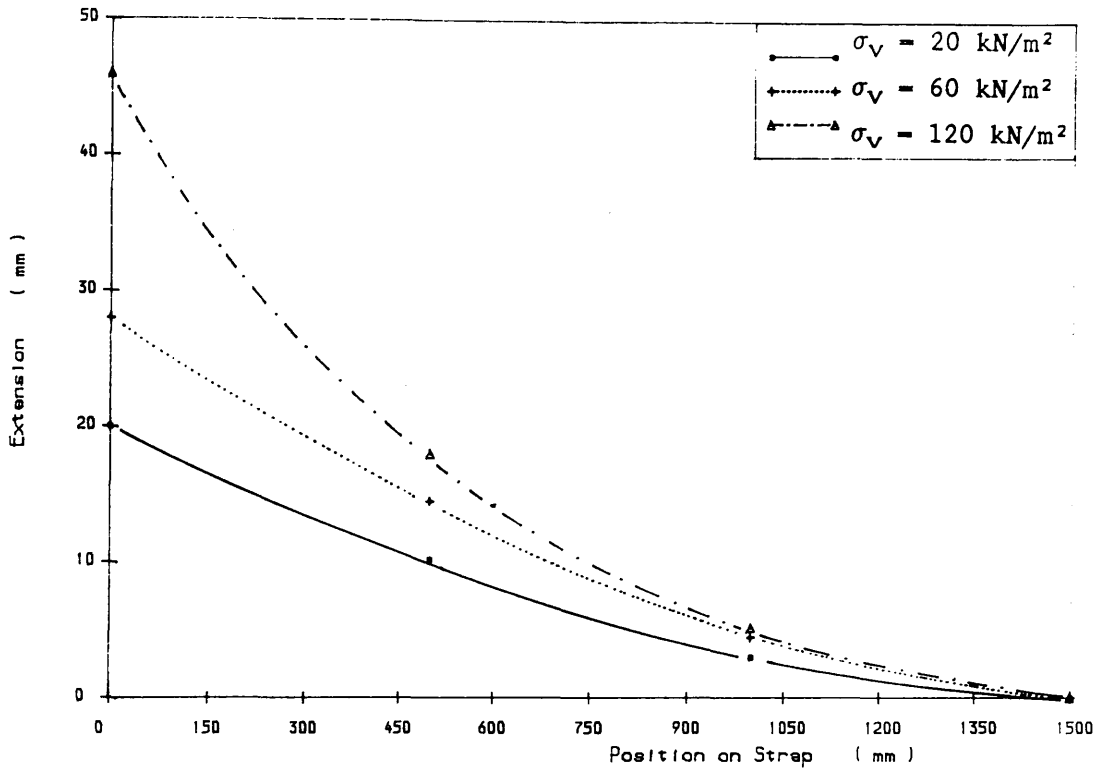


Figure 6.3 EXTENSION ALONG THE STRAP IN PULL-OUT TESTS

Wardley Minestone,  $\gamma_d=16.579 \text{ kN/m}^3$ , Paralink 300s,  $L=1.5\text{m}$

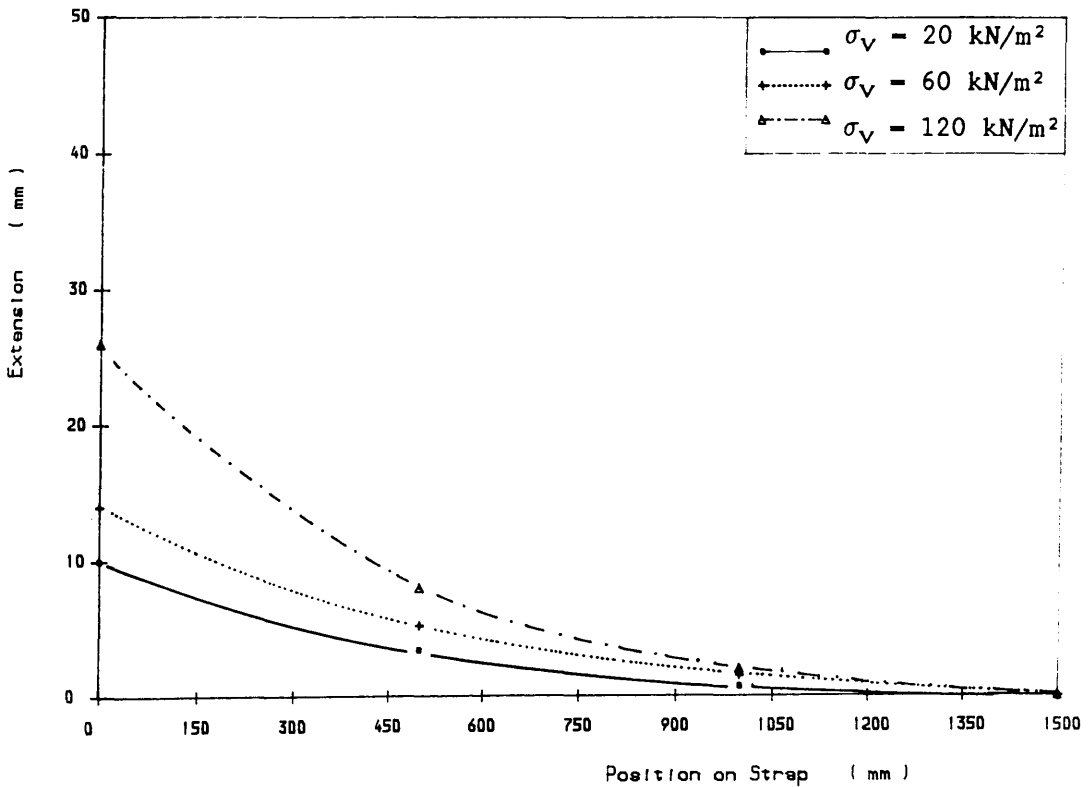


Figure 6.4 EXTENSION ALONG THE STRAP IN PULL-OUT TESTS

Wardley Minestone,  $\gamma_d=16.579 \text{ kN/m}^3$ , Paralink 500s,  $L=1.5\text{m}$

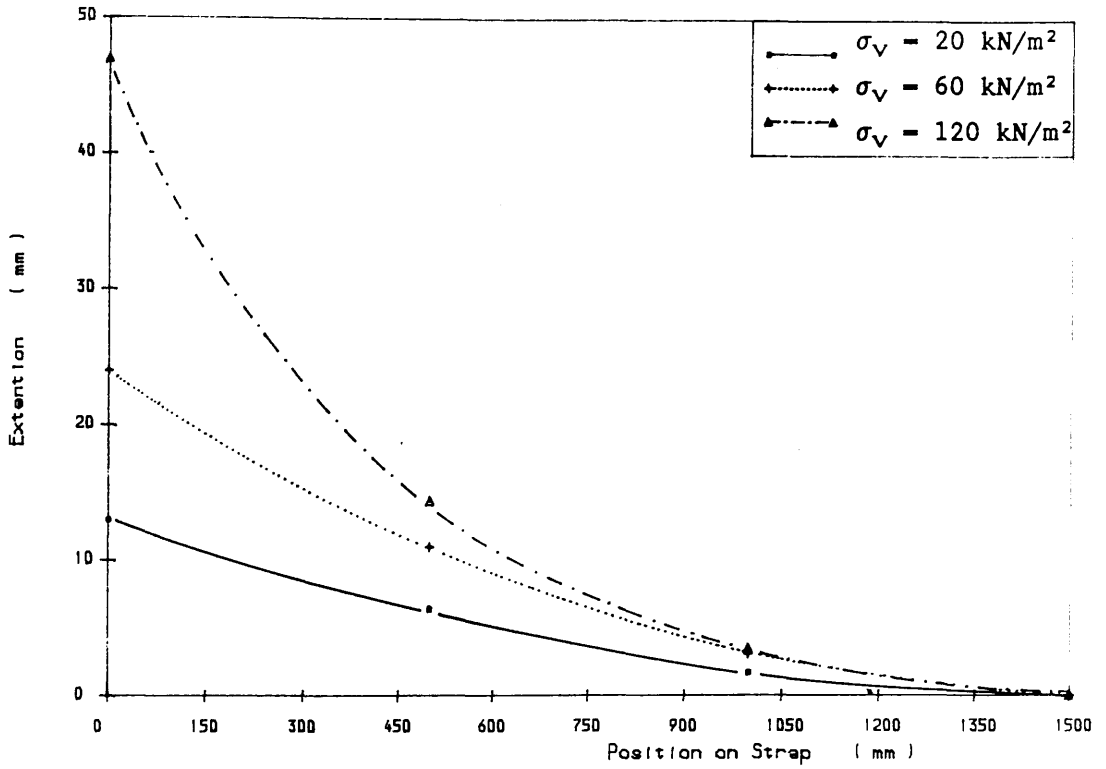


Figure 6.5 EXTENSION ALONG THE STRAP IN PULL-OUT TESTS

Wearmouth Minestone,  $\gamma_d=16.380\text{kN/m}^3$ , Paralink 300s, L=1.5m

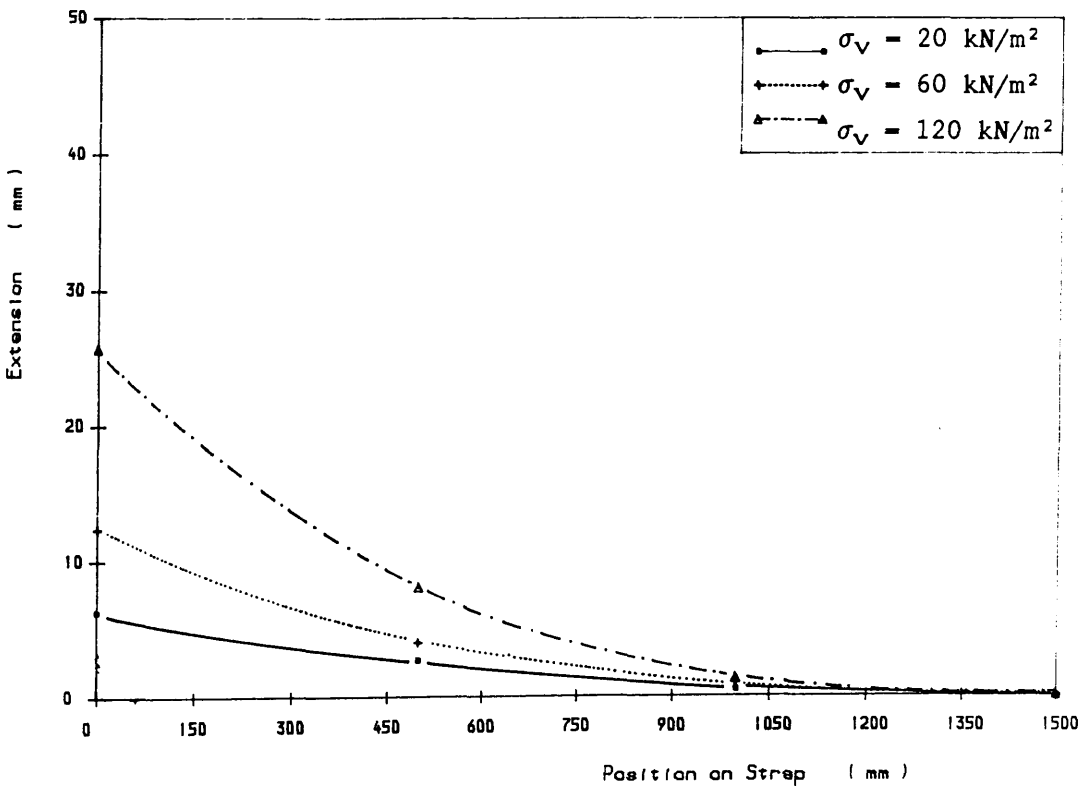


Figure 6.6 EXTENSION ALONG THE STRAP IN PULL-OUT TESTS

Wearmouth Minestone,  $\gamma_d=16.380\text{kN/m}^3$ , Paralink 500s, L=1.5m

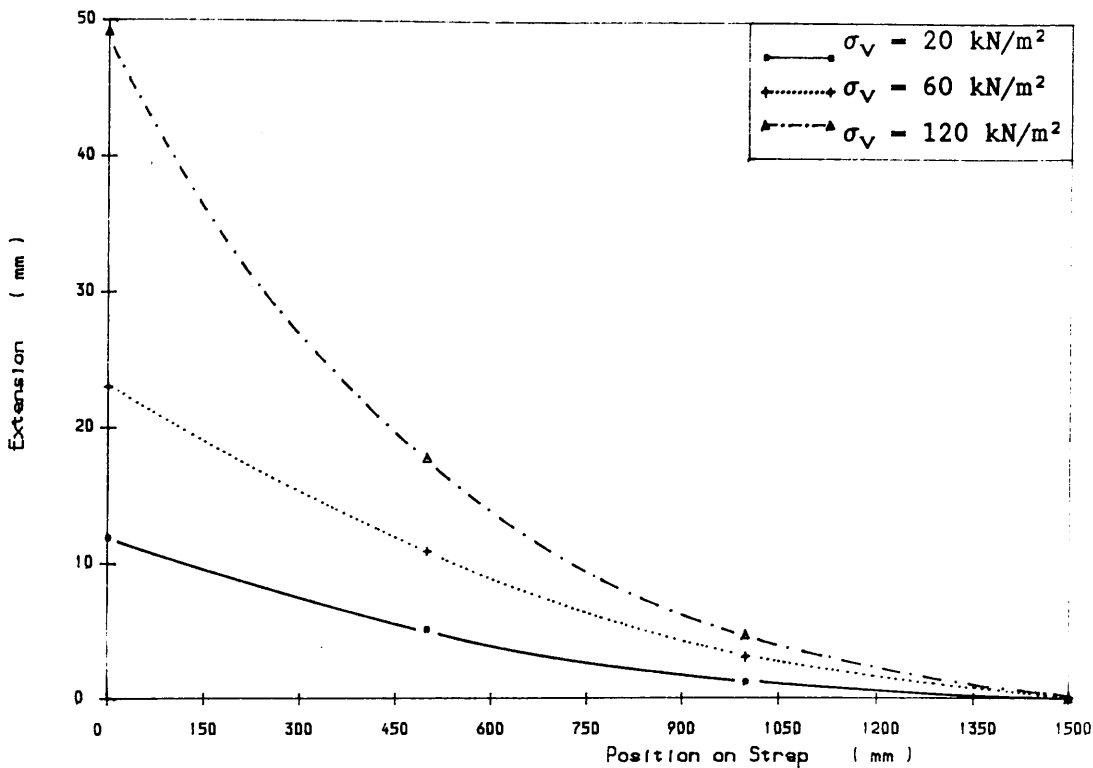


Figure 6.7 EXTENSION ALONG THE STRAP IN PULL-OUT TESTS  
 Loudon Hill Sand,  $\gamma_d=16.190\text{kN/m}^3$ , Paralink 300s,  $L=1.5\text{m}$

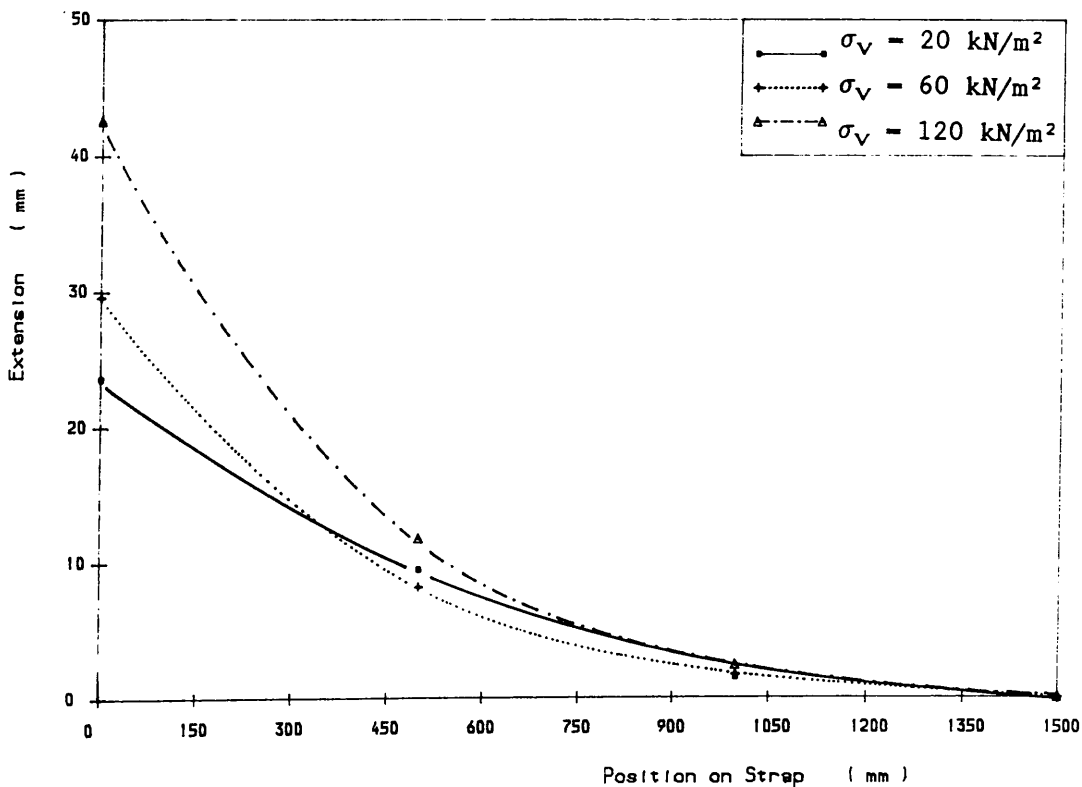


Figure 6.8 EXTENSION ALONG THE STRAP IN PULL-OUT TESTS  
 Loudon Hill Sand,  $\gamma_d=16.190\text{kN/m}^3$ , Paralink 500s,  $L=1.5\text{m}$

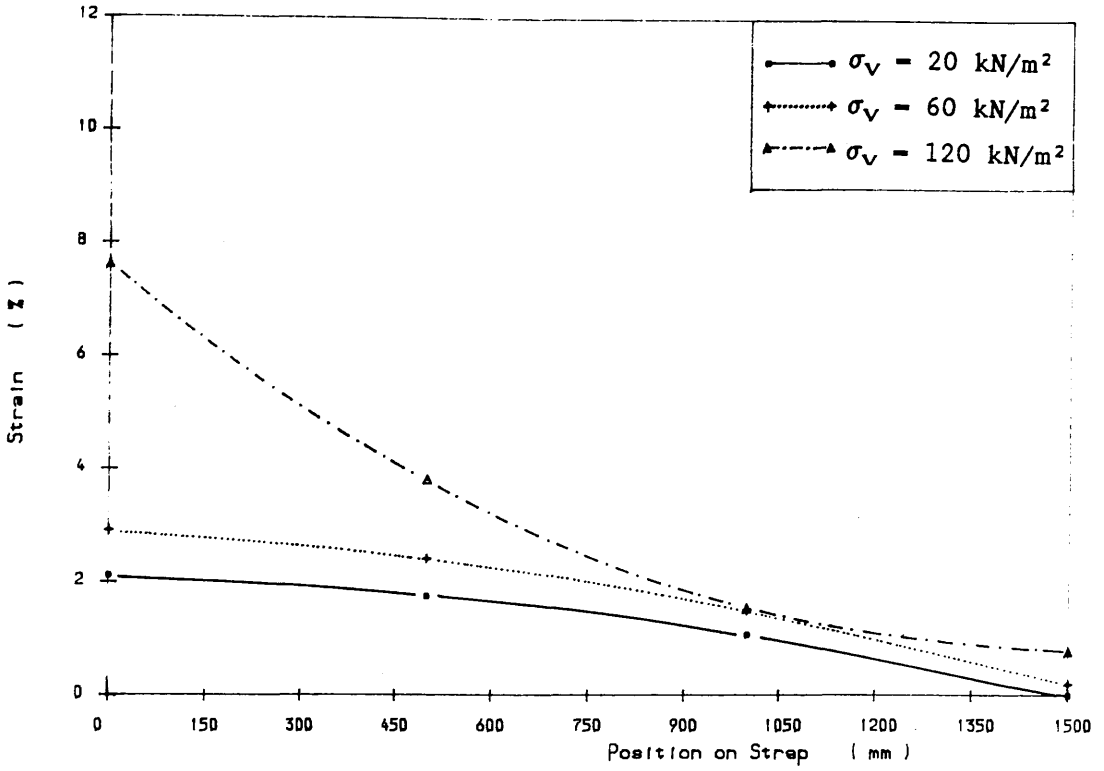


Figure 6.9 STRAIN ALONE THE STRAP IN PULL-OUT TESTS

Wardley Minestone,  $\gamma_d=16.579\text{kN/m}^3$ , Paralink 300s,  $L=1.5\text{m}$

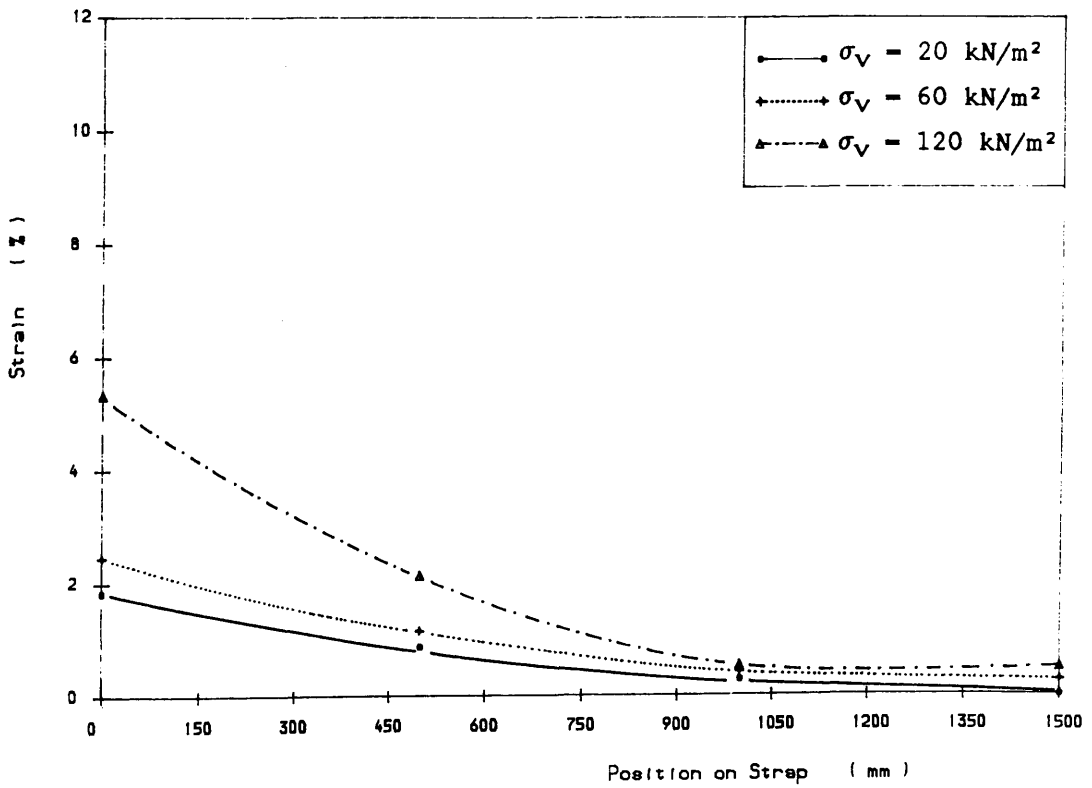


Figure 6.10 STRAIN ALONE THE STRAP IN PULL-OUT TESTS

Wardley Minestone,  $\gamma_d=16.579\text{kN/m}^3$ , Paralink

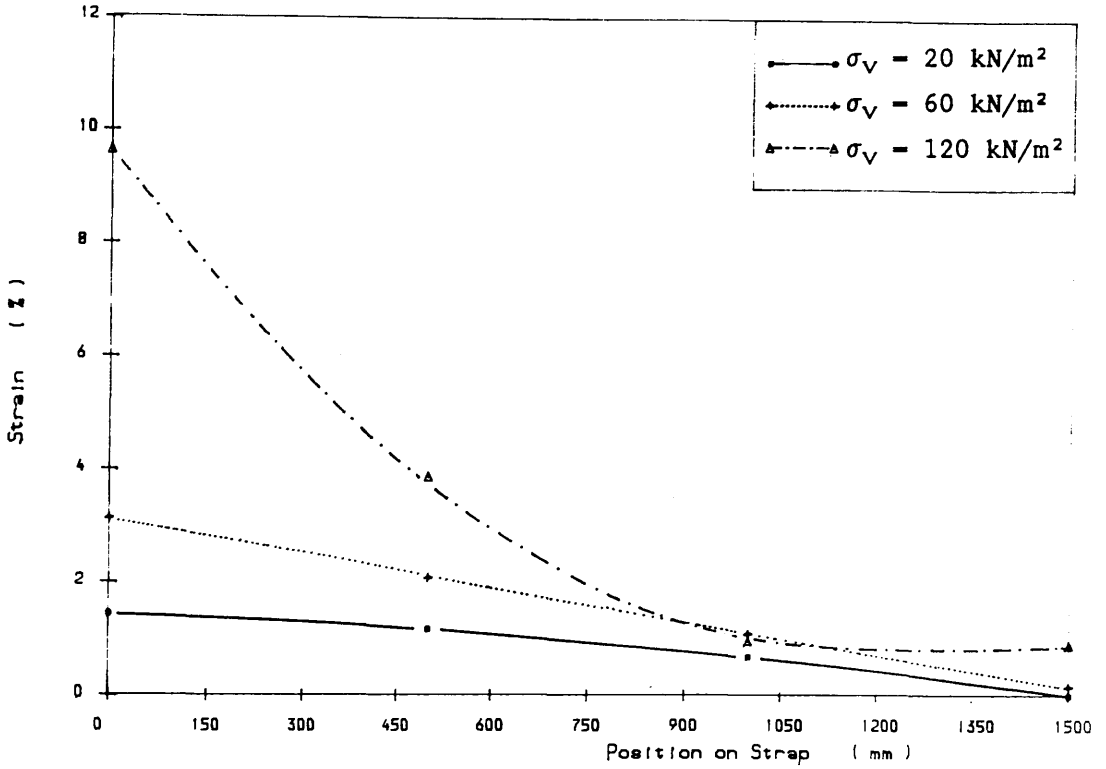


Figure 6.11 STRAIN ALONG THE STRAP IN PULL-OUT TESTS

Wearmouth Minestone,  $\gamma_d=16.380\text{kN/m}^3$ , Paralink 300s, L=1.5m

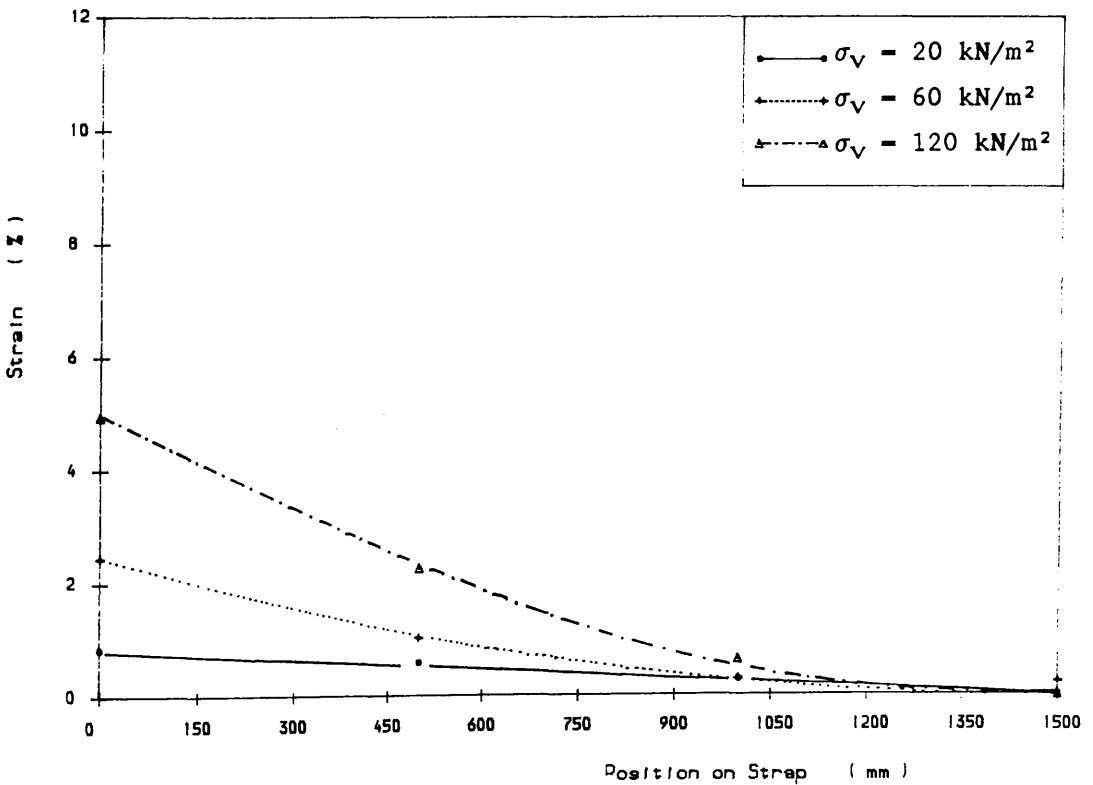


Figure 6.12 STRAIN ALONG THE STRAP IN PULL-OUT TESTS

Wearmouth Minestone,  $\gamma_d=16.380\text{kN/m}^3$ , Paralink 500s, L=1.5m

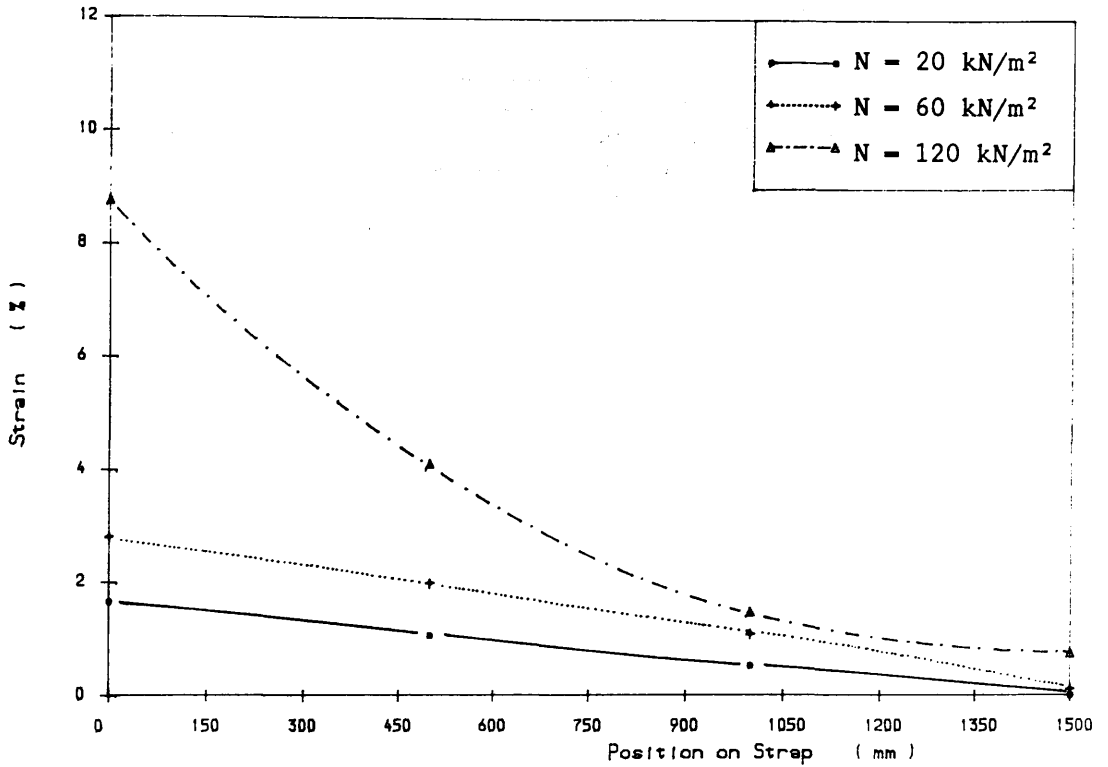


Figure 6.13 STRAIN ALONG THE STRAP IN PULL-OUT TESTS

Loudon Hill Sand,  $\gamma_d=16.190\text{kN/m}^3$ , Paralink 300s,  $L=1.5\text{m}$

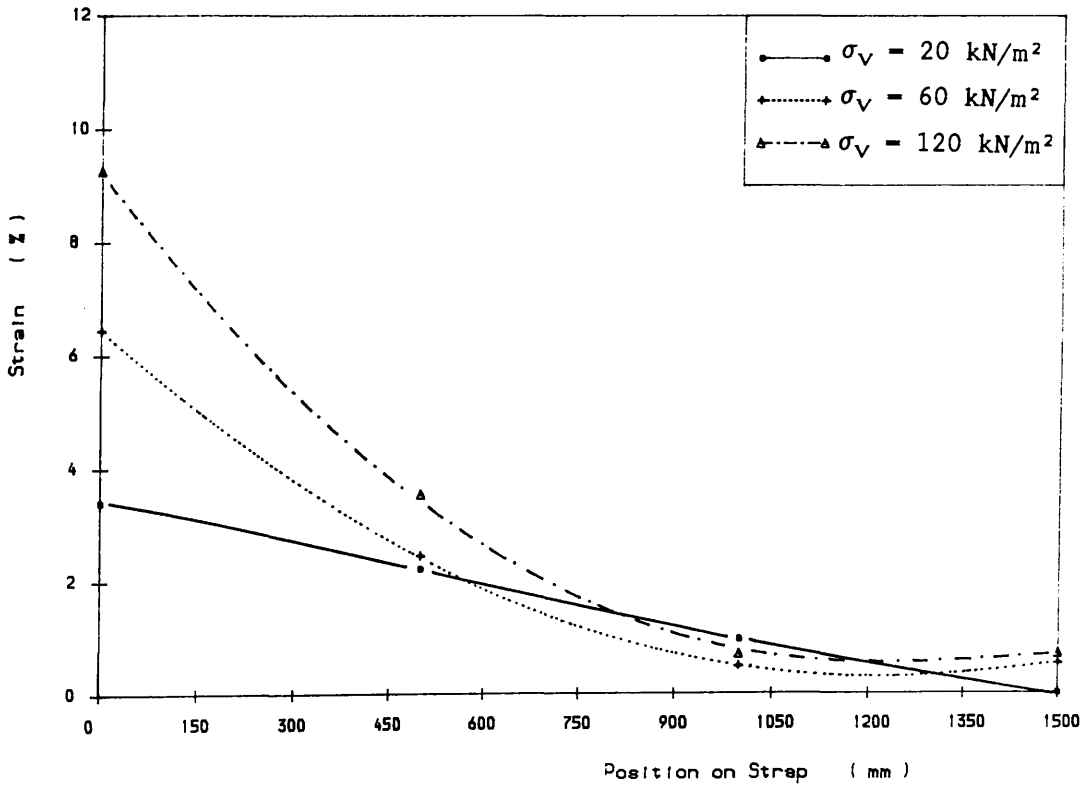


Figure 6.14 STRAIN ALONG THE STRAP IN PULL-OUT TESTS

Loudon Hill Sand,  $\gamma_d=16.190\text{kN/m}^3$ , Paralink 500s,  $L=1.5\text{m}$

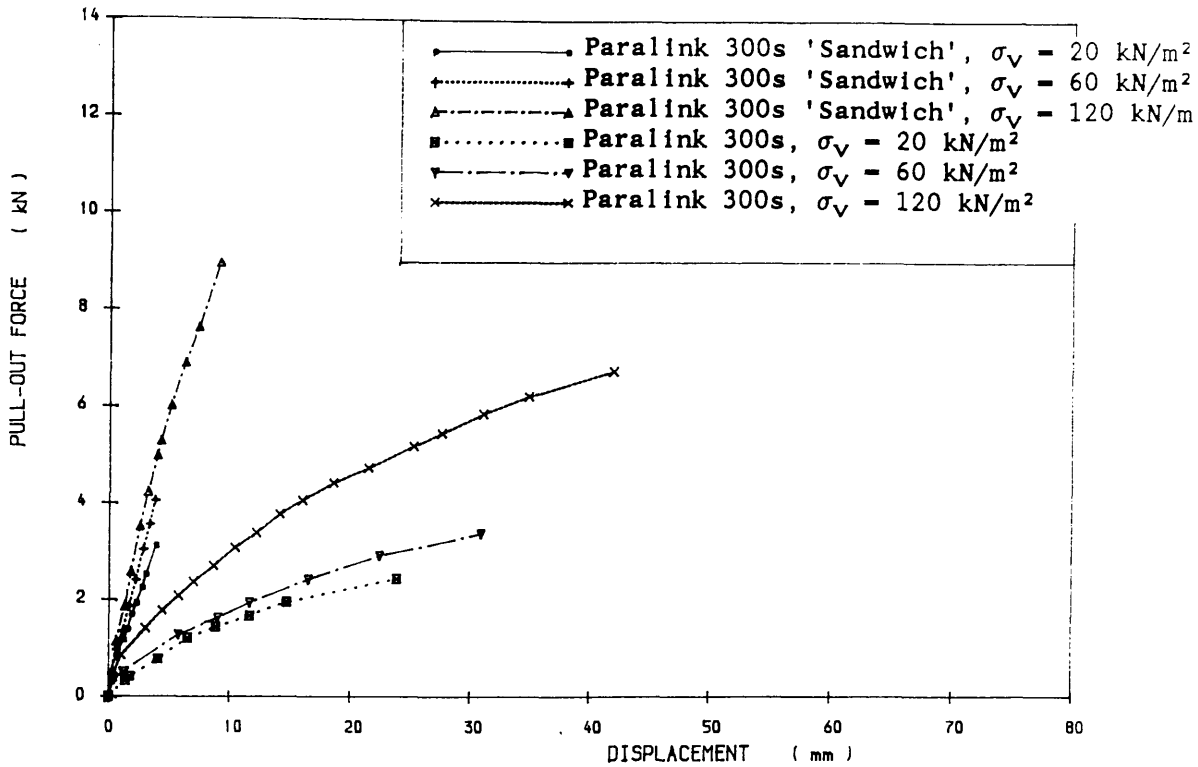


Figure 6.15 PULL-OUT FORCE VS. STRAP DISPLACEMENT

Laboratory Test, Wardley Minestone,  $\gamma_d=16.579\text{kN/m}^3$ ,  $L=1.5\text{m}$

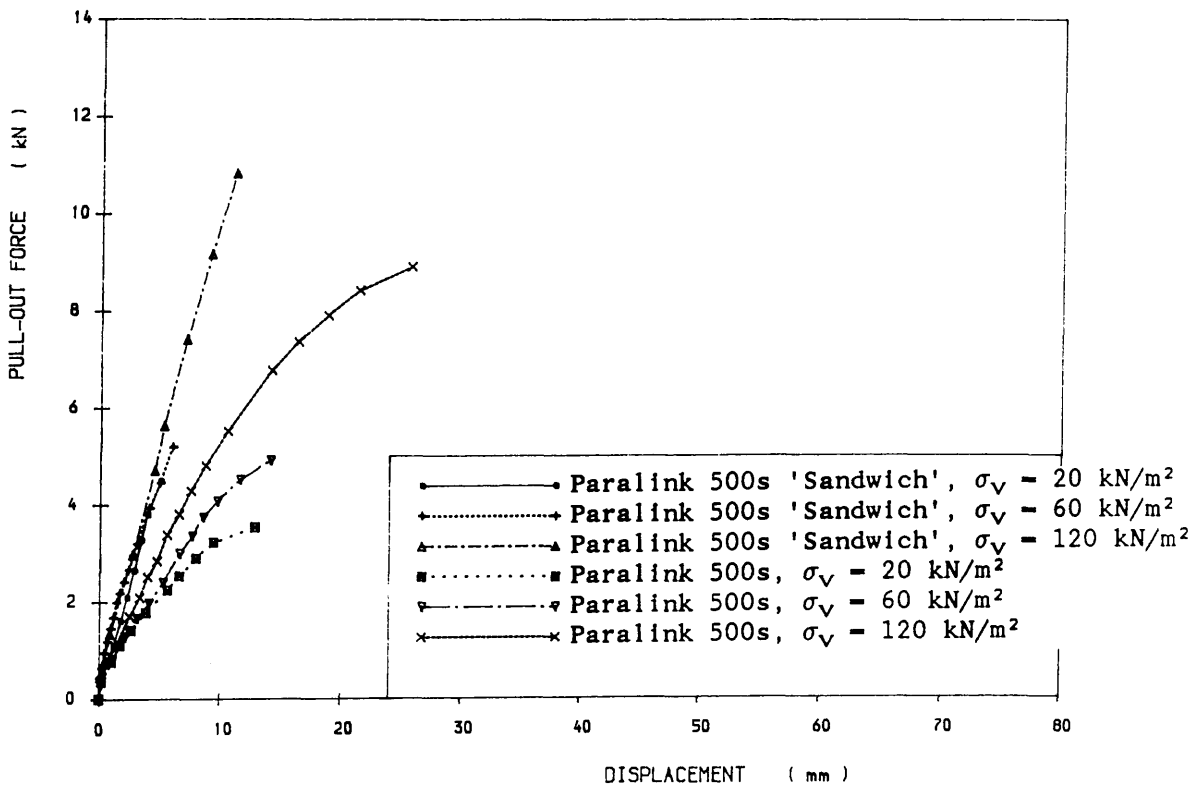


Figure 6.16 PULL-OUT FORCE VS. STRAP DISPLACEMENT

Laboratory Test, Wardley Minestone,  $\gamma_d=16.579\text{kN/m}^3$ ,  $L=1.5\text{m}$

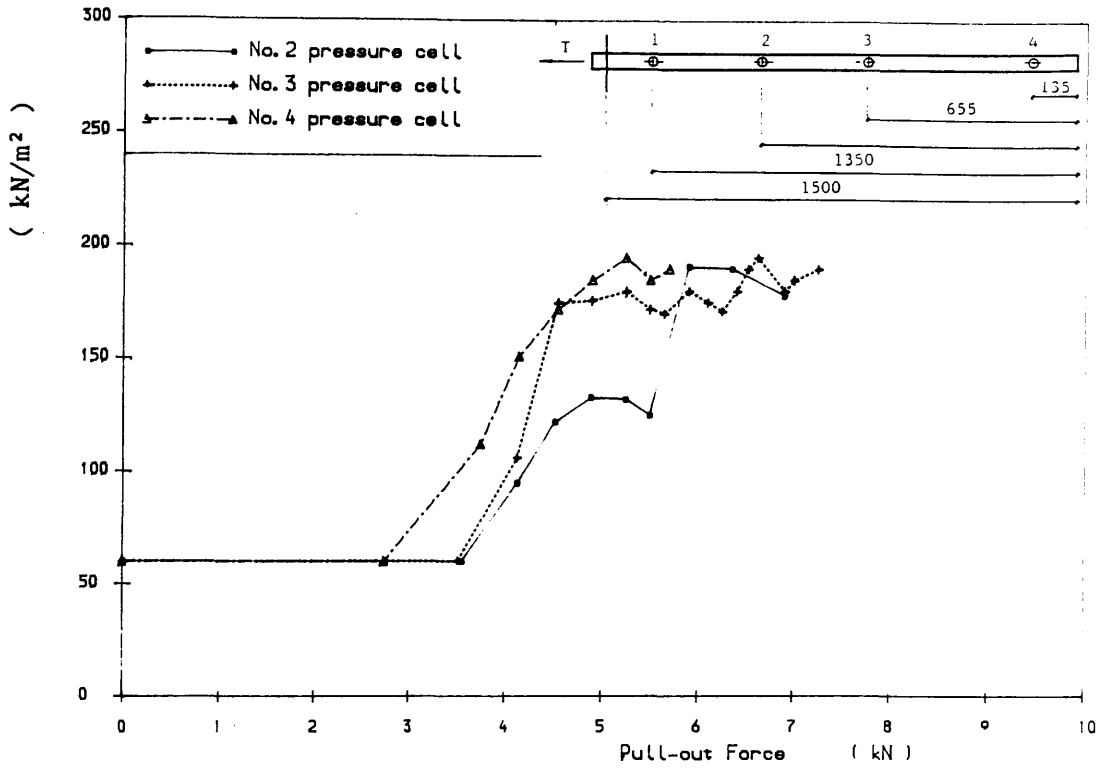


Figure 6.17 PRESSURES MONITORED DURING PULLING IN A PULL-OUT TEST  
 Loudon Hill Sand,  $\gamma_d=16.190\text{kN/m}^3$ , Ribbed Steel,  $L=1.5\text{m}$ ,  $\sigma_v=60\text{kN/m}^2$

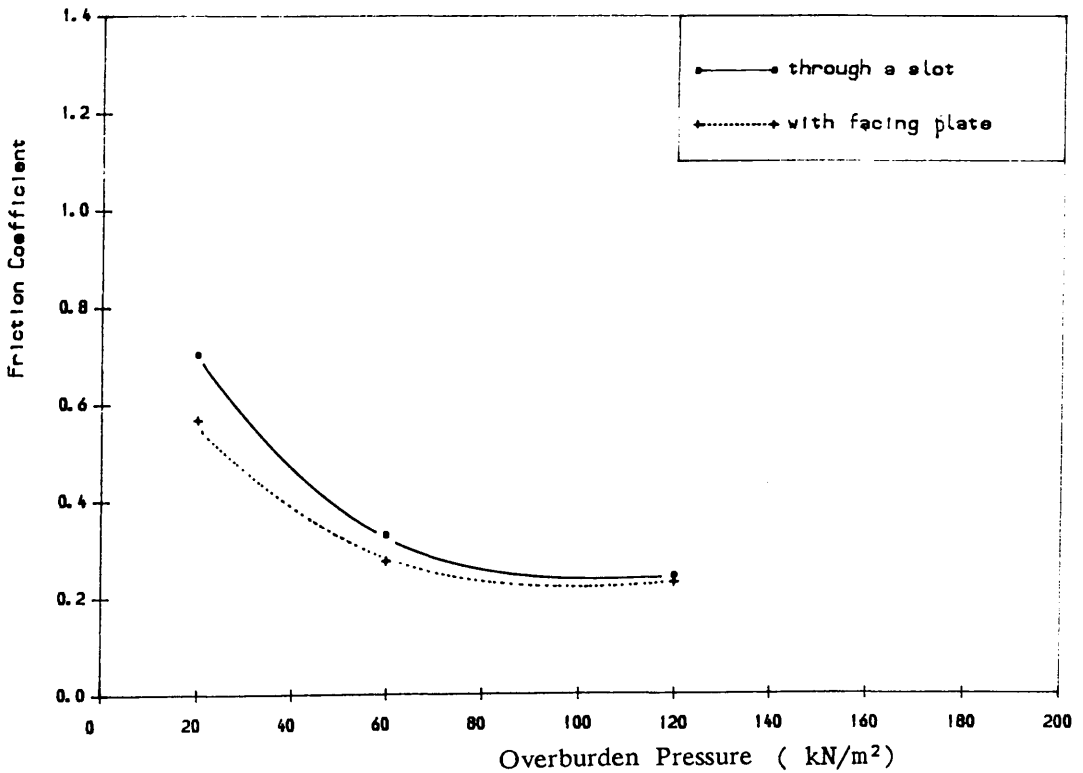


Figure 6.18 FRICTION COEFFICIENT VS. OVERBURDEN PRESSURE  
 Laboratory pull-out Test, Wardley Minestone,  $\gamma_d=17.847\text{kN/m}^3$ , Paralink 500s

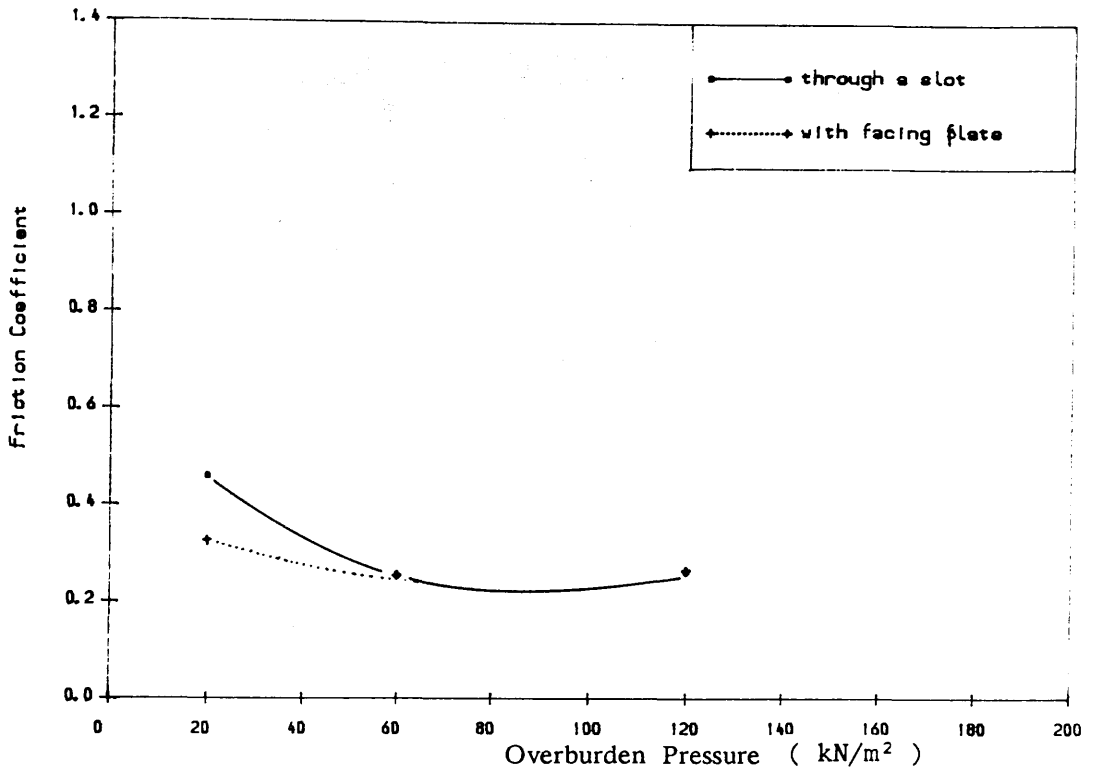


Figure 6.19 FRICTION COEFFICIENT VS. OVERBURDEN PRESSURE

Laboratory pull-out Test, Wearmouth Minestone,  $\gamma_d=17.658\text{kN/m}^3$ , Paralink 500s

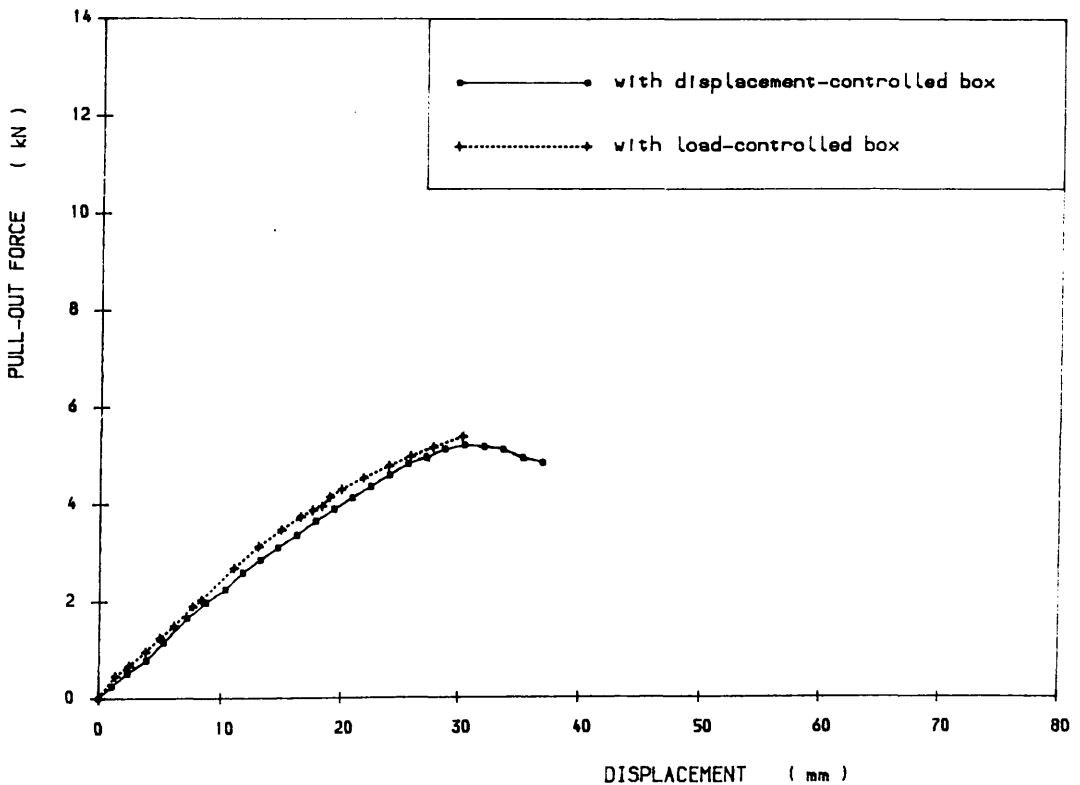


Figure 6.20 PULL-OUT FORCE VS. STRAP DISPLACEMENT

Horden Red Shale,  $\gamma_d=14.327\text{kN/m}^3$ , Paralink 300s,  $L=1.5\text{m}$ ,  $\sigma_v=60\text{kN/m}^2$

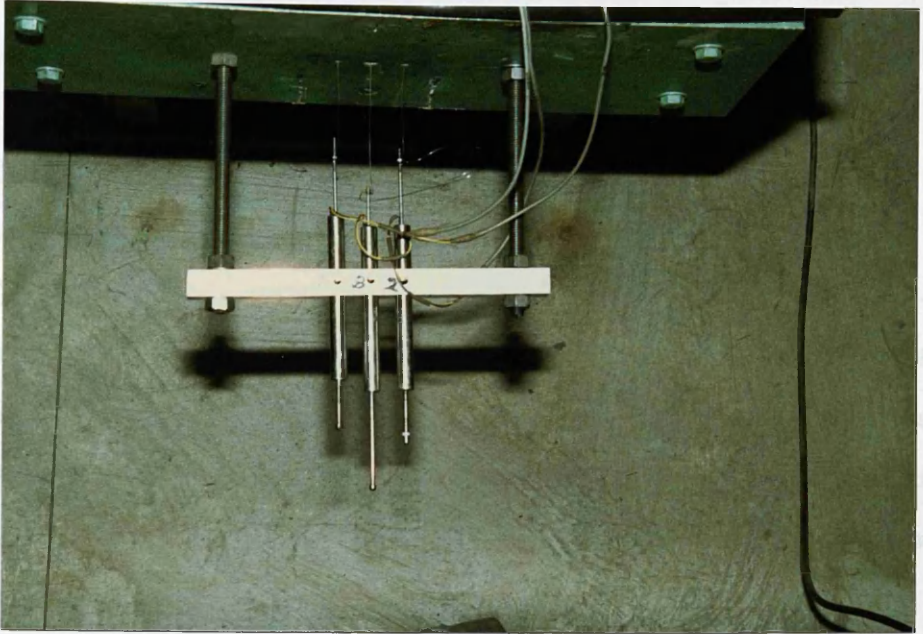


Plate 6.1 PIANO WIRES CONNECTED TO THE TRANSDUCERS

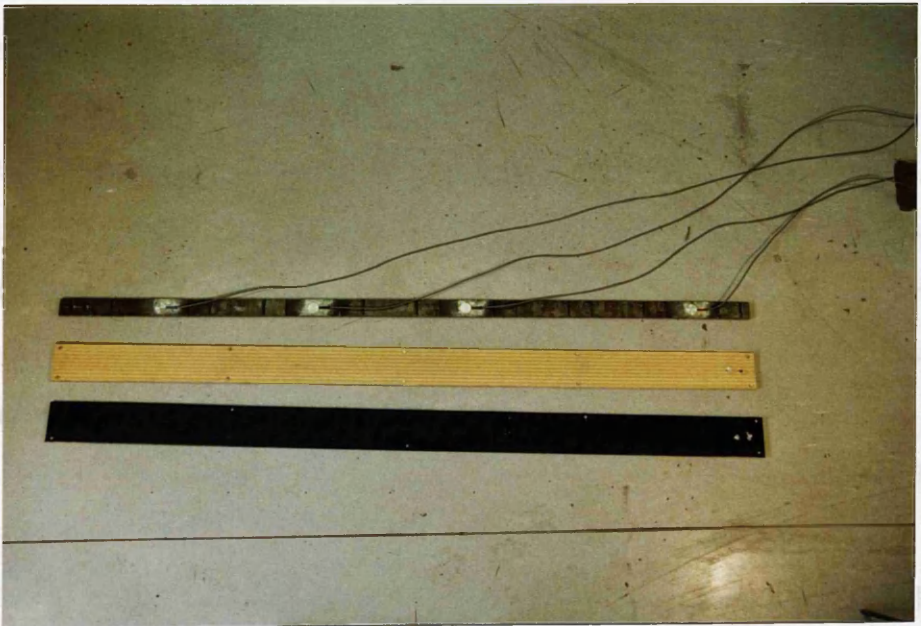


Plate 6.2 PARALINK "SANDWICH" STRAPS AND THE RIBBED STEEL STRAP WITH PRESSURE CELLS

## CHAPTER 7

### FIELD FULL-SCALE PULL-OUT TESTS

#### 7.1 INTRODUCTION

To investigate the bond resistance between fill and reinforcement, pull-out tests from a real reinforced earth structure have been regarded as a method which can reflect the actual case, and have been used widely by previous investigators (Chang 1974, Schlosser and Long 1973). Instead of a real reinforced earth structure, a full-scale box was used in the present work. This field full-scale pull-out test is one of the three main test methods used in the present project, the other two test methods, i.e. shear box test and laboratory pull-out test having been discussed in the previous chapters. The present chapter describes the full-scale pull-out tests and the results are presented.

#### 7.2 FIELD TEST BOX, DEVICES AND TEST PROCEDURES

##### 7.2.1 The Full-Scale Boxes and Test Devices

A box 5m long by 2m wide by 4.5m high, made from timber planks and rolled steel sections had been constructed by British Coal Minestone Services at Wardley Colliery near Sunderland in England. This box was open at the rear to allow fill to be transported and compacted inside. When the box was demolished after a change of use of the site, another box 5.5m long by 3.1m wide by 4.5m high was erected at Barony Colliery in Scotland, from the same materials. Both boxes are shown in *Plates 7.1 and 7.2*.

The pull-out device employed was a patented strain-control motorised jack (see *Plate 7.3*) supplied by British Coal. A load cell and a displacement transducer were both fixed to the jack and connected to a data logger and a plotter (see *Plate*

7.4) which could monitor the pull-out force and displacement during testing.

### 7.2.2 Test Procedures

All the tests were prepared with the assistance of British Coal. For the preparation of each test, the fill material was placed in the box using a mechanical shovel (at the lower level) or a conveyor belt (at the higher level). In the Wardley Colliery box, the straps were embedded in six or ten layers for tests in Wardley minestone, Wearmouth minestone and Horden red shale (see *Figures 7.1 and 7.2*). For the Barony Colliery box the straps were embedded in eight layers for tests in Loudon Hill sand and Methil PFA (see *Figure 7.3*). The three types of straps with different lengths were used in all these tests. Each layer of the fill between the straps was divided into two layers for compaction with a vibrating compactor using six passes. The same degree of compaction was used for all the tests. The densities and moisture contents were checked for each compacted layer, the core cutter method being employed for this purpose.

During the preparation one end of the strap with a buckle fixed to it was led out of the box through gaps between the timber planks. These buckles were to be connected to the pull-out jack at the start of the test. To do this a strap was fastened tightly round the buckle and the buckle was then fixed to the jack with a bolt through the holes in the buckle and the jack. For the ribbed steel, the strap was connected to the jack directly through the hole in the strap. The pull-out jack was set on a scaffold (in Wardley Colliery tests) or a hydraulic platform (in Barony Colliery tests) both of which could be adjusted to the appropriate heights. During testing a strap was pulled out with the jack at a constant rate of 3 mm/min until failure. The pull-out force and displacement were monitored and recorded through the load cell and displacement transducer connected to the data logger and the plotter.

Using the buckle connection in the field tests was quite convenient since it was easier to fix than the clamps. However, some large displacements occurred,

caused by the strap sliding through the buckle during pulling (see chapter 3), therefore the displacements obtained were not reliable.

### 7.3 TEST RESULTS

Five sets of field full-scale pull-out tests were carried out using the two types of Paralink and a few ribbed steel straps with the five different fill materials, i.e. Wardley minestone, Wearmouth minestone, Horden red shale, Loudon Hill sand and Methil PFA. All the fill materials were compacted at their natural moisture content, and the same compaction effort as described in the last section was adopted for all the tests. The results obtained from each of the fill materials are presented in this section.

#### 7.3.1 Results with Wardley Minestone

The natural moisture content of this minestone was found to be 9.7%, and the density achieved by the compaction effort was 17.847 kN/m<sup>3</sup>. The natural moisture content (9.7%) was quite close to the optimum (10%), and the density was 98% of the maximum density as obtained from the BS 1377:1975 Test 12.

As shown in Figure 7.1, the straps were arranged at six different levels, three straps being embedded at each level. The maximum forces and displacements were obtained from the tests and the apparent friction coefficients were calculated. These are presented in Table 7.1 and shown in Figures 7.4 to 7.8.

Figures 7.4 and 7.5 show the maximum pull-out force and apparent friction coefficient versus overburden pressure, the data obtained from 4 metre long straps being shown. The overburden pressure was calculated from the bulk density of the fill material and the height above the strap ( $\gamma H$ ). Although the data were quite scattered, a trend could still be observed. Assuming that the pull-out force was zero when there was no overburden pressure, then the fitting curves for these data of  $T_{\max}$  versus  $\sigma_v$  can start from the origin (see Figure 7.4). The curves show an

increase in maximum pull-out force with an increase in overburden pressure. However, the magnitude of the increase became very small when  $\sigma_v$  was over 20 kN/m<sup>2</sup>.

The apparent friction coefficients versus overburden pressure are shown in *Figure 7.5* for both types of Paralink strap. The decrease of  $f^*$  with increasing overburden pressure was observed for both of the straps. Paralink 500s was found to be superior to Paralink 300s, giving a higher value of  $f^*$ .

Some results are shown of apparent friction coefficient versus strap length (see *Figures 7.6* and *7.7*). *Figure 7.6* shows an increase of  $f^*$  with an increase in strap length for Paralink 300s, the value of  $f^*$  was found to increase by about 0.08 when the strap length increased from 2m to 4m, whereas very little increase or even some decrease in  $f^*$  was obtained for Paralink 500s.

Neglecting the influence of strap length, and gathering all the results from the three different types of strap together, a comparison can be made (see *Figure 7.8*). Although this shows a scattered data distribution, it can be seen that higher values of  $f^*$  were obtained for ribbed steel strap, with Paralink 500s being slightly superior to Paralink 300s, and the trend of declining  $f^*$  with increase in  $\sigma_v$  is obvious.

### 7.3.2 Results with Wearmouth Minestone

For this minestone a natural moisture content of 5.6% and a density of 17.658 kN/m<sup>3</sup> (98% of the maximum density) were obtained from the field tests. These straps, mainly Paralink with two ribbed steel, were arranged at ten different levels, and with three straps (except the top layer) embedded at each level. The overall view of this arrangement can be seen from *Figure 7.2*.

All the results from these tests are presented in *Table 7.2*, and in *Figures 7.9* to *7.13*.

*Figures 7.9* and *7.10* show the results obtained from the two types of Paralink strap with maximum pull-out force and apparent friction coefficient versus

overburden pressure. As observed from the previous minestone, an increase in  $T_{\max}$  with increase in  $\sigma_v$  is shown in *Figure 7.9*, and *Figure 7.10* indicates the trend of decrease of  $f^*$  with increasing overburden pressure. Very close results of  $T_{\max}$  or  $f^*$  are indicated from the two different Paralink straps.

*Figures 7.11* and *7.12* show the influence of strap length on the apparent friction coefficient for the two types of Paralink straps. Some small increases of  $f^*$  could be found with increasing strap length.

All the results obtained in this set of tests are shown together with apparent friction coefficient against overburden pressure (see *Figure 7.13*), and neglecting any influences caused by the various lengths. One can see that the two points obtained from the ribbed steel straps clearly lie above the others, while the results from the two Paralink straps can hardly be separated. However, the trend is clear, i.e. the value of  $f^*$  decreases with an increase in overburden pressure.

### 7.3.3 Results with Horden Red Shale

In this field full-scale test, the red shale was compacted to a density of  $17.640 \text{ kN/m}^3$  at a moisture content of 12.5%. The same box as used for the previous tests, with Wardley and Wearmouth minestones, was also employed in this set of test. The three different types of reinforcing strap were tested, their arrangement being identical with the test on Wearmouth minestone (see *Figure 7.2*). Twenty six pull-out tests were carried out, and the results are presented in *Table 7.3* and in *Figures 7.14* to *7.18*.

The same trend as from the previous tests was observed, i.e. the maximum pull-out force increased with increasing overburden pressure, and the apparent friction coefficient was found to decrease with increasing  $\sigma_v$ . However, the  $f^*$  remained almost constant at  $\sigma_v$  over about  $30 \text{ kN/m}^2$ .

*Figures 7.16* and *7.17* show some results of tests with different lengths of Paralink straps. The influence of strap length was varied, some increases and some decreases in  $f^*$  with increasing strap length were produced. Therefore it is hard to

draw a general conclusion about the influence of the strap length from this group of tests.

Neglecting the difference of strap lengths, all the results from this set of tests were plotted with apparent friction coefficient against overburden pressure, and are shown in *Figure 7.18*. When comparing the results from the same level, slightly higher apparent friction coefficients were produced from ribbed steel straps than the Paralinks, with Paralink 500s superior to Paralink 300s. The trend of declining  $f^*$  with increasing  $\sigma_v$  was very obvious at low overburden pressure, but as  $\sigma_v$  increased,  $f^*$  remained almost constant. At very low  $\sigma_v$  (4 kN/m<sup>2</sup> or 0.2m height), considerably larger values of  $f^*$  were obtained for both the Paralink straps.

#### 7.3.4 Results with Loudon Hill Sand

This sand was at its natural moisture content of 7.1% and a density of 16.19 kN/m<sup>3</sup> was achieved by the compaction effort in the field test. Twenty four reinforcing straps, mainly Paralinks and two ribbed steel, were embedded at eight different levels, the arrangement being illustrated diagrammatically in *Figure 7.3*. The box at Barony Colliery was employed in these tests. The results obtained are presented in *Table 7.4*, and shown in *Figures 7.19* to *7.25*.

*Figures 7.19* and *7.20* show that the maximum pull-out force increased with increasing overburden pressure, and these results were obtained from both 4m and 3m long Paralink straps. The difference in the results from the two types of Paralink straps was quite obvious, Paralink 500s being much superior to Paralink 300s in terms of pull-out resistance. This point was also indicated in terms of apparent friction coefficient (see *Figures 7.21* and *7.22*). The values of  $f^*$  obtained from Paralink 500s were about 0.1 to 0.3 higher than from Paralink 300s. The same trend as with the previous fill materials was also indicated, i.e. the apparent friction coefficient decreased with increase in overburden pressure, this decrease, however, becoming very small when  $\sigma_v$  was over 40kN/m<sup>2</sup>.

The influence of various lengths of Paralink straps is shown in *Figures 7.23*

and 7.24. As with Horden red shale, there was some uncertainty attached to these since both a decrease and an increase in  $f^*$  were found with increments of strap length on Paralink 500s. For Paralink 300s higher values of  $f^*$  were produced from 1.5m than from 3m long straps.

*Figure 7.25* shows all the results from this set of tests with apparent friction coefficient against overburden pressure. The difference of strap length was neglected in this graph. From this figure one can see that all the points produced with Paralink 500s lie above those with Paralink 300s, while the ribbed steel strap produced the highest value of  $f^*$  among the three. However, the ribbed steel strap did not show the same high value produced with the two minestone materials (see *Figures 7.8* and *7.13*). As with the others, the trend indicated that the apparent friction coefficient decreased with increase in overburden pressure.

### 7.3.5 Results with Methil PFA

This set of tests was carried out with the Barony Colliery box. This fine fill material achieved a dry density of  $11.59 \text{ kN/m}^3$  at the natural moisture content of 27% with the same compaction effort as used for the previous tests. The arrangement of these reinforcing straps was identical with the tests on Loudon Hill sand (see *Figure 7.3*). The results produced in this test are presented in *Table 7.5* and also shown in *Figures 7.26* to *7.32*.

As with the results obtained with the other previous materials, the trend also observed with the PFA was that the maximum pull-out force increased with increase in overburden pressure (see *Figures 7.26* and *7.27*) and the value of  $f^*$  decreased with increasing  $\sigma_v$  (see *Figures 7.28* and *7.29*). The decrease of  $f^*$  became very small when  $\sigma_v$  was over about  $40 \text{ kN/m}^2$ . Higher results of  $T_{\max}$  and  $f^*$  were obtained from Paralink 500s than from Paralink 300s.

*Figures 7.30* and *7.31* show some results produced from different lengths of Paralink strap, and although the influence of strap length did not show up significantly, smaller values of  $f^*$  were, however, obtained with shorter lengths of

straps.

Finally, all the results, neglecting the difference of strap lengths, are gathered together with apparent friction coefficient against overburden pressure (see *Figure 7.32*). The trend of decrease of  $f^*$  with increasing  $\sigma_v$  is quite obvious, and most of the points obtained from Paralink 500s are above those produced from Paralink 300s. The high results from the ribbed steel strap can be seen from this figure.

## 7.4 COMPARISON AND DISCUSSION

### 7.4.1 Comparison of the results from the Various Fill Materials

Field pull-out tests with five different fill materials have been performed and the results obtained from the tests with each of these materials have been described in section 7.3. In this section the results produced with the various fill materials are collected together, to allow a direct comparison to be made, and these are shown in *Figures 7.33 to 7.37*.

*Figures 7.33 and 7.34* show these results with maximum pull-out force against overburden pressure on the two types of Paralink straps respectively. These results appeared quite scattered. However, it can be observed that most of the data obtained from Horden red shale lies above the others, and the points obtained from Methil PFA lie at the bottom of the data band, while the results from the other three materials, i.e. Wardley minestone, Wearmouth minestone and Loudon Hill sand, are mixed up in the middle of this band and cannot readily be separated. These results also indicate a trend of increase of maximum pull-out force with increasing overburden pressure.

*Figures 7.35 and 7.36* show all the results of apparent friction coefficient against overburden pressure. Likewise these indicate the higher results from Horden red shale and the lower results from Methil PFA with those from the other materials lying between. The trend of these data show a decrease of  $f^*$  with increase in overburden pressure. Above about 30 to 40  $\text{kN/m}^2$  of  $\sigma_v$ , the value of  $f^*$

remained almost constant, for Paralink 300s the value of  $f^*$  was in a band about 0.15 to 0.4, while for Paralink 500s this was discovered to be between 0.2 to 0.4.

Some data produced from ribbed steel straps are shown in *Figure 7.37*, above 30 kN/m<sup>2</sup> of  $\sigma_v$  the value of  $f^*$  could be found between 0.4 to 0.7.

#### 7.4.2 Discussion of the Field Test Results

Although the present field pull-out tests were not carried out from an actual reinforced earth structure, the box was analogous to a real structure, and most of the conditions occurring in a reinforced earth structure could be represented in the full sized box. Compared to the laboratory pull-out box test, this field pull-out test was a full-scale case. Therefore unlike a laboratory test, the overburden pressure was not mobilized by an artificially applied pressure, but by the selfweight of the fill ( $\gamma H$ ), as happens in an actual structure. In addition, since this test was performed in the field at large scale, the preparation was similar to the construction of a reinforced earth wall, therefore some conditions, such as the density state in the field could represent the real case of an actual structure. However, there were some differences between this full scale box and an actual structure. For example unlike the facing in a structure, the front part of the box consisted of wooden planks fixed firmly to both sides of the box. Also the existence of the sides of the box which are not included in a structure might cause some side friction resistance on the fill.

From the presentation of the results above, it can be seen that the data obtained from the field tests were rather scattered. This was not unexpected. Because of the large scale of these tests, the control of the testing was not as good as in the smaller box used in the laboratory tests; in particular the density achieved by the compaction effort might not have been uniform, nor the moisture content, and this might influence the test results. As discussed in Chapter 5, density is a factor which influences the bond resistance of fill-reinforcement, particularly when the overburden pressure is low, therefore this influence could be significant. Some results such as with Wardley minestone at 8 kN/m<sup>2</sup> of  $\sigma_v$ , produced very low results

(see *Figure 7.5*). This was probably caused by poor compaction at these areas. On the other hand, *Figure 7.15* shows very high values of  $f^*$  at the overburden pressure of 4 kN/m<sup>2</sup> when tested with Horden red shale. This might be attributed to a very dense state achieved by high local compaction in this area.

Although the data were rather scattered, the trend could be seen that the maximum pull-out force increased with increase in overburden pressure, while the apparent friction coefficient decreased with it. This trend was encountered no matter which of the materials and reinforcements were used. This phenomenon coincided with that observed in the laboratory pull-out tests. The explanation of this phenomenon could be the same as that proposed for the laboratory tests. Further, when comparing the three types of reinforcement, it was found that Paralink 500s produced higher friction coefficient than Paralink 300s, this also being consistent with the laboratory test results. Especially when tested with Loudon Hill sand the value of  $f^*$  obtained from Paralink 500s was found about 0.1 to 0.3 higher than Paralink 300s. With Wearmouth minestone both reinforcements produced very close results. The reason for the two types of strap behaving differently with different fill materials is difficult to explain. However, it was probably due to the texture form of the strap surface. In these field tests although only a few ribbed steel straps were examined, the results indicated higher friction coefficient than the Paralink straps, no matter which fill materials were used. This was also consistent with the laboratory pull-out tests, as well as with the shear box test results.

The tests from various lengths of Paralink straps at the same overburden pressure showed some anomalies in the results. Increases and decreases of  $f^*$  with increasing strap length were encountered, and the variation of the values of  $f^*$  could be about 0.1 with a change in length from two metres to four metres. The undulation of a longer strap was supposed to be the reason for an increase in the pull-out resistance, leading to a higher value of  $f^*$  with a longer strap. The results showing an increase of  $f^*$  with an increase in the length of the strap was coincident with that obtained in the laboratory tests on Loudon Hill sand, but it is difficult to explain how a shorter strap could produce a higher value of  $f^*$ . The author believes

that the extension of Paralink straps under pulling action might at the same time reduce the cross section of the strap, and in turn this could probably reduce the pulling resistance (Chapter 6). Normally the longer the strap, the higher the pull-out force produced, consequently the higher force would cause a larger strap extension or cross section reduction. Therefore when considering the friction coefficient, a smaller value of  $f^*$  might be obtained from a longer Paralink strap. In addition the non-uniformity of the density in the field tests was also a reason which could cause a variation in results. Hence the case of a strap in pull-out testing is quite complex. From the present field test results, the conclusion about the influence of strap length was quite uncertain.

Comparing the various fill materials, Horden red shale was the most efficient in producing bond resistance when tested with any of the three types of the reinforcement. This coincided with what had been obtained in the laboratory pull-out tests as well as in the shear box tests. For the other fill materials the conclusion of superiority was difficult to draw.

## 7.5 CONCLUSIONS

Some conclusions drawn from the field tests are summarized:

- (1) The data obtained from field tests are rather scattered compared with the laboratory tests.
- (2) Among the three types of the reinforcement, ribbed steel produces the highest bond resistance, with Paralink 500s being slightly superior to Paralink 300s.
- (3) Comparing the five different types of fill material, Horden red shale appears more efficient in producing bond resistance no matter which of the straps is used. The efficiency of the other fill materials varies with the reinforcements. The varying range of the scattered values of  $f^*$  from these various materials is about 0.3 to

0.4.

(4) The maximum pull-out force increases with increasing overburden pressure ( $\gamma H$ ).

(5) The apparent friction coefficient decreases with increasing overburden pressure ( $\gamma H$ ).

(6) The influence of the strap length on the apparent friction coefficient is uncertain from the field tests.

Table 7.1

## FIELD PULL-OUT TEST RESULTS

## Wardley Minestone

Normal Stress $\sigma_v$ (kN/m <sup>2</sup> )	Strap Type	Strap Length L (m)	Pull-out Force $T_{max}$ (kN)	Displacement at Failure $\Delta L$ (mm)	Shear Stress $\tau$ (kN/m <sup>2</sup> )	Friction Coefficient $f^*$
8	C	2.5	1.6	20	8.00	1.000
	A	4.0	1.7	73	2.50	0.313
	B	4.0	2.2	40	3.13	0.391
20	A	2.0	3.0	35	8.82	0.464
	B	4.0	9.0	120	12.78	0.673
	A	4.0	7.0	114	10.29	0.542
32	A	3.0	5.0	60	9.80	0.327
	A	4.0	7.2	110	10.59	0.353
	A	2.0	2.7	36	7.94	0.265
42	B	4.0	6.6	57	9.38	0.229
	A	4.0	6.6	111	9.71	0.237
	C	4.0	7.4	48	23.13	0.564
54	B	3.0	1.6	20	8.00	1.000
	B	4.0	1.7	73	2.50	0.313
	B	2.0	2.2	40	3.13	0.391
64	A	4.0	7.7	123	11.32	0.180
	B	4.0	7.4	70	10.51	0.167
	B	2.0	4.7	24	13.35	0.212

A — Paralink 300s; B — Paralink 500s; C — Ribbed Steel.

Table 7.2

## FIELD PULL-OUT TEST RESULTS

## Wearmouth Minestone

Normal Stress $\sigma_v$ (kN/m <sup>2</sup> )	Strap Type	Strap Length L (m)	Pull-out Force $T_{max}$ (kN)	Displacement at Failure $\Delta L$ (mm)	Shear Stress $\tau$ (kN/m <sup>2</sup> )	Friction Coefficient $f^*$
4	B	4.0	1.6	16	2.27	0.568
	A	4.0	2.6	71	3.82	0.956
15	A	4.0	4.8	80	7.06	0.471
	B	4.0	5.4	32	7.67	0.511
	A	2.0	2.2	46	6.47	0.431
20	A	2.0	3.3	48	9.71	0.485
	A	4.0	6.6	111	9.71	0.485
	A	3.0	6.0	96	11.77	0.588
27	B	2.0	3.1	22	8.81	0.339
	B	4.0	8.2	70	11.65	0.448
	B	3.0	6.1	58	11.55	0.444
32	A	4.0	7.7	131	11.32	0.354
	B	4.0	10.6	88	15.06	0.470
	C	4.0	7.0	28	21.88	0.684
44	B	2.0	3.3	20	9.38	0.218
	B	4.0	9.6	61	13.64	0.317
	B	3.0	6.5	65	12.31	0.286
49	A	2.0	3.1	58	9.12	0.186
	A	4.0	8.5	127	12.50	0.255
	A	3.0	5.6	73	10.98	0.224
55	B	2.0	4.0	21	11.36	0.210
	B	4.0	8.9	81	12.64	0.234
	A	4.0	9.0	142	13.24	0.245
67	A	1.5	2.5	34	9.80	0.151
	B	1.5	4.1	19	15.53	0.239
	C	2.5	7.1	46	35.50	0.546
72	B	2.0	4.7	37	13.35	0.191
	A	4.0	11.6	214	17.06	0.244
	B	4.0	9.8	98	13.92	0.199

A — Paralink 300s; B — Paralink 500s; C — Ribbed Steel.

Table 7.3

## FIELD PULL-OUT TEST RESULTS

## Horden Red Shale

Normal Stress $\sigma_v$ (kN/m <sup>2</sup> )	Strap Type	Strap Length L (m)	Pull-out Force $T_{max}$ (kN)	Displacement at Failure $\Delta L$ (mm)	Shear Stress $\tau$ (kN/m <sup>2</sup> )	Friction Coefficient $f^*$
4	B	4.0	13.30	100	18.89	4.723
	A	4.0	9.70	137	14.26	3.566
16	A	4.0	8.7	134	12.79	0.800
	B	4.0	16.0	141	22.73	1.421
	A	2.0	4.8	43	14.12	0.882
22	A	2.0	4.1	54	12.06	0.548
	A	4.0	8.9	120	13.09	0.595
	A	3.0	6.3	80	12.35	0.562
28	B	2.0	5.4	23	15.34	0.547
	B	4.0	9.7	75	13.78	0.492
	B	3.0	6.3	40	11.93	0.426
34	A	4.0	6.6	120	9.71	0.286
	B	4.0	11.6	83	16.48	0.485
	C	4.0	8.1	50	25.31	0.744
46	B	2.0	7.2	32	20.46	0.445
	B	4.0	17.9	147	25.43	0.553
	B	3.0	15.7	116	29.74	0.646
52	A	2.0	7.9	50	23.24	0.447
	A	4.0	12.1	155	17.79	0.342
	A	3.0	11.0	128	21.57	0.415
58	B	2.0	8.7	34	24.72	0.426
	B	4.0	20.1	153	28.55	0.492
	A	4.0	14.4	200	21.18	0.365
70	A	1.5*	—	—	—	—
	B	1.5	7.2	30	27.27	0.390
	C	2.5	8.4	26	42.00	0.600
76	B	2.0	7.9	39	22.44	0.295
	A	4.0	13.2*	125*	—	—
	B	4.0	13.5*	115*	—	—

A — Paralink 300s; B — Paralink 500s; C — Ribbed Steel.

\* — Test stopped. Never finished due to technical fault.

Table 7.4

## FIELD PULL-OUT TEST RESULTS

Loudon Hill Sand

Normal Stress $\sigma_v$ (kN/m <sup>2</sup> )	Strap Type	Strap Length L (m)	Pull-out Force $T_{max}$ (kN)	Displacement at Failure $\Delta L$ (mm)	Shear Stress $\tau$ (kN/m <sup>2</sup> )	Friction Coefficient $f^*$
11	A	4.0	3.5	73	5.15	0.468
	B	4.0	5.9	40	8.38	0.762
	B	1.5	1.8	18	6.82	0.620
19	A	1.5	1.6	22	6.28	0.331
	A	3.0	2.4	35	4.71	0.248
	B	3.0	6.4	42	12.12	0.638
27	C	1.5	2.0	22	16.67	0.617
	A	4.0	6.2	53	9.12	0.338
	B	4.0	10.6	39	15.06	0.558
34	A	3.0	4.5	54	8.82	0.259
	B	1.5	2.4	8	9.09	0.267
	B	3.0	5.0	23	9.47	0.279
42	C	4.0	5.8	28	18.13	0.432
	A	4.0	6.1	85	8.97	0.214
	B	4.0	9.1	40	12.93	0.308
50	A	1.5	2.6	24	10.20	0.204
	A	3.0	3.9	45	7.65	0.153
	B	3.0	8.5	40	16.10	0.322
58	A	4.0	10.3	63	15.15	0.261
	B	1.5	7.4	32	28.03	0.483
	B	4.0	14.4	100	20.46	0.353
67	A	1.5	3.8	31	14.90	0.222
	A	3.0	5.4	63	10.59	0.158
	B	3.0	8.8	45	16.67	0.249

A — Paralink 300s; B — Paralink 500s; C — Ribbed Steel.

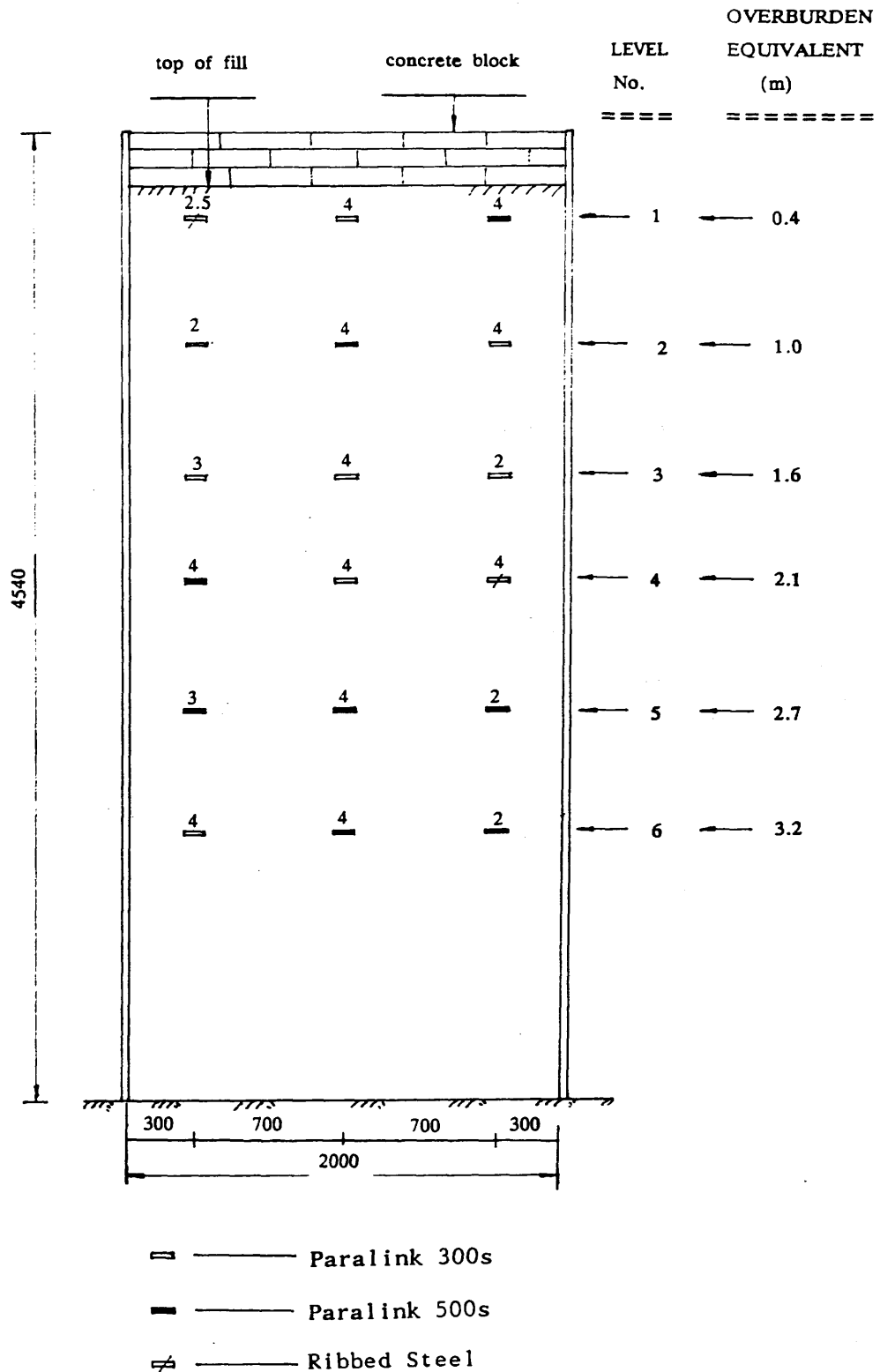
Table 7.5

## FIELD PULL-OUT TEST RESULTS

Methil PFA

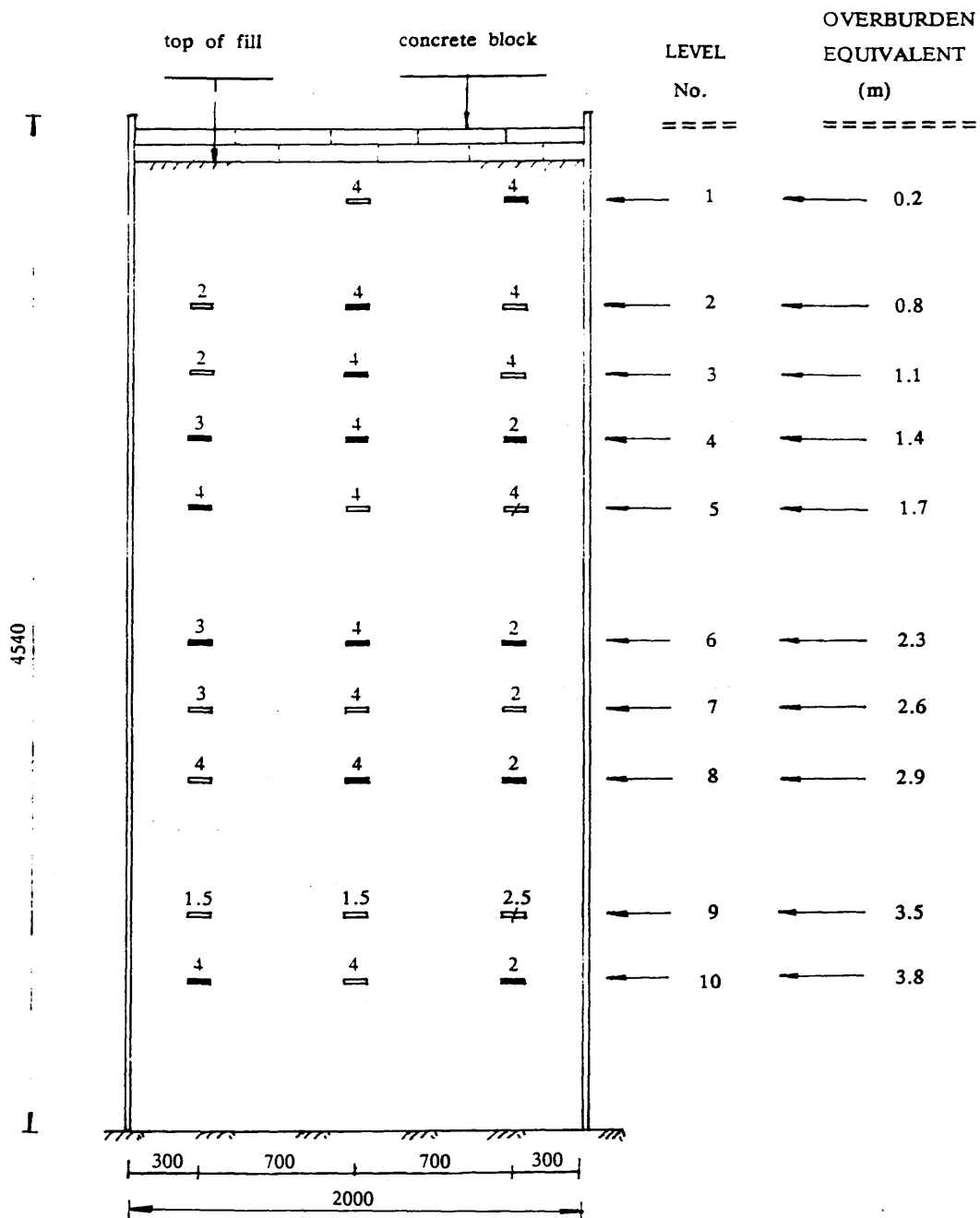
Normal Stress $\sigma_v$ (kN/m <sup>2</sup> )	Strap Type	Strap Length L (m)	Pull-out Force $T_{max}$ (kN)	Displacement at Failure $\Delta L$ (mm)	Shear Stress $\tau$ (kN/m <sup>2</sup> )	Friction Coefficient $f^*$
9	A	4.0	3.5	110	5.15	0.572
	B	4.0	6.2	78	8.81	0.979
	B	1.5	2.5	17	9.47	1.052
16	A	1.5	1.7	50	6.67	0.417
	A	3.0	3.1	55	6.08	0.380
	B	3.0	2.0	20	3.79	0.237
23	C	1.5	0.8	6	6.67	0.290
	A	4.0	4.7	82	6.91	0.300
	B	4.0	4.5	37	6.39	0.278
29	A	3.0	3.2	63	6.27	0.216
	B	1.5	3.4	31	12.88	0.444
	B	3.0	5.1	22	9.66	0.333
36	C	4.0	6.6	10	20.63	0.573
	A	4.0	4.6	77	6.77	0.188
	B	4.0	5.7	47	8.10	0.225
43	A	1.5	1.9	35	7.45	0.173
	A	3.0	3.4	79	6.67	0.155
	B	3.0	4.7	27	8.90	0.207
50	A	4.0	5.1	74	7.50	0.150
	B	1.5	3.1	14	11.74	0.235
	B	4.0	7.5	43	10.65	0.213
56	A	1.5	2.2	33	8.63	0.154
	A	3.0	4.1	65	8.04	0.144
	B	3.0	5.6	38	10.61	0.190

A — Paralink 300s; B — Paralink 500s; C — Ribbed Steel.



The number above the strap represent the strap length.

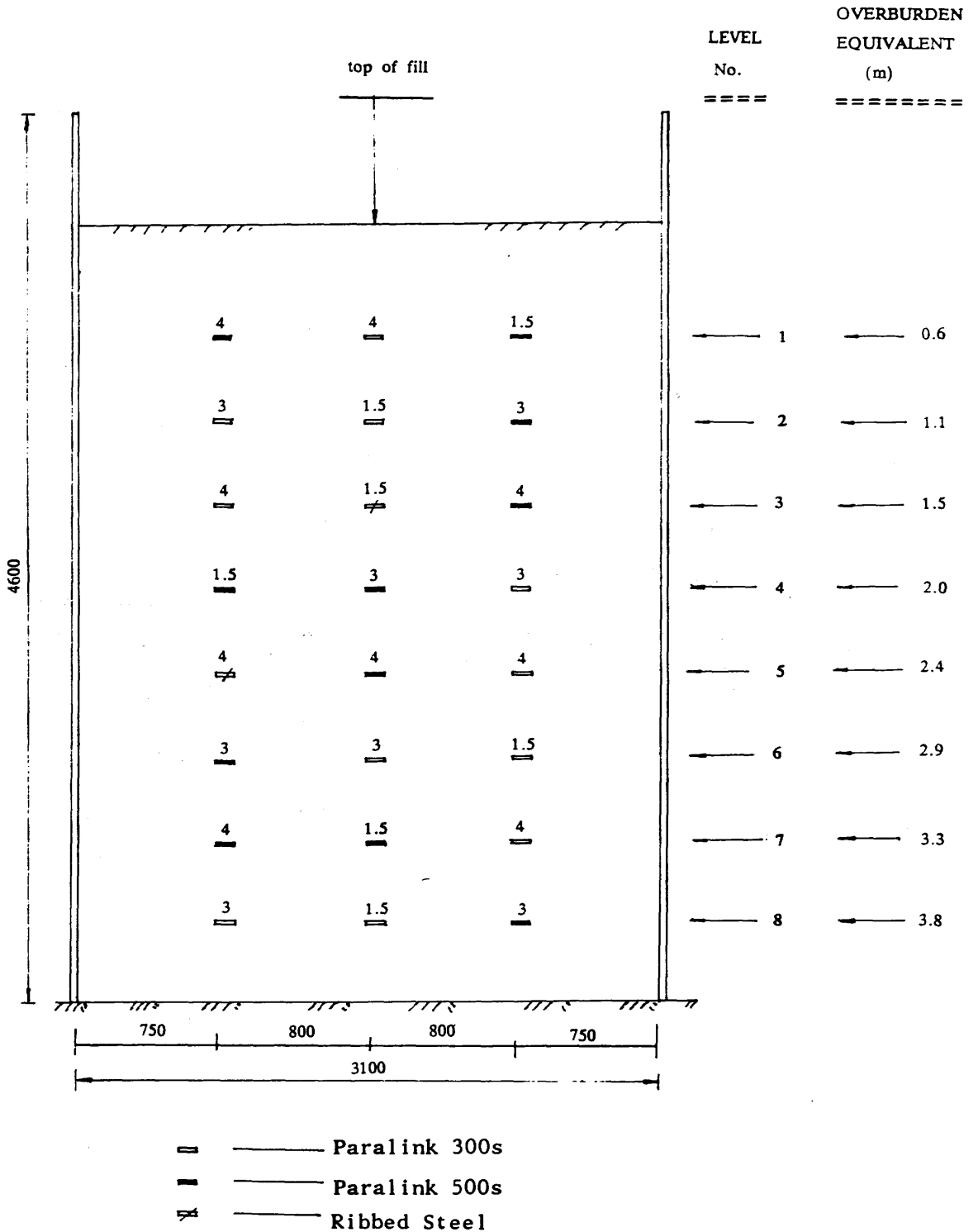
Figure 7.1 ARRANGEMENT OF VARIOUS STRAPS IN THE FIELD FULL-SCALE BOX IN WARDLEY COLLIERY ( for the Test with Wardley Minestone )



- ▬ ————— Paralink 300s
- ▬ ————— Paralink 500s
- ▬ ————— Ribbed Steel

The number above the strap represent the strap length.

Figure 7.2 ARRANGEMENT OF VARIOUS STRAPS IN THE FIELD FULL-SCALE BOX IN WARDLEY COLLIERY ( for the Test with Wearmouth Minestone and Horden red shale )



The number above the strap represent the strap length.

Figure 7.3 ARRANGEMENT OF VARIOUS STRAPS IN THE FIELD FULL-SCALE BOX IN BARONY COLLIERY ( for the Test with Loudon Hill sand and Methil PFA )

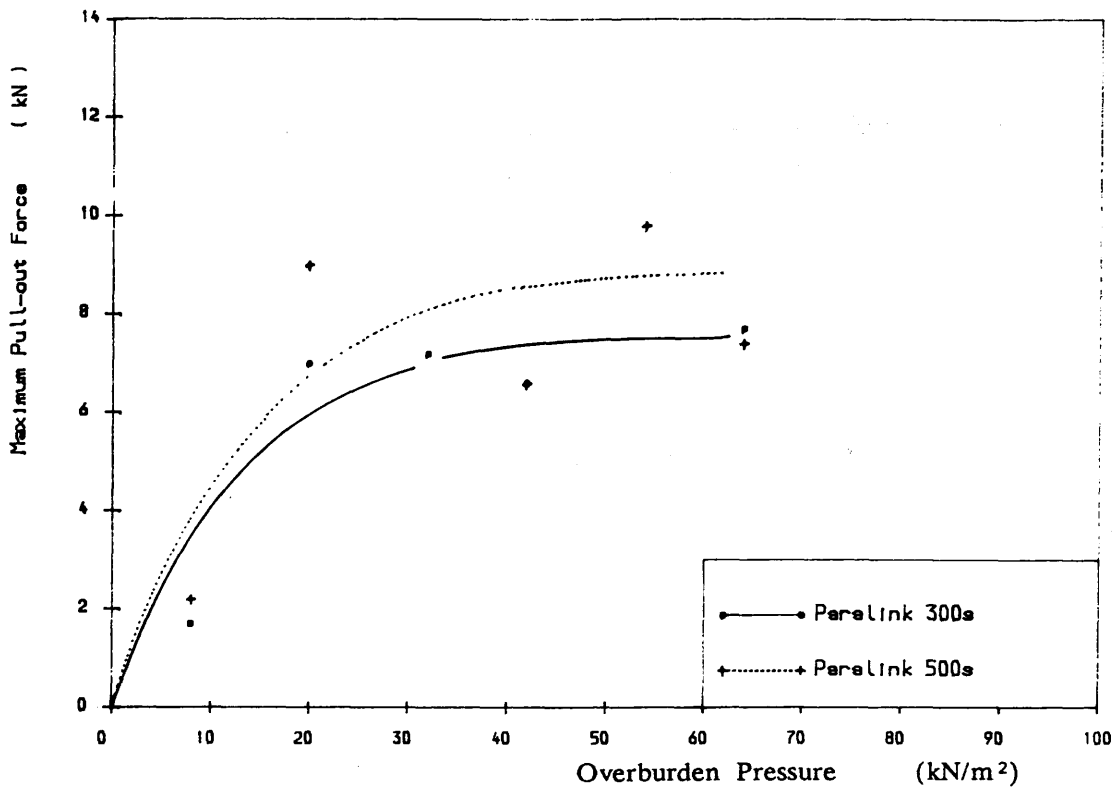


Figure 7.4 MAXIMUM PULL-OUT FORCE VS. OVERBURDEN PRESSURE

Field Pull-out Test, Vardley Minestone, L=4m

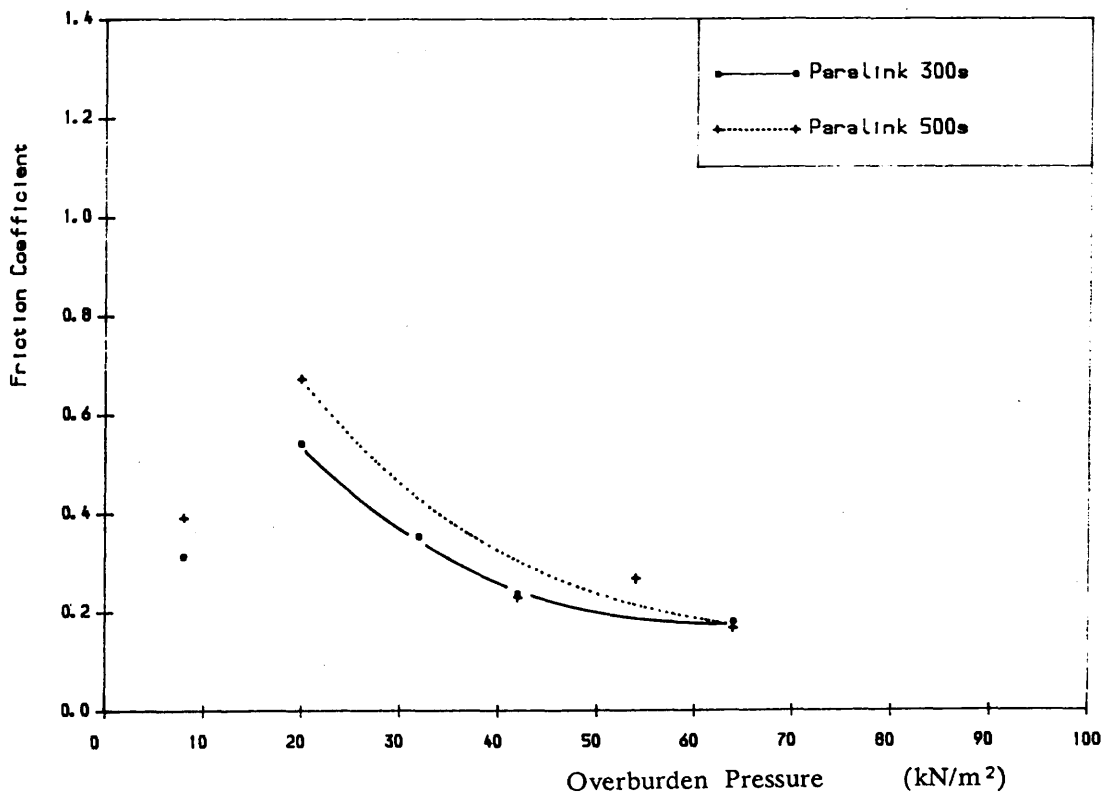


Figure 7.5 FRICTION COEFFICIENT VS. OVERBURDEN PRESSURE

Field Pull-out Test, Vardley Minestone, L=4m

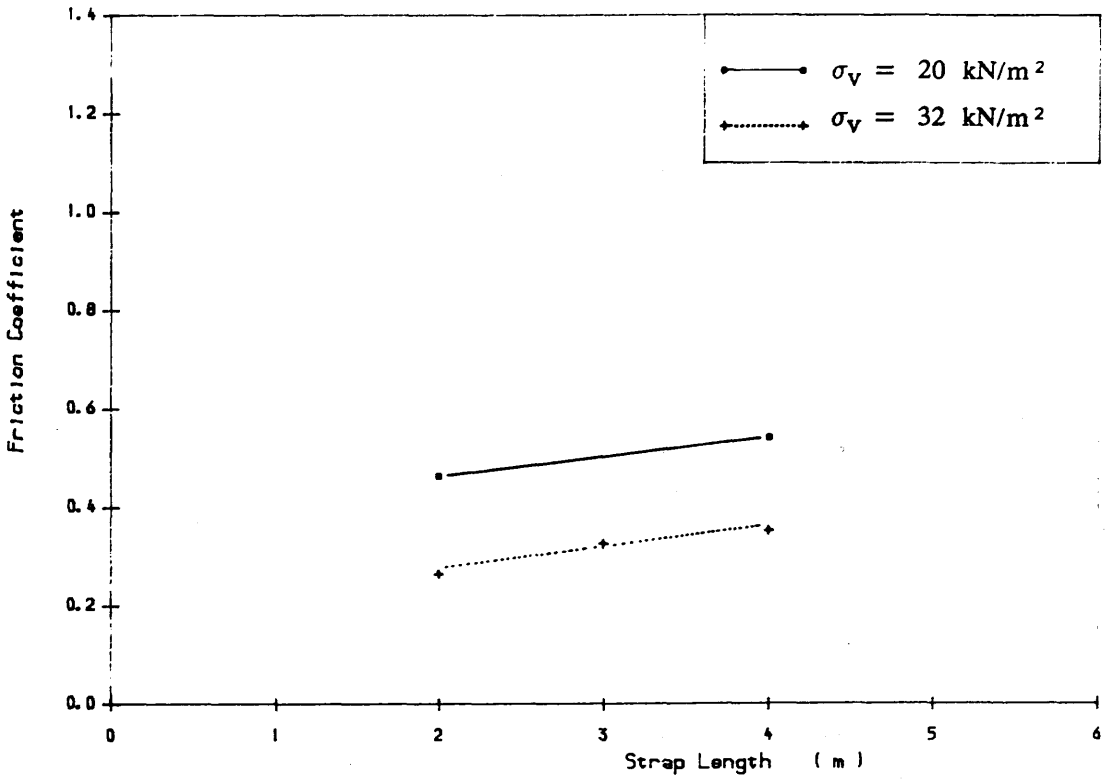


Figure 7.6 FRICTION COEFFICIENT VS. STRAP LENGTH  
Field Pull-out Test, Vardley Minestone, Paralink 300s

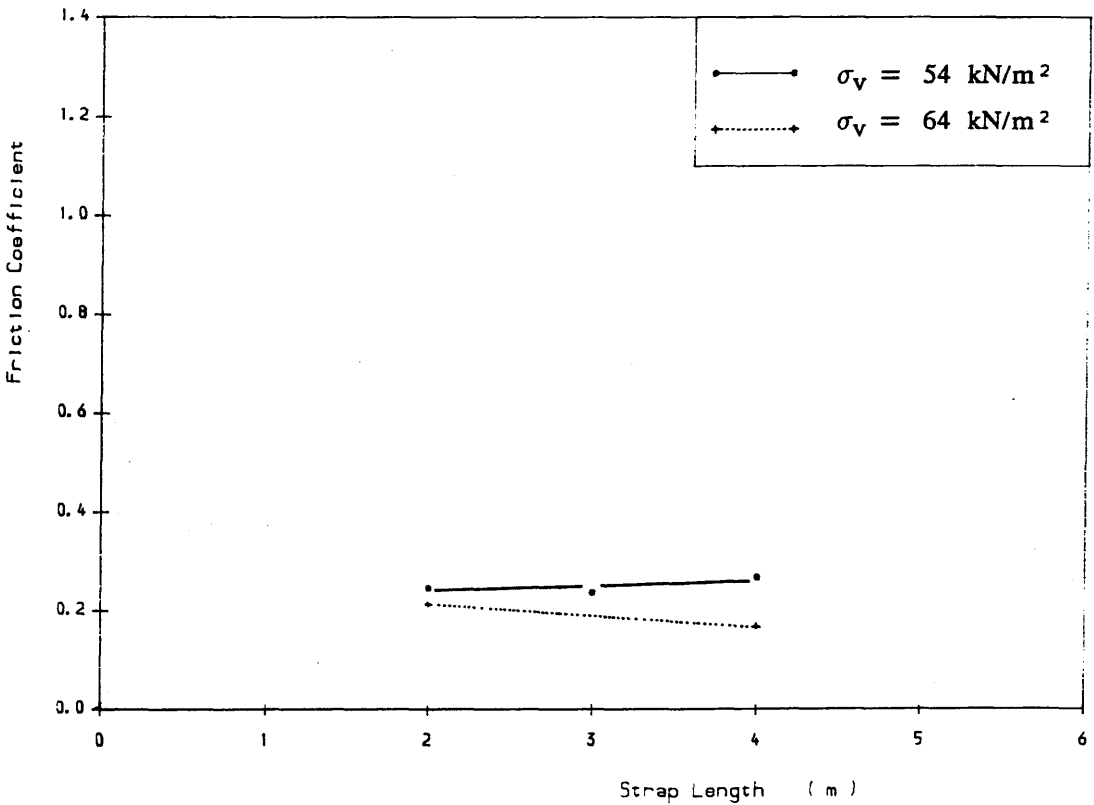


Figure 7.7 FRICTION COEFFICIENT VS. STRAP LENGTH  
Field Pull-out Test, Vardley Minestone, Paralink 500s

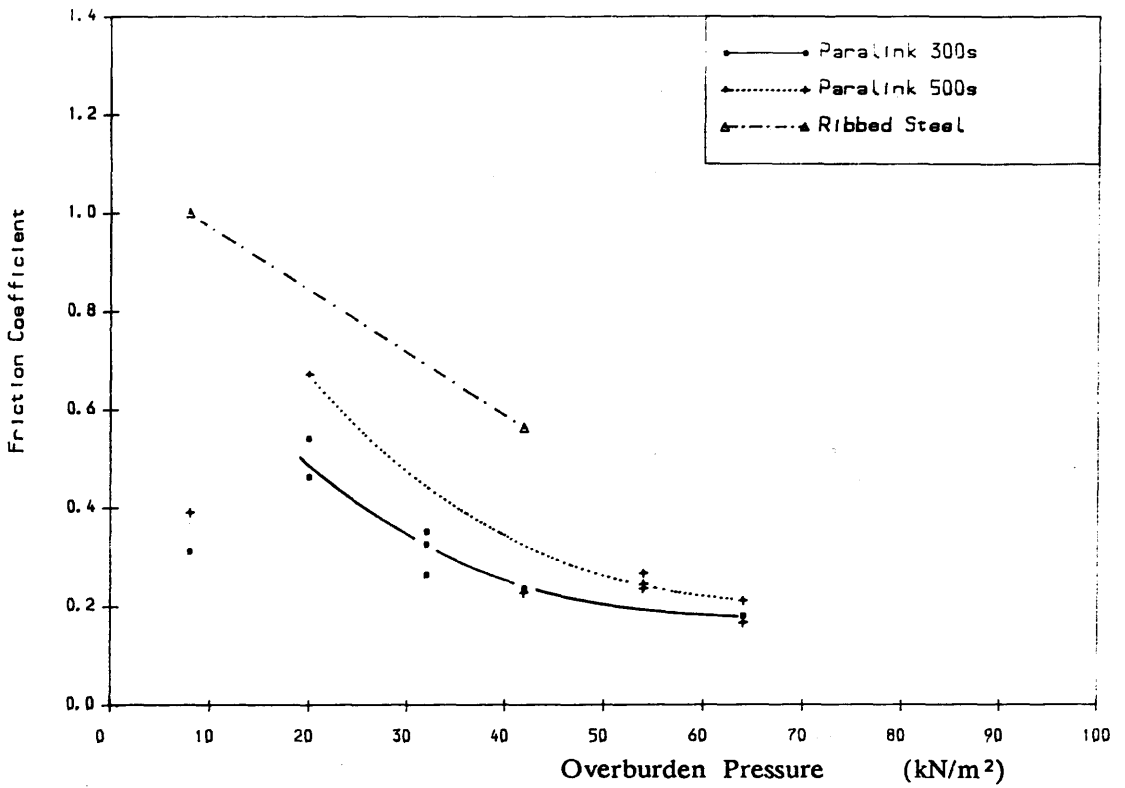


Figure 7.8 FRICTION COEFFICIENT VS. OVERBURDEN PRESSURE

Field Pull-out Test, Wardley Minestone, with Various Lengths

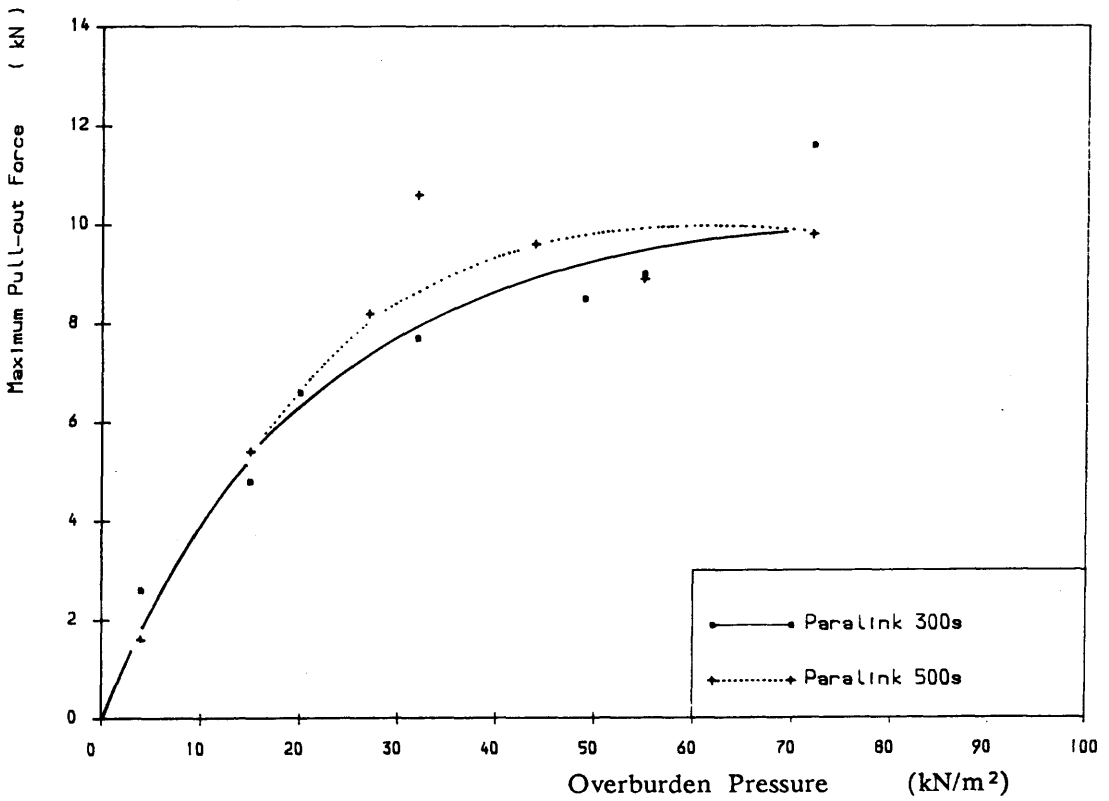


Figure 7.9 MAXIMUM PULL-OUT FORCE VS. OVERBURDEN PRESSURE

Field Pull-out Test, Wearmouth Minestone, L=4m

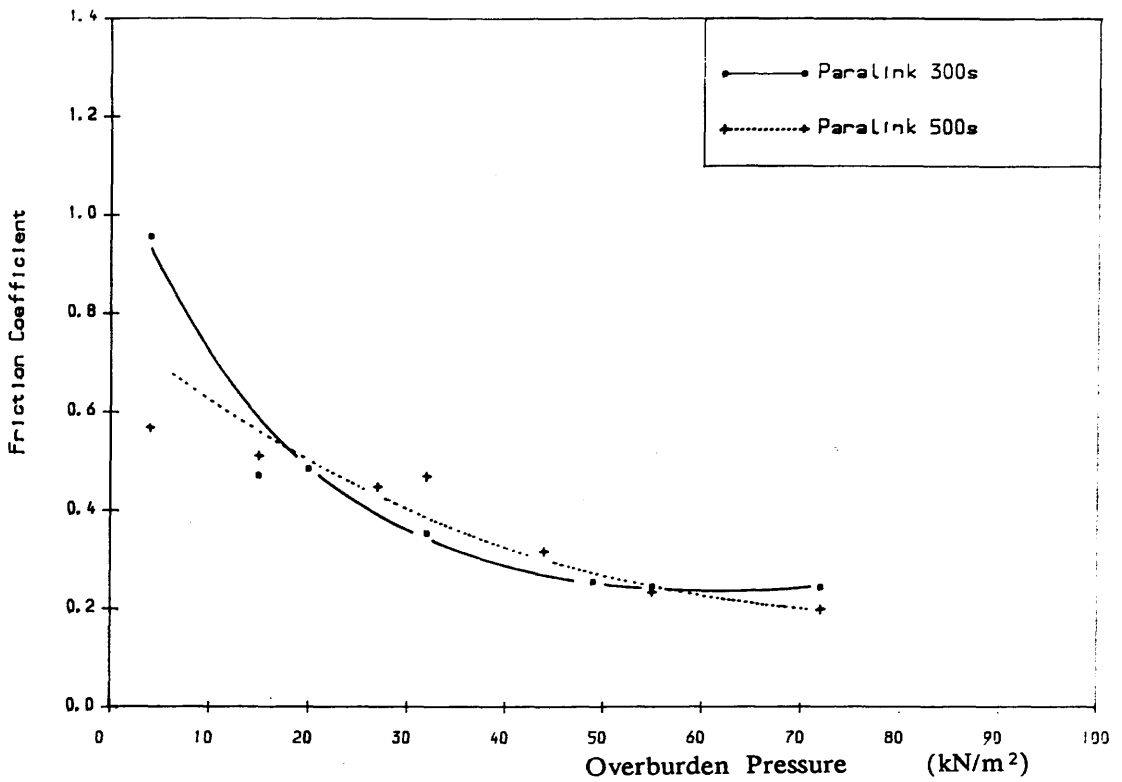


Figure 7.10 FRICTION COEFFICIENT VS. OVERBURDEN PRESSURE  
Field Pull-out Test, Wearmouth Minestone, L=4m

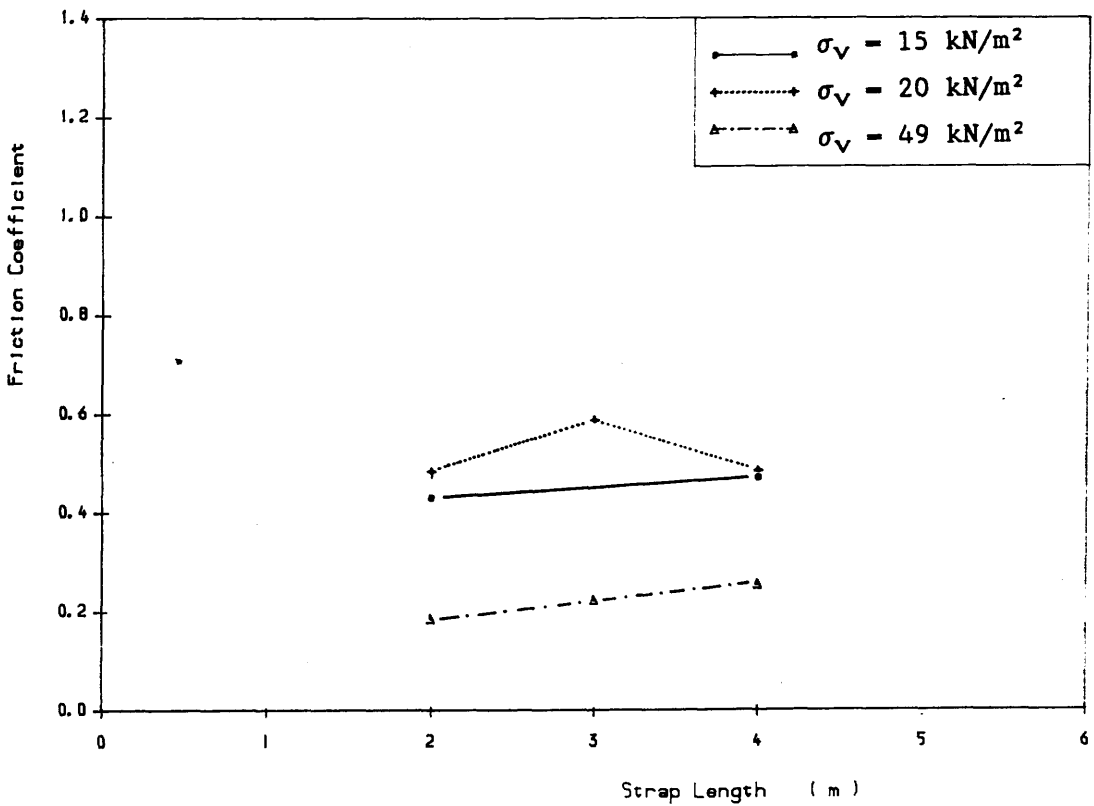


Figure 7.11 FRICTION COEFFICIENT VS. STRAP LENGTH  
Field Pull-out Test, Wearmouth Minestone, Paralink 300s

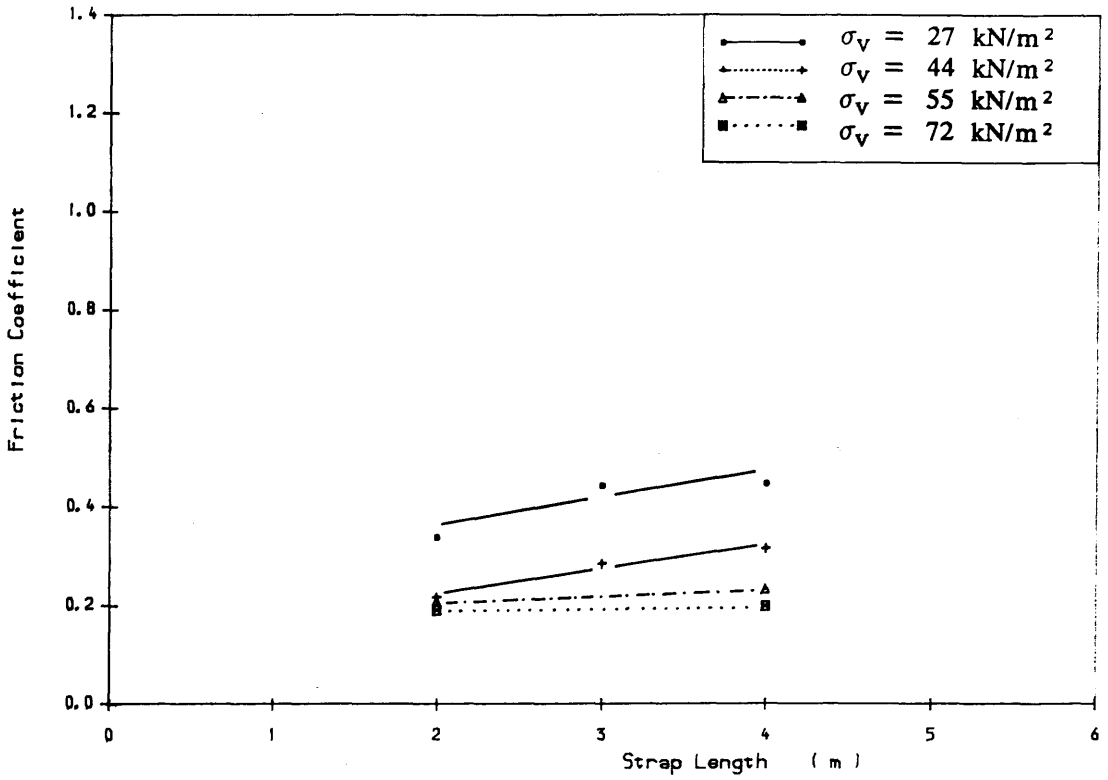


Figure 7.12 FRICTION COEFFICIENT VS. STRAP LENGTH  
Field Pull-out Test, Veermouth Minestone, Paralink 500s

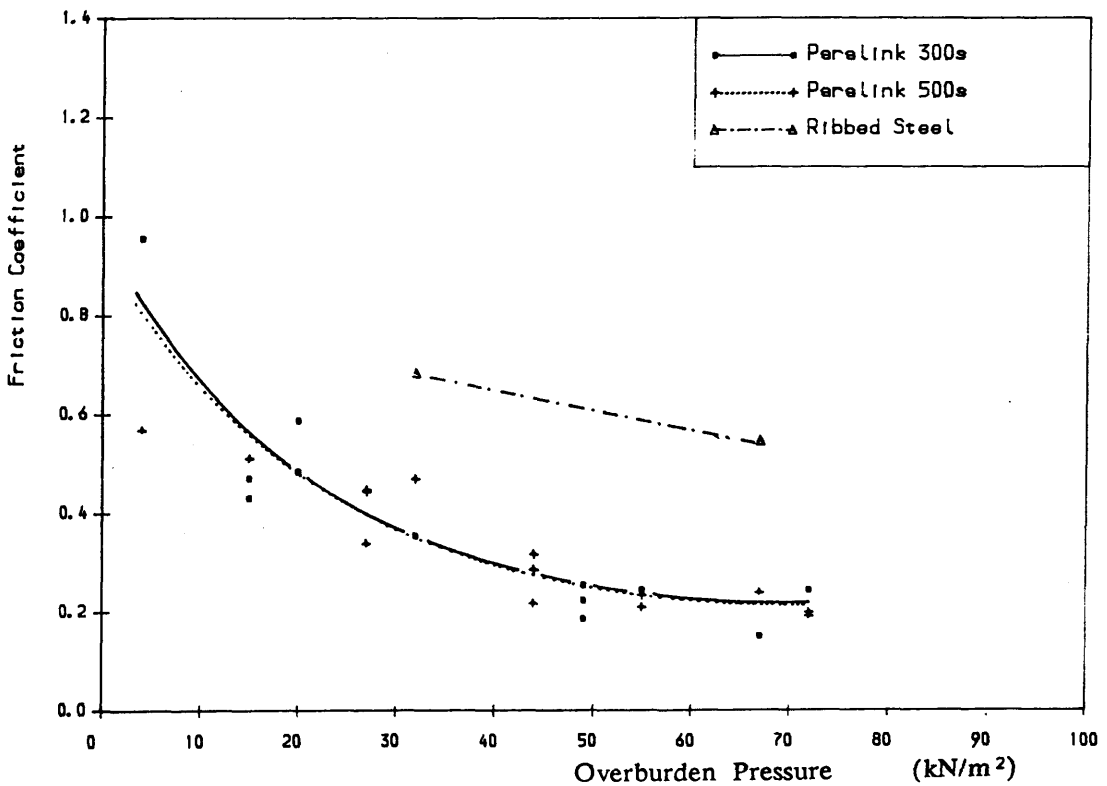


Figure 7.13 FRICTION COEFFICIENT VS. OVERBURDEN PRESSURE  
Field Pull-out Test, Veermouth Minestone, with Various Lengths

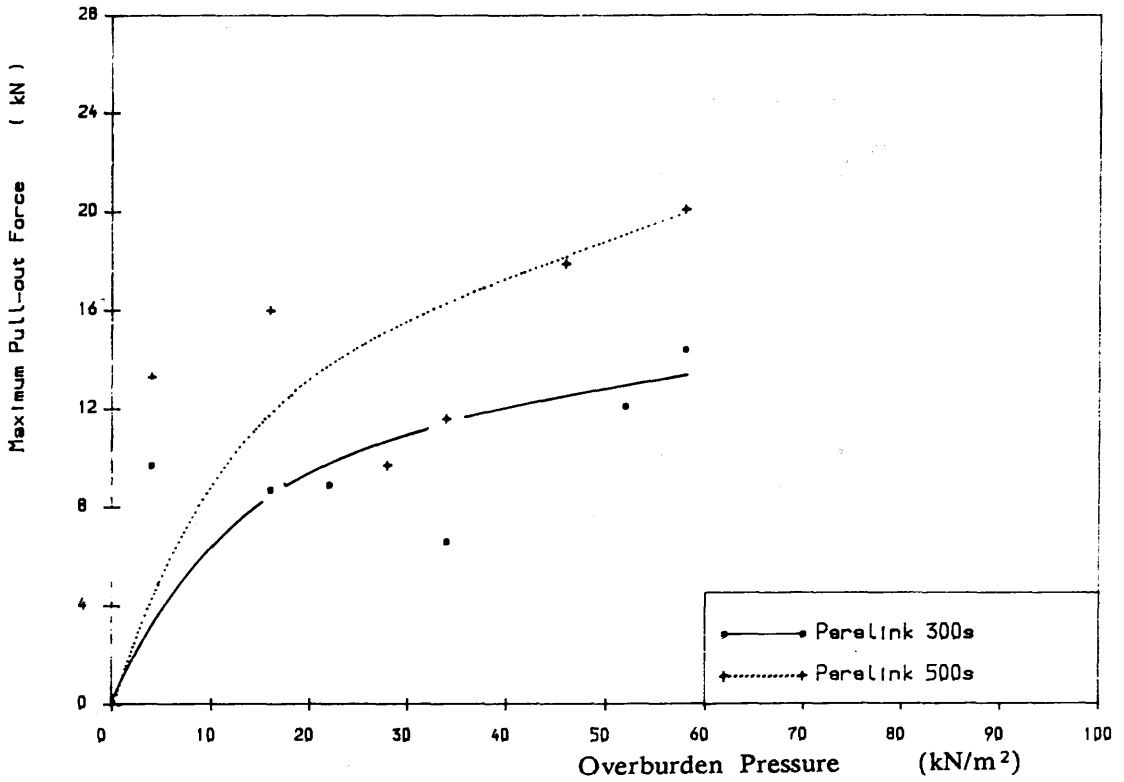


Figure 7.14 MAXIMUM PULL-OUT FORCE VS. OVERBURDEN PRESSURE  
Field Pull-out Test, Horden Red Shale, L=4m

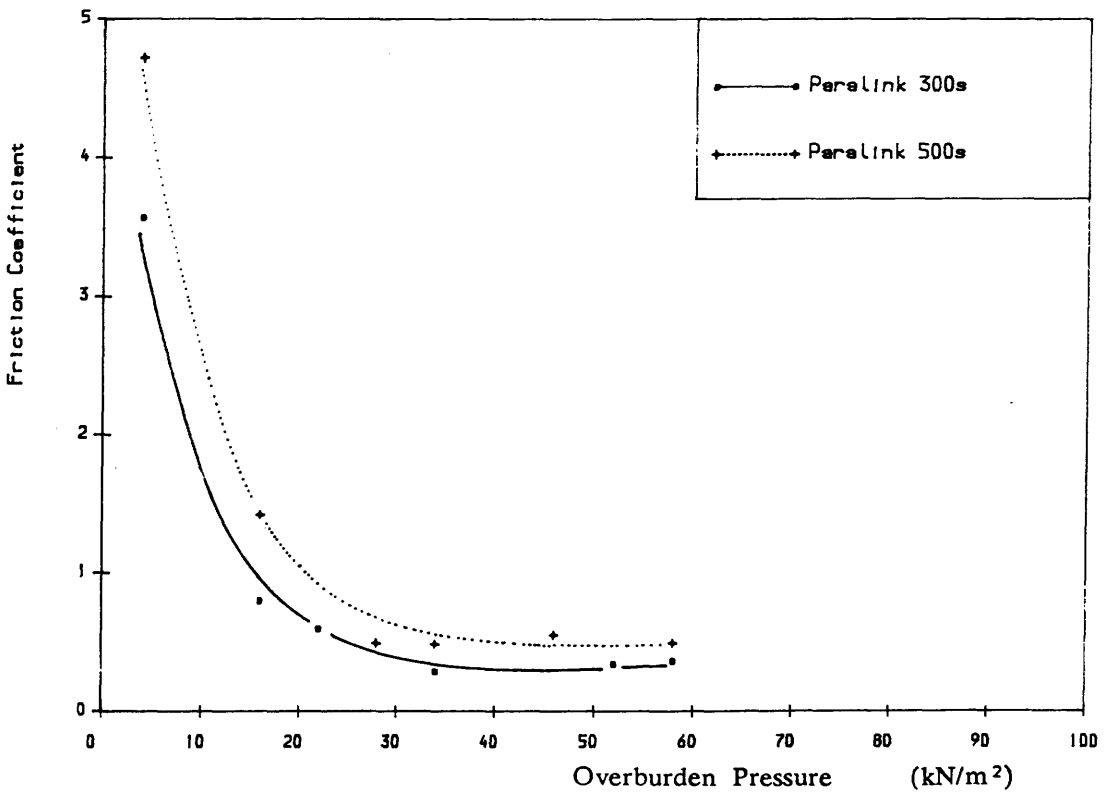


Figure 7.15 FRICTION COEFFICIENT VS. OVERBURDEN PRESSURE  
Field Pull-out Test, Horden Red Shale, L=4m

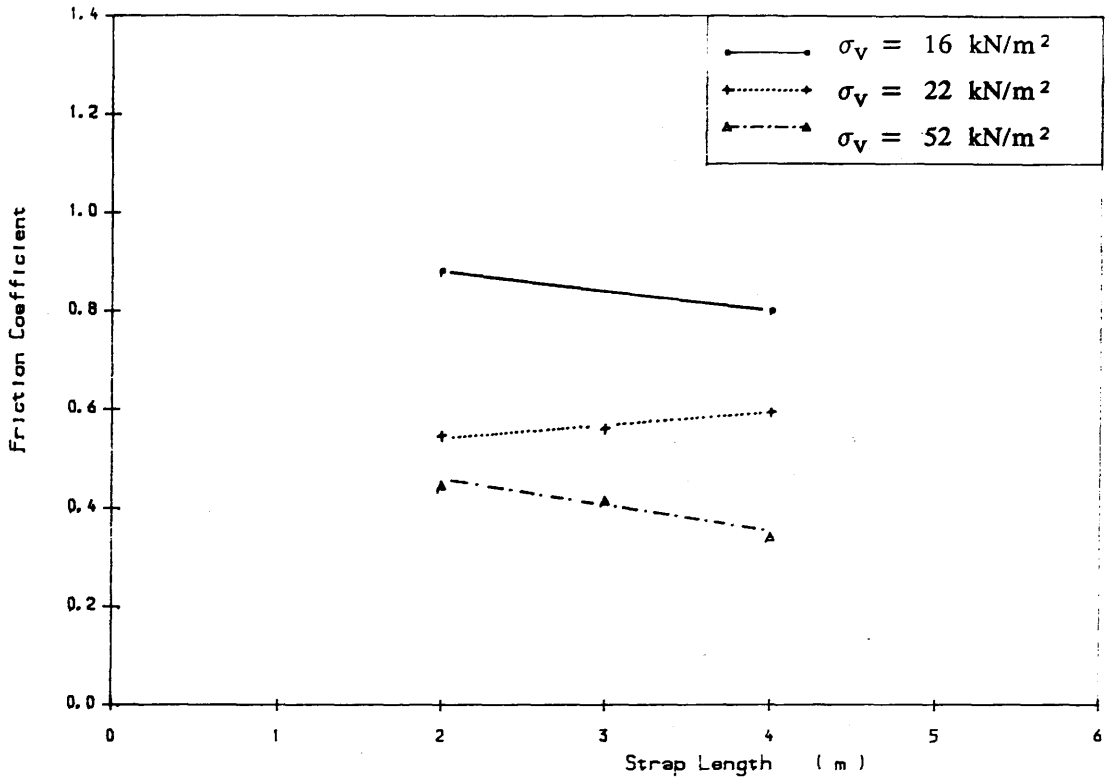


Figure 7.16 FRICTION COEFFICIENT VS. STRAP LENGTH  
Field Pull-out Test, Horden Red Shale, Paralink 300s

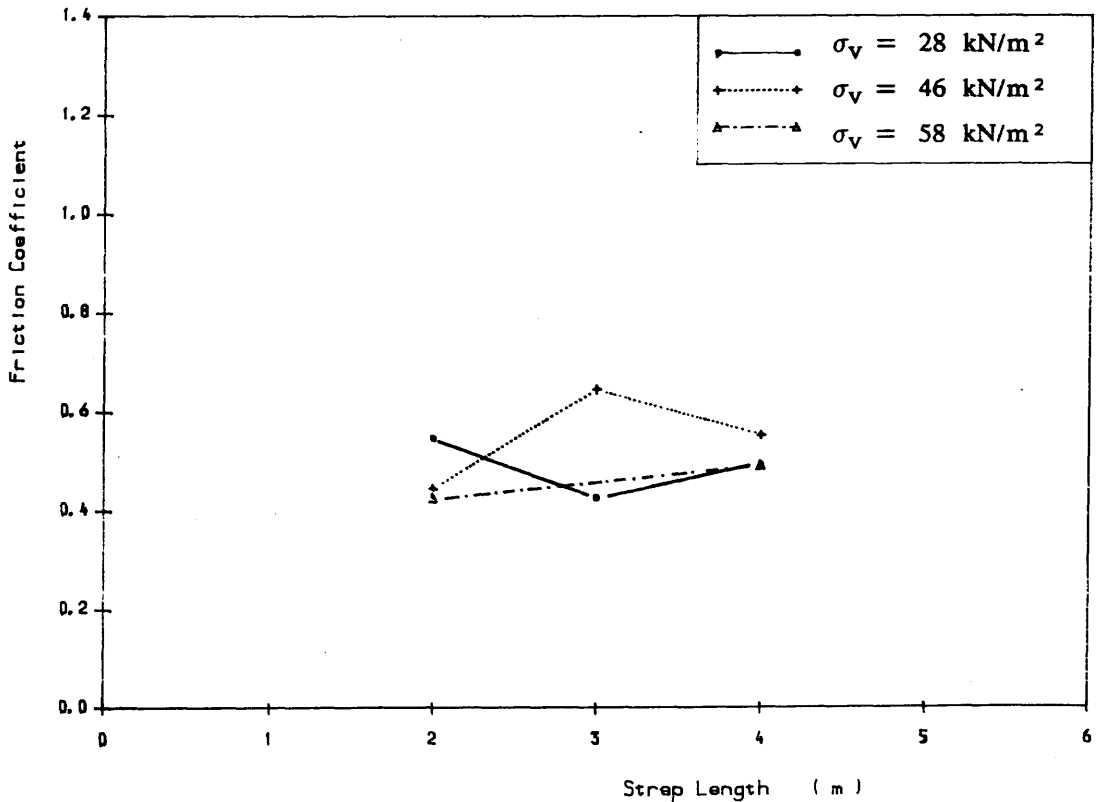


Figure 7.17 FRICTION COEFFICIENT VS. STRAP LENGTH  
Field Pull-out Test, Horden Red Shale, Paralink 500s

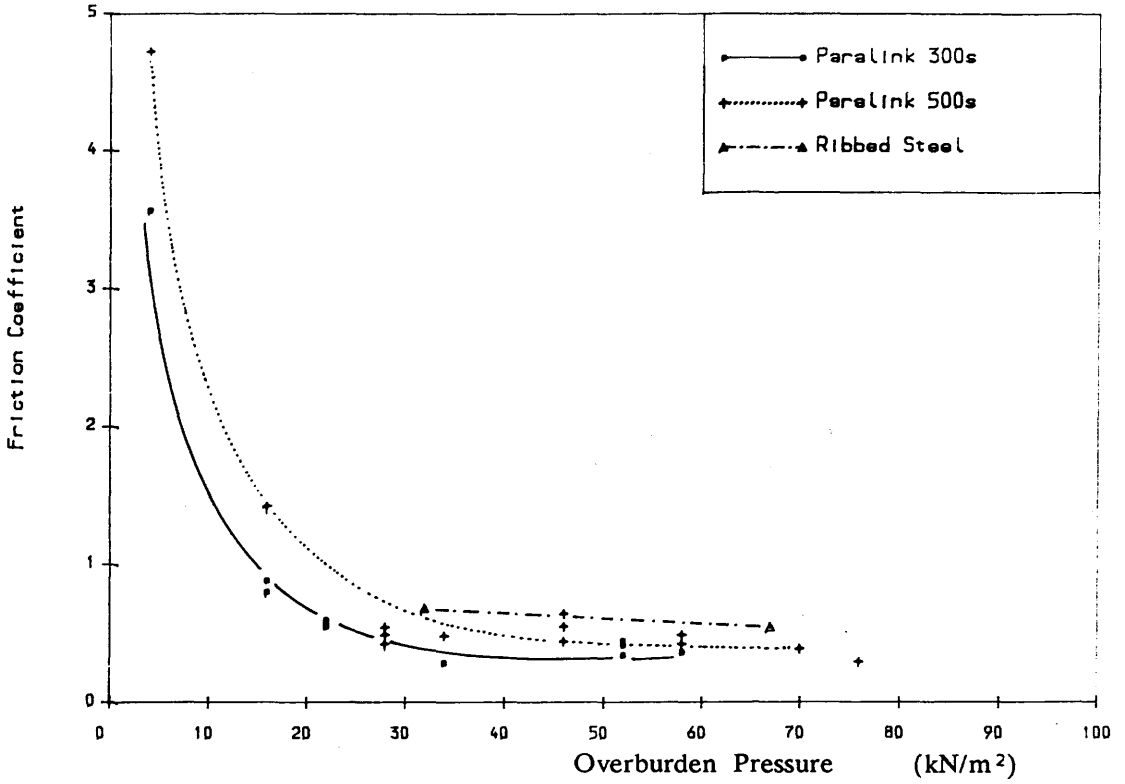


Figure 7.18 FRICTION COEFFICIENT VS. OVERBURDEN PRESSURE

Field Pull-out Test, Horden Red Shale, with Various Lengths

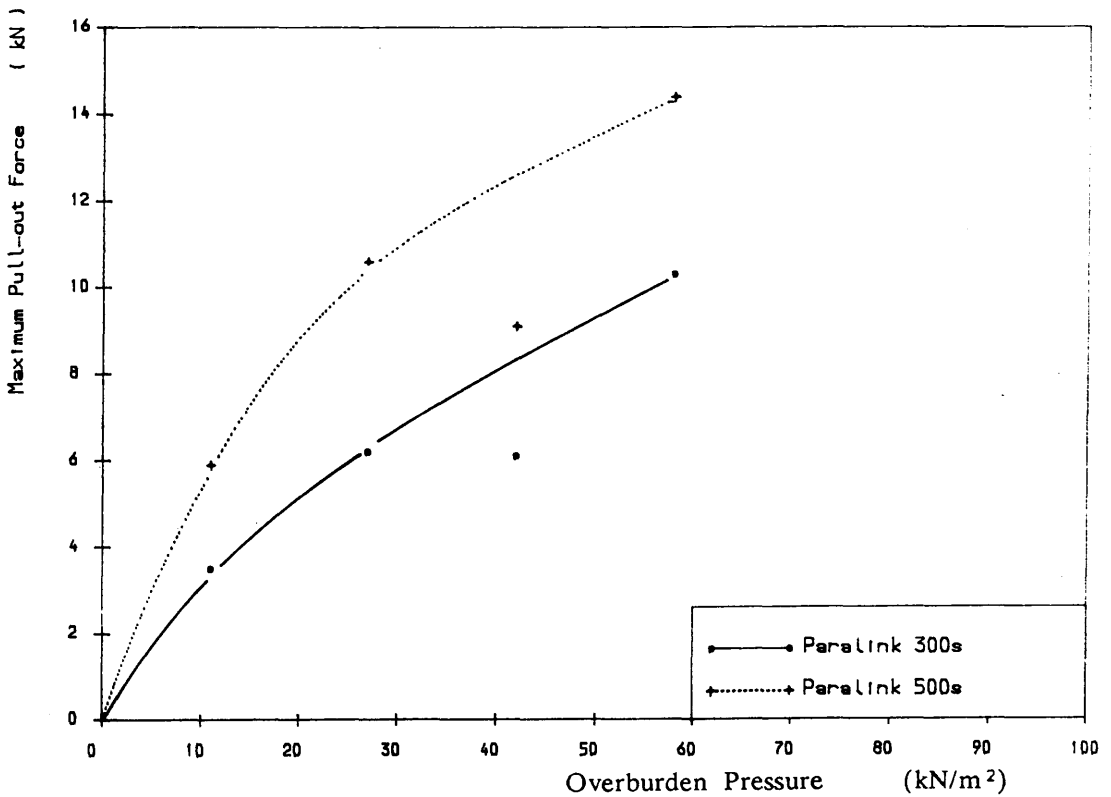


Figure 7.19 MAXIMUM PULL-OUT FORCE VS. OVERBURDEN PRESSURE

Field Pull-out Test, Loudon Hill Sand, L=4m

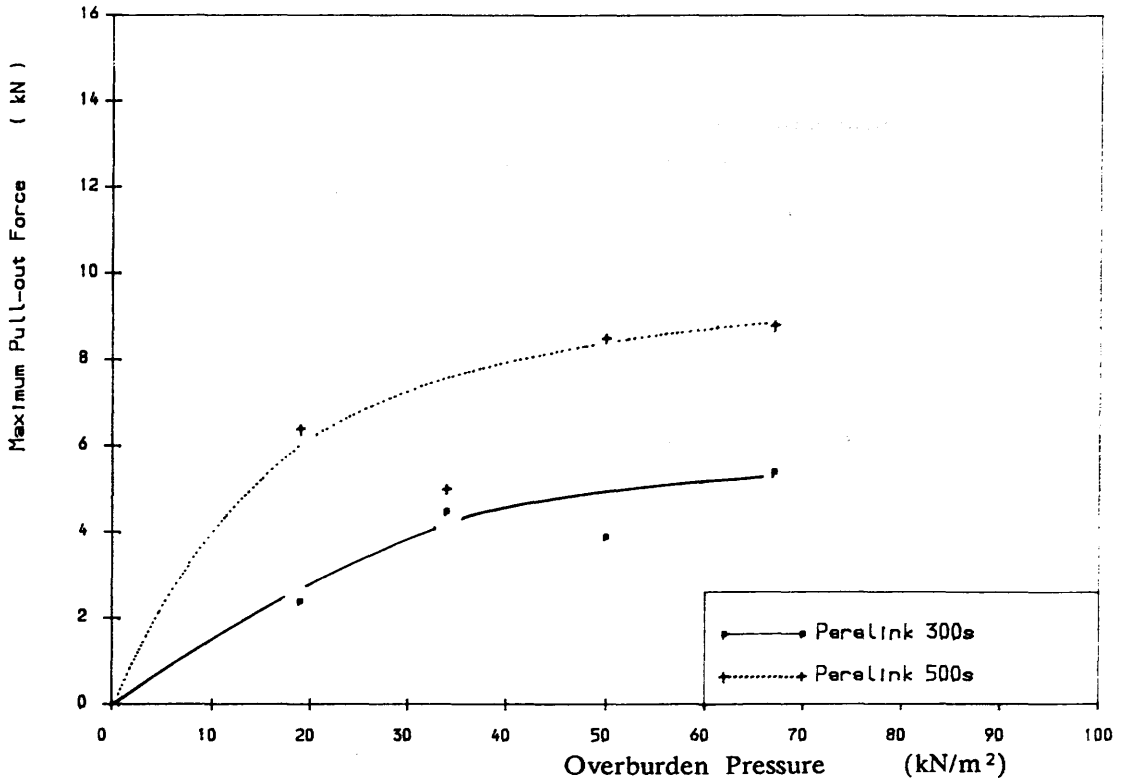


Figure 7.20 MAXIMUM PULL-OUT FORCE VS. OVERBURDEN PRESSURE  
Field Pull-out Test, Loudon Hill Sand, L=3m

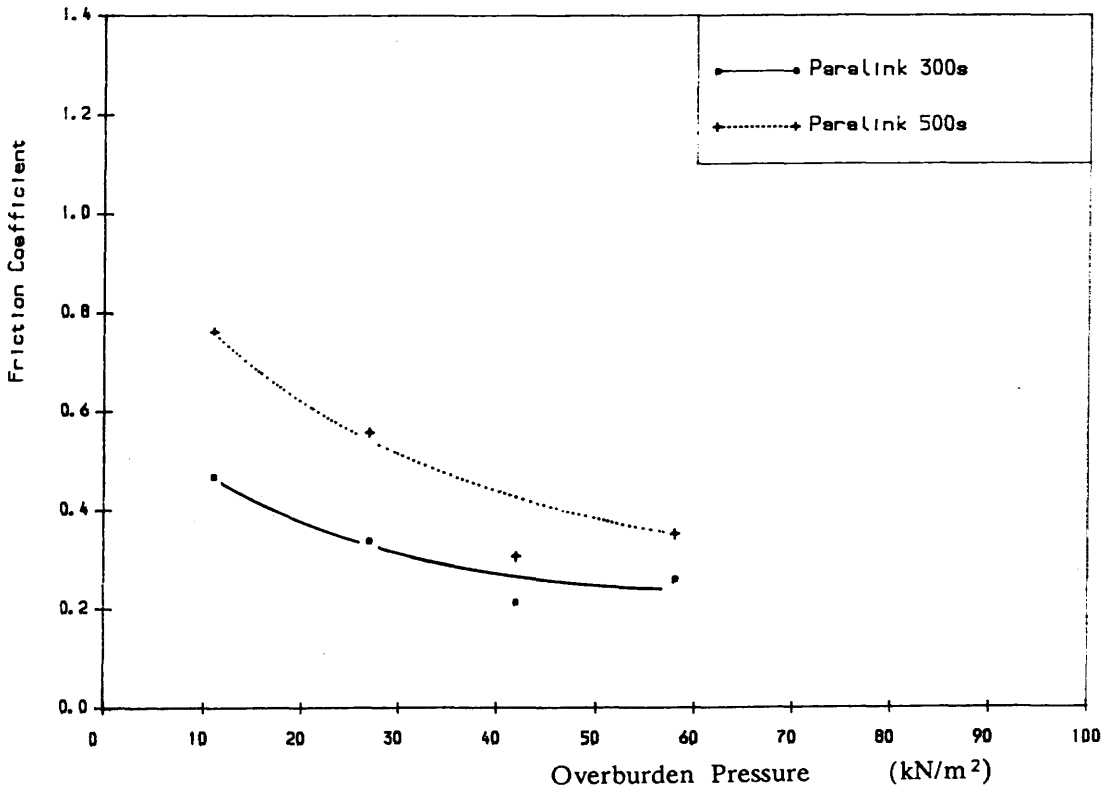


Figure 7.21 FRICTION COEFFICIENT VS. OVERBURDEN PRESSURE  
Field Pull-out Test, Loudon Hill Sand, L=4m

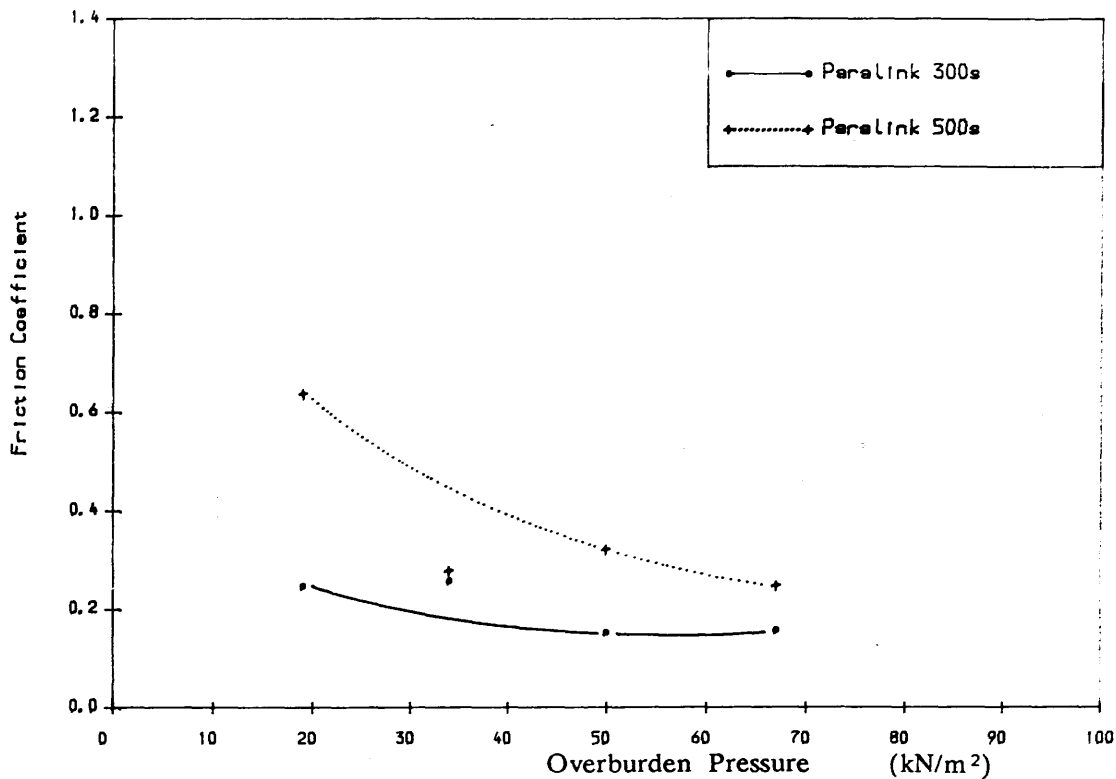


Figure 7.22 FRICTION COEFFICIENT VS. OVERBURDEN PRESSURE  
Field Pull-out Test, Loudon Hill Sand, L=3m

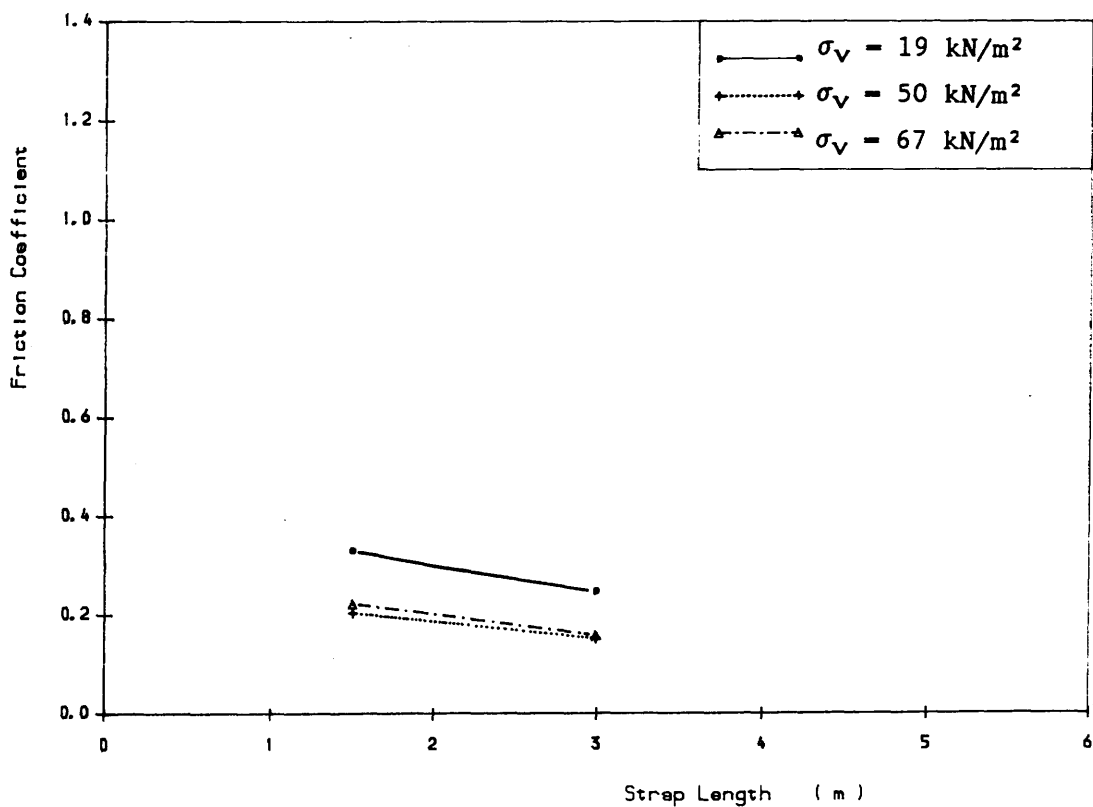


Figure 7.23 FRICTION COEFFICIENT VS. STRAP LENGTH  
Field Pull-out Test, Loudon Hill Sand, Paralink 300s

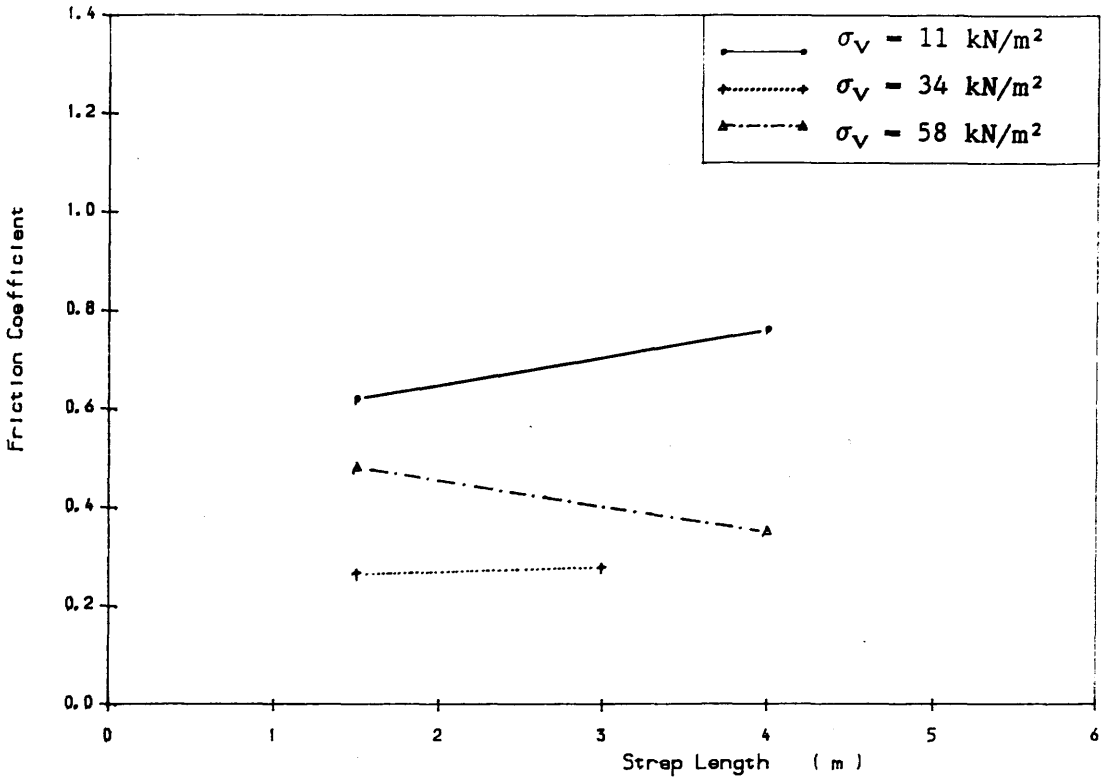


Figure 7.24 FRICTION COEFFICIENT VS. STRAP LENGTH  
Field Pull-out Test, Loudon Hill Sand, Paralink 500s

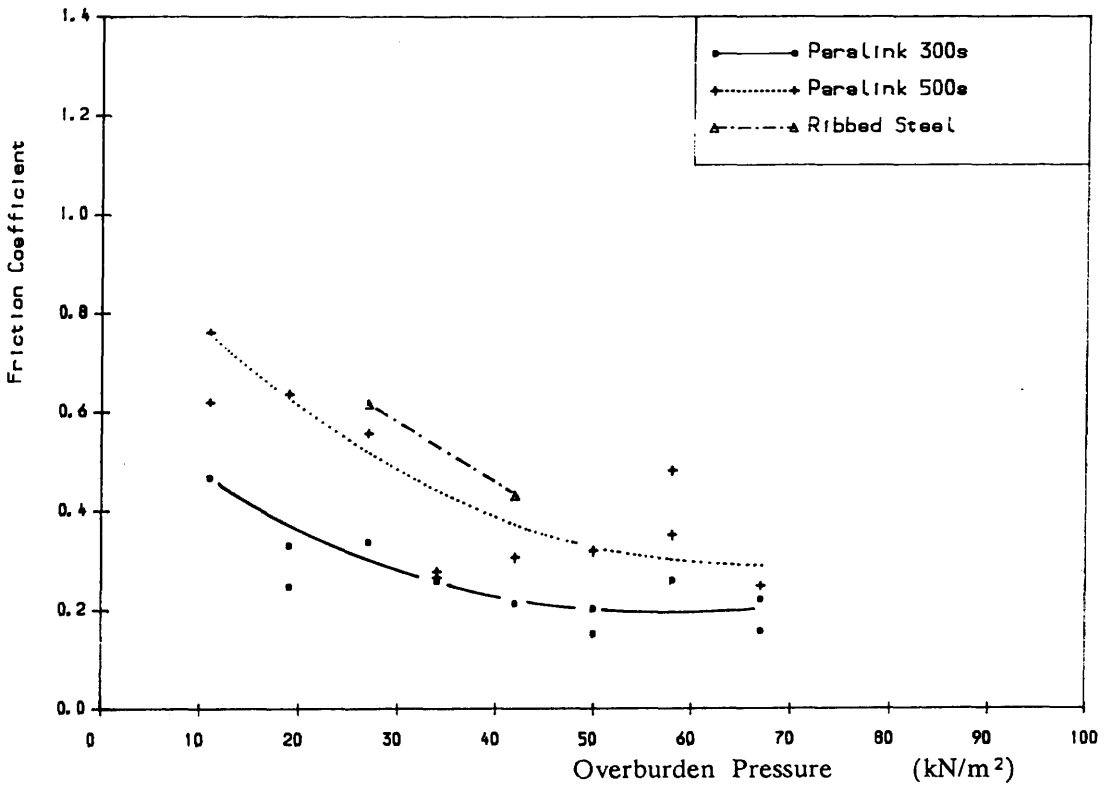


Figure 7.25 FRICTION COEFFICIENT VS. OVERBURDEN PRESSURE  
Field Pull-out Test, Loudon Hill Sand, with Various Lengths

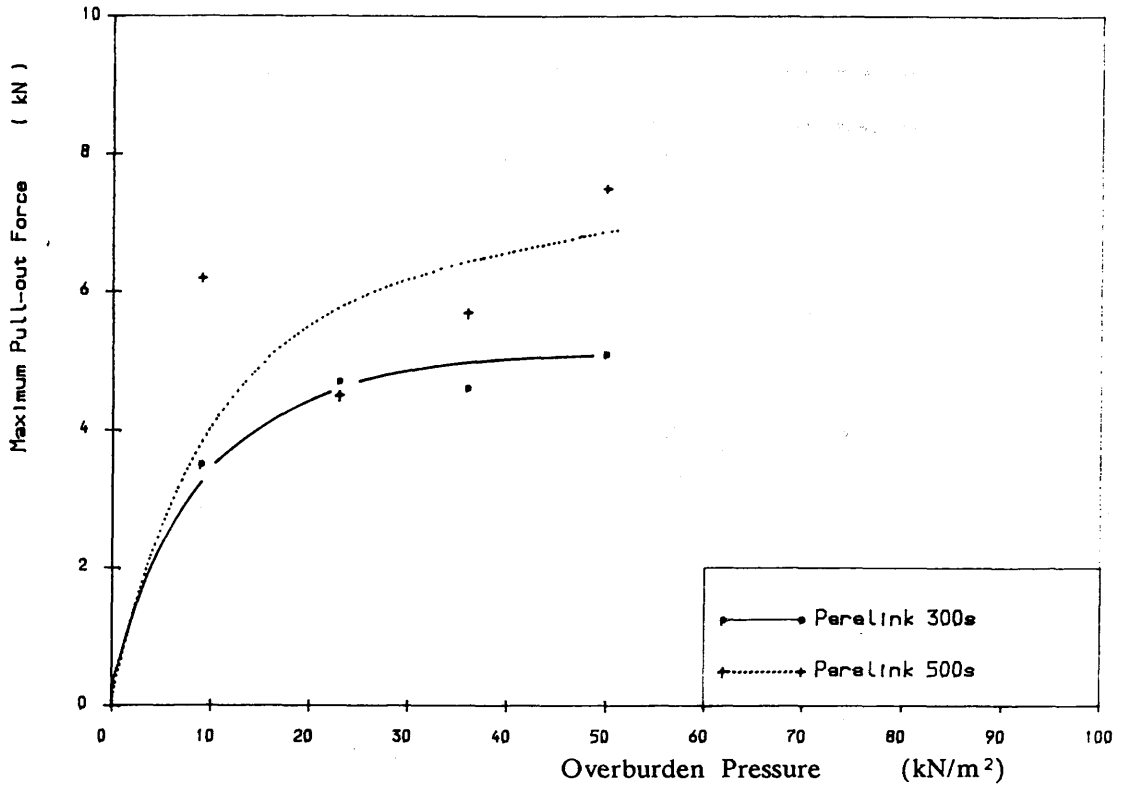


Figure 7.26 MAXIMUM PULL-OUT FORCE VS. OVERBURDEN PRESSURE  
Field Pull-out Test, Methil PFA, L=4m

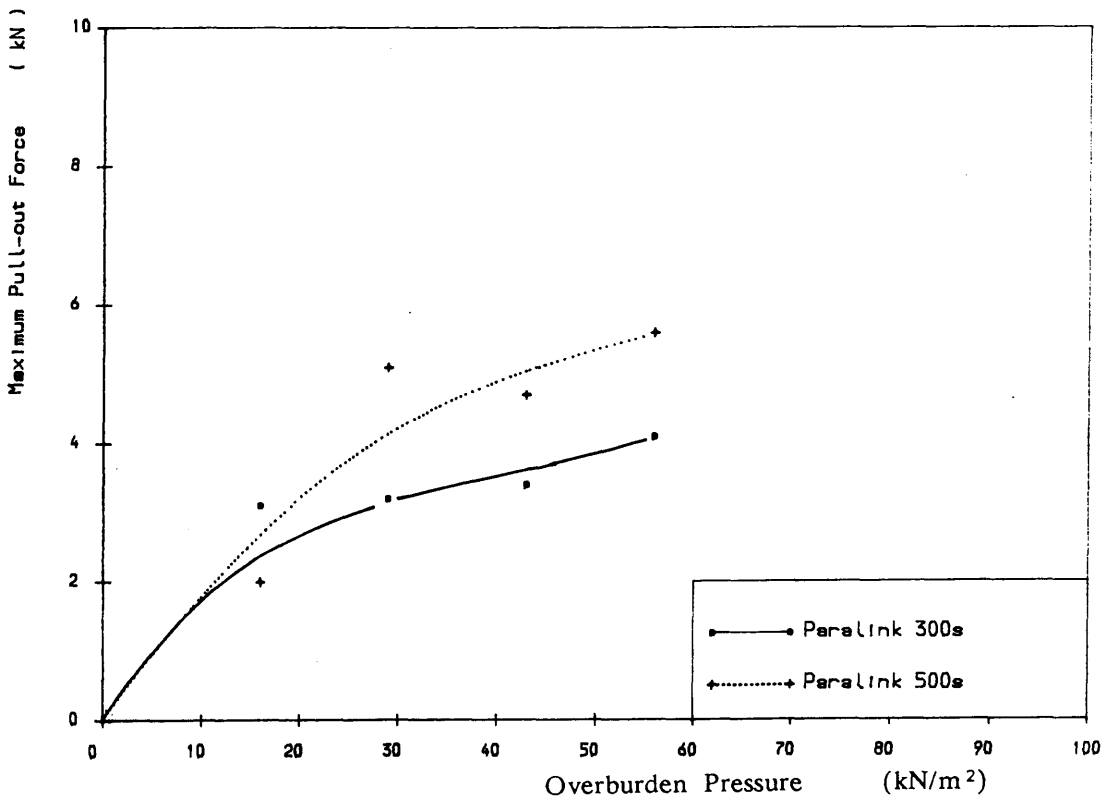


Figure 7.27 MAXIMUM PULL-OUT FORCE VS. OVERBURDEN PRESSURE  
Field Pull-out Test, Methil PFA, L=3m

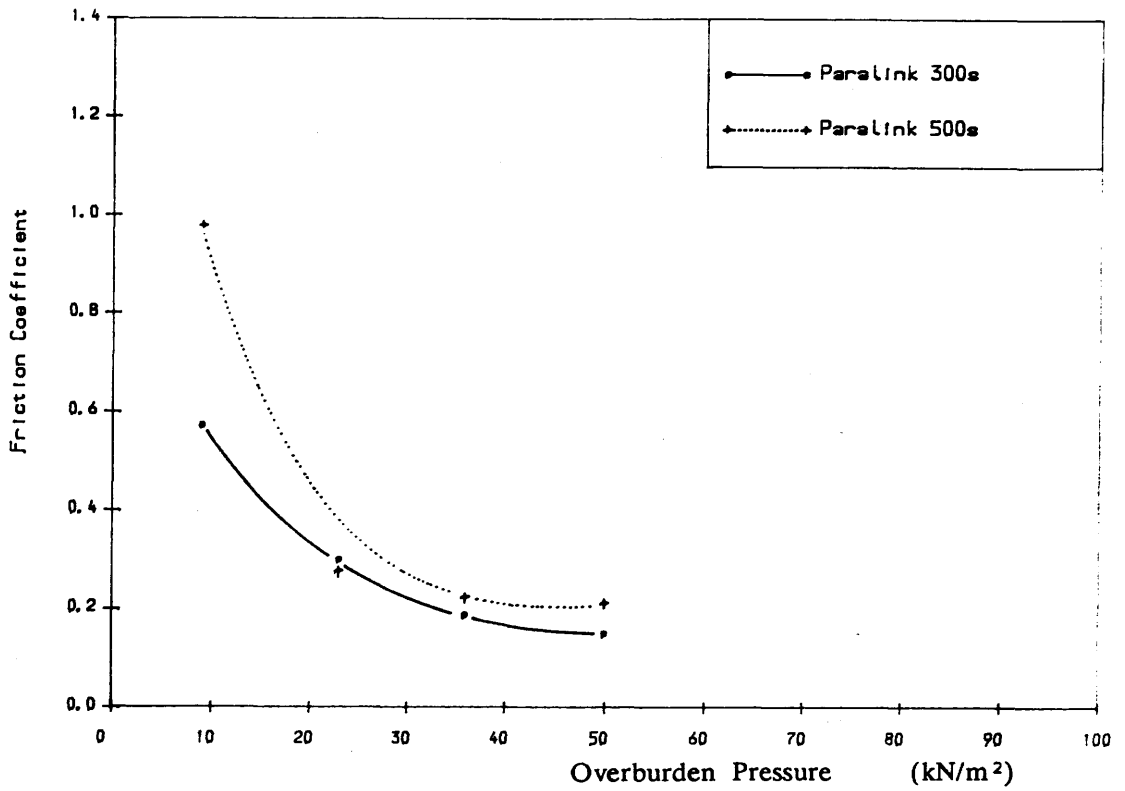


Figure 7.28 FRICTION COEFFICIENT VS. OVERBURDEN PRESSURE  
Field Pull-out Test, Methil PFA, L=4m

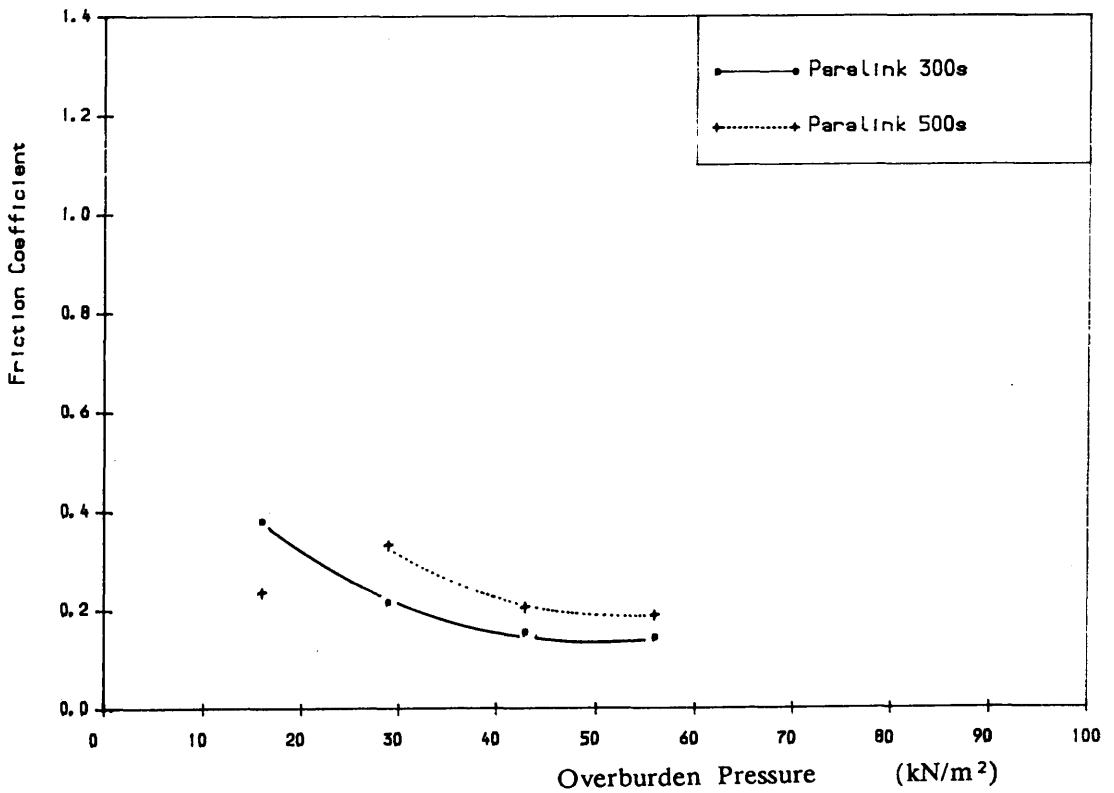


Figure 7.29 FRICTION COEFFICIENT VS. OVERBURDEN PRESSURE  
Field Pull-out Test, Methil PFA, L=3m

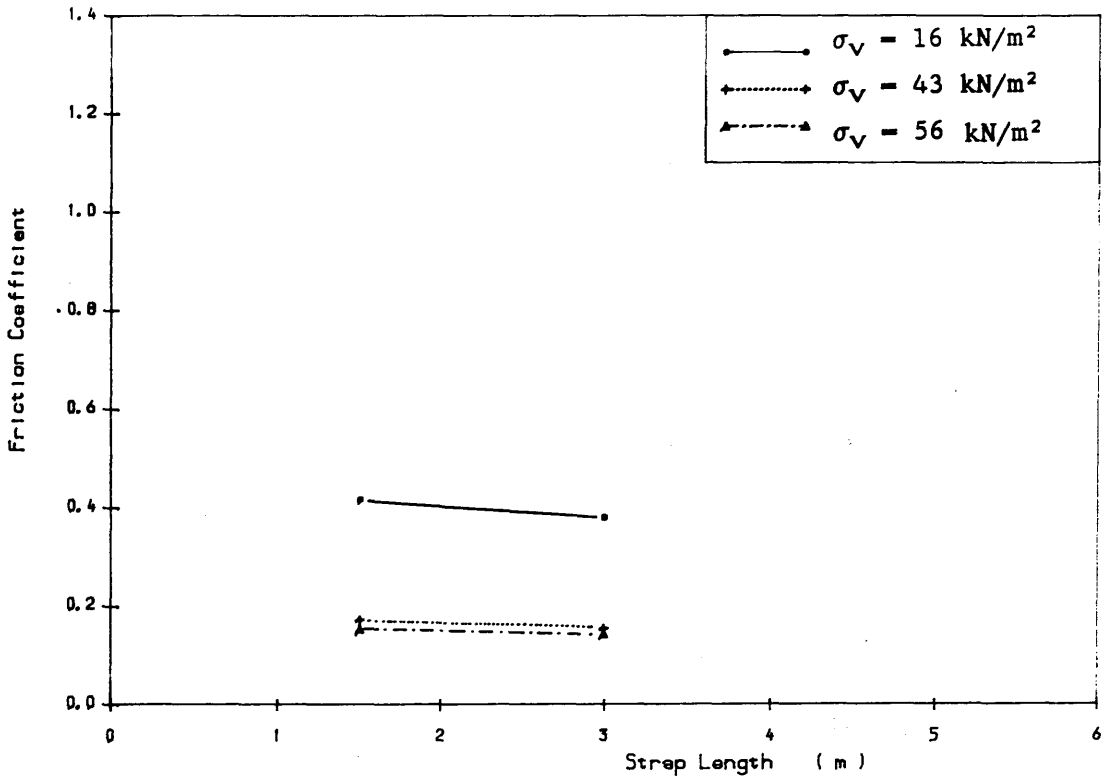


Figure 7.30 FRICTION COEFFICIENT VS. STRAP LENGTH  
Field Pull-out Test, Methil PFA, Paralink 300s

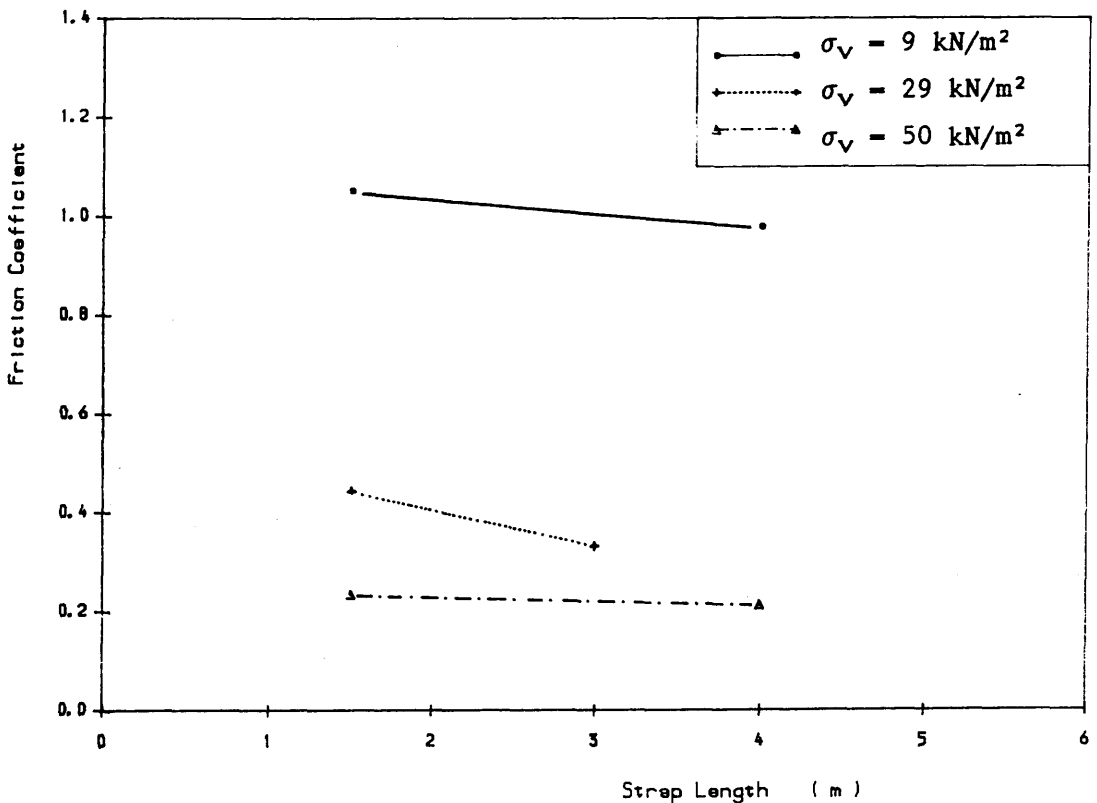


Figure 7.31 FRICTION COEFFICIENT VS. STRAP LENGTH  
Field Pull-out Test, Methil PFA, Paralink 500s

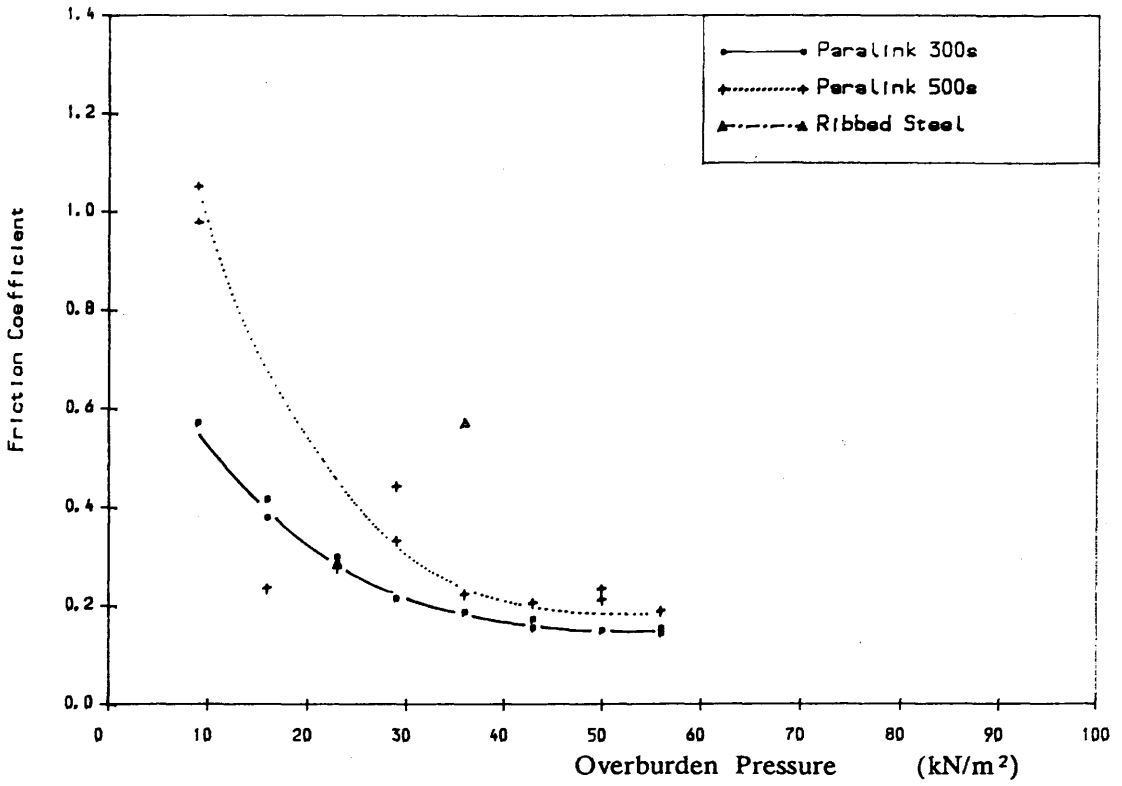


Figure 7.32 FRICTION COEFFICIENT VS. OVERBURDEN PRESSURE  
Field Pull-out Test, Methil PFA, with Various Lengths

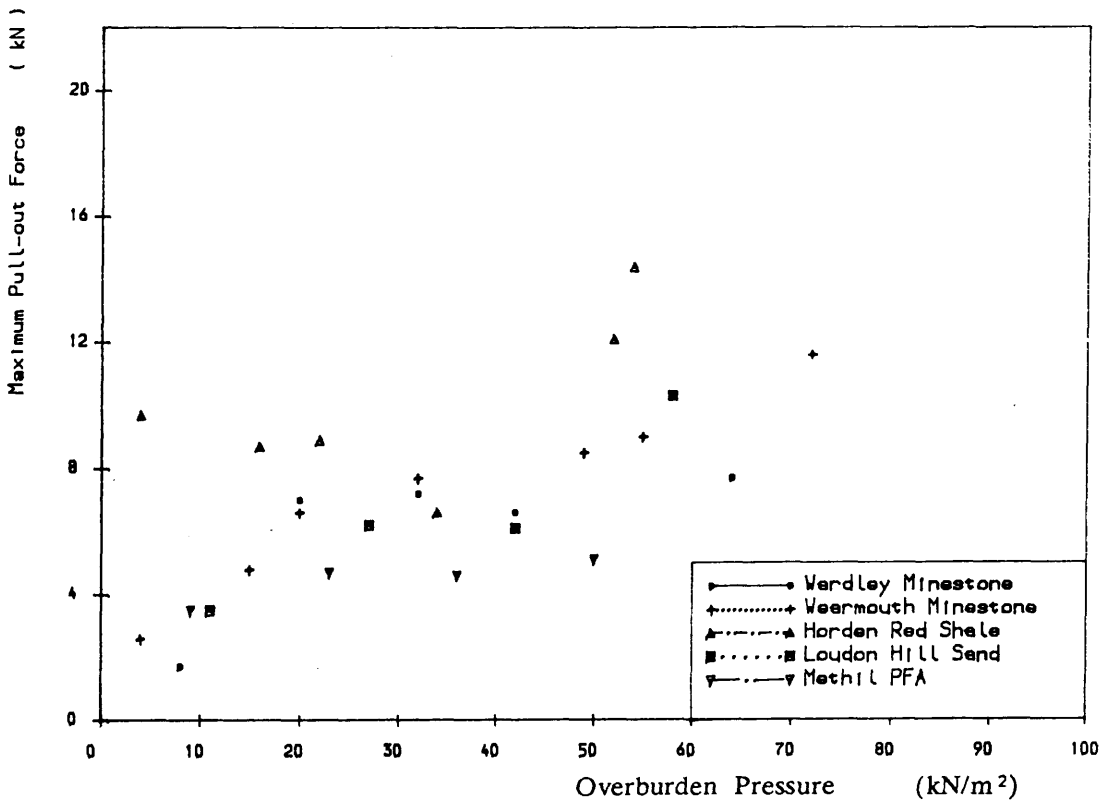


Figure 7.33 MAXIMUM PULL-OUT FORCE VS. OVERBURDEN PRESSURE  
Field Pull-out Tests, Paralink 300s, L=4m

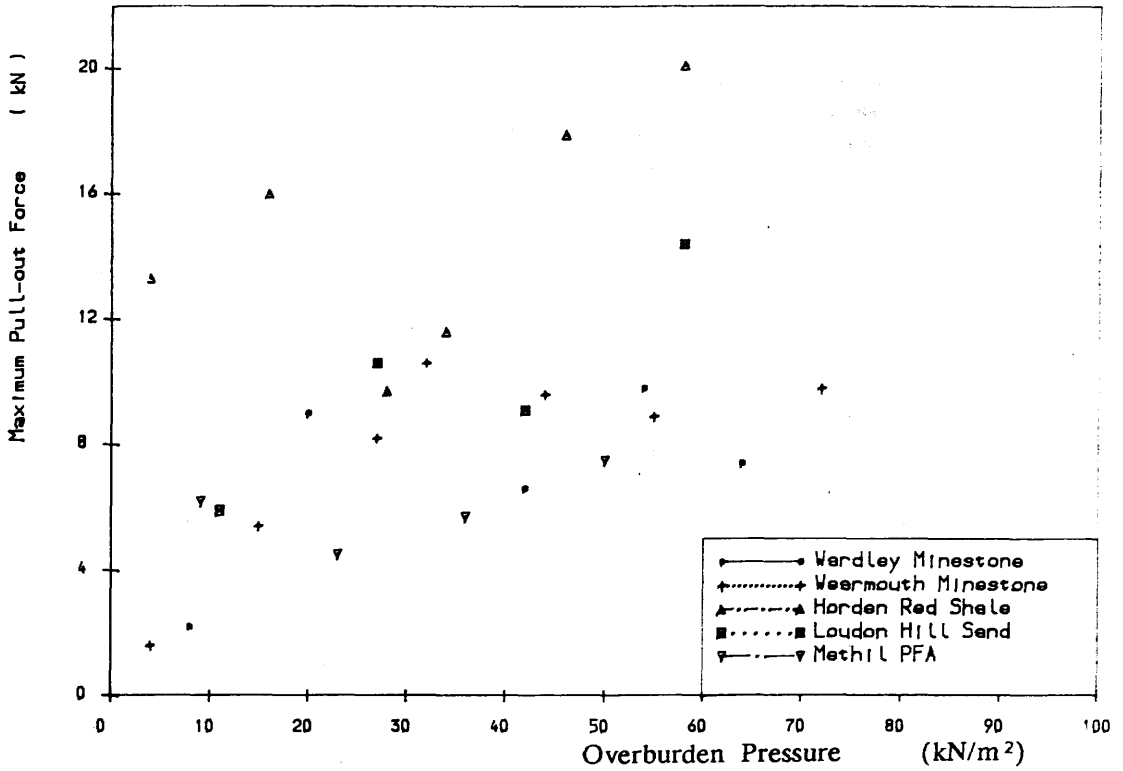


Figure 7.34 MAXIMUM PULL-OUT FORCE VS. OVERBURDEN PRESSURE  
Field Pull-out Tests, Paralink 500s, L=4m

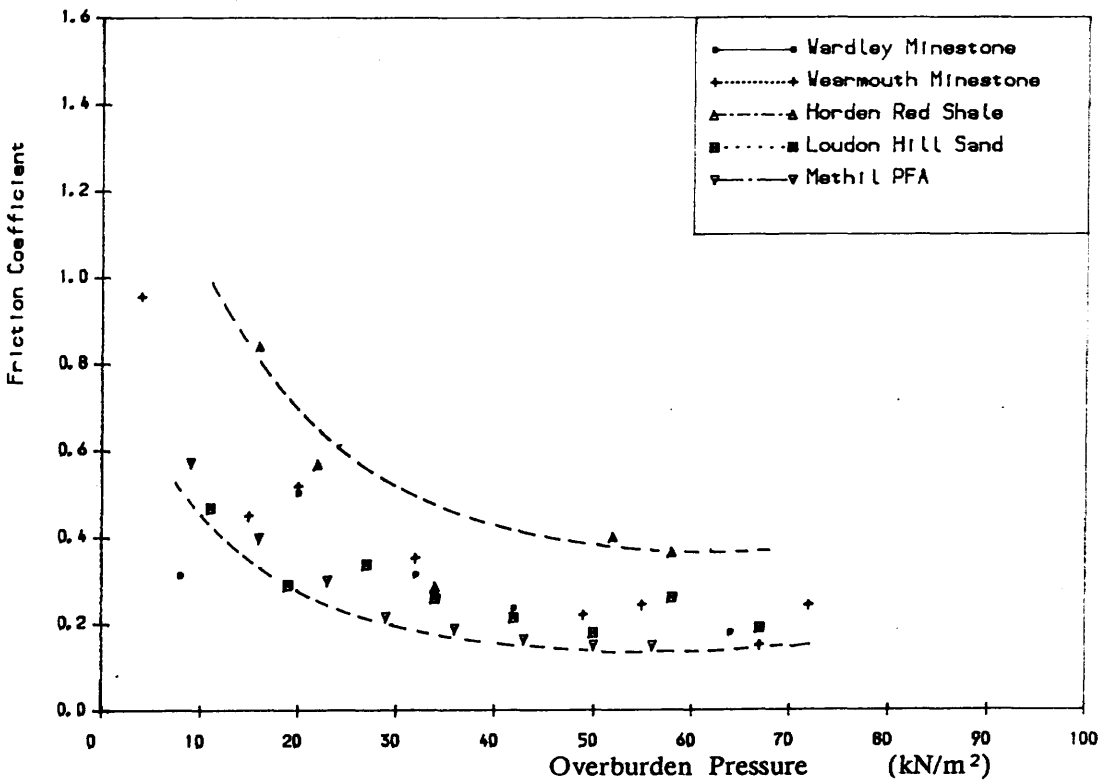


Figure 7.35 FRICTION COEFFICIENT VS. OVERBURDEN PRESSURE  
Field Pull-out Tests, Paralink 300s

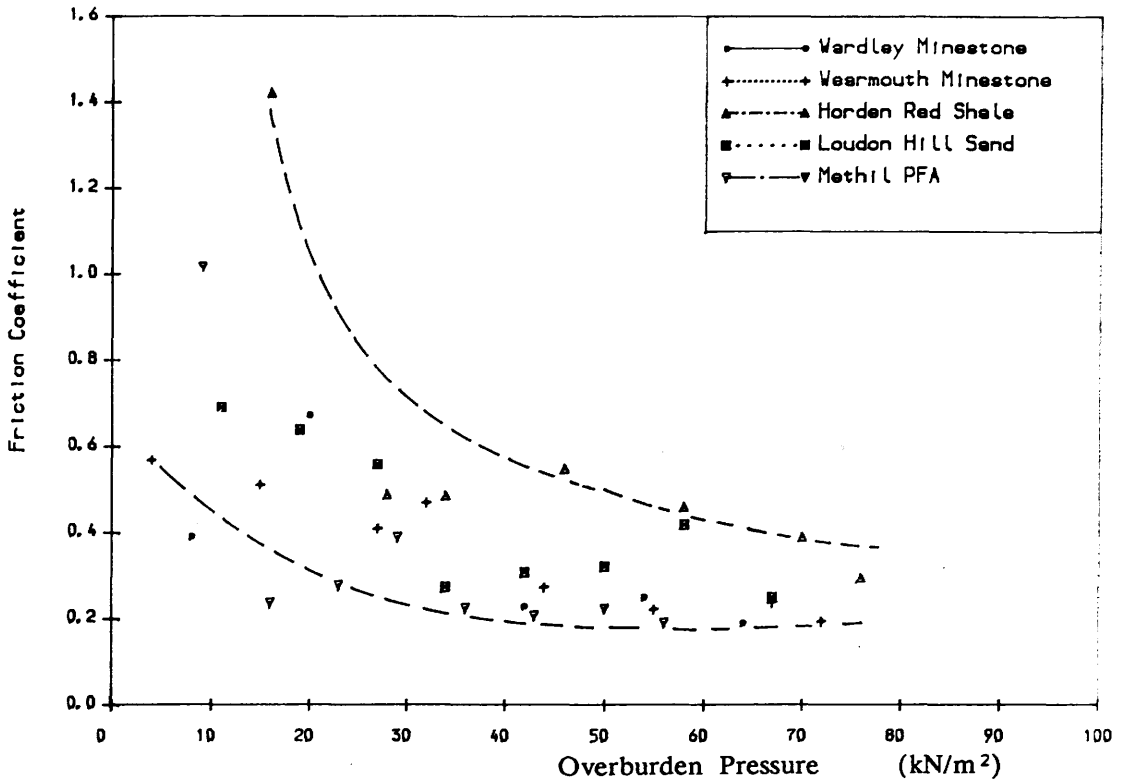


Figure 7.36 FRICTION COEFFICIENT VS. OVERBURDEN PRESSURE  
Field Pull-out Tests, Parallel 500s

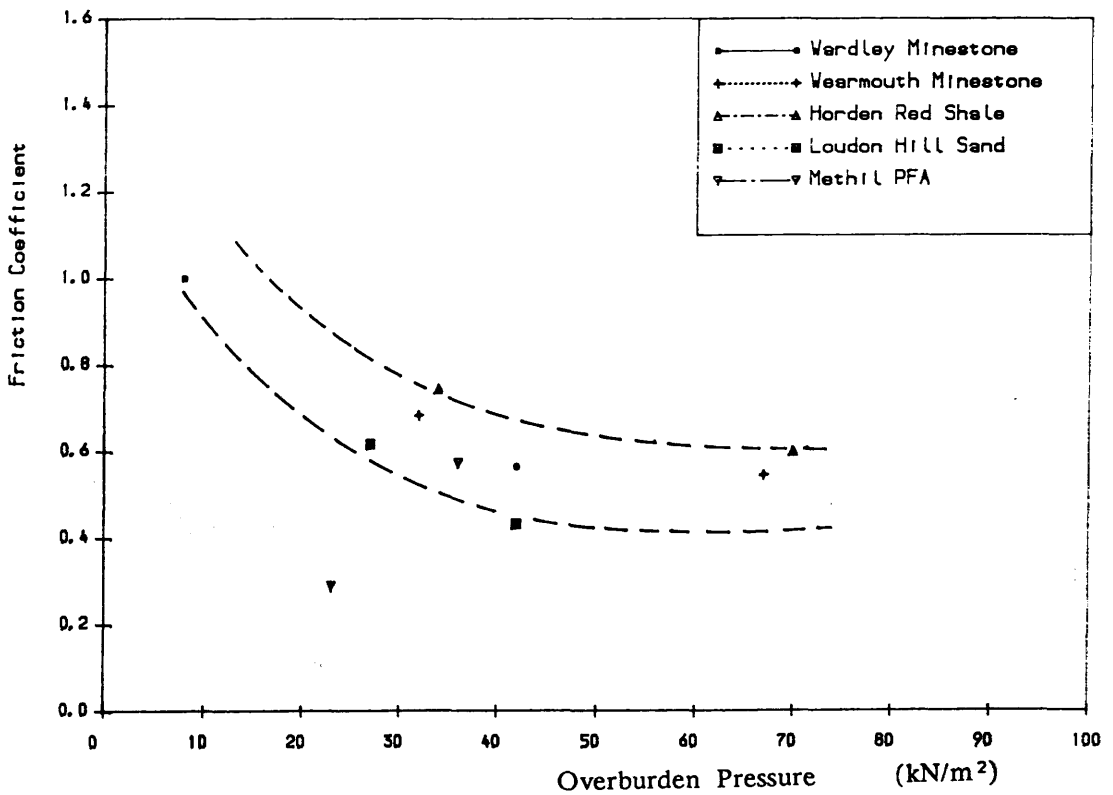


Figure 7.37 FRICTION COEFFICIENT VS. OVERBURDEN PRESSURE  
Field Pull-out Tests, Ribbed Steel



Plate 7.1 THE FIELD FULL-SCALE BOX AT WARDLEY



Plate 7.2 THE FIELD FULL-SCALE BOX AT BARONY



Plate 7.3 THE STRAIN-CONTROL MOTORISED PULL-OUT JACK

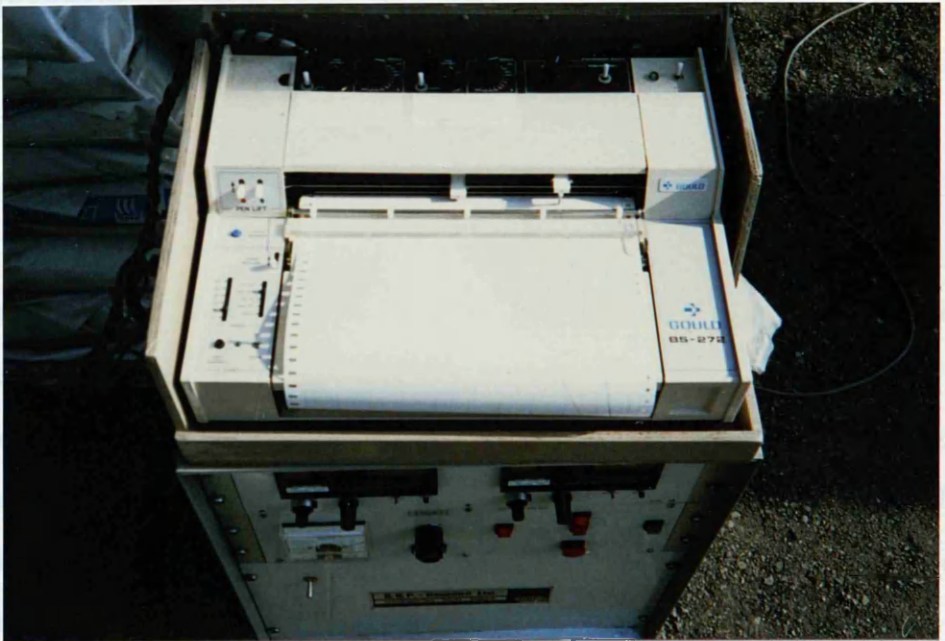


Plate 7.4 THE DATA LOGGER AND PLOTTER USED IN FIELD TESTS

## CHAPTER 8

### COMPARISON OF THE TEST METHODS AND DESIGN CONSIDERATION

#### 8.1 INTRODUCTION

As has been discussed in the previous chapters, three different types of test have been employed to investigate the fill–reinforcement bond resistance of three different types of reinforcement in five different fill materials. The test results from each of the tests have been presented and discussed. In the present chapter, the data obtained by means of the different testing methods are collected together, so that a direct comparison can be made. The friction coefficients obtained from the present work are summarized and some relationships are established between the friction coefficient and some of the affected factors.

#### 8.2 COMPARISON OF THE RESULTS FROM THE DIFFERENT TEST METHODS

##### 8.2.1 Test Results

The laboratory pull–out and direct shear box tests were conducted at various different conditions of density and moisture content of the fill materials, one of these corresponding to that in the field tests. Therefore the results from the three different testing methods under the same conditions could be compared directly. The results obtained from these tests are shown with friction coefficient against the overburden pressure in *Figures 8.1 to 8.15*.

*Figures 8.1 to 8.3* show these obtained from the tests with Wardley minestone. Comparing the different testing methods, it can be seen that the data

obtained in the field pull-out tests lie below the others, and hence produced the lowest friction coefficient. When comparing the laboratory pull-out box tests with the shear box tests, although higher results from pull-out tests were found when ribbed steel strap was used, consistent with results reported by previous investigators (Alimi et al 1977), contrary results were discovered when Paralink straps were used, i.e. the shear box tests produced higher friction coefficient than pull-out tests except when the overburden pressure was very low.

The results with Wearmouth minestone indicated a similar trend (see *Figures 8.4 to 8.6*), with the ribbed steel strap, lower values of  $f^*$  were produced from the shear box tests, but when the Paralink straps were used the shear box tests produced higher results than pull-out tests. For example, with Paralink 500s the value of the friction coefficient obtained from shear box tests was up to about 0.2 higher than from the pull-out tests. The field pull-out tests produced results close to the laboratory pull-out tests in this case.

In the case of Horden red shale (see *Figures 8.7 to 8.9*), when the ribbed steel was used the laboratory pull-out tests produced higher values of  $f^*$  than the shear box tests. For Paralink straps at low overburden pressure, higher results were encountered from the laboratory pull-out tests, but when  $\sigma_v$  was over 40 kN/m<sup>2</sup> higher values were obtained in the shear box tests than the laboratory pull-out tests. No matter which reinforcement was used, the lowest results were produced from the field pull-out tests.

The results obtained with Loudon Hill sand are shown in *Figures 8.10 to 8.12*. Similar to the previous fill materials, the field tests gave smaller values of friction coefficient than the other two testing methods. Comparing the shear box and laboratory pull-out tests, the former produced higher values than the latter at higher overburden pressure when Paralink straps were used, but in the case of ribbed steel straps higher values of friction coefficient were encountered from the laboratory pull-out tests.

When Methil PFA was used (see *Figures 8.13 to 8.15*), no matter which reinforcement was used, the results obtained from both shear box and laboratory

pull-out box tests were rather close, whereas the field tests showed lower values.

From the description of these results above, one can see the variation in the friction coefficient when different test methods were used. These results can be summarized as follows: Comparing the field pull-out tests with the others, no matter what types of reinforcing elements and fill materials were used, the field test always produced the lowest results of friction coefficient. But when the two tests, laboratory pull-out and direct shear box tests, were compared the conclusion was uncertain with different materials. However, it was found in general that in the case of ribbed steel reinforcement, most of the results obtained from the pull-out box tests were higher than from the shear box tests. On the contrary, for the two Paralink reinforcements it appeared that the higher results were produced mostly with shear box tests, except when the overburden pressure was very low. It is believed that the extensibility and compressibility of the reinforcement were factors which caused the reduction in the pull-out force, and in turn produced lower friction coefficients in the pull-out tests (see Chapter 6). Besides in a shear box test friction is mobilized on one side of the reinforcement, whereas in a pull-out test this is mobilized on two sides of the strap, therefore any difference in the surface nature between the both sides of reinforcement can also cause a difference in the results from the two types of test method.

One point which appeared to be consistent from the above three testing methods was that the friction coefficient decreased with increasing overburden pressure, although the magnitude of the decrease was small from the shear box tests when using Loudon Hill sand.

### 8.2.2 Analyses of The Test Methods

The bond resistance mobilized between the fill material and reinforcements is a fundamental mechanism in a reinforced earth structure. In the design based on the adhesion failure mode, the friction coefficient plays a very important part which influences the safety as well as the economy of the design. Therefore it is obviously

important to obtain the appropriate friction coefficient which represents the character of bond resistance occurring in a real structure. Both direct shear box and pull-out tests have been the methods currently used to investigate the bond resistance characteristics, and both are also adopted to obtain the friction coefficients used for the purpose of design. However, a remarkable lack of agreement exists between the pull-out and direct shear box test results. Most of the results reported by the previous investigators indicated that pull-out tests always produced higher friction coefficient than shear box tests. Some surprising results were encountered which showed that the angle of friction between the soil and reinforcement from pull-out tests was greater than the shear strength angle from soil alone in shear box tests. Some dispute has therefore arisen around the adoption of the two testing methods, and a number of investigations have been carried out to analyze the reasons which cause the differences when using the two different tests.

In the case of a direct shear box test, the normal stress and shear stress exerted on the reinforcement surface are considered to be accurately known, therefore this test is expected to give a quite accurate value of the soil-reinforcement friction coefficient. Hence it is considered that it represents the fundamental mechanism of friction occurring between the soil and reinforcement. However, this test represents the two dimensional case of an infinite reinforcement sheet, and it does not represent the different phenomena involved in the complex three-dimensional mechanism of the soil-reinforcement interaction in actual reinforced earth structures, because some factors such as arching do not occur in this case. Moreover, in a shear box test, the reinforcing elements are fixed on a wooden or metal block, therefore the tensile behaviour of reinforcement which occurs in a real structure does not happen in this test. Particularly for extensible reinforcements, such as Paralink, a tensile stress causes extension, and in turn this influences the behaviour of the frictional mechanism. Nevertheless this extension behaviour is not modelled in a shear box test.

In a pull-out test, the reinforcing strap embedded in the fill materials is extracted. The applied pull-out force is imposed directly on the strap, therefore the

strap is subjected to tensile load during the testing. It can be extended by the pulling action if the reinforcement is an extensible strap. On the other hand, this test represents the three-dimensional mechanism of the soil-reinforcement interaction which happens in actual reinforced earth structures. It was suggested by Mitchell and Schlosser (1979) that the pull-out test is an adequate representation of the real phenomenon which actually occurs in reinforced earth structures and gives values of the soil-reinforcement friction coefficient which should be used in the design of structures. However, there exist a number of complex factors which affect the pull-out test results, such as soil arching, dilatancy, soil compaction, the length and undulation in the strap. The dilatancy effect develops in the granular mass and modifies the distribution of the vertical stresses in the vicinity of the reinforcement so that the actual normal stress exerted on the reinforcement surface is unknown. However, Schlosser (1977) considered that the factors included in a pull-out test also occurred in real structures, and therefore the friction coefficient obtained in a pull-out test could be applied to a real structure.

Opposite conclusions were drawn by Jewell (1980) after observing the displacement field and the strain field which develops in sand reinforced by a bar or a grid reinforcement and loaded in shear. He discovered that these were not the same as in a test in which the reinforcement is pulled out of the sand. Therefore he concluded that the results of pull-out tests might have no direct relevance or bearing on the action of reinforcement in reinforced sand. Further he made two conclusions: (1) the pull-out test does not model the action of reinforcement placed in sand undergoing shear deformation, and (2) a theoretical analysis for the interpretation of pull-out tests is likely to be extremely complex (especially for rough reinforcement in dense sand); even the careful use of a simple interpretation in terms of the applied boundary stresses in the test are likely to lead to values of friction in excess of the basic angle of friction between soil and reinforcement relevant to a limit equilibrium analysis of reinforced earth. In other words the maximum force generated in a pull-out test often greatly exceeds the maximum force that can be generated in the same reinforcement (in the same sand and under

similar conditions of applied normal stress) when it acts to strengthen sand undergoing shear.

These arguments above made by the previous investigators both possess reasonable points. In particular the discovery by Jewell of a strain field in a reinforced sand undergoing shear is a significant contribution. However, these arguments lead to two completely conflicting conclusions on the adoption of the test methods, and these, in turn, considerably affect the results of design. Therefore careful consideration and discussion on the two test methods are still needed, especially when different materials (reinforcements and/or fills) are used.

Some interesting phenomena were discovered in the present work when comparing the shear box and laboratory pull-out tests. When the Paralink reinforcements were tested with the fills, contrary to what has been reported by most of the previous researchers, higher results of friction coefficient were mostly obtained from the shear box tests than from the pull-out tests. When the ribbed steel reinforcement was used, the results appeared consistent with the previous researchers, i.e. the pull-out tests produced higher results. When the fill material was changed to Methil PFA, for all the three reinforcements it gave very close results from the two test methods. These phenomena indicated very complex factors which affect the results when using the two different test methods. Hence one cannot draw a definite conclusion that the pull-out tests produce higher results than shear box tests, because this actually varies according to the different fill and reinforcing materials. One of the criticisms made by Jewell is that the pull-out test generates values of friction in excess of the basic angle of friction between soil and reinforcement relevant to a limit equilibrium analysis of reinforced earth. This criticism may not be suitable to reinforcing materials, such as Paralink straps.

According to the present results, three factors may influence the results from the two test methods: (1) the extensibility and compressibility of the reinforcement, (2) the properties of the fill materials, and (3) the difference of surface nature on both sides of reinforcing elements.

As has been discussed previously (Chapter 6), the extensibility and

compressibility of reinforcement has an influence on the pull-out test results. The non-uniform elongation along a strap during pulling action can cause a reduction in pull-out resistance. The maximum pull-out force for an extensible reinforcing strap (Paralink) is found to be smaller than the rigid strap ("sandwich" Paralink). The compressibility of a strap under normal stress can cause an arching effect in the soil when overburden pressure is applied, leading to a reduction of normal stress on the strap, which in turn can lead to a decrease in the pull-out force. When considering the reinforcement in a reinforced earth structure, one can understand that tensile stress must exist in the reinforcement. Therefore unlike the stiff reinforcements, the behaviour of the extensible reinforcements will play an important role in a reinforced earth structure when the friction resistance is considered. This behaviour should never be neglected.

When the performances of the two test methods are compared, one can see that in a pull-out test, the reinforcing strap is in tension because of the pull-out force imposes directly on it, therefore the influence of the extensible behaviour of the reinforcement is represented in the pull-out test. Whereas in a shear box test, since the reinforcing elements are fixed on a wooden block, there is no tensile stress exerted on it, the extensible behaviour is not reflected. In addition, the pull-out test represents a three dimensional case as in a reinforced earth structure, therefore the arching effect which occurs in a pull-out test will also occur in a real structure, whereas the shear box test represents only the two dimensional case. On the other hand, friction is mobilized on the both sides of a strap in a pull-out test which reflects the real case in an actual structure. Based on these points, pull-out tests may be considered as the preferred method to obtain the friction coefficient when extensible reinforcing straps are used. One important point is that it is on the safe side if pull-out test results are adopted when using Paralink reinforcements.

The strain fields in reinforced earth undergoing a shear force in a pull-out test condition are unknown when extensible Paralink straps and the present fill materials are used. However, Palmeira et al (1989) analysed a typical reinforced earth structure and divided it into three regions according to the mechanisms of

interaction between reinforcement and soil (see *Figure 8.16*). The mechanism represented in the interface direct shear tests is likely to occur in region **A**, pull-out tests would represent the mechanism in region **B**, while inclined reinforcement in unit cells would give information on factors that affect the mechanisms occurring in region **C**. Based on coherent gravity hypothesis there are two zones, active zone and resistant zone, in a reinforced earth structure (see *Figure 8.17*). The part of the reinforcement in the resistant zone plays an important role in stabilizing the structure, and the mechanisms of interaction in the resistant zone according to the discussion above can be represented by pull-out tests.

In the case of Methil PFA fill material, the two test methods produced quite close results for the three reinforcements. This is probably due to the properties of the very fine particles of this material. Some factors which occur with the other materials may not occur with the PFA. For example when ribbed steel strap is used, dilatancy, which is regarded as the main factor causing the different results between the two test methods, may not be apparent in a pull-out test with the PFA. In the case of Paralink reinforcements with PFA, the close results from the two different test methods may be due to the fact that this fill material is compressible, therefore the arching effect caused by the compressibility of the strap did not occur. On the other hand with the PFA material, no evident peak occurred at the maximum shear stress in the shear box test (see *Figures 4.22 and 4.23* in Chapter 4), therefore the reduction from the peak to the residual post-peak caused by the extensible behaviour in a pull-out test will not exist with this material.

The lowest value of friction coefficient was obtained from the field test, when compared with the results from the other two test methods. Between the field pull-out and the laboratory pull-out tests, the main differences were: (1) the field test was at a large scale, whereas the laboratory test was in a relatively small box, therefore control of density and moisture content could not be as good as in the laboratory. (2) In the field test, the overburden pressure exerted on the reinforcing straps was calculated according to the density and the depth of the fill ( $\gamma H$ ), whereas in the laboratory test this was simulated by imposing air pressure. Therefore

the pressures imposed on the strap may not be identical. The differences between the results produced from the two different tests were probably due to the last two factors. The condition in the field test can closely represent the condition in actual structures, therefore a safety factor ( $F_s = f^*_{lab}/f^*_{field}$ ) should be considered if friction coefficients from the laboratory test are adopted in a design. For the two polypropylene straps, this factor is found to vary from about 1.0 to 2.5 with present fill materials. When Wearmouth minestone is used  $F_s$  can be taken as 1.0, but with Wardley minestone and Horden red shale  $F_s$  is found to be around 1.45, a larger value of  $F_s$ , 2.5 can be taken when Loudon Hill sand and Methil PFA are used. Some differences in the friction coefficient between the field pull-out and the other two tests, laboratory pull-out and direct shear box, are presented in *Table 8.1*.

The different results from the shear box and pull-out box tests have been discussed above. For Paralink straps, it is believed that the pull-out box tests are more reliable than the shear box tests. However, unlike the shear box apparatus, a pull-out box is not always available soil mechanics laboratories. Therefore if the relations can be established between the two different tests, relevant pull-out test values can be assumed from shear box tests.

Some results from the ribbed steel and Paralink 300s tested with Wardley minestone and the sand are analysed. Equivalent pull-out forces were calculated from the shear box tests according to the shear stress and a strap surface area. These are plotted against the displacements and illustrated together with the curves obtained from the pull-out box tests in *Figures 8.18* and *8.19*. The curves with ribbed steel showed similar patterns from the two different tests. This is particularly clear with Loudon Hill sand (see *Figure 8.18*). Apparently lower results are shown in shear box tests. If we look at the curves produced from the pull-out test at  $20 \text{ kN/m}^2$  of  $\sigma_v$  and from shear box test at  $60 \text{ kN/m}^2$ , an interesting point is noted that the two curves have same patterns and very close values of pull-out forces. This implies that although an overburden pressure of  $20 \text{ kN/m}^2$  was applied, actually the normal stress imposed on the strap was up to  $60 \text{ kN/m}^2$  caused by dilatancy during pulling.

*Figures 8.20* and *8.21* show large differences in the curves from the two

different tests. The large displacements from the pull-out tests were due to the extension of the Paralink, which not reflected in the shear box tests.

Therefore it may be concluded that for rigid straps if normal stresses acting on the straps are identical in the two different test methods, similar force-displacement relations can be produced. Whereas in the case of extensible straps, these relations are apparently different, and larger displacements are produced in the pull-out tests. Ignoring this difference in force-displacement relations, a comparison of the results from the two tests can be made by introducing a ratio  $\rho$  which designates the ratio of pull-out force (or friction coefficient) from pull-out box tests to this from shear box tests, i.e.

$$\rho = T_{\max}/T_s \quad (8.1)$$

or 
$$\rho = f^*/\mu \quad (8.1')$$

The values of ratio  $\rho$  from the present tests are presented in Table 8.2 and also illustrated in *Figures 8.22 to 8.24*. It can be seen from the figures that the ratio  $\rho$  varies with different materials, hence the relation from the two test methods can not be certain. However, a trend is observed that  $\rho$  is also related to the overburden pressure, and no matter which material is used the value of  $\rho$  decreases with increasing  $\sigma_v$ . It seems that the influence of  $\sigma_v$  to  $\rho$  acts only up to a certain overburden pressure. When  $\sigma_v$  increases, the decreasing rate of  $\rho$  becomes smaller. For Paralink 300s, after 60 kN/m<sup>2</sup> of  $\sigma_v$ ,  $\rho$  tends to be about constant, and also the difference caused by the different fill materials becomes negligible. The value of  $\rho$  can be taken as 0.67 for Paralink 300s when  $\sigma_v$  is over 60 kN/m<sup>2</sup>. In the case of Paralink 500s, the effect of overburden pressure can be neglected after 120 kN/m<sup>2</sup> of  $\sigma_v$ , and the value of  $\rho$  at this overburden pressure is found to be about 0.65 with the two minestone fill materials, this value being very close to the value from Paralink 300s. Whereas with the sand and red shale,  $\rho$  is about 0.89 from Paralink 500s. Therefore it will be on the safe side if a conservative value 0.65 of

$\rho$  is adopted to assess an apparent friction coefficient ( $f^*$ ) from a shear box test result ( $\mu$ ) for the two polypropylene straps. For the ribbed steel strap the value of  $\rho$  may be taken as 1.25 (with Wearmouth minestone this can be taken as 1).

In this comparison above, PFA fill material is not included, because the results from the two different tests are very close, therefore the value of  $\rho$  can be taken as 1.

### 8.3 RELATIONSHIP BETWEEN THE FRICTION COEFFICIENT AND SOME OF THE FACTORS

The friction coefficient has been adopted to represent the character of fill–reinforcement bond resistance (or frictional resistance) in reinforced earth, and this is also used in the design. When considering a reinforced earth structure against adhesion failure, a number of design approaches have been developed (see Chapter 2), such as Rankine theory, Coulumb force, Coulumb moment methods and so on. No matter which theory is employed in the design, the factor of safety depends on the friction coefficient between the soil and the reinforcement, and this coefficient will significantly influence both the stability and economy of the final design. The friction coefficient obtained from the laboratory pull–out tests and shear box tests are summarized, and the relationship between friction coefficient and density and overburden pressure is established for the present materials.

#### 8.3.1 *Apparent Friction Coefficient of Fill–Reinforcement*

The term apparent friction coefficient ( $f^*$ ) is defined as the friction coefficient obtained from the pull–out tests. The description of and some discussion on this test has been made in the previous chapters (Chapters 5 and 6), as well as in the last section of this chapter. As has been discussed, the apparent friction coefficient is used in current design methods and it appears to represent the bond resistance characteristics more accurately when Paralink is used. The results of

apparent friction coefficients obtained in the present work are summarized.

It has been found from the previous discussion that the apparent friction coefficient was affected by the overburden pressure, particularly when the overburden pressure was low. When  $\sigma_v$  increased up to a certain amount, the value of  $f^*$  became almost constant. Based on this phenomenon, and from a semilogarithmic graph, if a linear relationship approximates to the decrease of  $f^*$  with the increase of  $\sigma_v$ , then the influence of overburden pressure to the apparent friction coefficient can be shown in figure (a):

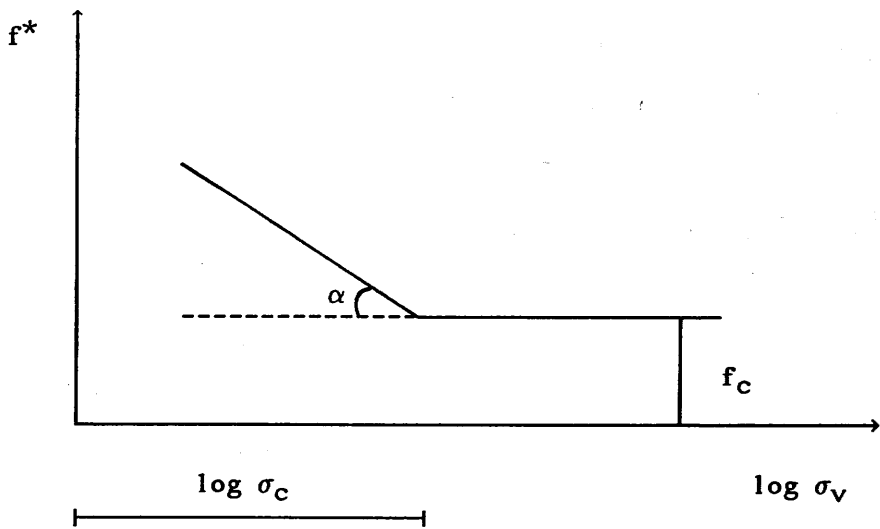


Fig. (a)

The following expressions can be derived from this figure:

$$f^* = \begin{cases} f_c + \tan\alpha \log(\sigma_c/\sigma_v) & \sigma_v < \sigma_c \\ f_c & \sigma_v \geq \sigma_c \end{cases} \quad (8.1)$$

where  $\sigma_c$  — the overburden pressure at which the  $f^*$  starts to be constant;

- $f_c$  — the constant value of the apparent friction coefficient;
- $\alpha$  — the angle of the decreasing line to the horizontal.

However, the influence of density on the apparent friction coefficient is not included in the above expressions. When the Paralink straps were tested with the fill materials provided, an interesting phenomenon was encountered, i.e. the influence of density on the value of  $f^*$  was also related to the overburden pressure. When  $\sigma_v$  was low, the influence of density was pronounced, but with the increase in  $\sigma_v$ , this influence tended to be modest and eventually  $f^*$  became constant when  $\sigma_v$  reached a certain amount, at about  $\sigma_c$ . This can be illustrated from the results obtained (see *Figures 8.25 to 8.29 and 8.31 to 8.32*). Therefore the value  $f^*$  influenced by the overburden pressure and the density can be generally shown in figure (b):

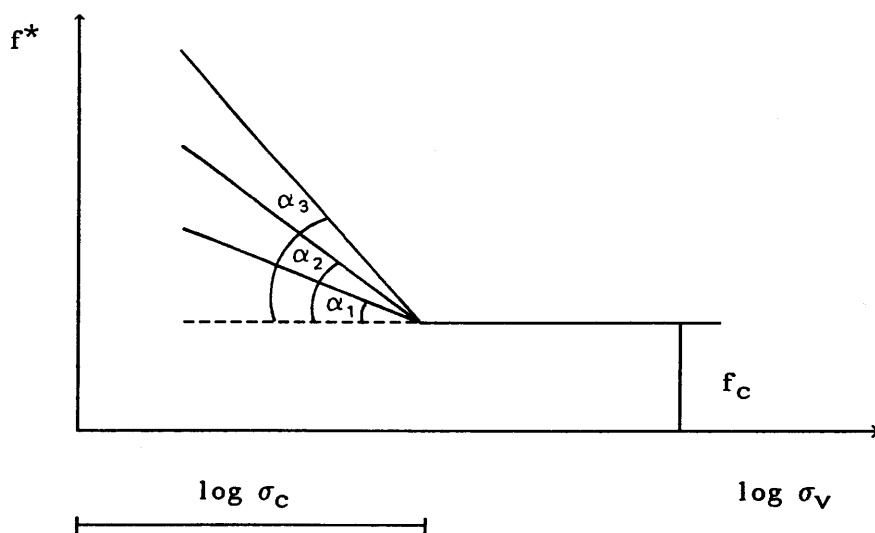


Fig. (b)

Comparing figure (a) and figure (b), it is apparent that the influence of the density actually causes a change of angle  $\alpha$ . Therefore, the value of  $\tan\alpha$  in expression (8.1) is a function of the density ( $\gamma_d$ ). If the relationship between  $\tan\alpha$

and  $\gamma_d$  is approximated by a straight line (see *Figures 8.34 to 8.37*) this can also be expressed as:

$$\tan\alpha = k ( \gamma_d - m ) \quad (8.2)$$

$k$  and  $m$  are constants which were obtained from each of the fill materials, and they were found to be very little different when the two types of Paralink straps were used with the minestones. Hence expression (8.1) can be rewritten as

$$f^* = \begin{cases} f_c + k ( \gamma_d - m ) \log( \sigma_c / \sigma_v ) & \sigma_v < \sigma_c \\ f_c & \sigma_v \geq \sigma_c \end{cases} \quad (8.3)$$

This expression can be used to obtain the apparent friction coefficient at various overburden pressures and densities when the Paralink straps are employed. These constants, i.e.  $f_c$ ,  $\sigma_c$ ,  $k$ , and  $m$  are presented in table 8.3 (a) for each of the materials.

For ribbed steel strap, equation (8.3) can also be adopted although it appears to be somewhat approximate (*Figures 8.38 and 8.39*). However, when this strap is used with Loudon Hill sand, the influence of density is still apparent at high overburden pressure (see *Figure 8.40*). Therefore varying the density does not only change the angle of  $\alpha$ , but also the value of  $f_c$  in equation (8.3). In this case  $f_c$  can be expressed as

$$f_c = w(\gamma_d - u) \quad (8.4)$$

and the constants  $w$  and  $u$  are presented in Table 8.3. The relationship between  $\tan\alpha$  and  $\gamma_d$ , and  $f_c$  and  $\gamma_d$  are shown in *Figures 8.41 and 8.42*.

In the case of Methil PFA, the tests were carried out at only one density, therefore the relationship between  $\tan\alpha$  and density was not discovered. However, the constants,  $f_c$ ,  $\sigma_c$ , and  $\tan\alpha$  obtained at the density corresponding to the field test

are presented in table 8.2 (b). Hence,  $f^*$  can be calculated according to expression (8.1), when the three straps are used with Methil PFA at the field test condition.

### 8.3.2 The Friction Coefficient from Shear Box Tests

The friction coefficient obtained from shear box tests is designated as  $\mu$  which can be calculated according to equation (2.16)

$$\mu = c_r/\sigma_v + \tan\delta \quad (2.16)$$

$c_r$  and  $\delta$  are the cohesion and frictional angle of fill–reinforcement produced directly from shear box tests for each specific reinforcement and fill material. The values of  $c_r$  and  $\delta$  for these materials used in the present work are presented in Tables 4.1 to 4.5 (see Chapter 4). The influence of the overburden pressure ( $\sigma_v$ ) has been included in equation (2.16). In addition to the overburden pressure, the density was also found to be a factor which affected the value of  $\mu$ . Moreover, the influence of density was found on the both values of  $c_r$  and  $\delta$ . This can be expressed as the following:

$$\delta = d\gamma_d + e \quad (8.5)$$

$$c_r = q\gamma_d + r \quad (8.6)$$

Where  $d$ ,  $e$ ,  $q$ , and  $r$  are constants. These have been obtained from each of these materials, except Methil PFA, and are presented in table 8.4. Therefore once  $\gamma_d$  is decided, the frictional angle ( $\delta$ ) and the cohesion ( $c_r$ ) can be obtained according to the two expressions (8.5) and (8.6). Eventually the friction coefficient  $\mu$  is calculated at each overburden pressure based on equation (2.16). Hence the two factors, overburden pressure and density which were observed to affect the result of friction coefficient have been taken into consideration in this calculation

For Methil PFA, the tests were carried out at only one density, therefore the relationship of the density with  $\delta$  and  $c_r$  was not observed.

### 8.3.3 The Relationship between Pull-out

#### Force and Strap Displacement

When extensible reinforcements are used in a reinforced earth structure the extensibility of the reinforcement, or in other words the behaviour of force-displacement in soil should also be considered. However, this behaviour under a confined pressure in soil is found to be different from that obtained from a tensile test (McGown et al 1982 and Fabian 1988). The stiffness of the reinforcements appeared to increase with increase in confining pressure. This phenomenon was also observed in the present work when the Paralink straps were used (see Chapter 5). Therefore when considering the force-displacement behaviour of these reinforcements, the influence of confining pressure or overburden pressure should not be neglected. On the other hand, this behaviour was also found to vary according to fill materials (see *Figures 5.66 and 5.67* in Chapter 5). However the stiffness seems independent of strap length (see *Figures 5.47 and 5.48* in Chapter 5). In order to obtain the displacement under a certain amount of force, the following equation is suggested:

$$D = \frac{T}{E_p} \quad (8.7)$$

where       $D$  — displacement of the reinforcement in metre;  
             $T$  — tensile force sustained by the reinforcement;  
             $E_p$  — the pull-out stiffness of the strap in soil.

The pull-out stiffness of the strap in soil is affected by overburden pressure, and the relationship between  $E_p$  and  $\sigma_v$  was found to be linear (see *Figures 5.66 and 5.67* in Chapter 5). This can be expressed by

$$E_p = i\sigma_v + j \quad (8.8)$$

According to the trend of the pull-out stiffness against overburden pressure, the constant  $i$  can be approximated as independent of the type of fill materials, and was found to be 1.483 (m) and 2.083 (m) for Paralink 300s and Paralink 500s respectively. The constant  $j$  varies according to the reinforcement combined with fill materials. The values produced for each of these materials from the present work are presented in Table 8.5.

Therefore once the tensile force ( $T$ ) and overburden pressure ( $\sigma_v$ ) imposed on a Paralink strap is known, the displacement (or stretching) of the strap can be estimated according to expressions 8.7 and 8.8.

Table 8.1 The Friction Coefficient from the Different Test Methods

( at the overburden pressure of 60 kN/m<sup>2</sup> )

type of fill	type of fill	shear box	laboratory pull-out	field pull-out
Wardley minestone	Paralink 300s	0.392	0.259	0.185
	Paralink 500s	0.431	0.330	0.215
	ribbed steel	0.787	1.555	0.450
Wearmouth minestone	Paralink 300s	0.375	0.230	0.200
	Paralink 500s	0.521	0.254	0.254
	ribbed steel	0.816	0.668	0.559
Horden red shale	Paralink 300s	0.566	0.396	0.283
	Paralink 500s	0.655	0.626	0.409
	ribbed steel	0.953	1.721	0.591
Loudon Hill sand	Paralink 300s	0.518	0.345	0.166
	Paralink 500s	0.582	0.644	0.286
	ribbed steel	0.813	1.003	0.241
Methil PFA	Paralink 300s	0.360	0.353	0.135
	Paralink 500s	0.451	0.477	0.196
	ribbed steel	0.709	0.666	—

Table 8.2 RATIO OF FRICTION COEFFICIENT FROM LABORATORY PULL-OUT TEST TO SHEAR BOX TESTS ( $\rho = f^*/\mu$ )

Type of Fill Material	Dry Density (kN/m <sup>3</sup> )	Moisture Content (%)	Ribbed Steel		Paralink 500s		Paralink 300s	
			Normal Stress (kN/m <sup>2</sup> ) 20      60      120					
Wardley minestone	17.847	9.7	2.949    1.976    1.240	1.192    0.733    0.592	1.214    0.660    0.513			
Wearmouth minestone	17.658	5.6	1.627    0.819    0.686	0.609    0.488    0.567	0.880    0.613    0.566			
Horden Shale	17.640	11.6	3.915    1.806    1.094	1.510    0.956    0.872	1.294    0.700    0.578			
Loudon Hill	16.190	7.1	2.078    1.335    1.421	1.706    1.208    0.930	0.954    0.708    0.695			
Methil PFA	11.590	27.0	1.357    0.939    0.825	1.208    1.058    1.160	1.214    0.981    1.163			

Table 8.3 The Constants in Expression (8.2) and (8.3)

a.

type of fill	type of reinforcement	$f_c$		$\sigma_c$ (kN/m <sup>2</sup> )	k (m <sup>5</sup> /kN <sup>2</sup> )	m (kN/m <sup>3</sup> )
Wardley minestone	Paralink 300s	0.20		70	0.250	14.23
	Paralink 500s	0.25		70	0.250	14.23
	Ribbed Steel	0.60		90	1.564	14.79
Wearmouth minestone	Paralink 300s	0.25		60	0.100	14.00
	Paralink 500s	0.28		60	0.100	14.00
	Ribbed Steel	0.50		90	0.250	14.23
Horden red shale	Paralink 300s	0.27		70	0.502	15.00
	Paralink 500s	0.50		70	0.502*	15.00*
Loudon Hill sand	Paralink 300s	0.32		100	0.835	15.29
	Paralink 500s	0.35		150	0.481	15.29
	Ribbed Steel	w	u	60	1.083	14.53
0.662		14.55				

b.

type of fill	density $\gamma_d$ (kN/m <sup>3</sup> )	type of reinforcement	$f_c$	$\sigma_c$ (kN/m <sup>2</sup> )	$\tan\alpha$ (m <sup>2</sup> /kN)
Methil PFA	11.590	Paralink 300s	0.35	60	0.796
		Paralink 500s	0.44	65	0.951
		Ribbed Steel	0.56	80	0.951

\* — the value referenced from Paralink 300s.

Table 8.4

The Constants in Expression (8.5) and (8.6)

type of fill	type of reinforcement	d (m <sup>3</sup> /kN)	e	q (m)	r (kN/m <sup>2</sup> )
Wardley minestone	Paralink 300s	1.212	-3.39	0.909	-12.14
	Paralink 500s	0.714	7.08	0.000	4.00
	ribbed steel	0.00	29.50	5.294	-12.75
Wearmouth minestone	Paralink 300s	0.760	4.60	0.000	3.00
	Paralink 500s	2.222	-17.33	1.143	-13.72
	ribbed steel	1.304	9.17	1.579	-18.26
Horden red shale	Paralink 300s	1.081	6.16	5.000	-81.25
	Paralink 500s	0.000	26.00	5.000	-79.75
	ribbed steel	1.667	9.16	4.762	-79.19
Loudon Hill sand	Paralink 300s	0.900	7.80	1.800	-25.00
	Paralink 500s	2.600	-17.60	1.600	-22.00
	ribbed steel	2.200	-2.80	3.600	-53.40

Table 8.5

The Constant (j) in Expression (8.8)

(kN/m)

type of fill	Paralink 300s	Paralink 500s
Wardley minestone	122	200
Wearmouth minestone	87	112
Horden red shale	222	344
Loudon Hill sand	157	495
Methil PFA	157	200

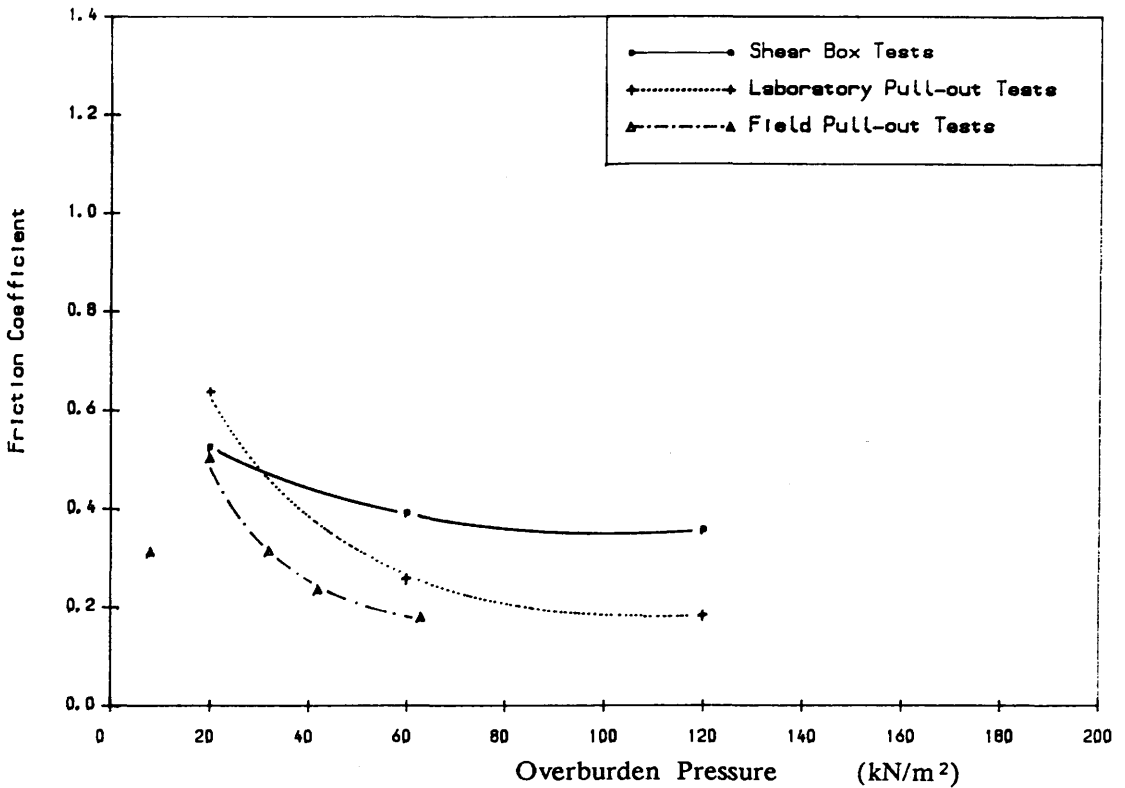


Figure 8.1 FRICTION COEFFICIENT VS. OVERBURDEN PRESSURE

Wardley Minestone,  $\gamma_d=17.847\text{kN/m}^3$ , Paralink 300s

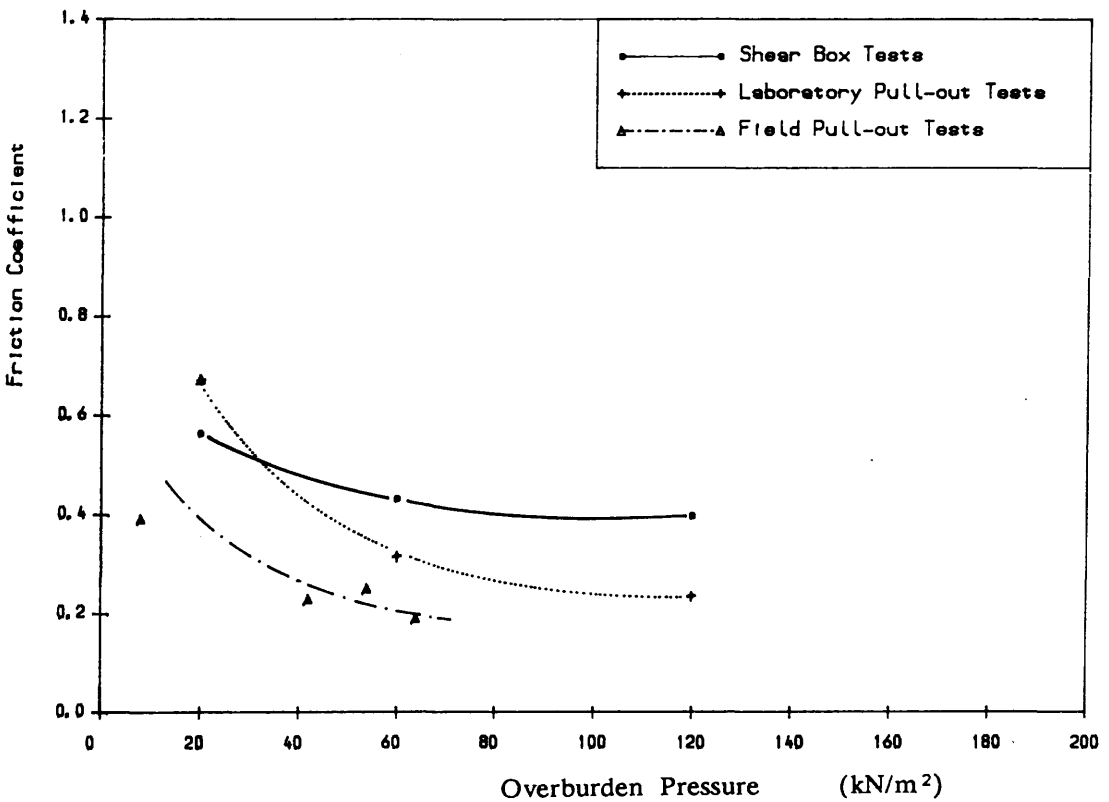


Figure 8.2 FRICTION COEFFICIENT VS. OVERBURDEN PRESSURE

Wardley Minestone,  $\gamma_d=17.847\text{kN/m}^3$ , Paralink 500s

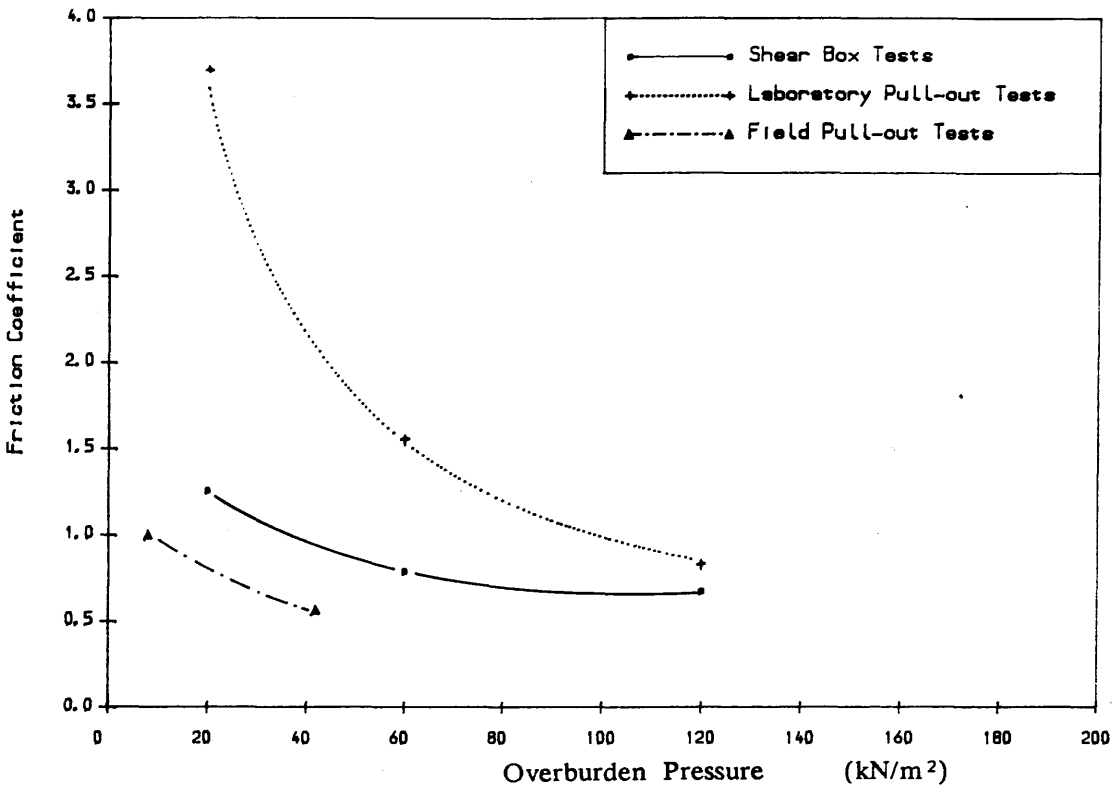


Figure 8.3 FRICTION COEFFICIENT VS. OVERBURDEN PRESSURE

Wardley Minestone,  $\gamma_d=17.847\text{kN/m}^3$ , Ribbed Steel

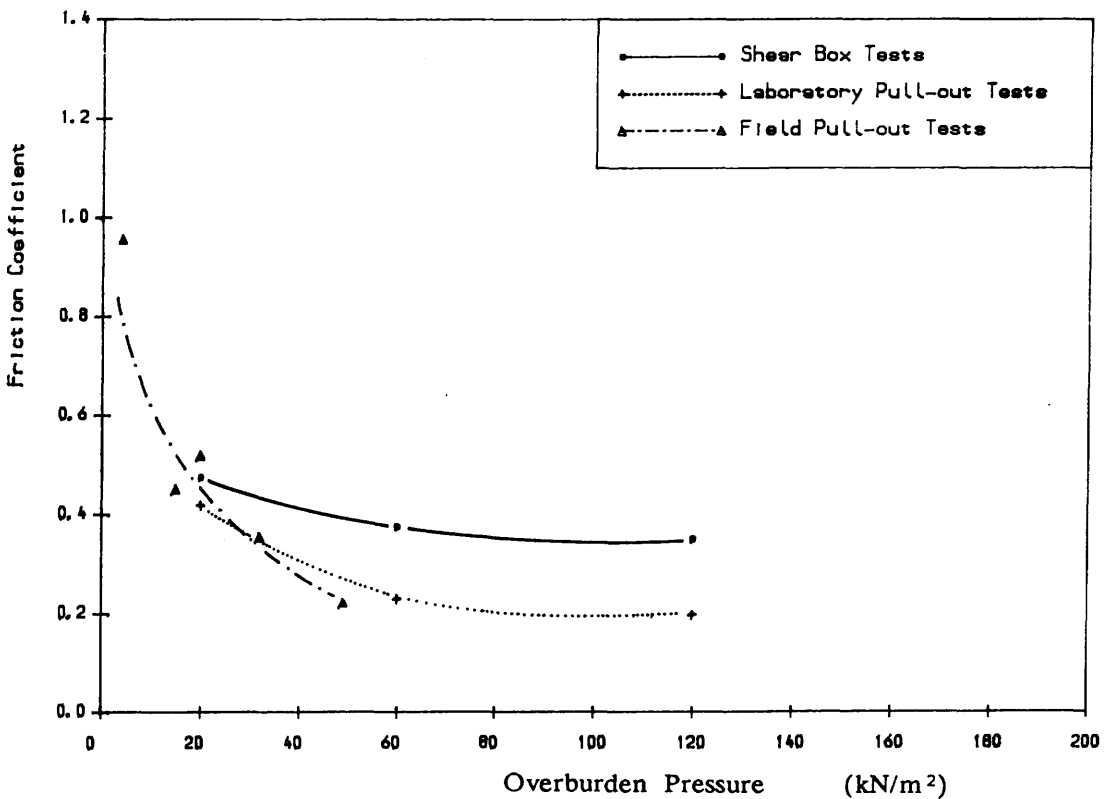


Figure 8.4 FRICTION COEFFICIENT VS. OVERBURDEN PRESSURE

Wearmouth Minestone,  $\gamma_d=17.658\text{kN/m}^3$ , Paralink 300s

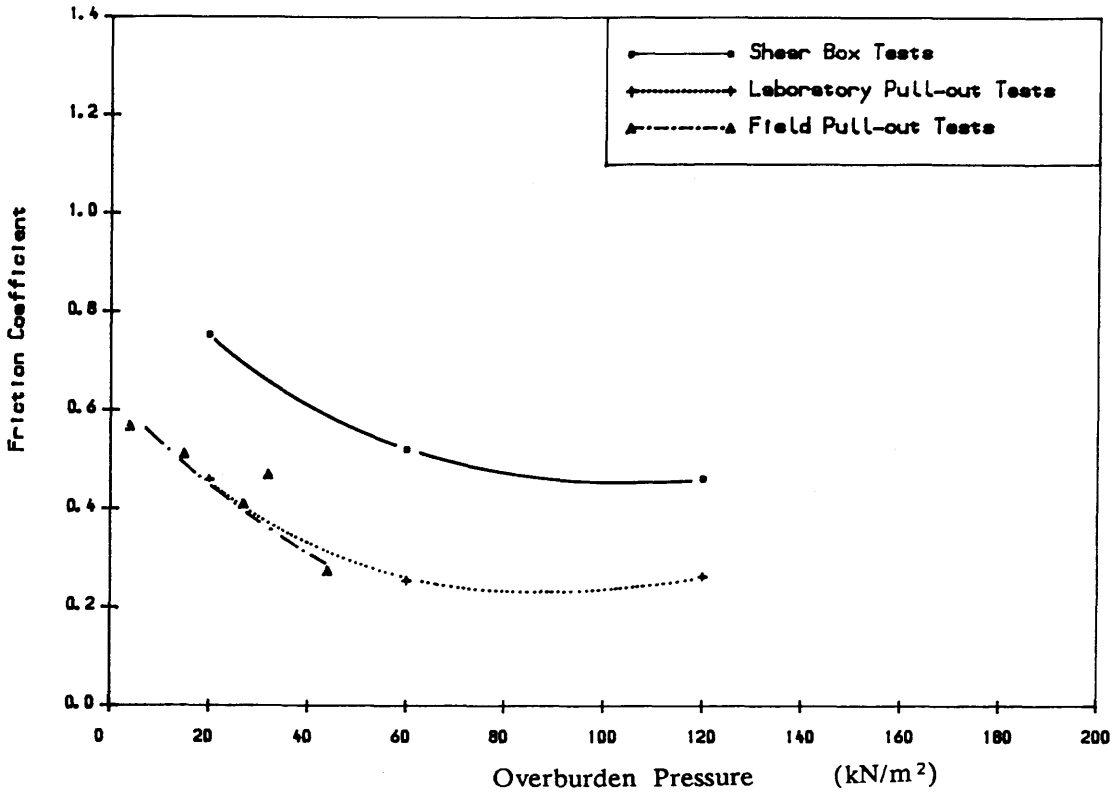


Figure 8.5 FRICTION COEFFICIENT VS. OVERBURDEN PRESSURE  
Wearmouth Minestone,  $\gamma_d=17.658\text{kN/m}^3$ , Paralink 500s

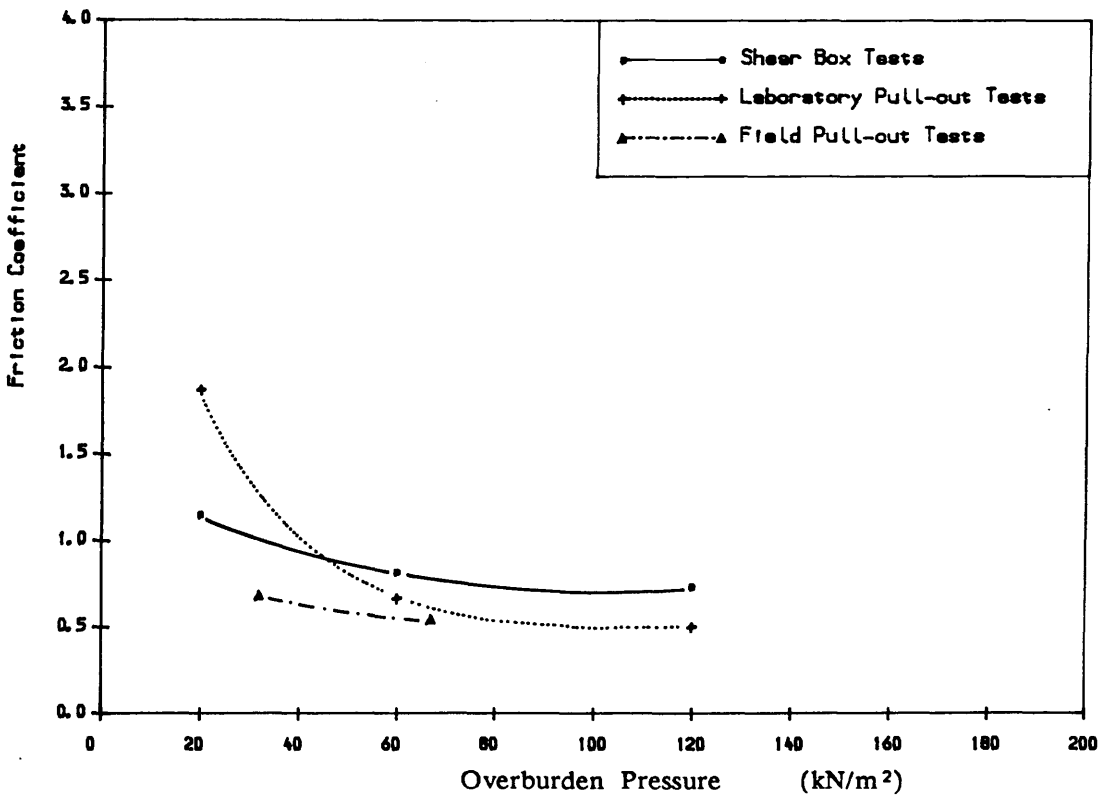


Figure 8.6 FRICTION COEFFICIENT VS. OVERBURDEN PRESSURE  
Wearmouth Minestone,  $\gamma_d=17.658\text{kN/m}^3$ , Ribbed Steel

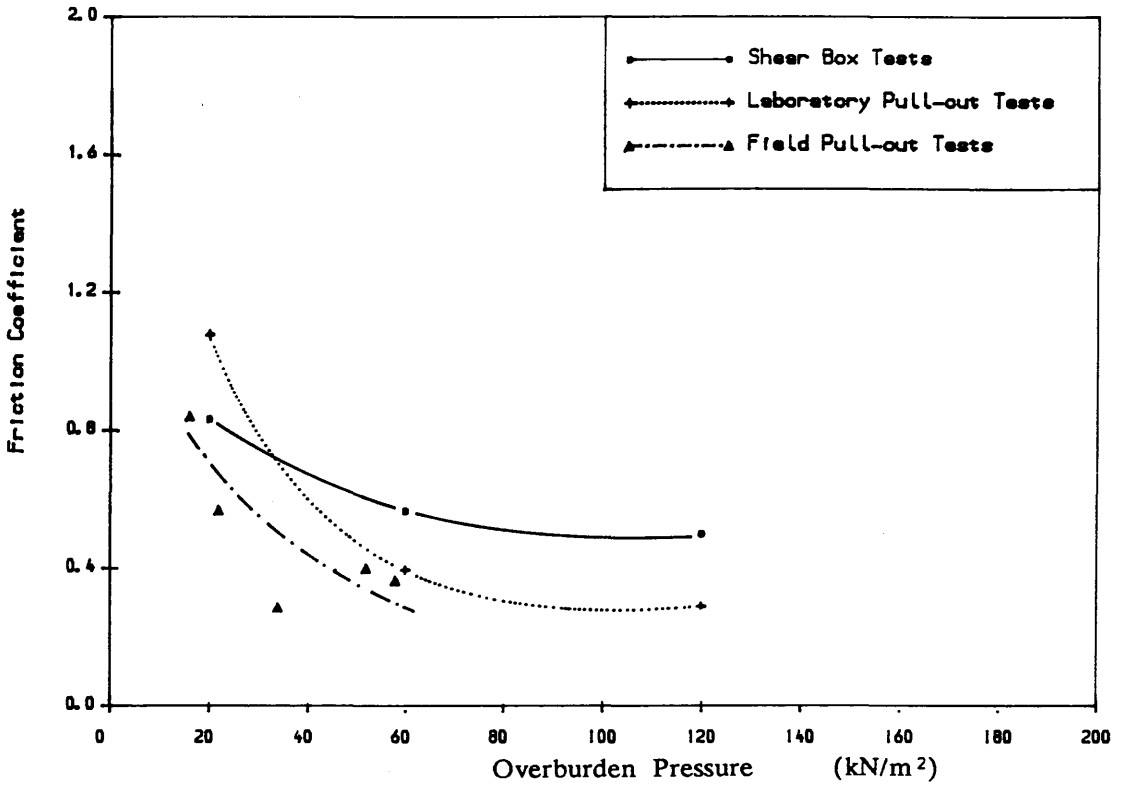


Figure 8.7 FRICTION COEFFICIENT VS. OVERBURDEN PRESSURE  
 Horden Red Shale,  $\gamma_d=17.640\text{kN/m}^3$ , Paralink 300s

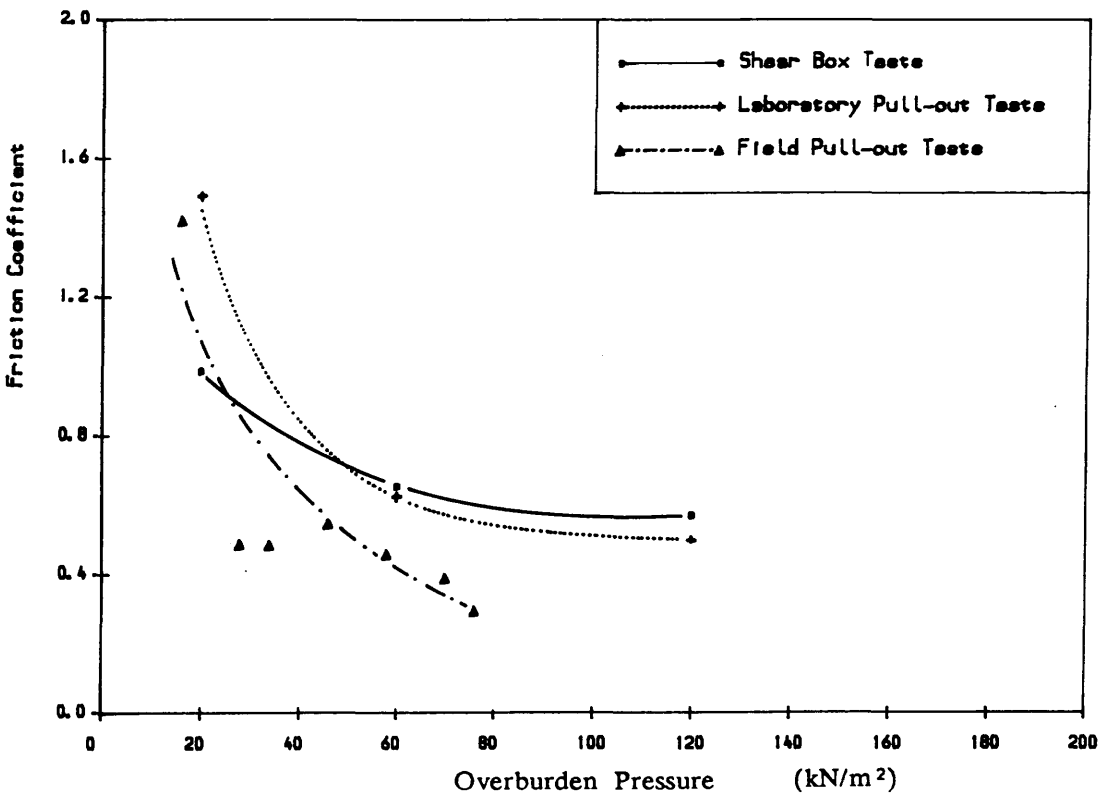


Figure 8.8 FRICTION COEFFICIENT VS. OVERBURDEN PRESSURE  
 Horden Red Shale,  $\gamma_d=17.640\text{kN/m}^3$ , Paralink 500s

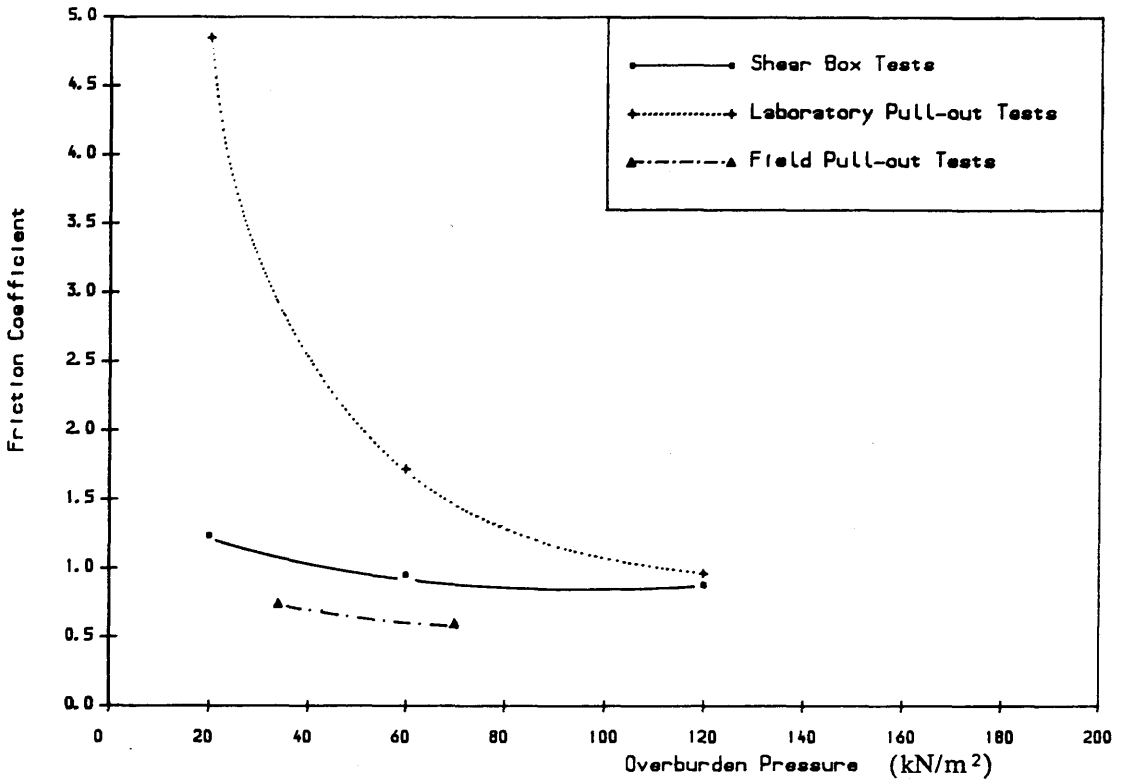


Figure 8.9 FRICTION COEFFICIENT VS. OVERBURDEN PRESSURE  
Horden Red Shale,  $\gamma_d=17.640\text{kN/m}^3$ , Ribbed Steel

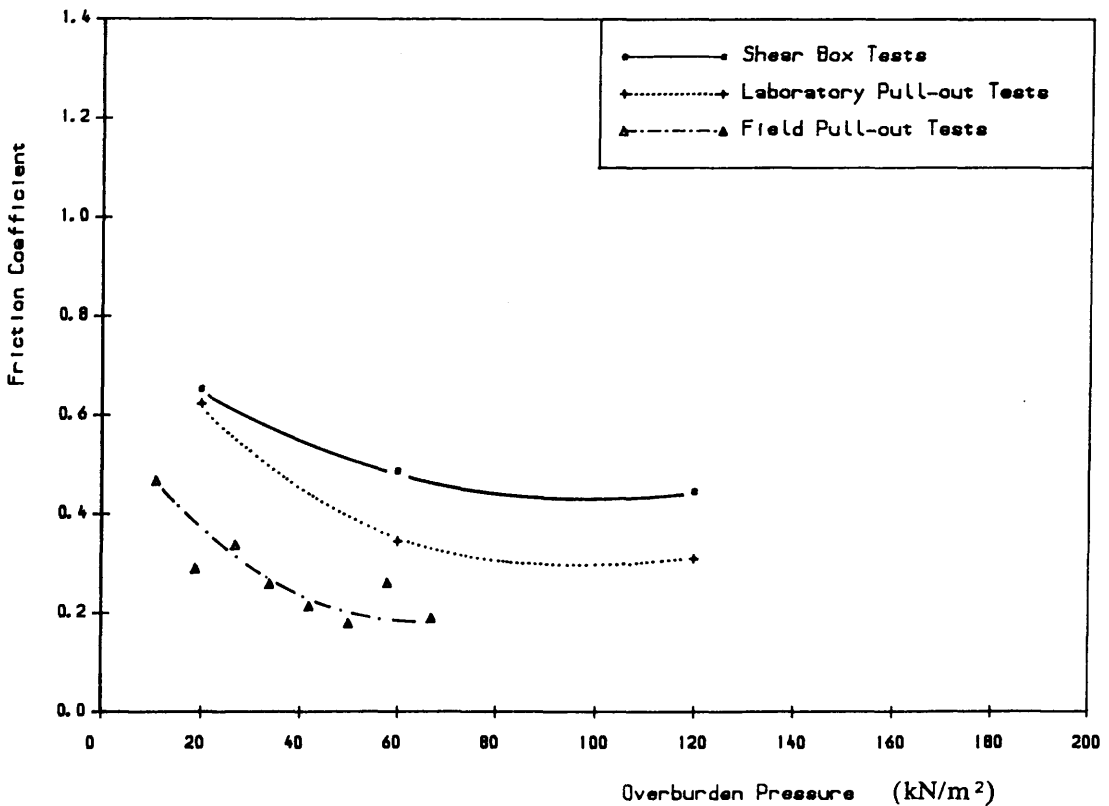


Figure 8.10 FRICTION COEFFICIENT VS. OVERBURDEN PRESSURE  
Loudon Hill Sand,  $\gamma_d=16.190\text{kN/m}^3$ , Paralink 300s

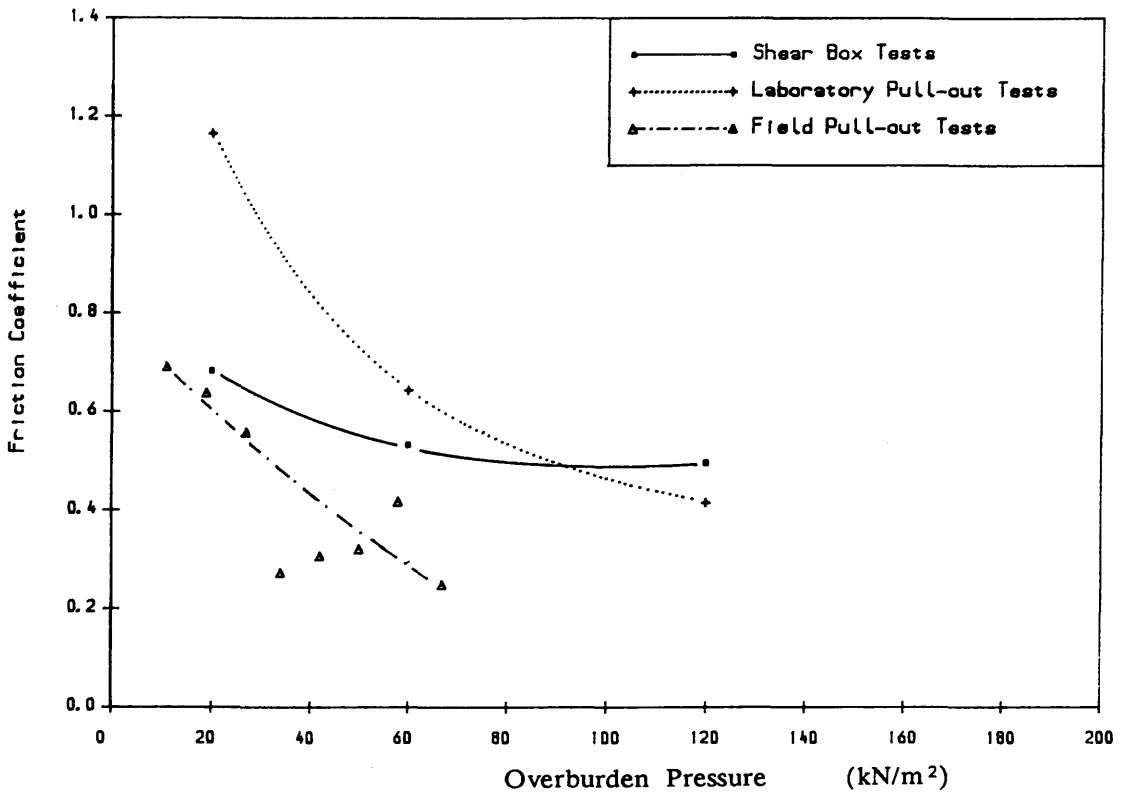


Figure 8.11 FRICTION COEFFICIENT VS. OVERBURDEN PRESSURE  
 Loudon Hill Sand,  $\gamma_d=16.190\text{kN/m}^3$ , Paralink 500s

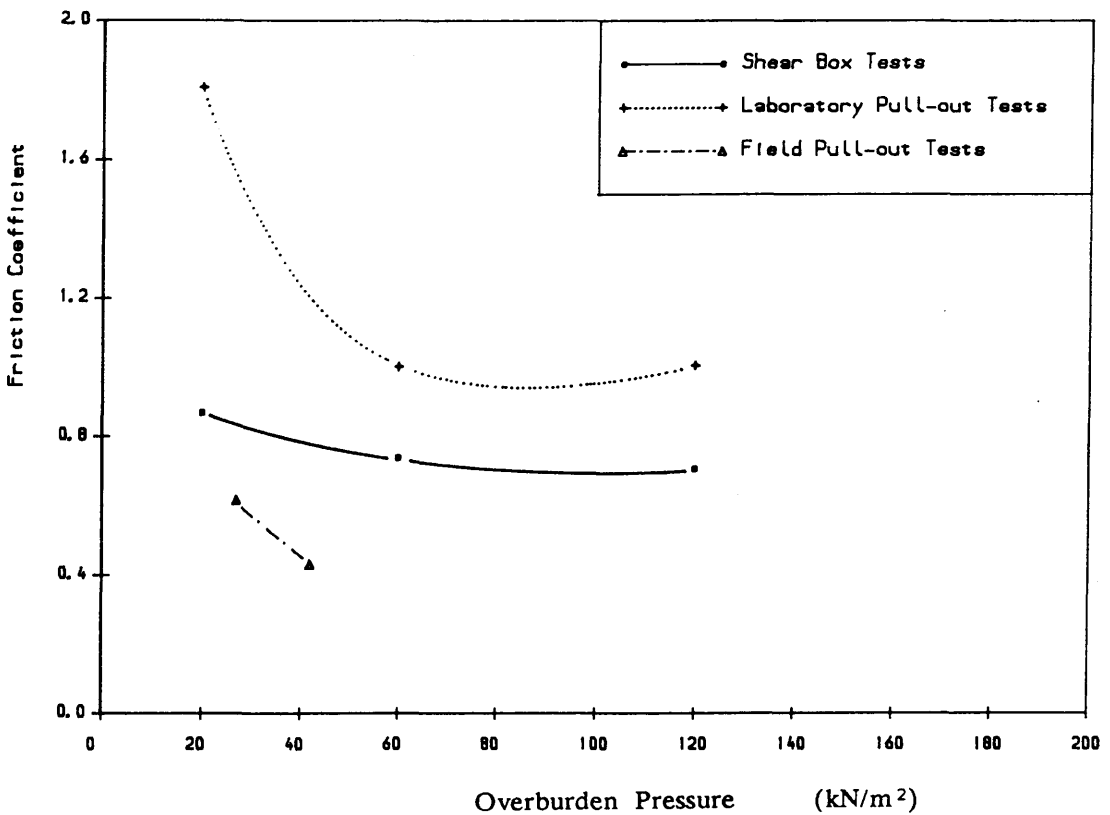


Figure 8.12 FRICTION COEFFICIENT VS. OVERBURDEN PRESSURE  
 Loudon Hill Sand,  $\gamma_d=16.190\text{kN/m}^3$ , Ribbed Steel

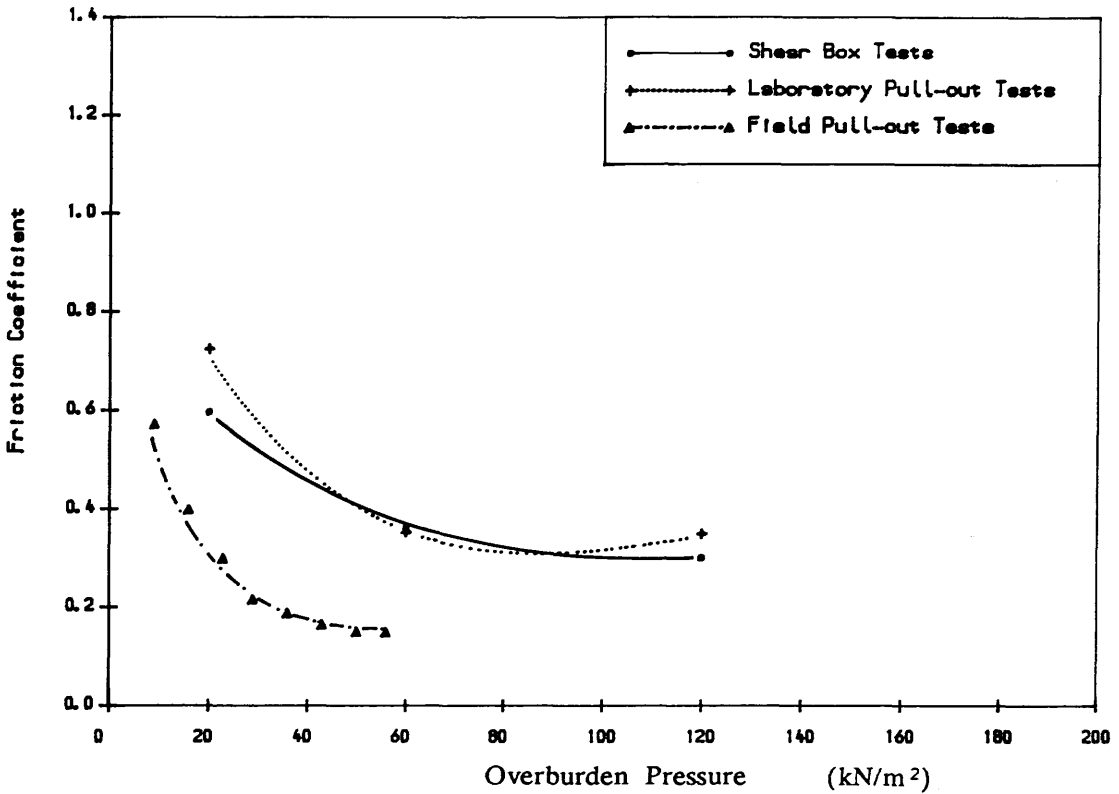


Figure 8.13 FRICTION COEFFICIENT VS. OVERBURDEN PRESSURE

Methyl PFA,  $\gamma_d=11.590\text{kN/m}^3$ , Paralink 300s

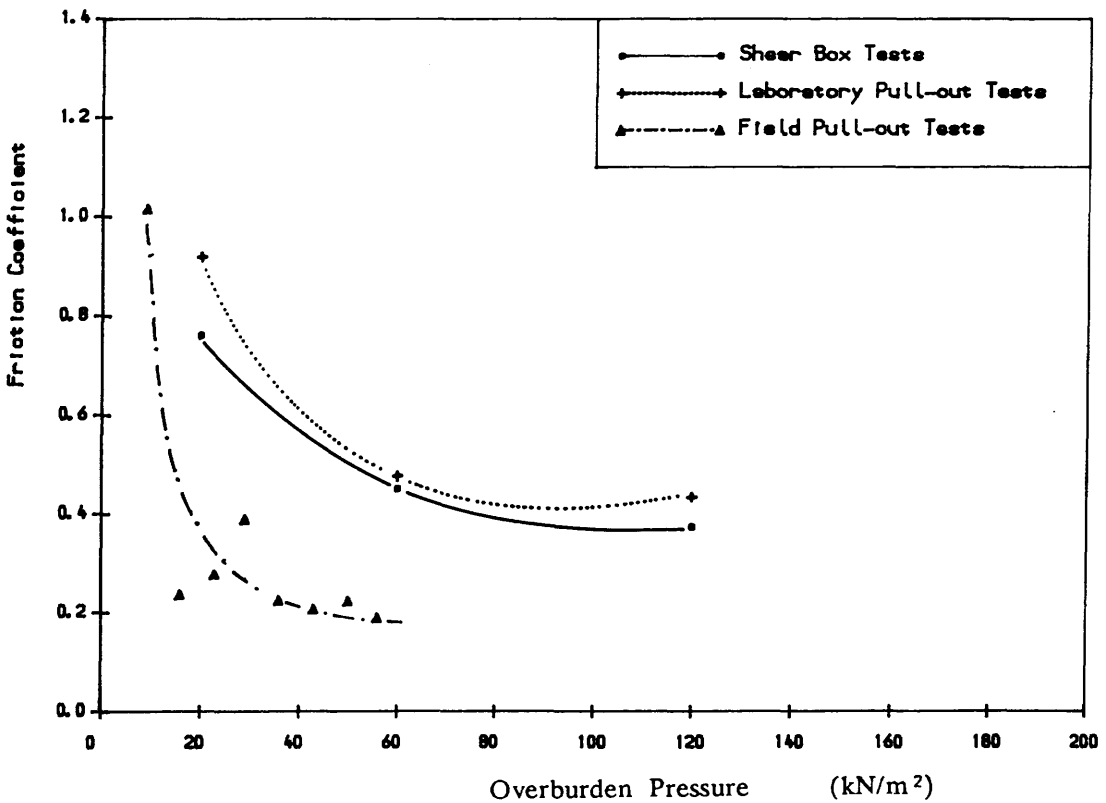


Figure 8.14 FRICTION COEFFICIENT VS. OVERBURDEN PRESSURE

Methyl PFA,  $\gamma_d=11.590\text{kN/m}^3$ , Paralink 500s

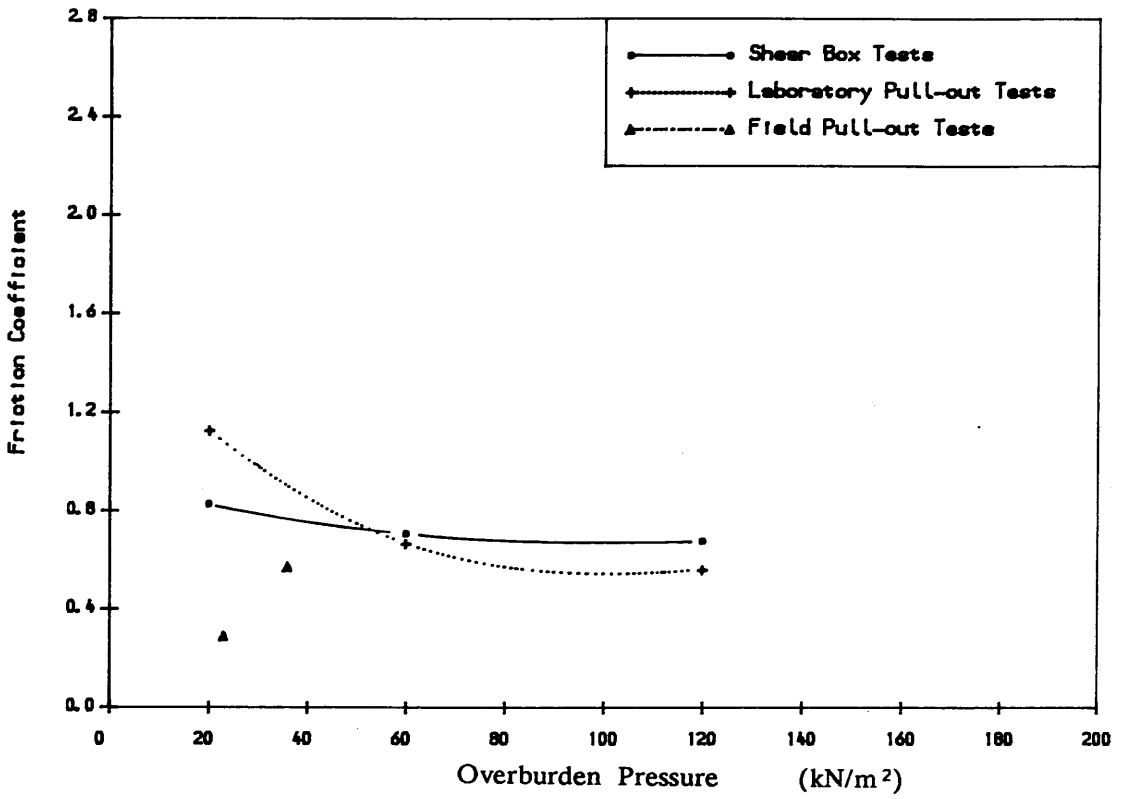


Figure 8.15 FRICTION COEFFICIENT VS. OVERBURDEN PRESSURE  
 Methil PFA,  $\gamma_d=11.590\text{kN/m}^3$ , Ribbed Steel

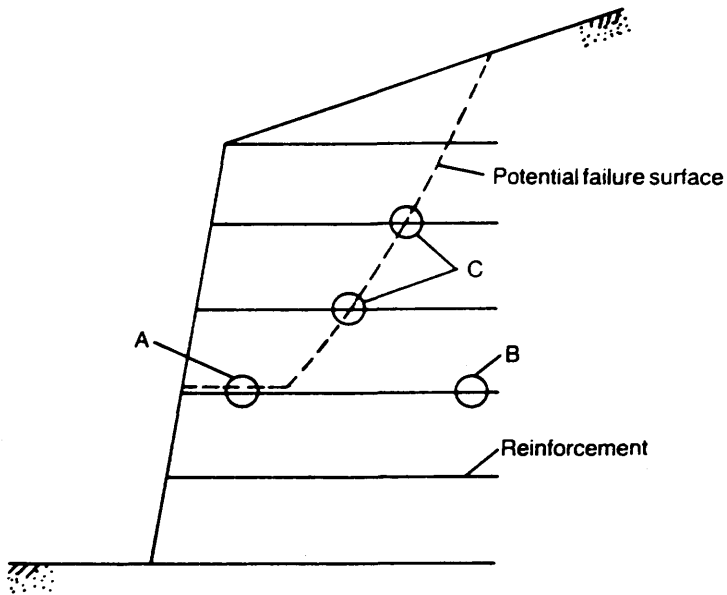


Figure 8.16 Mechanisms of Interaction in Reinforced Earth Structures  
(After Palmeria et al)

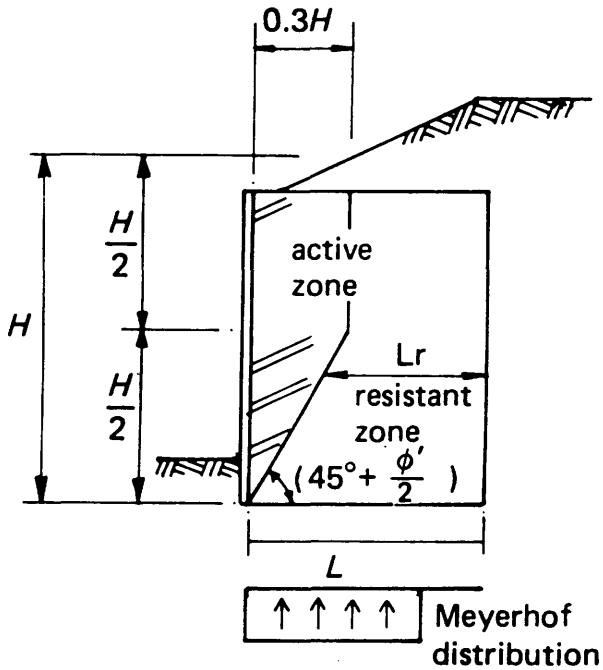


Figure 8.17 Coherent Gravity Hypothesis  
(After Jones)

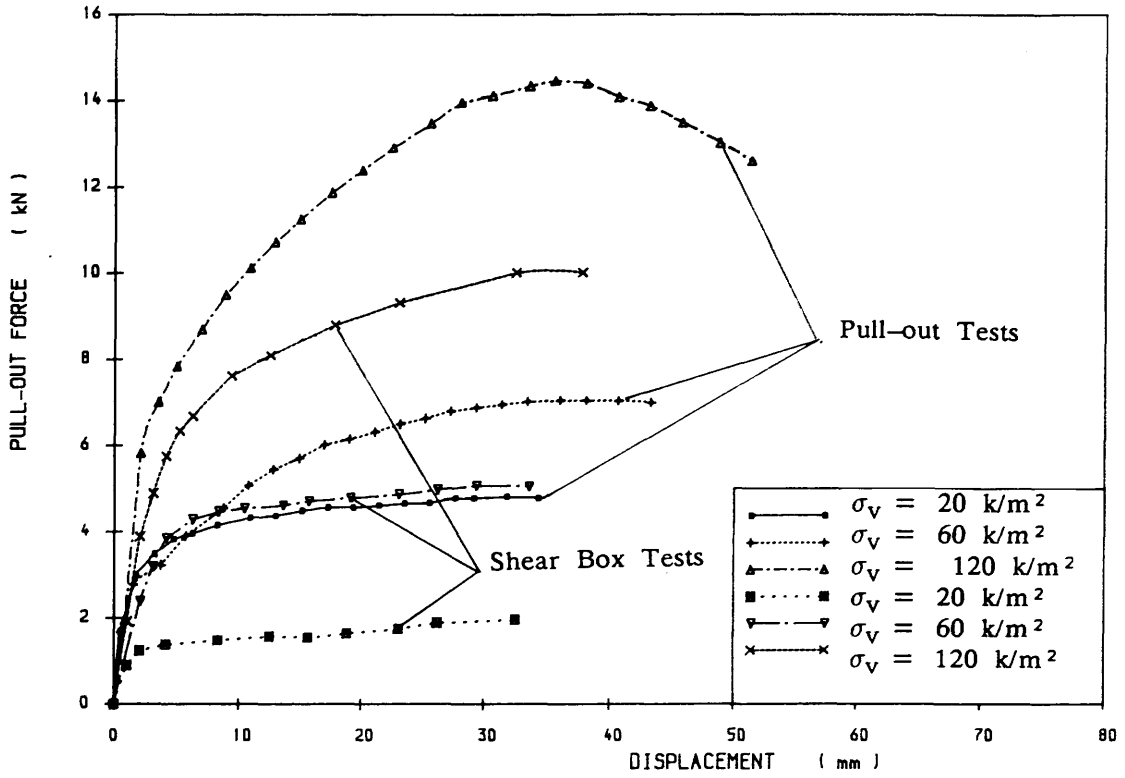


Figure 8.18 PULL-OUT FORCE VS. STRAP DISPLACEMENT

Loudon Hill Sand,  $L=1.5\text{m}$ ,  $\gamma=16.190\text{kN/m}^3$ , Ribbed Steel

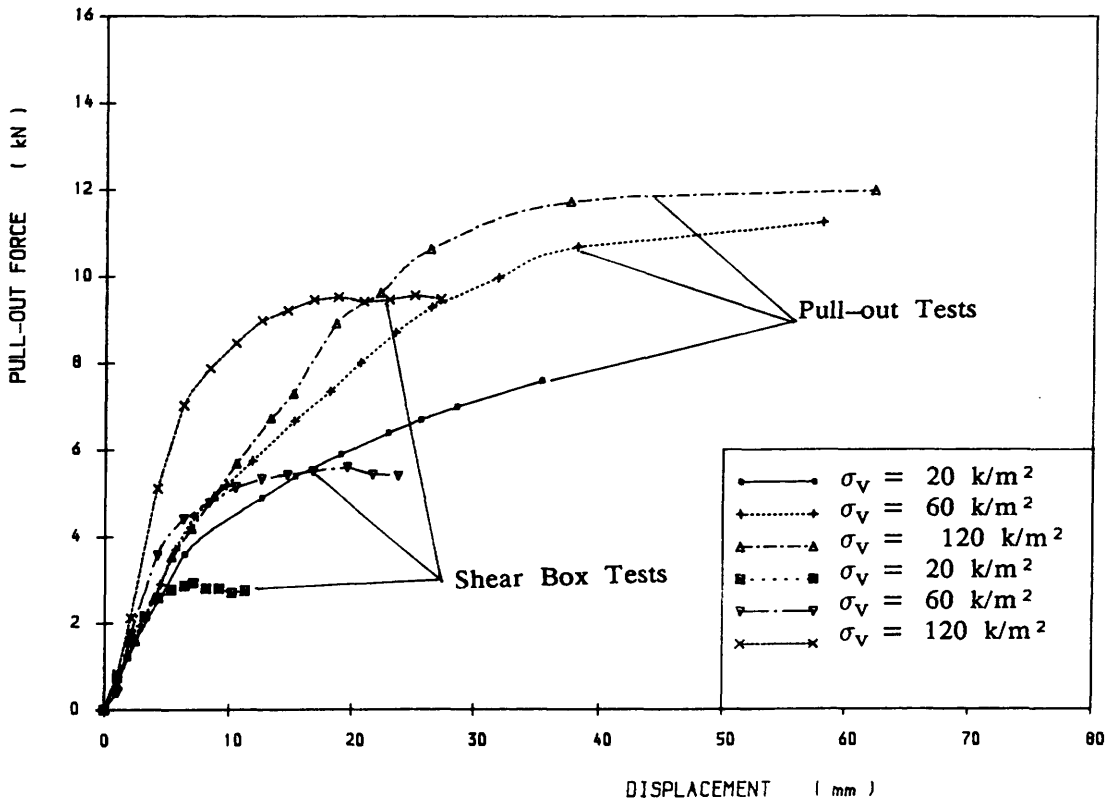


Figure 8.19 PULL-OUT FORCE VS. STRAP DISPLACEMENT

Vardley Minestone,  $L=1.5\text{m}$ ,  $\gamma=17.847\text{kN/m}^3$ , Ribbed Steel

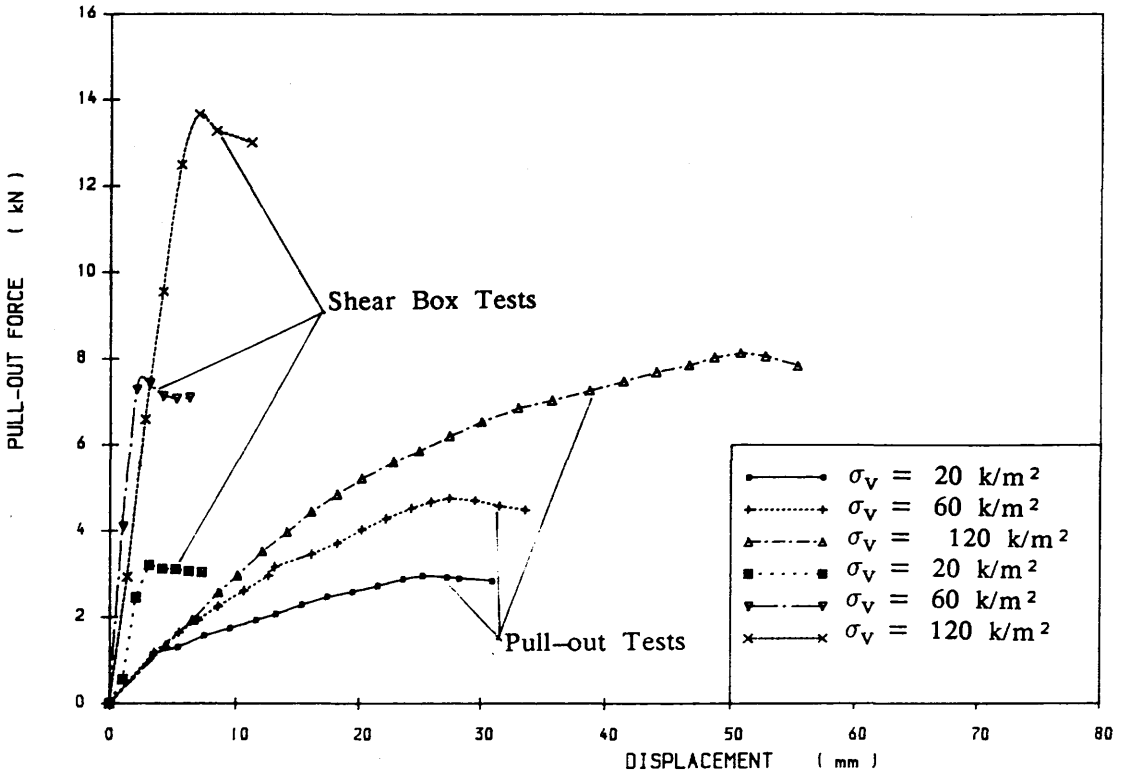


Figure 8.20 PULL-OUT FORCE VS. STRAP DISPLACEMENT

Loudon Hill Sand,  $L=1.5m$ ,  $\gamma=16.190 \text{ kN/m}^3$ , Paralink 300s

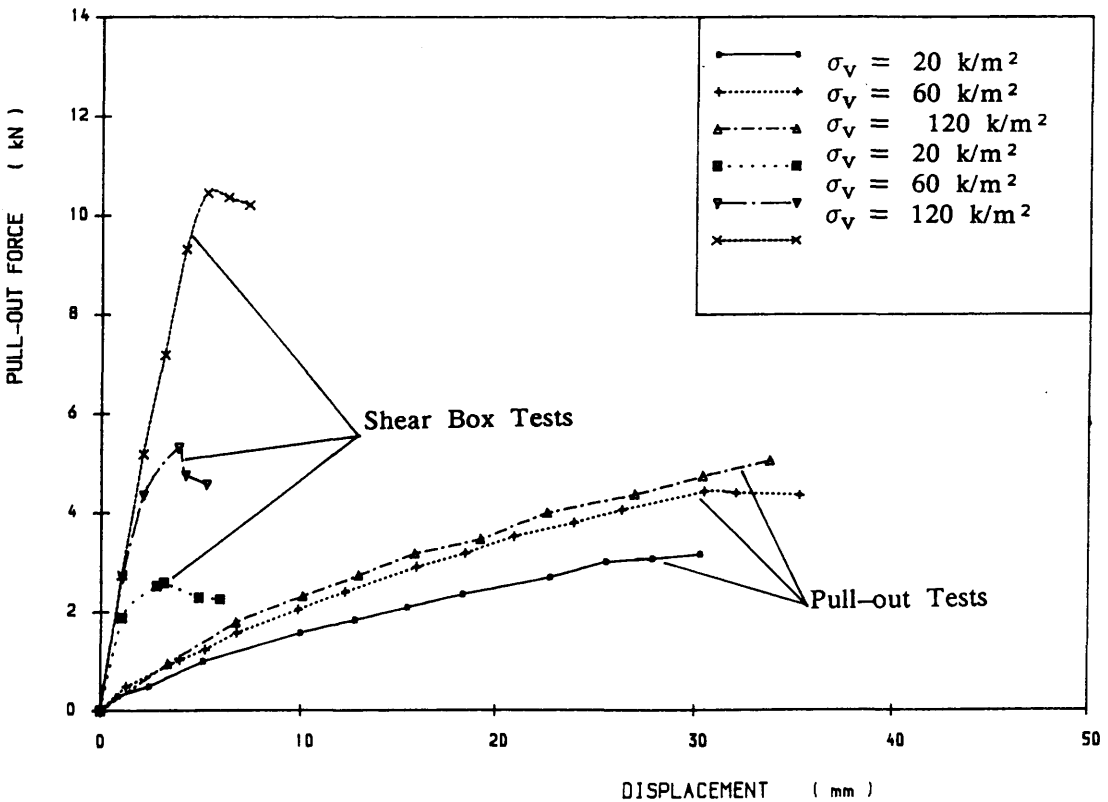
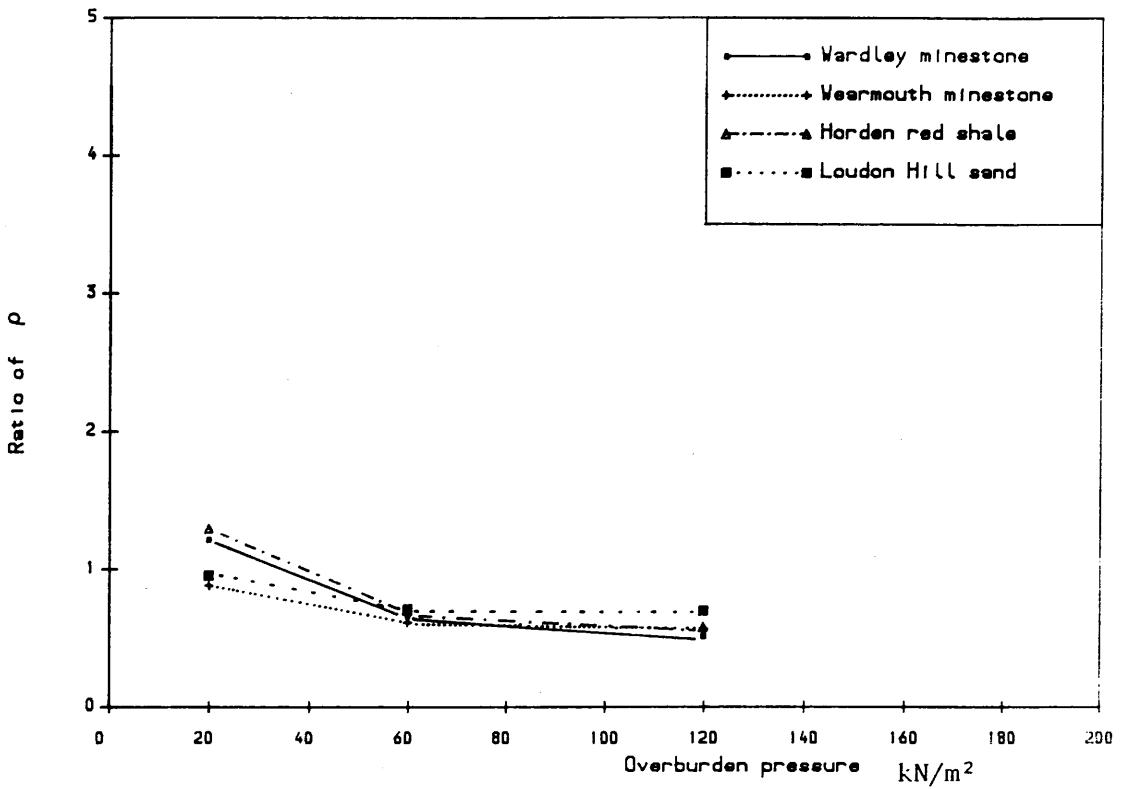
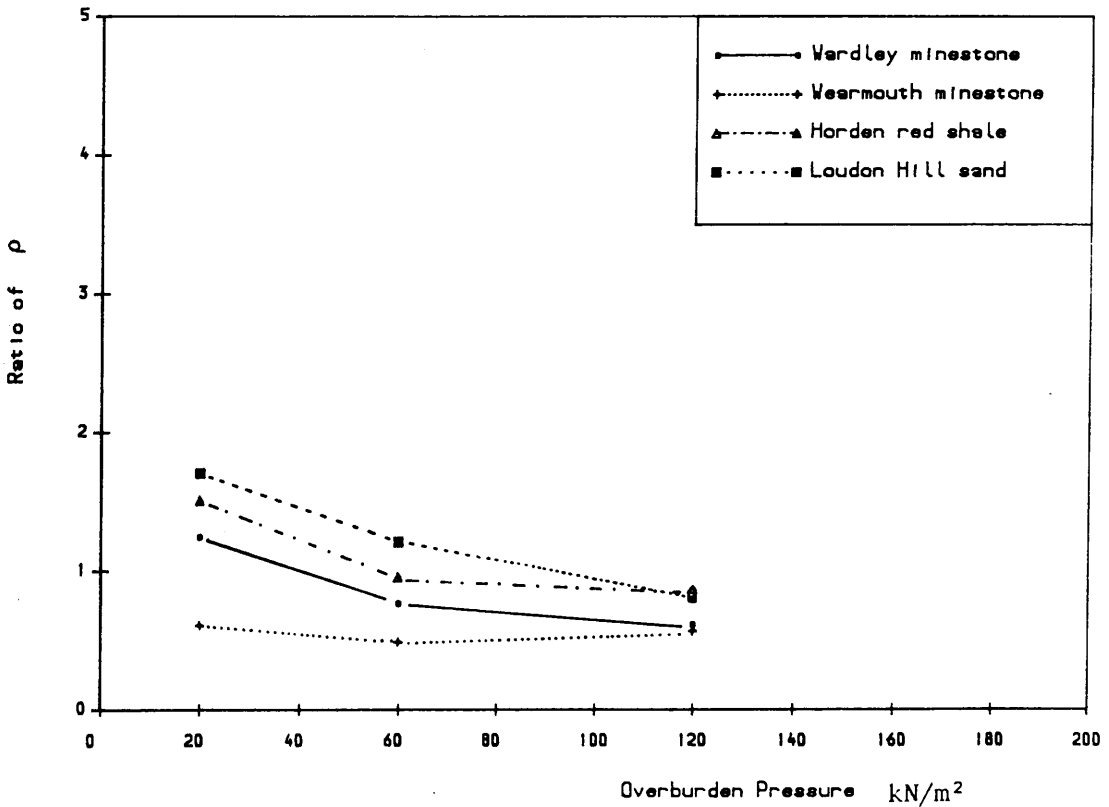


Figure 8.21 PULL-OUT FORCE VS. STRAP DISPLACEMENT

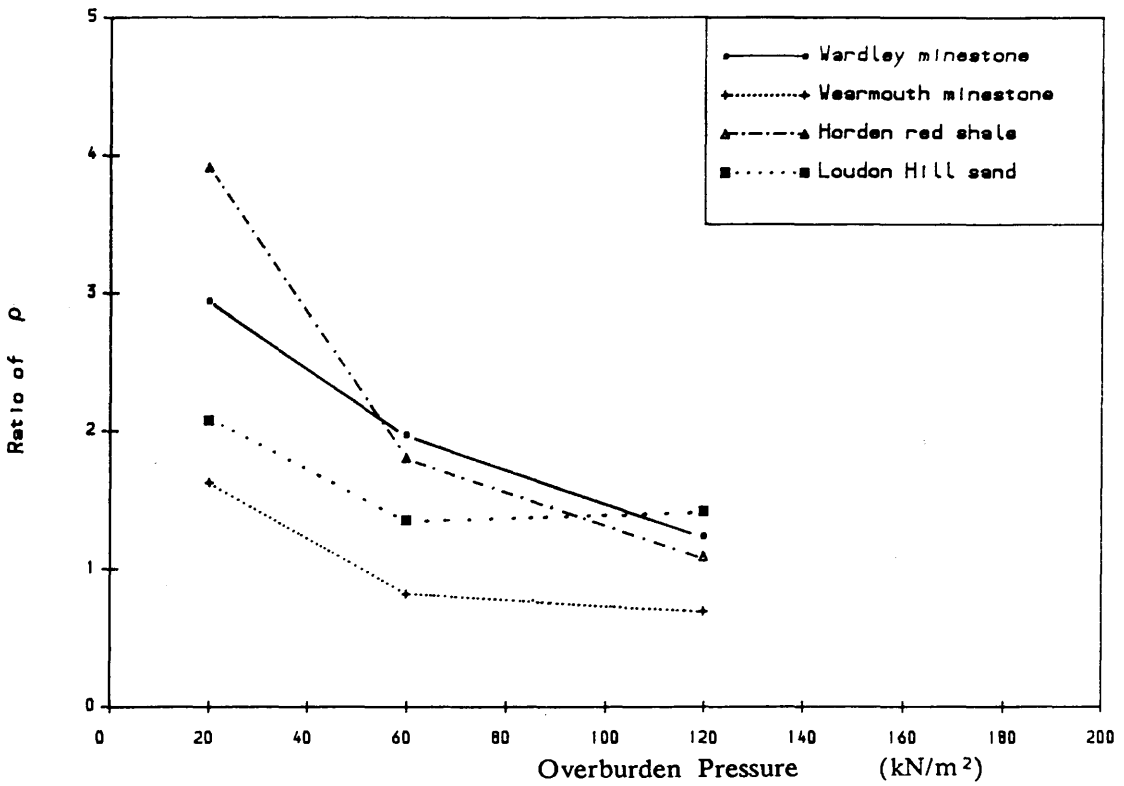
Vardley Minestone,  $L=1.5m$ ,  $\gamma=17.847 \text{ kN/m}^3$ , Paralink 300s



8.22 The Ratio of Friction Coefficient from Pull-out Test and Shear Box Test vs. Overburden Pressure, Paralink 300s



8.23 The Ratio of Friction Coefficient from Pull-out Test and Shear Box Test vs. Overburden Pressure, Paralink 500s



8.24 The Ratio of Friction Coefficient from Pull-out Test and Shear Box Test vs. Overburden Pressure, Ribbed Steel

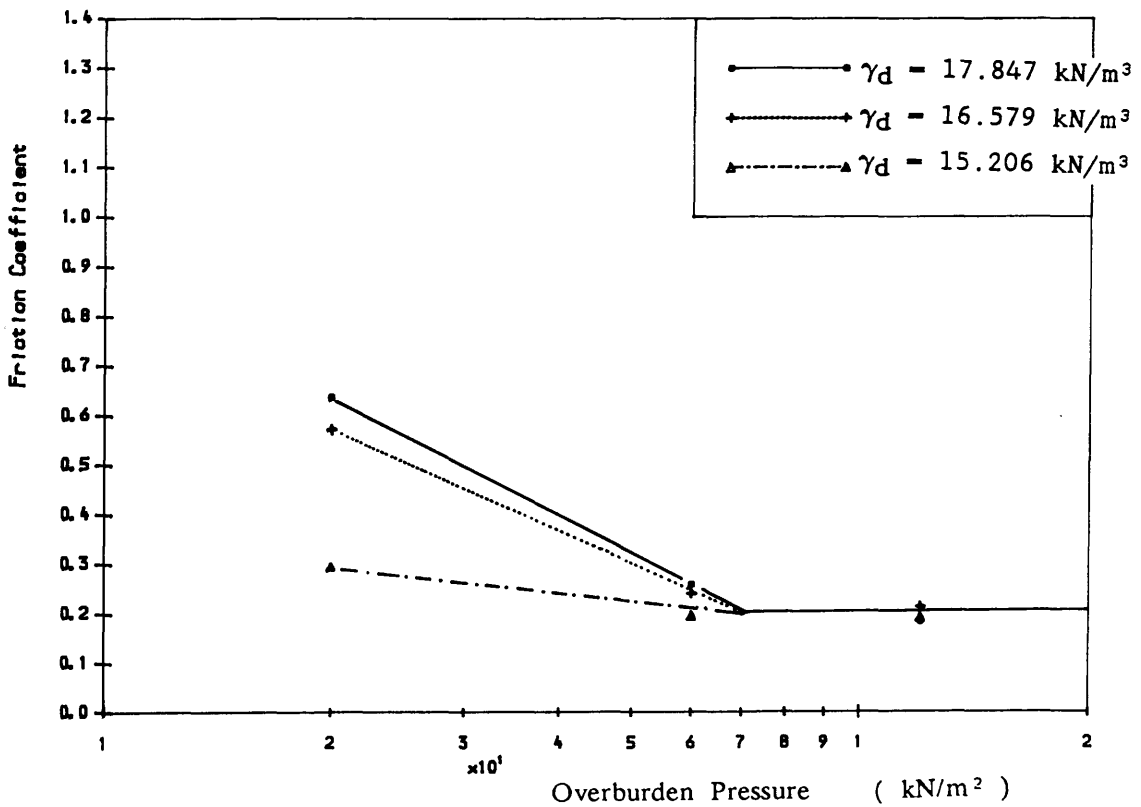


Figure 8.25 FRICTION COEFFICIENT VS. OVERBURDEN PRESSURE  
Laboratory Pull-out Test, Wardley Minestone, Paralink 300s, L=1.5m

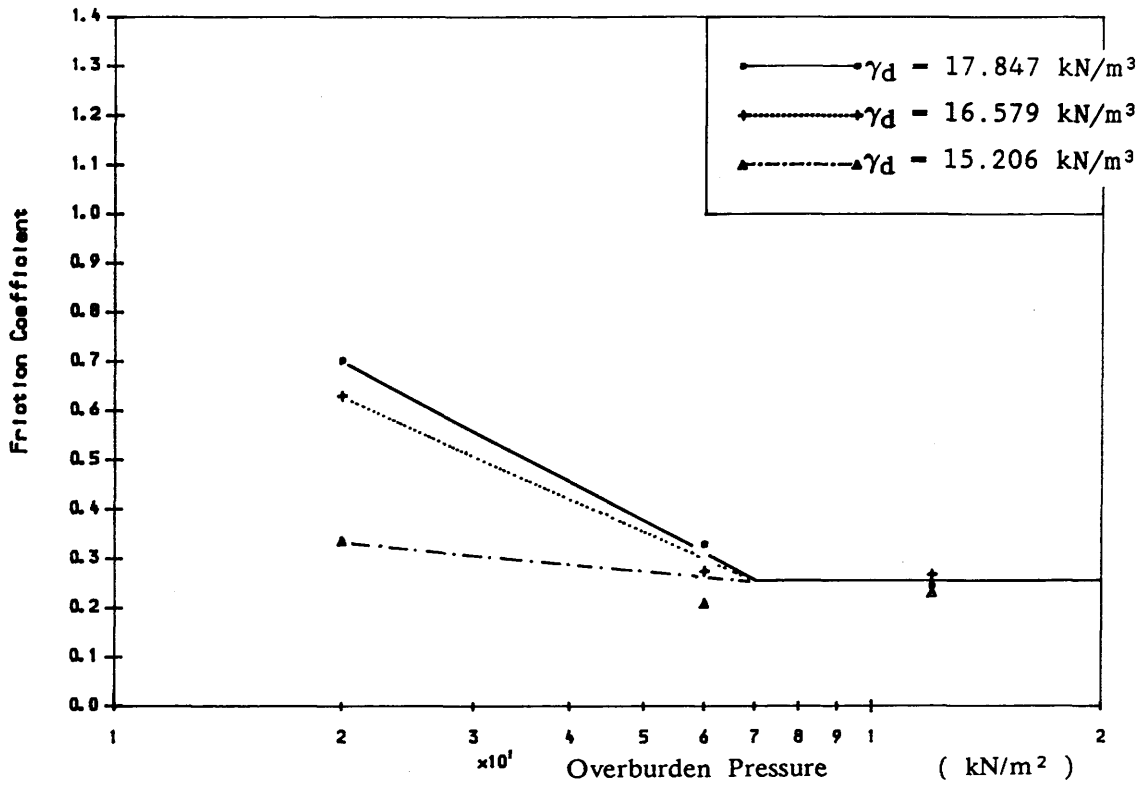


Figure 8.26 FRICTION COEFFICIENT VS. OVERBURDEN PRESSURE  
 Laboratory Pull-out Test, Vardley Minestone, Paralink 500s, L=1.5m

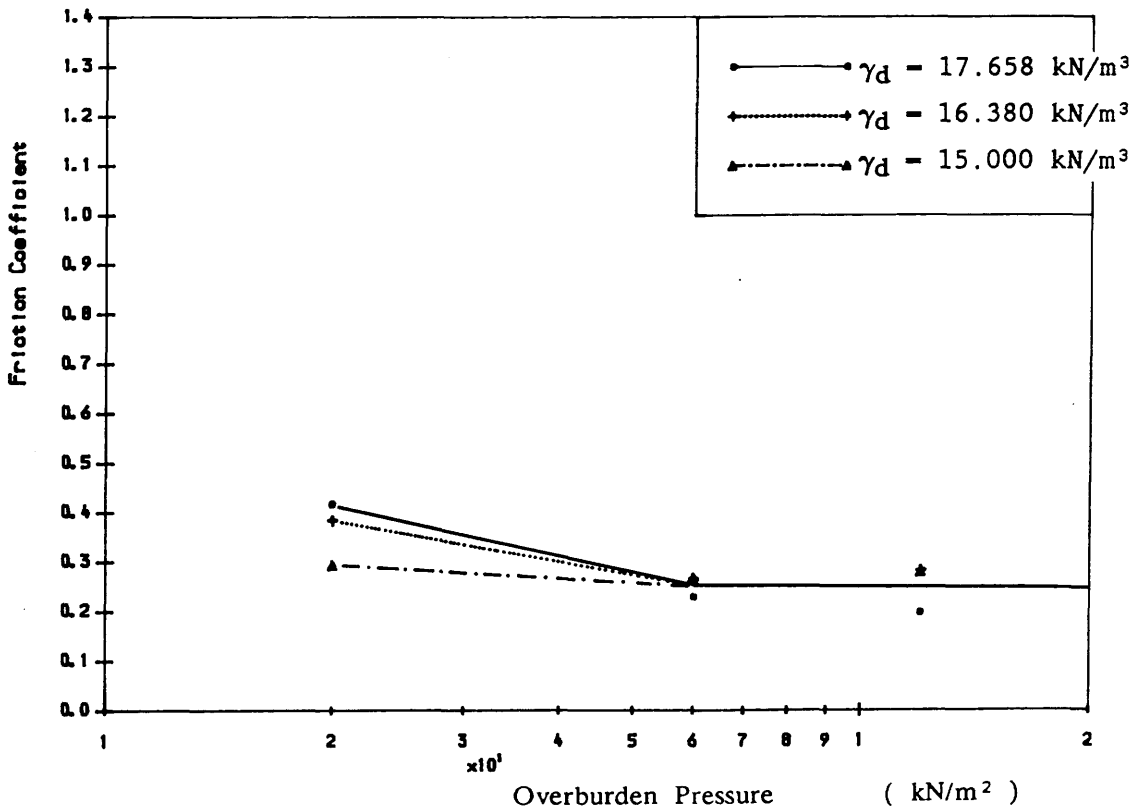


Figure 8.27 FRICTION COEFFICIENT VS. OVERBURDEN PRESSURE  
 Laboratory Pull-out Test, Vearmouth Minestone, Paralink 300s, L=1.5m

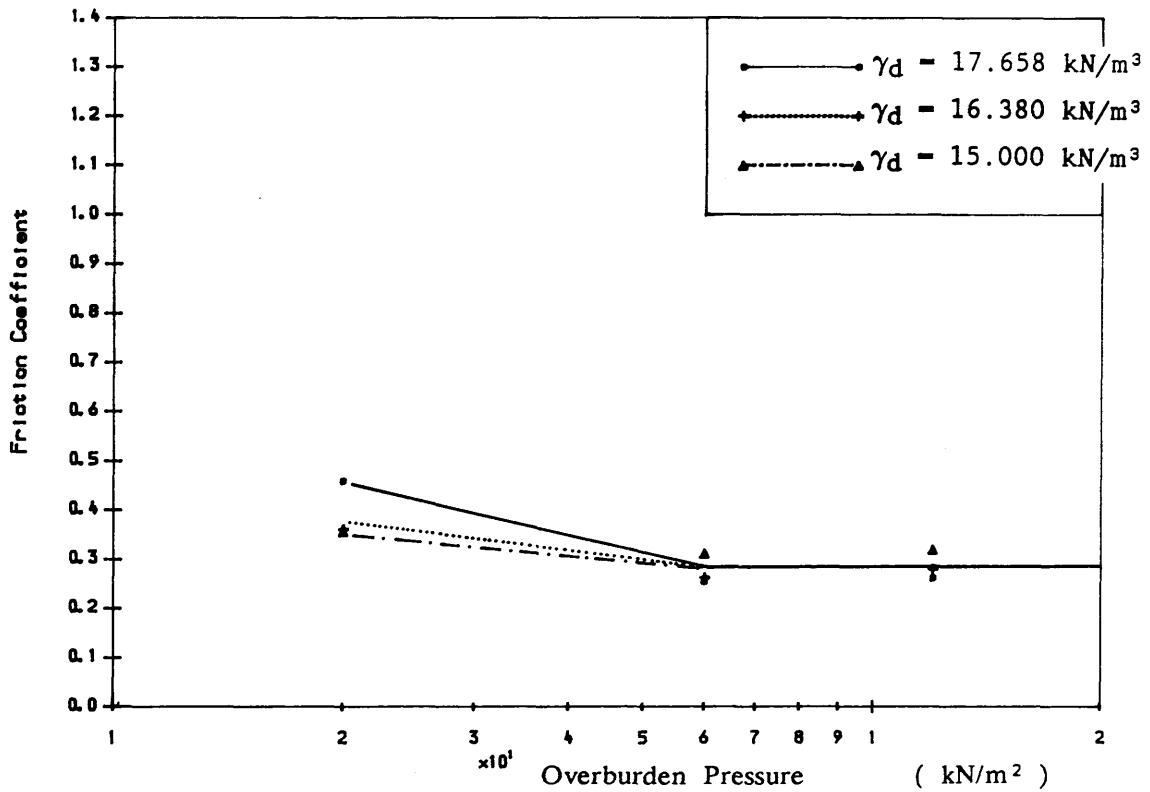


Figure 8.28 FRICTION COEFFICIENT VS. OVERBURDEN PRESSURE

Laboratoy Pull-out Test, Vearmorh Minestone, Paralink 500s, L=1.5m

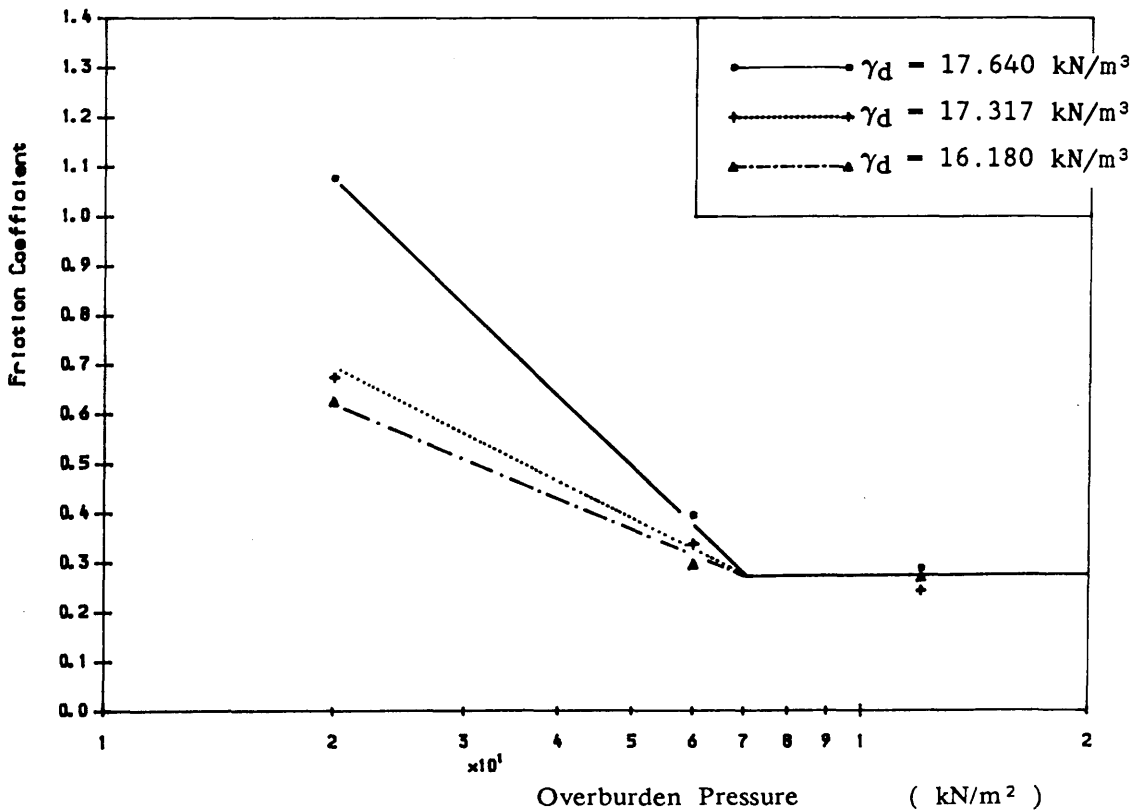


Figure 8.29 FRICTION COEFFICIENT VS. OVERBURDEN PRESSURE

Laboratoy Pull-out Test, Horden Red Shale, Paralink 300s, L=1.5m

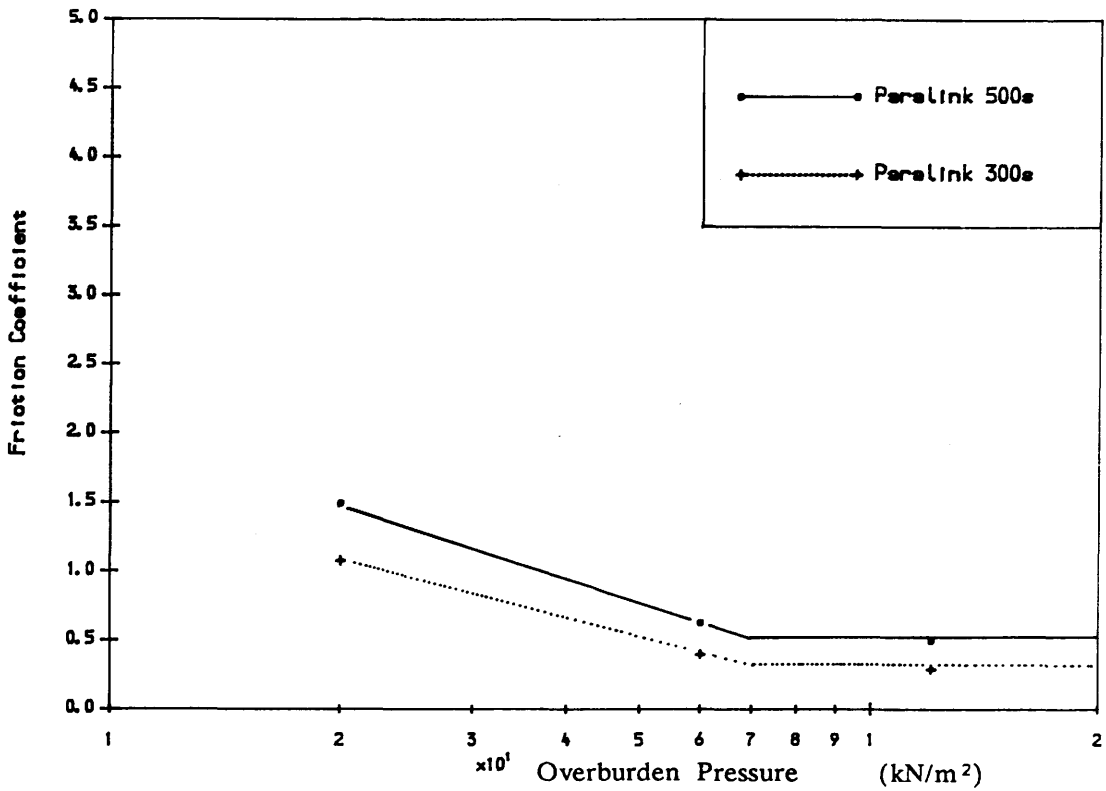


Figure 8.30 FRICTION COEFFICIENT VS. OVERBURDEN PRESSURE  
 Laboratory Pull-out Test, Horden Red Shale,  $\gamma_d=17.640\text{kN/m}^3$ ,  $L=1.5\text{m}$

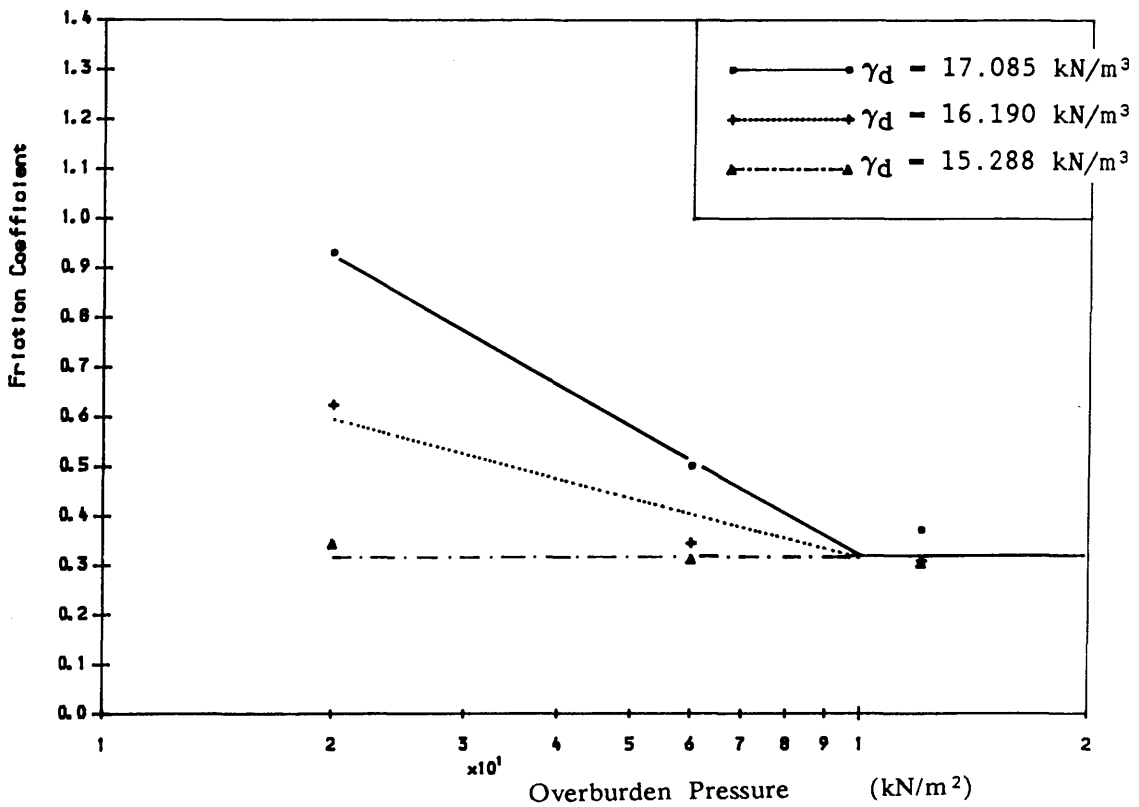


Figure 8.31 FRICTION COEFFICIENT VS. OVERBURDEN PRESSURE  
 Laboratory Pull-out Test, Loudon Hill Sand, Paralink 300s,  $L=1.5\text{m}$

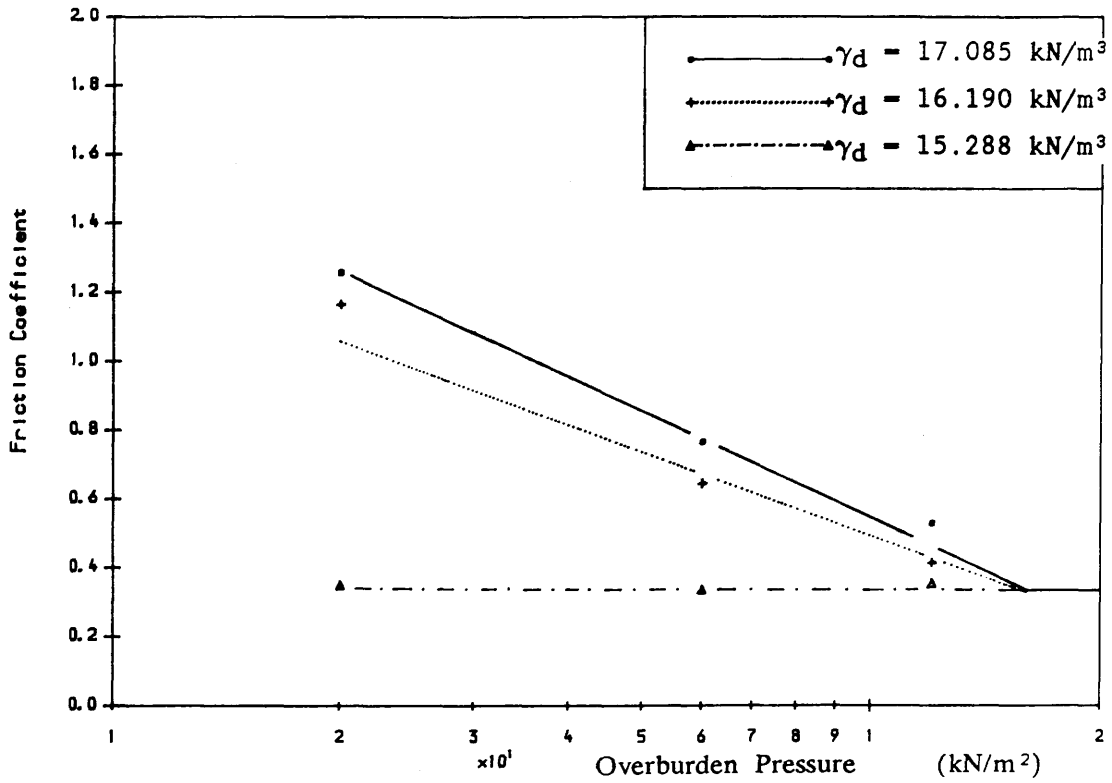


Figure 8.32 FRICTION COEFFICIENT VS. OVERBURDEN PRESSURE  
 Laboratory Pull-out Test, Loudon Hill Sand, Paralink 500s, L=1.5m

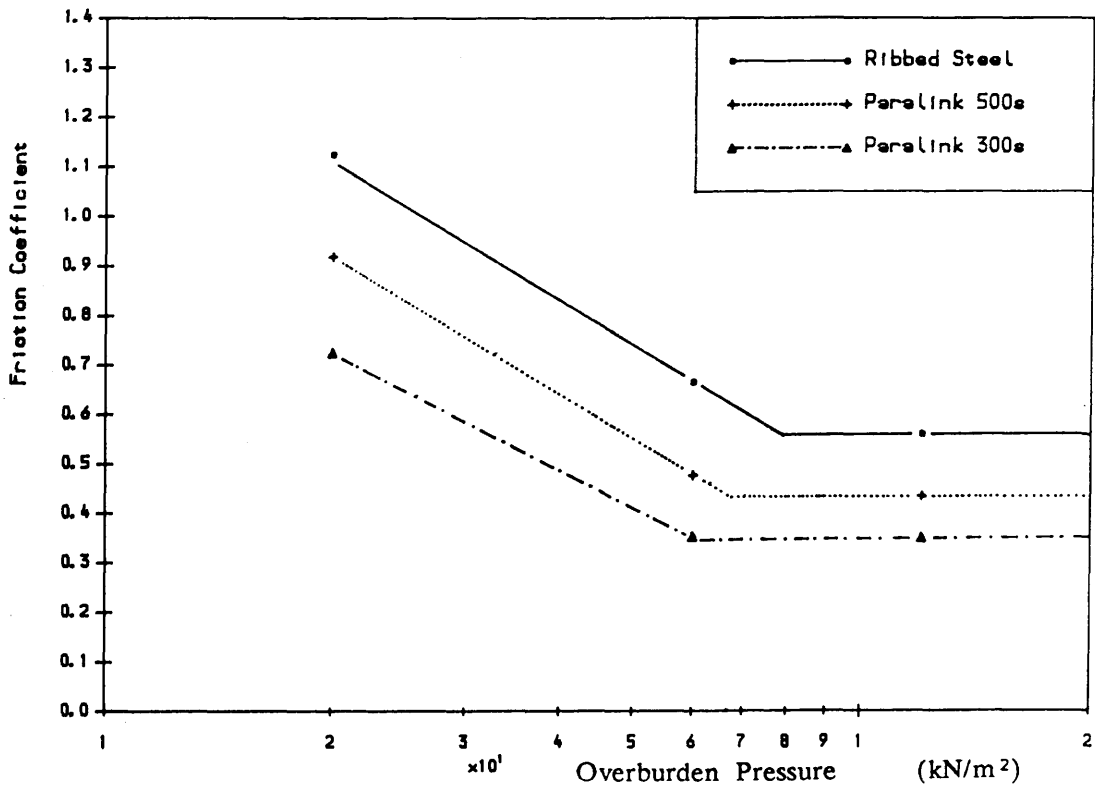


Figure 8.33 FRICTION COEFFICIENT VS. OVERBURDEN PRESSURE  
 Laboratory Pull-out Test, Methil PFA,  $\gamma = 11.590 \text{ kN/m}^3$ , L=1.5m

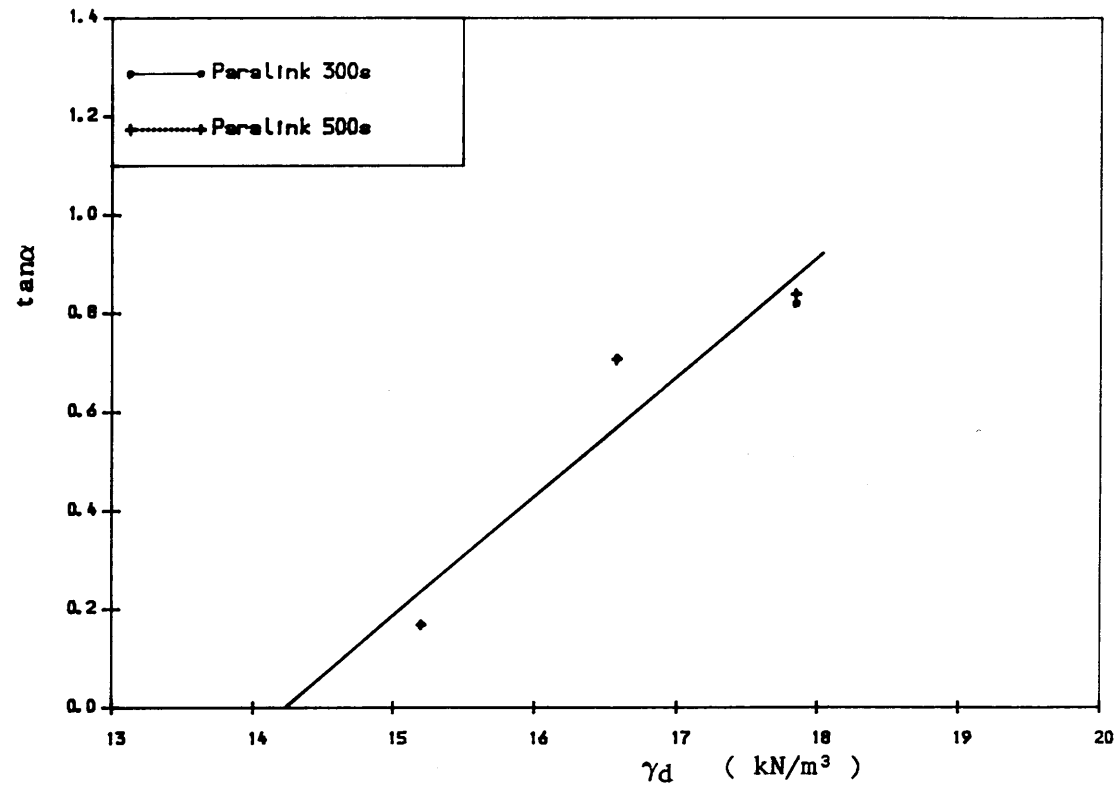


Figure 8.34 THE RELATIONSHIP BETWEEN  $\tan \alpha$  AND DENSITY  
Laboratory Pull-out Test, Wardley Minestone

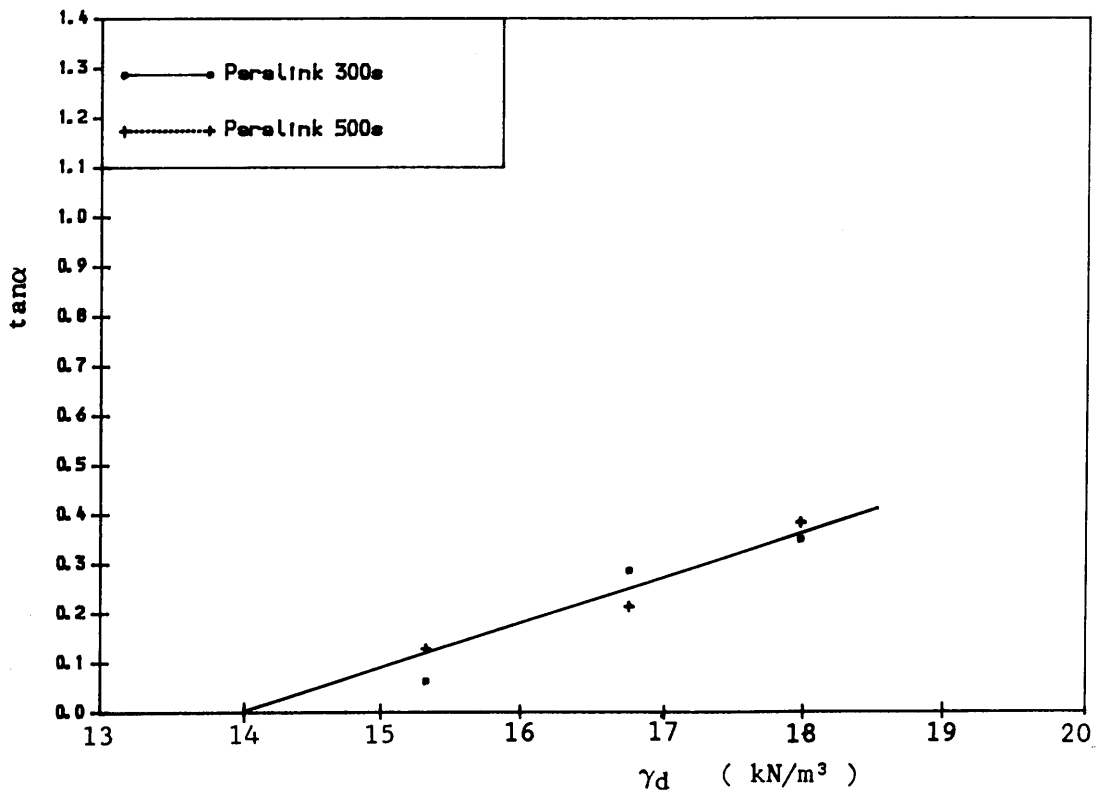


Figure 8.35 THE RELATIONSHIP BETWEEN  $\tan \alpha$  AND DENSITY  
Laboratory Pull-out Test, Wearmouth Minestone

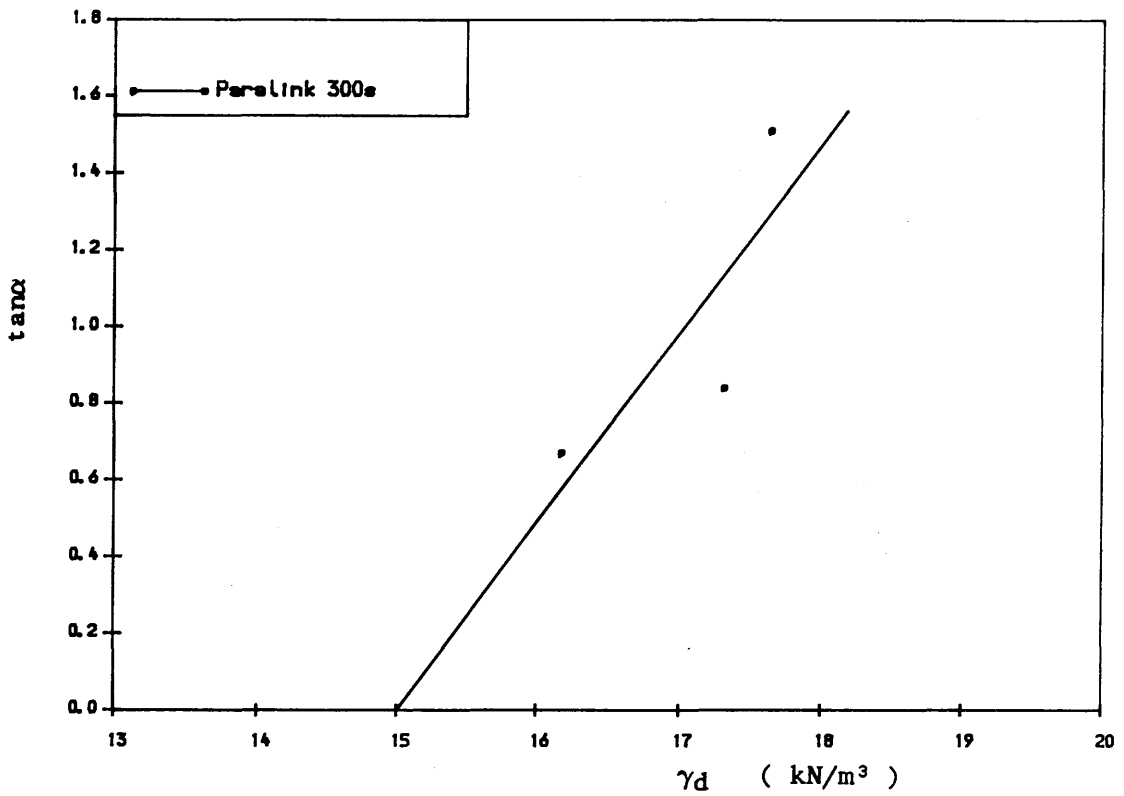


Figure 8.36 THE RELATIONSHIP BETWEEN  $\tan \alpha$  AND DENSITY  
Laboratory Pull-out Test, Horden Red Shale

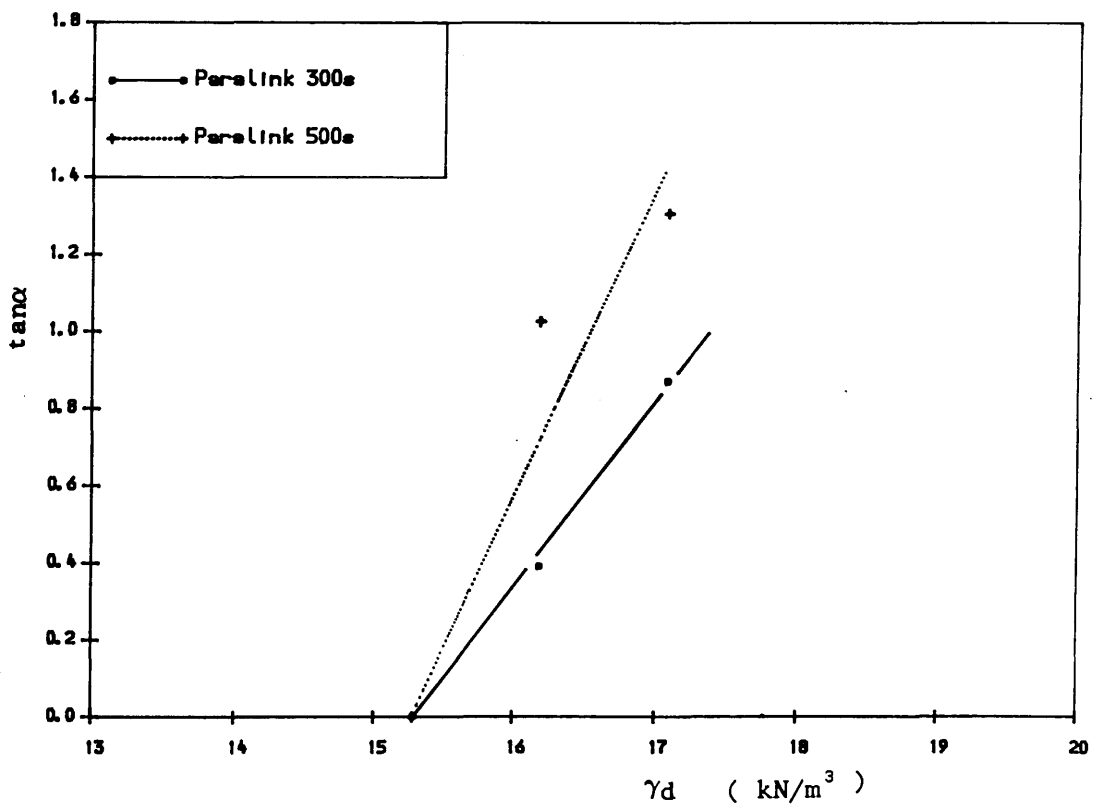


Figure 8.37 THE RELATIONSHIP BETWEEN  $\tan \alpha$  AND DENSITY  
Laboratory Pull-out Test, Loudon Hill Sand

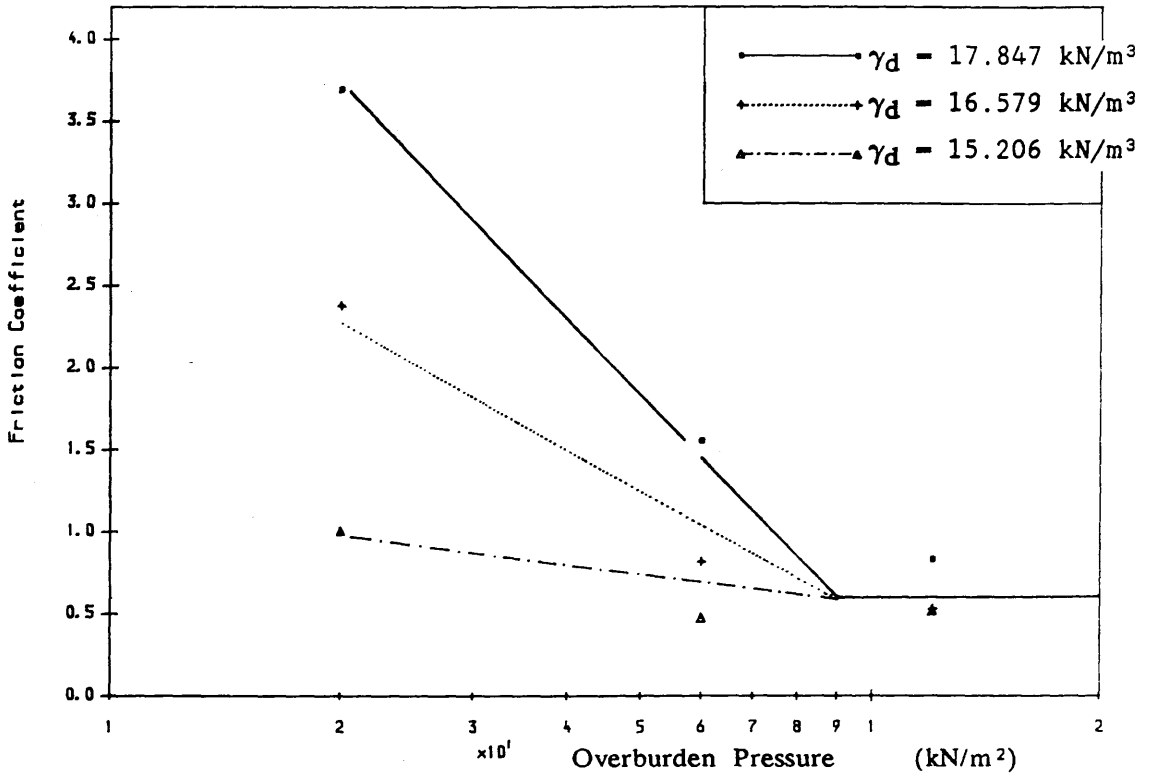


Figure 8.38 FRICTION COEFFICIENT VS. OVERBURDEN PRESSURE

Laboratory Pull-out Test, Wardley Minestone, Ribbed Steel, L=1.5m

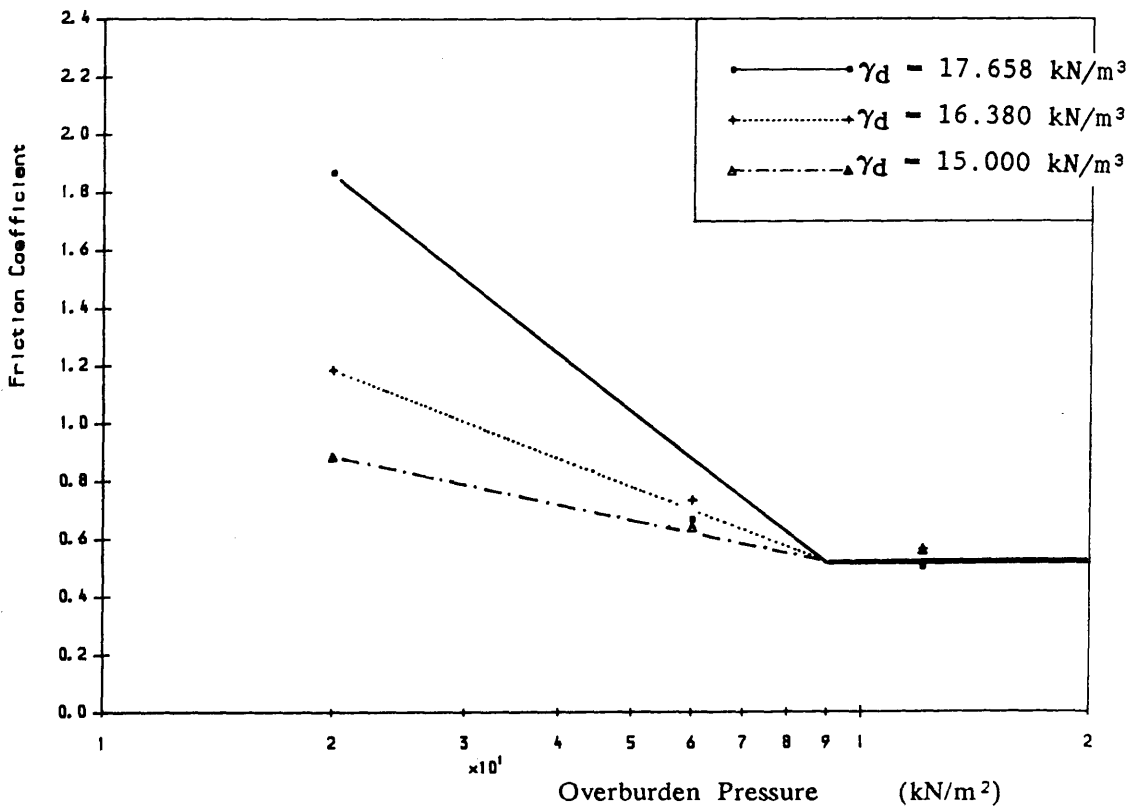


Figure 8.39 FRICTION COEFFICIENT VS. OVERBURDEN PRESSURE

Laboratory Pull-out Test, Wearmouth Minestone, Ribbed Steel, L=1.5m

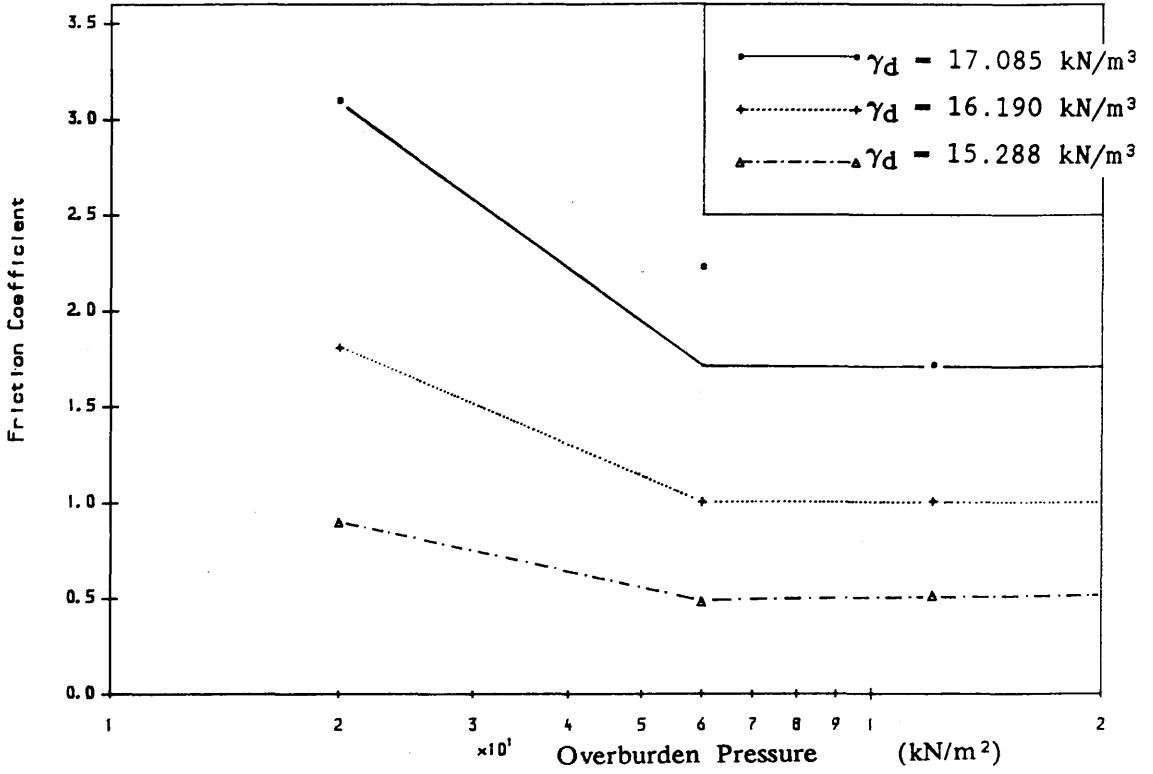


Figure 8.40 FRICTION COEFFICIENT VS. OVERBURDEN PRESSURE  
 Laboratory Pull-out Test, Loudon Hill Sand, Ribbed Steel, L=1.5m

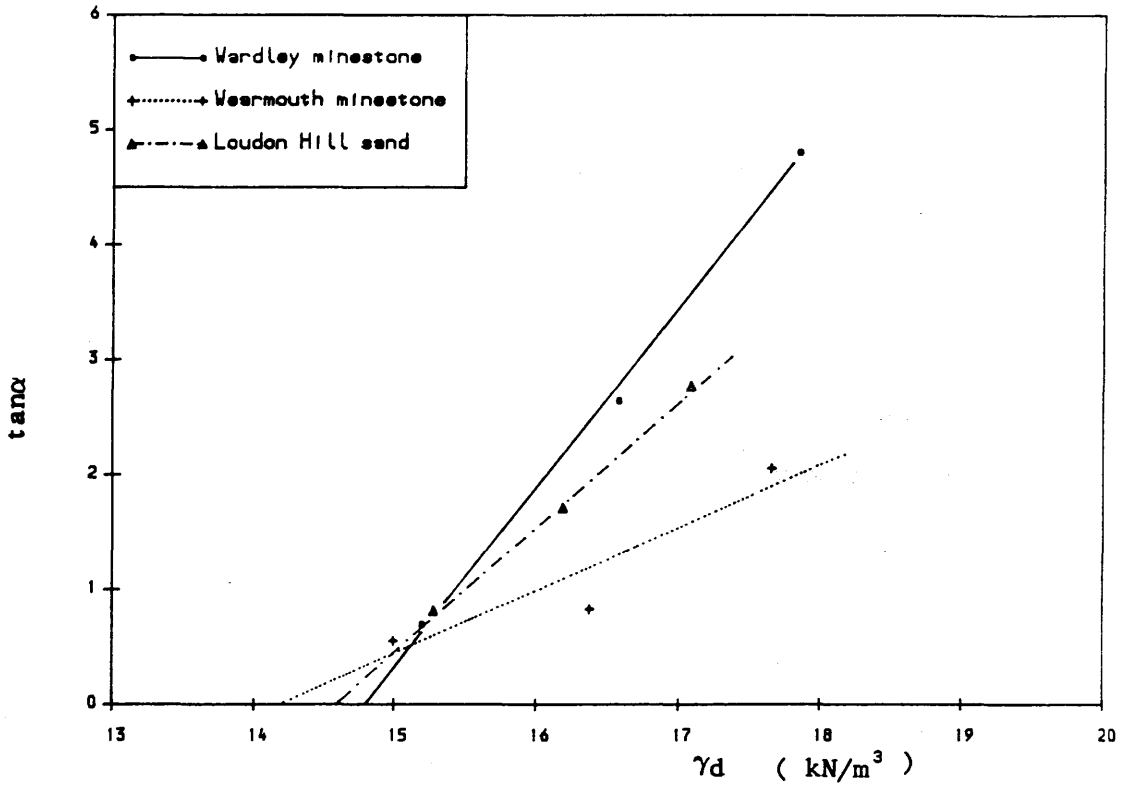


Figure 8.41 Laboratory Pull-out Test, Ribbed Steel

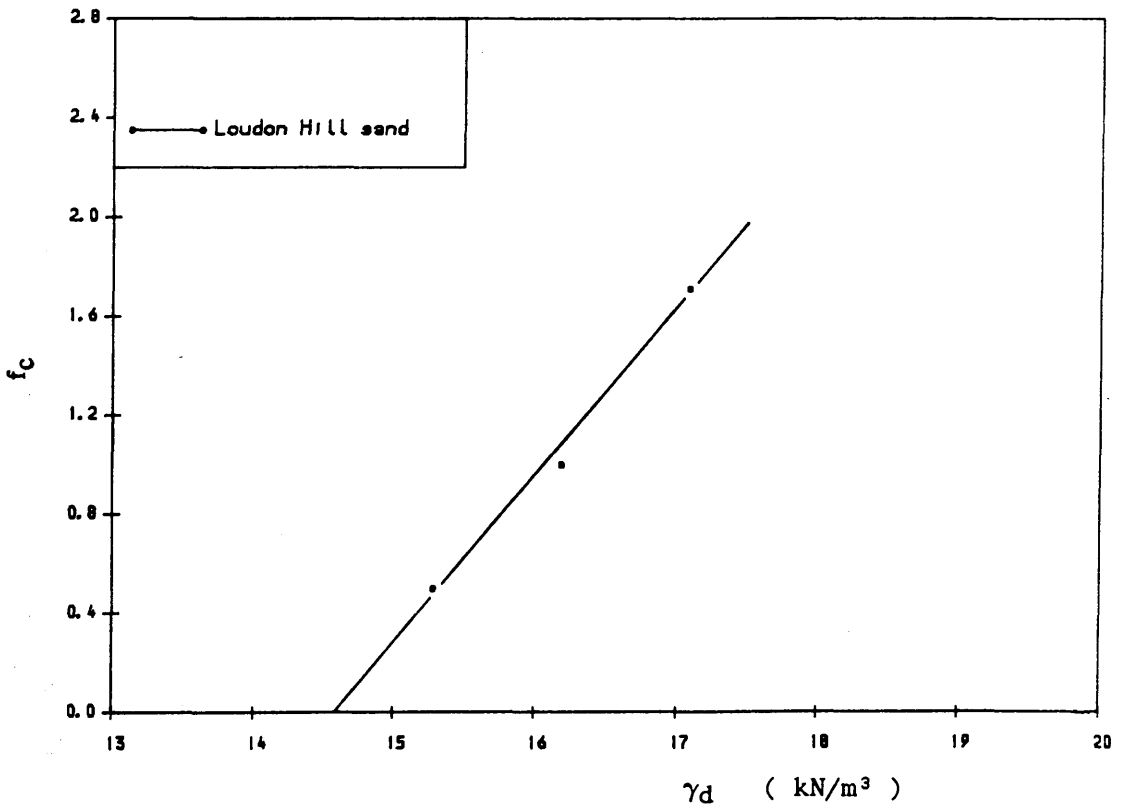


Figure 8.42 Laboratory Pull-out Test, Ribbed Steel

## CHAPTER 9

### GENERAL DISCUSSION, CONCLUSION AND FUTURE WORK

#### 9.1 INTRODUCTION

Specific discussion on the results obtained from the present work has been presented in the previous chapters. In this chapter these are summarized and a general discussion is given. The conclusions drawn from each of these chapters are also presented together. Finally, some future work is recommended.

#### 9.2 GENERAL DISCUSSION

##### 9.2.1 Reinforcing Materials

Among the three types of reinforcement, ribbed steel strap is the conventional reinforcement which has been widely used in reinforced earth structures. The other two straps, Paralink 300s and Paralink 500s are both plastic straps with polyester fibres enclosed in a durable polyethylene sheath. They possess similar forms, but are of different colours and have slightly different surfaces. Paralink straps are relatively new types of reinforcement, but have been currently used in practice (Brady, 1986). However they have been available for over 10 years.

The results of the present work show the superior characteristics of the ribbed steel strap to the Paralink straps in terms of friction resistance. The rigid behaviour of the ribbed steel is also an advantage in reducing any outwards deformation of a reinforced earth structure. This behaviour coincides with the mechanism of reinforced earth (Chapter 2) which proposed that the reinforcement be inextensible relative to soil, so that the lateral strain of the soil could be prevented. However, the corrosion affecting steel reinforcement when buried in soil is still a problem. This becomes even more severe when waste materials are

used as fill or even when the structure is constructed in an area such as a mine. Galvanized steel resists corrosion attack more than common steel, but it does not fully avoid it. Deterioration of reinforced earth walls in South Africa was reported by Blight and Dane (1989) where a wall was constructed with galvanized ribbed mild steel strips at a mine. After 8 years of the 30-year design life, it was found that the reinforcement was deteriorating, as a result of severe pitting corrosion. The wall was finally demolished and rebuilt. As O'Reilly stated (Brady, 1986), steel had nearly 5,000 years of development behind it, and had less scope for development than artificial plastics, which were discovered and developed in this century.

Hence when cheaper low quality backfills are used in reinforced earth structures, artificial plastic reinforcements, such as Geogrids and Paralink should be regarded as adequate reinforcing materials. Comparing the apparent friction coefficient of ribbed steel strap with the Paralinks, it was found that the value of  $f^*$  for the ribbed steel is about 1.4 to 6 times higher than that obtained for the Paralink straps when used with the fill materials in the present work. Whereas comparing the costs per unit area of the strap surface, ribbed steel is about double the price of Paralink. Therefore, if the friction coefficient and the costs are considered together, the superiority of the ribbed steel becomes less. In addition, the flexibility and light weight of the Paralink makes it easy to transport and handle in construction.

Considering the durability of the Paralink reinforcement, it was reported by Reilly (Brady, 1986) that straps removed from a seven year old reinforced earth structure at TRRL had not lost any of their original tensile strength. Research work at Strathclyde University has shown that the creep properties of plastics can be accounted for in design.

Although the extensibility of plastic reinforcement appears to differ from the fundamental mechanism, studies by McGown et al (1978) have provided useful information. It was concluded that the modification of soil behaviour is strain controlled with the reinforcement. Further they concluded that relatively inextensible tensile strain reinforcement, with in-situ rupture strains less than the maximum

tensile strains in soil without reinforcement, may impart a strength improvement which is limited by rupture of the reinforcement. Whereas extensible reinforcement, with rupture strains larger than the maximum tensile strains in the soil alone, would not rupture, no matter what their ultimate tensile strength, and would therefore always strengthen the soil. Lately, research has proposed that the extensibility of reinforcement could be an advantage in certain conditions, since it may relax the stress concentration and causes stress redistribution within a structure. All these have proved the advantages of using Paralink reinforcements in reinforced earth.

In addition to their use as reinforcing straps in reinforced earth structures, a new utilization of Paralink straps has been described by H. Murray (Brady, 1986). It was a system developed in Austria, in which continuous Paralink loops (Paraloops) were used as ties with concrete panels and anchors.

### 9.2.2 Fill Materials

Of the five different fill materials used in the present research, sand is a conventional material. Because of its cohesionless properties, high frictional resistance, good permeability and non-corrosion to metallic reinforcement, it has been regarded as the most adequate fill material and is widely used in reinforced earth structures.

Red shale, a well-burnt type of colliery spoil is also accepted as a high quality material for construction purposes, and many of the best deposits have been used up in U.K. This material is commonly much stronger than its unburnt equivalent.

PFA (Pulverised Fuel Ash) is a type of waste with light weight and fine particles. This material has also been used in reinforced earth as a fill material (Jones, 1984). The main advantages of using it are the reduction in cost and also its light weight, reducing bearing pressure on a very weak subsoil. But it is corrosive to steel, therefore the use of non-metallic reinforcement is required.

Minestones as coal mining wastes are reported to be the largest source of waste materials in the United Kingdom (Taylor 1978 and Rainbow 1982). These

materials have hitherto not been accepted for use in reinforced earth structures in the U.K., since it remains to be proven that their mechanical, physical characteristics are suited to backfill requirements in such structures. What affects the suitability of their utilization are the following natural properties.

Spontaneous ignition as an important character of colliery spoil has been of concern to civil engineers. In 1967 about 15% of the 2000 spoil heaps owned by the NCB alone were classified as burnt out and more than half as burning (Taylor, 1978). This phenomenon is in essence an atmospheric oxidation (exothermic) process of the coal content in minestones. Investigators found that spontaneous ignition occurred in loosely tipped spoils. The permeability to air is one of the controlling factors as to whether oxidation will be sustained and the temperature will rise. If the spoil is compacted, the permeability of air is reduced, and effectively excludes the supply of air into the spoil, therefore it is not prone to heating. Further, Taylor concluded that compaction in accordance with clause 609 of the Ministry of Transport's Specification relating to earth works has shown that previous fears about spontaneous heating were based on the behaviour of loose tipped materials. It implies that proper compaction can avoid the risk of spontaneous combustion.

Another factor which affects the suitability of minestone is the degradation due to chemical and physical weathering or due to compaction. Considering breakdown due to compaction Rainbow (1982) compared the particle size distribution before and after compaction and reported that although considerable degradation results from the compactive forces the final grading continues to fall within the specified grading envelope. For degradation due to weathering, it is generally considered that little chemical disintegration occurs on the surface whereas physical disintegration is at its peak at the surface. However, the evidence from old, initially loose, unburnt spoil heaps implies that intense weathering is limited to depths of about one metre (Taylor 1978).

The chemical properties of minestones make them corrosive to metallic reinforcement. However, with the development of non-metallic reinforcement, this problem can be readily solved.

In addition to the above factors, frictional resistance is one of the most fundamentally important aspects when considering the potential use of minestone for reinforced earth. The shear strength of the two minestones used in the present investigation were obtained from large shear box tests at their natural moisture content and field compaction conditions. As shown in table 3.1b (Chapter 3), both behaved as  $c-\phi$  soils. For Wardley minestone  $\phi = 33^\circ$  and  $c = 15 \text{ kN/m}^2$ , and for Wearmouth minestone  $\phi = 37^\circ$  and  $c = 11 \text{ kN/m}^2$ .

Comparing the mechanical characteristics of the fill materials used in the present work, it was found that the red shale produced the highest shear resistance, with the minestones being superior to the PFA and Loudon Hill sand. When considering the bond resistance between these fill materials and the reinforcements, difficulties are encountered in making a conclusion of superiority. Among the two minestones, Loudon Hill sand and Methil PFA, results are quite varied according to the type of reinforcement and the test method. However, Horden red shale proved to be superior to the others with all types of reinforcement in all the tests. For the two Paralink reinforcements with the minestones, the PFA and the sand, results from the field pull-out tests were scattered in the same range. Shear box tests also produced close results. These have shown that when Paralink straps are used the bond resistance with the minestones is as good as with the sand and the PFA. However, the laboratory pull-out test results showed a lower value with the minestones.

It is obviously attractive to make use of minestone both from an economic and an environmental point of view. Reinforced earth has been recognised as one of the new ways in which minestone could be used (Rainbow 1980), and it has actually been accepted in some countries, e.g. Belgium and France (Rainbow 1987). In Belgium over 50 reinforced minestone highway structures have been built. In the U.K. efforts have been made by British Coal to prove the suitability of minestones as backfill in reinforced earth construction. As part of the investigations, British Coal have built reinforced minestone retaining walls in lieu of conventional reinforced concrete retaining walls. These structures have been in operation for a number of

years without any sign of distress (Rainbow 1984 (2)). The reinforced elements employed in these structures include Paraweb, Tensar, Fibretain and high adherence galvanized mild steel. Hopefully minestones as fill materials will be accepted by the new code in the U.K. However, the properties of minestones vary from different collieries, therefore care should be taken to select the minestones which are most suitable.

### 9.2.3 Characteristics of Bond Resistance

The bond (or frictional) resistance mobilized at the fill–reinforcement interface is the essential phenomenon in the mechanism of reinforced earth, and it is also of major importance in reinforced earth structure design. However, this mechanism is quite complex, varies with different reinforcing or fill materials and is influenced by a number of factors such as overburden pressure, density, moisture content, reinforcement length and testing method. Lee (1978) described it as the most critical and least understood aspect of reinforced earth. This topic has attracted numerous studies in several countries over the last two decades. However, it is quite complex in character, and although significant research work has been carried out, it is not yet fully understood. On the other hand, with new reinforcements and fill materials being introduced, investigations about this characteristic are still required.

Investigations into the bond resistance of the fill and reinforcing materials provided in the present work have been carried out. The results obtained have been described and discussed in the previous chapters. These discussions are summarized in this section.

#### i) Influence of overburden pressure on friction coefficient

The influence of overburden pressure on apparent friction coefficient has been found from pull–out tests by previous investigators (Schlosser and Elias 1978). The apparent friction coefficient decreases with increase in overburden pressure. The

results from the present work agree with this conclusion. McKittrick (1978) and Guilloux et al (1979) analysed pull-out tests and believed that there exists an influence of dilatancy in pull-out tests. This dilatancy occurs in a comparatively small zone in the immediate vicinity of the reinforcing strap. Arching occurs across the strip by which the ambient backfill suppresses the volumetric expansion normally associated with dilatancy. This suppressed dilatancy results in locally enhanced vertical stress which gives rise to an increased pull-out resistance. At low overburden pressure the influence of the enhanced pressure is relatively large compared with the overburden pressure, thus making the apparent friction coefficient quite high, but when the overburden pressure is high, the enhanced vertical stress caused by dilatancy will be relatively small compared with the overburden pressure, hence its influence becomes small, as does the friction coefficient. This phenomenon of enhanced pressure is also proved in the present research when pressure cells were used with a ribbed steel strap in a pull-out test (Chapter 6). It was found that the pressure imposed on the strap increased during a pull-out test. In addition to the discussion above, it is believed that there is also another factor which enhances the vertical stress. When the fill material is compacted, some stress may be locked in the fill. If the fill materials behave like a  $c-\phi$  soil, this can be more apparent. This locked-in-stress will also impose an enhanced vertical stress on the reinforcement. This can also be proved by the results from the shear box tests (see table 4.7 in Chapter 4). The friction coefficient ( $\mu$ ) obtained from the shear box tests also decreases with increase in normal stress, due to the existence of the cohesion ( $c_f$ ) at the interface of the fill-reinforcement.

#### ii) Influence of density on friction coefficient

Density has been found to be one of the factors which affects the value of friction coefficient. Previous researchers (Alimi and Bacot 1977, Schlosser and Elias 1978) discovered after a series of pull-out tests with ribbed steel and bronze straps that the influence of density is significant, the friction coefficient increasing with

increase in density. Further Khattri (1982) reported that dense soil yielded higher values of apparent friction coefficient than loose soil from both shear box and pull-out tests with ribbed steel. With density variation along the length of the strip, the pull-out force is found to decrease with decrease in density. However, some contrary results were also reported, e.g. in full-scale pull-out tests with galvanized steel strip, Bacot and Iltis (1978) found that the apparent friction coefficient was smaller in a compacted fill than a non-compacted fill. Lee (1978) concluded that density has no influence on the value of angle of skin friction after carrying out shear box tests with aluminium foil.

The results from the present work are consistent with Alimi and Bacot, i.e. the friction coefficient increases with increase in density. This conclusion is proved from both shear box and pull-out tests and by using all the reinforcing and fill materials provided in the present work. The influence of density is more significant in the case of ribbed steel.

To explain the influence of density on the friction coefficient, the relation between strength and dilatancy of soils need to be introduced. Dilatancy will occur when a shearing force is imposed on a soil in a dense state, and the denser the soil, the more dilatancy will happen. A great deal of attention has been paid to the relation between strength and dilatancy in the 1960s. Rowe (1962) established a stress-dilatancy relation for plane strain:

$$\frac{\sigma'_1}{\sigma'_3} = \left( \frac{\sigma'_1}{\sigma'_3} \right)_{crit} \left( 1 - \frac{d\epsilon_v}{d\epsilon_1} \right) \quad (9.1)$$

in which  $\epsilon_v$  — the volumetric strain (positive in compression),

$\epsilon_1$  — the major principal strain,

the subscript (crit) represents the critical state.

The mechanical significance of the angle of dilation in plane strain deformation can be shown in the case of direct shear (see *Figure 9.1*). If rigid blocks of non-failure soil are assumed to bound the thin uniformly straining rupture zone ZZ, this must mean that for compatibility ZZ must be a zero extension line so that

$$d\epsilon_z = 0 \quad (9.2)$$

within the rupture zone. Also

$$d\gamma_{yz} = \frac{dz}{Y} \quad (9.3)$$

$$d\epsilon_y = -\frac{dy}{Y} \quad (9.4)$$

so in Figure (c)

$$\tan\psi = -\frac{d\epsilon_y}{d\gamma_{yz}} = \frac{dy}{dz} \quad (9.5)$$

where  $\gamma_{yz}$  — the shear strain,

$\epsilon_y$  — strain vertical to the shearing force,

$Y$  — the thickness of the soil,

$dy$  — the displacement vertical to the shearing force,

$dz$  — the displacement parallel to the shearing,

$\psi$  — the angle of dilation in plane shear.

Suppose that  $\varphi'_{\text{crit}}$  is the angle of shearing observed in a simple shear test on soil loose enough to be in a critical state, with zero dilation. Bolton (1986) introduced a saw blades model of dilatancy (see *Figure 9.2*). When the same soil is tested in dense, the overriding at points of contact must occur unless the particles crush. Suppose that the particles above the overall zero-extension line  $ZZ$  form one rigid zone sliding upwards at  $\psi$  over the rigid zone beneath, in accordance with the external observation of a dilatancy angle  $\psi$ . Assume that the angle of shearing developed on the inclined microfaces  $SS$ , on which there is zero dilation, remains at  $\varphi'_{\text{crit}}$ . Since all the sliding now takes place on surfaces parallel to  $SS$  it is permissible to view the observed angle of shearing  $\varphi'$  on the rupture surface as comprising the two components  $\varphi'_{\text{crit}}$  and  $\psi$  as shown in *Figure (9.2)*. This specifies

$$\varphi' = \varphi'_{\text{crit}} + \psi \quad (9.6)$$

Comparing equation (9.6) with (9.1), an overestimate by 20% was found by Bolton, then the  $\psi$  is modified by 0.8 and a good agreement was met (Bolton 1986). Therefore (9.6) becomes:

$$\varphi' = \varphi'_{\text{crit}} + 0.8\psi \quad (9.7)$$

This theory may also be applied to the present shear box tests for the fill–reinforcement bond resistance. An example can be made by taking the results of ribbed steel tested with Loudon Hill sand at two different density states ( $\gamma_1 = 17.63 \text{ kN/m}^3$  and  $\gamma_2 = 16.19 \text{ kN/m}^3$ ), and at the overburden pressure of  $60 \text{ kN/m}^2$ . From the tests the vertical movement ( $dy$ ) and the shearing displacement ( $dz$ ) were measured to be 2.9mm and 9.6mm for  $\gamma_1$ , and 1.3mm and 6.3mm for  $\gamma_2$  respectively. According to equation (9.5), the  $\psi_1$  and  $\psi_2$  for  $\gamma_1$  and  $\gamma_2$  were calculated to be  $16.8^\circ$  and  $11.6^\circ$  respectively. Instead of  $\varphi$ ,  $\delta$  is used here to designate the shearing angle between the soil and reinforcement.

The  $\delta'_{\text{crit}}$  (at very loose state) was not obtained, however from equation (9.7)

$$\delta'_1 = \delta'_{\text{crit}} + 0.8\psi_1 \quad (9.8)$$

$$\delta'_2 = \delta'_{\text{crit}} + 0.8\psi_2 \quad (9.9)$$

$$\text{therefore } (\delta'_1 - \delta'_2) = 0.8 (\psi_1 - \psi_2) \quad (9.10)$$

Substituting  $16.8^\circ$  and  $11.6^\circ$  into  $\psi_1$  and  $\psi_2$  respectively, then  $(\delta'_1 - \delta'_2)$  was found to be  $4.2^\circ$ . The results produced from the tests were  $\delta_1 = 34^\circ$  and  $\delta_2 = 30.3^\circ$ , thus  $\delta_1 - \delta_2 = 3.7^\circ$ . The comparison can be made if ignoring the difference

caused by the moisture content (i.e. at the effective stress), and results obtained from the tests and calculations are reasonably good.

In a pull-out test, when the pulling force is applied to the strap, it will also cause the potential of dilatancy. However, in this case rather than changing the volume of the soil, the dilatancy potential is transferred to an enhanced pressure, which can be quite significant. The results from the present pull-out test with pressure cells have proved this, i.e. the normal stress was found to increase during the pulling action. Therefore the denser the soil is the higher enhanced pressure can be produced, and in consequence a higher pull-out resistance is obtained.

A point discovered with the pull-out tests is that the magnitude of the influence of density on the apparent friction coefficient is also related to the overburden pressure ( $\sigma_v$ ). When  $\sigma_v$  is low the influence of density is significant, whereas with increasing  $\sigma_v$ , the effect of density becomes less, and some low values of  $f^*$  are encountered even from higher densities which agrees with the results from Bacot and Iltis. The reason for this has been explained in Chapter 5. It is similar to that discussed on the influence of overburden pressure.

After compaction a dense state is established, and the locked-in-stress and the dilatancy effect in the dense state act to give an enhanced normal stress. The denser the fill material is compacted, the higher the enhanced normal stress can be achieved, in turn high pull-out resistance can be produced, therefore higher apparent friction coefficient can be obtained. When the overburden pressure is low, as discussed previously, the enhanced normal stress is relatively high compared to the pressure, thus the effect of this stress appears significant. But with the increase in  $\sigma_v$ , the enhanced stress becomes relatively less compared to the pressure, therefore the influence of this stress becomes less. On the other hand, the prepared loose density state can only be kept under a low overburden pressure, since when the pressure is high, it compresses the fill material to a denser state which is probably close to a compacted higher density. Therefore the influence caused by the difference in prepared density becomes very small. Another factor which may lead to higher  $f^*$  values in material of low density with high overburden pressure is the

susceptibility of minestone to breakdown during compaction when the sharp edges of the stones may be abraded, leading to a reduction in friction.

The influence of density on the friction coefficient is different depending on the reinforcing and fill materials. The test results agree with the conclusion drawn by Khattri (1982) that the friction between soil-ribbed strip is much influenced by density, but in the case of soil-smooth strip, density has very little influence. The present work also shows that fill-ribbed steel is more influenced by density than fill-Paralink, because the existence of the protruding ribs can cause more dilatancy in the dense state. With the ribbed steel test, it is more likely that shear occurs within the fill rather than between the fill and the reinforcement, and thus an increase in density can increase the internal shear resistance of the fill, and hence increase the friction resistance.

### iii) Influence of reinforcement extensibility and

#### Compressibility on Apparent Friction Coefficient

Extensibility and compressibility of reinforcement have been found to affect the apparent friction coefficient from a pull-out test. Due to the elongation of an extensible strap, the displacements at different points along a strap were observed not to be uniform, but differential during the pulling. This behaviour is different from a rigid strap where all points move at the same time. It was also noticed that in most of the tests the free end of a strap did not move until the maximum pull-out force was produced. Therefore it can be understood that in the case of extensible strap testing, where the peak frictional resistance did not occur simultaneously at every point along the strap, due to the differential movement in the front part of the strap (near the pulling end) which had larger displacement, most likely the residual post-peak force was produced, and near the free end only a small force was generated at failure because of small displacements. Hence the extensibility of a strap causes a reduction of a pull-out force and in turn leads to a lower apparent friction coefficient. This discussion was proved by testing the Paralink

"sandwich" straps. Comparing a Paralink strap and a rigid "sandwich" strap, different patterns of force–displacement curves were encountered, i.e. the Paralink strap yielded a much larger displacement than the "sandwich" strap to achieve the ultimate pull–out force. In addition to this a higher friction coefficient was obtained from the "sandwich" strap than from the Paralink strap.

Besides, as has been discussed in chapter 6, the compressibility of Paralink straps under normal stress is also regarded as a factor which causes a lower pull–out test result. Because of the compressibility when overburden pressure is imposed, the strap yields, and leads to an arching effect which transfers the normal stress from the strap to the adjacent soil. As a result of this, the normal stress acting on the strap is reduced and in turn a lower pull–out force is produced.

iv) Influence of strap length on apparent friction coefficient

The influence of strap length has been reported by some previous researchers, e.g. Bacot and Iltis (1978) who showed that when galvanized steel strip was tested with sand, the friction coefficient increased with increase in strip length. In the present work, a few tests with various lengths of Paralink straps were carried out with Loudon Hill sand in laboratory pull–out tests. The same conclusion was drawn as Bacot and Iltis, i.e. higher values of  $f^*$  were obtained from longer straps. However, the results from field tests varied widely, and both increase and decrease of apparent friction coefficients were encountered with increasing strap length.

To explain the increase of apparent friction coefficient with strap length, one reason might be the influence of undulation of the reinforcement. The longer the strap is, the more it is prone to undulation, thus a higher pull–out force is produced because of the higher resistance caused by the undulations. But for the Paralink straps, one more point to be considered is the extensibility. As mentioned previously, the extensibility can reduce the friction resistance, and one of the reasons given was the reduction of the cross section of the strap during pulling. The higher pull–out force can lead to a greater more reduction in the cross section. With the increase in the strap length, more undulation occurs, but at the same time, a longer

strap produces a larger pull-out force which causes more reduction in the cross section of the strap. Therefore both factors may be offsetting each other. In the field tests, the nonuniformity of compaction may produce more influence on the friction coefficient compared with the strap length. Hence, uncertain results are produced. It can be seen that the influence of the strap length is a rather complex point, especially when extensible straps are used.

v) Influence of moisture content on bond resistance

A few tests were carried out with varying moisture content using the shear box apparatus. These were conducted with Paralink 500s and Wardley minestone materials. Some slightly reduction of shear resistance was observed with increase in moisture content. On the other hand, the displacement at the maximum shear stress was found to be larger with higher moisture content. It is believed that a higher moisture content can cause softening of the fill material, which can lead to larger displacement in the shear box test. The reduction of the shear resistance can probably be attributed to more moisture existing on the interface of the fill-reinforcement causing a reduction in the friction resistance.

vi) Influence of the facing plate in pull-out tests

Khatti investigated this influence using tests with ribbed steel strap and sand. He found the strip-with-facing plate pull-out testing method yielded lower values of apparent angle of skin friction by  $3.5^\circ$  and  $4^\circ$  in the case of dense and loose soil respectively than those from the strip pull-out testing method. The present tests with Paralink 500s straps and the two minestones show results consistent with Khattri, i.e. lower results were obtained from the tests with facing plate. In addition it was found that when the overburden pressure was high the differences became very small. When pulling a strap through a slot, the resistance of the rigid facing plate will develop a high lateral pressure which, in turn, enhances the vertical pressure on the

strap, causing a higher pull-out force (or a higher apparent friction coefficient). As discussed previously, the enhanced pressure has a larger influence when the overburden pressure is low, but when the overburden pressure is high this influence becomes less.

### 9.3 CONCLUSIONS

The conclusions drawn from the present work are summarized.

1. Comparing the three types of reinforcements, the ribbed steel strap produces the highest bond resistance, with Paralink 500s being superior to Paralink 300s, no matter which fill material or which test method is used.
2. Comparing the five different fill materials, Horden red shale is the most efficient material in producing a high bond resistance, but the efficiency of the other materials, i.e. Wardley minestone, Wearmouth minestone, Loudon Hill sand and Methil PFA, varies with the type of reinforcement and test method.
3. Comparing the three different test methods, no matter which reinforcing and fill material is used, the field full-scale pull-out tests produce the lowest value of bond resistance. The results from the two tests, laboratory pull-out and shear box, vary with different reinforcing and fill materials. When ribbed steel is used, the laboratory pull-out tests produce higher results than the shear box tests. On the contrary, if the extensible Paralink straps are used, lower results are produced more by the laboratory pull-out tests than the shear box tests. However, when the PFA fill material is used, the difference between the two different test methods, laboratory pull-out and shear box, is very small. For investigating the bond resistance of extensible reinforcements, pull-out tests appear to be more suitable than shear box tests.

4. No matter which reinforcing and fill material is used, the maximum pull-out force increases with increasing overburden pressure. On the other hand, the friction coefficient ( $f^*$  or  $\mu$ ) decreases with increase in overburden pressure. This is found from all three different test methods. However, from pull-out tests, this decrease is found to be modest when the overburden pressure is high. It can be seen that after 60 to 100 kN/m<sup>2</sup> of  $\sigma_v$ , the value of  $f^*$  becomes almost constant.

5. Density is a factor which influences the results of bond resistance between any of the three reinforcements and the fill materials (except the PFA). The higher the density, the higher the bond resistance is obtained. This is found from both laboratory pull-out and shear box tests. However, in pull-out tests the influence of density is related to the overburden pressure, when  $\sigma_v$  is low this influence is considerable, otherwise when  $\sigma_v$  is high this influence can be negligible. For ribbed steel strap, the influence of density is more significant.

6. The influence of moisture content is found in the case of Wardley minestone with Paralink 500s from shear box tests. Some reduction of bond resistance is caused by increasing moisture content. Moreover, greater displacement is required to achieve ultimate shear stress when moisture content increases.

7. From shear box tests, the internal shear resistance from soil alone is always higher than the bond resistance, no matter which fill material and what type of reinforcement is used.

8. Cohesion ( $c_r$ ) is found to be an important part of the bond resistance, especially when minestone is used as fill material. Therefore its contribution should be taken into account for design.

9. In the curve of shear stress versus displacement from shear box tests, no peak appeared for the ribbed steel, whereas peaks can be found for the Paralink

elements.

10. From shear box tests, in the case of ribbed steel there may exist a direct relation between the internal shear resistance and the bond resistance. The ratios of  $\tan \delta / \tan \varphi$  and  $c_r / c$  are both around 0.9. However, in the case of Paralink straps this relation does not exist, the ratios of  $\tan \delta / \tan \varphi$  and  $c_r / c$  vary according to the different fill materials.

11. The pull-out stiffness shown by the force-displacement curve with Paralink straps is influenced by the overburden pressure, and  $E_p$  increases with increasing  $\sigma_v$ . The relationship between  $E_p$  and  $\sigma_v$  is about linear. Pull-out stiffness is independent of strap length.

12. Pull-out test with "piano wire" monitoring is a readily available method to investigate the behaviour of a Paralink strap in pulling action. Until a more suitable technique of measuring the strain distribution along a Paralink strap is found, the measurement with "piano wire" can be used to determine the strain distribution in a pull-out test.

13. Due to the extensible characteristics of the Paralink straps, their performance in a pull-out test is different from a rigid steel strap. For a rigid strap once the pulling force is imposed, the whole strap, from the "clamped" end to the free end, will move simultaneously. In the case of a Paralink strap, the movement (or extension) is mobilized from the "clamped" end incrementally towards the free end, until eventually the free end starts moving, and bond failure occurs. This also implies that the stress in the strap generated by the pulling force is also transmitted from the "clamped" end towards the free end.

14. The extensibility of a strap affects the pull-out force displacement response, a larger displacement being required for an extensible strap to achieve the ultimate

pull-out force compared to a rigid strap. In addition to this, the apparent friction coefficient is also affected by the extensibility, and a lower value of  $f^*$  is obtained from an extensible strap than from a rigid strap.

15. Arching effect plays an important part in a pull-out test, but this effect acts differently with the ribbed steel and Paralink straps. In the case of a ribbed steel strap, arching effect is due to the soil dilatancy and it causes a transfer of normal stress on the strap during pulling. Whereas with a Paralink strap, because of its compressibility, the arching effect is mainly caused by the yield of the strap under the overburden pressure and this leads to a transfer of normal stress from the strap onto the adjacent fill. Results from the tests with pressure cells show that when a ribbed steel strap is tested with Loudon Hill sand, the normal stress acting on the strap increases during the pulling action.

16. With the two minestones and the Paralink strap tests, a lower value of  $f^*$  is produced from the pull-out with facing than through a slot. When  $\sigma_v$  is low the influence of facing resistance is apparent, when  $\sigma_v$  is high this influence does not appear.

17. Pull-out tests with load and displacement controlled systems produce very similar results.

#### 9.4 SUGGESTIONS FOR FUTURE STUDY

The following recommendations are made for future study:

1. Further investigation of the influence of reinforcement extensibility. The reason for the reduction in bond resistance with an extensible reinforcement still needs to be investigated. Pull-out tests with reinforcement of various stiffnesses but with the same surface and vertical compressibility may indicate the relationship between the

stiffness and the apparent friction coefficient.

2. Further investigation of the effect of dilatancy by means of a strap with pressure cells pull-out tests. Both ribbed and smooth steel strap can be used for tests with various fill materials at different overburden pressures and various densities. A strap possessing different vertical compressibility, but the same longitudinal stiffness and equivalent surface can be tested with various fill materials in a pull-out box. A comparison between the results obtained with this strap and these from shear box tests may indicate the relationship between normal stress ( $\sigma_v$ ) and the strap compressibility in pull-out tests.

3. Investigation of the influence of moisture content from pull-out tests as well as shear box tests.

4. Investigation of the long-term bond resistance characteristics between fill and Paralink reinforcement. Load-controlled pull-out box can be used for this purpose, a constant load can be applied and displacement with time observed at this load. Tests can be carried out with various materials at different conditions, such as different overburden pressures and different densities.

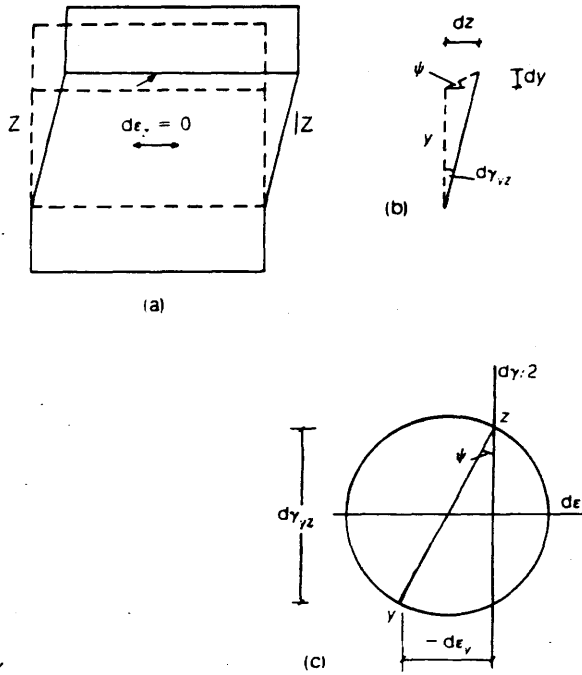


**Figure 9.1 ANGLE OF DILATION  $\psi$  IN PLANE SHEAR**  
 (After Bolton)

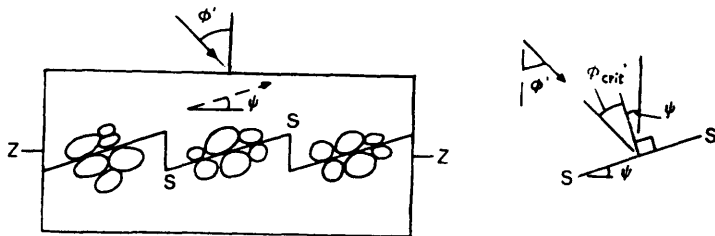


**Figure 9.2 THE SAW BLADES MODEL OF DILATANCY**  
 (After Bolton)

## REFERENCES

AL-HUSSAINI M. & PERRY E. B. 1978

"Analysis of a Rubber Membrane Strip Reinforced Earth Wall". Proc. Symp. Soil Reinforcing & Stabilising Techniques NSW. Inst. of Technology. 59 – 72.

ALIMI I., BACOT J., LAREAL P., LONG N. T. & SCHLOSSER F. 1977

"Adherence between Soil and Reinforcement insitu and in the Laboratory". Proc. IXth I.C.S.M.F.E. Vol.1. 11 – 14.

AL-YASSIN Z. & HERMANN L.R. 1977

"Finite Element Analysis of Reinforced Earth Walls". T.R.R.L./Heriot Watt Univ. Proc. Symp. Reinforced Earth, Edinburgh. 3 – 10.

BACOT J., ILTIS M., LAREAL P., PAUMIER T. & SANGLEREAT G. 1978

"Study of the Soil Reinforcement Friction Coefficient". Proc. ASCE Symp. Earth Reinforcement, Pittsburgh. 157 – 185.

BASSETT R.H. & LAST N.C. 1978

"Reinforcing Earth below Footings and Embankments". Proc. ASCE Symp. Earth Reinforcement, Pittsburg. 881 – 885.

BEATON J. L., FORSYTH R. A. & CHANG J. C. 1974

"Design and Field Behaviour of the Reinforced Earth Embankment Road 39". Report of California Dept. of Transportation, Div. of Highways.

BLIGHT G.E. & DANE M.S.W. 1989

"Deterioration of a Wall Complex Constructed of Reinforced Earth". Geotechnique 39, No. 1, 47–53.

BLIVET J.C. & GESTIN F. 1979

"Adherence de deux Geotextiles sur un Residu Fin, le Phosphogypse". Proc. Int. Conf. Soil Reinforcement, Paris. Vol.2. 403 – 408.

BOLTON M.D., CHOUDHURY S.P. & PANG P.L.R. 1977

"Modelling Reinforced Earth". T.R.R.L./Heriot Watt Univ. Proc. Symp. on Reinforced Earth, Edinburgh. 22 – 29.

BOLTON M.D., CHOUDHURY S.P. & PANG P.L.R. 1978

"Modelling Reinforced Earth". Ground Engineering, Vol.11, No.6. 19 – 24.

BOLTON M.D. 1986

"The Strength and Dilatancy of Sands". Geotechnique 36, No.1, 65–78.

BRADY K. 1986

"Reinforced and Anchored Earth". Report of a Meeting organised by the British Geotechnical Society Held at the Institution of Civil Engineers, Westminster, London. Ground Engineering Oct. 1986.

BROMS BENGT B. 1988

"Fabric Reinforced Retaining Wall". Int. Geotech. Symp. on Theory and Practice of Earth Reinforcement. Fukuoka, Japan. 3 – 31.

BS 1377:1975

"Methods of Testing for Soils for Civil Engineering Purposes". British Standards Institution.

CHANDRASEKARAN B. 1988

"An Experimental Evaluation of Fabric Strength Properties and Behaviour of Fabric Reinforced Soil". Master of Engrg. thesis. National Univ. of Singapore.

CHANG J. C., FORSYTH R. A. & SMITH T. 1972

"Reinforced Earth Highway Embankment Road 39". Highway Focus, Vol.4. No.1.

CHANG J. C. 1974

"Earthwork Reinforcement Techniques". California Dept. of Transportation, Transport Lab. Res. Rept. February.

CHANG J. C., DURR D. L. & FORSYTH R. A. 1974

"Earthwork Reinforcement Techniques". California Dept. of Transportation, Transport Lab. Res. Rept. February.

CHANG J.C., HANNON J.B. & FORSYTH R.A. 1977a

"Pull Resistance and Interaction of Earthwork Reinforcement and Soil". Presentation to 56th Annual Meeting Transp. Res. Board. Jan.

CHANG J.C., HANNON J.B. & FORSYTH R.A. 1977b

"Pull Resistance and Interaction of Earthwork Reinforcement and Soil". Transp.

CHAPUIS R. 1977

"Stabilite Interne des Murs en Terre Armee". Canadian Geot. Jnl. Vol.14.  
No.3. 389 – 398.

COYNE M.A. 1927

"Murs de Soutenenment et Murs de Quai a Echelle". Le Genie Civil, Thom  
XCI. October.

COYNE M.A. 1929

French Patent Specification No.656,692.

DEPARTMENT OF TRANSPORT 1977

"Reinforced Earth Retaining Walls for Embankment Including Abutments, Tech.  
Mem. BE (Interim), Dept. of Environment, Highways Directorate.

DEPARTMENT OF TRANSPORT 1978

"Reinforced Earth Retaining Walls and Bridge Abutments for Embankments".  
Tech. Memo. (Bridges) BE3/78.

DYER 1985

"Observation of the Stress Distribution in Crushed Glass with Applications to  
Soil Reinforcement". D.Phil. Thesis, University of Oxford.

FABIAN K.J. & FOURIE A.B. 1988

"Clay Geotextile Interaction in In-Soil Tensile Tests". Proc. Int. Geot. Symp.  
on Theory and Practice of Earth Reinforcement. Fucuoka Japan. 81 – 86.

FINLAY T. W. 1978

"Performance of a Reinforced Earth Structure at Granton". Ground Engineering,  
2, No.7, 42 – 44.

FINLAY T.W. & SUTHERLAND H.B. 1979

"Field Measurements on a Reinforced Earth Wall at Granton". Proc. 9th  
I.C.S.M.F.E. Vol.11.

FINLAY T.W., KHATTRI M.S. & SUTHERLAND H.B. 1984.

"The Friction Coefficient of Metallic Strip Reinforcement". Proc. 6th Conf. Soil  
Mech. and Found. Eng. Budapest. 619 – 624.

FINLAY T.W., WEI M.J. & HYTIRIS N. 1988

"Friction Characteristics of Polypropylene Straps in Reinforced Minestone". Proc. Int. Geotechnical Symp. Theory and Practice of Earth Reinforcement, Japan. 87-92.

FOURIE A.B. & FABIAN K.J. 1987

"Laboratory Determination of Clay-Geotextile Interaction". Geotextiles and Geomembranes. No.6. 275 - 294.

GUILLOUX A., SCHLOSSER F. & LONG N.T. 1979

"Etude du Frottement Sable-Armature en Laboratoire". Proc. Int. Conf. Soil Reinforcement, Paris. Vol.1. 35 - 40.

HANNA T.W. 1977

"Reinforced Earth". Informational Discussion I.C.E.

HARKER R.J. 1986

"Elastic Energy Methods of Design Analysis". New York, Oxford.

HAUSMANN M.R. 1976

"Strength of Reinforced Soil". Proc. 8th Australian Road Resh. Conf. Vol.8. Sect. 13. 1 - 8.

HOLTZ R.D. 1977

"Laboratory Studies of Reinforced Earth Using a Woven Polyester Fabric". Proc. Int. Conf. Fabrics in Geotechnics. Vol.3. 149 - 154.

HOSHIYA M. 1978

"Strength of Reinforced Earth Retaining Walls". Proc. ASCE Symp. Earth Reinforcement, Pittsburg. 459 - 472.

INGOLD T.S. & TEMPLEMAN J.E. 1979

"The Comparative Performance of Polymer Net Reinforcement". Proc. Int. Conf. on Soil Reinforcement, Paris, Vol.1. 65 - 70.

INGOLD T.S. 1980

"Reinforced Clay". Thesis of Ph.D. University of Surrey.

INGOLD T.S. 1981

"A Laboratory Simulation of Reinforced Clay Walls". Geotechnique 31, No.3.

INGOLD T.S. 1982

"Reinforced Earth". Thoams Telford Ltd., London.

JAKY J. 1944

"The Coefficient of Earth Pressure at Rest". J. Soc. Hungarian Architects and Engineers 78(22).

JEWELL R.A. 1980.

"Some Effects of Reinforcement on the Mechanical Behaviour of Soils". Ph.D. Thesis, University of Cambridge.

JEWELL R.A. & JONE C.J.F.P. 1981

"Reinforcement of Clay Soils and Waste Materials Using Grids". XICSMFE, Stockholm. 3, 701.

JONES C.J.F.P. 1984

"The Use of Ash in Reinforced Earth". Proc. 2nd Int. Conf. on the Use of PFA. London.

JONES C.J.F.P. 1985

"Earth Reinforcement and Soil Structures". Butterworths Advanced Series in Geotechnical Engineering.

JONES C.J.F.P. 1989

JONES G.A. & SMITH A.C.S. 1977

"Design, Construction and Monitoring of a Reinforced Earth Wall for Reconstruction of a Highway Slope Failure". T.R.R.L./Heriot Watt Univ. Proc. Symp. Reinforced Earth, Edinbugh. 551 – 556.

KHATTRI M.S. 1982

"Study of the Soil-Reinforcement Friction Coefficient". Thesis of M.Sc. Glosgow University.

KNIGHT P.G.K. 1979

"The Engineering Use of P.F.A.", Proc. Symp. on The Engineering Behaviour of Industrial and Urban Fill, Univ. of Birmingham. D63.

KUTARA K., AOYAMA N., YASUMAGA H. & KATO T. 1988.

"Long Term Pull-out Tests of Polymergrids in Sand". Proc. Int. Geotechnical Symp. Theory and Practice of Earth Reinforcement, Japan. 117 – 122.

LEE K.L. 1973

"Reinforced Earth Retaining Walls". Jrnl. S.M.F.E. Div. Proc. ASCE Vol.99. No.SM10. 745 –746. Discussion Vol.100, No.GT8. 958 – 966.

LEE K.L. 1978

"Mechanisms, Analysis and Design of Reinforced Earth, State of the Art Report". Proc. ASCE Symp. Earth Reinforcement, Pittsburg. 62 – 76.

MAKIZUCHI K. & MIYAMORI T. 1988

"Mobilization of Soil-Geofabric Interface friction". Proc. Int. Geotechnical Symp. Theory and Practice of Earth Reinforcement. 129 – 134.

MALLINDER F.P. 1977

"The Use of F.R.P. as Reinforcing Elements in Reinforced Soil Systems". T.R.R.L./Heriot-Watt Univ. Proc. Symp. Reinforced Earth, Edinburgh. 262 – 275.

McGOWN A., ANDRAWES K.Z. & AL-HASANI M. M. 1978

"Effects of Inclusion Properties on the Behaviour of Sand". Geot. 3. 327 –346.

McGOWN A., ANDRAWES K.Z. & KABIR M.H. 1982

"Load Extension Testing of Geotextiles Confined in Sand". Proc. 2nd Int. Conf. on Geotextile, 793 – 798.

McGOWN A., ANDRAWES K.Z. & YEO K.C. 1984

"The Load-Strain-Time Behaviour of Tensar Geogrids". Proc. Symp. on Poly Grid Reinforcement, ICE, London, Paper 1.2.

McKITTRICK D. 1978

"Reinforced Earth — Application of Theory and Research to Practice". Proc. Symp. Soil Reinforcing and Stabilising Techniques, NSW Inst. of Technology. 1 – 44 (Supplementary Volume).

McKITTRICK D. P. & DARBIN M. 1979

"World-Wide Development and Use of Reinforced Earth Structures". Ground Engineering, Vol.12 No.2. 15 – 21.

MITCHELL J.K. & SCHLOSSER F. 1979

"General Report", Proc. Int. Conf. Soil Reinforcement, Paris. Vol.3. 25 – 62.

MIYAMORI T., IWAI S. & MAIUCHI K. 1986

"Frictional Characteristics of Non-Woven Fabrics. Proc. 3rd Int. Conf. on Geotextiles, Vienna, Austris, Vol.3 701 – 705.

MUNSTER A. 1930

United States Patent Specification. No.1762343.

MURRAY & BODEN 1979

"Reinforced Earth Wall Constructed with Cohesive Fill". Proc. Int. Conf. on Soil Reinforcement. Paris, Vol.2, 569 –577

MYLES B. 1982

"Assessment of Soil Fabric Friction by Means of Shear". Proc. 2nd Int. Conf. on Geotextiles, Las Vegas, Nevada, Vol.3. 787 – 792.

NATIONAL COAL BOAD 1971

"Application of British Standard 1377:1967 to the Testing of Colliery Spoil". Technical Memorandum Issued on Soil Mechanics Testing by the Joint Working Party.

OSMAN M.A. 1977

"An Analytical and Experimental Study of Reinforced Earth Retaining Walls". Ph.D. Thesis, Glasgow University.

PALMEIRA E.M. 1987

"The Study of Soil Reinforcement Interaction by Means of Large Scale Laboratory Tests". DPhil. thesis, University of Oxford.

PALMEIRA E.M. & MILLIGAN G.W.E. 1989

"Scale and Other Factors Affecting the Results of Pull-out Tests of Grids Buried in Sand". Geotechnique, Vol.39, No.3. 511 – 524.

PASELY 1822

"Experiments on Revetments". Vol.2, Murray J, London.

POTYONDY J.G. 1961

"Skin Friction Between Various Soils and Construction Materials". *Geotechnique*, Vol.11. 339 – 353.

PRICE D.I. 1975

"Aspects of Reinforced Earth in the U.K.". *Ground Engineering*, March.

RAINBOW A.K.M. 1983

"An Investigation of Some Factors Influencing the Suitability of Minestone as the Fill in Reinforced Earth Structures". Ph.D. Thesis. National Coal Board, London.

RAINBOW A.K.M. 1984 a

"Research into Reinforced Minestone in United Kingdom". Symp. on the Reclamation. Treatment and Utilisation of Coal Mining Wastes, Durham, England. 7.1 – 7.12.

RAINBOW A.K.M. 1984 b

"Pull-out Tests Using Purpose Built Equipment". Symposium on the Reclamation. Treatment and Utilisation of Coal Mining Wastes, Durham, England. 8.1 – 8.15.

RAINBOW A.K.M. 1984 c

"Shear Strength of Minestone Under Low Normal Stress in Large Shear Box (Applied to Reinforced Minestone)". Sym. on the Reclamation. Treatment and Utilisation of Coal Mining Wastes. Durham, England. 36.1 – 36.8.

RAINBOW A.K.M. 1987

"Minestone Fill in Reinforced Earth Abutments". *Highway and Transportation*. June 1987. Vol.34. No.6. 25 – 31.

ROWE P.W. 1962

"The Stress–Dilatancy Relation for Static Equilibrium of an Assembly of Particles in Contact". *Proc. R.Soc.* 269A, 500–527.

ROWE P.W. 1969

"The Relation between the Shear Strength of Sands in Triaxial Compression, Plane Strain and Direct Shear". *Geotechnique* 19, No.1, 75–86.

SCHLOSSER F. & VIDAL H. 1969

"La Terre Armee". *Bull. Liason LCPC* No.41.

SCHLOSSER F. & LONG N.T. 1973

"Etude du Comportement du Materiau Terre Armee. Annales de L'Institut Technique du Batiment et des Travaux Publics. Supplement No. 304. Serie Materiaux No.45.

SCHLOSSER F. 1977

"Experience on Reinforced Earth in France". T.R.R.L./Heriot Watt Univ. Proc. Symp. on Reinforced Earth, Edinburgh. 195 – 203.

SCHLOSSER F. & ELIAS V. 1978

"Friction in Reinforced Earth". Proc. ASCE Symp. Earth Reinforcement. Pittsburgh 735 – 762.

SHEN C.K., MITCHELL J.F., DeNATALE J.S. & ROMSTAD K.M. 1979

"Laboratory Testing and Model Studies of Friction in Reinforced Earth". Proc. Int. Conf. on Soil Reinforcement. Paris, Vol.1. 169 – 174.

SHEN C.K., KIM O.Y., LI X.S. & SOHN J. 1988

"Soil-Reinforcement Interaction Determined by Extension Test". Proc. Int. Geotechnical Symp. Theory and Practice of Earth Reinforcement, Japan. 165 – 170.

SOYDEMIR C. & ESPINOSA A.E. 1979

"Model Behaviour of Reinforced Earth Walls". Proc. Int. Conf. on Soil Reinforcement. Paris Vol.1. 181 – 184.

STANFORD A.L. & TANMER J.M. 1985

"Physics for Students of Science and Engineering". Orlando London.

SWIGER W.F. 1978

"Summary Report". Proc. ASCE Symp. Earth Reinforcement, Pittsburg. 881 – 885.

TAYLOR R.K. 1978

"Properties of Mining Wastes with Respect to Foundations". Foundations Engrg. in Difficult Ground. Newnes – Butterworths, London. 175 – 203.

TAYLOR J.P. & DRIOUX J.C. 1979

"Utilisation de la Terre Armee Dans le Domaine des Barrages". Proc. Int.

TAYLOR R.K. 1984

"Design Shear Strengths for U.K. Coarse Colliery Discards". Symp. on the Reclamation. Treatment and Utilisation of Coal Mining Wastes. Durham, England. 34.1 – 34.14.

TERASHI M. & KITAZUME M. 1988

"Behaviour of a Fabric Reinforced Clay Ground under an Embankment". Centrifuge 88, corte (cd). 243 – 252.

TERZAGHI K. 1956

"Theoretical Soil Mechanics". John Wiler and Sons, INC.

TUMAY M.T., ARMAN A. & ANTONINIM. 1977

"Metal versus Fiber Fabric Earth Reinforcement in Dry Sands — A Comparative Statistical Analysis". T.R.R.L./Heriot Watt Univ. Proc. Symp. Reinforced Earth, Edinburgh. 197 – 210.

VIDAL H. 1966

"La Terre Armee". Annales de L'Inst. Tech de Batiment et des Travaux Publics. Serie Materiaux 30, Supplement. No.223 –224. Jul – Aug.

VIDAL H. 1969a

"The Principle of Reinforced Earth". Highway Res. Red. No.282. 1 – 16.

VIDAL H. 1969b

"La Terre Armee". Annales de L'Institut Technique Batiment et des Travaux Publec. Supplement Vol.22. No. 259 – 260. Serie Materiaux 38.

VIDAL H. 1978

"Development and Future of Reinforced Earth". Proc. ASCE Symp. Earth Reinforcement, Pittsburgh. 1 – 61.

WALTER P.D. 1978

"Performance of Comparison of Ribbed and Smooth Reinforcing strips", Proc. Symp. Soil Reinforcing and Stabilising Techniques, Sydney, Australia. 221 – 231.

WEATHERLY N. 1979

"Trench Filled P.F.A. in Colliery waste Supporting Old People's Bungalows",

Proc. Symp. on The Engineering Behaviour of Industrial and Urban Fill, Univ. of Birmingham.

WESTERGAARD H. M. 1938

"A Problem of Elasticity Suggested by a Problem in Soil Mechanics, Soft Material Reinforced by Numerous Strong Horizontal Sheets". Stephen Timoshenko 60th Anniversary Volume. McMillan. New York.

